



Sensor Design on Inexpensive Substrates for Biochemical Applications

**Thesis in fulfillment of the requirement for the degree of
Doctor of Philosophy in Chemical Engineering**

By

Miaosi Li

M.Sc. (Chem.)

Department of Chemical Engineering

Faculty of Engineering

MONASH UNIVERSITY

March 2015

To my parents
for raising me to believe that
anything was possible

And to my husband L.W.
for making everything possible

Copyright Notice

Under the Copyright Act 1968, this thesis must be used only under the normal conditions of scholarly fair dealing. In particular no results or conclusions should be extracted from it, nor should it be copied or closely paraphrased in whole or in part without the written consent of the author. Proper written acknowledgement should be made for any assistance obtained from this thesis.

I certify that I have made all reasonable efforts to secure copyright permissions for third party content included in this thesis and have not knowingly added copyright content to my work without the owner's permission.

..... 

Miaosi Li

This page is intentionally blank

TABLE OF CONTENTS

	Page
Table of Contents	iii
General Declaration	vii
Acknowledgments	ix
Abstract	xi
List of Publications and Awards	xiii
List of Figures	xvii
List of Tables	xxvi
List of Abbreviations	xxix
List of Nomenclature	xxxix
Chapter 1 Introduction and Literature Review	1
1.1 Introduction	3
1.2 Literature review	6
1.2.1 Current trend for developing diagnostics	6
1.2.2 Low-cost diagnostic devices	7
1.2.3 Review of blood groups	21
1.2.4 Low-cost devices for blood typing	29
1.2.5 Low-cost paper microfluidics for environmental sensing	40
1.3 Review summary	45
1.4 Research aims	47
1.5 Thesis outline	48
1.6 References	51
Chapter 2 Low-cost buffer-free device for forward and reverse blood typing	59
2.1 Abstract	65
2.2 Keywords	66
2.3 Introduction	66
2.4 Experimental	69
2.4.1 Materials	69
2.4.2 Methods	69
2.5 Results and disscussion	73

2.5.2 Antibody dissolution from the plastic slides.....	73
2.5.3 Sensitivity.....	78
2.5.4 Antibody longevity on the plastic slide.....	79
2.5.5 Reverse blood typing using the plastic slide assay	82
2.5.6 Proposed mechanism of RBC agglutination on the plastic slide	83
2.6 Conclusion	84
2.7 Acknowledgements	84
2.8 References	85
Chapter 3 Paper-Based Blood Typing Device that Reports Patient’s Blood Type “in Writing”	87
3.1 Abstract	93
3.2 Keywords	93
3.3 Introduction	93
3.4 Experimental	95
3.4.1 Materials, reagents and blood samples.....	95
3.4.2 Methods.....	96
3.5 Results and disscussion	101
3.6 Conclusion	105
3.7 Acknowledgements	105
3.8 References	106
Chapter 4 Paper-based device for rapid typing of secondary blood groups	107
4.1 Paper-based device for rapid typing of secondary human blood groups	113
4.1.1 Abstract	113
4.1.2 Keywords	113
4.1.3 Introduction	114
4.1.4 Experimental	116
4.1.5 Results and disscussion	119
4.1.6 Conclusion	127
4.1.7 Acknowledgements	128
4.1.8 References	128
4.2 The detection of blood group phenotypes using paper diagnostics	133
4.2.1 Abstract	133
4.2.2 Keywords	134
4.2.3 Introduction	134

4.2.4 Experimental	136
4.2.5 Results	141
4.2.6 Discussions	144
4.2.7 Conclusion	152
4.2.8 Acknowledgements	153
4.2.9 References	153
Chapter 5 Paper-based device for environmental sensing by text-reporting	155
5.1 Abstract	161
5.2 Keywords	161
5.3 Introduction	161
5.4 Experimental	164
5.4.1 Materials and apparatuses	164
5.4.2 Methods.....	164
5.4.3 Indicator solution concentration.....	166
5.5 Results and disscussion	167
5.5.1 Testing results	167
5.5.2 Interference study.....	169
5.5.3 Pseudo-environmental sample analysis	173
5.6 Conclusion	177
5.7 Acknowledgements	177
5.8 References	177
Chapter 6 Conclusions and future work.....	179

Appendix I Published First and Co-Authored Papers Included in the Main Body of This Thesis

I (1) A low-cost forward and reverse blood typing device – a blood sample is all you need to perform an assay	I-1
I (2) Paper-Based Blood Typing Device That Reports Patient’s Blood Type “in Writing”	I-9
I (3) Paper-based device for rapid typing of secondary human blood groups.....	I-15
I (4) The detection of blood group pherotypes using paper diagnostics.....	I-25

I (5) “Periodic-Table-Style” Paper Device for Monitoring Heavy Metals in Water ..	I-37
---	------

Appendix II Published First Authored Papers Not Included in the Main Body of This Thesis

II (1) Change transport between liquid marbles	II-1
--	------

Appendix III Published Co-Authored Papers Not Included in the Main Body of This Thesis

III (1) Understanding Thread Properties for Red Blood Cell Antigen Assays: Weak ABO Blood Typing.....	III-1
III (2) Superhydrophobic surface supported bioassay – An application in blood typing	III-9
III (3) Barcode-Like Paper Sensor for Smartphone Diagnostics: An Application of Blood Typing	III-15
III (4) A study of the transport and immobilisation mechanisms of human red blood cells in a paper-based blood typing device using confocal microscopy.	III-21
III (5) Strategy To Enhance the Wettability of Bioactive Paper-Based Sensors	III-29
III (6) Surface Modification of Cellulose Paper for Quantum Dot-based Sensing Applications	III-35

Monash University

Declaration for thesis based or partially based on conjointly published or unpublished work

General Declaration

In accordance with Monash University Doctorate Regulation 17.2 Doctor of Philosophy and Research Master's regulations the following declarations are made:

I hereby declare that this thesis contains no material which has been accepted for the award of any other degree or diploma at any university or equivalent institution and that, to the best of my knowledge and belief, this thesis contains no material previously published or written by another person, except where due reference is made in the text of the thesis.

This thesis includes 5 original papers published in peer reviewed journals and 0 unpublished publications. The core theme of the thesis is designing new platforms on inexpensive substrate for biochemical applications for end-users in developing countries. The ideas, development and writing up of all the papers in the thesis were the principal responsibility of myself, the candidate, working within the Department of Chemical Engineering, Monash University under the supervision of Prof. Wei Shen.

The inclusion of co-authors reflects the fact that the work came from active collaboration between researchers and acknowledges input into team-based research.

In the case of 4 chapters my contribution to the work involved the following:

Thesis chapter	Publication title	Publication status*	Nature and extent of candidate's contribution
2	A low-cost forward and reverse blood typing device — A blood sample is all you need to perform an assay	Published	Key ideas, experimental works, analysis of results, writing up.
3	Paper-Based Blood Typing Device That Reports Patient's Blood Type "in Writing"	Published	Key ideas, experimental works, analysis of results, writing up.
4	4.1 Paper-based device for rapid typing of secondary human blood groups 4.2 The detection of blood group phenotypes using paper diagnostics	Published	Key ideas, experimental works, analysis of results, writing up.
5	"Periodic-table-style" paper device for monitoring heavy metals in water	Published	Key ideas, experimental works, analysis of results, writing up.

I have / have not (circle that which applies) renumbered sections of submitted or published papers in order to generate a consistent presentation within the thesis.

Signed:



Date:

03-03-2015

This page is intentionally blank

ACKNOWLEDGEMENTS

I would like to express my sincere gratitude and thanks to my supervisor Prof. Wei Shen for his constant guidance, encouragement, support and patience throughout my PhD candidature. Prof. Shen is the one of most impressive and passionate supervisors I have ever worked with. He provided me the opportunity to start the excellent and interesting PhD project. During my PhD candidature, he trained me to think critically and independently; encouraged me to try innovative ideas; taught me to improve my writing skills for publication in top level journals and give attractive presentations; motivated me to do better than what I would expect from myself; supported me when I was in stress; inspired me to never afraid of failure. He is always there to help me and guide me to enjoy both research and life, which will be treasured all my life. I really appreciate his supervision and enjoy working with him.

I gratefully acknowledge Haemokinesis, ARC Linkage Grant, Faculty of Engineering and Monash University for providing me the living allowance and tuition fee scholarship which have made my PhD work possible.

I would like to acknowledge Prof. Gil Garnier, Assoc. Prof. Xiwang Zhang, Prof. Wenlong Cheng, Dr. Warren Batchelor and Dr. Lian Zhang in Bioresource Processing Research Institute of Australia (BioPRIA) and Department of Chemical Engineering at Monash University, for their kind help and suggestions about my project. I also would like to thank Dr. John Zhu in Melbourne Center of Nanofabrication for his technique training and result discussions.

I would like to thank Ms. Jane Moodie for her helpful discussions and suggestions about my thesis, as well as Dr. Alex McKnight and Ms. Whui Lyn Then for proofreading this thesis. I also would like to acknowledge the administrative staff and the technical staff at BioPRIA and Department of Chemical Engineering: Janette Anthony, Lilyanne Price, Jill Crisfield, Scot Sharman, Heather McIlesh, Kim Phu, Ron Graham, Gamini Ganegoda, for their support and assistance during my study.

I would like to express many thanks to Dr. Junfei Tian for his help and suggestions throughout my project, especially for his innovative inspirations when I just started my

candidature. I would like to thank Dr. Xu Li, Dr. David Ballerini, Whui Lyn Then, Lizi Li, Liyun Guan, Rong Cao, Azadeh Nilghaz, Baiqian Dai, and Windy Huang for their support and help during the experimental work and paper writing. I will also thank Natasha Yeow, Jielong Su, Ruoyang Chen, Liyuan Zhang, Tina Arbatan, Preveena Raj, Ying Hui Ngo, Hui Hui Chiam, Sigappi Narayanan, Rosiana Lestiani, Dr. Varanasi Swambabu, Matthew O'Connor, Zhiyong He and Uthpala Garusinghe at BioPRIA for their friendship throughout my PhD study.

I would like to express my deep yearning to my friend Miss Yuzhou Wu in the Department of Chemical Engineering. I will always appreciate and cherish her help, support and friendship during my life.

Last but most importantly, I would like to thank my parents and every member in my family for their deep, unconditional and lifetime love and support. I would like to express my deepest gratitude to my husband Liwei Wang, for he's always being my side to accompany, understand and support me during my entire PhD study.

ABSTRACT

This research project focuses on exploring new sensor design methods on inexpensive substrates for various biomedical and chemical applications, in order to improve the health and life quality of people living in less-industrialized countries and remote regions. People living in these areas are more susceptible to diseases due to shortage of funds, medical facilities, medical knowledge and professional staff. This project has noticed that for most existing point-of-care diagnostics designed for developing areas, although are affordable, sensitive, specific and rapid (“ASSR”), cannot be practically utilized in these areas, for they are not easily operated by non-professional and untrained personnel. In particular, a desirable user-oriented device is required to be user-friendly, equipment-free and delivered to end-users (“UED”), and achieving these demands, therefore, is the aim of this project.

This thesis includes two parts, presenting two original sensor design concepts respectively. One is the “sample-only” method, which only requires the user to introduce the sample to the sensor with no extra effort during the assay; the other one is the “text-reporting” method, which can report the assay result directly with unambiguous text messages to the user. Both of the two concepts effectively address the “UED” problems in existing devices.

The sensors developed by the new design concepts were conducted through fabrication on inexpensive substrates, which are cellulose paper and plastic (or glass) slides throughout this research. The patterning of these substrates is processed through traditional industrialized surface treatment, paper-sizing and printing techniques, making the devices affordable and easily-obtained.

The feasibility of these two concepts is then demonstrated through applying them to practical applications. The first application is blood typing. The “sample-only” method allows the user to get clear blood typing results by only introducing one blood drop during the assay. The “text-reporting” method designs the first paper-based blood typing device that reports a patient’s blood type in written text, which enables non-professional users to determine the blood types immediately. Furthermore, the “text-

reporting” method also presents its desirable features in another application: environmental monitoring. With the help of text-based information, even untrained users can quickly and simply obtain the testing result of contaminants in water at home, in the field, in emergency and many other areas where laboratories are not readily available. None of these applications requires supporting equipment and personnel for assay analysis and result interpretation.

The applications performed by the new sensor design methods in this project bring the test immediately and conveniently to the patients or end-users, and effectively reduce the high-dependency of testing on hospitals or central laboratories. The sensor design concepts explored in this project establish the “ASSURED” platform which is highly practical for use by non-professional users in developing countries. These methods also hold enormous potential for integration with future work, which would strongly drive the development of products for point-of-care, telemedicine and on-site environmental sensing.

LIST OF PUBLICATIONS AND AWARDS

Peer-Reviewed Journal Papers

The following published papers are included in the main body of this thesis as individual chapters. The sections of these published papers have been renumbered in order to generate a consistent presentation within the thesis. Papers in their published format are included as Appendix 1 in this thesis.

1. **Li, M.**, Cao R., Nilghaz, A., Guan L., Zhang, X., Shen, W., “Periodic-table-style” paper device for monitoring heavy metals in water, *Anal. Chem.*, 2015, **87**(5): 2555–2559
2. **Li, M.**, Tian, J., Cao., R., Guan, L., Shen, W., A low-cost forward and reverse blood typing device — A blood sample is all you need to perform an assay, *Anal. Methods*, 2015, **7**: 1186–1193.
3. **Li, M.**, Then, W., Li, L., Shen, W., Paper-based device for rapid typing of secondary human blood groups, *Anal. Bioanal. Chem.*, 2014, **406**: 669–677.
4. **Li, M.**, Tian, J., Al-tamimi, M., Shen, W., Paper-Based Blood Typing Device That Reports Patient's Blood Type "in Writing", *Angew. Chem. Int. Ed.*, 2012, **51**: 5497–5501.
5. Then, W., **Li, M.**, McLiesh, H., Shen, W., Garnier, G., The detection of blood group phenotypes using paper diagnostics, *Vox Sanguinis*, 2015, **108**: 186–196.

The following published papers are not included in the main body of this thesis and can be find in Appendix 2 and 3 in their published format.

6. **Li, M.**, Tian, J. Li, L., Shen, W., Charge Transport between Liquid Marbles, *Chem. Eng. Sci.*, 2013, **97**, 337–343.
7. Nilghaz, A., Zhang, L., **Li, M.**, Ballerini, D., Shen, W., Understanding Thread Properties for Red Blood Cells Antigen Assays: Weak ABO Blood Typing, *ACS Applied Materials & Interfaces*, 2014, **6**(24):22209–22215.

8. Li, L., Tian, J., **Li, M.**, Shen, W., *Superhydrophobic surface supported bioassay--an application in blood typing*, *Colloids and Surfaces B: Biointerfaces*, 2013, **106**, 176–180.
9. Guan, L., Tian, J., Cao, R., **Li, M.**, Wu, Z., Nilghaz, A., Shen, W., Surface Modification of Cellulose Paper for Quantum Dot-based Sensing Applications, *BioResources*, 2015, **10**(1): 1587–1598.
10. Guan, L., Tian, J., Cao, R., **Li, M.**, Cai, Z., Shen, W., Barcode-Like Paper Sensor for Smartphone Diagnostics: An Application of Blood Typing, *Anal. Chem.*, 2014, **86** (22): 11362–11367.
11. Li L., Tian, J., Ballerini, D., **Li, M.**, Shen, W., A study of the transport and immobilisation mechanisms of human red blood cells in a paper-based blood typing device using confocal microscopy, *Analyst*, 2013, **138**(17): 4933–4940.
12. Tian, J., Jarujamrus P., Li L., **Li, M.**, Shen, W., Strategy To Enhance the Wettability of Bioactive Paper-Based Sensors, *ACS Appl. Mater. Interfaces*, 2012, **4** (12): 6573–6578.

Conference Papers

Li, M., Tian, J., M, Al-Tamimi and Shen, W., A “Text reporting” Paper-Based Blood Typing Device, *MMT 2012*, Ariel Israel, 2012.

Patents

Shen, W., Al-Tamimi, Tian, J., **Li, M.**, Device and method for identifying and reporting blood sample test results, AU2011905163.

Awards

1. “Win in Suzhou” 2014 Australian Start-up Competition---Final list; Second Prize, Sydney, 2014.
2. Chinese non-government sponsored student scholarships, Melbourne, 2013.
3. The Australian Museum Eureka Prize of “Innovative Use of Technology”, Group member, Sydney, 2012.09.
4. IChemE award of “Dhirubhai Ambani Chemical Engineering Innovation for Resource-Poor People Award”, Group member, UK, 2012. 11.

This page is intentionally blank

LIST OF FIGURES

Chapter 1

- Figure 1:** Procedures of clinical test by central laboratory and POC testing. (With permission from ref. [11]. Copyright (2005) Elsevier)
- Figure 2:** The development of paper-based analytical and diagnostic devices since 1850.
- Figure 3:** The six-step fabrication procedure of μ PADs using lithographic method. (a) A pattern with SU-8 photoresist barrier was created on a piece of filter paper. (b) After plasma treatment, the patterned paper was loaded with reagents for bioassays. (With permissions from ref. [3]. Copyright (2007) John Wiley and Sons.)
- Figure 4:** Alkyl ketene dimer (AKD) sizing reaction with cellulose fibres to lower the surface energy and water-penetration rate in paper.
- Figure 5:** Ink jet printed paper fluidic pattern of a Chinese paper cut. Four liquid feeding zones were added to the four corners of the pattern. Water penetration at an early stage (a) and at the final stage (b) is shown. (With permissions from ref.[51]. Copyright (2010) Elsevier.)
- Figure 6:** (A) Schematic illustration of the processes to produce patterned paper with wax; (1) hand drawing with a wax pen; (2) printing with an inkjet printer followed by painting with a wax; (3) printing with a wax printer. (B) The fabricated microfluidic on filter paper with wax in three different ways: (a) hand painting with a wax pen; (b) printing with an inkjet printer followed by painting with a wax pen and (c) printing with a wax printer directly. (C) Comparison of the channel width of patterned paper produced by wax printing (a) before and (b) after heating in oven (1mm is the width of the micro-channels). (With permissions from ref.[52]. Copyright (2009) John Wiley and Sons)
- Figure 7:** (a) Schematic diagram of the fabrication step for wax screen-printing method. (b) Resolution of the wax screen-printing method showing the smallest hydrophilic channel width. (With permissions from ref.[53]. Copyright (2011) Royal Society of Chemistry)
- Figure 8:** Procedure for patterning paper by wax dipping in top view (left) and lateral view (right). (With permissions from ref. [54]. Copyright (2011) Elsevier)
- Figure 9:** Examples of colorimetric assay for the semi-quantitative detection of glucose and protein (a) (With permissions from ref. [3]. Copyright (2007) John Wiley and Sons), NO_2^- (b) (With permissions from ref. [51]. Copyright (2010) Elsevier), and glucose, lactate and uric acid (c) (With permissions from ref. [67]. Copyright (2010) Elsevier).
- Figure 10:** (a) Design of the electrochemical cell for paper-based microfluidics. WE, working electrode; RE, reference electrode; CE, counter electrode. (b) Three

electrode paper-based microfluidic devices for the EC detection of glucose, lactate and uric acid. (With permissions from ref. [80]. Copyright (2009) American Chemical Society)

Figure 11: Fabrication and operation of a paper-based microfluidic ECL sensor. (a) The patterned paper microfluidics by inkjet printer. (b) The individual paper fluidic elements were cut to size and the hydrophilic areas were filled with $\text{Ru}(\text{bpy})_3^{2+}$ solution. (c) The paper substrate was then aligned and combined with the screen printed electrode. (d) Camera phone captured ECL signals for further analysis. (With permission from ref. [86] Copyright (2011) American Chemical Society)

Figure 12: Recent thread-based microfluidic for biochemical and chemical analysis based on colorimetric result reporting methods: (a) various colorimetric detection for protein, nitrite and ketone; (b) colorimetric NO_2^- concentration series (0, 125, 250, 500, and 1000 μM) developed using a sensor array made of filter paper and cotton thread (With permissions from ref. [87]. Copyright (2010) American Chemical Society); (c) colorimetric protein assay ranging from 0-6 mg/mL conducted on the thread by distance measurement ; (d) colorimetric assay of nickel ion ranging from 0-1000 μM . (With permissions from ref. [93]. Copyright (2014) Elsevier)

Figure 13: The determination of ABO blood groups followed by Landsteiner's law.

Figure 14: Illustration of the Rh-induced haemolytic disease of the fetus and newborn.

Figure 15: Methods for blood typing based on the column agglutination in gel (i.e. Gel Card technology): blood sample interacts with the antibody and then passes through the gel matrix during centrifugation; agglutinated large RBC lumps are blocked by the gel, whereas the free cells with no antibody binding reaches to the bottom of the microtube after centrifugation, showing the different blood typing results.

Figure 16: Schematic diagram of the structure of IgM and IgG molecule.

Figure 17: Schematic diagram showing direct and indirect blood typing by antibodies of different structures: a) Antibody IgM causes the direct blood cell agglutination; b) IgG antibody cannot lead to a direct agglutination reaction but only the cell sensitisation after incubation with the RBCs; the excess of IgG need to be wash out after the incubation, and afterwards the AHG are added to induce the RBC agglutination for the blood group determination.

Figure 18: Testing with samples of whole blood of type A+, B+ and O- on antibody-treated polyester threads. Columns show results on threads A, B and D from left to right, whilst rows show the results for the different blood types, as labelled on the left. (With permissions from ref.[114]. Copyright (2011) Springer)

Figure 19: (a) A single-step blood grouping test prototype for proof of concept and (b) the results for typing a blood sample A+. (With permissions from ref.[114]. Copyright (2011) Springer)

- Figure 20:** Blood group detection using wicking of agglutinated colloids from specific antigen/antibody interaction on dry paper strips. Blood typing: (a) B+ and (b) O+. (With permissions from ref. [4]. Copyright (2010) American Chemical Society)
- Figure 21:** Agglutinated blood fixations on papers and chromatographically eluted with 0.9% NaCl buffer for 10 min. (With permissions from ref. [113]. Copyright (2012) American Chemical Society)
- Figure 22:** (a) The approach for simultaneously determining Rh typing and (b), the forward and reverse ABO blood groupings and the results based on the ratio of the distance. (With permissions from ref. [116]. Copyright (2015) Elsevier)
- Figure 23:** Assays of eight ABO/RhD blood types by the barcode-like paper-based blood typing device. (With permissions from ref. [117]. Copyright (2014) American Chemical Society)
- Figure 24:** Smartphone application for reading the blood typing information and displaying blood typing result on its screen. (With permissions from ref. [117]. Copyright (2014) American Chemical Society)
- Figure 25:** Protocol for the quantification of desorbed antibody from testing papers by the saline washing simulation. (With permissions from ref. [118]. Copyright (2012) Royal Society of Chemistry)
- Figure 26:** Protocols of testing RBCs agglutination in paper with both adsorbed and desorbed antibodies. (With permissions from ref. [118]. Copyright (2012) Royal Society of Chemistry)
- Figure 27:** Confocal images of non-agglutinated and agglutinated RBCs patterns inside antibody-treated paper: (a) image of non-agglutinated RBCs captured with 20 folds magnification; (b) image of non-agglutinated RBCs captured with 60 folds magnification. (c) 3D image of non-agglutinated RBCs captured with 60 folds magnification; (d), (e), (f) are images of agglutinated RBCs captured with the same condition from (a), (b) and (c), respectively. (With permissions from ref. [119]. Copyright (2013) Royal Society of Chemistry)
- Figure 28:** Antibody stability studies by protection of additives (A) and free-drying (B). For additive protection, the specific (+) and non-specific (-) test results of paper squares loaded with antibodies on day 0 (top) and day 28 (bottom) were tested by (a) without additives, (b) with 1 % PVP, (c) with 6 % dextran and (d) with 10 % glycerol. For freeze-drying, the specific and non-specific test results of freeze-dried paper squares loaded with antibodies were tested after stored for (a) 0 days, (b) 3 days, (c) 7 days, (d) 14 days, (e) 28 days, and (f) 42 days. (With permissions from ref. [120]. Copyright (2013) Springer)
- Figure 29:** Optical density from blood typing on different papers: a) filter papers; b) blotting and Kleenex towel papers; c) experimental papers made from long and short fibres. (With permissions from ref. [121]. Copyright (2012) Springer)
- Figure 30:** Detection principle and results of the sensor: (a) fabrication of the multiplexed sensor; (b) colorimetric assay of Hg (II) on the patterned paper

device in a concentration-dependent manner; (c) detection of four individual metals from a mixture of metals. (With permissions from ref. [5]. Copyright (2011) American Chemical Society)

Figure 31: The 3D paper microfluidic chip fabrication: (a) four wax-patterned paper layers stacked by three double-sided stick tape. The paper layers were patterned hydrophilic channels to deliver liquids while the tape layers were modified by holes that connected channels in each paper layer; (b) the detection of four metals enabled by the four sample inlets on the device; (c) colorimetric assays of the four heavy metals in the detection zone. (With permissions from ref. [126]. Copyright (2014) Springer)

Figure 32: The sensor modification and detection process: (a) fabrication of the paper-based device with different detection zone for colorimetric and electrochemical assays; (b) analytical procedure for metal testing on an air sampling filter. The anodic stripping voltametric method was used for detection of Cd and Pb and the colorimetric reaction was for Fe, Ni, Cr and Cu assays. (With permissions from ref. [129]. Copyright (2014) American Chemical Society)

Chapter 2

Figure 1: Demonstration of a blood typing assay of an A+ blood sample on a plastic slide substrate by: (a) placing a drop of blood sample on a drop of anti-A; (b) tilting the substrate to allow the blood sample and anti-A solution to spread into a film, immediately revealing the positive assay result; (c) a drop of A+ blood sample placed on a drop of anti-B; (d) tilting the substrate to reveal the negative assay result.

Figure 2: The designed procedure for blood typing on a plastic slide.

Figure 3: Schematics of the procedure for studying the antibody dissolution behaviour from the plastic slide. This procedure involves an antibody dissolution step by PBS, followed by quantifying the concentration of the antibodies washed off the plastic slide.

Figure 4: Assay results reported by the plastic slide device for all 8 ABO and RhD blood groups

Figure 5: Antibody dissolution behaviour study for anti-A: (a) Anti-A activity as a function of a series of dissolutions with PBS; antibody activity can be determined by the reflective optical density of the agglutinated A1 reagent red cell (concentrated from the commercial reagent to a hematocrit level of 45%) on paper. (b) The calibration curve of the A1 cell optical density as a function of anti-A dilution factor; the red curve is the fitting curve of a

natural logarithm function (formula 1); (c) anti-A dissolution behaviour of five consecutive PBS dissolution rinses collected from the plastic substrate.

Figure 6: Antibody dissolution behaviour study for anti-B: (a) anti-B activity as a function of series of dilution, tested by the agglutination colour density of the B reagent red cell (concentrated from the commercial reagent to a hematocrit level of 45%); (b) the standard curve of the B cell colour density as a function of anti-B dilution factor; (c) anti-B dissolution behaviour of five consecutive PBS dissolution rinses of the plastic device.

Figure 7: Antibody dissolution behaviour study for anti-D: (a) anti-D activity as a function of series of dilution, tested by the agglutination colour density of the C reagent red cell (concentrated from the commercial reagent to a hematocrit level of 45%); (b) the standard curve of the C cell colour density as a function of anti-D dilution factor; (c) anti-D dissolution behaviour of five consecutive PBS dissolution rinses of the plastic device.

Figure 8: Sensitivity tests of the plastic slide method by dilution of reagent red blood cell carrying known antigens: (a) A1 cells in the anti-A treated channel; (b) B cells in the anti-B treated channel; (c) C1 cell in the anti-D treated channel. The negative control channel was treated with BSA only.

Figure 9: Lifetime detection for blood group A interaction with anti-A treated device staying for different periods.

Figure 10: Antibody activity for its corresponding antigen after being deposited for 45 days on the device surface coated with an additive mixture of 10% of glycerol and 0.1% of Tween 20. Test was conducted under an ambient laboratory condition.

Figure 11: The reverse blood typing results for identifying ABO blood groups.

Chapter 3

Figure 1: Schematics of the two design solutions using composite text symbols to report blood test results in text. (a) Design solution 1: The composite text symbol for reporting the presence of RhD takes the form of “+”; it consists of a permanent “-” printed using water-insoluble ink and a “|” printed using Anti-D. (b) Design solution 2: The composite text symbol for reporting “O” and “non-O” types of blood samples takes the form of “⊗”; it consists of a permanent letter “O” printed using non-bioactive water-insoluble ink and a “×” printed using an equal-volume mixture of Anti-A and Anti-B.

Figure 2: The designed and printing of the text-reporting paper device.

Figure 3: (a) The Kleenex paper towel hydrophobized by AKD, leaving text patterns hydrophilic. (b) The hydrophilic text patterns become visible when wetted by antibody solutions.

Figure 4: Fabrication and testing procedures of the text-reporting blood-typing devices. Negative patterns of letters and symbols are printed using a heptane solution of an alkenyl ketene dimer; letters and symbols remain hydrophilic and are surrounded by hydrophobic areas. (a) Anti-A and Anti-B are introduced into the corresponding letters. An equal-volume mixture of Anti-A and Anti-B is introduced into “×”, and Anti-D is introduced into “|”. (b) Letter “O” and symbol “—” are printed over “×” and “—”, respectively, using a non-bioactive and water-insoluble ink. (c) A blood sample is introduced in the device for blood typing test. (d) After washing each pattern with 2×50 µL of saline solution, the blood typing result is reported by the device in text.

Figure 5: (a) The complete paper text-reporting device for blood typing. (b) After an A+ blood sample was introduced into all text patterns. (c) Text report of the blood typing assay result was obtained after washing the text patterns with NaCl buffer (2×50 µL).

Figure 6: (a) A schematic of the expected text patterns reported by the blood type device fabricated based on our design. The corresponding blood types are given to assist the reader. (b) The actual tests of all eight ABO RhD blood types. The device size is 25 mm×25 mm.

Figure 7: Blood sample dilution for the evaluation of the sensitivity of the method. Dilution was made to from 100% (i.e. undiluted) to 25% (i.e. ¼ blood sample mixed with ¾ NaCl buffer, (v/v)). (a) A+ sample; (b) B+ sample.

Figure 8: The test of weak blood samples using the paper-based text-reporting devices.

Chapter 4

Chapter 4.1

Figure 1: Schematics of design, fabrication, testing procedures and result reporting of paper diagnostics for secondary blood typing.

Figure 2: Paper-based blood group assay designed for identifying 11 antigens in 7 secondary blood groups. The grouping assay was performed under the same condition: reaction time was 30 seconds and the washing of free RBC was done using 0.9% NaCl PSS. Reference assays using the mainstream technology (Gel Card) showed that the secondary groups of this blood sample were: C(-), E(-), c(+), e(+), K(-), Jka(+), Jkb(+), M(+), N(+), S(+), P1(+), Lea(+).

Figure 3: Increasing degrees of heamagglutination of the second group e in antibody-treated paper as a function of time.

Figure 4: Haemagglutination behaviour of 3 blood groups investigated by confocal imaging (60× oil immersion lens): (a) RBCs of primary group D(+) agglutinated by D antibodies within 30 s; (b) RBCs of secondary group E(+) agglutinated by E antibodies within 30 s; (c) RBCs of secondary group e(+) did not show any sign of agglutination after reacting with e-antibody for 30s; (d) group e(+)RBCs showed clear agglutination when reacting with e-antibody for 3 mins.

Figure 5: The comparison of the effect of antibody structures (IgG and IgM) on the visual identification of the testing results: (a) for K antigen test; (b) for s antigen test. Confocal images show details of haemagglutination behaviours of K(+) and s(+) on paper treated with different antibodies: (c) anti-K IgG, (d) anti-s IgG, (e) anti-K IgM and (f) anti-s IgM. Reaction times of all assays were 2 min and 60× oil lens was used.

Figure 6: (a) Visual assay of a M(+) blood sample on paper and (b) confocal image taken for the same sample. A commercial Anti-M IgM obtained from human sera was used for the assay and 3 mins reaction time was allowed.

Figure 7: Identification for agglutinated RBCs of blood group c washed by: (a) distilled water; (b) 0.9% NaCl; (c) PBS. Two minutes RBC-antibody interaction time was allowed.

Chapter 4.2

Figure 1: Methodology for blood group phenotyping using paper via elution

Figure 2: Fabrication, testing procedures and result reporting of paper diagnostics for antigen detection using example: blood group K.

Figure 3: Blood group phenotyping using (a) elution, and (b) text reporting methods on paper. Blood spot (BS) and elution pathway (EP) are represented as density. Extent of coagulation is represented as optical density ratio (ODR) comparing density EP:BS. Positive is denoted by high density and ODR, negative has lower densities and ODR. (Fyb was not tested using the text reporting method.)

Figure 4: (a) Effect of time on the reaction period tested with c antigen, comparing elution method (E) and text-reporting method (T). ODR of E is compared to density of T. (b) Effect of time on the reaction period tested with c antigen using text-reporting

Figure 5: Comparison of antisera (polyclonal or IgM) affecting identification of testing results for K antigen.

Figure 6: Effect of anti-K polyclonal concentration on efficacy; (a) at stock solution, (b) double stock concentration by volume, and (c) quadruple stock concentration by volume.

Figure 7: Dispersion difference between the commercial product and FFMU antibody Lea.

Chapter 5

Figure 1: The electronically generated chemical symbol patterns of the three heavy metals in their true size.

Figure 2: Schematic diagram of the fabrication of patterns of heavy metal chemical symbols on chromatographic paper.

Figure 3: Colorimetric assay for the selection of indicator concentrations: a) bathocuproine concentration from 10 to 60 mg/mL for detection of 1.0 mg/L Cu(II) sample; b) 1,5-diphenylcarbazide concentration from 0.6 to 4.0 mg/mL for detection of 0.5 mg/L Cr(VI) sample; c) dimethylglyoxime concentration from 60 to 100 mM for detection of 1 mg/L Ni(II) sample.

Figure 4: Colorimetric assays showing heavy metal ions of different concentrations: (a) Cu(II); (b) Cr(VI) and (c) Ni(II).

Figure 5: Calibration curves fitted by the measured colour intensity versus the concentration of each ion: a) Copper, concentration from 0.8 to 8 mg/L; b) Chromium, from 0.5 to 4 mg/L; c) Nickel, from 0.6 to 6 mg/L.

Figure 6: Interference tolerant studies of the paper devices for the three target heavy metal ions in the presence of Cu(II), Cr(VI), Ni(II), Fe(III) and Zn(II) as interfering ions (5 parallel tests for each assay): a) Cu(II) assays of 0.8, 4 and 8 mg/L of Cu(II); b) Cr(VI) assays of 0.5, 2 and 4 mg/L Cr(VI); c) Ni(II) assays of 1, 4 and 6 mg/L of interfering ions; d) The responses of the Cu(II), Cr(VI) and Ni(II) indicator systems to non-target multiple interferent ions solutions. For assays in a) to c), the concentration of each interfering ion was 10 times higher than that of the target ion. For assays in d), samples contained no target ions; the concentrations of all non-target metal ions were 10 mg/L.

Figure 7: Interference tolerant studies of the paper devices for the three target heavy metal ions in the presence of 10 mg/L Cr (VI), Mn(II), Fe(III), Co(II),

Ni(II), Zn(II) for 1 mg/L Cu(II) assay; 10 mg/L Mn(II), Fe(III), Co(II), Ni(II), Cu(II), Zn(II) for 1.0 mg/L Cr(VI) assay; 10 mg/L Cr (VI), Mn(II), Fe(III), Co(II), Cu(II), Zn(II) for 1 mg/L Ni(II) assay, and 200 mg/L Na(I) and K(I), 100 mg/L Ca(II) and Mg (II) for all the three assays.

Figure 8: Pseudo-environmental samples analyzed by paper-based devices and ICP-AES method: a) tap water with spiking of 1mg/L Cu(II), 0.5 mg/L Cr(VI) and 1mg/L Ni(II); b) tap water with spiking of 5 mg/L Cu(II), 3 mg/L Cr(VI) and 5 mg/L Ni(II).

Figure 9: Text-reporting paper device for Cu(II), Ni(II) and Cr(VI) assay in a simulated environmental assay: tap water with striking of 5 mg/L Ni(II), 5 mg/L Cu(II), and 3 mg/L Cr(VI) respectively.

LIST OF TABLES

Chapter 1

Table 1: Other reported techniques for patterning paper-based microfluidics with their patterning reagents and principles.

Table 2: List of the common clinically important blood group systems

Table 3: Blood type determine principles by forward and reverse blood typing

Chapter 2

Table 1: Blood type confirmation by forward and reverse blood typing methods.

Table 2: The blood spot optical density data and the calculated concentrations of three antibodies of each dissolution from the plastic substrate.

Table 3: Additives effect on the surface hydrophilicity for blood flowing with the increase of time

Chapter 3

Table 1: Blood types that can be reported in text by specific antigen-antibody agglutination reactions before and after implementing our design solutions (See Figure. 1)

Table 2: Statistics of blood typing data obtained using paper text-reporting devices

Chapter 4

Chapter 4.1

Table 1: List of the common secondary blood group systems

Table 2: Agglutination reaction time required by each secondary blood group

Table 3: Statistics of secondary blood typing data obtained using paper devices

Chapter 4.2

Table 1: Blood groups and the corresponding antibodies used for blood group phenotyping on paper. The antibody structure and clone is also included.

Table 2: Blood group phenotyping using the Elution (E) and Text reporting (TR) methods on paper. Blood spot (BS) and elution pathway (EP) are represented as density. Optical density ratio (ODR) compares density EP:BS. Positive is denoted by high density and ODR, negative has lower densities and ODR.

Table 3: Results achieved for the MNS blood system using the Elution (E) and Text reporting (TR) methods on paper. Blood spot (BS) and elution pathway (EP) are represented as density. Optical density ratio (ODR) compares density EP:BS. Positive is denoted by high density and ODR, negative has lower densities and ODR.

Chapter 5

Table 1: Tolerance ratio of interference ions for detection of 1 mg/L Cu(II), Cr(VI) and Ni (II).

Table 2: Recovery rate of spike water sample determined by paper device and ICP-AES

This page is intentionally blank

LIST OF ABBREVIATIONS

3D	three dimension
AAS	atomic absorption spectrometer
AHG	anti-human globulin
AKD	alkyl ketene dimer
AR	analytical grade
ARC	Australian Research Council
ARCBS	Australian Red Cross Blood Service
ASA	alkenyl succinic acid anhydride
AuNP	gold nanoparticle
BioPRIA	Bioresource Processing Research Institute of Australia
BS	blood spot
BSA	bovine serum albumin
CAT	column agglutination test
CE	capillary electrophoresis
CL	chemiluminescence
CPRG	chlorophenol red β -galactopyranoside
DMG	dimethylglyoxime
DMSO	dimethyl sulphoxide
DNA	deoxyribonucleic acid
DPC	1,5-diphenylcarbazine
DPCA	1,5-diphenylcarbazon
EC	electrochemical
ECL	electrochemiluminescence
EP	elution pathway
FFMU	for further manufacturing use
FITC	fluorescein isothiocyanate
GC	gas chromatography

GAL	galactosidase
HDFN	haemolytic disease of the fetus and newborn
HTR	haemolytic transfusion reactions
IAT	indirect antiglobulin test
ICP-AES	inductively coupled plasma atomic emission spectroscopy
ICPMS	inductively coupled plasma mass spectroscopy
IgG	immunoglobulin G
IgM	immunoglobulin M
ISBT	international society of blood transfusion
ODR	optical density ratio
PBS	phosphate buffered saline
POC	point of care
PVP	polyvinylpyrrolidone
RBCs	red blood cells
Rh	rhesus
TR	Text-reporting
U.S.EPA	United States Environmental Protection Agency
WHO	world Health Organization
μPADs	microfluidic paper-based analytical devices
μTADs	microfluidic thread-based analytical devices

LIST OF NOMENCLATURE

C_A	original concentration of anti-A
C'_A	diluted concentration of anti-A
C_B	original concentration of anti-B
C'_B	diluted concentration of anti-B
C_D	original concentration of anti-D
C'_D	diluted concentration of anti-D
D	reflective optical density
f_A	dilution factor of anti-A
f_B	dilution factor of anti-B
f_D	dilution factor of anti-D
I	measured reflected light intensities
I_0	incident reflected light intensities
L	liter
l	liquid penetration distance
mg	milligram
min	minute
mL	milliliter
mM	millimolar
mm	millimetre
R^2	correlation coefficient
r	equivalent capillary pore radius
s	second
t	penetration time
W	watt
γ	surface tension
η	viscosity
θ	contact angle
μL	microlitre

μM

micromolar

$^{\circ}\text{C}$

degree Celsius

Chapter 1

Introduction and Literature Review

This page is intentionally blank

1.1 Introduction

In the world today, affordable health care, including early diagnosis and screening of diseases, environmental monitoring and food and water quality testing, are in increasing demand, especially in remote areas and in less industrialized countries, where the centralized laboratories and hospitals taken for granted in the cities of the developed world are absent. Due to the lack of established and affordable medical facilities for disease detection, disease treatment and infectious disease control, people become much more susceptible to diseases. To overcome these problems, the World Health Organisation (WHO) recognizes the development of inexpensive, self-contained and easy-to-use diagnostics as an imperative objective. The WHO has developed the concept “ASSURED” — affordable, sensitive, specific, user-friendly, rapid, equipment-free and delivered to end-users [1], which clarifies critical criteria that must be met by potential diagnostics designed for use in developing countries.

Low-cost diagnostics for home users are also in increasing demand in industrialized countries. Factors driving this demand are the ageing of the population and the steady increase of so-called life-style diseases in western countries. These factors put high pressure on the current medical systems of these countries, forcing governments and research institutions to develop strategies to cope with such pressure. An effective way to alleviate the pressure is to develop point-of-care (POC) diagnostics to enable patients to perform their personal health-care evaluations at home. They may then communicate their test results to experts in central laboratories and hospitals for further evaluation and medical instructions [2].

POC has been proven to be a workable approach to control some of the worst lifestyle diseases. An example of a POC diagnostic device is the blood glucose monitoring device. Patients can monitor their blood glucose level at home without any assistance from professionals. From the health care point of view, the glucose device enables patients to monitor and thus control their own condition without having to frequently visit doctors for medical intervention. Clearly, POC devices, which meet the “ASSURED” criteria, will play a significant role in future human health care and disease control in both developing and developed countries. In this thesis, the terms

low-cost diagnostics and POC diagnostics are used interchangeably to refer to user-operated devices designed for non-professional users such as home users.

A number of POC systems involving microfluidic diagnostic technology (MDT) have become cost-effective in recent years. The market for POC products for diagnosis has significantly increased, particularly for those products designed for use in developing countries and less-industrialized areas. Inexpensive materials, including plastics, paper, and thread are applied in new POC devices which have been demonstrated in research laboratories for tests such as bioassays, blood typing, and food and water quality control [3-5]. These devices present high “ASSR” (affordable, sensitive, specific and rapid) performance in their intended analytical and diagnostic applications. However, the “UED” criteria, i.e., user-friendly, equipment free and delivered (to end users), still present an impassable barrier for the innovations to be developed into reliable user-operated devices. In order to achieve “UED” features, equipment-free devices should be designed in a such way that not only the users’ efforts to operate the devices are significantly reduced, but also the test results can be presented in a clear way to minimize possible misinterpretations by non-professional users.

Of these criteria, user-friendliness (U), which builds the connections between diagnostic devices and their users, is one of the major hurdles preventing many current diagnostic methods from being commercially available. Although many diagnostic and analytical assays can be performed rapidly on inexpensive substrates with high sensitivity and selectivity, the assays require a certain professional level of operating skill. As a result, a non-professional user cannot operate the assays without training and the results reported by these assays are also not straightforward enough for non-professional users to interpret without assistance from professional medical workers. Secondly, the criteria equipment-free (E) and delivered (D), i.e., accessible to end-users, are also absent from many reported methods demonstrated in research laboratories. In these methods, supporting equipment including electrochemical stations and colour intensity analysers has to be used to capture signals and analyse results [3-5]. Such equipment often requires a high level of professional skills which is usually beyond the capability of general non-professional users. Therefore, although most current POC devices are well-designed as “ASSR” devices, considerable efforts are

urgently required to improve their “UED” features.

The broad aim of the research reported here is to design novel ASSURED devices, focusing on the communication between a POC device and its users. Two original concepts were developed in this research: the “sample-only” method and the “text-reporting” method. The devices designed using these two novel concepts can overcome the existing “UED” obstacles in previously developed methods and are ideal for use by non-professional users as “ASSURED” platforms in developing countries, in impoverished areas, in field locations, and for emergencies. Details of the innovations in device fabrication and in diagnostic applications are discussed in Chapters 2 – 5.

The objective of this chapter is to give a comprehensive review of the “ASSR” low-cost diagnostics developed for different applications. Based on this review, the advantages, limitations and knowledge gaps of developed diagnostics will be identified. The first section (1.2) provides a review of the development of low-cost microfluidic diagnostic devices, focussing on their fabrication procedures and result reporting methods. This section gives specific emphasis to the development of low-cost devices designed for blood analysis and environmental sensing. The second section (1.3) summarises the literature review and outlines the current research limitations and knowledge gaps. The third section (1.4) lists the specific research aims of this research project on the design of novel ASSURED diagnostics. The last section (1.5) outlines the thesis structure.

1.2 Literature review

1.2.1 Current trend for developing diagnostics

One of the continuing endeavours throughout human history has been the goal of controlling serious diseases that threaten the health and development of the human race. Diagnosis is a critical step to identify the existence of a disease and to assess the outbreak potential of the disease. Current development of diagnostics has two different directions: one is toward extensive automation and consolidation of testing in central laboratories [6], and the other toward developing point-of-care (POC) products for decentralizing the diagnosis to various near-patient sites [7, 8]. The procedure for these two different clinical approaches are shown in Figure 1 and it is clear that the POC diagnostics are much more suitable for use in resource-limited area or in situations where the test results are needed rapidly, such as developing counties, rural areas, field, emergencies, home, schools, workplaces, travelling departments, mobile nursing practices and so on [7-11], for in these circumstances the clinical tests in centralized laboratories and hospitals taken for granted in the cities of the developed world are absent. As such the design and fabrication of the ASSURED [1] POC platforms have become an important research area world-wide.

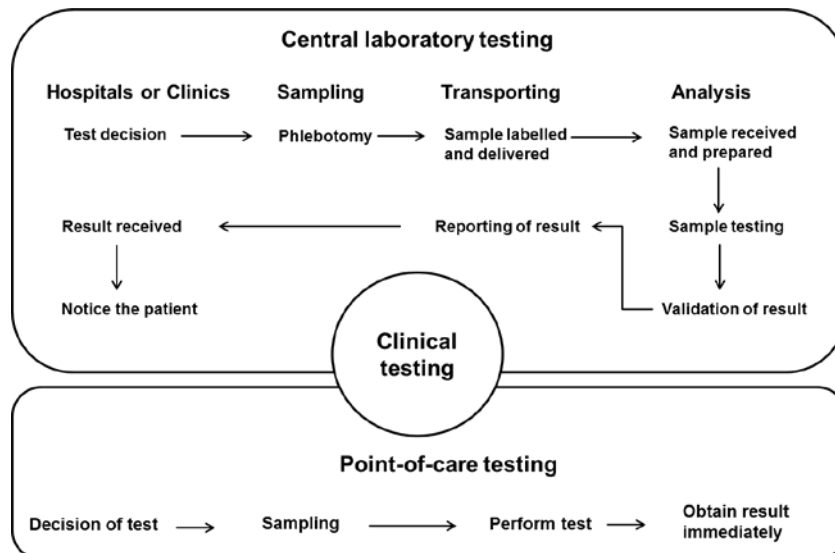


Figure 1. Procedures of clinical test by central laboratory and POC testing. (With permission from ref. [11]. Copyright (2005) Elsevier)

1.2.2 Low-cost diagnostic devices

Many inexpensive testing devices based on the microfluidic diagnostic technology have been fabricated using engineering methods. A POC product for analysis and diagnosis typically consists of two procedures: sensor fabrication and result reporting. Therefore in this section, new concepts for POC systems involving paper-based and thread-based microfluidics will be introduced with their fabrication and result reporting features for different applications in biochemical diagnosis, blood typing and environmental monitoring.

1.2.2.1 Microfluidics

The microfluidics originated from its use in gas chromatography (GC), capillary electrophoresis (CE) [12] and then high-performance liquid chromatography (HPLC) [13]. The microfluidic is a miniaturized system using channels with tens to hundreds of micrometer length in dimension to manipulate minute amounts (10^{-9} to 10^{-18} L) of liquids [14]. The increased development of microelectronics during the mid-20th century substantially promoted the application of microfluidics. Research using microfluidics was flourished since the early 1990s due to their reoutation as an attractive “lab-on-a-chip” (LOC) [15] system for use in the fields of biology, chemistry, physics and multidisciplinary engineering. Microfluidics applied in sample separation [16], cell and protein analysis [17, 18], DNA sequencing [19, 20], drug delivery [21-23] and many other applications have been successfully conducted. Microfluidic technology is flexible, easily-modified and low-cost because it reduces consumption of samples and reagents, and are therefore becoming the potential “ASSURED” platform to provide POC analysis and diagnosis [24,25].

1.2.2.2 Paper-based microfluidic devices (μ PADs)

Paper is a raw material typically made of cellulose and can offer various applications in chemical/biochemical analysis and diagnosis. Since the cellulose is well-compatible with proteins and biomolecules, and the porous structure of paper can rapidly deliver the liquids by capillary wicking [26]. Besides, the low-cost, renewable and easy-modification properties of paper make it a robust and attractive material for use as POC

microfluidic devices [27-34]. Figure 2 summarizes the development process of paper-based testing devices. The first application of paper in terms of analytical tests was as chromatographic substrates in 1850 [35, 36]. Then the development of paper strip tests for diagnostic and biodetection purposes started in 1950s. It was driven by the fact that paper strip testing of biologically relevant species (e.g., glucose in urine) was as simple as measuring pH with pH paper [37]. In recent decades, paper and other fibrous nonwoven materials (e.g., nitrocellulose membranes) have been widely used as substrates for POC diagnostics [38]. Nowadays, many paper strip tests are commercially available for POC diagnostics, such as pregnancy tests. Although these strip tests are simple and low cost, they are not sufficient for operating multiplex and quantitative analyses. Several years ago, a research group from Harvard University led by Professor George Whitesides introduced a new concept of fabricating paper-based microfluidic devices which can be utilised to simultaneously detect multiple analytes in liquid samples [3]. Their work overcame some drawbacks of the conventional paper strip tests, and most importantly, this new concept has led to the rise of a new research area of patterned paper substrate as a low-cost, portable microfluidic platform for bio/chemical/medical applications.

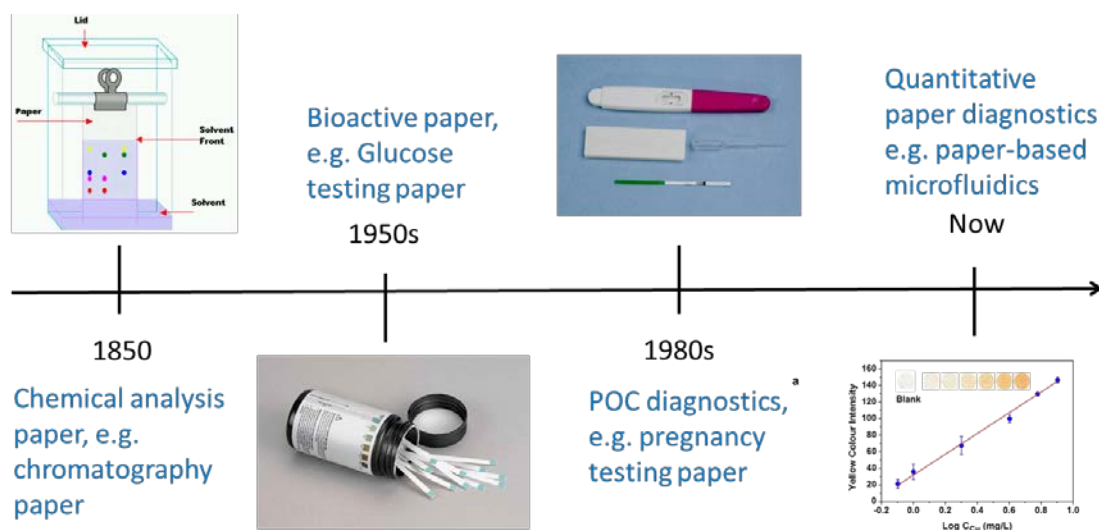


Figure 2. The development of paper-based analytical and diagnostic devices since 1850.

1.2.2.2.1 Fabrication of paper-based microfluidics diagnostics

Paper is made by filtering a dilute (1 wt%) aqueous suspension of fibres, colloidal filler particles and soluble polymers. Cellulose fibres are the major component of many paper types, which are porous, hydrophilic materials and are able to take up more than their own mass of water. Therefore the naturally hydrophilic property of paper makes it favourable for the fabrication of low-cost microfluidic devices through paper hydrophobization.

Paper hydrophobization can be achieved routinely through “sizing” during the papermaking process, which lowers surface energy, as evidenced by increased water-contact angle [39]. Through the process of alkyl ketene dimer (AKD) sizing treatment, the paper samples are strongly hydrophobic and have contact angles of typically between 110-125° with water [40], whereas unsized cellulose has a water contact angle of only 25° [41]. The penetration of liquids in paper can be characterized by the Washburn equation (equation 1) [42]:

$$l = \sqrt{\frac{\gamma r \cos\theta}{2\eta} t} \quad (1)$$

Where l is the distance of liquid penetration of the pore in paper, r is the equivalent capillary pore radius of paper, γ is the liquid surface tension, η is the liquid viscosity, θ is the contact angle and t is the time of penetration. According to equation (1), if a paper surface sustains an apparent contact angle with a liquid of greater than 90°, the liquid will not penetrate in the paper.

Patterned paper with hydrophilic channels demarcated by hydrophobic borders can provide a good platform for controlling capillary penetration of aqueous solutions. Various methods of patterning paper for the fabrication of PADs have been achieved.

Photolithography method

In 2007, Martinez et al. [3] created barrier patterns on the filter papers using photolithographic techniques. This work overcame some drawbacks of the conventional paper strip tests and introduced the new concept of fabricating paper-based microfluidic devices which can be utilised to simultaneously and quantitatively

detect multiple analytes in liquid samples. As is shown in Figure 3, they patterned filter paper with SU-8 2010 photoresist to generate the hydrophilic channels with the width of 3 mm bound by a hydrophobic barrier, and then modified the paper for biological assays by adding appropriate reagents to the test areas. In this study, the glucose and protein in an artificial urine sample was detected with established colour reactions, to test the feasibility and sensitivity of applying this system to clinical diagnosis.

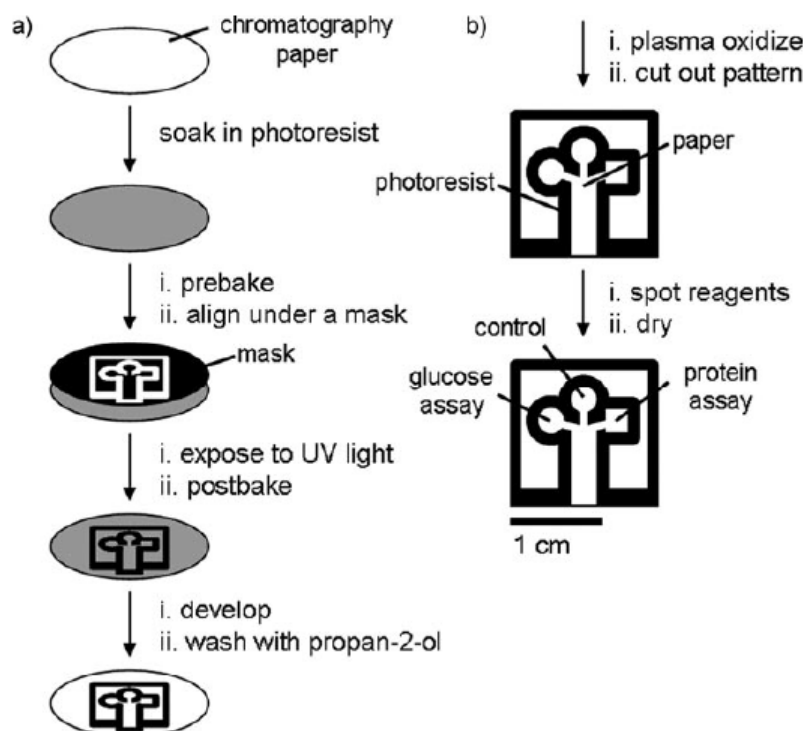


Figure 3. The six-step fabrication procedure of μ PADs using lithographic method. (a) A pattern with SU-8 photoresist barrier was created on a piece of filter paper. (b) After plasma treatment, the patterned paper was loaded with reagents for bioassays. (With permissions from ref. [3]. Copyright (2007) John Wiley and Sons.)

The paper-based microfluidics developed by the photolithographic method were suitable to many applications for semi-quantitative diagnosis [43-45]. However, because of the easily-damaged photoresist barriers, expensive equipment and complicated fabrication process, some other alternative methods were explored during the subsequent studies.

AKD ink-jet printing method

In the paper-sizing industry, alkyl ketene dimer (AKD) is one of the commonly used agents for cellulose hydrophobization agent which provides the paper with a high level

of water-resistance. Figure 4 shows the cellulose-coupling chemistry of AKD; with the formation of beta-keto ester linkage under heating, the hydrophobic tail of the molecule turns from the surface, providing paper with hydrophobicity [46].

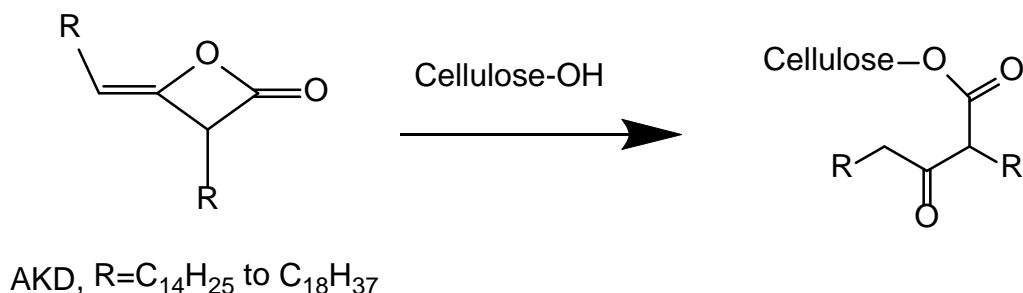


Figure 4. Alkyl ketene dimer (AKD) sizing reaction with cellulose fibres to lower the surface energy and water-penetration rate in paper.

Ink-jet printing is one among many commercial processes, but owing to its time-saving and low-cost, which allows the direct patterning of the substrate surface, it has become a versatile tool for various industrial fabrication processes [47]. The current commercial digital ink jet printers are capable of issuing small droplets of a few picolitres and small amounts of ink for generating an electronically created image [48]. In recent years, commercially available printers are modified to dispense various biomolecule solutions instead of ink [49, 50]. The reconstructed printers also inherit the frugal ink management feature of the normal printers and are capable of depositing hydrophobization agents onto paper surface. This provides a cost-effective solution for patterning and fabricating channels on paper. Li et al. [51] explored the ink-jet printing method to generate hydrophilic-hydrophobic contrast on paper based on AKD hydrophobization. Hydrophilic filter papers were printed using a reconstructed commercial digital ink jet printer with electronically generated patterns of an alkenyl ketene dimer–heptane solution (5%, v/v). The modification of the printer involved replacing the ink in cartridge with the AKD-heptane solution. Printing did not leave any visible mark on paper samples which retain their original flexibility. The printed filter paper samples were then heated in an oven at 100 °C for 8 min to cure AKD onto the cellulose fibres. A well-defined hydrophilic–hydrophobic border can then be created for forming the μ PAD (Figure 5). This ink-jet printing method was then used to print microfluidic sensor patterns on filter paper, as well as print the colourless

indicator for NO_2^- into the circular detection zone. NO_2^- sample solution was introduced into the channel and was detected by this sensor.

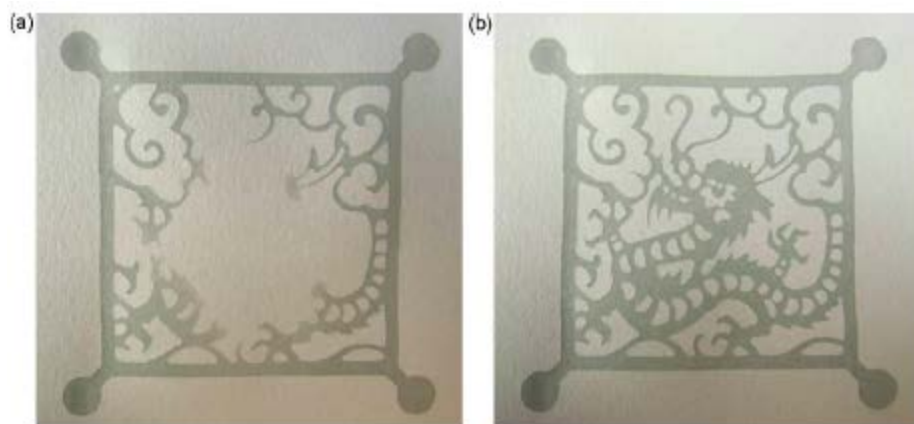


Figure 5. Ink jet printed paper fluidic pattern of a Chinese paper cut. Four liquid feeding zones were added to the four corners of the pattern. Water penetration at an early stage (a) and at the final stage (b) is shown. (With permissions from ref.[51]. Copyright (2010) Elsevier.)

Wax-coating methods

The wax patterning method was employed to develop paper-based microfluidic devices for portable bioassays by Lu et al. [52] Three different ways of wax patterning were studied in this paper (Figure 6): (1) Wax pen painting, which used a wax pen to draw the desired pattern on both sides of a filter paper. The painted wax will penetrate the paper to form the hydrophobic wall when melted at 150 C; (2) ink-jet printing followed by wax pen painting, which was suitable for the cases when complicated pattern design is required; and (3) wax ink-jet printing directly. The third method generated stable hydrophilic channels of 1 mm bordered by the hydrophobic barrier as defined by wax. Enzyme reactiond between tetra-methyl benzidine (TMB) and horseradish peroxidase (HRP), glucose and BSA protein were chosen to demonstrate colorimetric detection of analytes for verifying the performance of the wax-printed paper-based device.

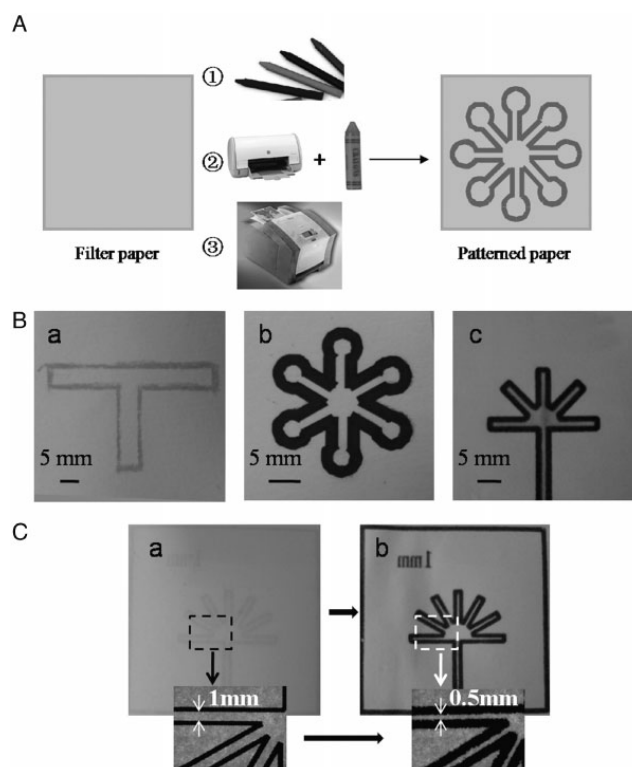


Figure 6. (A) Schematic illustration of the processes to produce patterned paper with wax; (1) hand drawing with a wax pen; (2) printing with an inkjet printer followed by painting with a wax; (3) printing with a wax printer. (B) The fabricated microfluidic on filter paper with wax in three different ways: (a) hand painting with a wax pen; (b) printing with an inkjet printer followed by painting with a wax pen and (c) printing with a wax printer directly. (C) Comparison of the channel width of patterned paper produced by wax printing (a) before and (b) after heating in oven (1mm is the width of the micro-channels). (With permissions from ref.[52]. Copyright (2009) John Wiley and Sons)

Dungchai et al. [53] reported the paper microfluidics fabricated by wax-screen-printing technology. As is shown in Figure 7a, solid wax was rubbed through a screen onto the paper. The printed wax was then melted by a hot plate under 100 °C for 60s, allowing the melted wax to penetrate into the paper to form hydrophobic barriers. The patterned paper was ready for use when it was cool to room temperature after removed from the hot plate. After the fabrication of paper microfluidics by wax screen printing, red food dye was added to the paper devices to visualize the resolution of this method. The widths of hydrophilic channel were studied in the range of 550-1000 μm at the optimal melting temperature and time, and the smallest channel width allowing solution to flow the entire length of a 12 μm channel was found to be $650 \pm 71 \mu\text{m}$ (Figure 7b). It also showed in this study the thickness, porosity, and orientation of paper fibres, as well as the smallest features printable on the screen, affected the resolution of this method.

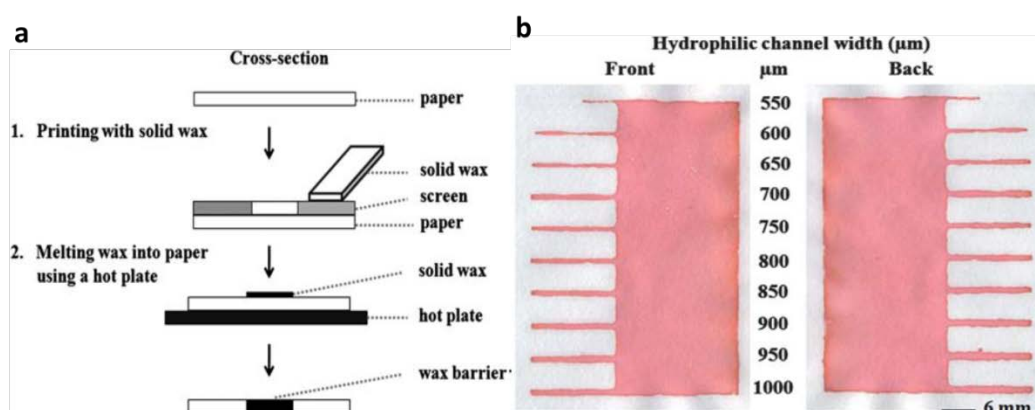


Figure 7. (a) Schematic diagram of the fabrication step for wax screen-printing method. (b) Resolution of the wax screen-printing method showing the smallest hydrophilic channel width. (With permissions from ref.[53]. Copyright (2011) Royal Society of Chemistry)

Songiaroen et al. [54] developed another wax-patterned paper microfluidics by wax-dipping. In their study an iron mould with designed patterns for wax dipping was created by a laser cutting technique. The designed pattern was transferred onto paper by dipping an assembly mould into melted wax under the temperature of 120-130°C. The whole fabrication process took within 1 min without the use of complicated instruments or organic solvents. Bioassays for simultaneous detection of glucose and protein in real samples were performed by this μ PAD to verify the performance (Figure 8).

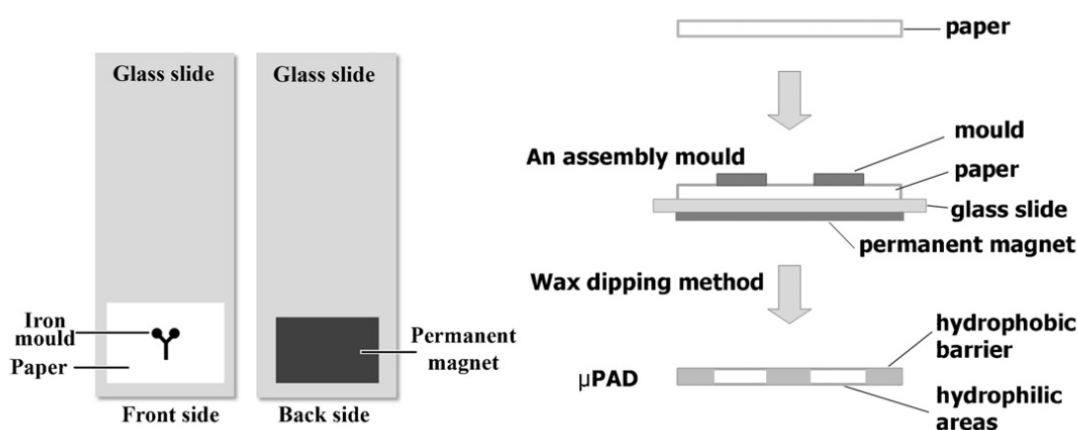


Figure 8. Procedure for patterning paper by wax dipping in top view (left) and lateral view (right). (With permissions from ref. [54]. Copyright (2011) Elsevier)

Other fabrication methods

Apart from the AKD and wax fabrication methods, other reported techniques for patterning paper-based microfluidics includes: plotting, ink jet etching, plasma treatment, flexography printing, laser treatment and paper-cutting techniques [55-62]. Table 1 lists these methods with their patterning reagents and principles. In summary, the reagents play three sorts of rules for paper patterning: 1) physical blocking of the paper pores (e.g. polydimethylsiloxane (PDMS) and silicone), 2) water-resistant reagents physically deposited on the cellulose fibre surfaces (e.g., polystyrene and wax), and 3) chemical modification of fibre surfaces (e.g., cellulose reactive agent AKD). Further, the paper patterning strategies can be classified into two approaches: one is the selective hydrophobization on the naturally hydrophilic paper surface, which is a one-step approach; the other one is the two-steps approach involving hydrophobization of the entire paper followed by selective hydrophilization [63].

Table 1. Other reported techniques for patterning paper-based microfluidics with their patterning reagents and principles.

<i>Fabrication methods</i>	<i>Patterning reagents</i>	<i>Patterning principles</i>
Plotting [55]	PDMS	Physical blocking of pores in paper for selective hydrophobization
Ink jet etching [56, 57]	Polystyrene (PS)	Physical deposition of reagent on fibre surface for entire hydrophobization followed by selective dehydrophobization through dissolving the PS
Plasma treatment [58, 59]	AKD	Chemical modification of fibre surface for entire hydrophobization followed by selective dehydrophobization through plasma
Flexography printing [60]	PS	Physical deposition of reagent on fibre surface for selective hydrophobization
Laser treatment [61]	Silicone or wax	Physical blocking of pores in paper for entire hydrophobization followed by selective laser dehydrophobization
Paper cutting [62]	Computer controlled knife	Shaped microfluidics through computer controlled cutting

1.2.2.2.2 Result reporting methods used for paper-based microfluidics

After effective sampling on the patterned paper microfluidics, the result reporting is another important aspect to evaluate the functionality and feasibility of the diagnostics. As an ideal diagnostic performing low-cost and high-performance assays, result reporting by such a μ PAD should involve but not limited on the abilities of: 1) delivering stable and clear contrast results after sampling; 2) instantaneous response without driven by complicated equipment; 3) reliable and accurate data analysis support tools; 4) comparable detection limit and selectivity with the standard methods. Currently developed methods on result-reporting were limited on colorimetric reactions for most of the μ PADs, and nanoparticle-enhanced colorimetry, electrochemistry and chem/electrochemiluminescence methods for some of the μ PADs.

Colorimetric methods

Currently, colorimetric methods are the preferred assay for obtaining qualitative and semi-quantitative results for most paper-based microfluidic devices. Colorimetric detection chemistries are typically related to enzymatic or chemical colour-change reactions. In most cases, colorimetric reactions generated strong contrast on paper after sampling and the results can be visually assessed by the unaided eye [64, 65]. The assay signals with colour intensities related to analyte concentrations can then be captured by optical devices and measured by software to perform the semi-quantitative analysis. Various biomarkers of health diagnosis has been identified and semi-quantitatively detected through colorimetric methods including the glucose [3, 45, 52, 54-56, 60, 63, 66-69], protein [3, 45, 52, 54-56, 62, 68, 70, 71], nitrite[51, 59, 66, 68, 72], uric acid [59, 67, 72], ketones [66, 68], lactate [67], pH [56, 57], human IgG [57], total iron [53], pathogenic bacteria [73], Alkaline phosphatase [51, 58] and so on. Figure 9 shows some examples of the colorimetric assay conducted on paper devices.

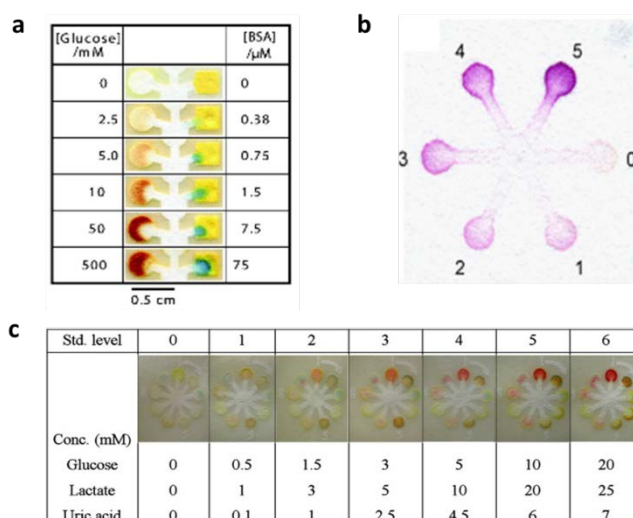


Figure 9. Examples of colorimetric assay for the semi-quantitative detection of glucose and protein (a) (With permissions from ref. [3]. Copyright (2007) John Wiley and Sons), NO_2^- (b) (With permissions from ref. [51]. Copyright (2010) Elsevier), and glucose, lactate and uric acid (c) (With permissions from ref. [67]. Copyright (2010) Elsevier).

Nanoparticle-enhanced colorimetry

Although simple and fast, the main drawback of the colorimetric method is its sensitivity usually does not reach the requirement of current biological and clinical analyses. Therefore strategies to enhance the sensitivity of colorimetric detection need to be explored, one method of which was the nanoparticle technology.

Gold nanoparticles (AuNPs) is one of the desirable materials to enhance the sensitivity and selectivity of colorimetric detection [74-77]. AuNP suspensions lead to different colours related to the interparticle distance. Liu et al. [78] utilized the DNA-functionalized AuNPs to detect adenosine and cocaine through the enhanced-colorimetry. Zhao et al. [79] also reported the assay with immobilized DNA-cross-linked AuNPs to detect endonuclease and adenosine .

Electrochemical detection

Unlike colorimetry, electrochemistry (EC) detection has higher sensitivity and less prone to interference from certain types of contaminants. By employing the screen-printed electrode technique for paper microfluidics, result reporting through the EC

detection can significantly enhance the sensitivity and selectivity of the paper device [80-84].

Dungchai et al. [80] reported the first EC detection on paper-based microfluidics. Photolithography was used to generate microfluidic channels on filter paper, while screen-printing technology was used to fabricate a three-electrode system attached to the microfluidic detection zones (Figure 10a). Three bioassays including the detection of glucose, lactate and uric acid have been conducted simultaneously on this device through the cyclic voltammetry response of each assay (Figure 10b).

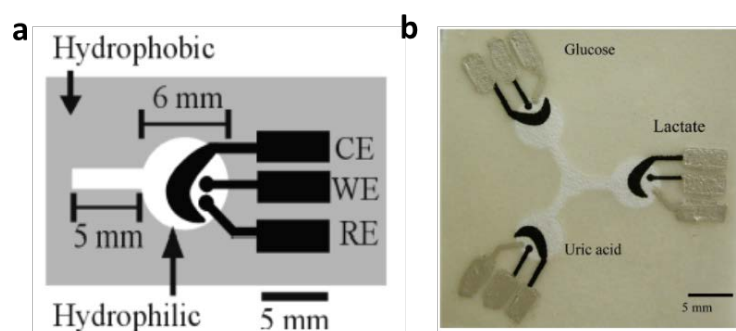


Figure 10. (a) Design of the electrochemical cell for paper-based microfluidics. WE, working electrode; RE, reference electrode; CE, counter electrode. (b) Three electrode paper-based microfluidic devices for the EC detection of glucose, lactate and uric acid. (With permissions from ref. [80]. Copyright (2009) American Chemical Society)

Chemiluminescent and electrochemiluminescent detection

Chemiluminescent (CL) and electrochemiluminescent (ECL) are another two optical detection approaches for result reporting in paper microfluidics. The chemistries of CL and ECL rely on the luminescence as the result of chemical reactions and electrochemical potential controlled reaction, respectively. Since the CL and ECL detections are performed in dark, they are independent of ambient light. Yu et al. [85] firstly demonstrated the CL methods for detection on a paper-based microfluidic sensor. A chromatography paper was patterned with microfluidic through the paper plotter method with the generation of one sample injection area, two bioactive channels and two CL detection areas. The sensor was then fabricated by sandwiching this patterned chromatography paper between two layers of impermeable single-sided adhesive tape. Quantitative detections of glucose and uric acid with the glucose oxidase- and urate oxidase-treated channels were approached on this device based on CL detection.

The first ECL detection on μ PADs was reported by Delaney et al. [86], with the analysis of 2-(dibutylamino)-ethanol (DBAE) and nicotinamide adenine dinucleotide (NADH) at levels of 0.9 μ M and 72 μ M, respectively. The paper was patterned through AKD ink jet printing method [68] and attached to a screen-printed electrode. And the sensing chemistry was orange luminescence emitted from the ECL reaction of tris (2, 2'-bipyridyl) ruthenium (II) ($\text{Ru}(\text{bpy})_3^{2+}$) with certain analytes. A mobile camera phone was used to capture the ECL signals and proposed the further quantitative analysis (Figure 11).

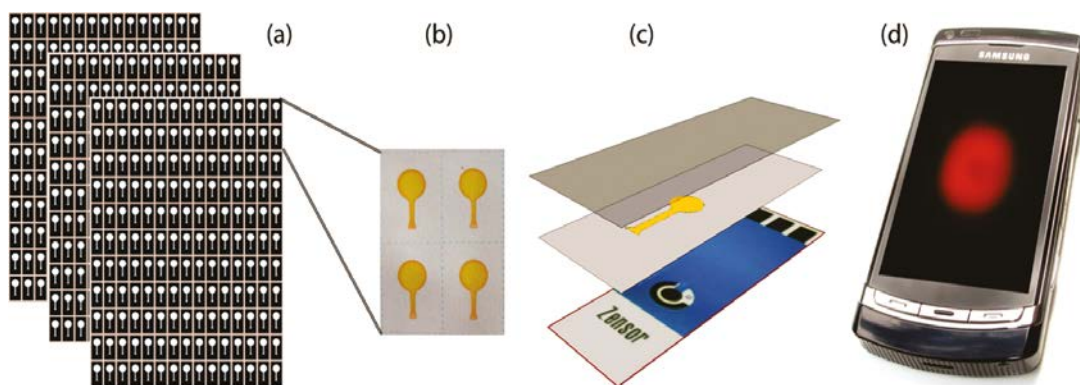


Figure 11. Fabrication and operation of a paper-based microfluidic ECL sensor. (a) The patterned paper microfluidics by inkjet printer. (b) The individual paper fluidic elements were cut to size and the hydrophilic areas were filled with $\text{Ru}(\text{bpy})_3^{2+}$ solution. (c) The paper substrate was then aligned and combined with the screen printed electrode. (d) Camera phone captured ECL signals for further analysis. (With permission from ref. [86] Copyright (2011) American Chemical Society)

1.2.2.3 Thread-based microfluidic devices (μ TADs)

Thread and thread-based microfluidics are another material and technique for producing the diagnostics with high affordability, functionality and availability. Similar to paper, thread is a porous and fibrous material which requires only micro-liters of reagents and analytes for performing the chemical and biochemical assays. Besides, the thread acts as capillaries with the voids between its fibres, which enable fluids wicking along the channel [87-89]. These characters make thread attractive for fabrication as microfluidics for diagnosis.

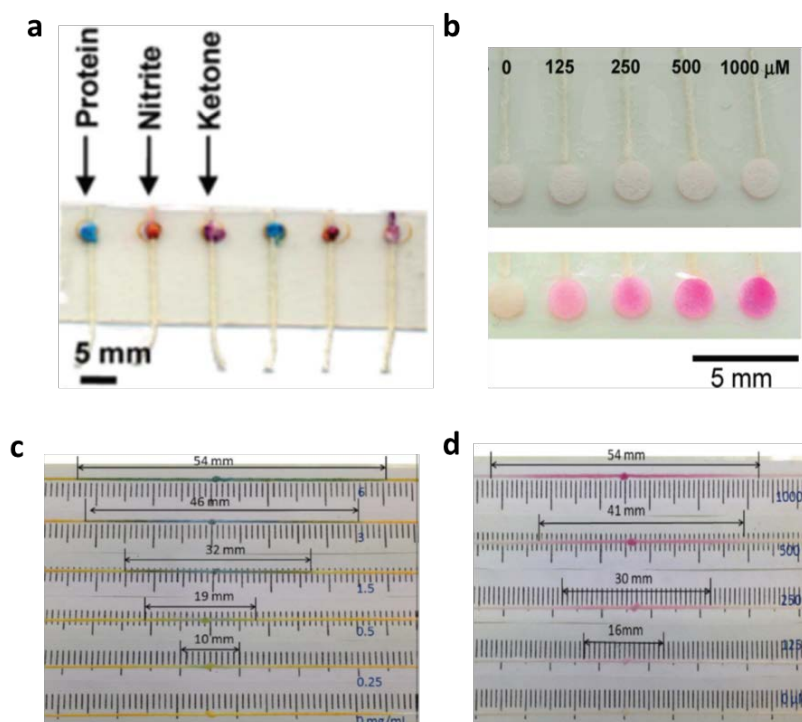
1.2.2.3.1 Fabrication of μ TADs with flow-control

Thread is actually a “ready-made” microfluidic device for the liquid wicking occurs instantaneously and rapidly. Liquid wicking one dimensionally in the thread resulted in the liquid penetration along the thread faster than cross the thread. Therefore the flow-control of thread microfluidic is an important concept for improve the functionality of the sensor.

Ballerini et al. [90] employed a selected switch for the flow-control of thread, by introducing the adhesive glue as the blocking reagent to fill into the interfibre gaps, thus restricting capillary flow of liquids. Besides, it was found that the knots of the thread can simply affect the pathways of the liquid penetration, thus the fluid combining, mixing and splitting can be controlled by these knots [91]. Li et al. further investigated the relationship between the volume of liquid and the wicking distance. Results showed liquid penetration distance along the thread increased linearly for small volumes of the solution. Therefore there is no need to precisely control sample volume when conducting the quantification tests on thread in this linear range [92].

1.2.2.3.2 Result-reporting by μ TADs for diagnosis

Results reporting of thread diagnostics typically relies on the colorimetric assay. Since the thread can be easily made in white colour, it provides desirable background for the colour intensity measurement. Reches et al. [89] and Li et al. [87] developed the thread-paper microfluidics by which thread was as the liquid sample transport channel which filter paper carried out the colorimetric assay for the semi-quantitative detection of protein, NO_2^- and ketone (Figures 12a and 12b). Recently Nighaz et al. [93] developed a thread-based “ruler” device for semi-quantitative identification of protein and nickel ions by distance measurement, also based on the colorimetric reaction of these two analytes (Figures 12c and 12d).



Landsteiner firstly discovered the ABO blood group, with his experiments indicating two different antigens existing on the surface of the human red blood cells (RBCs), i.e. A and B. And during the following years, a huge amount of antigens has been recognized and each of them has been determined as a blood group. To date, 30 blood group systems, including 328 authenticated blood groups, have been classified and recognized by the international society of blood transfusion (ISBT) [94, 95].

1.2.3.2 Clinical significance of blood typing

Over the past century, the discovery of almost every blood system was accompanied by clinical events that could be fatal. The finding of ABO blood groups is the consequence of the hemolysis disease after the blood transfusion. By cross-testing the RBCs and serum from different person's blood, Landsteiner found out that the blood of two people under contact agglutinates, which was due to contact of blood with blood serum. As a result he stated the law to describe the relationship between antigens on the red blood cells and antibodies in the serum for ABO blood system: 1. If an agglutinin is present in the red cells of a blood, the corresponding agglutinin must be absent from the plasma; 2. If an agglutinin is absent in the red cells of a blood, the corresponding agglutinin must be present in the plasma [96]. This law and the determination of a blood group are illustrated in Figure 13. By this figure the reason of the haemolytic transfusion reactions (HTRs), as well as the importance of blood typing before blood transfusion are clear, for the interaction of antigen on RBCs with its corresponding antibody in the serum would happen once the receptor's blood type mismatches the donor's.

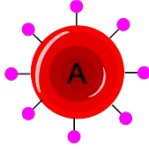
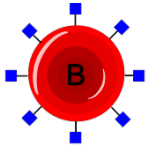
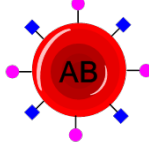
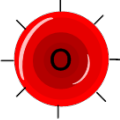


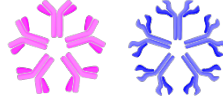
Blood groups	Group A	Group B	Group AB	Group O
Antigens on the RBCs	 Antigen A	 Antigen B	 Antigen A and B	 None
Antibodies in the plasma	 Anti-B	 Anti-A	None	 Anti-A and Anti-B

Figure 13. The determination of ABO blood groups followed by Landsteiner's law.

The discovery of the ABO blood groups has made blood transfusion feasible. Whilst antibodies A and B are naturally present in human blood serum corresponding to the antigens which they lack, the other blood antibodies in serum are only generated as a result of an immunisation response triggered by transfused RBCs that carry other antigens, or by fetal red cells leaking into the maternal circulation during pregnancy or during birth. [97] Thus the later discovery of the RhD antigens has led to the understanding and subsequent prevention of haemolytic disease of the fetus and newborn (HDFN) [95, 97-100]. The HDFN shows alloimmune fetal haemolytic anemia and many other blood antigens, such as RhCcEe, K, JKab, Fyab, P1, etc. has been gradually identified to cause this disease (Figure 14) [95, 99]. However, as for M, N blood systems, their antibodies are inactive below 37 °C and are therefore not considered clinically important [99, 100]. Table 2 summarizes the blood systems of clinical significance including their antigens. The correct typing of these blood groups is extremely important for blood transfusion, transplantation, blood banking and may other medical procedures.

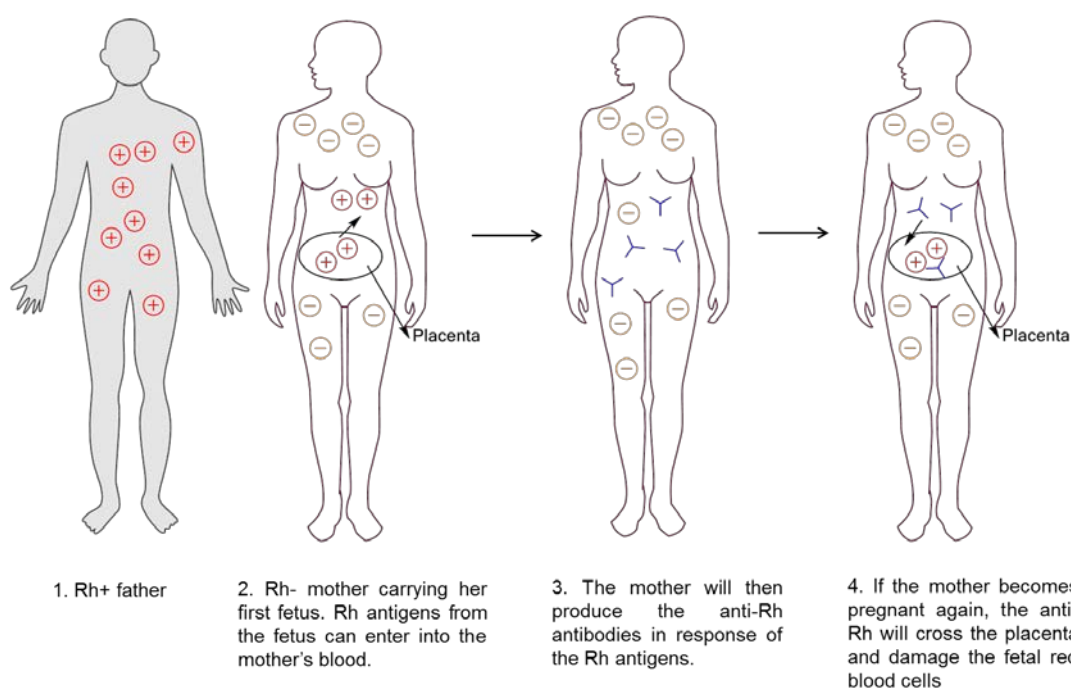


Figure 14. Illustration of the Rh-induced haemolytic disease of the fetus and newborn.

Table 2. List of the common clinically important blood group systems

<i>Blood group systems</i>	<i>Antigens</i>
Rhesus	D, C, c, E, e
Kell	K, k
P	P1
Kidd	Jk ^a , Jk ^b
MNS	M, N, S, s
Lewis	Le ^a , Le ^b
Lutheran	Lu ^a , Lu ^b
Duffy	Fy ^a , Fy ^b

1.2.3.3 Blood typing principle and methods

1.2.3.3.1 Blood typing for ABO blood groups

ABO blood groups which can cause immediate and severe HTRs are considered as the most important human blood groups. According to Landsteiner's law, the typing of ABO blood groups relies on the determination of the presence or absence of certain antigens on the surface of red blood cells (RBCs), as well as certain antibodies in the serum of the blood. The blood typing process which is based on antigen detection is

referred to as forward blood typing; whereas the blood typing through antibody detection is the method of reverse blood typing [95]. The typing principle for determining an individual's blood type is shown in Table 3, where the positive sign “+” means the observation of agglutination, while the negative sign “-” refers to the absence of the agglutination reaction. It shows that the results determined by forward and reverse blood typing follow different principles.

Table 3. Blood type determine principles by forward and reverse blood typing methods.

<i>Reaction of antibodies with blood</i>		<i>Forward blood type</i>	<i>Reaction of reagent cells with serum</i>		<i>Reverse blood type</i>
Anti-A	Anti-B		A1 Cells	B Cells	
+	-	A	-	+	A
-	+	B	+	-	B
+	+	AB	-	-	AB
-	-	O	+	+	O

Forward blood typing

Forward blood typing determines the presence or absence of certain antigens on the surface of red blood cells (RBCs). Commercial antibodies are used to test the presence of the corresponding antigens on RBCs. This is clinically performed by introducing antibody into a blood sample; the appearance of RBC agglutination indicates the presence of the corresponding antigens on RBC. On the other hand, the absence of agglutination indicates the absence of the antigen. The haemagglutination reaction immediately occurs as the formation of antigen-antibody complexes and then blood typing results can be reported by this visible reaction.

In the routine laboratory, ABO blood typing can be performed using the tube [101], micro plate [102-104] and the column agglutination systems [105, 106]. Among them, the column agglutination system is the mostly commonly-used method nowadays, which relies on the different migration rates of agglutinated RBC lumps and non-agglutinated RBCs in a gel column of uniform pore size [107]. The column agglutination assay is performed in a gel matrix contained within a microtube. As is shown in Figure 15, this gel technology is a solid phase testing method inspired from

the principle of gel filtration for separation of red blood cells from human blood [106]. This method standardizes RBC agglutination reactions by trapping the agglutinates and can permit simple and reliable reading.

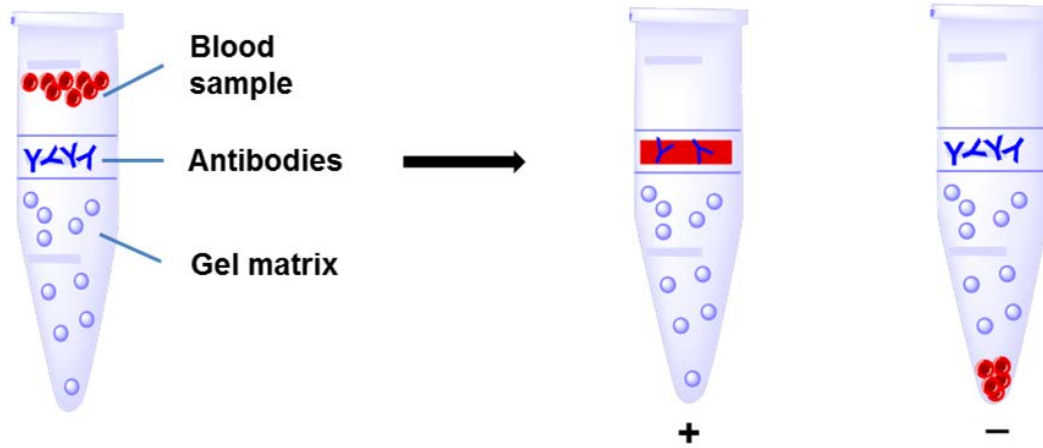


Figure 15. Methods for blood typing based on the column agglutination in gel (i.e. Gel Card technology): blood sample interacts with the antibody and then passes through the gel matrix during centrifugation; agglutinated large RBC lumps are blocked by the gel, whereas the free cells with no antibody binding reaches to the bottom of the microtube after centrifugation, showing the different blood typing results.

Reverse blood typing

Although reverse blood typing is generally regarded as a supplement for the forward blood typing, it is still considered as a compulsory assay for matching the forward tests to confirm the patient's blood type before transfusion in many countries, including Australia. This blood typing assay determines the antibodies in the serum by using the reagent RBCs with known antigens. Since a reversed blood typing assay determines the interactions between the reagent RBCs and the antibodies in a patient's serum, it also relies on observation of RBC agglutination. Therefore as same as the forward blood typing, methods for reversed blood typing are also based on microplate [104] and gel technology [106], with results identified by the laws in Table 3.

1.2.3.3.2 Blood typing for other blood groups

RhD and other clinically significant blood groups which can lead to severe HDFN also require the accurate blood typing. Unlike the ABO blood groups, these blood groups only follow the first part of Landsteiner's law, rather than the second part. So the typing

of these blood groups is a forward assay which determines the antigens on the surface of RBCs using the commercial antiserum products with known antibody types. Depending on the different antibody structure, the direct and indirect testing methods are performed for the blood typing assay of these blood groups.

Direct blood test

The blood typing for ABO, Rh, Kell, and many other blood groups are based on the direct agglutination assay, which occurs as a direct result of interaction between antigen and IgM antibody. Generally in blood serology, antibody commonly existed in two different classes, one is immunoglobulin M (IgM) and the other is immunoglobulin G (IgG). The commercial antibody products of IgM are monoclonal immunoglobulin which has a pentameric form; each has two binding sites and ten sites in total, as Figure 16 shows. The molecular dimension of an IgM molecule can reach to the maximum of 30 nm between antigen binding sites [100], thus leading to a strong direct hemagglutination reaction in the blood typing assay. The hemagglutination induced by IgM can also occur at a low temperature. As a result, blood typing methods for Rh, Kell, P1 and other blood group systems whose agglutination reaction are induced by IgM antibody are still commonly based on the gel card technology [100], as same as the ABO blood typing.

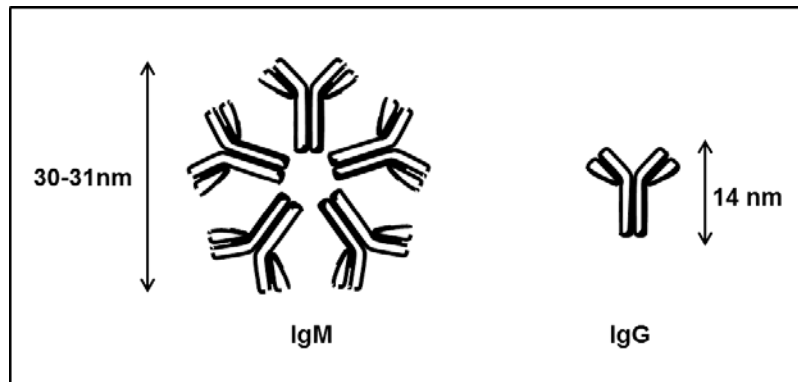


Figure 16. Schematic diagram of the structure of IgM and IgG molecule.

Indirect antiglobulin test

While the antibody products IgM for blood grouping can easily identify the corresponding group antigens through RBC hemagglutination, the IgG antibody cannot. Unlike IgM, IgG can only induce the sensitisation of the RBCs at the

temperature of 37°C [100], rather than a visible agglutination reaction. This is due to the different structure and dimension that IgG possess. As is shown in Figure 16, IgG antibodies are monomers with only 2 binding sites in total and the molecular dimension is 14 nm. This distance between the two binding sites of an IgG molecule is too small to allow it to simultaneously bind with antigens on two RBCs and cause direct agglutination. As a result most IgG antibodies require anti-human globulin (AHG) to effect the visible agglutination of RBCs. The AHG-performed blood test by IgG is regarded as the indirect antiglobulin test (IAT). Figure 17 shows the principle of the IAT and the RBC response by IgM as a comparison. Commonly conducted methods for IAT include the spin tube technique [94, 100], solid-phase microplate method[108, 109], gel method[110, 111] and low ionic polybrene technique[112, 113], all based on the IAT principle.

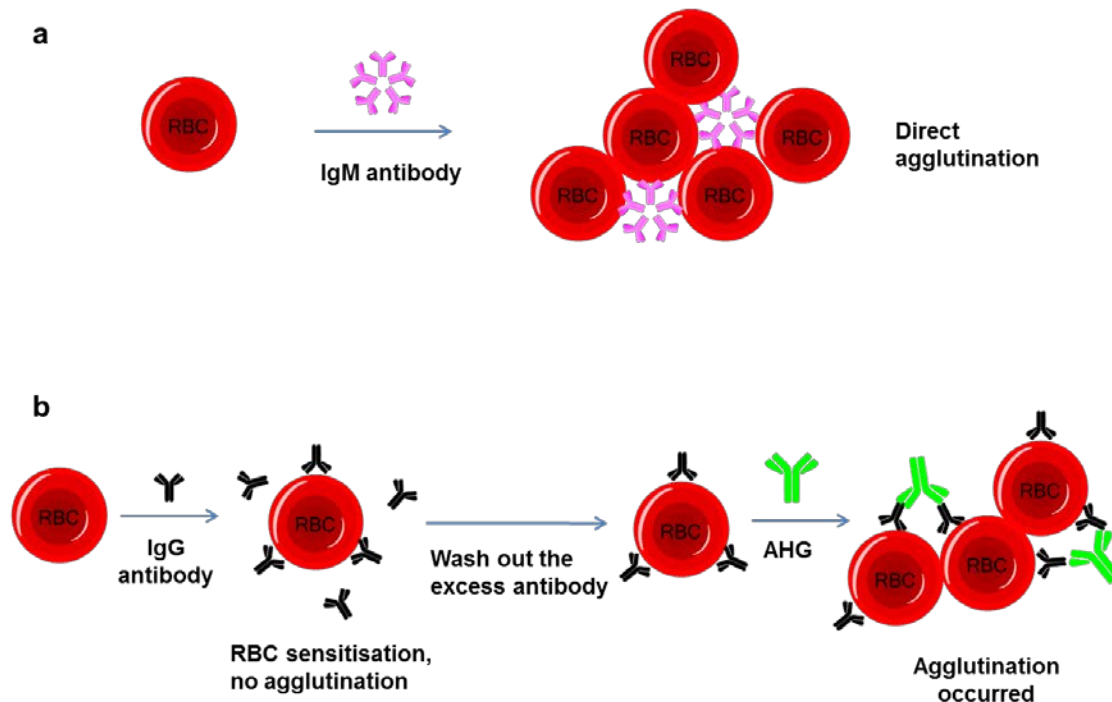


Figure 17. Schematic diagram showing direct and indirect blood typing by antibodies of different structures: a) Antibody IgM causes the direct blood cell agglutination; b) IgG antibody cannot lead to a direct agglutination reaction but only the cell sensitisation after incubation with the RBCs; the excess of IgG need to be wash out after the incubation, and afterwards the AHG are added to induce the RBC agglutination for the blood group determination.

1.2.4 Low-cost devices for blood typing

As the first stage of diagnosis for many clinical procedures, blood typing strongly requires the “ASSURED” platform for conducting the assay in the developing regions of the world and for home-users, hospitals, paramedics and pathological laboratories in developed countries, since the routine blood typing methods need expensive materials and equipment, as well as professional personnel in the laboratories. Recently some low-cost bioactive thread- and paper-based methods have been reported for rapid human blood typing based on the principle of haemagglutination reactions.

1.2.4.1 Thread-based blood typing methods

Ballerini et al.[114] investigated the use of thread as a flexible and low-cost substrate for the rapid grouping of blood. This method used the increased flow resistance of large agglutinated RBCs lumps in narrow capillary channels to separate agglutinated red blood cells (RBCs) from plasma phase on the capillary substrate (i.e. thread). Large and discrete lumps formed in a continuous serum phase do not provide capillary wicking driving force and fall behind the capillary wicking front, leading to their separation from the wicking liquid. In the experiments, the cotton thread was pre-treated by plasma treatment to remove surface contaminants, and then soaked in the grouping antibodies, Anti-A, Anti-B and Anti-D, followed by dosing a blood sample on each antibody-treated thread, which were referred to as thread A, B, D, respectively. For positive results, the separations of agglutinated RBCs and serum were showed; for negative results, however no separation could be seen (Figure 18). Based on this observation, blood type can be confirmed. The authors then designed a single-step prototype for rapid blood typing. By immobilising the threads A, B and D in a small square of polymer film in a criss-cross arrangement, it is possible to determine a person's ABO and Rh blood groups with a single dose of whole-blood (Figure 19).

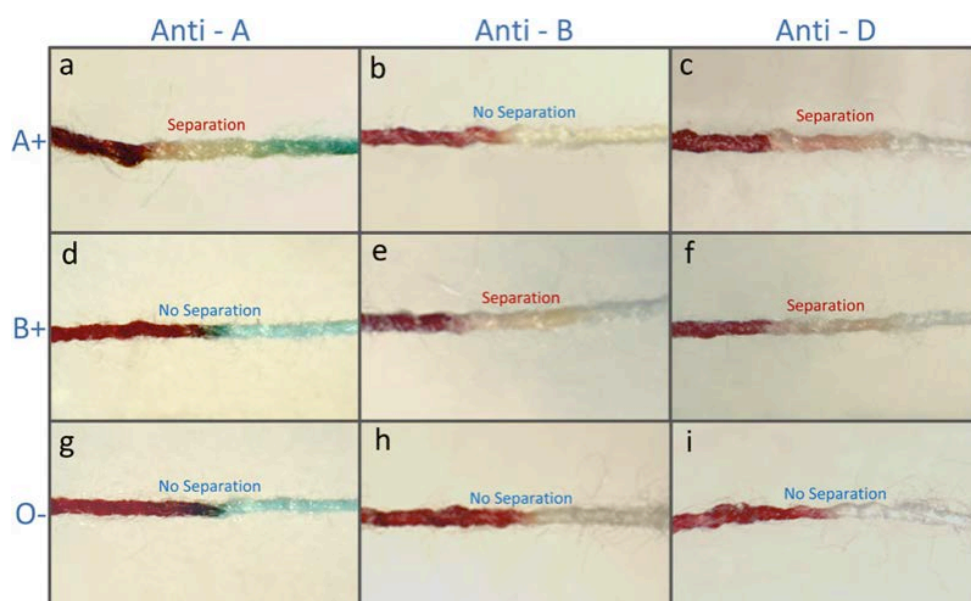


Figure 18. Testing with samples of whole blood of type A+, B+ and O- on antibody-treated polyester threads. Columns show results on threads A, B and D from left to right, whilst rows show the results for the different blood types, as labelled on the left. (With permissions from ref.[114]. Copyright (2011) Springer)

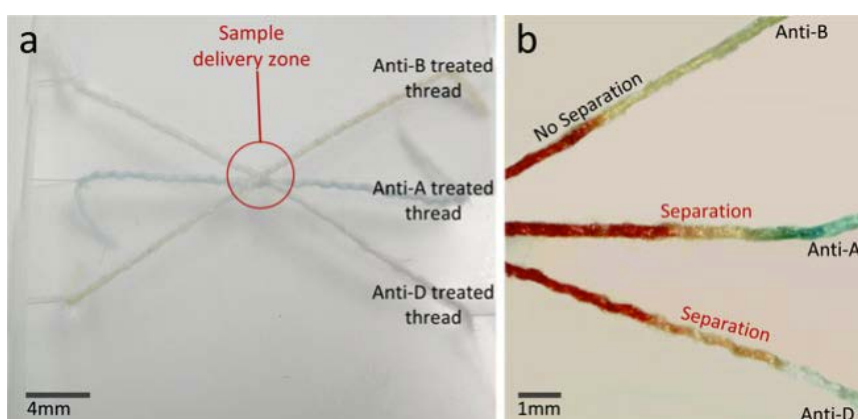


Figure 19. (a) A single-step blood grouping test prototype for proof of concept and (b) the results for typing a blood sample A+. (With permissions from ref.[114]. Copyright (2011) Springer)

1.2.4.2 Paper-based blood typing methods

Based on the difference of capillary wicking rates of agglutinated blood and non-agglutinated blood, paper-based instantaneous blood typing tests using specific antibody-antigen interactions to trigger blood agglutination were investigated [4]. Paper strips were soaked into the three ABO and Rh antibody solutions; then blood droplets were introduced at the centre of the paper strip, leading to different wicking behaviour.

Agglutinated blood sample shows a chromatographic separation from the wicking serum (Figure 20). The agglutinated red cells show very little wicking while the serum wicks for a much longer distance than the agglutinated red cells. The mechanism of such separation was studied and explained as followed: Agglutinated red blood cells form large lumps that contact with fibre surface in paper and become immobilized while the serum still wicks. The separation of agglutinated red blood cells from the serum phase occurs and can be easily observed. In contrast, stable blood suspensions wicked uniformly and no separation of RBCs and serum phase occurs. This concept was explored to engineer paper diagnostics for instantaneous blood typing.

Al-Tamini et al. [115] developed another paper-based diagnostic for rapid blood typing based on the agglutinated and non-agglutinated red blood cells showing different behaviour when eluted with a saline solution. Three spots of Anti-A, Anti-B and Anti-D solutions were dosed and dried on the Filter paper, followed by spotting blood onto the antibodies and eluted with 0.9% NaCl buffer. Agglutinated RBCs were fixed on the

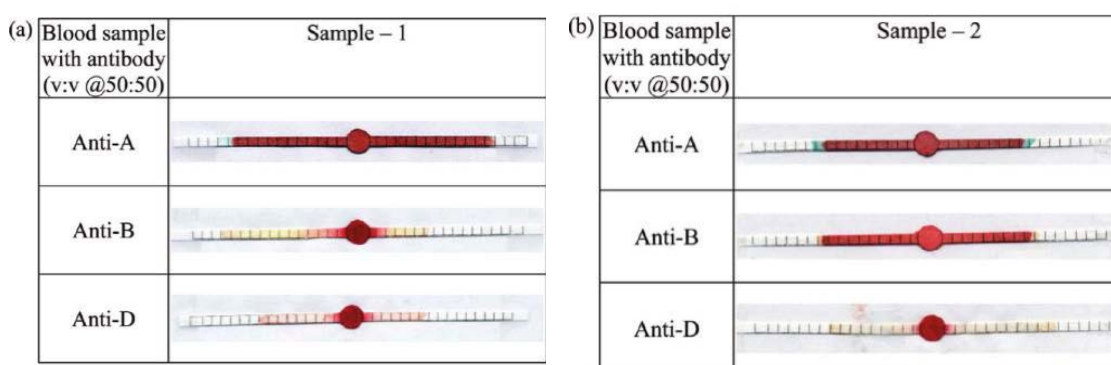


Figure 20. Blood group detection using wicking of agglutinated colloids from specific antigen/antibody interaction on dry paper strips. Blood typing: (a) B+ and (b) O+. (With permissions from ref. [4]. Copyright (2010) American Chemical Society)

paper substrate, resulting in a high optical density of the spot, with no visual trace in the buffer wicking path. Conversely, non-agglutinated RBCs could easily be eluted by the buffer and had low optical density of the spot and clearly visible trace of RBCs in the buffer wicking path (Figure 21). RBCs fixation on paper accurately detected blood groups (ABO and RhD) using ascending buffer for 10 min or using a rapid elution step in 100/100 blood samples including 4 weak AB and 4 weak RhD samples.

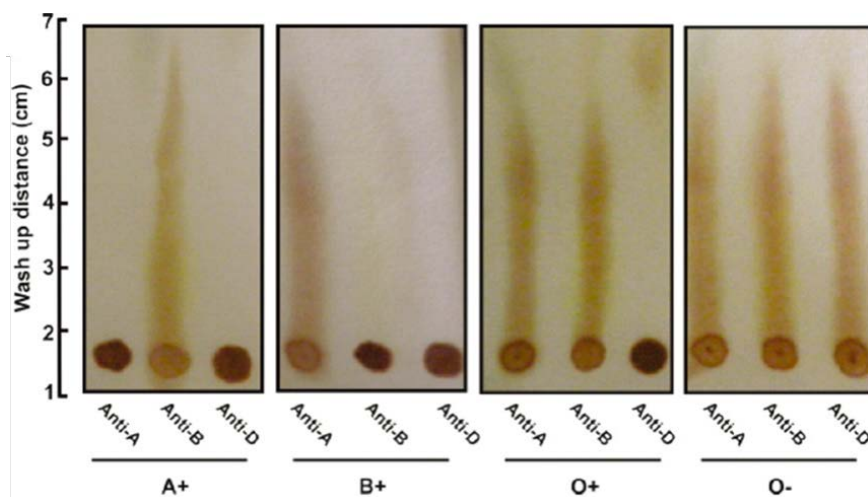


Figure 21. Agglutinated blood fixations on papers and chromatographically eluted with 0.9% NaCl buffer for 10 min. (With permissions from ref. [113]. Copyright (2012) American Chemical Society)

Noiphung et al. [116] reported a paper-based device for simultaneous determination of Rh typing and forward and reverse ABO blood groups. The paper device was fabricated by the wax-printing and dipping method, to generate a two-sided device for forward and reverse blood typing assay. In the forward blood typing side, blood sample was diluted to 50% to flow through the antibody-immobilized channel; in the reverse blood typing side, MF1 blood separation paper was employed as the blood dropping zone and so the whole blood sample can be used. Then separated plasma with certain antibody can be recognized by the reagent RBCs in the channels. The ratio between the distance of red blood cell movement and plasma separation is the criterion for agglutination and indicates the presence of the corresponding antigen or antibody, as shown in Figure 22. This study shows the haematocrit of the sample effects the accuracy of the results, and appropriate dilution is suggested before typing. The total assay time was 10 min and the accuracy for detecting blood group A, B, AB, O, and Rh typing were 92%, 85%, 89%, 93%, and 96%, respectively.

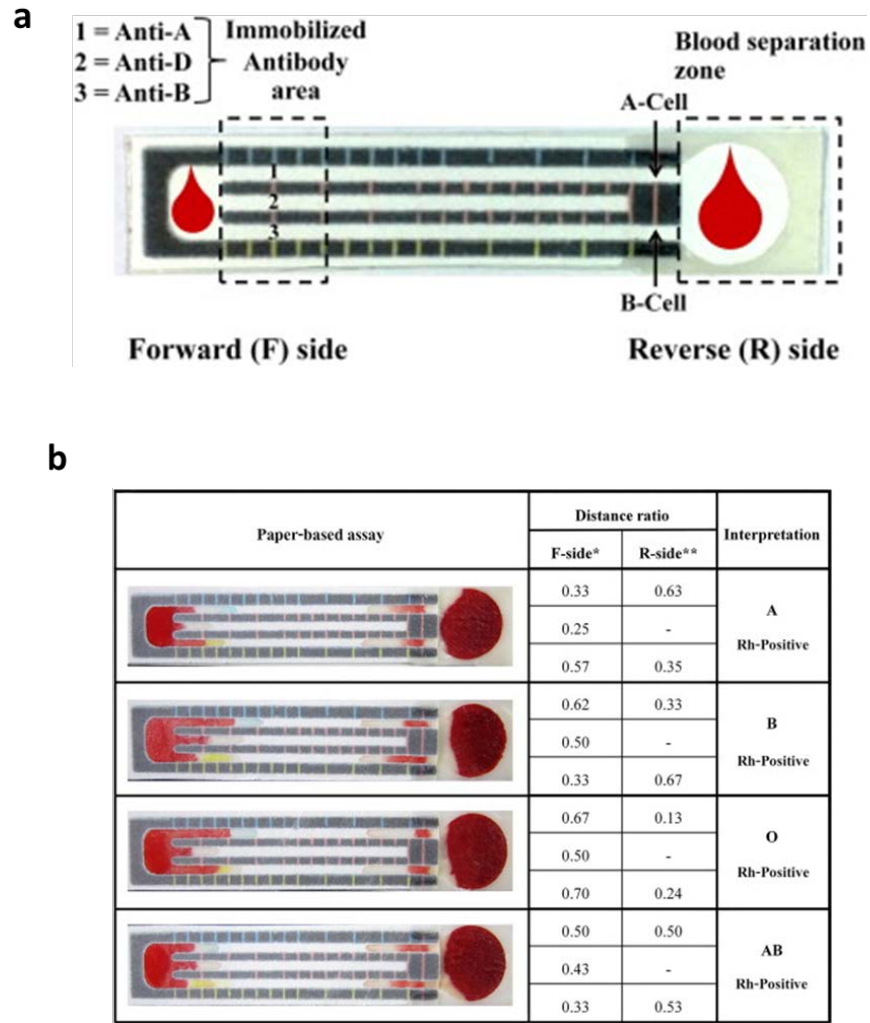


Figure 22. (a) The approach for simultaneously determining Rh typing and (b), the forward and reverse ABO blood groupings and the results based on the ratio of the distance. (With permissions from ref. [116]. Copyright (2015) Elsevier)

Recently, Guan et al. [117] reported the ABO and RhD blood typing by patterning the paper microfluidic as a barcode: AKD ink jet printing technique was used to define hydrophilic bar channels with subsequently treated blood typing antibodies A, B and D. Blood typing assay was then performed by the introduction of blood sample, followed by the buffer elution along the channel. Therefore blood types can be visually identified from eluting lengths in bar channels (Figure 23).

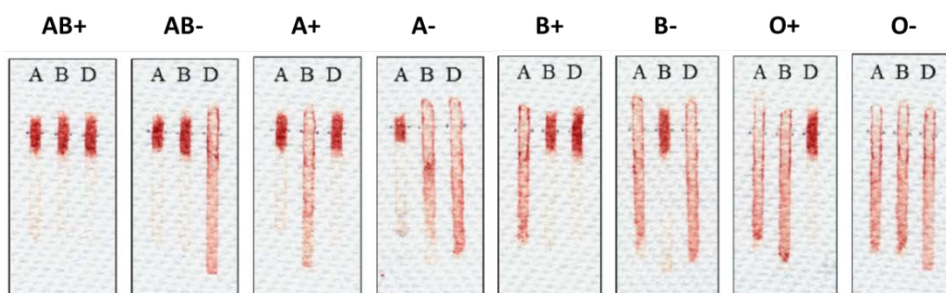


Figure 23. Assays of eight ABO/RhD blood types by the barcode-like paper-based blood typing device. (With permissions from ref. [117]. Copyright (2014) American Chemical Society)

A breakthrough for this work was that a smartphone-based analytical application was designed to read the barcode-like blood typing pattern. Since the blood penetration along the channel gives the distinguishable distance difference between a positive and negative result, a smartphone application based on the Android system was designed to identify length information in each bar channel and interpreted them into the corresponding blood types through coding (Figure 24).

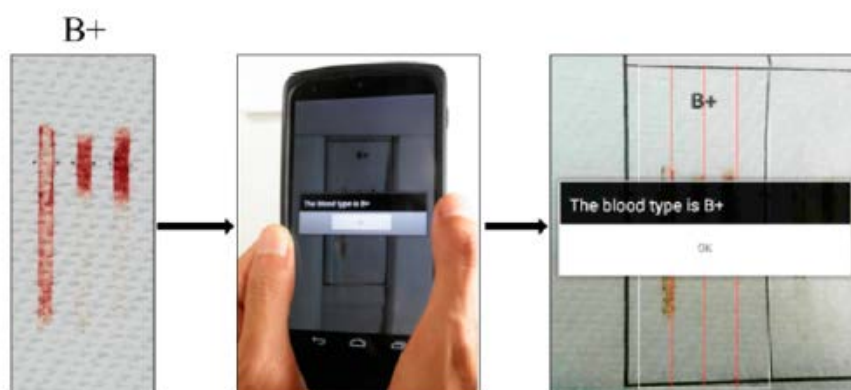


Figure 24. Smartphone application for reading the blood typing information and displaying blood typing result on its screen. (With permissions from ref. [117]. Copyright (2014) American Chemical Society)

1.2.4.3 Mechanism study of ABO blood typing on paper

Recent literatures on bioactive paper indicate its desirable ability for performing blood typing assays. Therefore the mechanism study of blood typing on the porous structure of paper is an important aspect for understanding the RBC haemagglutination behaviours, and more significantly, for building the bridge to connect paper and cellulose engineering with biomedical diagnosis applications. Currently, mechanism

related studies include cellulose-absorbed antibodies for RBC agglutination investigation [118], RBC agglutination behaviours on paper fibre structure obtained from microscopic level [119], antibody stabilization on paper for blood typing [120] and the effect of paper structure on blood typing visualization [121]. The mechanism studies of these works are helpful for designing and engineering new bio-active paper-based devices for blood analysis and other bioassays with improved sensitivity, specificity, stability and longevity.

1.2.4.3.1 Mechanisms of RBC agglutination in the antibody-loaded paper

The principle of paper-based blood typing devices is based on the separation of agglutinated RBC lumps from the wicking blood samples in the porous matrices of antibody-treated paper. For understanding the mechanisms of the RBC-antibody interaction and the separation of agglutinated RBCs in the porous matrices in a quantitative manner, Jarujamrus et al. [118] reported a method focusing on semi-quantitative study of the adsorption and desorption of antibody molecules in the antibody-treated paper matrices, as well as the RBC-antibody interactions in such matrices. Figure 25 shows the method for quantifying desorbed antibody from paper by the Bradford total protein assay. And the desorbed percentages for anti-A, anti-B and anti-D by buffer washing were calculated of $42.5 \pm 1.9\%$, $40.4 \pm 5.1\%$ and $34.2 \pm 2.4\%$, respectively.

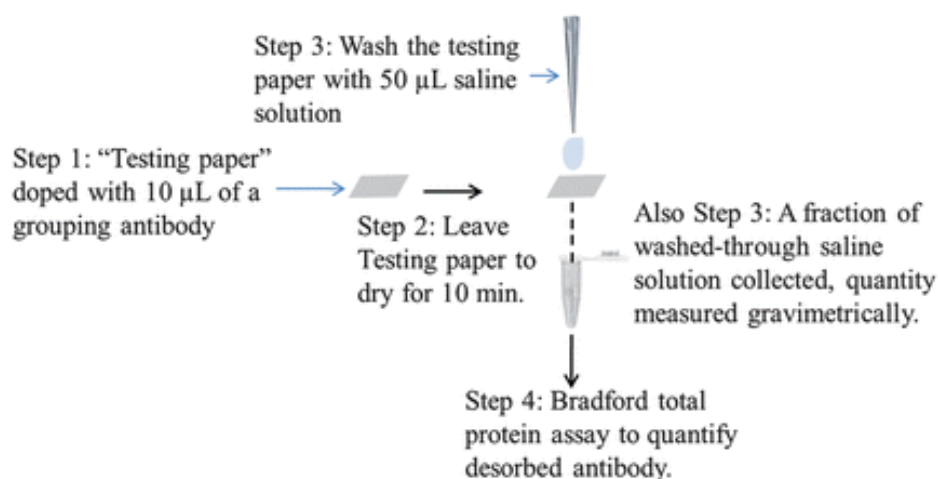


Figure 25. Protocol for the quantification of desorbed antibody from testing papers by the saline washing simulation. (With permissions from ref. [118]. Copyright (2012) Royal Society of Chemistry)

In their work, the author also studied the RBCs agglutination in paper with adsorbed and desorbed antibodies, as the protocols shows in Figure 26. The results suggested that the adsorbed antibody molecules alone on paper matrix are not sufficient to immobilize RBCs into large agglutinated lumps. However, paper containing both adsorbed and desorbed antibody molecules was able to agglutinate the RBCs more efficiently under interaction. The proposed mechanism was concluded due to the phenomenon: antibody-RBC interaction is resulted in the desorbed antibody molecules diffusing into the blood sample which penetrates into the pores of the paper; adsorbed antibodies on the cellulose fibre surface immobilized a certain proportion of RBCs while the released antibody from the fibre into the blood sample agglutinates the remaining ones; in one way the antibody molecules can bridge RBCs onto the adsorbed RBC layers on the cellulose fibre surface, in another way they enable the formation of agglutinated RBC particles in the blood sample bulk.

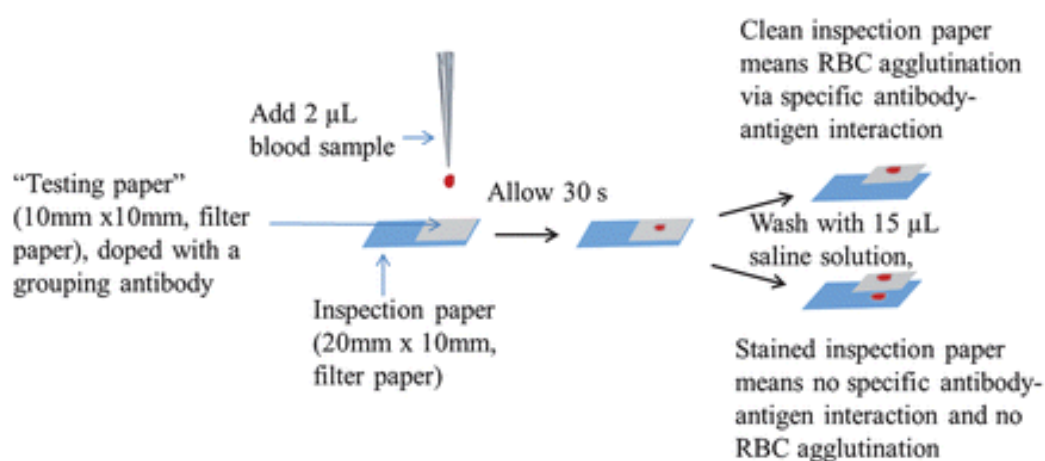


Figure 26. Protocols of testing RBCs agglutination in paper with both adsorbed and desorbed antibodies. (With permissions from ref. [118]. Copyright (2012) Royal Society of Chemistry)

1.2.4.3.2 RBC immobilisation and transport mechanisms inside paper

Li et al. [119] provided the information of RBCs haemagglutination inside the fibre network of paper, to understand the immobilization behaviour of RBCs, as well as transport behaviour under chromatographic elution on paper for the free and agglutinated RBCs. In this study, confocal microscopy was employed to observe the

morphology of the free and agglutinated RBCs that are labelled with fluorescein isothiocyanate (FITC). As is shown in Figure 27, observations were described in terms of the mechanism of RBC haemagglutination inside paper: (1) haemagglutination of RBCs caused the deformation RBCs to form agglutinated lumps with various sizes, rather than massive haemolysis; (2) the movement of red cells due to agglutination freed large area of the fibre surface from cell coverage, which was in accordance with results obtained from the previous work [118], confirming RBC agglutination inside an antibody-treated paper was through the haemagglutination caused by the released antibody molecules from the fibre surface; (3) the formation of red cells lumps tended to attach with the fibre network of paper, which suggests the immobilisation of the agglutinated RBC lumps inside the fibre network is due to the strong adhesion of lumps to the fibres and mechanical entrapment. Dimensions of large agglutinated RBC lumps were close to those of the interfibre pores when the lumps were formed inside the paper. The entrapment and adhesion of those lumps occurred mostly at the gaps and pores between fibres, making the chromatographic elution of the lumps impossible. The confocal results are in full agreement with the conclusion by Al-Tamimi et al. [115] and they provide detailed microscopic evidence of the working mechanism blood typing method using bioactive paper.

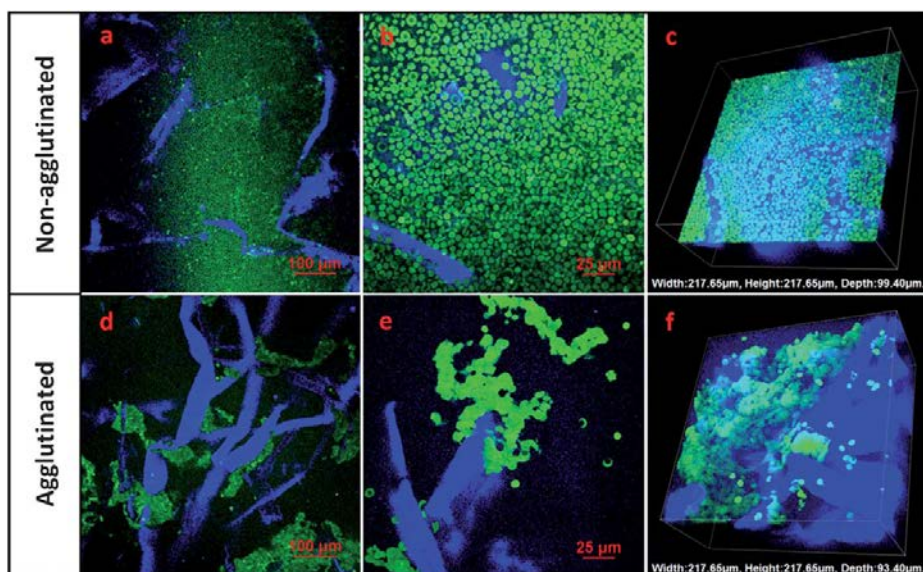


Figure 27. Confocal images of non-agglutinated and agglutinated RBCs patterns inside antibody-treated paper: (a) image of non-agglutinated RBCs captured with 20 folds magnification; (b) image of non-agglutinated RBCs captured with 60 folds magnification. (c) 3D image of non-agglutinated RBCs captured with 60 folds magnification; (d), (e), (f) are images of agglutinated RBCs captured with the same condition from (a), (b) and (c), respectively. (With permissions from ref. [119]. Copyright (2013) Royal Society of Chemistry)

1.2.4.3.3 Stabilization of blood typing antibodies sorbed into paper

The study of stability of blood typing antibodies on paper is important for making paper-based blood typing devices with antibody activity that remains for extended periods. Stabilization of antibody molecules requires the prevention of the formation of intermolecular aggregation, as well as alteration of certain intra molecular conformation.

Guan et al. [120] introduced two strategies for the stabilization of IgM antibodies A, B and D. One was using the chemical additives, such as polyvinylpyrrolidone (PVP), dextran and glycerol for the protection of antibodies; the other is the freeze-drying method for antibody-coated paper (Figure 28). As for the additive strategies, agglutination patterns of RBCs in paper with the absence and presence of pre-mixed additives on Day 0 and Day 28 had been compared. Antibodies without the protection of additives lost their activity for agglutination RBCs while the antibodies mixed with

additives retained a reasonable level of activity for effective RBCs agglutination, after 28 days of storage at room temperature. However the protection by additives for storage at room temperature was limited with the slow loss of antibody activity; dextran provided the longest protection, followed by PVP and then glycerol. For the freeze-drying strategy, freeze dried antibodies sorbed into paper could be stored for a much longer periods at ambient conditions without significant loss of their activity, showing more efficient stabilization of antibodies than additive protection. The thermal stability of freeze-dried antibodies in paper was also studied under a selection of temperatures. After freeze-drying, antibodies in paper can retain most of their activities after incubation under 4, 25, 40 and 60 °C for 6 h.

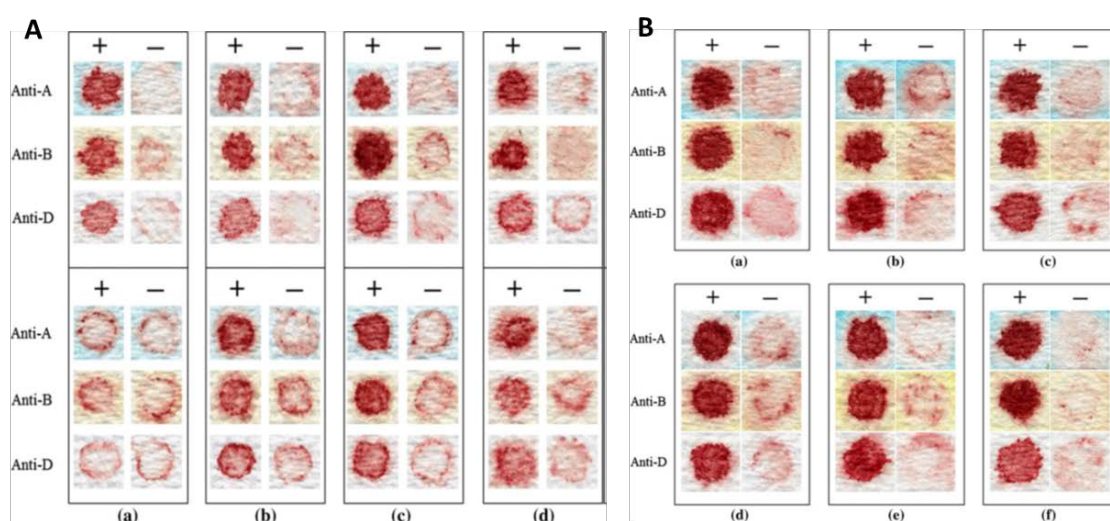


Figure 28. Antibody stability studies by protection of additives (A) and free-drying (B). For additive protection, the specific (+) and non-specific (-) test results of paper squares loaded with antibodies on day 0 (top) and day 28 (bottom) were tested by (a) without additives, (b) with 1 % PVP, (c) with 6 % dextran and (d) with 10 % glycerol. For freeze-drying, the specific and non-specific test results of freeze-dried paper squares loaded with antibodies were tested after stored for (a) 0 days, (b) 3 days, (c) 7 days, (d) 14 days, (e) 28 days, and (f) 42 days. (With permissions from ref. [120]. Copyright (2013) Springer)

1.2.4.3.4 Effect of paper structure on blood typing visualization

Understanding the effect of paper structure on blood typing visualization is crucial for engineering new paper based devices for performing not only blood typing, but also for many other biochemical assays. For this purpose, Su et al. [121] analysed the commercial and experimental papers with different fibre composition, basis weight,

density and porosity for their performance on the separation of agglutinated RBCs from non-agglutinated ones, by optical density measurements of the blood spot under each character. Results indicated that the type of fibres neatly effected the blood typing visualization while the basis weight, density and porosity of paper significantly effected on the separation of agglutinated and non-agglutinated RBCs (Figure 29). Thin and porous papers provided the best performance of blood typing whereas thick and dense papers were improper for blood typing as they tended to retain indiscriminately both free RBCs and aggregated RBCs. Thus an ideal paper substrate for blood typing can be achieved from the low basis weight papers made from softwood fibres. Also the porous cellulose webs modified with cationic polymers could further optimize blood typing analysis.

1.2.5 Low-cost paper microfluidics for environmental sensing

Water and air contamination from human activities is one of the most serious problems attracting the world-wide attentions nowadays. Heavy metal polluted water is considered as one of the critical human health issues [122-124]. When these ions enter into the human body, they could easily bind to vital cellular components and accumulate in organisms due to the difficulty in degradation, resulting in a series of diseases and disorders (e.g., cancers, osteomalacia, and kidney malfunction.) As a low-cost, easy-patterned and bio/chemical-friendly substrate, paper is also an attractive platform for point-of-care and on-site environmental monitoring for use in resource-limited settings [125].

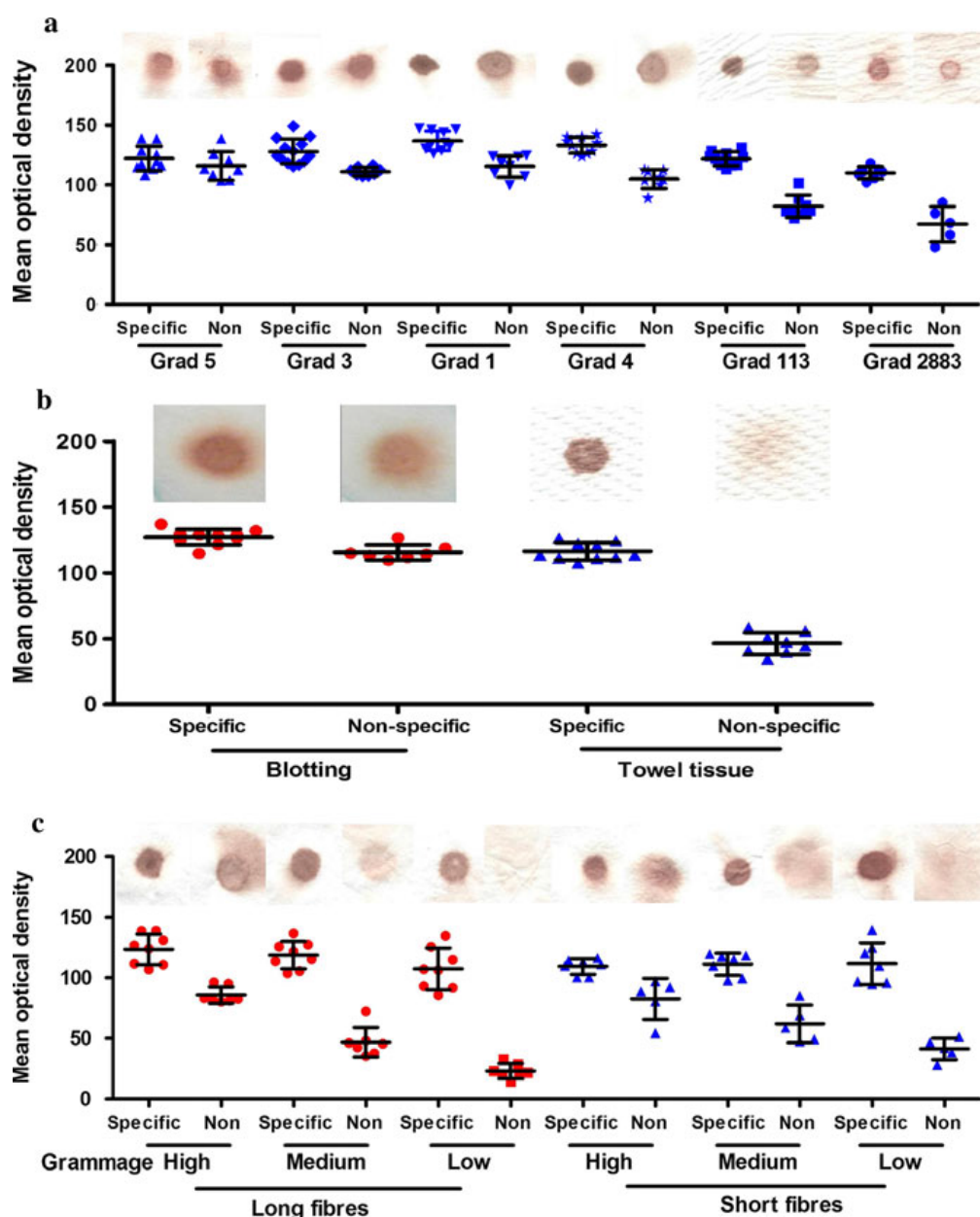


Figure 29. Optical density from blood typing on different papers: a) filter papers; b) blotting and Kleenex towel papers; c) experimental papers made from long and short fibres. (With permissions from ref. [121]. Copyright (2012) Springer)

Hossain et al. [5] described a β -galactosidase (B-GAL)-based paper microfluidics which provides rapid and sensitive determination of multiple heavy metals in water. The sensor was fabricated by inkjet printing of sol-gel based bioinks to propose multiplexed detection assay (Figure 30): the hydrophobic barrier (HB zone) of this sensor was modified by a wax printer in which B-GAL and chlorophenol red β -galactopyranoside (CPRG) were entrapped within silica materials in the circular region

(CR zone) and arm (CG zone), respectively; and the sensing zones (CR zones) were incubated with a drop of sample for 10 min followed by lateral flow chromatography. CPRG is a chromogenic substrate which can be hydrolyzed by B-GAL to form a red-magenta coloured product. A loss of the red-magenta colour is induced by the presence of heavy metals in the sample. The colour intensity in a concentration-dependent manner can then be monitored after a 10 min incubation time at room temperature (Figure 30). Individual metals in a mixture of metal samples can also be screened by this sensor based on different colorimetric complexes produced by Hg (II), Cu (II), Cr (VI) and Ni (II) assays. The detection limits for seven heavy metal ions performed in this work ranging from 0.001 to 0.230 ppm, which are well below or equal to the maximum allowable limits.

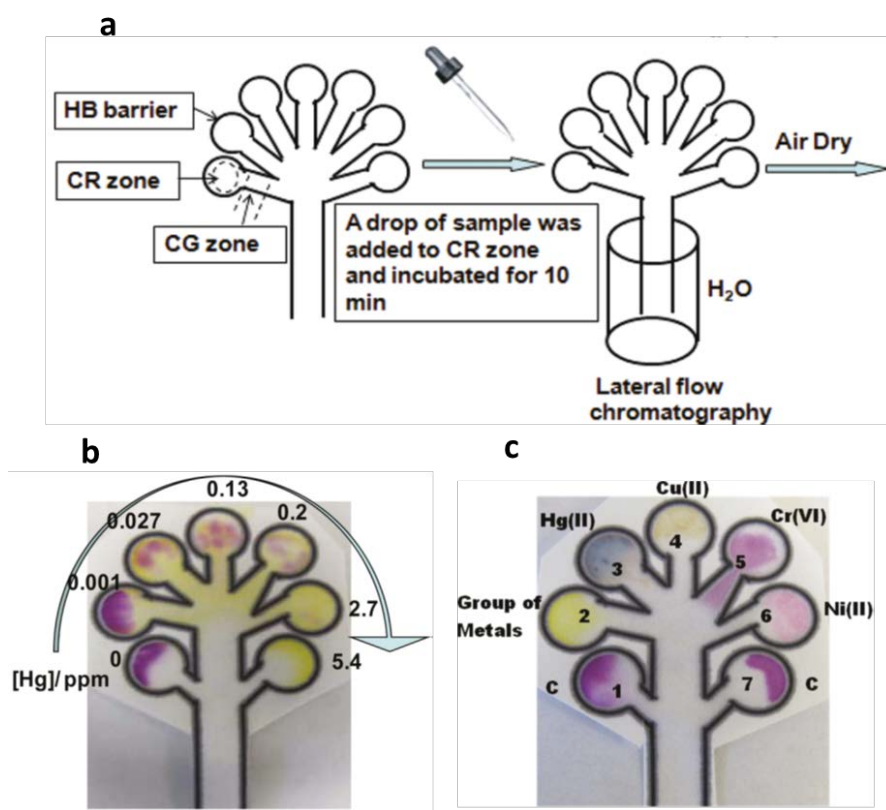


Figure 30. Detection principle and results of the sensor: (a) fabrication of the multiplexed sensor; (b) colorimetric assay of Hg (II) on the patterned paper device in a concentration-dependent manner; (c) detection of four individual metals from a mixture of metals. (With permissions from ref. [5]. Copyright (2011) American Chemical Society)

Wang et al. [126] developed a three-dimensional μ PAD for the determination of four heavy metals, Cu(II), Ni(II), Cd(II) and Cr(VI), through wax-patterned paper layers stacked by double-sided adhesive tape, as is shown in Figure 31. Fluids passed both laterally and vertically through the layers of the device, distributing the reagents into each layer. Chromogenic assays of the four heavy metal ions can then be performed through the four samples inlets on the device. The chromogenic signals were collected by a cell phone camera for further quantitative analysis in the computer. The colour intensity estimated by the software showed the identification limit ranging from 0.19 to 0.35 ppm of the four heavy metals. This device can also detect individual metal ions from real environmental samples, including reservoirs and beach water, with comparable results from the atomic absorption spectrometer (AAS).

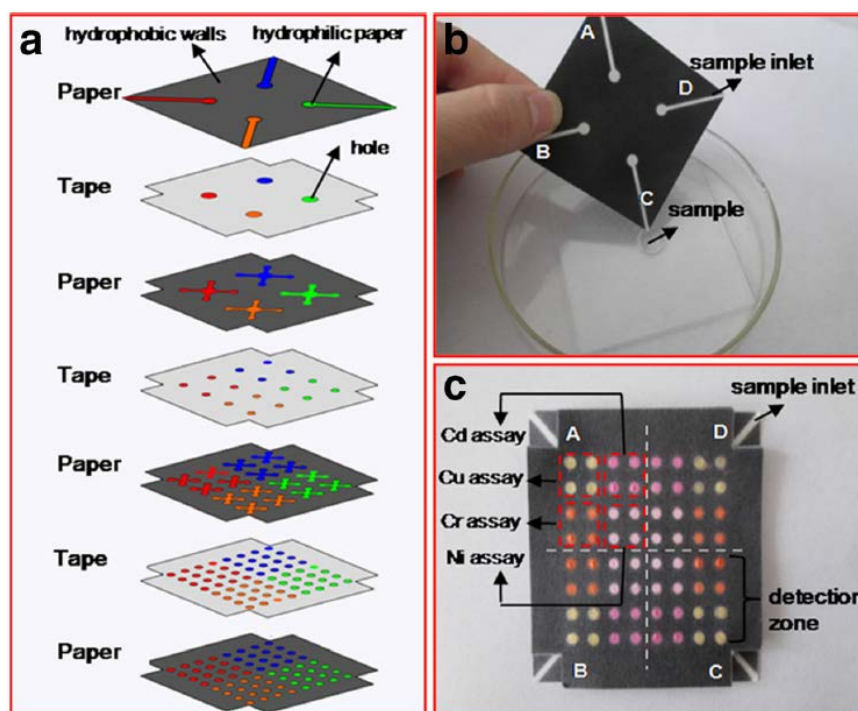


Figure 31. The 3D paper microfluidic chip fabrication: (a) four wax-patterned paper layers stacked by three double-sided stick tape. The paper layers were patterned hydrophilic channels to deliver liquids while the tape layers were modified by holes that connected channels in each paper layer; (b) the detection of four metals enabled by the four sample inlets on the device; (c) colorimetric assays of the four heavy metals in the detection zone. (With permissions from ref. [126]. Copyright (2014) Springer)

Besides water contamination, pollutants exposure to particulate matter (air pollution) is another issue that leads to a variety of serious respiratory and cardiovascular disorders. The Henry group has reported several paper-based microfluidics for the monitoring of air quality, including the detection of aerosol oxidative activity and heavy metals in air [127-129]. One of their recent works introduced a multilayer paper microfluidic device for quantification of six heavy metals through the combination of colorimetric and electrochemical processes [129]. As is shown in Figure 32, the device consists of two layers with one for colorimetric assays, and another for electrochemical testing with screen-printed three-electrode system. The detection for Ni, Fe, Cu and Cr were achieved through colorimetric reaction and the Pb and Cd were identified by electrochemical assay. Detection limit of each metal was comparable with traditional methods. Particulate metals accumulated on air sampling filters were tested as an example of the device utility.

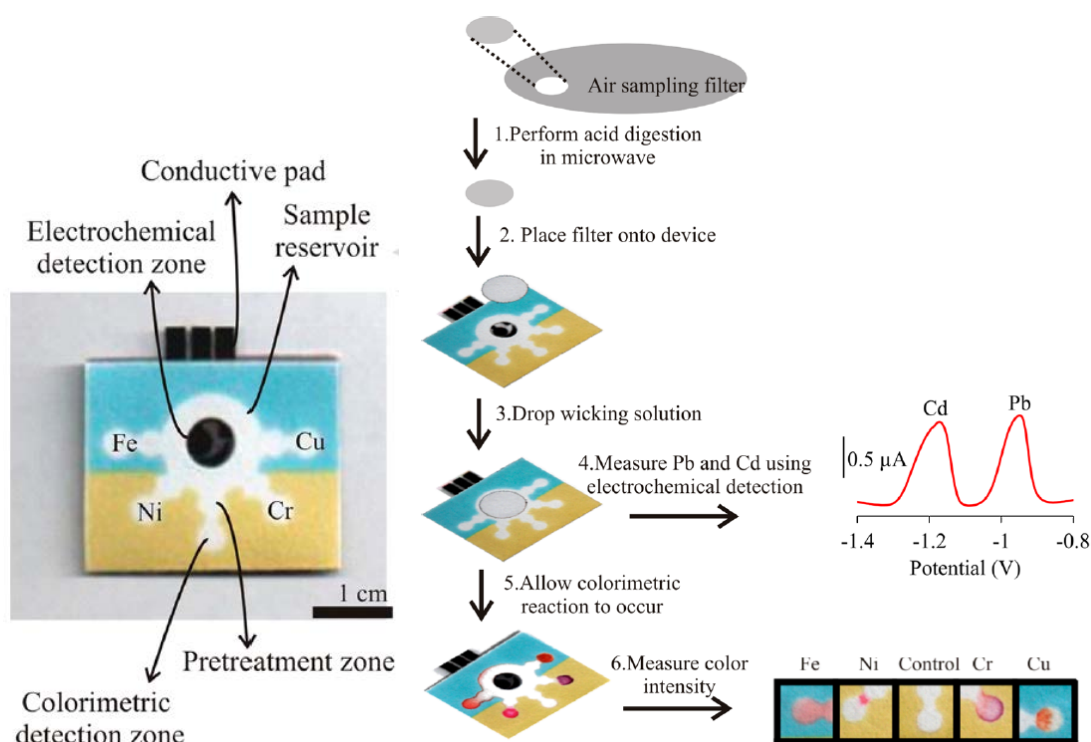


Figure 32. The sensor modification and detection process: (a) fabrication of the paper-based device with different detection zone for colorimetric and electrochemical assays; (b) analytical procedure for metal testing on an air sampling filter. The anodic stripping voltametric method was used for detection of Cd and Pb and the colorimetric reaction was for Fe, Ni, Cr and Cu assays. (With permissions from ref. [129]. Copyright (2014) American Chemical Society)

1.3 Review summary

From the literature review, it is clear that there are many reported methods of designing low-cost devices for blood typing, environmental sensing and other analytical applications. However, these methods have some drawbacks which limit their use as desirable ASSURED platforms. The summary of these drawbacks is presented below.

First of all, minimizing users' efforts in operating the sensor, handling the reagent during the bioanalytical assays for example, is still challenging. Typically in a blood typing assay, although many recently reported devices no longer require their users to operate complicated equipment such as centrifugal machine, handling the supported reagent is still compulsory. Therefore, a highly adaptable blood-typing device with minimum users' efforts is strongly demanded.

Secondly, supporting equipment, such as colour intensity measurement devices and electrochemical stations, cannot be avoided in the interpretation of the results obtained from these reported low-cost diagnostics. Whilst a colorimetric or voltametric signal can report the test results, in most situations the results need to be interpreted by trained personnel. The situation would become more complicated if an assay could generate multiple outcomes and therefore, requires careful comparison and examination before the conclusion of the diagnosis can be made. As the matter of fact, the well-trained professional personnel will be necessary to perform these assays at all time, which largely compromise the value of low-cost diagnostics. Therefore, it is critical to develop an unambiguous reporting method for sensors, so that the results can be easily and clearly understood even by unskilled users.

Thirdly, environmental problems, such as water contamination, are now attracting world-wide attention of not only the governments and professionals, but the general public. However, few studies have been made focusing on the sensor design for untrained users to perform on-site environment monitoring. While several published methods performed the environmental monitoring on inexpensive platforms including paper, none of these methods can deliver the analytical results directly to the users,

either professional or non-professional, without data analysis tools and other assistance. Thus, in addition to high sensitivity, specificity and rapid detection, easy result interpretation without equipment and professional assistance are also highly desirable as one of the most important performance feature in designing new improved devices for public environmental monitoring.

1.4 Research aims

The overall aims of this research are to explore novel and non-conventional sensor design concepts, in order to establish innovative platforms to meet the “user-friendly, equipment-free and delivered” (UED) criteria for conducting chemical and biomedical assays on inexpensive substrate for end-users. Blood typing and on-site environmental monitoring are two pioneering applications to demonstrate these sensor design concepts in this thesis. By achieving these aims, devices designed using these new concepts can be developed for use in locations such as less-industrialized areas, rural regions, home care, field operations and emergency situations.

In particular, the specific aims of this research were:

1. To explore a “sample-only” method which reduces the users’ efforts when assays are performed, providing a simplified assay procedure to the untrained or non-professional users.
2. To explore a novel communication method — “text-reporting” — between the device and its user, which enable the users to understand the testing result through unambiguous text-based messages.
3. To investigate novel low-cost sensing concepts in diagnostic and environmental monitoring applications, and to demonstrate functionality and feasibility of these devices in blood analysis and water quality evaluation.

1.5 Thesis outline

Based on the research aims, the studies that were conducted, as well as the successful outcomes, are outlined chapter by chapter.

- **Chapter 2. Low-cost sample-only device for forward and reverse blood typing**

(Published paper: Li, M., Tian, J., Cao., R., Guan, L., Shen, W., A low-cost forward and reverse blood typing device — A blood sample is all you need to perform an assay, *Anal. Methods*, **2015**, 7: 1186–1193.)

The sample-only method is developed in this chapter, which focuses on the design of a new user-operated blood typing device that requires minimum effort from the user to perform a blood typing assay under non-laboratory conditions. Specifically, it presents a new device to perform forward and reverse blood typing assays without the buffer-activation or buffer-washing steps that are necessary in conventional assays. Two significant original contributions are included in this study. First, a new method using patterned plastic slides is able to deliver the assay result to the user in one minute. The device simply requires the user to put a drop of blood into the patterned channels of the device, with no further operational effort required. Second, a simple and reliable approach for quantitatively measuring the antibody dissolution rate on the slides has been designed using paper chromatography elution. In addition, to increase the longevity of the device, a new method of preserving the activities of antibodies is presented. These designs present a vivid example of improving the sensor's "UED" capability by reducing user's effort while performing the assay.

- **Chapter 3. Paper-based blood typing device that reports patient's blood type "in writing"**

(Published paper: Li, M., Tian, J., Al-tamimi, M., Shen, W., Paper-Based Blood Typing Device That Reports Patient's Blood Type "in Writing", *Angew. Chem. Int. Ed.*, **2012**, 51: 5497–5501.)

The development of the text-reporting method is commenced in this chapter, in which a break-through concept in reporting assay results to the user in text is presented. It prevents the possible misinterpretation of the results obtained using the current colorimetric and electrochemical methods. As an example of the application of this concept, a bioactive-paper blood typing device is designed to be capable of fast reporting ABO and RhD blood types in written text. It is also the first demonstration of an equipment-free device for blood type reporting using paper text and symbols [130]. This text-reporting method significantly improves the “UED” features of the POC diagnostics and will be valuable for making “ASSURED” devices in developing countries. Using this device, a new communication method between the sensor and its user is established, and this text-reporting method can be incorporated into many other applications.

- **Chapter 4. Paper-based device for rapid typing of secondary blood groups**

(Published paper 1: Li, M., Then, W., Li, L., Shen, W., *Paper-based device for rapid typing of secondary human blood groups*, *Anal. Bioanal. Chem.*, **2014**, 406, 669–677; and Published paper 2: Then, W., Li, M., McLiesh, H., Shen, W., Garnier, G., *The detection of blood group phenotypes using paper diagnostics*, *Vox Sanguinis*, **2015**, 108: 186–196.)

This chapter extends blood typing of ABO and RhD blood groups to secondary blood groups using paper sensors, represented by two published papers. The first paper applies the text-reporting concept to a paper-based device, so that a number of clinically important secondary blood groups can be identified. On a single piece of paper, twenty secondary groups can be reported simultaneously in unambiguous written text. Moreover, for the purpose of designing highly efficient paper-based secondary blood grouping devices, secondary group antibody-RBC interactions in the fibre network of the paper were also investigated. The confocal microscopy method developed for paper-based blood grouping assays [119] was employed to obtain the mechanism of the interactions of RBC with the secondary group antibodies. The second paper presents the use of paper chromatography elution as a method for secondary blood groups typing. In this paper, the influence of RBC-antibody reaction

times, reagent concentrations and antibody structure on the clarity of the blood typing results using the paper-based device is reported.

- **Chapter 5. Paper-based device for environmental sensing by text-reporting**
(Published: Li, M., Cao R., Nilghaz, A., Guan L., Zhang, X., Shen, W.,
“Periodic-table-style” paper device for monitoring heavy metals in water, *Anal. Chem.*, **2015**, 87 (5): 2555–2559)

This chapter presents an effective extension of the text-reporting concept to environmental monitoring. With the employment of this concept, on-site water monitoring can be simply and inexpensively performed by users at home or under other conditions where laboratories are not available. The paper-based microfluidic device is patterned with unambiguous text to form a periodic table-style device, which is used for monitoring heavy metal contamination in water. Three common heavy metals, Cu(II), Ni(II) and Cr(VI), were chosen as testing examples. If any of their concentrations exceeds the legislated safe-to-use level, it is indicated directly in the corresponding chemical symbols on the device. Semi-quantitative measurements of the three ions were also conducted to identify the reliable detection limit and accuracy of this device. This method successfully further extends the text-reporting concept to instantaneous on-site environmental monitoring.

- **Chapter 6. Conclusions and future work**

This chapter summarizes the major contributions of this thesis and recommends future research approaches to building paper-based sensors for real-world applications.

1.6 References

- [1] WHO, *Mapping the landscape of diagnostics for sexually transmitted infections*: <http://www.who.int/tdr/publications/documents/mapping-landscape-sti.pdf>.
- [2] A. W. Martinez, S. T. Phillips, E. Carrilho, S. W. Thomas, H. Sindi, G. M. Whitesides, "Simple Telemedicine for Developing Regions: Camera Phones and Paper-Based Microfluidic Devices for Real-Time, Off-Site Diagnosis", *Anal. Chem.*, 2008, **80** (10): 3699–3707.
- [3] A. W. Martinez, S. T. Phillips, M. J. Butte, G. M. Whitesides, "Patterned paper as a platform for inexpensive, low-volume, portable bioassays", *Angew. Chem. Int. Ed.*, 2007, **46**: 1318–1320.
- [4] M. S. Khan, G. Thouas, W. Shen, G. Whyte, G. Garnier, "Paper diagnostic for instantaneous blood typing", *Anal. Chem.*, 2010, **82**: 4158–4164.
- [5] S. M. Z. Hossain, J. D. Brennan, " β -Galactosidase-based colorimetric paper sensor for determination of heavy metals", *Anal. Chem.* 2011, **83**: 8772–8778.
- [6] K. E. Blick, "Current trends in automation of immunoassays", *J. Clin. Ligand. Assay.*, 1999, **22**: 6–12.
- [7] P. St-Louis, "Status of point-of-care testing: promise, realities, and possibilities", *Clin. Biochem.*, 2000, **33**: 427–440.
- [8] C. P. Price, A. St John, J. M. Hicks, *Point-of-care testing*, 2nd ed, 2004, Washington' AACC Press.
- [9] R. W. Hardy, G. L. Hortin, *Point-of-care testing*, 2nd ed, 2004, Washington' AACC Press: 221–225.
- [10] R. E. Kirkbride, *Point-of-care testing*, 2nd ed, 2004, Washington' AACC Press: 353–360.
- [11] P. von Lode, "Point-of-care immunotesting: Approaching the analytical performance of central laboratory method", *Clin. Biochem.*, 2005, **38**: 591–606.
- [12] W. C. Tian, E. Finehout, *Microfluidics for biological applications*, 2008, Springer Publishing Company Incorporated.
- [13] A. Manz, N. Graber, H.M. Widmer, "Miniaturized total chemical analysis systems: A novel concept for chemical sensing", *Sens. Act. B Chem.*, 1990, **1**: 244–248.
- [14] G. M. Whitesides, "The origins and the future of microfluidics", *Nature*, 2006, **442**: 368–373.
- [15] D. Mark, S. Haeberle, G. Roth, F.von Stetten, R. Zengerle, "Microfluidic lab-on-a-chip platforms: requirements, characteristics and applications", *Chem. Soc. Rev.*, 2010, **39**: 1153–1182.
- [16] M. Kersaudy-Kerhoas, R. Dhariwal, M. Desmulliez, L. Jouvét, "Hydrodynamic blood plasma separation in microfluidic channels", *Microfluidics and Nanofluidics*, 2010, **8**: 105–114.

- [17] P. J. Hung, P. J. Lee, P. Sabounchi, R. Lin, L. P. Lee, "Continuous perfusion microfluidic cell culture array for high-throughput cell-based assays", *Biotech. Bioengineering*, 2005, **89**: 1–8.
- [18] R. Gómez-Sjöberg, A. A. Leyrat, D. M. Pirone, C. S. Chen, S. R. Quake, "Versatile, fully automated, microfluidic cell culture system", *Anal. Chem.* 2007, **79**: 8557–8563.
- [19] B. M. Paegel, C. A. Emrich, G. J. Weyemayer, J. R. Scherer, R. A. Mathies, "High throughput DNA sequencing with a microfabricated 96-lane capillary array electrophoresis bioprocessor", *Proc. Natl. Acad. Sci. U.S.A.*, 2002, **99**: 574–579.
- [20] C. W. Kan, C. P. Fredlake, E. A. S. Doherty, A. E. Barron, "DNA sequencing and genotyping in miniaturized electrophoresis systems", *Electrophoresis*, 2004, **25**: 3564–3588.
- [21] J. T. Santini, M. J. Cima, R. Langer, "A controlled-release microchip", *Nature*, 1999, **397**: 335–338.
- [22] D. A. LaVan, T. McGuire, R. Langer, "Small-scale systems for in vivo drug delivery", *Nat. Biotech.*, 2003, **21**: 1184–1191.
- [23] W. M. Saltzman, W. L. Olbricht, "Building drug delivery into tissue engineering design", *Nat. Rev. Drug Discov.*, 2002, **1**: 177–186.
- [24] J. West, M. Becker, S. Tombrink, A. Manz, "Micro total analysis systems: Latest achievements", *Anal. Chem.*, 2008, **80**: 4403–4419.
- [25] K. Ohno, K. Tachikawa, A. Manz, "Microfluidics: Applications for analytical purposes in chemistry and biochemistry", *Electrophoresis*, 2008, **29**: 4443–4453.
- [26] S. Mendez, E.M. Fenton, G.R. Gallegos, D.N. Petsev, S.S. Sibbett, H.A. Stone, Y. Zhang, G.P. Lopez, "Imbibition in porous membranes of complex shape: quasi-stationary flow in thin pectangular segments", *Langmuir*, 2010, **26** : 1380–1385.
- [27] A. W. Martinez, S. T. Phillips, G. M. Whitesides, E. Carrilho, "Diagnostics for the developing world: microfluidic paper-based analytical devices", *Anal. Chem.*, 2010, **82**: 3–10.
- [28] R. Pelton, "Bioactive paper provides a low-cost platform for diagnostics", *Trac Trends Anal. Chem.*, 2009, **28**: 925–942.
- [29] A. C. Siegel, S. T. Phillips, B. J. Wiley, G. M. Whitesides, "Thin, lightweight, foldable thermochromic displays on paper", *Lab Chip*, 2009, **9**: 2775–2781.
- [30] B. Balu, A. D. Berry, D. W. Hess, V. Breedveld, "Patterning of superhydrophobic paper to control the mobility of micro-liter drops for two-dimensional lab-on-paper applications", *Lab Chip*, 2009, **9**: 3066–3075.
- [31] M. M. Ali, S. D. Aguirre, Y. Q. Xu, C. D. M. Filipe, R. Pelton, Y. F. Li, "Detection of DNA using bioactive paper strips", *Chem. Commun.*, 2009, 6640–6642.
- [32] S. V. Vaeck, "Quantitative inorganic paper chromatography direct determination of cobalt by a scanning method", *Anal. Chim. Acta.*, 1955, **12**: 443–454.

- [33] W. A. Zhao, M. M. Ali, S. D. Aguirre, M. A. Brook, Y. F. Li, "Paper-based bioassays using gold nanoparticle colorimetric probes", *Anal. Chem.*, 2008, **80**: 8431–8437.
- [34] W. A. Zhao, A. van den Berg, "Lab on paper", *Lab Chip*, 2008, **8**: 1988–1991.
- [35] R. Stock, C. B. F. Rice, *Chromatographic Methods*, 3rd ed., John Wiley & Sons: New York, 1974.
- [36] P. Atkins, L. Jones, *Chemistry-Molecules, Matter, and Change*, 3rd ed., W.H. Freeman & Company: New York, 1997.
- [37] J. P. Comer, "Semiquantitative Specific Test Paper for Glucose in Urine", *Anal. Chem.*, 1956, **28**: 1748–1750.
- [38] P. von Lode, "Point-of-care immunotesting: approaching the analytical performance of central laboratory methods", *Clin. Biochem.*, 2005, **38**, 591–606.
- [39] Neimo, L., *Papermaking Chemistry, Book 4 of Papermaking Science and Technology*, Helsinki: Fapet Oy, 1999, 184–197.
- [40] W. Shen, Y. Filonanko, Y. Truong, I. H. Parker, N. Brack, P. Pigram, J. Liesegang, "Contact angle measurement and surface energetics of sized and unsized paper", *Colld. Surf. A: Phys. Eng. Asp.*, 2000, **173**: 117–126.
- [41] D. Kannangara, H. Zhang, W. Shen, "Liquid-paper interactions during liquid drop impact and recoil on paper surfaces", *Colld. Surf. A: Phys. Eng. Asp.*, 2006, **280**: 203–215.
- [42] K. T. Hodgson, J. C. Berg, "The effect of surfactants on wicking flow in fiber networks", *J. Colloid Interface Sci.*, 1988, **121**: 22–31.
- [43] A. W. Martinez, S. T. Phillips, B. J. Wiley, M. Gupta, G. M. Whitesides, "FLASH: A rapid method for prototyping paper-based microfluidic devices", *Lab Chip*, 2008, **8**: 2146–2150.
- [44] A. W. Martinez, S. T. Phillips, E. Carrilho, S. W. Thomas, H. Sindi, G. M. Whitesides, "Simple telemedicine for developing regions: Camera phones and paper-based microfluidic devices for real-time, off-site diagnosis", *Anal. Chem.*, 2008, **80**: 3699–3707.
- [45] A. W. Martinez, S. T. Phillips, G. M. Whitesides, "Three-dimensional microfluidic devices fabricated in layered paper and tape", *Proc. Natl. Acad. Sci. U.S.A.*, 2008, **105**: 19606–19611.
- [46] M. A. Hobbe, "Paper's resistance to wetting—A review of internal sizing chemicals and their effect", *BioResources*, 2006, **2**(1): 106–145.
- [47] H. P. Le, "Progress and Trends in Ink-jet Printing Technology", *J. Imag. Sci. Tech.*, 1998, **42**: 49–62.
- [48] H. Kipphan, *Handbook of Print Media*, Springer, 2001.
- [49] L. R. Allain, M. Askari, D. L. Stokes, T. Vo-Dinh, "Microarray sampling-platform fabrication using bubble-jet technology for a biochip system", *Fresenius J. Anal. Chem.*, 2001, **371**: 146–150.

- [50] T. Xu, J. Jin, C. Gregory, J. J. Hickman, T. Boland, "Inkjet printing of viable mammalian cells", *Biomaterials*, 2005, **26**: 93–99.
- [51] X. Li, J. Tian, G. Garnier, W. Shen, "Fabrication of Paper-Based Microfluidic Sensors by Printing", *Colloids Surf. B Biointerfaces*, 2010, **76**(2): 564–570.
- [52] Y. Lu, W.W. Shi, L. Jiang, J.H. Qin, B.C. Lin, "Rapid prototyping of paper-based microfluidics with wax for low-cost, portable bioassay", *Electrophoresis*, 2009, **30**: 1497–1500.
- [53] W. Dungchai, O. Chailapakul, C. S. Henry, "A low-cost, simple, and rapid fabrication method for paper-based microfluidics using wax screen-printing", *Analyst*, 2011, **136**(1): 77–82.
- [54] T. Songjaroena, W. Dungchaib, O. Chailapakulc,d, W. Laiwattanapaisal, "Novel, simple and low-cost alternative method for fabrication of paper-based microfluidics by wax dipping", *Talanta*, 2011, **85**: 2587–2593.
- [55] D. A. Bruzewicz, M. Reches, G. M. Whitesides, "Low-cost printing of poly(dimethylsiloxane) barriers to define microchannels in paper", *Anal. Chem.*, 2008, **80**(9): 3387–3392.
- [56] K. Abe, K. Suzuki, D. Citterio, "Inkjet-printed microfluidic multianalyte chemical sensing paper", *Anal. Chem.*, 2008, **80**(18): 6928–6934.
- [57] K. Abe, K. Kotera, K. Suzuki, and D. Citterio, "Inkjet-printed paperfluidic immuno-chemical sensing device", *Anal. Bioanal. Chem.*, 2010, **398**(2): 885–893.
- [58] X. Li, J. Tian, T. Nguyen, W. Shen, "Paper-based microfluidic devices by plasma treatment", *Anal. Chem.*, 2008, **80**(23): 9131–9134.
- [59] X. Li, J. Tian, W. Shen, "Progress in patterned paper sizing for fabrication of paper-based microfluidic sensors", *Cellulose*, 2010, **17**(3): 649–659.
- [60] J. Olkkonen, K. Lehtinen, T. Erho, "Flexographically printed fluidic structures in paper", *Anal. Chem.*, 2010, **82**(24): 10246–10250.
- [61] G. Chitnis, Z. Ding, C. L. Chang, C. A. Savran, B. Ziaie, "Laser-treated hydrophobic paper: an inexpensive microfluidic platform", *Lab Chip*, 2011, **11**(6): 1161–1165.
- [62] E. M. Fenton, M. R. Mascarenas, G. P. Lopez, S. S. Sibbett, "Multiplex lateral-flow test strips fabricated by two-dimensional shaping", *ACS Appl. Mater. Interfaces*, 2009, **1**: 124–129.
- [63] X. Li, D. Ballerini, W. Shen, "A perspective on paper-based microfluidics: Current status and future trends", *Biomicrofluidics*, 2012, **6**: 11301–1130113.
- [64] Y. Liu, Y. Sun, K. Sun, L. Song, X. Jiang, "Recent developments employing new materials for readout in lab-on-a-chip", *J. Mater. Chem.*, 2010, **20**(35): 7305–7311.
- [65] R. F. Carvalhal, E. Carrilho, L. T. Kubota, "The potential and application of microfluidic paper-based separation devices", *Bioanalysis*, 2010, **2**(10): 1663–1665.
- [66] S. Klasner, A. Price, K. Hoeman, R. Wilson, K. Bell, C. Culbertson, "Paper-based microfluidic devices for analysis of clinically relevant analytes present in urine and saliva", *Anal. Bioanal. Chem.*, 2010, **397**(5): 1821–1829.

- [67] W. Dungchai, O. Chailapakul, C. S. Henry, "Use of multiple colorimetric indicators for paper-based microfluidic devices", *Anal. Chim. Acta.*, 2010, **674**(2): 227–233.
- [68] A. W. Martinez, S. T. Phillips, Z. Nie, C. M. Cheng, E. Carrilho, B. J. Wiley, G. M. Whitesides, "Programmable diagnostic devices made from paper and tape", *Lab Chip*, 2010, **10**(19): 2499–2504.
- [69] H. Noh, S. T. Phillips, "Fluidic timers for time-dependent, point-of-care assays on paper", *Anal. Chem.*, 2010, **82**(19): 8071–8078.
- [70] W. Wang, W. Y. Wu, J. J. Zhu, "Tree-shaped paper strip for semiquantitative colorimetric detection of protein with self-calibration", *J. Chromatogr. A.*, 2010, **1217**(24): 3896–3899.
- [71] A. K. Ellerbee, S. T. Phillips, A. C. Siegel, K. A. Mirica, A. W. Martinez, P. Striehl, N. Jain, M. Prentiss, G. M. Whitesides, "Quantifying colorimetric assays in paper-based microfluidic devices by measuring the transmission of light through paper", *Anal. Chem.*, 2009, **81**(20): 8447–8452.
- [72] X. Li, J. Tian, W. Shen, "Quantitative biomarker assay with microfluidic paper-based analytical devices", *Anal. Bioanal. Chem.*, **396**(1): 495–501.
- [73] C. Z. Li, K. Vandenberg, S. Prabhulkar, X. Zhu, L. Schneper, K. Methee, C. J. Rosser, E. Almeida, "Paper based point-of-care testing disc for multiplex whole cell bacteria analysis", *Biosens. Bioelectron.*, 2011, **26**(11): 4342–4348.
- [74] W. Zhao, M. M. Ali, S. D. Aguirre, M. A. Brook, Y. Li, "Paper-based bioassays using gold nanoparticle colorimetric probes", *Anal. Chem.*, 2008, **80**: 8431–8437.
- [75] S. S. Agasti, S. Rana, M. H. Park, C. K. Kim, C. C. You, V. M. Rotello, "Nanoparticles for detection and diagnosis", *Adv. Drug Deliv. Rev.*, 2010, **62**: 316–328.
- [76] Y. H. Ngo, D. Li, G. P. Simon, G. Garnier, "Paper surfaces functionalized by nanoparticles", *Adv. Colloid Interface Sci.*, 2011, **163**: 23–38.
- [77] S. M. Z. Hossain, R. E. Luckham, M. J. McFadden, J. D. Brennan, "Reagentless bidirectional lateral flow bioactive paper sensors for detection of pesticides in beverage and food samples", *Anal. Chem.*, 2009, **81**: 9055–9064.
- [78] Y. Liu, Y. Liu, Z. Liang, X. Li, S. Liu, J. Yu, "Enhanced sensitivity and selectivity of chemosensor for malonate by anchoring on gold nanoparticles", *Chinese J Chem.*, 2011, **29**: 531–538.
- [79] W. Zhao, M. A. Brook, Y. Li, "Design of gold nanoparticle-based colorimetric biosensing assays", *Chem. Bio. Chem.*, 2008, **9**: 2363–2371.
- [80] W. Dungchai, O. Chailapakul, C. S. Henry, "Electrochemical detection for paper-based microfluidics", *Anal. Chem.*, 2009, **81**(14): 5821–5826.
- [81] Z. Nie, F. Deiss, X. Liu, O. Akbulut, G. M. Whitesides, "Integration of paper-based microfluidic devices with commercial electrochemical readers", *Lab Chip*, 2010, **10**(22): 3163–3169.

- [82] A. Apilux, W. Dungchai, W. Siangproh, N. Praphairaksit, C. S. Henry, O. Chailapakul, "Lab-on-paper with dual electrochemical/colorimetric detection for simultaneous determination of gold and iron", *Anal. Chem.*, 2010, **82**(5): 1727–1732.
- [83] Z. Nie, C. A. Nijhuis, J. Gong, X. Chen, A. Kumachev, A. W. Martinez, M. Narovlyansky, G. M. Whitesides, "Electrochemical sensing in paper-based microfluidic devices", *Lab Chip*, 2010, **10**(4): 477–483.
- [84] R. F. Carvalhal, M. S. Kfoury, M. H. de Oliveira Piazzetta, A. L. Gobbi, L. T. Kubota, "Electrochemical detection in a paper-based separation device", *Anal. Chem.*, 2010, **82**(3): 1162–1165.
- [85] J. Yu, L. Ge, J. Huang, S. Wang, S. Ge, "Microfluidic paper-based chemiluminescence biosensor for simultaneous determination of glucose and uric acid", *Lab Chip*, 2011, **11**: 1286–1291.
- [86] J. L. Delaney, C. F. Hogan, J. Tian, W. Shen, "Electrogenerated chemiluminescence detection in paper-based microfluidic sensors", *Anal. Chem.*, 2011, **83**: 1300–1306.
- [87] X. Li, J. Tian, W. Shen, "Thread as a Versatile Material for Low-Cost Microfluidic Diagnostics", *ACS Appl. Mater. Interfaces.*, 2009, **2**(1): 1–6.
- [88] R. Safavieh, M. Mirzaei, M. A. Qasaimeh, D. Juncker, "Yarn based microfluidics: from basic elements to complex circuits", *Proceedings of MicroTAS.*, 2009, 1–5.
- [89] M. Reches, K. A. Mirica, R. Dasgupta, M. D. Dickey, M. J. Butte, G. M. Whitesides, "Thread as a Matrix for Biomedical Assays", *ACS Appl. Mater. Interfaces.*, 2010, **2**(6): 1722–1728.
- [90] D. R. Ballerini, X. Li, W. Shen, "Flow control concepts for thread-based microfluidic devices", *Biomicrofluidics*, 2011, **5**: 014105–014113.
- [91] R. Safavieh, G.Z. Zhou, D. Juncker, "Microfluidics made of yarns and knots: from fundamental properties to simple networks and operations", *Lab Chip*, 2011, **11**: 2618–2624.
- [92] X. Li, D. Ballerini, J. Tian, W. Shen, "Thread as a Substrate for Low-Cost Point-of-Care Diagnostics", *Sustainable Chemistry*, 2011.
- [93] A. Nilghaz, D. R. Ballerini, X. Fang, W. Shen, "Semiquantitative analysis on microfluidic thread-based analytical devices by ruler", *Sens. Act. B Chem*, 2014, **191**: 586–594.
- [94] G. Daniels, *Human Blood Groups*, 2nd ed., Oxford: Blackwell Science, 2002.
- [95] G. Daniels, M. E. Reid, "Blood groups: the past 50 years", *Transfusion*, 2010, **50**(2): 281–289.
- [96] P. Rous, K. Landsteiner, *Obituary Notices of Fellows of the Royal Society*, 1947, **5**(15): 294–226.
- [97] N. D. Avent, M. E. Reid, "The Rh blood group system: a review", *Blood*, 2000, **95**(2): 375–387.
- [98] C. M. Westhoff, "The Rh blood group system in review: A new face for the next decade", *Transfusion*, 2004, **44**(11): 1663–1673.

- [99] G. Daniels, J. Poole, M. de Silva, T. Callaghan, S. MacLennan, N. Smith, "The clinical significance of blood group antibodies", *Transfusion Med.*, 2002, **12**: 287–295.
- [100] G. Daniels, I. Bromilow, *Essential Guide to Blood Groups*, Wiley-Blackwell: Hoboken, 2007.
- [101] B. H. Estridge, A. P. Reynolds, N. J. Walters NJ, Basic medical laboratory techniques, Delmar Engage Learning, Albany, NY, USA, 2002.
- [102] F. Llopis, F. Carbonell-Uberos, M. C. Montero, S. Bonanad, M. D. Planelles, I. Plasencia, C. Riola, T. Planells, C. Carrillo, A. De Miguel, "A new method for phenotyping red blood cells using microplates", *Vox Sang.*, 1999, **77**:143–148.
- [103] F. Llopis, F. Carbonell-Uberos, M. Planelles, M. Montero, N. Puig, T. Atienza, E. Alba, J. Montoro, "A monolayer coagglutination microplate technique for typing red blood cells", *Vox Sang.*, 1997, **72**: 26–30.
- [104] J. H. Spindler, H. ter Kl, M. Kerowgan, "A novel microplate agglutination method for blood grouping and reverse typing without the need for centrifugation", *Transfusion*, 2001, **41**: 627–632.
- [105] M. M. Langston, J. L. Procter, K. M. Cipolone, D. F. Stroncek, "Evaluation of the Gel System for ABO Grouping and D Typing", *Transfusion*, 2001, **39**: 300–305.
- [106] Y. Lapierre, D. Rigal, J. Adam, D. Josef, F. Meyer, S. Greber, C. Drot C, "The gel test: a new way to detect red cell antigen-antibody reactions", *Transfusion*, 1990, **30**: 109–113.
- [107] D. M. Harmening, *Modern Blood Banking and Transfusion Practices*, 6th ed., Philadelphia, PA: F. A. Davis Company, 2003.
- [108] H. Moore, "Automated reading of red cell antibody identification tests by a solid phase antiglobulin technique", *Transfusion*, 1984, **24**(3): 218–221.
- [109] F. Plapp, L. Sinor, J. Rachel, M. Beck, W. Coenen, W. Bayer, "A solid phase antibody screen", *Am. J. Clin. Pathol.*, 1984, **82**(6): 719–721.
- [110] Y. Lapierre, D. Rigal, J. Adam, D. Josef, F. Meyer, S. Greber, C. Drot, "The gel test: a new way to detect red cell antigen-antibody reactions", *Transfusion*, 1990, **30**(2): 109–113.
- [111] J. D. Tissot, C. Kiener, B. Burnand, P. Schneider, "The direct antiglobulin test: Still a place for the tube technique?" *Vox sang.*, 2000, **77**(4): 223–226.
- [112] M. Crawford, F. Gottman, C. Gottman, "Microplate system for routine use in blood bank laboratories", *Transfusion*, 1970, **10**(5): 258–263.
- [113] P. Lalezari, A. Jiang, "The manual polybrene test: a simple and rapid procedure for detection of red cell antibodies", *Transfusion*, 1980, **20**(2): 206–211.
- [114] D. R. Ballerini, X. Li, W. Shen, "An inexpensive thread-based system for simple and rapid blood grouping", *Anal. Bioanal. Chem.*, 2011, **399**: 1869–1875.
- [115] M. Al-Tamimi, W. Shen, R. Zeineddine, T. Huy, G. Garnier, "Validation of paper-based assay for rapid blood typing", *Anal. Chem.*, 2012, **84**: 1661–1668.
- [116] J. Noiphung, K. Talalak, I. Hongwarittorn, N. Pupinyo, P. Thirabowonkitphithan, W. Laiwattanapaisa, "A novel paper-based assay for the

- simultaneous determination of Rh typing and forward and reverse ABO blood groups", *Biosens. Bioelectron.*, 2015, **67**:485-489.
- [117] L. Guan, J. Tian, R. Cao, M. Li, Z. Cai, W. Shen, "Barcode-like paper sensor for smartphone diagnostics: an application of blood typing", *Anal. Chem.*, 2014, **86**(22): 11362–11367.
- [118] P. Jarujamrus, J. Tian, X. Li, A. Siripinyanond, J. Shiowatanab, W. Shen, "Mechanisms of red blood cells agglutination in antibody-treated paper", *Analyst*, 2012, **137**, 2205–2210.
- [119] L. Li, J. Tian, D. Ballerini, M. Li, W. Shen, "A study of the transport and immobilization mechanisms of human red blood cells in a paper-based blood typing device using confocal microscopy", *Analyst*, 2013, **138**: 4933–4940.
- [120] L. Guan, R. Cao, J. Tian, H. McLiesh, G. Garnier, W. Shen, "A preliminary study on the stabilization of blood typing antibodies sorbed into paper", *Cellulose*, 2014, **21**:717–727.
- [121] J. Su, M. Al-Tamimi, G. Garnier, "Engineering paper as a substrate for blood typing bio-diagnostics", *Cellulose*, 2012, **19**:1749–1758.
- [122] K. Jomova, M. Valko, "Advanced in metal-induced oxidative stress and human disease", *Toxicology*, 2011, **283**(2): 65–87.
- [123] R. S. Boyd, "Heavy metal pollutants and chemical ecology: exploring new frontiers", *J. Chem. Ecol.*, 2010, **36**(1): 46–58.
- [124] N. Johri, G. Jacquillet, R. Unwin, "Heavy metal poisoning: the effects of cadmium on the kidney", *Biomaterials*, 2010, **23**(5):783–792.
- [125] C. Sicard, J. D. Brennan, "Bioactive paper: biomolecule immobilization methods and applications in environmental monitoring", *MRS Bulletin*, 2013, **38**: 331–334.
- [126] H. Wang, Y. J. Li, J. F. Wei, J. R. Xu, Y. H. Wang, G. X. Zheng, "Paper-based three-dimensional microfluidic device for monitoring of heavy metals with a camera cell phone", *Anal. Bioanal. Chem.*, 2014, **406**: 2799–2807.
- [127] Y. Sameenoi, P. Panymeesamer, N. Supalakorn, K. Koehler, O. Chailapakul, C. S. Henry, J. Volckens, "Microfluidic paper-based analytical device for aerosol oxidative activity", *Environ. Sci. Technol.*, 2013, **47**(2): 932–940.
- [128] M. M. Mentele, J. Cunningham, K. Koehler, J. Volckens, C. S. Henry, "Microfluidic paper-based analytical device for particulate metals", *Anal. Chem.*, 2012, **744**: 1–7.
- [129] P. Rattanarat, W. Dungchai, D. Cate, J. Volckens, O. Chailapakul, C. S. Henry, "Multilayer paper-based device for colorimetric and electrochemical quantification of metals", *Anal. Chem.*, 2014, **86**(7): 3555–3562.
- [130] A. Yetisen, M. Akrama, C. Lowe, "Paper-based microfluidic point-of-care diagnostic devices", *Lab Chip*, 2013, **13**: 2210–2251
- .

Chapter 2

*Low-cost buffer-free device for forward and
reverse blood typing*

This page is intentionally blank

The low-cost blood typing devices currently available allow users to conduct assays rapidly, but they are complex and require great effort to gain the results. Therefore, effectively minimizing user's efforts during an assay is one of the priorities of this research project. This chapter presents a new blood typing device that is designed to eliminate the requirement of buffer. The device has also proved to have the desirable longevity with pre-treated antibody reagents. As a result, the user simply needs to introduce a drop of blood sample into the device and the blood type can be easily determined within one minute. Both forward and reverse blood typing assays can be performed using this device. In addition, a method to quantify antibody dissolution rate on the device has been developed. With this sample-only concept, this device provides a user-friendly, equipment-free and deliverable design that requires minimum effort from users to perform blood typing assays rapidly.

This page is intentionally blank

Monash University

Declaration for Thesis Chapter 2

Declaration by candidate

In the case of Chapter 2, the nature and extent of my contribution to the work was the following:

Nature of contribution	Extent of contribution (%)
Initiation, key ideas, experimental works, analysis of results, writing up	80

The following co-authors contributed to the work. If co-authors are students at Monash University, the extent of their contribution in percentage terms must be stated:

Name	Nature of contribution	Extent of contribution (%) for student co-authors only
Junfei Tian	Experimental works, analysis of results	
Rong Cao	Assisted in experimentation	5
Liyun Guan	Assisted in experimentation	5
Wei Shen	Key ideas, paper reviewing and editing	Supervisor

The undersigned hereby certify that the above declaration correctly reflects the nature and extent of the candidate's and co-authors' contributions to this work*.

Candidate's Signature

	Date 03-03-2015
---	---------------------------

Main Supervisor's Signature

	Date 04-03-2015
--	---------------------------


*Note: Where the responsible author is not the candidate's main supervisor, the main supervisor should consult with the responsible author to agree on the respective contributions of the authors.

This page is intentionally blank

A low-cost forward and reverse blood typing device— A blood sample is all you need to perform an assay

Miaosi Li, Junfei Tian, Rong Cao, Liyun Guan and Wei Shen,*

BioPRIA, Department of Chemical Engineering,
Monash University, Clayton Campus, Vic. 3800, Australia

*Corresponding Author 

This paper has been published in *Analytical Methods*

2.1 ABSTRACT

For all user-operated blood typing devices in today's market, a buffer-activation or buffer-washing step is required. The buffer-activation step, as is employed in some commercial blood typing devices, involves dissolving the antibodies deposited in the assaying zones of the device before the introduction of a blood sample for an assay. The buffer-washing step involves washing the blood sample in the assay zone in the end of the assay for result reporting. While all these devices work well, the activation or washing step does reduce the adaptability of those devices to resource-poor areas and under emergent circumstances. In this study, we designed a new device to perform forward and reverse blood typing assays without the buffer-activation or buffer-washing. Low-cost plastic slides were patterned to form channels containing dried grouping antibodies. Blood typing assays can be performed by simply placing a few micro Litres of a blood sample into the channels and then tilting the slide. The sample flows along the channel under gravity, dissolving dried antibody and then spreading into a film, unveiling the reaction of red blood cells (RBCs) and antibodies. This device enables easy visual identification of the agglutinated and non-agglutinated RBCs in typically 1 minute. Both forward and reverse blood typing assays can be performed using this device. To optimize the device design, antibody dissolution profile, assay sensitivity, and the device longevity were investigated in this work.

2.2 KEYWORDS

Buffer-free, minimum user's efforts, blood typing, sensor longevity, antibody dissolution rate

2.3 INTRODUCTION

In today's world there is an increasing need for affordable healthcare devices which would enable many conventional diagnostic assays to be carried out from home. The home-based and patient-operated assays, if made reliable and rapid, can significantly alleviate the pressure on hospitals and pathological laboratories in developed countries [1, 2]. At the same time, these technologies also carry the hope to minimize the impact of disease outbreaks and to increase drinking water safety in impoverished areas [3-7]. This is because the centralised laboratories and hospitals taken for granted in the cities of the developed world are absent in remote and impoverished areas. In the past few years, novel diagnostic devices built on low-cost substrates such as paper, thread, and plastic and glass slides have demonstrated the possibility for such a hope to become reality [8-21]. These innovations showed the potential impact of low-cost analytical technologies on future human health and environmental care. Among those innovations, a series of blood typing diagnostics based on paper and thread platforms have been developed [19, 22-28]. The paper- and thread-based devices have significant advantages over the current laboratory- and hospital-based technologies due to their high adaptability to unsupported field conditions, user-friendliness and assaying speed.

Blood typing is a routine clinical test, but also a test of paramount importance for avoiding fatal haemolytic transfusion reactions (HTRs) during surgeries, clinical emergencies and blood transfusions. Equally important, since the world annual blood donations are around 75 million units [1], routine and rigorous sorting of blood types must to be performed in large numbers and speedily. These healthcare and clinical requirements urge the continuous development of accurate, user-friendly and low-cost blood typing technologies [29-31].

For ABO and Rh blood groups most clinical techniques are based on the visual observation of heamagglutination reactions; although advanced gene-sequencing

technology providing precise determination of blood type through DNA analysis is now available [32]. Upon the contact of RBCs with an antibody, the absence of RBC agglutination indicates that there is no hemagglutination reaction; this observation confirms that there are no corresponding antigens on the RBC surface to the grouping antibody. Conversely, if agglutination is observed, it confirms that corresponding antigens to the antibody are present on RBC surface.

Furthermore, for the ABO blood system the Landsteiner's rule applies [31], which states that, for an individual, if an antigen is present on the surface of his RBCs, the corresponding antibody will be absent from his blood plasma. Instead, the reciprocal antibody will be present in the plasma or serum. For example, an individual of blood type A has A antigen on his RBCs and antibody B in his serum. The normal blood typing assay, also known as the forward blood typing assay, uses blood grouping antibodies to identify the specific antigens on RBCs. Conversely, there is another blood typing assay which determines the antibodies in the serum by using the reagent RBCs with known antigens. This blood typing assay is known as reverse blood typing. Since a reversed blood typing assay determines the interactions between the reagent RBCs and the antibodies in a patient's serum, it also relies on observation of RBC agglutination. Details to explain the forward and reverse blood typing can be found in Figure 13 in Chapter 1. In many countries, both forward and reverse blood typing are required to confirm the patient's blood type before a blood transfusion or transplantation is allowed to proceed. The laws that determine blood types by forward and reverse blood typing are shown in Table 1.

Table 1. Blood type determination by forward and reverse blood typing methods.

<i>Reaction of antibodies with blood</i>		<i>Forward blood type</i>	<i>Reaction of reagent cells with serum</i>		<i>Reverse blood type</i>
Anti-A	Anti-B		A1 Cells	B Cells	
+	–	A	–	+	A
–	+	B	+	–	B
+	+	AB	–	–	AB
–	–	O	+	+	O

Technical designs of blood typing assays therefore focus on using a variety of different methods to differentiate the agglutinated RBCs from the non-agglutinated RBCs.

Common methods include the tube test [33], slide test [34], and column agglutination system (e.g. Gel Card) [35, 36]. These methods rely on the different sedimentation velocities of agglutinated RBC lumps and non-agglutinated RBCs in a serum suspension, or different migration rates of agglutinated RBC lumps and non-agglutinated RBCs in a gel column of uniform pore size [31]. The recently reported paper- and thread-based blood typing devices function as a size-based filtration device. Since within these devices the interactions of RBCs and antibodies occur inside the fibre networks of paper and thread, the fibre networks of paper and thread restrict the movement of agglutinated RBC lumps, but do not restrict non-agglutinated RBCs from moving with the serum phase or a carrier phase of buffer. Paper- and thread-based assays allow a short incubation of RBCs with the grouping antibody (typically 20 seconds for ABO and RhD tests), followed with a saline wash [19, 25-26]. The inability of agglutinated RBC lumps to move in a paper fibre network during saline washing makes them easily differentiated from the non-agglutinated RBCs, which can be readily washed out of the fibre network.

In order to further improve the adaptability of paper-based devices to non-laboratory condition, future designs will need to explore new concepts that can significantly reduce the effort of the user required to perform the blood typing assay. In this work we present a new concept of a blood typing device which does not require the user to apply the saline buffer for activating or washing the device in order to perform an assay. This concept relies on the dissolution of blood grouping antibodies deposited on a non-absorbing substrate by a blood sample, and the subsequent thinning of the sample into a film for blood typing result identification. In the fabrication of the device, channels are formed to guide the blood sample flow. Furthermore, we investigated two factors that affect the performance and sensitivity of the device: the thickness of the blood sample film and the antibody dissolution behaviour. A chromatographic elution method was designed to provide a semi quantitative estimation of the antibody dissolution profile from the device surface. The antibody longevity on the plastic substrate was studied for one month under ambient laboratory conditions. Apart from performing the general forward blood typing assays, we have also demonstrated the use of our new device to perform reverse blood typing. Presently, reverse blood typing can only be performed in central laboratories and hospitals. This study is the first one to demonstrate reverse

blood typing using a low-cost device. We believe that our device concept will allow forward and reverse blood typing to be combined into one user-friendly device.

2.4 EXPERIMENTAL

2.4.1 Materials

Polyester plastic slides were purchased from 3M (3M Visual Systems Division, USA). Blood samples were sourced from Red Cross Australia, Sydney. They were stored at 4°C and used within 7 days of collection. All the antibodies were purchased from ALBA Bioscience, Edinburgh, UK.

The red blood cells required for reverse blood typing, including 15% A1 cells, 15% B cells and 3% C1 cells, were obtained from CSL, Australia; they were concentrated to 45% hematocrit level (the average human whole blood) by centrifugation, stored at 4°C and used within 30 days. The 0.9% (w/v) NaCl saline solution and the phosphate-buffered saline (PBS) were prepared with AR grade NaCl (Univar) and Phosphate (Aldrich), using MilliQ water. Glycerol and Tween 20 were purchased from Aldrich. Surface treatment of the plastic slides was carried out using a plasma reactor (K1050X plasma asher (QuorumEmitech, UK)).

2.4.2 Methods

2.4.2.1 Blood typing procedure

A blood typing device for use in impoverished regions must allow for direct visual identification of test results; the device should function with a minimum effort from the user and without the need of any equipment. Following these requirements, we explored a new device design concept which provides direct and rapid visual identification of the test result, while minimizing the effort from the user to perform the test. It focuses on eliminating the saline washing step. Figure 1 describes the advantage of forming a blood sample film on an antibody treated plastic slide for blood typing assays and the device design. Figures 1a and 1c show the result of adding a drop of blood sample into a drop of antibody solution on a plastic slide. Although agglutination of RBCs by the corresponding antibodies had occurred, it could not be visually

observed. However, if the slide is tilted to allow the drop to flow under gravity and form a thin film, the user can immediately identify the agglutination of the RBCs by an antibody. Figures 1b and 1d show the flowing blood sample and the grouping antibodies on a tilted plastic slide, clearly showing agglutinated and non-agglutinated RBCs, respectively. In order to reduce the users' efforts to perform the assay, blood grouping antibodies were coated onto the plastic slide so that users are not required to administer antibodies for forward blood typing. This device design principle requires the rapid dissolution of a sufficient quantity of grouping antibodies by the blood sample; therefore the antibody dissolution profile must be verified experimentally.

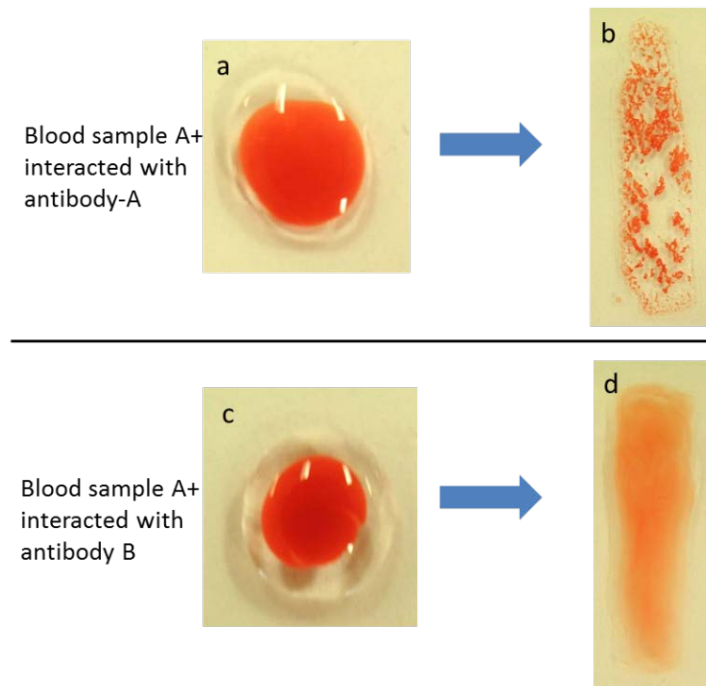


Figure 1. Demonstration of a blood typing assay of an A+ blood sample on a plastic slide substrate by: (a) placing a drop of blood sample on a drop of anti-A; (b) tilting the substrate to allow the blood sample and anti-A solution to spread into a film, immediately revealing the positive assay result; (c) a drop of A+ blood sample placed on a drop of anti-B; (d) tilting the substrate to reveal the negative assay result.

Plastic slides were first treated with plasma at an intensity of 50 W for 1 minute; a water-resistant pen was then used to draw the boundaries to demarcate the sample flow channels. Three micro Litres of antibodies (anti-A, anti-B and anti-D) were dropped respectively on top of the three channels designated to these antibodies, and slide was tilted to allow antibodies to flow through the channel under gravity. After the antibodies covered the entire length of the channels and were completely dried, 3 μ L of blood sample was dropped from the top of each channel, following the same procedure.

Typically, it takes up to 1 minute for the blood sample to flow through the entire channel. Antibody-specific agglutination of RBCs can be identified immediately as the blood sample flows through the channels treated with antibodies and forms films. A schematic protocol of the test is shown in Figure 2.

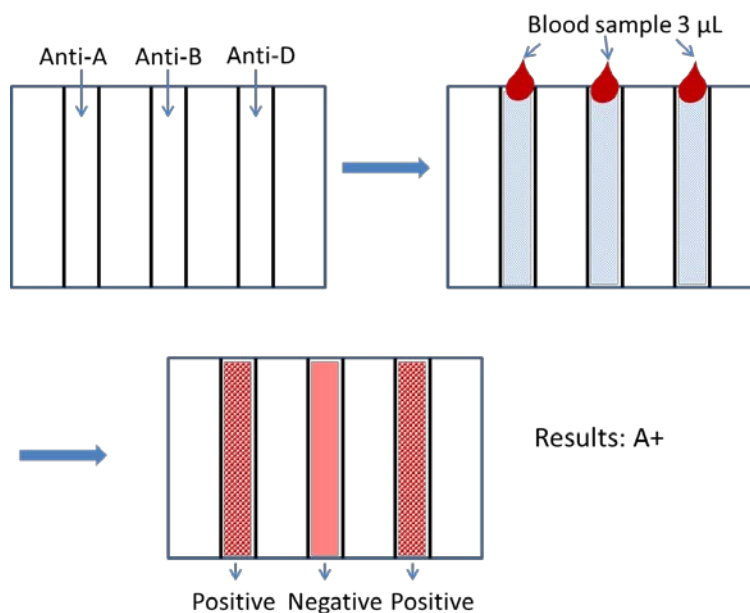


Figure 2. The designed procedure for blood typing on a plastic slide.

2.4.2.2 Quantification of antibody dissolution rates from plastic slides

Since the working principle of the plastic slide device relies on the rapid dissolution of the antibodies deposited on the slide, it is necessary to characterize the dissolution rates of all three antibodies employed for the device design. To do this, PBS buffer was used to perform a controlled dissolution study of all antibodies from the plastic slide surface. Figure 3 shows the experimental procedure: Channels on a plastic substrate were pre-treated with antibody and allowed to dry under ambient condition. A 10 μL PBS was used to flow through each channel to dissolve the antibody; the contact time was controlled at 30 s. The flow-through PBS solutions containing the dissolved antibodies were collected using Kleenex paper towel; the solutions wetted the paper towel and formed circular wetting zones as shown in Figure 3.

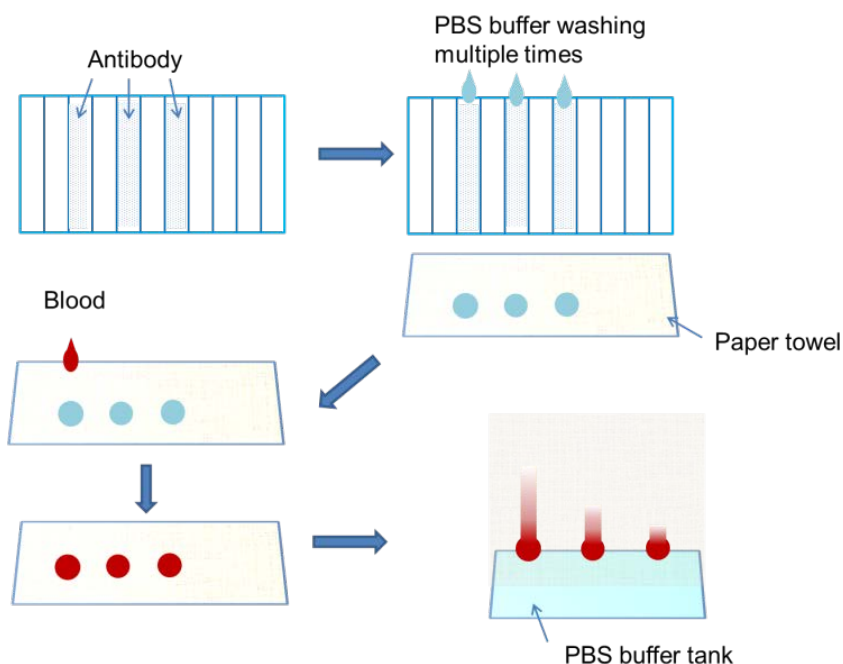


Figure 3. Schematics of the procedure for studying the antibody dissolution behaviour from the plastic slide. This procedure involves an antibody dissolution step by PBS, followed by quantifying the concentration of the antibodies washed off the plastic slide.

In order to quantify the dissolved antibodies, antibody concentrations of the collected PBS washing solution were analysed. We designed the quantification step as follows: A blood sample carrying the corresponding antigen to an antibody was introduced into the zone of the collected PBS washing solution on paper towel. After 30 seconds of incubation time under ambient condition, the paper was immersed into a chromatography tank containing PBS for elution (Figure 3), following the method we reported previously [24]. If the antibody concentration is high enough, the RBCs of the blood sample will agglutinate, forming a blood stain with a strong colour which cannot be eluted away by BPSPBS. The elution pattern was scanned into a computer and then converted to a monocolour mode (Grey scale mode) with the ImageJ software. The optical density of the grey scale image of the blood spot was determined using the software. The gray scale is digitized into 256 steps, which represent different tones from dark to bright in ascending manner, with 0 being the darkest and 255 being the brightest tone. The optical density of the blood spot therefore provides a simple and semi-quantitative method for determining the antibody dissolution behaviour. An antibody dilution standard calibration curve can be established by determining the optical densities of agglutinated blood spots by a series of step dilutions of an antibody.

2.5 RESULTS AND DISCUSSION

2.5.1 Blood typing results

There are in total eight different blood types in the ABO and RhD blood groups; all of them can be clearly identified by the plastic slide method (Figure 4). After a blood sample was introduced into the channels, it takes typically up to 1 minute for the 3 μ L of blood sample to flow through the entire length of the channel. During this process, antibody-specific agglutination of RBCs form large lumps, which become clearly identifiable when the blood sample flows halfway through the channels, making the assay time with the plastic slide shorter than 1 minute.

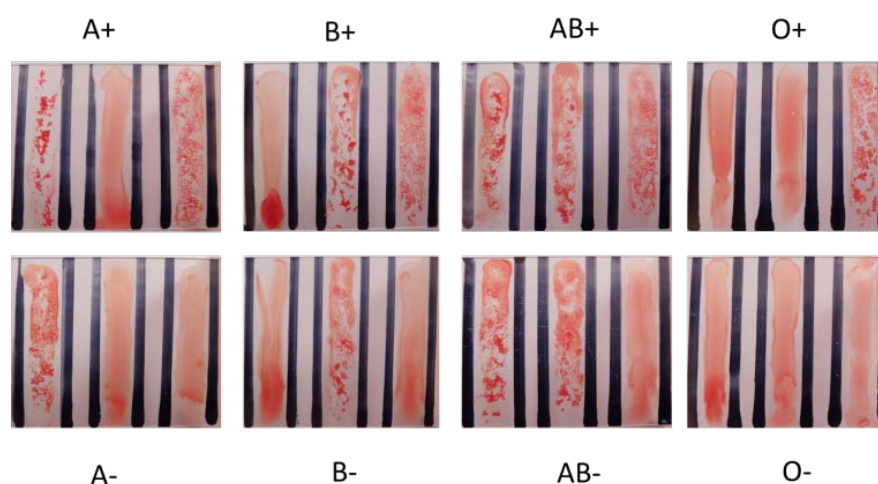


Figure 4. Assay results reported by the plastic slide device for all 8 ABO and RhD blood groups

2.5.2 Antibody dissolution from the plastic slides

Figure 5a shows the chromatographs of agglutinated type A blood sample by a serially diluted anti-A; the dilution was made from 1 (original anti-A) to 512 folds. The serial dilution data show that the anti-A retained its activity after being diluted 128 folds. Further dilution, however, weakens the antibody activity, causing weak RBC agglutination. Figure 5b presents the anti-A dilution curve of the blood spot colour density against the dilution factor. Since the concentration of the commercial antibody was unknown, the dilution factor was used as the relative antibody concentration. Figure 5c shows the result of a serial dissolution of anti-A from the plastic slide; the

anti-A standard solution was gradually diluted into a series of concentrations and dropped onto the paper towel, followed by the introducing of reagent red blood cell A onto each antibody spot. Then the chromatographic elution method was applied to the paper towel and the colour intensity of each blood spot was tested for building the standard curve of anti-A dilution behaviour, as is shown in Figures 5a and 5b. The standard curve in Figure 5b shows that a significant loss of anti-A activity to A antigen on the RBC surface by visual evaluation occurred only when it was diluted to 1/128 of its original concentration. This result suggests that the dissolving rate of anti-A is slow, and the following phenomenon provided reasoning. The standard curve in Figure 5b can be fitted to a logarithmic formula (Formula (1)) to establish the relationship of the colour density and the relative concentration of the antibody. This standard curve provides a way to quantify the antibody that was washed off the plastic substrate by the saline solution. Since the precise original antibody concentrations were unknown, we could assume that they were C_A , C_B and C_D , and measure the concentration changes caused by the saline dissolution [37]. Through measuring the colour density of each blood spot in Figure 5c, the relative concentration of anti-A released from the substrate after each saline wash can be calculated; the results are shown in Table 2. Anti-A deposited on the plastic substrate dissolved only 11.1% by the first wash, the remaining anti-A on the substrate still retained sufficient bioactivity for blood typing after another three such washes.

$$\text{Optical Density } A = 26.5 - 14.6 \times \ln(f_A - 5.42 \times 10^{-4}); f_A = \frac{C'_A}{C_A} \quad (1)$$

Where f_A is the dilution factor of anti-A; C'_A is the concentration of anti-A of each dilution.

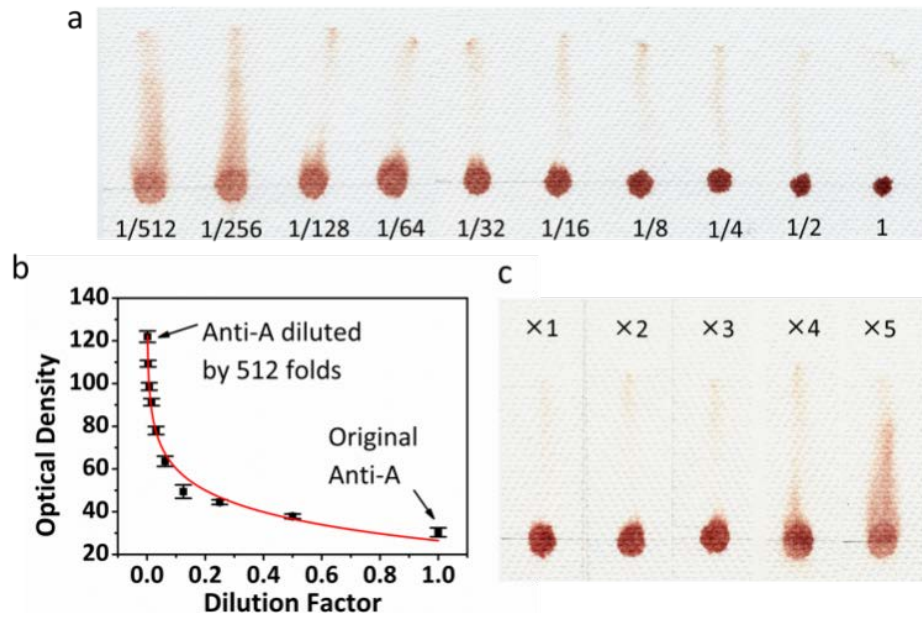


Figure 5. Antibody dissolution behaviour study for anti-A: (a) Anti-A activity as a function of a series of dissolutions with PBS; antibody activity can be determined by the reflective optical density of the agglutinated A1 reagent red cell (concentrated from the commercial reagent to a hematocrit level of 45%) on paper. (b) The calibration curve of the A1 cell optical density as a function of anti-A dilution factor; the red curve is the fitting curve of a natural logarithm function (formula 1); (c) anti-A dissolution behaviour of five consecutive PBS dissolution rinses collected from the plastic substrate.

Table 2. The blood spot optical density data and the calculated concentrations of three antibodies of each dissolution from the plastic substrate.

Antibody		Number of dissolution washes				
		x1	x2	x3	x4	x5
Anti-A	Colour density	58.7±2.3	62.0±2.8	66.3±2.4	75.8±1.8	99.6±2.6
	Relative concentration	(11.1±1.7)%C _A	(8.9±1.7)%C _A	(6.6±1.1)%C _A	(3.5±0.4)%C _A	(0.7±0.1)%C _A
Anti-B	Colour density	68.3±1.9	76.1±1.6	86.8±2.5	100.5±2.8	
	Relative concentration	(23.1±2.4)%C _B	(15.6±1.3)%C _B	(9.4±1.1)%C _B	(5.5±0.5)%C _B	
Anti-D	Colour density	82.4±1.7	110.6±3.2	143.9±2.2		
	Relative concentration	(92.0±14.3)%C _D	(9.5±1.9)%C _D	(3.2±0.1)%C _D		

Following the same procedure for quantifying anti-A, the dissolution behaviour of antibodies B and D have also been quantified. The calibration curve of anti-B dilution showed that anti-B lost its activity after a dilution of 1/16, indicating a weaker activity compared with anti-A (Figure 6a). The calibration curve was fitted with formula (2) (Figure 6b), which quantitatively showed that the concentration of anti-B in the first saline wash was 23.1% of its original concentration C_B (Table 2). The more efficient dissolution of anti-B by saline solution than of anti-A confirms that anti-B can be dissolved more easily from the plastic slide, therefore anti-B weakened more rapidly than anti-A with the number of washes by saline (Figure 6c). As shown in Figure 6c, anti-B could sustain three washes and the residual anti-B on the plastic substrate still had sufficient activities for unambiguous blood typing. However, as for anti-D, the dissolution was even more efficient (Figures 7a and 7b), our measurement showed that 92.0% of its original concentration was dissolved (Formula (3) and Table 2) and removed from the plastic substrate in the first saline wash; anti-D lost its activity at 1/8 dilution (Figure 7c).

$$\text{Optical Density } B = 41.4 - 17.2 \times \ln(f_B - 0.02); f_B = \frac{C'_B}{C_B} \quad (2)$$

$$\text{Optical Density } D = 81.1 - 10.7 \times \ln(f_D - 0.03); f_D = \frac{C'_D}{C_D} \quad (3)$$

Where f_B and f_D are the dilution factors of anti-B and anti-D; C'_B and C'_D are the concentrations of anti-B and anti-D after each dilution.

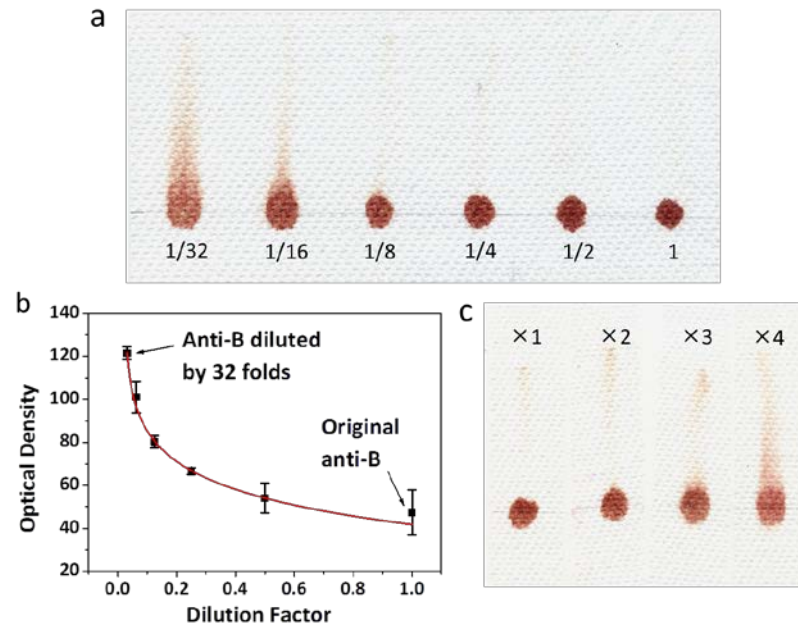


Figure 6. Antibody dissolution behaviour study for anti-B: (a) anti-B activity as a function of series of dilution, tested by the agglutination colour density of the B reagent red cell (concentrated from the commercial reagent to a hematocrit level of 45%); (b) the standard curve of the B cell colour density as a function of anti-B dilution factor; (c) anti-B dissolution behaviour of five consecutive PBS dissolution rinses of the plastic device.

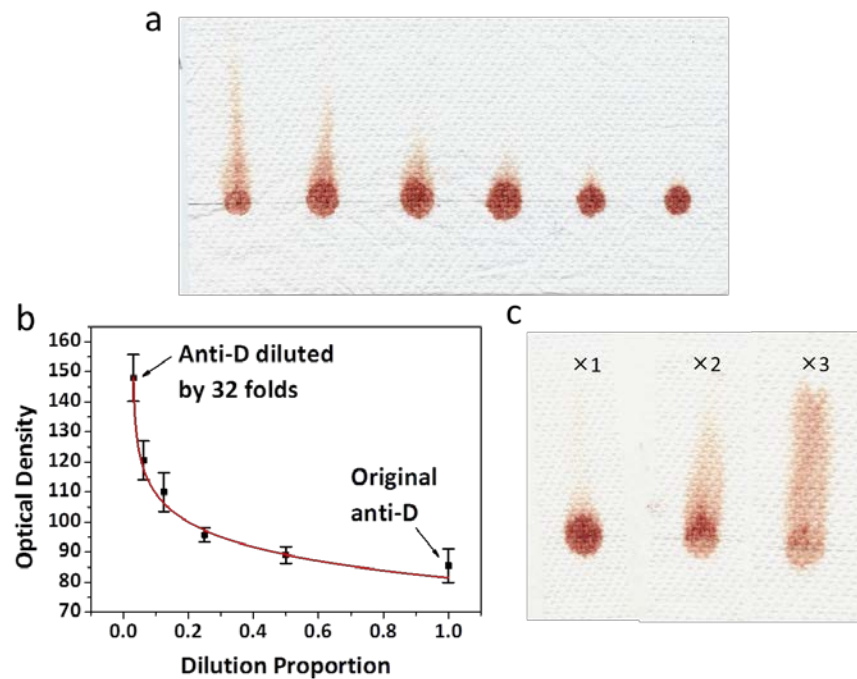


Figure 7. Antibody dissolution behaviour study for anti-D: (a) anti-D activity as a function of series of dilution, tested by the agglutination colour density of the C reagent red cell (concentrated from the commercial reagent to a hematocrit level of 45%); (b) the standard curve of the C cell colour density as a function of anti-D dilution factor; (c) anti-D dissolution behaviour of three consecutive PBS dissolution rinses of the plastic device.

anti-D dissolution behaviour of five consecutive PBS dissolution rinses of the plastic device.

According to the definition of reflective optical density used in the printing industry [40], the reflective optical density is defined as a logarithmic ratio of the reflected radiation from a printed grey tone on paper to the reflected radiation from the unprinted paper. This is usually presented in the form of logarithm based to 10 [40], but can be easily converted to the form of natural logarithm:

$$D = -\ln \frac{I}{I_0} \quad (4)$$

Where D is the reflective optical density, usually measured with a reflective densitometer in the printing industry, I and I_0 are the reflective radiation intensity from a printed grey tone and from unprinted paper, respectively. In this study grey tones generated by the agglutinated blood spot on paper loaded with different amount of antibodies, creates a similar concept for the tones to be quantified by reflective optical density.

Since blood spot optical density data (Figure 5 – Figure 7) can also be correlated with concentrations of corresponding antibody (or dilution) data by logarithm functions, it suggests that optical density data can be correlated to the concentration ratios of the dissolved antibodies. Such correlations have been experimentally given in equations (1) – (3) and are expected to provide semi-quantitative results for antibody dissolution evaluation.

2.5.3 Sensitivity

The sensitivity of any blood typing device must be investigated for typing blood samples with low concentrations of RBCs. This requirement is essential, as clinically the RBC concentration from blood samples of anaemia patients could be more than 50% lower than those from a healthy patient. Since almost all commonly used blood typing assays rely on the development of large agglutinated RBC lumps, those method can be less sensitive to samples with low RBC concentrations.

The sensitivity study of the plastic slide method was conducted by identifying the agglutination patterns of serially diluted reagent RBCs that carry known antigens. The

original RBC samples used for testing were the red cells A1, B and C1. To prepare samples with low RBC concentrations, the suspension media of the reagent red cells was first removed by centrifugation and then the red cells were diluted to haematocrit of 45% with PBS; this RBC concentration simulates the blood RBC concentration of a healthy individual. Low RBC concentration samples were prepared by diluting this sample by factors of 75%, 50% and 25% with PBS. The diluted blood samples were then used for the sensitivity tests of the device and results are shown in Figure 8. All positive tests of diluted blood samples A, B and D can still be clearly identified via RBC agglutination, even though they were diluted to 25%. These results confirm that the plastic slide blood typing device is able to deliver the equivalent sensitivity of a high performance blood typing device. The film forming process of the blood sample provides a simple way to enhance the sensitivity of blood typing using the plastic slide method.

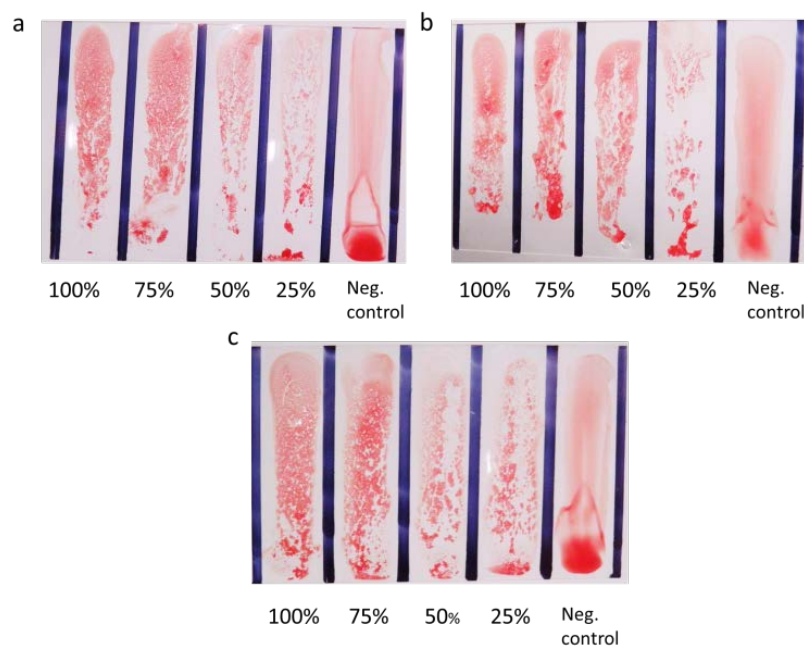


Figure 8. Sensitivity tests of the plastic slide method by dilution of reagent red blood cell carrying known antigens: (a) A1 cells in the anti-A treated channel; (b) B cells in the anti-B treated channel; (c) C1 cell in the anti-D treated channel. The negative control channel was treated with BSA only.

2.5.4 Antibody longevity on the plastic slide

It was found that the original antibodies gradually lost their activity within 10 days of being deposited on plastic slides and allowed to dry. This is because the dried

antibodies dehydrated after long exposure to air. As a result, the surface of the channel became more hydrophobic (contact angle reached to 85 °C) and this significantly reduces the speed of blood flow in the channel. Figure 9 shows the hydrophobic development of the slide surface with time. To solve this problem, glycerol and Tween 20 were chosen as additives to prevent antibody dehydration and to increase the channel surface wettability. Glycerol has been used as a traditional additive for protecting biomolecules from denaturing [38]. Its high humectant effect attracts water molecules and prevents biomolecules from dehydration; such a protective effect is most likely related to the presence of 3 hydroxyl groups in the glycerol molecule and its small molecular size. Apart from attracting water molecules, glycerol may also provide direct hydrogen-bonding, like many sugar molecules, to stabilize the biomolecule [39]. The addition of Tween 20 as a biologically compatible surfactant is intended to enhance the wettability of the deposited antibody layer on the plastic slide after ageing. Additives with a series of different proportions of glycerol and Tween 20 were mixed with the antibodies to form solutions to treat the channels of the device; the wettability of the channels was tested at different storage times by measurement of the flow length of blood samples in the channels in 30 seconds; results are presented in Table 3. Our results show that antibody solutions containing 20% glycerol, or 10% Glycerol and 0.1% Tween 20 enhanced the channel wettability; testing after 30 days of storage showed that the device's wettability was unchanged and all antibodies still retained their activity. We chose the 10% Glycerol and 0.1% Tween 20 as the preferred additive formulation to perform further experiment. Figure 10 shows the blood test results obtained after 45 days of storage under ambient temperature and open to air; all the antibodies were still active and gave accurate blood typing within 30 seconds (Figure 10).

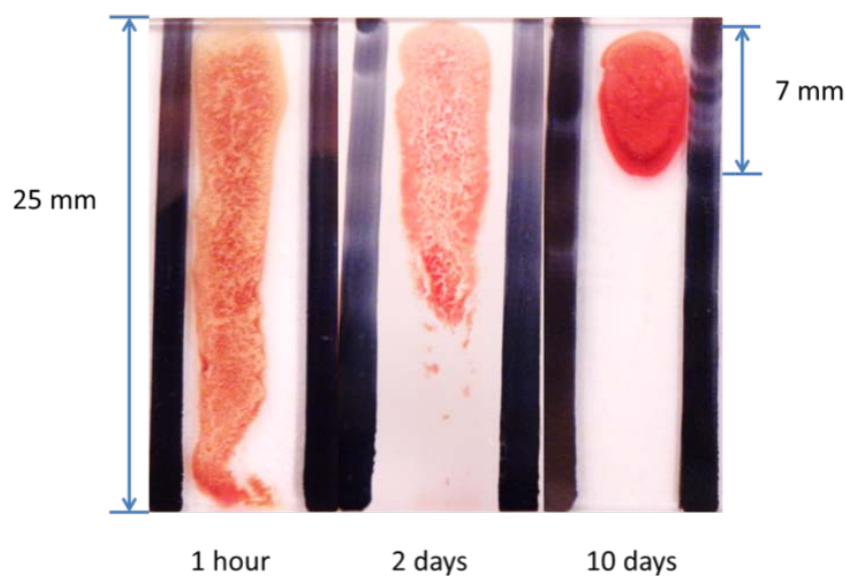


Figure 9. Lifetime detection for blood group A interaction with anti-A treated device staying for different periods.

Table 3. Additives effect on the surface hydrophilicity for blood flowing with the increase of time

<i>Additives</i>	<i>Blood sample flow distance (mm)</i>			
	<i>1 hour</i>	<i>2 days</i>	<i>10 days</i>	<i>30 days</i>
Pure antibody	21	13	8	4
Tween 20 (0.1%)	25	14	3	3
Tween 20 (0.5%)	25	12	3	3
Tween 20 (1%)	20	8	3	3
Glycerol (1%)	25	15	8	4
Glycerol (5%)	25	17	12	6
Glycerol (10%)	25	25	22	20
Glycerol (10%) + Tween 20 (0.1%)	25	25	25	25
Glycerol (20%)	25	25	25	25

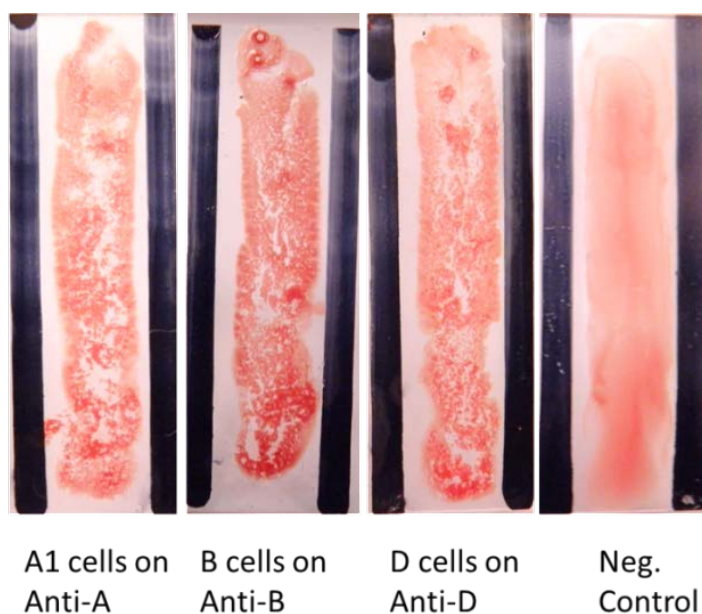


Figure 10. Antibody activity for its corresponding antigen after being deposited for 45 days on the device surface coated with an additive mixture of 10% of glycerol and 0.1% of Tween 20. Test was conducted under an ambient laboratory condition.

2.5.5 Reverse blood typing using the plastic slide assay

The reverse blood typing assays were also performed using the plastic slide method. Patients' blood serum was first separated from the whole blood sample, which can be prepared by the traditional centrifugation or the new low-cost POC methods on membrane [41, 42] or paper [43]. Then the serum samples were dropped into the channels on the plastic slide and allowed to spread throughout the channel. Reagent red blood cells A and B were then pipetted into separate serum-coated channels. By allowing the reagent RBCs to spread in the channel and form a film, the agglutination RBCs can be clearly identified by the naked eye without any aid (Figure 11).

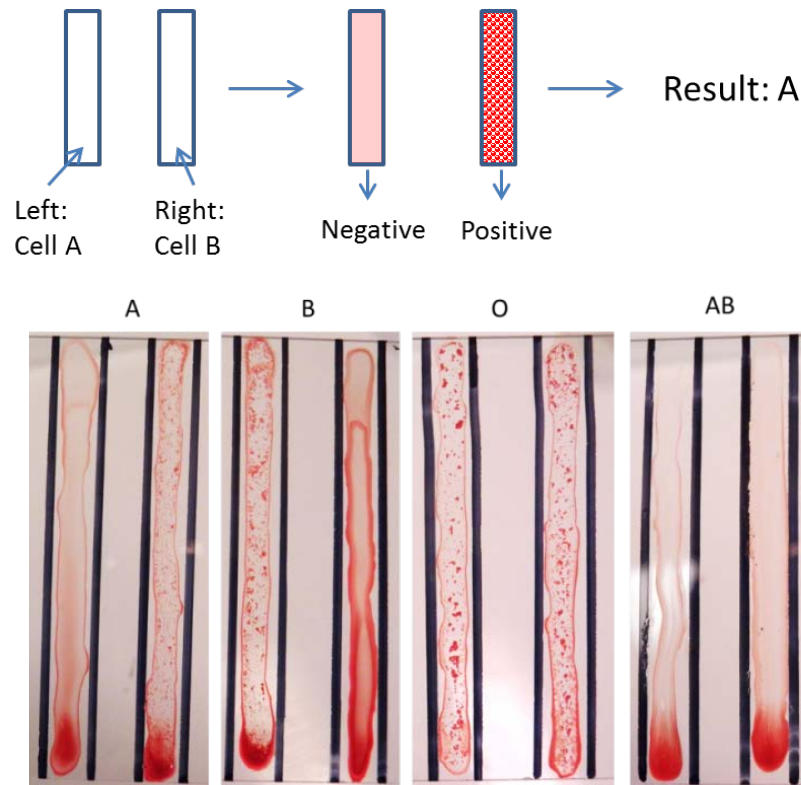


Figure 11. The reverse blood typing results for identifying ABO blood groups.

2.5.6 Proposed mechanism of RBC agglutination on the plastic slide

The use of film formation as a sensitive method for blood typing takes advantage of the following two processes: Firstly, the spreading of blood sample over the antibody coated channel surface provides a large contact area between the blood sample and antibody. The large contact area promotes interactions between the RBCs in the blood sample and the antibodies on the plastic slide; agglutination of RBCs by their corresponding antibodies can therefore form quickly. Secondly, the relatively slow spreading of blood samples in an antibody treated channel is likely to give sufficient time for blood sample and antibody to interact and incubate. This, combined with the small thickness of the blood sample film, tends to lead to the formation of sheet-like agglutination lumps, which are very easy to visually identify. The plastic slide device thus offers a sensitive means for rapidly performing both forward and reverse blood typing assays.

2.6 CONCLUSIONS

In this work we designed and demonstrated a new user-friendly blood typing device. The device was fabricated by patterning the plastic slide with channels treated with different blood grouping antibodies; this design requires the user to simply introduce the blood sample into the channels to complete the blood typing assay, without the need of buffer washing or stirring operations. This device functions by letting the blood sample spread under gravity over a surface treated with blood grouping antibodies. The agglutinated RBC lumps can be rapidly and clearly differentiated from the non-agglutinated RBCs, providing unambiguous visual identification of the positive and negative blood typing assays. This method provides a user-friendly design concept that requires minimum effort from the user to perform an assay to determine the blood type of a patient within 1 minute.

The film-forming principle of this method provides a high level of sensitivity to identify blood types of samples with low RBC concentrations. Preliminary investigation of the longevity of the device was also conducted; a mixture of glycerol and Tween 20 was chosen as an effective additive mixture to maintain the bioactivity of the antibodies on the device for the testing period of 30 days.

2.7 ACKNOWLEDGEMENTS

This work is supported by the Australian Research Council (ARC). Funding received from ARC through grant numbers DP1094179 and LP110200973 is gratefully acknowledged. The authors thank Haemokinesis for its support through ARC Linkage Project, and Mr Hansen Shen for proof-reading the manuscript. Ms. Miaosi Li also thanks the Monash University Research and Graduate School and the Faculty of Engineering for postgraduate research scholarships.

2.8 REFERENCES

- [1] R. H. Müller, D. L. Clegg, *Anal. Chem.*, 1949, **21**: 1123-1125.
- [2] A. W. Martinez, S. T. Phillips, M. J. Buttle, G. M. Whitesides, *Angew. Chem. Int. Ed.*, 2007, **46**: 1318-1320.
- [3] S. M. Z. Hossain, J.D. Brennan, *Analytical Chemistry*, 2011, **83**: 8772-8778.
- [4] S. M. Z. Hossain, C. Ozimok, C. Sicard, S. D. Aguirre, M. Ali, Y. Li, J. D. Brennan, *Analytical and Bioanalytical Chemistry*, 2012, **403**: 1567-1576.
- [5] H. Wang, Y. J. Li, J. F. Wei, J. R. Xu, Y. H. Wang, G. X. Zheng, *Anal. Bioanal. Chem.*, 2014, **406**: 2799-2807.
- [6] P. Rattanarat, W. Dungchai, D. Cate, J. Volckens, O. Chailapakul, C. S. Henry, *Anal. Chem.*, 2014, **86**: 3555-3562.
- [7] S. M. Z. Hossain, R. E. Luckham, M. J. McFadden, J. D. Brennan, *Anal. Chem.*, 2009, **81**: 9055-9064.
- [8] X. Li, J. Tian, G. Garnier, W. Shen, *Colloids Surf. B: Biointerfaces*, 2010, **76**: 564-570.
- [9] X. Li, J. Tian, W. Shen, *Anal. Bioanal. Chem.*, 2010, **396**: 495-501.
- [10] J. L. Delaney, C.F. Hogan, J. Tian, W. Shen, *Anal. Chem.*, 2011, **83**: 1300-1306.
- [11] X. Li, J. Tian, W. Shen, *Cellulose*, 2010, **17**: 649-659.
- [12] R. Pelton, *TrAC Trends in Anal. Chem.*, 2009, **28**: 925-942.
- [13] S. J. Vella, P. Beattie, R. Cademartiri, A. Laromaine, A. W. Martinez, S. T. Phillips, K. A. Mirica, G. M. Whitesides, *Anal. Chem.*, 2012, **84**: 2883-2891.
- [14] D. Mabey, R. Peeling, A. Ustianowski, M. Perkins, *Nat. Rev. Microbiol.*, 2004, **2**: 231-240.
- [15] X. Li, J. Tian, T. Nguyen, W. Shen, *Anal. Chem.*, 2008, **80**: 9131-9134.
- [16] X. Li, J. Tian, W. Shen, *Lab Chip*, 2011, **11**: 2869-2875.
- [17] J. Tian, D. Kannangara, X. Li, W. Shen, *Lab Chip*, 2010, **10**: 2258-2264.
- [18] A. W. Martinez, S. T. Phillips, E. Carrilho, S. Thomas, H. Sindi, G. M. Whitesides, *Anal. Chem.*, 2008, **80**: 3699-3707.
- [19] D. Ballerini, X. Li, W. Shen, *Anal. Bioanal. Chem.*, 2011, **399**: 1869-1875.
- [20] A. Nilghaz, D. Ballerini, W. Shen, *Biomicrofluidics*, 2013, **7**: 1-13.
- [21] A. Nilghaz, D. Ballerini, X. Fang, W. Shen, *Sensors and Actuators B: Chemical*, 2014, **191**: 586-594.
- [22] L. Li, J. Tian, D. Ballerini, M. Li, W. Shen, *Colloids and Surfaces B: Biointerfaces*, 2013, **106**: 176-180.
- [23] M. S. Khan, G. Thouas, W. Shen, G. Whyte, G. Garnier, *Anal. Chem.*, 2010, **82**: 4158-4164.
- [24] M. Al-Tamimi, W. Shen, R. Zeineddine, H. Tran, G. Garnier, *Anal. Chem.*, 2011, **84**: 1661-1668.
- [25] M. Li, J. Tian, M. Al-Tamimi, W. Shen, *Angew. Chem. Int. Ed.*, 2012, **51**: 5497-5501.
- [26] L. Li, J. Tian, D. Ballerini, M. Li, W. Shen, *Analyst*, 2013, **138**: 4933-4940.
- [27] T. Songjaroen, W. Dungchai, O. Chailapakul, C. S. Henry, W. Laiwattanapaisal, *Lab Chip*, 2012, **12**: 3392-3398.
- [28] M. Li, W. L. Then, L. Li, W. Shen, *Anal. Bioanal. Chem.*, 2014, **406**: 669-677.
- [29] G. Daniels, M. E. Reid, *Transfusion*, 2010, **50**: 281-289.
- [30] N. D. Avent, M. E. Reid, *Blood*, 2000, **95**: 375-387.
- [31] G. Daniels, I. Bromilow, *Essential Guide to Blood Groups*, Wiley-Blackwell: Hoboken, 2007.

- [32] W. Malomgré, B. Neumeister, *Anal. Bioanal. Chem.*, 2009, **393**: 1443-1451.
- [33] B. H. Estridge, A. P. Reynolds and N. J. Walters, Basic medical laboratory techniques, Delmar Cengage Learning, Albany: USA, 2000.
- [34] D. Pramanik, Principles of physiology, 3rd ed., Academic: Kolkata, 2010.
- [35] J. H. Spindler, K. H. Ter, M. Kerowgan, *Transfusion*, 2001, **41**: 627-632.
- [36] M. M. Langston, J. L. Procter, K. M. Cipolone, D. F. Stroncek, *Transfusion*, 2001, **39**: 300-305.
- [37] P. Jarujamrus, J. Tian, X. Li, A. Siripinyanond, J. Shiowatana, W. Shen, *Analyst*, 2012, **137**: 2205-2210.
- [38] I. M. Klotz, G. P. Royer and I. S. Scarpa, Proceedings of the National Academy of Sciences of the United States of America, 1970, **68**: 263-264
- [39] C. Manta, N. Ferraz, L. Betancor, G. Antunes, F. Batista-Viera, J. Carlsson, K. Caldwell, *Enzyme and Microbial Technology*, 2003, **33**: 890-898.
- [40] H. Kipphan, Handbook of printing media, Springer-Verlag, Berlin, 2001: 100.
- [41] X. Yang, O. Forouzan, T. P. Brown, S. S. Shevkoplyas, *Lab Chip*, 2012, **12**: 274-280.
- [42] C. Liu, M. Mauk, R. Gross, F. D. Bushman, P. H. Edelstein, R. G. Collman, H. H. Bau1, *Anal. Chem.*, 2013, **85**: 10463-10470.
- [43] T. Songjaroen, W. Dungchai, O. Chailapakul, C. S. Henry, W. Laiwattanapaisal, *Lab Chip*, 2012, **12**: 3392-3339

Chapter 3

*Paper-Based Blood Typing Device that Reports
Patient's Blood Type “in Writing”*

This page is intentionally blank

In the last chapter, an effective solution to minimize users' efforts while they are handling the blood typing device was presented. However, communication of assay results given by a diagnostic device to its users is another common issue in current blood typing devices. This issue will be mainly discussed in this chapter. This work presents a novel concept of result reporting by a paper-based device to the user. At present, in most cases, users can only observe the colorimetric or electrochemical signals from the device, and in order to obtain the final result, they need to interpret all these signals based on their knowledge and experience. For most untrained and non-professional users, this is an impossible mission to accomplish without assistance from professionals. The research reported in this chapter explores a novel concept of assay result reporting – text reporting. This mechanism delivers the assay results in text messages that can be readily understood by the users. Text reporting is a non-conventional concept; it is a platform concept that has potential implications in many other low-cost sensor designs. The blood typing device with this novel text-reporting concept presented in this chapter is currently under commercial development.

This page is intentionally blank

Monash University

Declaration for Thesis Chapter 3

Declaration by candidate

In the case of Chapter 3, the nature and extent of my contribution to the work was the following:

Nature of contribution	Extent of contribution (%)
Initiation, key ideas, experimental works, analysis of results, writing up	30

The following co-authors contributed to the work. If co-authors are students at Monash University, the extent of their contribution in percentage terms must be stated:

Name	Nature of contribution	Extent of contribution (%) for student co-authors only
Junfei Tian	Initiation, key ideas, experimental works, analysis of results, writing up	
Mohammad Al-Tamimi	Initiation, key ideas, experimental works, analysis of results, writing up	
Wei Shen *	Key ideas, reviewing and editing of the paper	Supervisor

The undersigned hereby certify that the above declaration correctly reflects the nature and extent of the candidate's and co-authors' contributions to this work*.

Candidate's Signature		Date 03-03-2015
------------------------------	---	---------------------------

Main Supervisor's Signature		Date 04-03-2015
------------------------------------	--	---------------------------


*Note: Where the responsible author is not the candidate's main supervisor, the main supervisor should consult with the responsible author to agree on the respective contributions of the authors.

This page is intentionally blank

Paper-Based Blood Typing Device that Reports Patient's Blood Type “in Writing”

*Miaosi Li, Junfei Tian, Mohammad Al-Tamimi and Wei Shen**

Australian Pulp and Paper Institute, Department of Chemical Engineering,
Monash University, Clayton Campus, Vic. 3800, Australia

*Corresponding Author 

This paper has been published in *Angewandte Chemie International Edition*

3.1 ABSTRACT

The British author, J. K. Rowling, presented a visionary idea in her novel “Harry Potter and the Chamber of Secrets” that one can interrogate a piece of paper for information and get unambiguous answers from the paper in writing. Here we report a study, following her vision, on using a low-cost bioactive paper device to perform ABO and rhesus (RhD) blood typing tests and obtain test results from the paper in writing. Paper text patterns are designed and printed to allow interactions between grouping antibodies and red blood cells. Composite text patterns consisting of the bioactive and non-bioactive sections are used to form the letters and symbols for the final display of the testing report. This paper-based blood typing device rapidly reports patient's blood type in unambiguous written text.

3.2 KEYWORDS

Text-reporting, Bioactive paper, Blood typing, Low-cost diagnostics

3.3 INTRODUCTION

The use of patterned bioactive paper as a tool for biochemical analysis has become a platform for making low-cost and user-operated devices for diagnosis [1], point of care

(POC),[1,2,3-6] pathogen and biomarker detection [1,4,5], food and drinking water quality testing [7], etc. The potential of this platform to deliver affordable, rapid, and user-friendly diagnostic sensors for disease screening, healthcare and drinking water quality evaluation to the developing countries has become increasingly clear.[1,4,8-10] Over the last five years, there has been an explosion of research in bioactive-paper-based low-cost sensor fabrication [1,3,4,11-16], electronic transmission of colorimetric assays for real-time diagnosis [6,17], as well as new diagnostic and environmental applications using low-cost sensors [6,7,18-21]. Colorimetric and electrochemical methods are the preferred analytical approaches for bioactive-paper sensors, since these methods are proven to be effective in qualitative and semi-quantitative sensing and can be easily adapted onto paper [3,6,21,22]. However, those studies also revealed certain limitations of those new concepts in their practical applications. Whilst a colorimetric or voltammetric signal can report the test results, in most situations the results need to be interpreted by trained personnel. This is particularly true if an assay has multiple outcomes and requires careful examination in order for the diagnosis to be made. Therefore, among the many challenges in low-cost diagnostics, unambiguous reporting of the test results by the sensors to the users is critical. Where sensors are used in developing regions for large-scale disease screening, even if we can fabricate sensors that are robust enough to function under an unsupported field condition, misinterpretation of the assay results may still be a significant factor that can compromise the value of low-cost diagnostics.

Are there other means by which we can design and interrogate bioactive paper sensors for diagnostic results? An inspiration can be found in the movie adapted from J.K. Rowling's novel *Harry Potter and the Chamber of Secrets* [23]; Potter interrogated Tom Riddle's Diary by writing on a page of paper in the Diary "Do you know anything about the Chamber of Secrets?"; the paper responded with a "Yes" in writing, instead of with a colour change. The artist's vision shows that non-conventional mechanisms of reporting assay results using paper-based sensors should be explored. To the authors' best knowledge, equipment-free bioactive-paper-based diagnostic devices capable of reporting multiple conditions in written text from a single test is currently not available. In this study, we present a bioactive-paper blood typing device that is capable of reporting ABO RhD blood types rapidly and in written text.

Correct typing of human blood is extremely important in blood transfusion and in events of medical emergency. The blood type of an individual is determined by the presence or absence of certain antigens on the surface of a red blood cell (RBC). In addition, antibodies existed in blood serum protect the body from incompatible and hostile antigens [24]. The vast majority of techniques for ABO and RhD typing of blood to date have been based upon the principle of haemagglutination reactions between RBCs and antibodies. The absence of agglutination indicates no haemagglutination reaction [24]. Recently low-cost bioactive paper [19] and bioactive thread [18,25] microfluidic sensors have been reported for human blood grouping applications. These devices are also based on the principle of haemagglutination reactions. Through observing the differences in wicking distances of the agglutinated red blood cells and the blood serum, an indication of haemagglutination reaction can be identified. However, paper- and thread-based technologies still require users who have the blood typing knowledge to interpret the result. In order for the blood typing devices to be more adaptable to conditions in developing countries, they must be able to report results unambiguously to users who may not have the knowledge to interpret the results based on the first principle. An easy way to bridge this application gap is to design paper-based devices that can report blood typing results to the users in written text.

3.4 EXPERIMENTAL

3.4.1 Materials, reagents and blood samples

The paper substrate employed in this study was Kleenex paper towel (Optimum, Kimberly-Clark). Kleenex paper towel is made with primarily softwood fibres; it has larger interfibre pore than filter papers. Our recent study shows that non-agglutinated RBCs can be easily washed out of a more open paper sheet such as paper towel than a dense paper sheet such as filter paper. Alkyl ketene dimer (AKD) was received from BASF. AKD is a cellulose reactive hydrophobization reagent used in papermaking industry; it has a 4-member lactone ring connected to two hydrocarbon chains of C₁₆ to C₂₀. When AKD is introduced onto cellulose fibres, its four-member lactone ring reacts with an OH group on cellulose, imparting strong hydrophobic effect to the cellulose fibre surface with its two long hydrocarbon chains. AR grade n-heptane was obtained from Aldrich; it was used to formulate an ink-jet-printable solution for patterning text

on paper by forming a strong hydrophilic-hydrophobic contrast. Blood samples were sourced from Dorevitch Pathology, Australia. They were stored at 4 °C and used within 5 days of collection. The blood types of all samples were determined by the pathological laboratory using the current mainstream blood typing technology. The blood type information was used for purpose of comparison with the results obtained in this study following the ethical protocols. Grouping antibodies, Anti-A, clone 10090; Anti-B, clone 10091 and Anti-D, clone 20093, were received from Lateral Grifols, Australia. They were used as received. A saline solution containing 0.9% (w/v) NaCl was prepared with MilliQ water and AR grade NaCl (Univar); it was used as the washing solution to remove only the non-agglutinated RBCs from the text patterns, but not the agglutinated RBCs (see sections below).

3.4.2 Methods

The text-reporting blood typing device we present here is partly based on the principle of haemagglutination reactions. Its fabrication involves the use of hydrophobic–hydrophilic contrast to form text patterns and to use these text patterns as sites for RBC and antibody interactions. The hydrophobic-hydrophilic contrast will ensure the unambiguous legibility of the text pattern of agglutinated blood to be displayed. In our design the text patterns are made hydrophilic, and antibody solutions are introduced into the corresponding text patterns (e.g. Anti-A into text pattern “A”). In a blood typing assay a blood sample is introduced to all text patterns. To clearly identify the occurrence of haemagglutination reactions inside the hydrophilic text patterns, a saline-washing step is employed. If the antibody in a text pattern is not the corresponding antibody to the antigens carried by RBCs, there will be no haemagglutination reaction; the non-agglutinated RBCs can be easily washed out of the text pattern with the saline solution. Contrary to this, if RBCs have haemagglutination reaction through the antibody-antigen interaction, agglutinated RBC lumps will form inside the fiber matrix of the paper and cannot be washed out by the saline solution.²⁶ Those text patterns occupied by the agglutinate RBC lumps therefore have unambiguous legibility with high resolution and contrast.

Table 1. Blood types that can be reported in text by specific antigen-antibody agglutination reactions before and after implementing our design solutions (See Figure. 1)

No.	Agglutination or non-agglutination observations (see text below)	Blood types determined by RBC agglutination	RBC Antigens CANNOT be expressed in text by RBC agglutination (and reasons)	RBC Antigens CANNOT be expressed in text after implementing design solution 1	States CAN be expressed in text after implementing design solutions 1 & 2
1	ABD	AB+			✓
2	$\overline{A}BD$	A+			✓
3	$\overline{A}\overline{B}D$	AB-	✗ (\overline{D})		✓
4	$\overline{A}\overline{B}\overline{D}$	A-	✗ (\overline{D})		✓
5	$\overline{A}B\overline{D}$	B+			✓
6	$\overline{A}\overline{B}\overline{D}$	O+	✗ (\overline{A} , \overline{B})	✗ (\overline{A} , \overline{B})	✓
7	$\overline{A}\overline{B}D$	B-	✗ (\overline{D})		✓
8	$\overline{A}B\overline{D}$	O-	✗ (\overline{D} , \overline{A} , \overline{B})	✗ (\overline{A} , \overline{B})	✓

In devices for ABO RhD blood typing, three antibodies (Anti-A, Anti-B, and Anti-D) are used to display blood typing results by text. The interaction of each antibody with RBCs can have two possible outcomes, that is, “Agglutination” and “No agglutination”. The total number of blood types determinable by the three antibodies will be $2^3=8$. Taking an A+ blood sample, for example, the interaction of the A+ blood sample with the three antibodies can be expressed as $\overline{A}BD$, that is, A (agglutination with antibody A occurs), \overline{B} (no agglutination with antibody B), and D (agglutination with antibody D occurs). Following this expression, all different blood types (column 3) determinable by these antibodies through the presence and absence of RBC agglutination (column 2) can be listed in Table 1.

If we use only haemagglutination reactions to design a text-reporting device for blood typing, many blood types cannot be unambiguously reported by text. This situation includes two circumstances where blood types have no haemagglutination reactions with the grouping antigens, therefore no visually perceivable text patterns can be formed to make the text report. The first circumstance involves all Rh(−) blood types; the lack of interactions of RBCs with Anti-D results in no haemagglutination reaction (i.e. \overline{D}) and therefore cannot form visually perceivable text patterns. The second circumstance involves O-type blood. Since red cells of O-type blood do not carry A and B antigens, they do not have haemagglutination reactions with either Anti-A or Anti-B (i.e. \overline{AB}). O-type blood cannot be reported in written text formed by haemagglutination

reaction only. Table 1 (column 4) lists all five blood types that are associated with these two circumstances. Further design of the devices must overcome these obstacles.

In this study we present a design of a composite text symbol that can report both D and \bar{D} unambiguously. This symbol takes the form of “+”; it consists of a permanent “−” printed using a non-bioactive water-insoluble ink and a bioactive “|” printed using Anti-D (Figure 1 a). In a blood test when a sample is introduced into “|”. If the sample carries D antigen, haemagglutination reaction will occur inside “|” and saline washing will not be able to remove the agglutinated RBCs out of pattern “|”. The composite text symbol will report “+”. On the other hand, if the sample does not carry the RhD antigen, then no haemagglutination reaction will occur. After saline washing, no agglutinated blood sample will be perceivable in “|”; the composite text symbol will report “−” (Figure 1 a). This design fulfills the requirement of using one composite pattern to unambiguously report RhD(+) and RhD(−) in text.

For O-type blood samples, we again employ another composite text symbol to report both “O” and “non-O” types of blood samples. This composite text symbol takes the form of “⊗”; it consists of a permanent letter “O” printed using water-insoluble ink and a “×” printed using an equal-volume mixture of Anti-A and Anti-B (see Figure 1b). In a blood test when a sample is introduced into “×”, the sample is mixed with Anti-A and Anti-B inside “×”. If the sample carries A-antigen or B-antigen, or both, then haemagglutination reaction will occur inside “×” and saline washing will not be able to remove the agglutinated RBCs out of the pattern. The composite text symbol will report “⊗”. On the other hand, if the sample does not carry A-antigen and B-antigen, then no haemagglutination reaction will occur inside “×”. After saline washing, the composite text symbol will report “O” (Figure 1b). This design fulfills the requirement of using one composite pattern to unambiguously report “O” and “non-O” types of blood samples in text. The three blue dots in the printed device are for positioning purpose.

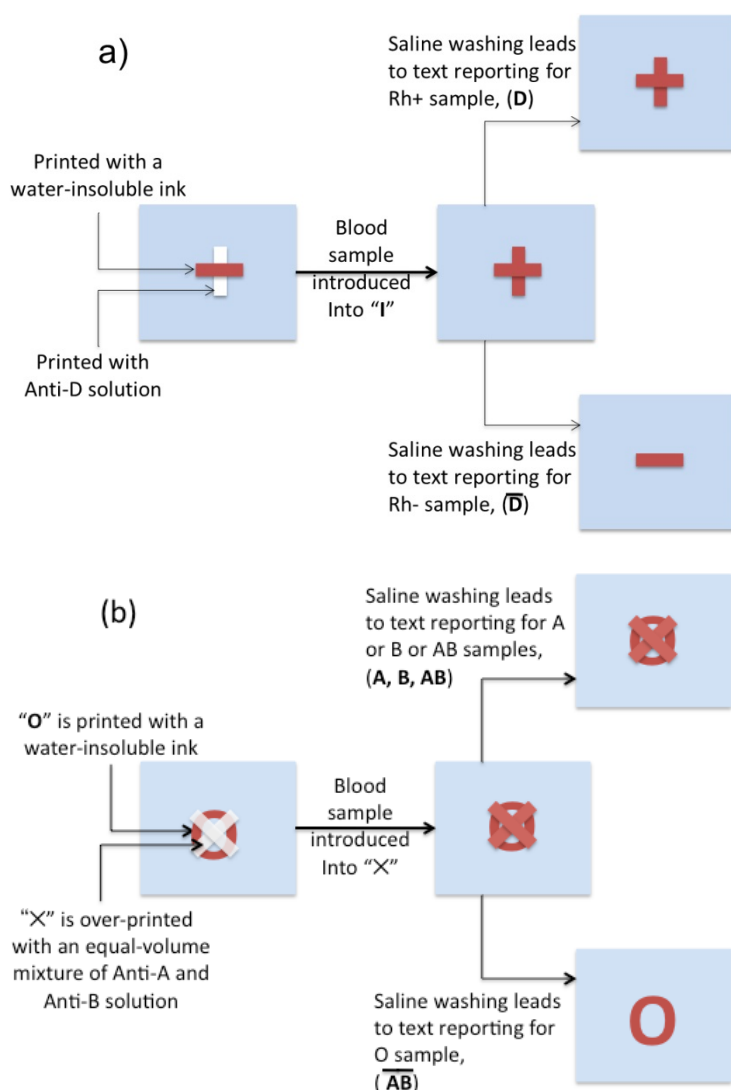


Figure 1. Schematics of the two design solutions using composite text symbols to report blood test results in text. (a) Design solution 1: The composite text symbol for reporting the presence of RhD takes the form of “+”; it consists of a permanent “-” printed using water-insoluble ink and a “I” printed using Anti-D. (b) Design solution 2: The composite text symbol for reporting “O” and “non-O” types of blood samples takes the form of “⊗”; it consists of a permanent letter “O” printed using non-bioactive water-insoluble ink and a “x” printed using an equal-volume mixture of Anti-A and Anti-B.

Negative text patterns consisting of letters “A” and “B” and two text symbols, “x” and “I” were created electronically (Figure 2). A reconstructed Canon ink jet printer (Pixma iP3600) was used to print a 2 % (w/v) heptane solution of an alkenyl ketene dimer (AKD) onto a Kleenex paper sheet followed by a heat treatment to cure the hydrophobic effect, forming the negative patterns of letters and symbols (Figure 3).

Printing of negative patterns of letters and symbols ensures that these patterns remain hydrophilic and are surrounded by hydrophobic areas.

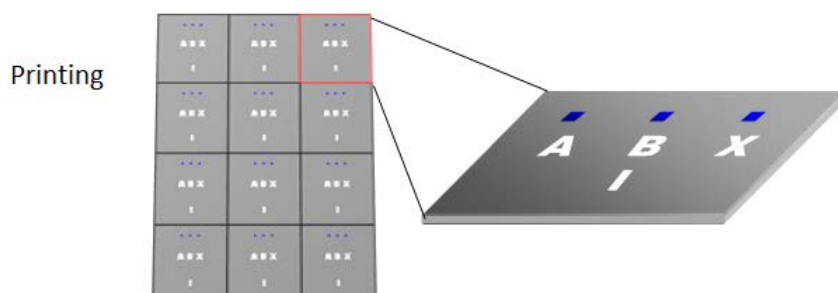


Figure 2. The designed and printing of the text-reporting paper device.

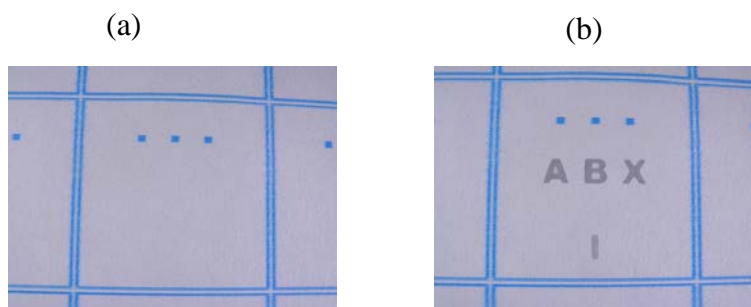


Figure 3. (a) The Kleenex paper towel hydrophobized by AKD, leaving text patterns hydrophilic. (b) The hydrophilic text patterns become visible when wetted by antibody solutions.

The hydrophilic patterns are, however, invisible. After printing of the hydrophilic patterns, 2.5 μL of Anti-A, clone 10 090; Anti-B, clone 10 091; and Anti-D, clone 20 093 were introduced into the hydrophilic patterns “A”, “B”, and “I”, respectively, by ink jet printing or writing with a pen (Figure 4a). Two and a half microlitres of an equal-volume mixture of Anti-A and Anti-B were introduced into the pattern “x” (Figure 4a). Then letter “O” was printed using a water-insoluble ink over the hydrophilic and invisible “x” symbol; symbol “—” was also printed with a water-insoluble ink over the hydrophilic and invisible “I” symbol as shown in Figure 4b. The strong hydrophilic–hydrophobic contrast ensures a high resolution of the text patterns formed by antibody solutions. After drying under ambient conditions the device is ready for use.

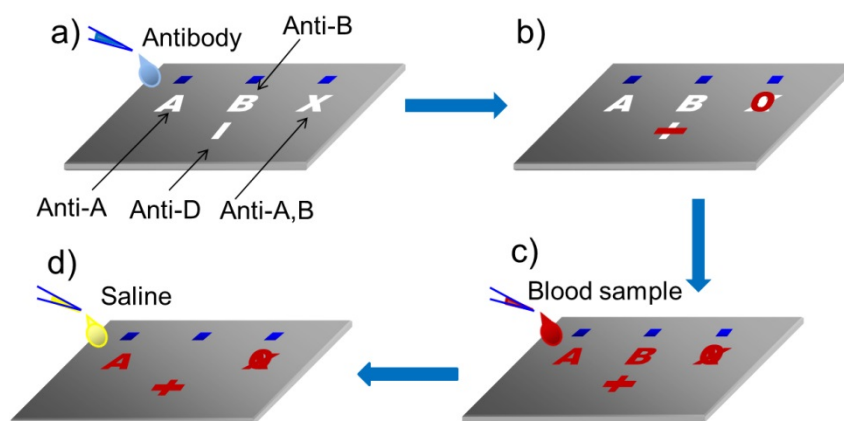


Figure 4. Fabrication and testing procedures of the text-reporting blood-typing devices. Negative patterns of letters and symbols are printed using a heptane solution of an alkenyl ketene dimer; letters and symbols remain hydrophilic and are surrounded by hydrophobic areas. (a) Anti-A and Anti-B are introduced into the corresponding letters. An equal-volume mixture of Anti-A and Anti-B is introduced into “×”, and Anti-D is introduced into “|”. (b) Letter “O” and symbol “−” are printed over “×” and “−”, respectively, using a non-bioactive and water-insoluble ink. (c) A blood sample is introduced in the device for blood typing test. (d) After washing each pattern with $2 \times 50 \mu\text{L}$ of saline solution, the blood typing result is reported by the device in text.

In a blood typing assay, $2.5 \mu\text{L}$ of blood sample were introduced into each of the antibody-loaded patterns (i.e. A, B, ×, and |) with a micropipette (Figure 4c). Twenty seconds were allowed for the antibodies in the letter and symbol patterns to react with the antigens carried by the RBCs. After 20 seconds, two aliquots of $50 \mu\text{L}$ saline solution were introduced into each of the letter and symbol patterns. In cases where haemagglutination reactions occur in certain text or symbol patterns, the agglutinated blood sample could not be washed out of those patterns. The agglutinated RBCs formed legible text patterns that report the occurrence of the specific haemagglutination reaction. On the other hand, if the haemagglutination reaction does not occur, the non-agglutinated blood can be easily washed out of the patterns through the vertical flow, leaving no visible trace of the blood sample (Figure 4d). The legible letter and symbol patterns, in combination, form the text report of the blood type of the sample.

3.5 RESULTS AND DISCUSSION

Figure 5 shows a practical process for completing a typical typing assay of blood sample A+ followed by the procedures described in Figure 4 on the paper device.

Results of the eight ABO and RhD blood types were collected and shown in Figure 6. Figure 6a shows the expected reports for the eight blood types by the device, and Figure 3b shows a photo of the actual blood type tests of all eight blood types.

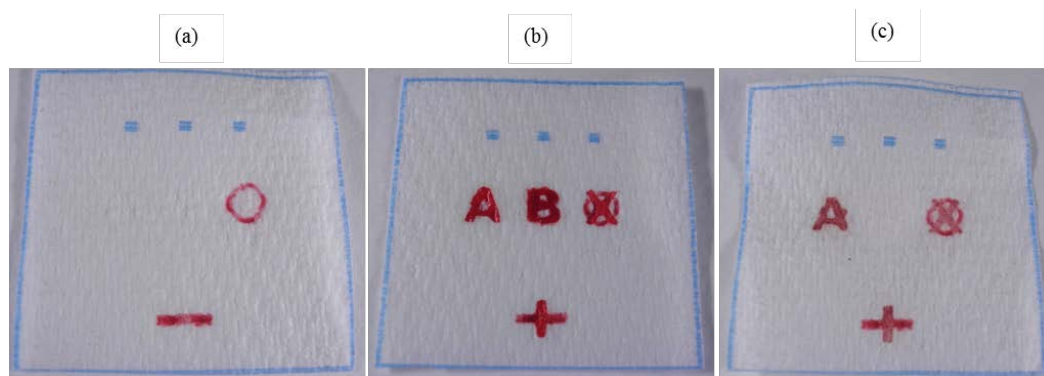


Figure 5. (a) The complete paper text-reporting device for blood typing. (b) After an A+ blood sample was introduced into all text patterns. (c) Text report of the blood typing assay result was obtained after washing the text patterns with NaCl buffer (2×50 μL).

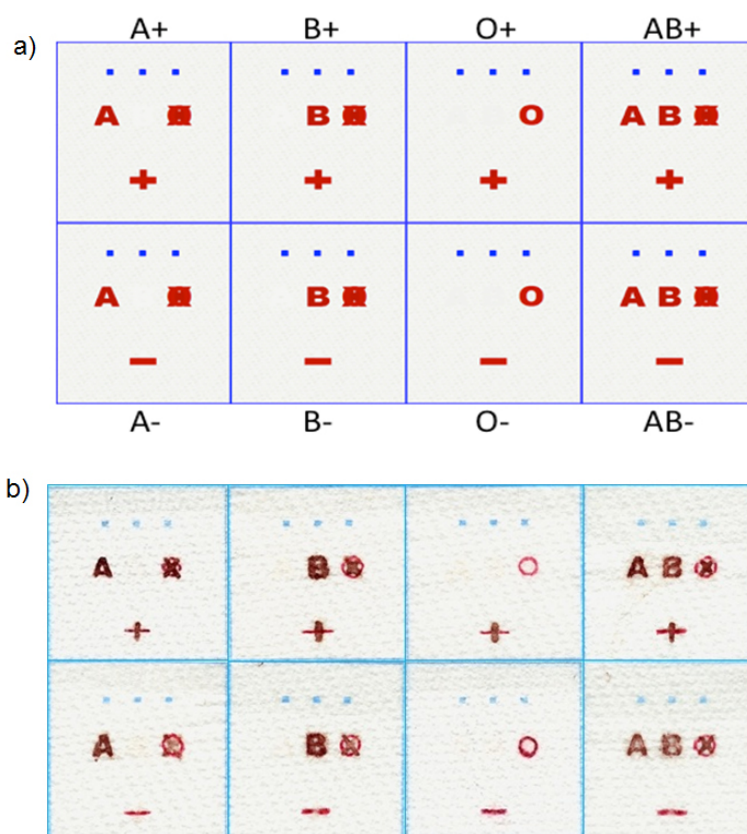


Figure 6. (a) A schematic of the expected text patterns reported by the blood type device fabricated based on our design. The corresponding blood types are given to assist the reader. (b) The actual tests of all eight ABO RhD blood types. The device size is 25 mm×25 mm.

The sensitivity of the bioactive paper text-reporting device was evaluated by testing blood samples (A+ and B+) diluted with saline solution (Figure 7). This method is used to evaluate the sensitivity of blood typing assays for samples from patients with anemia conditions; these samples have a decreased RBC colour intensity. The bioactive paper text-reporting device can confidently identify A and B antigens on RBCs after the blood samples were diluted by a factor of four and D antigens by a factor of two. This level of sensitivity is sufficient, since dilution by a factor of two is considered an adequate threshold for anemia samples.

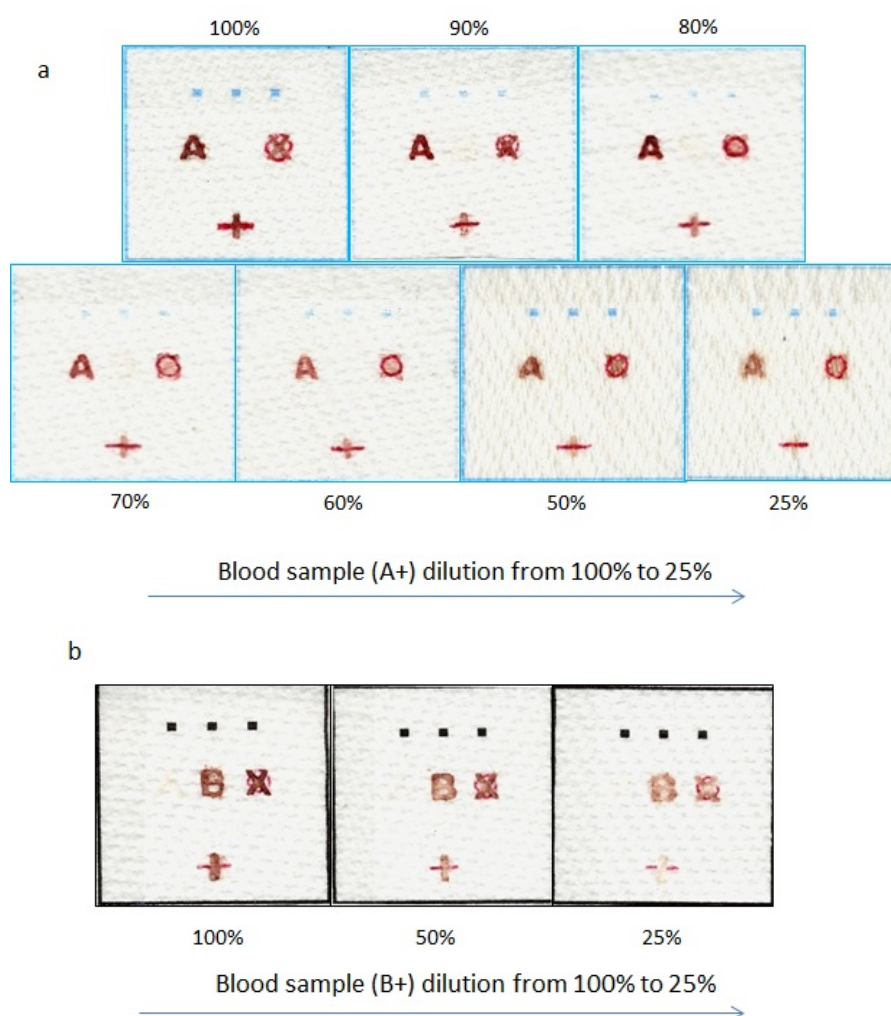


Figure 7. Blood sample dilution for the evaluation of the sensitivity of the method. Dilution was made to from 100% (i.e. undiluted) to 25% (i.e. $\frac{1}{4}$ blood sample mixed with $\frac{3}{4}$ NaCl buffer, (v/v)). (a) A+ sample; (b) B+ sample.

It is a known phenomenon that blood samples from some individuals have weak interactions with the antibodies, which may cause false negative blood typing results. This phenomenon is either related to low surface antigen concentration on RBCs or the interaction of the antigens with the antibody is weak [27]. In the present study there were two confirmed weak samples. One was a weak AB sample and the other was a weak D. Gel test showed that they were between +2 and +1 (+2 is considered as weak sample). The types of these samples were then confirmed by the pathology laboratory following the protocol using tube test. These two weak samples were tested using the text-reporting paper devices, the results obtained are unambiguous and in agreement with the tube test results, i.e. AB positive and D positive (Figure 8). The results show that text-reporting devices are sensitive enough to provide correct and unambiguous report to weak blood samples. The results are also in agreement with our recent study on the validation of using paper-based assay for blood typing that paper-based assay can detect weak blood samples, even though the antibodies in paper cannot completely agglutinate RBCs in weak samples [28].

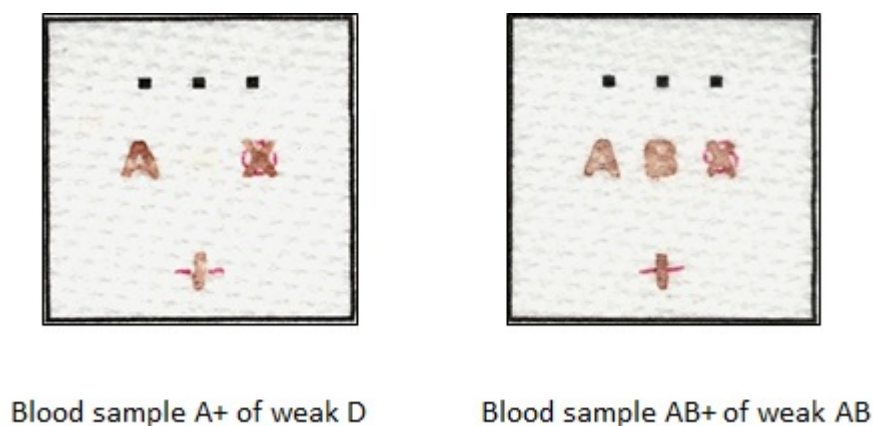


Figure 8. The test of weak blood samples using the paper-based text-reporting devices.

A total of 99 samples were tested using the text-reporting device; this sample set contained all eight blood types. All samples were also assayed in the pathological laboratory using the current mainstream blood typing technologies. It was found in our early work of the text-reporting device that a single wash with 50 μ L NaCl solution could not entirely eliminate the problem of false positive; one sample had a very weak but discernable blood stain colour. This problem has been solved by using two saline washes (i.e., 2 \times 50 μ L NaCl solution). All test results using the bioactive paper text-

reporting devices matched with the results obtained by the pathological laboratory using the gel card technology, and no false negative or false positive result has been obtained. Details of the tested samples are presented in Table 2 .

Table 2. Statistics of blood typing data obtained using paper text-reporting devices

<i>Blood Type</i>	A+	A-	B+	B-	AB+	AB-	O+	O-	Total
<i>Number of samples and their typing</i>	24	9	17	2	6	2	26	13	99
<i>Results by paper text-reporting devices</i>	24	9	17	2	6	2	26	13	99
<i>False positive</i>	0	0	0	0	0	0	0	0	0
<i>Matching with the Laboratory results (%)</i>	100	100	100	100	100	100	100	100	100

3.6 CONCLUSION

We show in this study that this bioactive paper text-reporting blood typing device meets the basic requirements of sensitivity, specificity, and text legibility. It is capable of reporting all blood types in the ABO RhD system. This reporting method significantly increases the ability of the device to report the results unambiguously to non-professional users. It is expected that an expansion of text-reporting bioactive paper sensors beyond the ABO RhD blood typing application may be possible. The concept of text-reporting using paper-based devices for low-cost diagnostic applications will be valuable for making affordable, sensitive, specific, rapid, equipment-free, and user-friendly (ASSURED) [10] devices for developing countries.

3.7 ACKNOWLEDGEMENT

This work is supported by the Australian Research Council (ARC). Funding received from ARC through DP1094179 and LP110200973 is gratefully acknowledged. Authors thank Haemokinesis for its support through ARC Linkage Project. M. L. and J. T. thank Monash University Research and Graduate School and the Faculty of Engineering for their postgraduate research scholarships. The authors would like to specially thank Dr.

E. Perkins and Dr. W. Mosse of the Department of Chemical Engineering, Monash University for proof reading the manuscript.

3.8 REFERENCES

- [1] A. W. Martinez, S. T. Phillips, M. J. Buttle, G. M. Whitesides, *Angew. Chem.Int. Ed.*, 2007, **46**: 1318-1320.
- [2] R. H. Müller, D. L. Clegg, *Anal. Chem.*, 1949, **21**: 1123-1125.
- [3] X. Li, J. Tian, W. Shen, *Cellulose*, 2010, **17**: 649-659.
- [4] X. Li, J. Tian, G. Garnier, W. Shen, *Colloids and Surf. B: Biointerfaces*, 2010, **76**: 564-570.
- [5] X. Li, J. Tian, W. Shen, *Anal. Bioanal. Chem.*, 2010, **396**: 495-501.
- [6] J. L. Delaney, C. F. Hogan, J. Tian, W. Shen, *Anal. Chem.*, 2011, **83**: 1300-1306.
- [7] S. M. Z. Hossain, R. E. Luckham, M. J. McFadden, J. D. Brennan, *Anal. Chem.*, 2009, **81**: 9055-9064.
- [8] R. Pelton, *TrAC Trends in Anal. Chem.*, 2009, **28**: 925-942.
- [9] <http://www.bioactivepaper.ca>
- [10] D. Mabey, R. Peeling, A. Ustianowski, M. Perkins, *Nat. Rev. Microbiol.*, 2004, **2**: 231-240.
- [11] X. Li, J. Tian, T. Nguyen, W. Shen, *Anal. Chem.*, 2008, **80**: 9131-9134.
- [12] X. Li, J. Tian, W. Shen, *Lab Chip*, 2011, **11**: 2869-2875.
- [13] J. Tian, D. Kannangara, X. Li, W. Shen, *Lab Chip*, 2010, **10**: 2258-2264.
- [14] K. Abe, K. Suzuki, D. Citterio, *Anal. Chem.*, 2008, **80**: 6928-6934.
- [15] E. M. Fenton, M. R. Mascarenas, G. P. Lo'pez, S. S. Sibbett, *ACS Appl. Mater. Interfaces*, 2009, **1**: 124-129.
- [16] Y. Lu, W. Shi, L. Jiang, J. Qin, B. Lin, *Electrophoresis*, 2009, **30**: 1497-1500.
- [17] A. W. Martinez, S. T. Phillips, E. Carrilho, S. Thomas, H. Sindi, G. M. Whitesides, *Anal. Chem.*, 2008, **80**: 3699-3707.
- [18] D. Ballerini, X. Li, W. Shen, *Anal. and Bioanal. Chem.*, 2011, **399**: 1869-1875.
- [19] M. S. Khan, G. Thouas, W. Shen, G. Whyte, Garnier, G. *Anal. Chem.*, 2010, **82**: 4158-4164.
- [20] V. Leung, A. Shehata, C. Filipe, R. Pelton, *Colloids and Surf. A: Physicochem. Eng. Aspects.*, 2010, **364**: 16-18.
- [21] A. Apilux, W. Dungchai, W. Siangproh, N. Praphairaksit, C. Henry, O. Chailapakul, *Anal. Chem.*, 2010, **82**: 1727-1732.
- [22] E. Carrilho, S. T. Phillips, S. J. Vella, A. W. Martinez, G. M. Whitesides, *Anal. Chem.*, 2009, **81**: 5990-5998.
- [23] J. K. Rowling, *Harry Potter and the Chamber of Secrets*, ©2002 Miracle Productions GmbH and Co. KG.
- [24] V. Joshi, A. Nandedkar, S. Mendburwar, *Anatomy and physiology for nursing and health care*, 2006, BI Publications Pvt. Ltd.
- [25] D. Ballerini, X. Li, W. Shen, *Anal. and Bioanal. Chem.*, 2011, **399**: 1869-1875.
- [26] X. Li, J. Tian, W. Shen, *ACS Appl. Mater. Interfaces.*, 2010, **2**: 1-6.
- [27] G. Daniels, I. Bromilow, *Essential Guide to Blood Groups*, 2nd ed., Wiley-Blackwell: Chichester, West Sussex, U.K., 2010.
- [28] M. Al-Tamimi, W. Shen, R. Zeineddine, H. Tran, G. Garnier, *Anal. Chem.*, 2012, **84**: 1661 – 1668.

Chapter 4

*Paper-based device for rapid typing of secondary
blood groups*

This page is intentionally blank

In the previous two chapters, effective solutions were provided for designing ABO and RhD blood group typing devices. Many other blood groups have been found during the past century and some are clinically significant, because of the likelihood of causing haemolytic transfusion reactions and haemolytic disease of the newborn (HDN). Therefore, investigations of novel techniques of rapid and low-cost secondary blood typing diagnostics are necessary and significant.

In this chapter, paper-based devices for rapid typing of secondary blood groups are presented in two published papers. The first published paper focuses on the design of a user-friendly secondary blood typing device with the novel text-reporting concept. Due to the weaker haemagglutination reactions of secondary blood groups compared to the primary blood groups, haemagglutination patterns under different conditions for the secondary blood groups are studied for optimization of the assay conditions. In addition, the confocal microscopy method was also employed to obtain mechanistic details of RBC behaviour in the interactions with secondary group antibodies, which established a deeper understanding of secondary blood grouping. The second published paper describes another method for secondary blood typing based on paper chromatography elution. In this paper, the reaction times, reagent concentrations, and antibody structures of different blood group systems of the elution methods were compared with those of the flow-through method reported in the first study.

This page is intentionally blank

Monash University

Declaration for Thesis Chapter 4.1

Declaration by candidate

In the case of Chapter 4.1, the nature and extent of my contribution to the work was the following:

Nature of contribution	Extent of contribution (%)
Initiation, key ideas, experimental works, analysis of results, writing up	70

The following co-authors contributed to the work. If co-authors are students at Monash University, the extent of their contribution in percentage terms must be stated:

Name	Nature of contribution	Extent of contribution (%) for student co-authors only
Whui Lyn Then	Paper editing	10
Lizi Li	Assisted in experimentation	10
Wei Shen *	Key ideas, paper reviewing and editing	Supervisor

The undersigned hereby certify that the above declaration correctly reflects the nature and extent of the candidate's and co-authors' contributions to this work*.

**Candidate's
Signature**

	Date 03-03-2015
--	---------------------------

**Main
Supervisor's
Signature**

	Date 04-03-2015
--	---------------------------

*Note: Where the responsible author is not the candidate's main supervisor, the main supervisor should consult with the responsible author to agree on the respective contributions of the authors.

This page is intentionally blank

4.1 Paper-based device for rapid typing of secondary human blood groups

*Miaosi Li, Whui Lyn Then, Lizi Li and Wei Shen**

Australian Pulp and Paper Institute, Department of Chemical Engineering,
Monash University, Clayton Campus, Vic. 3800, Australia

*Corresponding Author 

This paper has been published in *Analytical and Bioanalytical chemistry*

4.1.1 ABSTRACT

In this article we report the use of bioactive paper for typing secondary human blood groups. Our recent work on using bioactive paper for human blood typing has led to the discovery of a new method for identifying haemagglutination of red blood cells. The primary human blood groups, i.e. ABO and RhD groups, have been successfully typed with this method. Clinically, however, many secondary blood groups can also cause fatal blood transfusion accidents, despite the fact that the haemagglutination reactions of secondary groups are generally weaker than those of the primary groups. This paper describes the design of a user-friendly sensor for rapid typing of secondary blood groups using bioactive paper. It also presents the mechanistic insights of interactions between secondary group antibodies and red blood cells using confocal microscopy. Haemagglutination patterns under different conditions are revealed for optimization of the assay conditions.

4.1.2 KEYWORDS

Bioactive paper, blood typing, secondary blood groups, confocal microscopy, haemagglutination

4.1.3 INTRODUCTION

Blood groups were discovered at the beginning of the twentieth century, and for many years they have been considered the best human genetic markers since they carry a significant amount of information for mapping the human genome. To date, 30 blood group systems, including 328 authenticated blood groups, have been classified [1, 2]. The discovery of the ABO blood groups by Landsteiner has first made blood transfusion feasible. The later discovery of the RhD antigens has led to the understanding and subsequent prevention of haemolytic disease of the newborn (HDN) [3-5]. Although ABO and RhD groups are the most important systems in transfusion medicine, many other blood group antibodies are also capable of causing haemolytic transfusion reactions or HDN. These blood groups, known as minor or secondary blood groups, are also of great clinical and biological importance in blood transfusion and transplantation [5, 6]. Each of these blood groups contains unique sub-type antigens and has a different weight of distribution in human population [7]. Furthermore, secondary blood groups do not follow the second part of Landsteiner's law – "If an agglutinin is absent in the red cells of a blood, the corresponding agglutinin must be present in the plasma." – which is only true of the ABO groups. Whilst antibodies A and B are naturally present in human blood serum corresponding to the antigens which they lack, the Rh and secondary antibodies in serum are only generated as a result of an immunisation response triggered by transfused red blood cells (RBCs) that carry secondary antigens, or by foetal red cells leaking into the maternal circulation during pregnancy or during birth [5]. Table 1 summarizes the common secondary blood groups and their sub-type antigens. Among these blood groups, some antibodies, such as Anti-M, N, Lewis and Lutheran system antibodies, are inactive below 37 °C and are therefore not considered clinically important [5]. Others, however, are as clinically significant as primary blood groups. The mismatching of these blood groups may cause immediate and severe haemolytic transfusion reactions (HTRs) and HDN.

Table 1 List of the common secondary blood group systems

<i>Secondary Blood group systems</i>	<i>Antigens</i>
Rhesus	D*, C, c, E, e
Kell	K, k
P	P1
Kidd	Jk ^a , Jk ^b
MNS	M, N, S, s
Lewis	Le ^a , Le ^b
Lutheran	Lu ^a , Lu ^b

Accurate and rapid identification of human secondary blood groups is important for blood banking and medical procedures either under laboratory or field conditions [8]. Routine minor blood grouping methods rely primarily on the haemagglutination reactions between antigens and antibodies that are either performed manually or by automatic means [9, 17]. Currently, the commonly used method for secondary blood grouping is based on a gel card test procedure, which requires concentrated RBCs and centrifugation [9]. Owing to the fact that there are a large number of antigens in secondary blood groups, a full identification of the antigens in those groups using this procedure is expensive and requires central laboratory conditions. Other methods, such as slide techniques, although low-cost and equipment-free, are insensitive and therefore are not recommended for initial or definitive antigen determinations, particularly when dealing with neonatal samples [5]. Investigations into novel techniques of rapid and low-cost secondary blood typing diagnostics are therefore necessary and significant, especially for use in less-industrialized areas, home care, and for local and temporary blood banking in disaster response missions.

Recent research on the use of bioactive paper for human blood typing has established a new method for identifying haemagglutination of red blood cells (RBCs) [10-15], which relies on using fibre networks in paper with controlled pore sizes to filter out and retain the agglutinated RBC lumps. When a blood sample is introduced onto a piece of paper pre-treated with the corresponding grouping antibody, haemagglutination will occur, leading to the formation of agglutinated RBC lumps inside the fibre network. [16] The agglutinated lumps of RBCs are captured by the fibre network and cannot be

removed by chromatographic elution with PBS or saline solution, leaving a clearly visible bloodstain on the paper. Conversely, if a blood sample is introduced onto paper treated with non-corresponding grouping antibodies, haemagglutination will not occur and free RBCs can be easily washed out of the fibre network, leaving no discernable stain. This phenomenon forms the foundation of using paper to make low-cost, rapid and user-friendly devices for ABO and RhD blood typing assays [15].

The antigens of some secondary blood groups are found to be less antigenic than the primary blood groups [18]. Those antigens show weaker interactions with their corresponding antibodies, resulting in increased difficulty in their identification in blood grouping assays. Different antibodies (i.e. immunoglobulin G (IgG) instead of immunoglobulin M (IgM)) available to certain secondary red cell group antigens present further difficulties in blood grouping assays. Although the capabilities of IgG and IgM antibodies in the blood typing of secondary groups have been well understood, red cell responses to bonding with those antibodies are not. In this study, we investigate the secondary group antibody-RBC interactions in the fibre network of paper for the purpose of designing highly efficient paper-based secondary blood grouping devices. The confocal microscopy method we developed for paper-based blood grouping assays [16] was employed to obtain mechanistic details of RBC behaviour in the interactions with secondary group antibodies. Our results elucidate: (1) the differences of antibody-specific RBC haemagglutination caused by primary and secondary group antibodies; (2) the responses of red cells to bonding with IgG and IgM antibodies; (3) the time-dependent antibody-antigen interactions in secondary blood grouping; (4) a concept of secondary group assay result reporting using symbols. The protocols and conditions of assaying have also been established and discussed. The outcome of this work provides microscopic details for the engineering of low-cost, sensitive, specific and rapid paper-based blood grouping devices for secondary human blood groups.

4.1.4 EXPERIMENTAL

4.1.4.1 Materials and appliances

The paper substrate used in this study was Kleenex paper towel (Kimberly-Clark, Australia). Alkyl ketene dimer (AKD) as a paper hydrophobization reagent was

obtained from BASF (Wax 88 Konz). AR grade n-heptane was obtained from Sigma-Aldrich, Australia; it was used to formulate an ink-jet-printable solution for patterning text on paper through forming hydrophobic borders. Blood samples were sourced from Red Cross Australia, Sydney. They were stored at 4°C and used within 7 days of collection. All antibodies were purchased from ALBA Bioscience, Edinburgh, UK. The 0.9% (w/v) NaCl saline solution and the phosphate-buffered saline (PBS) were prepared with AR grade NaCl (Univar) and Phosphate (Sigma-Aldrich), using MilliQ water. Fluorescein isothiocyanate (FITC, isomer I, Product number: F7250, from Sigma-Aldrich) was used for labelling RBCs [16,19,20]. Anhydrous dimethyl sulphoxide (DMSO, from 95 MERCK Chemicals Ltd, Australia) was employed to dissolve the FITC. Anhydrous D-glucose was provided by AJAX Chemicals Ltd., Australia.

A reconstructed Canon ink jet printer (Pixma iP3600) was used to print the AKD-heptane solution onto a Kleenex paper sheet to form the required patterns defined by the hydrophilic-hydrophobic contrast. A series of micropipettes (Eppendorf Research[®], 2.5–50 µL) were used to transfer antibodies, blood samples, and saline solutions onto the paper device. A Nikon Ai1Rsi Confocal Microscope in the Melbourne Centre for Nanofabrication was used for obtaining the confocal micrographs. The objective lens employed for imaging was a 60× oil immersion lens.

4.1.4.2 Symbol patterning onto paper

In our previous work for ABO and RhD blood group tests [15], the fabrication of a paper-based blood grouping device involved patterning letters and symbols as hydrophilic sites for RBC and antibody interactions, surrounded by hydrophobic borders, onto paper. It was done with ink-jet printing of AKD on paper to selectively hydrophobize it. The hydrophobic-hydrophilic contrast allows unambiguous legibility of text patterns of agglutinated blood to be displayed. Following the international convention, the blood types of the ABO group are reported directly with letters, whereas Rh and other secondary groups are reported with the symbols “+” or “-” to indicate either their presence or absence in RBCs. In this work, for patterning paper for secondary blood grouping, we used “+” and “-” to indicate either the positive or

negative of an assay. The symbol consists of a vertical hydrophilic channel and an overlapping horizontal bar printed with water insoluble ink, as shown in Figure 1.

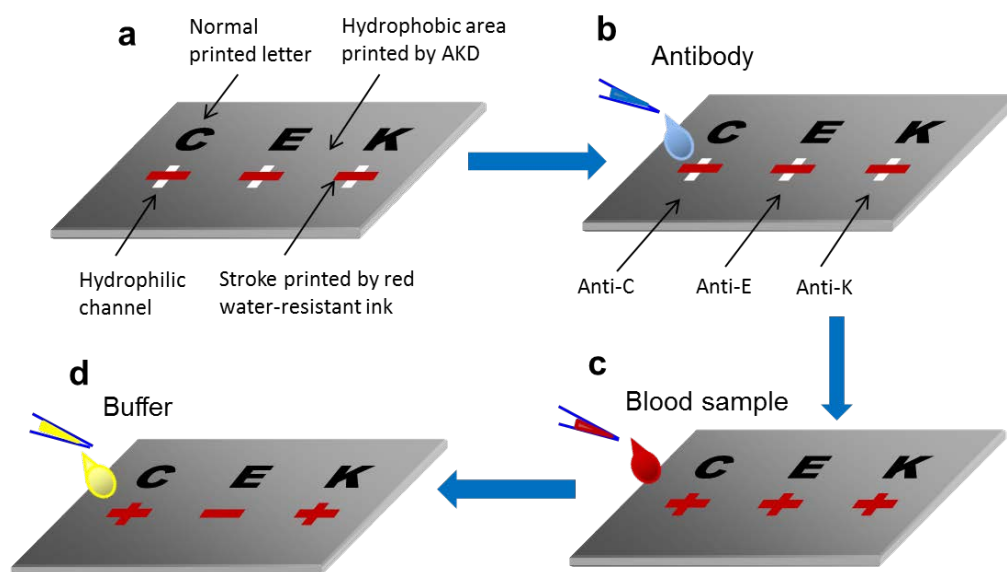


Figure 1. Schematics of design, fabrication, testing procedures and result reporting of paper diagnostics for secondary blood typing.

An assay for identifying multiple secondary blood groups was performed by introducing aliquots of 2.5 μL of the corresponding antibodies onto the vertical section of the symbols, and allowing the antibodies to dry under ambient condition. Two and half microlitres of a blood sample were then introduced onto the vertical channel of all the symbols; a pre-determined reaction time was allowed for the antibodies to interact with the RBCs. Subsequently, two 30 μL aliquots of saline solution were introduced onto the vertical section of the cross symbol to wash out the non-agglutinated RBCs. After washing, the results can be directly read from the device – “+” indicating positive and “-”, negative.

For confocal imaging, RBCs were labelled with FITC using the method reported by Li et al. [16], Hauck et al. [19] and Hudetz et al. [20]. The whole blood sample was first centrifuged at 1300g/RCF for 3 minutes to separate the RBCs from the plasma. The plasma layer was then removed and the RBCs layer was washed with the physical saline solution (PSS) once. FITC was dissolved in DMSO at a high concentration (40mg/mL), and then diluted with the Cell-Stab solution to 0.8 mg/mL. This FITC solution and a D-glucose solution in PBS were then added into the RBCs, until the

concentrations of FITC and D-glucose reached 0.5mg/mL and 0.4 mg/mL respectively. This RBC suspension was then incubated in the dark for 2 hours to allow FITC to attach onto the cell surface. After incubation, the cell suspension was washed with PSS 13 times to remove unattached FITC and then re-suspended at a hematocrit of around 35% for further use.

Kleenex paper towel was cut into 10 mm × 10 mm square pieces for use as the testing substrate. Ten microlitres of antibody solution was dropped onto paper pieces and allowed to dry, and then 6 µL of labelled RBCs was dropped onto them. A pre-set reaction time was allowed. After that, 20 µL of PSS was pipetted onto the sample and the sample was immediately placed onto a glass slide for confocal imaging.

4.1.5 RESULTS AND DISCUSSION

4.1.5.2 Secondary blood typing results

Following the testing procedure illustrated in Figure 1, a number of secondary blood groups can be assayed on a paper strip; the typical assay results of one blood sample is shown in Figure 2 by putting the assaying papers together. Gel Card tests of the same blood sample performed in the laboratory of Red Cross Australia were used to compare with the results obtained using our paper-based assays.

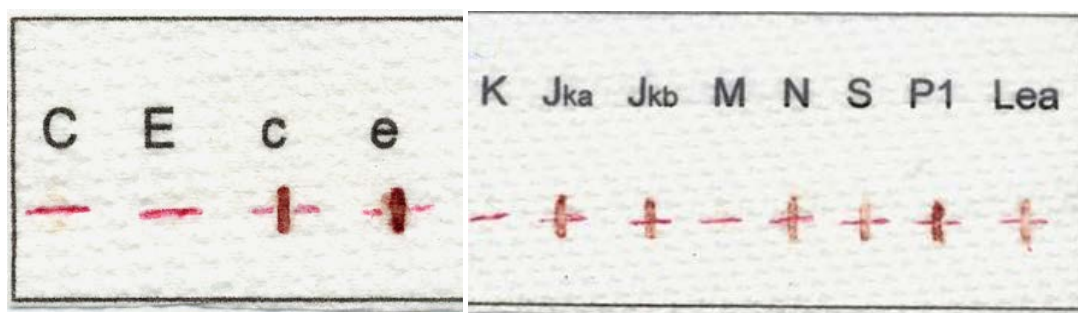


Figure 2. Paper-based blood group assay designed for identifying 11 antigens in 7 secondary blood groups. The grouping assay was performed under the same condition: reaction time was 30 seconds and the washing of free RBC was done using 0.9% NaCl PSS. Reference assays using the mainstream technology (Gel Card) showed that the secondary groups of this blood sample were: C(-), E(-), c(+), e(+), K(-),Jka(+), Jkb(+), M(+), N(+), S(+), P1(+), Lea(+).

Two observations can be made: First, with the exception of blood group M, the secondary blood grouping results reported by our paper-based assays matched with the Gel Card results. Second, like the Gel Card where the clarity of the results of secondary blood groups are less consistent than those of primary groups, on paper-based assays the colour intensity of antigen-positive red blood cells varies significantly despite all tests being conducted under the same condition. These results suggest that paper-based sensors are capable of performing assays for secondary blood grouping, and the reaction conditions of secondary group antigens and antibodies vary. To further understand the antigen-antibody interactions of secondary blood groups, and to optimize the assay conditions, we focused on the influence of the following factors on RBC agglutination: the antibody-antigen reaction time, antibody types, as well as washing conditions. Microscopic information obtained with confocal microscopy was compared with the visual assays to study the interactions of RBCs in paper.

4.1.5.2 The effect of interaction period

The bonding of ABO and RhD antigens with their corresponding antibodies normally occurs instantaneously [15], therefore haemagglutination can be visually identified within 30 seconds [16]. This reaction time, however, is not sufficient for some secondary blood group antigens as they are less antigenic. As a result, time required for secondary blood group agglutinations to be visually identifiable varies from 30 seconds to 3 minutes, depending on the antibody-antigen pair. For example, blood groups C and E have strong interactions with their corresponding antibodies within 30s, whereas blood groups c and e would show false negative results if the same interaction time of 30 s was given. It was found in our study that longer interaction times (i.e. 2-3 min) must be allowed for secondary groups to improve the clarity of their results (Figure 3). However, a prolonged reaction time can lead to false positive results, as excessive exposure of a blood sample to atmosphere causes aggregation of RBCs. Our study showed that a reaction time up to 3 min is appropriate and adequate for the unambiguous identification of the weaker haemeagglutinations.



Figure 3. Increasing degrees of haemagglutination of the second group e in antibody-treated paper as a function of time.

Confocal microscopy was used to gain a microscopic understanding of haemagglutination processes of RBCs carrying secondary group antigens. For comparison, haemagglutination of RBCs by corresponding primary and secondary group antibodies was investigated to show differences in the strength of RBC agglutination. Figure 4 shows four confocal microscopic images taken with a 60 \times oil immersion lens. RBCs carrying D(+) (primary) and E(+) (secondary) antigens showed rapid agglutination within 30 seconds after contact with their corresponding antibodies. RBCs carrying primary group D antigens interacted strongly with their corresponding antibodies, leading to strong deformation of RBCs, which formed large lumps; individual RBCs in the lump could not be identified (Figure 4a). RBCs carrying secondary group E antigen showed weaker agglutination than the D group. Although E(+) RBCs also formed lumps upon reacting with the E antibody, cell deformation was less severe than that of the D(+) RBCs (Figure 4b). The e(+)-RBCs showed even weaker agglutination; no agglutination was observable when 30 seconds of reaction time was given (Figure 4c). However, when 3 minutes of reaction time was allowed, the e(+)-RBCs clearly showed agglutination, even though the degree of agglutination was much weaker than RBCs of the D(+) and E(+) groups (Figure 4d). These results correlate with the visual assays performed on paper (Figure 3). More importantly, the confocal results confirmed the time-dependent haemagglutination reaction of some secondary blood groups. Table 2 summaries the reaction time required by different secondary groups.

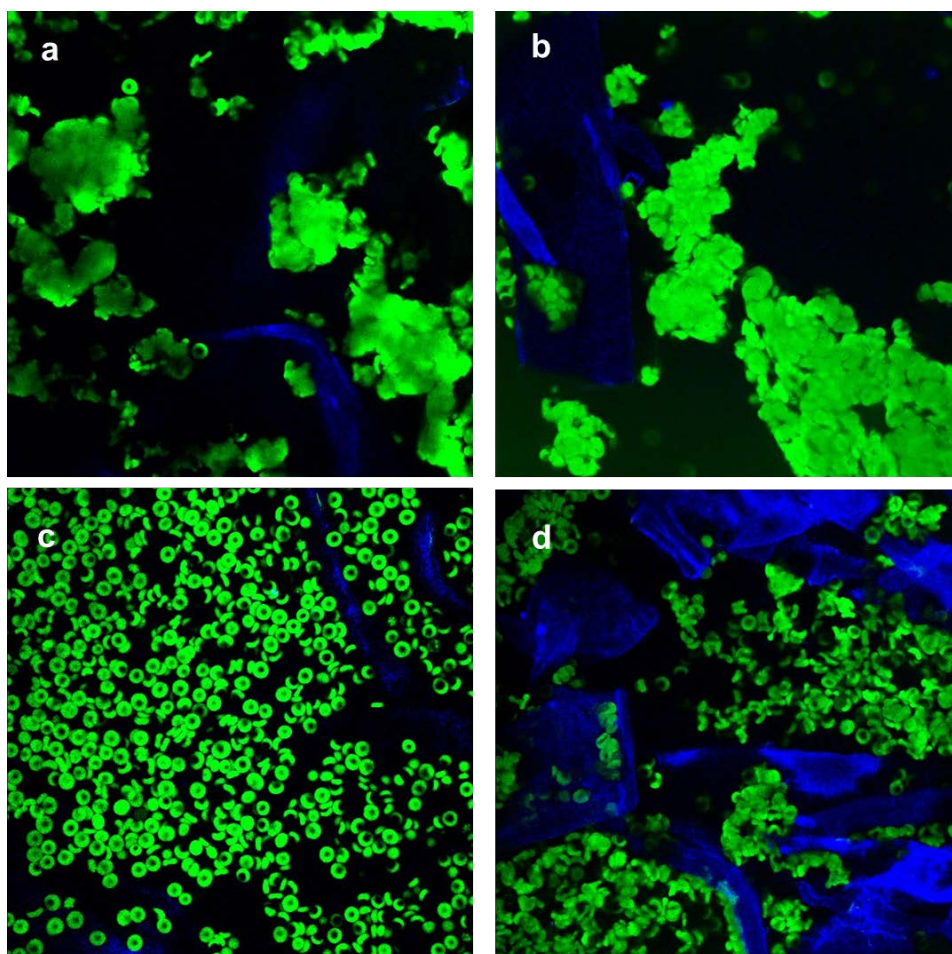


Figure 4. Haemagglutination behaviour of 3 blood groups investigated by confocal imaging (60× oil immersion lens): (a) RBCs of primary group D(+) agglutinated by D antibodies within 30 s; (b) RBCs of secondary group E(+) agglutinated by E antibodies within 30 s; (c) RBCs of secondary group e(+) did not show any sign of agglutination after reacting with e-antibody for 30s; (d) group e(+)RBCs showed clear agglutination when reacting with e-antibody for 3 mins.

Table 2. Agglutination reaction time required by each secondary blood group*

<i>Blood groups</i>	C	c	E	e	K	k	Jka	Jkb	P1	S	s
<i>Required reaction period</i>	30s	3min	30s	3min	2min	30s	2min	2min	30s	2min	2min

* For Alba antibodies specified in this study

4.1.5.3 The effect of antibody structure

While some commercial antibodies for secondary blood grouping can easily identify the corresponding secondary group antigens through RBC haemagglutination, others

cannot. This is partially due to the structure of antibodies; the IgM and IgG antibodies show a strong performance contrast in causing heamagglutination of RBCs. The commercial products of IgM are monoclonal immunoglobulin which has a pentameric form; each has two binding sites and ten sites in total. IgG antibodies, however, are monomers with only 2 binding sites in total. The molecular dimension of an IgM molecule is also greater than an IgG molecule, being 30 nm and 14 nm, respectively [5]. Consequently, The distance between the two binding sites of an IgG molecule is too small to allow it to simultaneously bind with antigens on two RBCs and cause direct agglutination. Generally, IgM antibodies will directly agglutinate antigen-positive red cells, whereas most IgG antibodies require potentiators or anti-human globulin (AHG) to effect agglutination [5].

For secondary blood grouping on paper, the IgM antibodies can simultaneously bind to antigens on two RBCs, thus producing sufficiently large agglutinated RBC lumps that can be immobilized in the porous structure of paper. In contrast, agglutination reactions between IgG and RBC antigens without AHG are either extremely weak or do not occur at all, leading to false negative results. An example of K antigen in the Kell system is used to illustrate the different performance of antibodies with different structures. Both IgM and IgG antibodies corresponding to K antigen are commercially available. Figure 5a shows a distinct difference in RBC agglutination patterns: whilst IgM causes strong agglutination of the K-positive sample, IgG shows little or no effect. Another example of detecting s antigen (of the MNS system, Table 1) using IgM and IgG antibodies also shows very similar results to that of the K-antigen in the Kell system, confirming that the different structures of antibodies can lead to extremely different agglutination behaviours (Figure 5b).

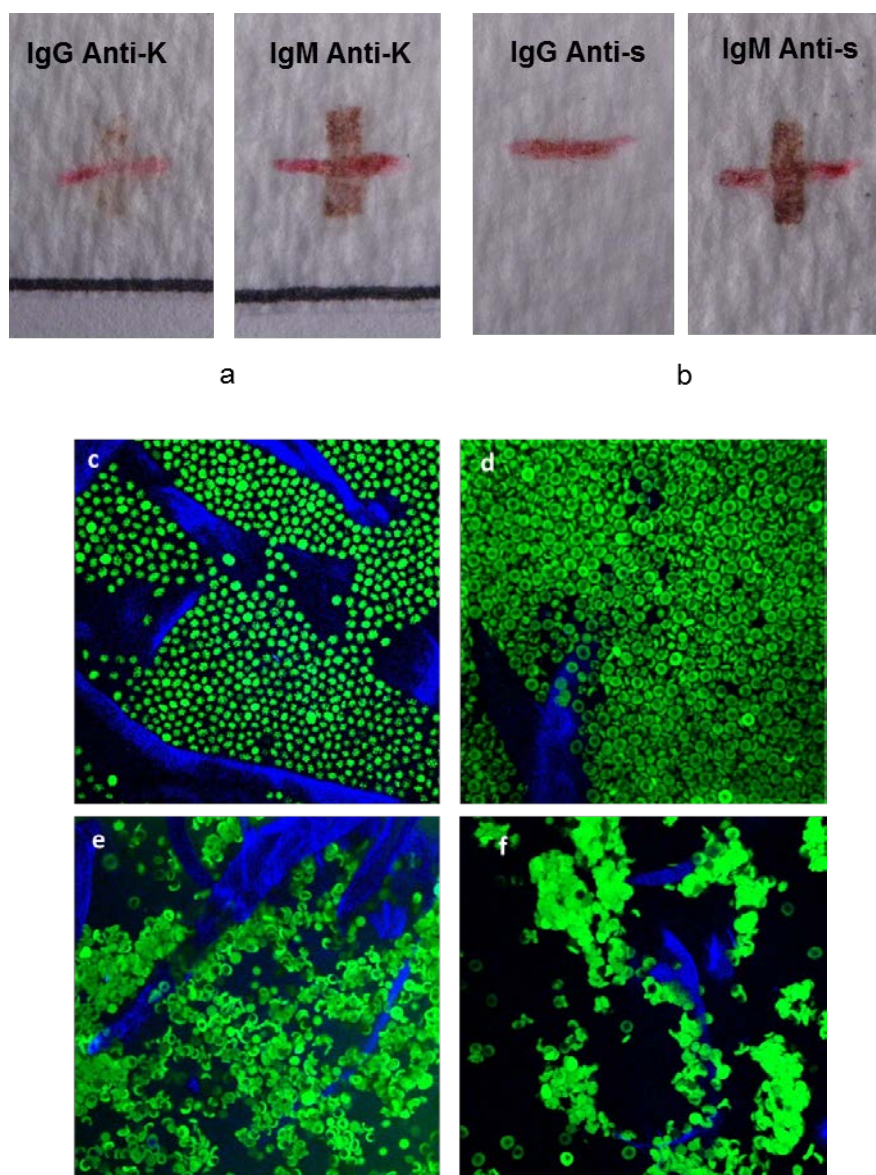


Figure 5. The comparison of the effect of antibody structures (IgG and IgM) on the visual identification of the testing results: (a) for K antigen test; (b) for s antigen test. Confocal images show details of haemagglutination behaviours of K(+) and s(+) on paper treated with different antibodies: (c) anti-K IgG, (d) anti-s IgG, (e) anti-K IgM and (f) anti-s IgM. Reaction times of all assays were 2 min and 60 \times oil lens was used.

Confocal microscopy was used to capture the agglutination patterns of the K(+) and s(+) RBCs by IgM and IgG antibodies. Figures 5c and 5d show agglutination patterns of K(+) and s(+) RBCs after being introduced onto papers treated with anti-K IgG and anti-s IgG, respectively. In both cases, no discernable RBC agglutination could be observed. An interesting observation was that K(+) RBCs show strong deformation and crenation when mixed with anti-K IgG. This is due to fact that the commercial IgG anti-K reagent was directly obtained and prepared from a donor's plasma. The impurity

of the antibody solution might have caused the red blood cell deformation. After a drop of 10 μL Cell-Stab solution was added to the paper, RBCs regained their natural biconcave disc shape (result not presented), but agglutination of RBCs never occurred. In contrast, when K(+) and s(+) RBCs were introduced onto papers treated with the anti-K IgM (Figure 5e) and anti-s IgM (Figure 5f), agglutination of RBCs can be clearly observed under confocal microscope. The confocal results also show that anti-s IgM causes a stronger degree of agglutination than anti-K IgM (Figures 5e and 5f); these results concur with the visual assay on the paper surface (Figures 5a and 5b). They provided a clear understanding of the effects of antibody structures on the efficiency of RBC agglutination; such effects were further confirmed on a microscopic level.

In another study, antibody-antigen interactions of the secondary blood group M were investigated using confocal microscopy. The motivation of this investigation was to understand why a false negative was observed for this blood group in our screening test (Figure 2). A repeat of the assay on paper showed no RBC agglutination, even though 3 min of reaction time was allowed (Figure 6a). The confocal image showed that M(+) RBCs could not be agglutinated by anti-M IgM (Figure 6b). Although anti-M is IgM antiserum, it is considered as a naturally occurring antibody in the human body, rather than an antibody generated by immunoreactions [21]. This type of antibody is a cold-reacting antibody which is not active at 37°C, and therefore is regarded as clinically insignificant [5, 21]. In general, the detection of anti-M can be ignored for transfusion purposes.

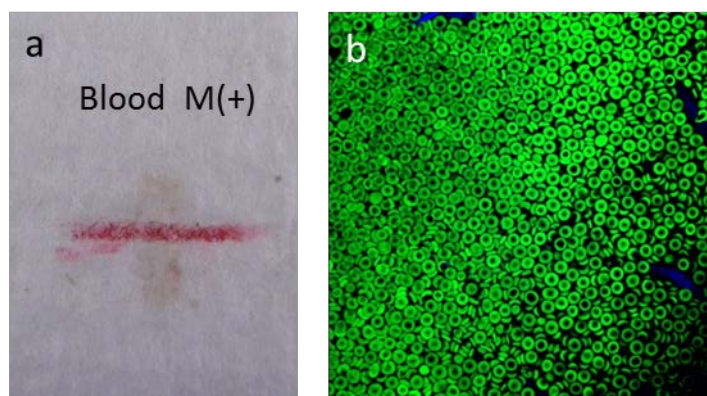


Figure 6. (a) Visual assay of a M(+) blood sample on paper and (b) confocal image taken for the same sample. A commercial Anti-M IgM obtained from human sera was used for the assay and 3 mins reaction time was allowed.

4.1.5.4 The effect of washing conditions

The selection of the washing solution affects the result of secondary blood grouping assays. Firstly, water cannot be used for removing the non-agglutinated blood due to the osmotic effect. Under the osmotic pressure, water penetrates into the red cell through its membrane, causing red cell haemolysis by bursting. The agglutinated red cells therefore can also be removed from the paper (Figure 7a). Secondly, pH is also an important factor in washing. Under normal circumstances, washing solution with a pH of about 7 is acceptable because red cells carry a negative charge and at pH 7–7.5 most antibody molecules bear weak positive charges. This enhances the attraction between the RBCs and antibody molecules during the first stage of interaction. Significant lowering of pH increases the dissociation of the antigen-antibody complexes. This influence of pH levels on the assay result was found to be much more important for secondary blood groups than for primary groups; this is due to the weaker antibody-antigen interactions of secondary blood groups. Figures 7b and 7c show the washing of the agglutinated RBCs from the paper. Our results show that for the best results of secondary blood grouping assays, PBS should be used for washing.

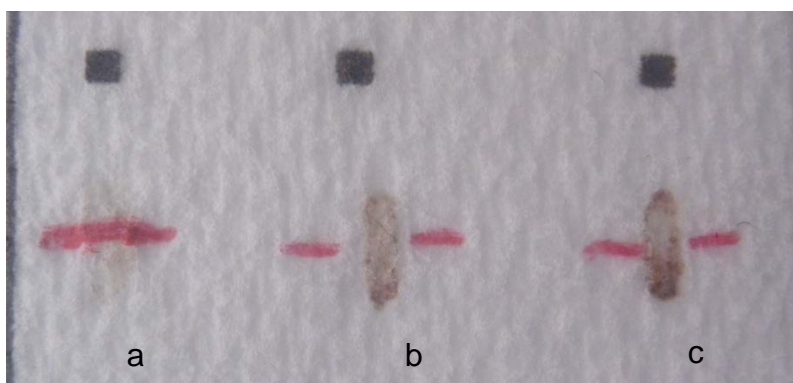


Figure 7. Identification for agglutinated RBCs of blood group c washed by: (a) distilled water; (b) 0.9% NaCl; (c) PBS. Two minutes RBC-antibody interaction time was allowed.

A total of 10 clinically important secondary blood group systems, including 12 blood groups have been tested under their optimum conditions. Each blood group involved from 11 to more than 100 samples and all test results using the bioactive-paper devices matched the results obtained in a pathological laboratory using Gel Card technology.

Details of the tested samples are presented in Table 3. The accuracy of this paper diagnostic assay for 127 blood samples is 100%.

Table 3. Statistics of secondary blood typing data obtained using paper devices

<i>Blood type</i>	C	E	c	e	P1	K	k	Jk ^a	Jk ^b	S	s
<i>Antibody type</i>	IgM	IgM	IgM	IgM	IgM	IgM	IgM	IgM	IgM	IgM	IgM
<i>Incubation time</i>	30s	30s	3m	3m	30s	2m	30s	2m	2m	2m	2m
<i>Number of samples</i>	127	127	127	127	79	79	19	30	30	11	11
<i>Matching with the Laboratory result (%)</i>	100	100	100	100	100	100	100	100	100	100	100

4.1.6 CONCLUSION

We show in this study that paper-based diagnostics are capable of testing various clinical important secondary blood types. Compared to the typing of primary blood groups, the major challenges in secondary blood group assaying were identified to be the antibody-RBC interaction time, antibody types, and pH of the washing buffer. Visual observation of the agglutination pattern on paper was used to evaluate the degree of agglutination under the conditions of investigation, whilst confocal microscopy was employed to obtain microscopic information on the agglutination patterns in fibre network at a cellular level. The microscopic and macroscopic results presented in this work establish a detailed understanding of secondary blood grouping in paper. First, RBCs carrying some secondary group antigens require a longer time to react with their corresponding antibodies in order to form a sufficient level of agglutination for unambiguous visual identification on paper. Second, the types of antibodies are important in secondary blood group typing. This work confirmed, at a cellular level, that while IgM antibodies are able to cause direct agglutination of RBCs, IgG antibodies are unable. In that case an indirect method must be used. Third, the pH

of the washing buffer must be controlled at neutral, or at a slightly basic level, to prevent the undesirable dissociation of the agglutinated RBC lumps during washing.

This work is the first research on using paper-based diagnostics for secondary blood typing. Of the 12 clinically important secondary blood groups we investigated in this study (Table 3), the results obtained by paper-based devices showed 100% match with the mainstream Gel Card technology. The design concept of the paper assay enables both professionals and non-professionals to easily understand and archive the assay.

4.1.7 ACKNOWLEDGEMENT

This work is supported by the Australian Research Council (ARC). Funding received from ARC through grant numbers DP1094179 and LP110200973 is gratefully acknowledged. The authors thank Haemokinesis for its support through ARC Linkage Project. Authors also thank Dr. John Zhu of Monash Center for Nanofabrication (MCN) for Confocal imaging and technical help, and Mr Hansen Shen for proof-reading the manuscript. Ms Miaosi Li, Ms Whui Lyn Then and Ms. Lizi Li thank the Monash University Research and Graduate School and the Faculty of Engineering for postgraduate research scholarships.

4.1.8 REFERENCE

- [1] G. Daniels, Human Blood Groups, 2nd edn. Oxford: Blackwell Science, 2002.
- [2] G. Daniels, M. E. Reid, Blood groups: the past 50 years, *Transfusion*, 2002, **50**(2): 281-289.
- [3] N. D. Avent, M. E. Reid, The Rh blood group system: a review, *Blood*, 2000, **95**(2): 375-387.
- [4] C. M. Westhoff, The Rh blood group system in review: A new face for the next decade, *Transfusion*, 2004, **44**(11): 1663-1673.
- [5] G. Daniels, I. Bromilow (2007) Essential Guide to Blood Groups. Wiley-Blackwell: Hoboken.
- [6] G. Daniels, J. Poole, M. de Silva, T. Callaghan, S. MacLennan, N. Smith, The clinical significance of blood group antibodies, *Transfusion Med*, 2002, **12**: 287 – 295.
- [7] B. Thakral, K. Saluja, R. R. Sharma, N. Marwaha, Phenotype frequencies of blood group systems (Rh, Kell, Kidd, Duffy, MNS,P, Lewis, and Lutheran) in north Indian blood donors, *Transfusion and Apheresis Science*, 2010, **43**(1): 17-22.

- [8] W. Malomgré, B. Neumeister, Recent and future trends in blood group typing, *Analytical and Bioanalytical Chemistry*, 2009, **393**(5): 1443-1451.
- [9] D. M. Harmening, Modern blood banking and transfusion practices, 4th Edition ed. Philadelphia: F.A. Davis, 1999.
- [10] R. Pelton, Bioactive paper provides a low-cost platform for diagnostics, *Trends in Analytical Chemistry*, 2009, **28**(8): 925-942.
- [11] X. Li, J. Tian, W. Shen, Paper as a Low-Cost Base Material for Diagnostic and Environmental Sensing Applications, *Appita Conference and Exhibition. Appita Inc. Melbourne*, 2009: 267-271.
- [12] D. Ballerini, X. Li, W. Shen, Patterned paper and alternative materials as substrates for low-cost microfluidic diagnostics, *Microfluidics and Nanofluidics*, 2012, 1-19.
- [13] M. S. Khan, G. Thouas, W. Shen, G. Whyte, G. Garnier., Paper Diagnostic for Instantaneous Blood Typing, *Analytical Chemistry*, 2010, **82**(10): 4158-4164.
- [14] M. Al-Tamimi, W. Shen, R. Zeineddine, H. Tran, G. Garnier, Validation of Paper-Based Assay for Rapid Blood Typing, *Analytical Chemistry*, 2011, **84**(3): 1661-1668.
- [15] M. Li, J. Tian, M. Al-Tamimi, W. Shen, Paper-Based Blood Typing Device That Reports Patient's Blood Type "in Writing", *Angewandte Chemie International Edition*, 2012, **51**: 5497-5501.
- [16] L. Li, J. Tian, D. Ballerini, M. Li, W. Shen, A study of the transport and immobilisation mechanisms of human red blood cells in a paper-based blood typing device studied using confocal microscopy, *Analyst*, 2013, **138**: 4933-4940.
- [17] L. Li, J. Tian, D. Ballerini, M. Li, W. Shen, Superhydrophobic surface supported bioassay-An application in blood typing, *Colloids and Surfaces B: Biointerfaces*, 2013, **106**: 176-180.
- [18] L. Dean, Blood Groups and Red Cell Antigens, Bethesda (MD): National Center for Biotechnology Information, USA, 2005.
- [19] E. F. Hauck, S. Apostel, J. F. Hoffmann, A. Heimann, O. Kempfski, J. Cereb, Capillary flow and diameter changes during reperfusion after global cerebral ischemia studied by intravital video microscopy, *Blood Flow Metab*, 2004, **24**: 383-391.
- [20] A. G. Hudetz, G. Feher, C. G. M. Weigle, D. E. Knuese, J. P. Kampine, Video microscopy of cerebrocortical capillary flow: response to hypotension and intracranial hypertension, *Am J Physiol: Heart Circ Physiol*, 1995, **268**: H2202-H2210.
- [21] D.D. Mais, ASCP Quick Compendium of Clinical Pathology, 2nd Ed. Chicago: ASCP Press, 2009.

This page is intentionally blank

Monash University

Declaration for Thesis Chapter 4.2

Declaration by candidate

In the case of Chapter 4.2, the nature and extent of my contribution to the work was the following:

Nature of contribution	Extent of contribution (%)
Initiation, key ideas, experimental works, analysis of results, paper editing	44

The following co-authors contributed to the work. If co-authors are students at Monash University, the extent of their contribution in percentage terms must be stated:

Name	Nature of contribution	Extent of contribution (%) for student co-authors only
Whui Lyn Then	Initiation, key ideas, experimental works, analysis of results, writing up	44
Heather Mcliesh	Assisted in experimentation	
Wei Shen	Key ideas, paper reviewing and editing	Supervisor
Gil Garnier*	Key ideas, paper reviewing and editing	Supervisor

The undersigned hereby certify that the above declaration correctly reflects the nature and extent of the candidate's and co-authors' contributions to this work*.

Candidate's Signature

	Date 03-03-2015
--	---------------------------

Main Supervisor's Signature

	Date 04-03-2015
--	---------------------------

*Note: Where the responsible author is not the candidate's main supervisor, the main supervisor should consult with the responsible author to agree on the respective contributions of the authors.

This page is intentionally blank

4.2 The detection of blood group phenotypes using paper diagnostics

Whui Lyn Then, Miaosi Li, Heather McLiesh, Wei Shen and Gil Garnier**

BioPRIA, Australian Pulp and Paper Institute, Department of Chemical Engineering,
Monash University, Clayton Campus, Vic. 3800, Australia

*Corresponding Author

This paper has been published in *Vox Sanguinis*

4.2.1 ABSTRACT

Paper biodiagnostics for blood typing are novel, cheap, fast and easy to use. Agglutinated red blood cells cannot travel through the porous structure of paper, indicating a positive antibody-antigen interaction has occurred. Conversely, non-agglutinated blood can disperse and wick through the paper structure with ease to indicate a negative result. This principle has been demonstrated to detect blood group phenotypes: ABO and RhD. However, typing for red blood cell antigens such as Rh, Kell, Duffy, and Kidd, have not yet been explored on paper. In this work, two paper testing methods – an elution and a direct flow-through method – were investigated to detect red blood cell antigens excluding the ABO system and RhD. Antigens explored include: C, c, E, e, K, cellano (k), Fya, Fyb, Jka, Jkb, M, N,S and s, P1, Lea and Leb. The variables tested include: reaction time, reagent concentration. The importance of antibody type/structure for successful agglutination on paper was confirmed. Some blood group phenotypes showed less agglutination due to weaker antibody-antigen interactions. Most blood groups with antibodies available as IgM, such as C/c, E/e, K and cellano, and Jka and Jkb, and P1, were successful using both methods. However, other blood groups, especially those with antibodies only available as polyclonal antibodies were unsuccessful and require further scrutiny. As a result, this study confirms that paper can be used as an alternative blood grouping diagnostic tool for selected blood group phenotypes.

4.2.2 KEYWORDS

Paper diagnostics, blood typing, haemagglutination , blood groups, antibodies, IgM, IgG, Rh, Kell, Kidd, Duffy.

4.2.3 INTRODUCTION

Although ABO and RhD are the most important blood group systems in transfusion medicine, many other blood group antibodies can cause serious or fatal haemolytic transfusion reactions (HTRs) or haemolytic disease of the foetus and newborn (HDFN). Current blood typing techniques rely on antibody-antigen interactions to cause red blood cell agglutination for positive identification. Techniques, such as gel columns, are well established. Common methods for phenotyping blood groups are the tube test and column agglutination test (CAT), which require centrifugation only available under laboratory conditions, unsuitable for in-field and remote testing [1]. Currently CATs are more widely used, relying on gels or glass beads to visualize agglutination. However, the process requires trained personnel, is more expensive, lengthy and time consuming to operate,. Low-cost and equipment-free methods, such as the glass slide test, can be insensitive and are unsuitable for antigen identification, particularly for neonatal samples [2]. This is especially true when testing for the wide array of clinically significant blood group phenotypes.

For many years, blood groups were the best genetic markers, and have played a key role in the mapping of the human genome [3]. Blood group antigens are found on the surface of red blood cells (RBCs). These dictate an individual's blood type. Blood group antibodies are present in the blood plasma and generally result from an immune response triggered by prior exposure, such as previous transfusion or during pregnancy, to the corresponding antigen not located on that individual's RBC surface (alloantibody). There are now 35 blood group systems recognised, with over 300 blood group antigens, many of which are clinically significant, requiring detection and the identification of antibodies to be performed prior to blood transfusions [3, 4]. The discovery of the ABO blood groups made blood transfusions safe; the disclosure of the RhD antigens led to the understanding and prevention of HDFN [2, 5, 6]. Each of the blood group phenotype systems contain antigens which are unique and have a different

frequency depending on the patient's ethnicity [7]. The blood groups and their corresponding alloantibody examined in this study are summarized in Table I. Aside from these blood groups, some alloantibodies, such as Anti-M, N, P1 and Lewis antibodies, are seldom active at body temperature (37 °C) and are generally not considered clinically significant [2]. The mismatching of a blood group antigen in the presence of a clinically significant antibody could cause immediate, delayed or severe HTRs or HDFN, necessitating tests to identify or confirm the presence of these antigens. Prior to blood transfusion, the accurate and fast identification of the blood group phenotypes is essential for patients who possess an alloantibody [8].

Further development in low-cost minor blood typing methods is necessary, especially for testing in developing countries and the battlefield. Novel paper diagnostic for human blood typing through the haemagglutination of the RBCs was developed [9-17]. Paper can be pre-treated with a blood typing antibody reagent. When a blood sample is subsequently introduced onto the antibody pre-treated paper, if positive, a haemagglutination reaction will occur between the RBCs and corresponding antibody. These blood agglutinates are formed within the porous structure of paper and cannot be removed when washed with solutions such as phosphate buffered saline (PBS) or 0.9% NaCl saline. Inversely, during negative reactions, the RBCs do not agglutinate and the cells are easily washed away. This phenomenon is the foundation of paper substrates for blood typing which was used to design diagnostics for ABO and RhD blood testing [12].

In this study, paper diagnostics were engineered to identify blood groups using haemagglutination, focusing on common clinically significant blood group phenotypes. The method for phenotyping these blood groups proved not to be as simplistic as the ABO and RhD groups; time-dependant reactions became evident [10, 17]. The influences of antibody types, reaction time, washing conditions, and antisera concentration on the identification of blood group phenotype were investigated.

Two separate testing methods were developed using paper, each using different principles regarding the interactions of the analytes, samples and washing method. One method follows the principles of chromatography, allowing the washing solution to

elute unbound blood cells laterally along the paper structure (wicking). This method was used for ABO and RhD groups [11]. The second uses the flow-through method [12, 18, 19], which washes through the paper, rather than along, utilizing a filtration mechanism. While each method has been successful when testing ABO and RhD blood types, this is the first report testing paper diagnostics for the detection of blood group phenotypes other than ABO and RhD using both methods.

4.2.4 EXPERIMENTAL

4.2.4.1 Materials and Equipment

Professional Kleenex paper towel from Kimberly-Clark, Australia, was employed as paper. Antisera blood typing antibodies were purchased from ALBA bioscience, Edinburgh, United Kingdom and used as received (Table 1). Washing solutions 0.9% (w/v) NaCl saline and phosphate-buffered saline (PBS) were prepared using MilliQ water, analytical grade NaCl (Univar) and PBS tablets (Sigma-Aldrich), respectively. Alkyl ketene dimer (AKD) from BASF was used for paper hydrophobization. Analytical grade n-heptane from Sigma-Aldrich was used to formulate ink-jet solution to print text on paper. EDTA blood samples were sourced from Australian Red Cross Blood Service (ARCBS); stored at 4°C and used within 7 days of collection.

Micropipettes (Eppendorf research®, 2.5–50 µL) were used to introduce the antibodies, blood samples, and saline solutions on paper. Millipore centrifugation tubes (50kD cutoff) from Merck, Australia were used to remove supernatant and increase concentration of the antibodies by filtration.

4.2.4.2 Methods

Two methods were tested. The first was the elution methodology for high-throughput diagnostics in laboratory settings [11]. The second flow-through method used the direct reporting method suited for remote and emergent situations [12]. These methods differ by the direction of liquid transport within paper during the washing step. The elution method relies on the paper structure to wick saline solution laterally and separate by chromatography along paper, while direct-reporting washes via a flow-through filtration-like method.

Table 1. Blood groups and the corresponding antibodies used for blood group phenotyping on paper. The antibody structure and clone is also included.

<i>Blood System</i>	<i>Blood Type</i>	<i>Reagent Type</i>	<i>Clone</i>
Rh	C	IgM	P3X25513G8
	E	IgM	DEM1
	c	IgM	H48
	e	IgM	MS-36 and P3FD512
Kell	K	Polyclonal	Polyclonal (Human Source)
	K	IgM	MS-56
	k	IgM	Lk1
Kidd	Jk ^a	IgM	P3HT7
	Jk ^b	IgM	P3.143
Duffy	Fy ^a	Polyclonal	Polyclonal (Human Source)
	Fy ^b	Polyclonal	Polyclonal (Human Source)
MNS	M	IgM	LM1
	N	IgM	LN3
	S	IgM	P3S13JS123
	s	Polyclonal	Polyclonal (Human Source)
P	P1	IgM	650
Lewis	Le ^a	IgM	LEA2
	Le ^b	IgM	LEB2

1) Elution

A known antibody reagent is dotted along the bottom of paper (10µL) before the addition of mixed EDTA blood sample (3µL) [11]. After a reaction period, ranging from 30 to 120 seconds, the substrate was hung in a vertical-standing elution tank containing 0.9% NaCl saline solution at a depth of 1cm. Following an elution period of 5 min., the substrate was removed and dried in the laboratory ($T = 22 \pm 1^\circ\text{C}$; relative humidity = 30-50%) (Figure 1). Qualitative evaluation of results was conducted visually. Agglutination showed a distinct bloodspot, while non-agglutinated RBCs were defined by the absence of a blood spot and by a clear elution path on paper. Quantitative analysis was achieved using ImageJ software to measure colour densities of the blood spot (BS) and elution pathway (EP). Kleenex paper towel was selected for performance, attainability and cost. Compared with other paper, such as Whatman filter, the results achieved were clearer and more reliable [11,16].

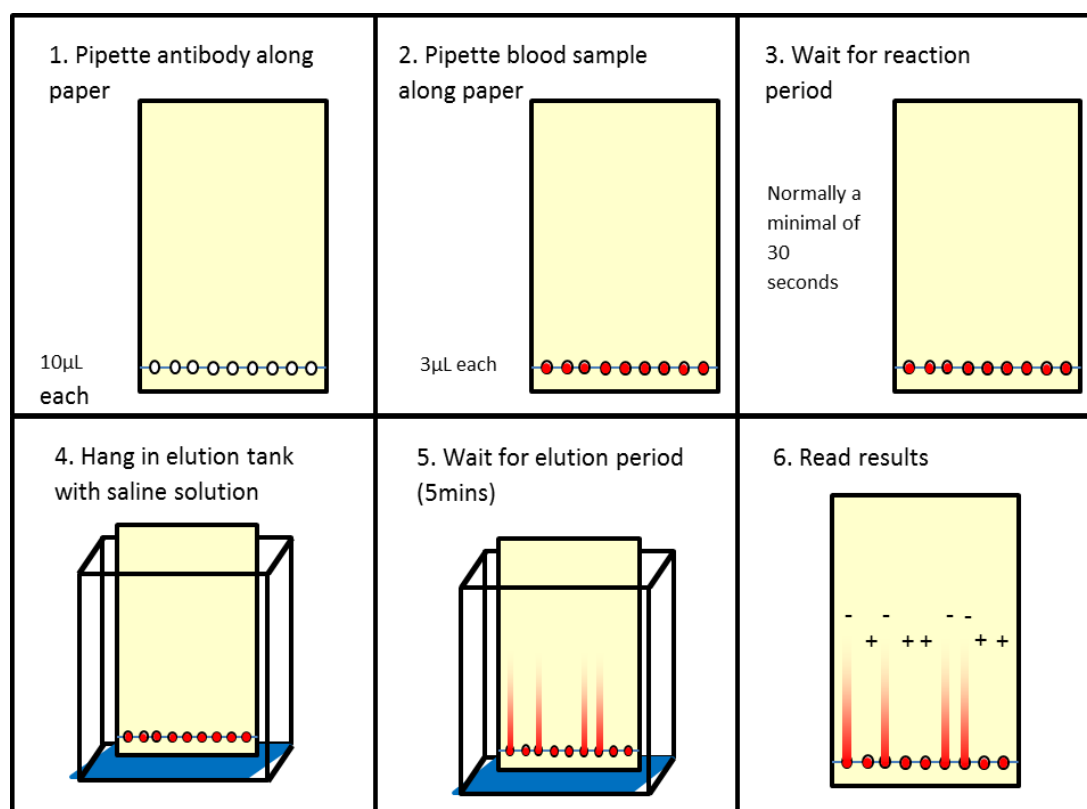


Figure 1. Methodology for blood group phenotyping using paper via elution

2) Flow-Through Direct reporting

Agglutinated cells can form patterns to resemble text or signs. This can be achieved by hydrophobic barriers printed onto the paper prior to the addition of cells. The hydrophobic barrier guides where antisera will be absorbed into the paper. This strong hydrophobic-hydrophilic contrast can be used to border the RBC-antibody interactions on paper, forming shapes or 'text' that can be easily read when fabricating a user friendly blood group device [15]. A reconstructed Canon ink jet printer (Pixma iP3600) was used to print channels onto paper with an AKD-heptane solution (Figure 2). Aliquots of 2.5 μ L of antibody solutions were introduced into the corresponding patterns. After the antibody solution was dried, 2.5 μ L of blood sample was introduced into the vertical channel. A reaction period was allowed for the antibodies to interact with the RBCs inside the channels. Washing was performed with two 30 μ L aliquots of saline solution introduced into the patterns to wash out non-agglutinated RBCs. The blood types were then read directly. Quantitative analysis used ImageJ to measure channel density.

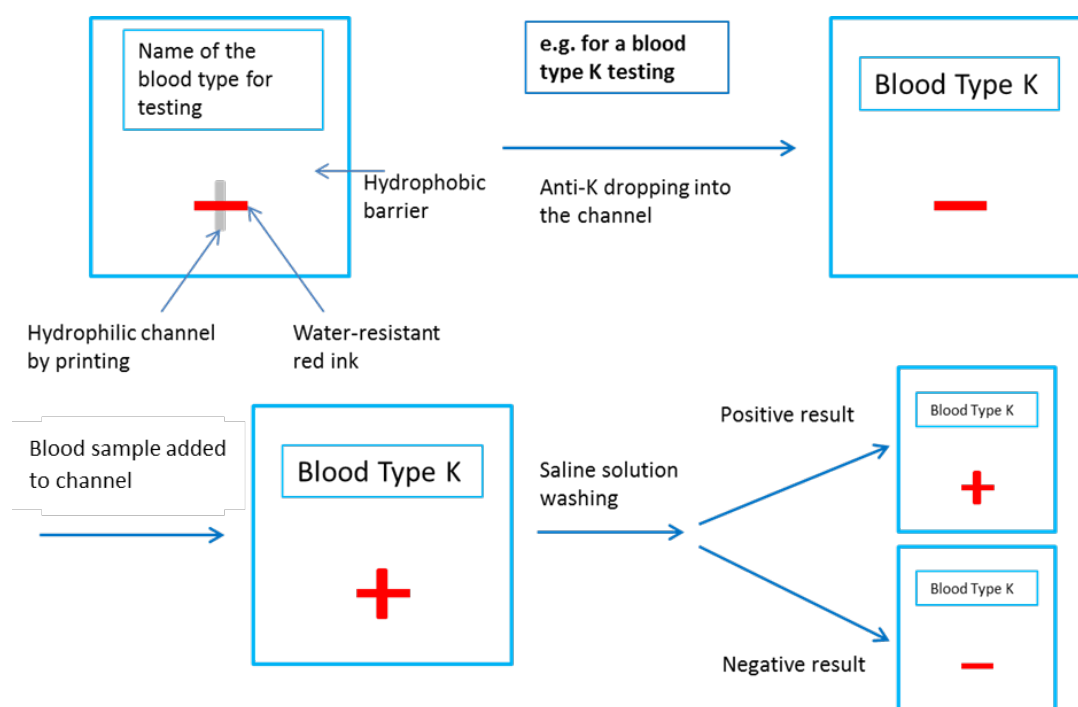


Figure 2. Fabrication, testing procedures and result reporting of paper diagnostics for antigen detection using example: blood group K.

4.2.4.3 Analysis Criteria

Successful testing should easily distinguish positive from negative, while preventing false positive and false negative results. For the elution method, a positive result should report a well-defined blood spot (BS) with no RBCs in the elution pathway (EP); conversely, a negative result would have no BS, but show distinct wicking in the EP. The direct reporting method prints a positive "+" sign, while a negative in absence of RBCs, leaves a negative "-" sign. 236 different patient samples were tested. However, not all samples were fully phenotyped. The number of samples for each antigen tested was restrained by blood availability, outlined in table 2.

Table 2. Blood group phenotyping using the Elution (E) and Text reporting (TR) methods on paper. Blood spot (BS) and elution pathway (EP) are represented as density. Optical density ratio (ODR) compares density EP:BS. Positive is denoted by high density and ODR, negative has lower densities and ODR.

ANTIGEN		C	E	c	e	K	K	k	
Antibody Type		IgM	IgM	IgM	IgM	IgM	Polyclonal	IgM	
No. of Samples		76	67	54	8	11	53	25	
Reaction Time	(s)	30	30	E:120, TR:180	E:60, TR:180	E:60, TR:120	120	120	
Buffer		NaCl	NaCl	PBS	PBS	NaCl	NaCl	NaCl	
		+	-	+	+	-	+	-	
No. of Samples		31	45	17	50	40	14	23	
Elution Method		BS	BS	BS	BS	BS	BS	BS	
		123 ±9.1	51 ±9.4	118 ±5.1	42 ±7.9	105 ±4.3 44.0 ±2.4	107 ±4.63	38 ±4.1 82 ±3.6 41 ±7.7	
		EP	EP	EP	EP	EP	EP	EP	
		8.2 ±3.1 ±6.8	32 ±6.8	8.5 ±3.0 49 ±11	5.8 ±1.0 32 ±6.5	6.1 ±0.48	54 ±6.5 13 ±8.8	27 ±4.3 15.8 ±9.43 33.5 ±7.11	
		ODR	ODR	ODR	ODR	ODR	ODR	ODR	
		17 ±2.7 ±0.55	2.9 ±0.55	16 ±3.6 1.0 ±1.4	12 ±3.7 1.8 ±0.39	18 ±1.5 ±0.12	0.72 8.4 ±5.5 2.0 ±0.46 0.183 ±0.126 179	0.585 ±0.126 6.4 ±1.5 ±0.25	
Text Method		152 ±7.4	28 ±3.8	145 ±7.1	30 ±4.9	154 ±5.7 30 ±3.7	135 ±9.2	30 ±4.2 106 ±5.0 34 ±4.0 46 ±4.1	35 ±7.1 131 ±8.3 31 ±5.0
ANTIGEN		Fy ^a	Fy ^b	JK ^a	JK ^b	PI	Le ^a	Le ^b	
Antibody Type		Polyclonal	Polyclonal	IgM	IgM	IgM	IgM	IgM	
No. of Samples		12	8	30	25	40	46	23	
Reaction Time	(s)	120	30	120	120	30	180	180	
Buffer		NaCl	NaCl	NaCl	NaCl	NaCl	PBS	PBS	
		+	-	+	+	-	+	-	
No. of Samples		9	3	7	1	22	8	15	
Elution Method		BS	BS	BS	BS	BS	BS	BS	
		60 ±13	60 ±23	37 ±5.6	40	106 ±8.7	48 ±4.0	100 ±7.5	
		EP	EP	EP	EP	EP	EP	EP	
		39 ±15	38 ±13	33 ±5.8	35	14 ±3.6	40 ±4.2	15 ±3.6	
		ODR	ODR	ODR	ODR	ODR	ODR	ODR	
		1.6 ±0.17	2.0 ±0.028	1.1 ±0.19	1.1	8.3 ±2.7	1.2 ±0.13	6.8 ±1.8	
Text Method		36 ±11	27 ±4.0	N/A	N/A	95 ±6.2	37 ±4.8	122 ±9.8	

To compare the strength of each blood group's antibody/antigen reactions and the testing conditions, the colour densities of the resulting BS were measured using ImageJ. Distinct patterns emerged when comparing positive and negative results. Higher density values indicated a positive result (usually >100), while lower values indicated negative samples (<40). Densities between this range (40-100) could be classified as weaker reactions. This distinction was used for the text-reporting method.

However, to analyse the elution method results, the BS alone was insufficient to indicate the interactions of certain blood groups. In such instances, the BS optical densities bordered the weak reaction threshold. In some cases, the BS for negative and positive looked too similar for accurate determination by the naked eye. It was the presence/absence of an EP that confirmed the result. Therefore, in addition to BS density, an area of the EP 2cm above the BS was measured. Positive results contained little or no RBCs in EP with low density values. Conversely, negative results showed high densities representing unbound RBCs travelling through paper after washing. This difference was translated into a fraction, the optical density ratio (ODR), comparing density of BS to EP. A higher ODR value (>6.0) indicated positive, while low values (<3.0) indicated negative, with weak reactions between indicated in between (3.0-6.0).

$$ODR = \frac{BS}{EP}$$

4.2.5 RESULTS

A series of antibody/antigen reaction tests were performed using both procedures to detect blood group phenotypes (Figures 1 and 2). As each antibody/antigen pair behaves differently when tested, each needed to be analysed individually. This differs from the major blood groups (A, B, O and RhD), which react strongly and clearly for most patients; exceptions include the weak subgroup variants [10, 11, 16]. It was found that several factors impacted the interaction strengths observed for each antigen tested. These factors are: 1) reagent type, 2) reaction time, 3) antibody concentration, and 4) washing conditions. The washing conditions were found to affect the results of the text-reporting method, but not the elution method. This is due to the effects of directional flow during washing. Horizontal flow in elution method uses the chromatographic

effect to elute the red blood cells away from its original spot, while vertical flow in text-reporting approach uses the filtration effect to remove individual blood cells from paper. As a result, the proportion of red blood cells removed from the paper substrate in text-reporting method can be significantly affected by the washing conditions. Table 2 and Figure 3 depict the results achieved for both the elution and text-reporting method for the blood groups investigated (Table 1). However, testing for Duffy groups, Fya and Fyb, MNS groups, and Lewis groups, Lea and Leb, was unsuccessful.

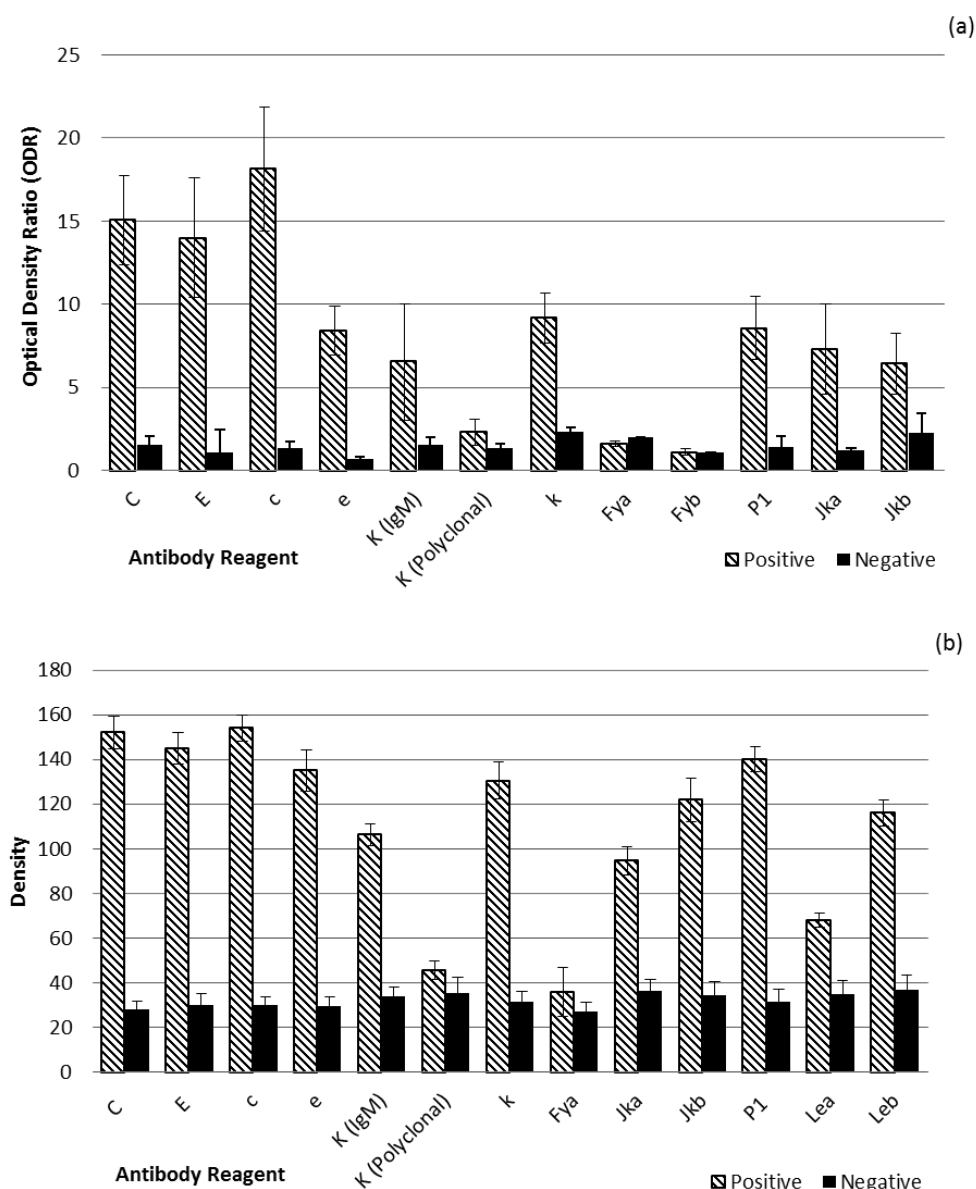


Figure 3. Blood group phenotyping using (a) elution, and (b) text reporting methods on paper. Blood spot (BS) and elution pathway (EP) are represented as density. Extent of coagulation is represented as optical density ratio (ODR) comparing density EP:BS. Positive is denoted by high density and ODR, negative has lower densities and ODR. (Fyb was not tested using the text reporting method.)

4.2.5.1 Testing conditions

The main variables investigated for optimization include: 1) reagent type, 2) reaction time, and 3) antibody concentration, and 4) washing conditions.

Reagent type – The effect of reagent type was investigated. Certain antibodies are only commercially available as polyclonal (human source), not immunoglobulin M (IgM). IgM antibody reagents are generally monoclonal, containing a pentameric structure, with ten binding sites. IgG antibodies are monomers, containing only two-binding sites. Whilst IgM antibodies show strong agglutination, IgG antibodies generally only sensitise cells without agglutination. This is due to electrostatic repulsion between RBCs. IgM antibodies provide over twice the bridging distance, overcoming the electrostatic double layer surrounding RBCs. IgM antibodies are expected to exhibit better binding capabilities compared to IgG antibodies, allowing direct agglutination rather than only sensitization to occur. The identification of certain blood groups by direct agglutination using paper is therefore constrained by the commercial availability of IgM antisera.

Reaction time – The time allowed for the antibody sera and RBCs to react. Haemagglutination between ABO and RhD antigens and antibodies can be achieved within 30s. However, some minor blood group antigens take longer than 30s to bind with their antibodies to show strong haemagglutination for clear identification. Thus, the time the RBC antigens had to bind was extended and compared. Reaction times 30, 60, 120 and 180s were tested, with optimum conditions reported in Table 2. Reaction times beyond 180s were not explored as longer reaction times could increase the potential of false positives.

Antibody concentration – The effect of antibody concentration was explored. Antibody concentration was increased by filtering the reagent using Millipore centrifugation tubes. These tubes retain biomolecules 50kDa or larger, and remove supernatant. Increased concentration allows faster collision rate and resulted in stronger agglutination for positive tests. However, this raises the possibility of provoking the

prozone effect where agglutination does not occur due to an excess of antibody or antigen.

Washing conditions – Varying the washing buffer was investigated to determine the effect of pH, ionic strength and specificity has on the elution of RBCs and clarity of results. Using the text reporting method, washing using PBS yielded clearer results, while the effects were nominal for the elution method.

4.2.6 DISCUSSION

Each blood group typing reaction behaved differently when tested, and therefore each required individual analysis.

4.2.6.1 Rh Blood Group System

Apart from the ABO blood groups, the antibodies against the Rh blood group system are the most common clinically significant antibodies. Of these, D is the most immunogenic antigen. The additional antigens investigation within the Rh system which are important when screening patient or donor blood are C, c, E, and e. Testing using paper for these four antigens was successful using the commercial antibody reagent at a standard reaction time of 30 seconds. The Rh antisera used were all monoclonal IgM (Table 1).

Using the elution method, the C and E antigens were strongly detected (ODR pos: 17 ± 2.7 , neg: 2.9 ± 0.55 ; pos: 16 ± 3.6 , neg: 1.0 ± 1.4 , respectively) (Figure 3(a)), only needing 30s reaction time. However, c and e antigens showed a slightly less clear BS with higher density in the EP. The clarity of tests for c and e improved with longer reaction times of 120s (ODR pos: 12 ± 3.7 , neg: 1.8 ± 0.39 ; pos: 18 ± 1.5 , neg: 0.72 ± 0.12 , respectively). Extending the RBC-antibody contact time to two minutes or more showed better agglutination with less unbound RBCs able to migrate through the paper structure.

A maximum reaction time of 180s was selected as longer reaction times could increase false positives. For the elution method for c and e, a 180s reaction time provided less distinct results with negative ODRs of 1.8 ± 0.39 and 3.0, respectively. While above the threshold, a lower ODR for negative results provides a clearer result (Figure 4).

The text-reporting method was similar. C and E had clear and distinct densities (pos: 152 ± 7.4 , neg: 28 ± 3.8 ; pos: 145 ± 7.1 , neg: 30 ± 4.9 respectively). When compared to the BS data of the elution method, the text-reporting method showed a clearer distinction between positive and negative. The c and e tests similarly improved with a longer reaction time of 180s (pos: 154 ± 5.8 , neg: 30 ± 3.7 ; pos: 135 ± 9.2 , neg: 29 ± 4.2 respectively) (Figure 4).

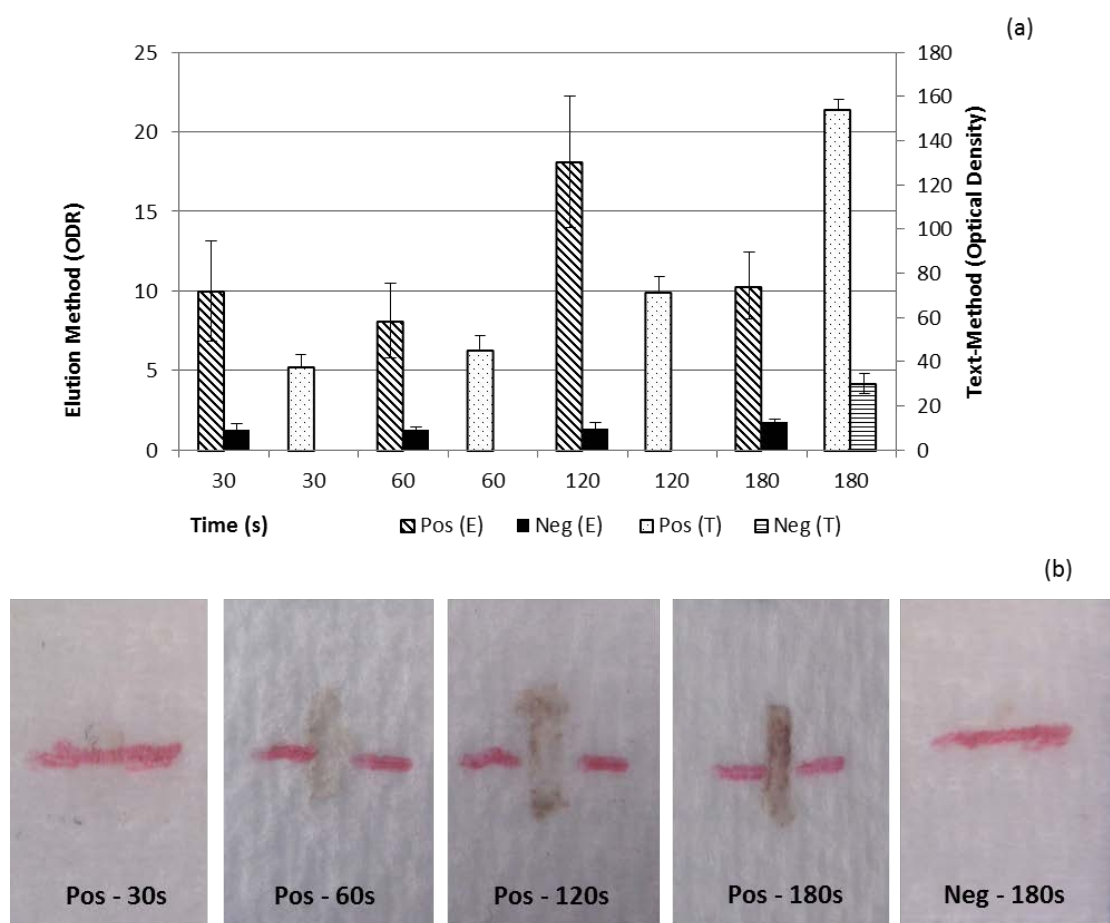


Figure 4. (a) Effect of time on the reaction period tested with c antigen, comparing elution method (E) and text-reporting method (T). ODR of E is compared to density of T. (b) Effect of time on the reaction period tested with c antigen using text-reporting.

4.2.6.2 Kell Blood Group System

Two clinically significant blood group antigens from the Kell system were explored: K and Cellano (k). Two types of K reagents commercially available were tested: monoclonal IgM and polyclonal (Table 1). The anti-K polyclonal reagents manufactured from human plasma is expected to be composed of IgG antibodies since the immune response against the Kell system produce predominantly IgG antibodies [2]. The efficiency of both reagents was tested with both paper testing methods.

The elution method reported ODR pos: 8.4 ± 5.5 , neg: 2.0 ± 0.46 ; pos: 2.3 ± 0.11 , neg: 1.4 ± 0.39 , for IgM and polyclonal respectively. The text-reporting method had densities of pos: 106 ± 4.9 , neg: 34 ± 4.0 ; pos: 46 ± 4.1 , neg: 35 ± 7.1 , for IgM and polyclonal respectively. Interactions between IgM antibodies and the RBCs are strong and there is no overlap between a positive and a negative test. While both paper methods were accurate with the anti-K IgM antibody, they both failed with polyclonal anti-K (Figure 5). A clear distinction between positive and negative is fundamental for blood group testing, and only IgM antibodies have systematically achieved such distinction.

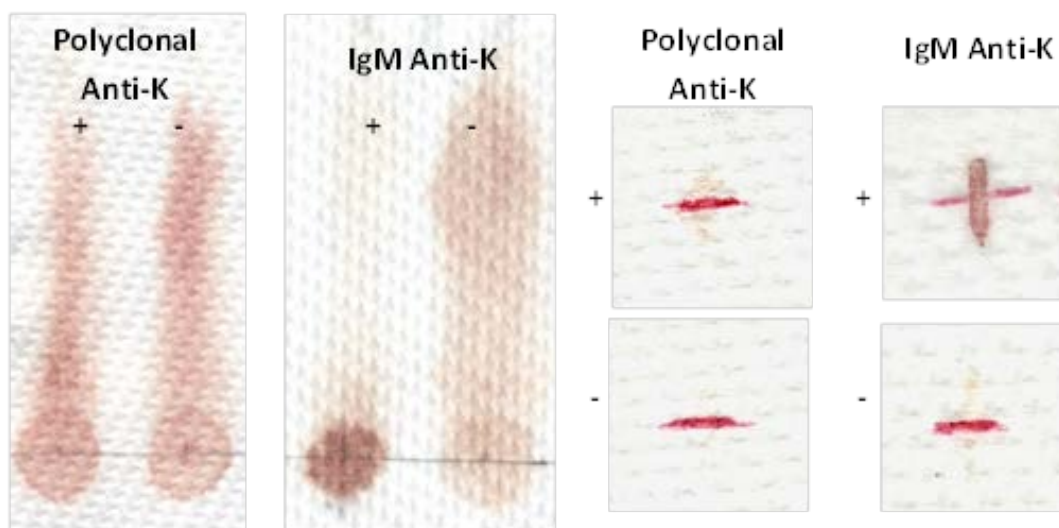


Figure 5. Comparison of antisera (polyclonal or IgM) affecting identification of testing results for K antigen.

In the Saline tube test, IgM antibodies can directly agglutinate antigen-positive red cells, whereas IgG antibodies require anti-human globulin (AHG) to effect agglutination. For both paper testing methods, agglutination between IgG antibodies and RBC antigens

without AHG led to false negative results. As in saline tube testing, this is explained by the greater size of the IgM pentamer able to bridge red cells for electrostatic stabilization. To achieve bridging, the critical length of the antibody must be greater than the thickness of the electrical layer surrounding the RBC. While IgM antibodies can bridge red cells, where IgG monomers cannot. This allows IgM antibodies to agglutinate red cells in saline solution.

Buffer washing solution affected the clarity of results for the text-reporting method. Using Phosphate buffered saline (PBS) improved the density compared to 0.9% NaCl saline. This is likely due to the directional flow when washing. Only nominal effects were observed for the elution method.

Testing with polyclonal anti-K antisera was used to determine the effect of increasing antibody concentration. Surprisingly, increasing the concentration of the commercial polyclonal antibodies by removing excess serum enhanced reaction clarity. Antibody concentration was increased by filtering the serum to retain biomolecules 50 kDa or larger.

Increasing antibody concentration improved the stoichiometric ratio between antibody and antigen (or RBCs). A higher stoichiometry ratio allows for more antigen-antibody interaction; however, it is costly. This provides a counterpoint to reaction kinetics, as a longer reaction time decreases rapidity and could increase potential false positives.

This worked unexpectedly well, enhancing the clarity for polyclonal anti-K when concentration was doubled (pos: 6.8, neg: 1.4 ± 0.46 with a reaction time of 60s), with optimum at 120s (pos: 7.8, neg: 0.61 ± 0.18) (Figure 6). However, the same method applied to other polyclonal reagents was unsuccessful. Polyclonal anti-K antisera, while predominantly IgG antibodies, could contain residual IgM from the original source. Removing the excess supernatant probably increased the IgM concentration in addition to the IgG, thus promoting agglutination. To test this hypothesis, a simple immediate spin tube test and an Indirect Antiglobulin Test (IAT) were performed with the original polyclonal reagent, against K positive cells. Surprisingly, cell agglutination was observed with both tests, albeit significantly weaker in the immediate spin test.

This result indicates that the polyclonal reagent used was predominantly IgG antibodies with some residual IgM antibodies present. Drawbacks of increasing concentration are: antibody sera are expensive, and not all polyclonal reagents have an IgM component.

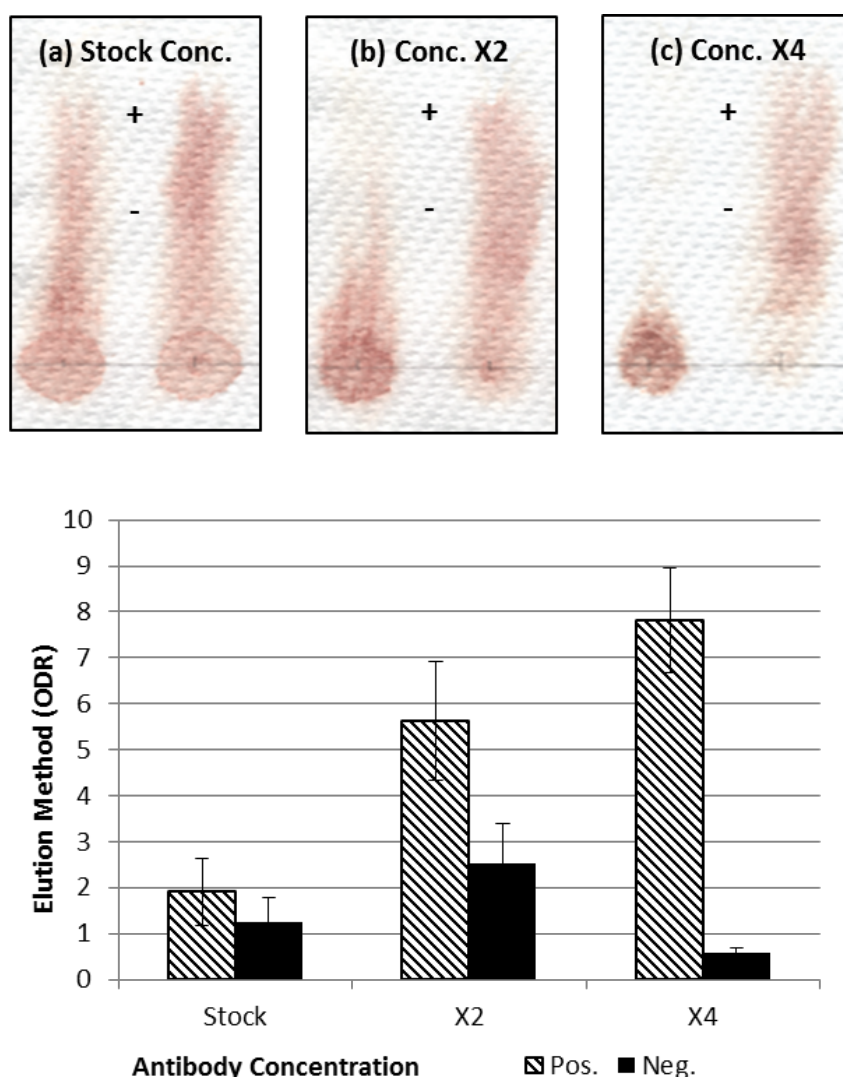


Figure 6. Effect of anti-K polyclonal concentration on efficacy; (a) at stock solution, (b) double stock concentration by volume, and (c) quadruple stock concentration by volume.

Testing for blood group k typing using a monoclonal IgM antibody was straightforward. Much like the Rh groups, results for both the elution and text reporting methods were clear. For the elution method, positive and negative ODR was 6.4 ± 1.5 and 1.5 ± 0.25 , respectively. Density results for text-reporting method were 131 ± 8.3 and 31 ± 5.0 for positive and negative respectively (Table 2 and Figure 3).

4.2.6.3 Duffy Blood Group System

Unlike the anti-K antibody reagent, Duffy antibodies, anti-Fya and Fyb, are not available as IgM. Polyclonal Duffy antibody reagents are predominantly IgG[1]. No optimization techniques could achieve clear results as positives reported as (false) negatives. When reaction time was varied, despite an increased density for positive results, tests for negatives showed an equal increase in density. Attempts to duplicate the improved results seen when the concentrating the polyclonal anti-K were unsuccessful for both anti- Fya and Fyb. All results were negative, showing the inability of IgG antibodies to form RBC agglutinates retainable within paper. The antibody structure (IgM versus IgG) is crucial for successful identification.

4.2.6.4 Kidd Blood Group System

The Kidd blood groups studied are Jka and Jkb. The corresponding typing reagents are available as monoclonal IgM antisera, and generally showed a clear distinction between positive and negative results. However, the BS achieved was not as defined as desired, requiring optimization. Extending reaction time improved results. Reaction time of 120s was determined for group Jka (ODR pos: 8.3 ± 2.7 , neg: 1.2 ± 0.13 ; pos: 95 ± 6.2 , neg: 37 ± 4.8 ; elution and text-reporting methods, respectively) and Jkb (ODR pos: 6.8 ± 1.8 , neg: 2.9 ± 1.2 ; pos: 122 ± 10 , neg: 34 ± 6.2 ; elution and text-reporting methods, respectively). Both elution and text-reporting results were accurate.

4.2.6.5 MNS Blood Group System

Paper testing for the M, N, S and s antigens was unsuccessful for both methods. The M and N blood groups often reported falsely as 'weak' positives. Numerical data are available in table 3.

Table 3. Results achieved for the MNS blood system using the Elution (E) and Text reporting (TR) methods on paper. Blood spot (BS) and elution pathway (EP) are represented as density. Optical density ratio (ODR) compares density EP:BS. Positive is denoted by high density and ODR, negative has lower densities and ODR.

<i>Antigen</i>	M		N		S		s		
<i>Antibody type</i>	IgM		IgM		IgM		IgM		
<i>No. of samples</i>	54		39		54		8		
<i>Reaction time (s)</i>	30		30		30		30		
<i>Buffer</i>	NaCl		NaCl		NaCl		NaCl		
<i>No. of samples</i>	+	−	+	−	+	−	+	−	
	34	20	20	19	40	14	7	1	
	BS	90±7.0	66±6.6	107±7.8	90±8.6	76±5.8	73±6.0	43±2.6	45
	EP	44±6.4	42±5.9	23±4.0	38.0±5.1	44±5.9	48±8.4	39±4.0	30
<i>Elusion method</i>	ODR	2.1±0.29	1.6±0.10	4.8±0.73	2.5±0.4	1.7±0.17	1.6±0.36	1.1±0.16	1.5
<i>Text method</i>		66±16	96±9.3	96±18	86±25	72±12	42±5.1	N/A	N/A

4.2.6.6 P Blood Group System

P1 antigen was tested using a monoclonal IgM antibody. Like the C and E antigens, no special optimization was required. The results were clear and easy to distinguish between positive and negative results for both elution and text-reporting (pos: 12±1.9, neg: 1.7±0.63 ODR; pos: 140±5.7, neg: 31±5.5 S respectively) (Figure 3a and b).

4.2.6.7 Lewis Blood Group System

Testing the Lewis blood system revealed the importance of the antibody solution composition. Unlike other blood groups, testing with anti-Lea and anti-Leb, showed anomalous patterns using the elution method. Rather than displaying a clear BS or EP, the blood dispersed irregularly with important tailing (Figure 7). This is likely due to potentiators, such as dextran, often added to formulation. Potentiators, consisting of polymers, are often used to enhance the extent of RBC agglutination for low potency antibodies. Potentiators can become problematic for paper tests should they non-specifically retain individual RBC on paper. Instead of absorbing into paper, the antibody solution created a film above the surface, affecting elution and causing irregular dispersion. There was no distinction between positive and negative. The irregular dispersion pattern in paper caused by potentiators was confirmed using “For Further Manufacturing Use” (FFMU) anti-Lea, the raw material without potentiators.

However, the FFMU anti-Lea was still unsuccessful for distinguishing positive or negative, due to the lack of potentiators to affect agglutination.

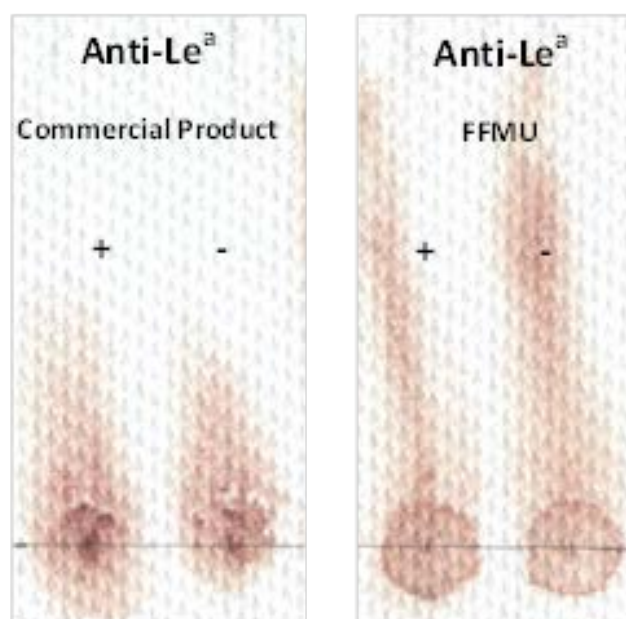


Figure 7. Dispersion difference between the commercial product and FFMU antibody Lea.

Unlike the elution method, the flow through method distinguished both positive and negative samples. This is due to directionality and the strength of washing, unaffected by potentiators. The perpendicular washing allowed the saline solution to flow through paper and filtrate, rather than eluting RBCs. Instead, unbound cells could flow through paper. Colour density for Lea and Leb using the text-reporting method were pos: 68 ± 3.1 , neg: 35 ± 6.2 ; and pos: 116 ± 5.9 , neg: 37 ± 6.2 , respectively.

4.2.6.8 Perspective

More than half of the clinically significant blood group phenotypes explored within this study were successfully optimised; the exceptions being Fya, Fyb, S and s. This demonstrates the potential for paper biodiagnostics as a viable alternative for blood group phenotyping. Both testing methods are unique and designed for varying purposes. Successful results for the elution method were more definitive than the flow-through method, better designed for high throughput testing. Meanwhile, the flow-through method is ideal for point-of-care testing, especially in remote areas or developing

countries. Although in-field testing is unlikely to achieve standard laboratory conditions for temperature and humidity, paper blood typing diagnostics would still provide a cheap, fast and easy to use alternative to current conventional blood grouping methods.

4.2.7 CONCLUSION

Two paper methods - an elution and a flow through direct-reporting method – were investigated to determine the blood group phenotype of red blood cells. Clinically significant antigens tested include C, c, E, e, K, cellano (k), Fya, Fyb, Jka, Jkb, S and s antigens. The M, N, P1, Lea and Leb antigens were also tested. As each group behaved differently, optimization for each antigen was required. This optimization was achieved by controlling the main variables: antibody-antigen reaction time, antibody concentration and changing the washing buffer solution. Antibody class is of the utmost importance on paper. Most antigens with antibodies available as IgM monoclonal antisera were successful with both paper methods (Rh, K (IgM), k (Cellano), Kidd, P1), though to varying degrees of clarity. Testing with polyclonal antisera was unsuccessful (K and Duffy). Unexpectedly, increasing the antibody concentration of polyclonal anti-K showed a discernible difference between positive and negative results; this was due to increasing the concentration of IgM component. Results were not replicated using polyclonal Duffy antibodies (IgG). Increasing reaction time between antibody and antigens (RBC) showed increased clarity with both methods, while changing washing solution improved testing using the flow-through method. The formulation of the antibody solution is also an important variable for paper testing; any additive able to non-specifically bind RBC to paper affects test sensitivity; this was observed with the Lewis antibodies.

While successful detection was achieved with most IgM antibodies, except Lewis, M, N and S, using both paper assays, polyclonal antibodies, consisting predominantly of IgG, resulted in inconsistent results.

4.2.8 ACKNOWLEDGEMENTS

ARC LP110200973, Haemokinesis and Monash University for funding and D. Bashforth for discussion.

4.2.9 REFERENCES

- [1] D.M.Harmening, Modern blood banking and transfusion practices. 4th Edition ed. 1999, Philadelphia: F.A. Davis.
- [2] G. Daniels, I. Bromilow, Essential Guide to Blood Groups, 2007, Wiley-Blackwell: Hoboken.
- [3] G. Daniels, M.E. Reid, Blood groups: the past 50 years, *Transfusion*, 2010, **50**(2): 281-289.
- [4] G. Daniels, Human blood groups. 2008: John Wiley & Sons.
- [5] N. D. Avent, M. E. Reid, The Rh blood group system: a review, *Blood*, 2000, **95**(2): 375-87.
- [6] C.M. Westhoff, The Rh blood group system in review: A new face for the next decade, *Transfusion*, 2004, **44**(11): 1663-1673.
- [7] B. Thakral, et al., Phenotype frequencies of blood group systems (Rh, Kell, Kidd, Duffy, MNS, P, Lewis, and Lutheran) in north Indian blood donors, *Transfusion and Apheresis Science*, 2010, **43**(1): 17-22.
- [8] W. Malomgré, B. Neumeister, Recent and future trends in blood group typing, *Analytical and Bioanalytical Chemistry*, 2009, **393**(5): 1443-1451.
- [9] R. Pelton, Bioactive paper provides a low-cost platform for diagnostics, *Trends in Analytical Chemistry*, 2009, **28**(8): 925-942.
- [10] M.S. Khan, et al., Paper Diagnostic for Instantaneous Blood Typing, *Analytical Chemistry*, 2010, **82**(10): 4158-4164.
- [11] M. Al-Tamimi, et al., Validation of Paper-Based Assay for Rapid Blood Typing, *Analytical Chemistry*, 2011, **84**(3): 1661-1668.
- [12] M. Li, et al., Paper-Based Blood Typing Device That Reports Patient's Blood Type "in Writing", *Angewandte Chemie International Edition*, 2012, **51**(22): 5497-5501.
- [13] X. Li, J. Tian, W. Shen, Paper as a Low-Cost Base Material for Diagnostic and Environmental Sensing Applications in Appita Conference and Exhibition 2009, Appita Inc.: Melbourne, 267-271.
- [14] D. Ballerini, X. Li, W. Shen, Patterned paper and alternative materials as substrates for low-cost microfluidic diagnostics, *Microfluidics and Nanofluidics*, 2012, **13**(5): 769-787.
- [15] J. Su, M. Al-Tamimi, G. Garnier, Engineering paper as a substrate for blood typing bio-diagnostics, *Cellulose*, 2012, **19**(5): 1749-1758.
- [16] M.E. Reid, C. Lomas-Francis, M. L. Olsson, The blood group antigen factsbook. 2012: Academic Press.
- [17] L. Li, et al., A study of the transport and immobilisation mechanisms of human red blood cells in a paper-based blood typing device using confocal microscopy, *Analyst*, 2013, **138**(17): 4933-4940.
- [18] P. Jarujamrus, et al., Mechanisms of red blood cells agglutination in antibody-treated paper, *Analyst*, 2012, **137**(9): 2205-2210.

[19] M. Li, et al., Paper-based device for rapid typing of secondary human blood groups, *Analytical and bioanalytical chemistry*, 2014, **406**(3): 669-677.

Chapter 5

*Paper-based device for environmental sensing by
text-reporting*

This page is intentionally blank

Text reporting as a novel communication method between sensors and users provides a platform concept for low-cost diagnostics and analytical devices. In previous chapters, the demonstration of this concept for making blood typing devices has highlighted its advantages over conventional colorimetric and electrochemical methods in delivering analytical results that can be understood by non-professional users. Clearly, the text-reporting concept can be further expanded beyond blood typing, and one of the promising applications is environmental monitoring.

In this chapter, a new paper-based microfluidic device (μ -PAD) for monitoring heavy metal ions in water via text messages is presented. This device was fabricated using letter-based microfluidics and it can report the presence and safety threshold of heavy metal ions in water simultaneously by displaying the chemical symbols of the target heavy metal ions. The device is a novel “periodic table-style” paper device. To prove this concept, Cu(II), Cr(VI) and Ni (II) were chosen as examples and were tested on this newly designed device. The reliability, sensitivity and selectivity were all shown to meet the general requirements of legislated water quality guidelines.

This page is intentionally blank

Monash University

Declaration for Thesis Chapter 5

Declaration by candidate

In the case of Chapter 5, the nature and extent of my contribution to the work was the following:

Nature of contribution	Extent of contribution (%)
Initiation, key ideas, experimental works, analysis of results, writing up	60

The following co-authors contributed to the work. If co-authors are students at Monash University, the extent of their contribution in percentage terms must be stated:

Name	Nature of contribution	Extent of contribution (%) for student co-authors only
Rong cao	experimental works, analysis of results, editing of the paper	30
Azadeh	Assisted in experimentation	5
Xiwang Zhang	reviewing and editing of the paper	Co-supervisor
Wei Shen *	Key ideas, reviewing and editing of the paper	Supervisor

The undersigned hereby certify that the above declaration correctly reflects the nature and extent of the candidate's and co-authors' contributions to this work*.

Candidate's Signature

		Date 03-03-2015
--	--	---------------------------

Main Supervisor's Signature

		Date 04-03-2015
--	--	---------------------------

*Note: Where the responsible author is not the candidate's main supervisor, the main supervisor should consult with the responsible author to agree on the respective contributions of the authors.

This page is intentionally blank

“Periodic-table-style” paper device for monitoring heavy metals in water

*Miaosi Li, Rong Cao, Azadeh Nilghaz, Liyun Guan, Xiwang Zhang and Wei Shen**

Australian Pulp and Paper Institute, Department of Chemical Engineering,
Monash University, Clayton Campus, Vic. 3800, Australia

*Corresponding Author 

This paper has been published in *Analytical Chemistry*

5.1 ABSTRACT

If a paper-based analytical device (μ -PAD) could be made by printing indicators for detection of heavy metal ions in chemical symbols of the metals in a style of the periodic table of elements, it could be possible for such μ -PAD to report the presence and the safety level of heavy metal ions in water simultaneously and by text message. This device would be able to provide easy solutions to field-based monitoring of heavy metal ions in industrial wastewater discharges and in irrigating and drinking water. Text-reporting could promptly inform even nonprofessional users of the water quality. This work presents a proof of concept study of this idea. Cu(II), Ni(II), and Cr(VI) were chosen to demonstrate the feasibility, specificity, and reliability of paper-based text-reporting devices for monitoring heavy metal ions in water.

5.2 KEYWORDS

Heavy metals, periodic-table-style, paper sensor, on-site water monitoring, lay users.

5.3 INTRODUCTION

Water contamination is one of the most serious environmental problems facing the world today. The increasing human activities and rapid industrializations are

introducing a huge amount of pollutants into the environment, which will undoubtedly contaminate natural water bodies and put human health and ecosystems at risk [1]. Among various pollutants, heavy metal ions are always one of big concerns due to their severe toxicities so that they have been included in “Blacklist” by the United States Environmental Protection Agency (U.S. EPA) [2]. When these heavy metal ions enter into the human body, they could easily bind to vital cellular components and accumulate in organisms, resulting in a series of diseases and disorders (e.g., cancers, osteomalacia, kidney malfunction, etc.) [3,4]. As the first step of water pollution prevention, accurate and rapid monitoring of the heavy metal ions is vital. Ideally monitoring methods are expected to identify point sources of pollutants and the variation of nonpoint sources of pollutants in the environment.

Several methods are widely used for identification and quantification of heavy metal ions, including colorimetry, atomic absorption spectroscopy (AAS), inductively coupled plasma atomic emission spectroscopy (ICP-AES), inductively coupled plasma mass spectroscopy (ICPMS), and so on [5-7]. Although these methods are capable of achieving highly sensitive detection, identification and quantification of heavy metal ions, they always require the support of well-equipped laboratories and skilled operators, which can be very expensive. Therefore, alternative and inexpensive methods are in demand for field-based or on-site water monitoring by personnel with limited training or even unskilled home-users.

Patterned paper, as a platform technology for making low-cost and user-operated analytical devices, offers a possibility to construct new heavy metal sensors that meet the abovementioned desirable features. Patterned paper has been used to make sensing devices for disease screening, point of care (POC), pathogen and biomarker detection, and food and water quality testing [8-15]. In environment monitoring, research works using paper-based microfluidic devices have, to date, demonstrated the possibility of providing quantification of heavy metal ions, including Cu, Cd, Hg, Pb, Cr(VI), Ni, etc. [18-23]. These works provide a new approach to monitor heavy metal ions in water in situations where designated laboratories are not available. However, the assay procedures and result interpretation (involving colorimetric or electrochemical signals) cannot be easily followed and understood by untrained or home users without

professional assistance. Besides the high sensor sensitivity and specificity, high portability, rapid detection, and easy result interpretation are highly desirable performance features for new sensing devices. Most recently, researchers have demonstrated that paper-based sensors can be designed to communicate assay results with users via text message, removing errors in assay result interpretation [16,17].

One imaginative way to significantly improve the performance of a future paper-based sensor in detecting, quantifying, and reporting heavy metal ions in water could be to print the chemical symbols of heavy metal ions with their corresponding and specific indicator systems in a format of the periodic table of elements. Testing of heavy metal ions in water would simply involve dipping the paper sensor in water, the sensor could then reveal the testing results if the concentrations of heavy metal ions are higher than legislated standards by showing the chemical symbols of the heavy metal ions present in water. Such a chemically responsive periodic-table-style paper sensor could be designed to not only provide qualitative answers of what is the water but also provide quantitative (i.e., safe-to-use) information on the heavy metal ions in water.

Following this idea, we demonstrate the feasibility of paper-based heavy metal sensors, capable of reporting text messages to users if heavy metal concentrations in water reach a legislated unsafe level. We “print” indicator systems for target heavy metal ions on a patterned paper in chemical symbols of the target metals. This concept can promptly inform even nonprofessional users with clear and unambiguous written warnings against unsafe water. We also demonstrate another use of the same indicator systems to quantify heavy metal concentrations in water. This will enable environmental workers to obtain reliable semiquantitative heavy metal analysis under non-laboratory conditions and at low-cost.

An ideal paper-based heavy metal sensor for text-reporting has to meet the following performance requirements. First of all, the indicator must be sensitive and form the specific complex with the metal ion to be detected and shows a distinctive colour. Second, the indicator system as well as the indicator-metal complex must not be easily leachable into water. Third, the non-detection area of the sensor must be water-repellent. On the basis of these requirements, we chose Cu(II), Cr(VI), and Ni(II) as

model heavy metal ions to demonstrate our idea. The indicator systems for these heavy metal ions meet the above requirements reasonably well.

5.4 EXPERIMENTAL

5.4.1 Materials and apparatuses

The paper substrate employed in this study was chromatography 1# paper manufactured from WhatmanTM (GE Healthcare UK Limited) and the wax for coating the paper was a “Paraffin Wax50 FRJ” purchased from Dussek Campbell Pty.Limited, Australia. Reagents including sodium chloride (NaCl), potassium chloride (KCl), calcium chloride dehydrate ($\text{CaCl}_2 \cdot 2\text{H}_2\text{O}$), magnesium sulphate (MgSO_4), cobalt chloride (CoCl_2), copper sulphate (CuSO_4), hydroxylammonium chloride ($\text{H}_3\text{NO} \cdot \text{HCl}$), glacial acetic acid (CH_3COOH), bathocuproine, chloroform, PEG 400, 1,5-diphenylcarbazine, sulfuric acid (H_2SO_4), acetone, potassium dichromate ($\text{K}_2\text{Cr}_2\text{O}_7$), dimethylglyoxime, ethanol, nickel chloride (NiCl_2), sodium fluoride (NaF), sodium thiosulfate ($\text{Na}_2\text{S}_2\text{O}_3$), iron chloride (FeCl_3), and zinc sulphate (ZnSO_4) were all analytical-grade and purchased from Sigma-Aldrich. Manganese Chloride tetrahydrate ($\text{MnCl}_2 \cdot 4\text{H}_2\text{O}$) was analytical-grade and purchased from MERCK. MilliQ water was used throughout this experiment unless the tap water was mentioned for the real environmental sample testing. Epson photo scanner 2450 was used to capture the colorimetric signals with 600 dpi and Photoshop CS6 was used to measure the colour intensity of each colour spot. The ICP-AES method for measuring the pseudo-environmental samples was conducted by the Optima 7000 DV from PerkinElmer.

5.4.2 Methods

Before fabrication on paper, chemical symbols of Cu, Cr and Ni was generated by Microsoft Word with font of “Ariel Black” and size of “31”, as is shown in Figure 1. The average width of each channel is approximate 2.5 mm, and in the experiment, 10 μL of liquids are adequate for penetrating into each channel.

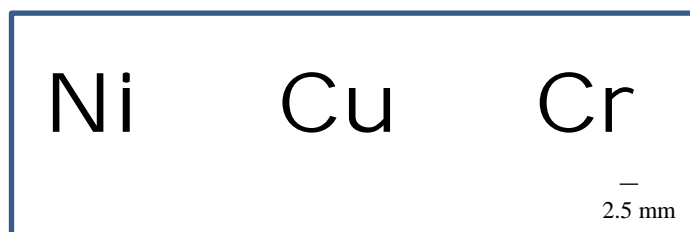


Figure 1. The electronically generated chemical symbol patterns of the three heavy metal ions in their true size.

Chromatography no. 1 paper was employed to pattern the chemical symbols of Cu, Cr, and Ni by means of generating hydrophilic and hydrophobic boundaries on paper. Computer-generated chemical symbols were first printed on office paper and then soaked in molten wax. After wax treatment, the office paper was allowed to cool down to room temperature. The letters on the wax-loaded office paper was then cut out, forming the cut-out pattern. This office paper was then put on to a piece of chromatography paper and heated with an electric iron, and the wax was transferred to the chromatography paper to form hydrophilic symbols of Cu, Cr, and Ni, surrounded by wax [24]. The so-patterned chromatography paper was the final patterned substrate for further construction of the analytical devices. Figure 2 shows the process of fabrication of the patterned chromatography paper. Indicator systems were then added into the chemical symbols of the metals to make the device active.

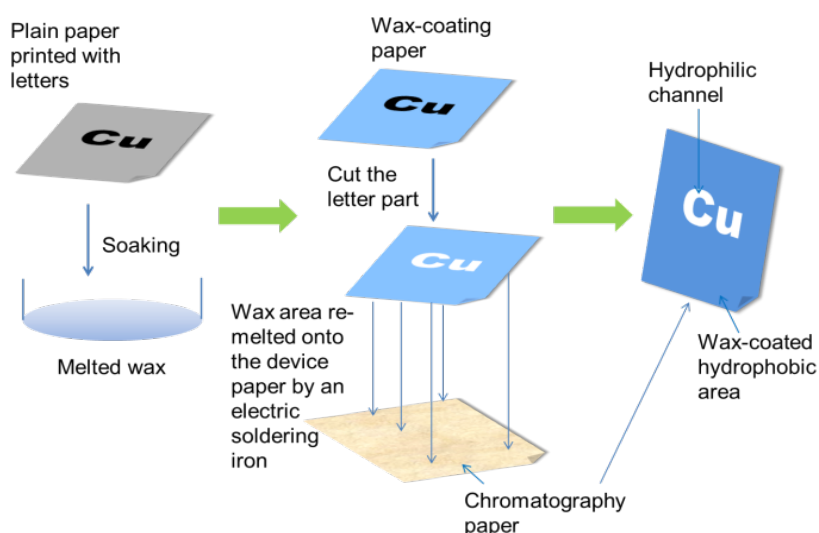


Figure 2. Schematic diagram of the fabrication of patterns of heavy metal chemical symbols on chromatographic paper.

5.4.3 Indicator solution concentration

These three heavy metal ions are identified via the colorimetric assays of metal ions and their specific indicators. When Cu(II) is reduced to Cu(I) by hydroxylamine, Cu(I) forms an orange chelate with its indicator bathocuproine. Similar to the copper assay, the reduced metal ion Cr(III) from Cr(VI) forms a purple complex with indicator 1,5-diphenylcarbazine under acidic condition. As for the determination of Ni(II), a pink-magenta chelate is produced through the interaction between Ni(II) and its indicator dimethylglyoxime. The concentrations of indicators were reported to have influences to the sensitivity and clarity of colorimetric assay for detection of the heavy metal ions. According to the reported concentrations of indicators previously in studies of Cu(II) [21], Cr(VI) [19] and Ni(II) [23] analyses using sensors made of paper and other substrates, therefore, in our work, a preliminary study was carried out to understand the influence of indicator concentrations to heavy metal assay results through the colorimetric assays of these three metal ions. As are shown in Figure 3, different concentrations of the indicators

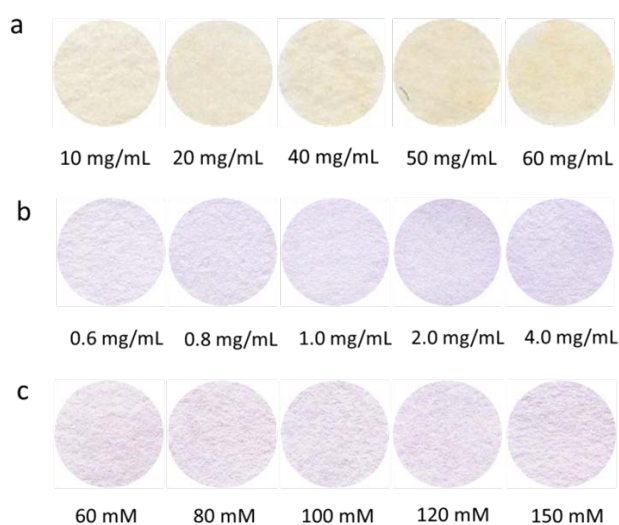


Figure 3. Colorimetric assay for the selection of indicator concentrations: a) bathocuproine concentration from 10 to 60 mg/mL for detection of 1.0 mg/L Cu(II) sample; b) 1,5-diphenylcarbazine concentration from 0.6 to 4.0 mg/mL for detection of 0.5 mg/L Cr(VI) sample; c) dimethylglyoxime concentration from 60 to 100 mM for detection of 1 mg/L Ni(II) sample.

were used to test the three heavy metal ions to evaluate the sensitivity of different concentrations. The heavy metal concentrations in these tests were fixed at 1.0 mg/L,

0.5 mg/L and 1.0 mg/L for Cu(II), Cr(VI) and Ni(II), respectively. For all the three metals, concentrations of the indicators in the selected range were capable to identify the ions clearly, and very small differences on the colour clarity and intensity were observed. The results show that the concentration of each indicator in this range is sufficient for the identification of the heavy metal ions. Therefore during the main experiments of this work, the concentration of the indicators were chosen as 50 mg/mL bathocuproine for Cu(II) assay, 1.0 mg/mL 1,5-diphenylcarbazide for Cr(VI) assay and 80 mM dimethylglyoxime for Ni(II) assay.

5.5 RESULTS AND DISCUSSION

5.5.1 Testing results

Cu(II) is one of the most common heavy metal ions in water, and according to the Australian drinking water guidelines for fresh and marine water quality, Cu concentration in drinking water must not be higher than 1 mg/L [25]. Also, the Australian and New Zealand guidelines for fresh and marine water quality set the standard of Cu(II) in water for irrigation and livestock drinking between 0.2 mg/L (long-term use) and 5 mg/L (short-term use) [26]. To fabricate a text-reporting Cu(II) sensor, a 10 μ L aliquot of hydroxylamine (0.1 g/mL) in acetic buffer (6.3 M, pH 4.3) was first added into the letter channel. In total, 50 mg of bathocuproine was dissolved in 1 mL of chloroform as the indicator for Cu, and 40 mg PEG 400 was also added into this solution to prevent the detection channel from becoming hydrophobic [20]. Before the addition of each solution, the paper device was air-dried for 10 min. Cu(II) forms Cu-bathocuproine complex which has an orange to brown colour; the complex is not highly soluble in water.

In a Cu(II) assay, the formation of an orange to brown Cu-bathocuproine complex became visible after 10 μ L aliquot of water sample containing higher than 0.8 mg/L Cu (II) was dropped onto the device, which displays the “Cu” symbol (Figure 4a). Otherwise, if Cu(II) concentration is below 0.8 mg/L, the symbol remains colourless. The use of 10 μ L of sample is that it just fills the symbol. The colour of the symbol became brighter as the copper concentration increases. This appearance of the “Cu”

symbol on the device informs users that Cu(II) concentration is higher than the drinking water standard. In practical use, the device can be simply dipped into a water sample to “read out” the result.

Hexavalent chromium, Cr(VI), is considered as a highly toxic heavy metal ion. A water system contaminated by Cr(VI) can be severely harmful to the environment and humans. For the chromium assay on the paper device, 1,5-diphenylcarbazide (DPC) was dissolved into 50% (v/v) acetone to make the 1 mg/mL solution. The solution was introduced into the “Cr” symbol on paper, followed by an addition of 1% H_2SO_4 . Under the acidic conditions, a magenta to purple complex will form when a 10 μL of Cr(VI) solution is added into the “Cr” symbol. Like the Cu(II) assay, the Cr(VI) assay showed a purple symbol of “Cr” when the Cr(VI) concentration exceeded 0.5 mg/L. By

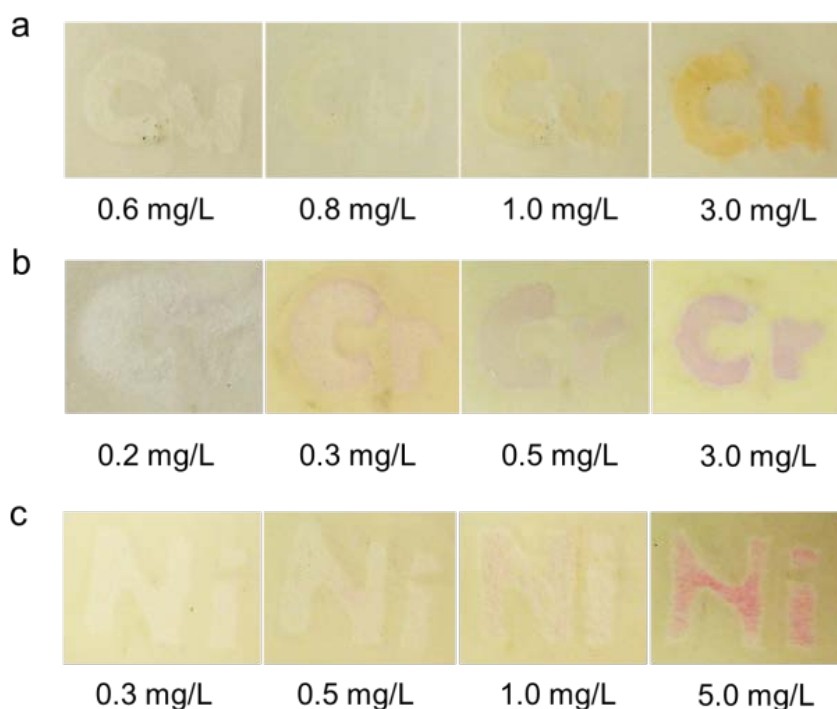


Figure 4. Colorimetric assays showing heavy metal ions of different concentrations: (a) Cu(II); (b) Cr(VI) and (c) Ni(II).

the Australian and New Zealand guidelines for fresh and marine water quality, the trigger value of Cr(VI) in the water resources for purpose of irrigation, livestock drinking and other industries is between 0.1 mg/L (long-term use) and 1 mg/L (short-term use) [26], the appearance of “Cr” on the paper (Figure 4b) warns the users against long-term use of the water for their industrial activities.

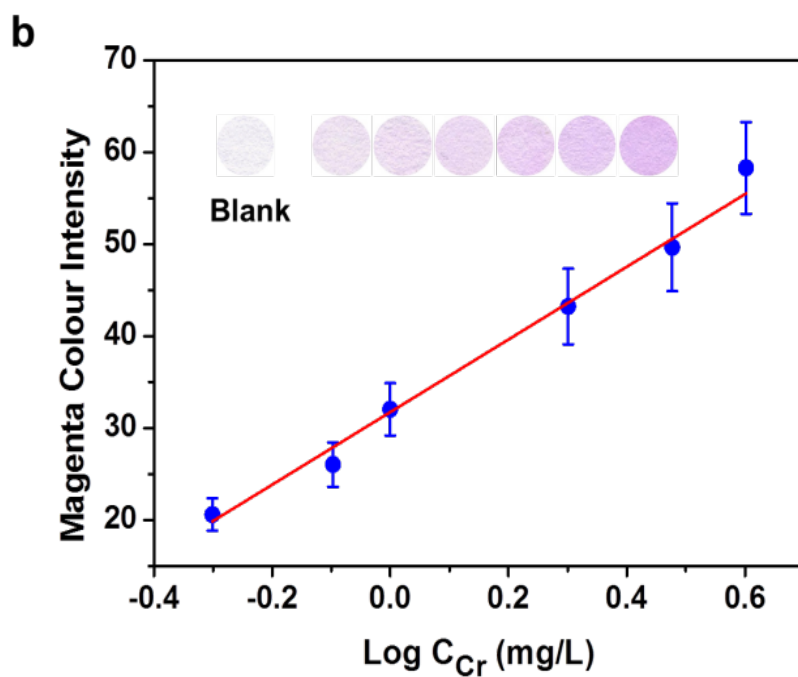
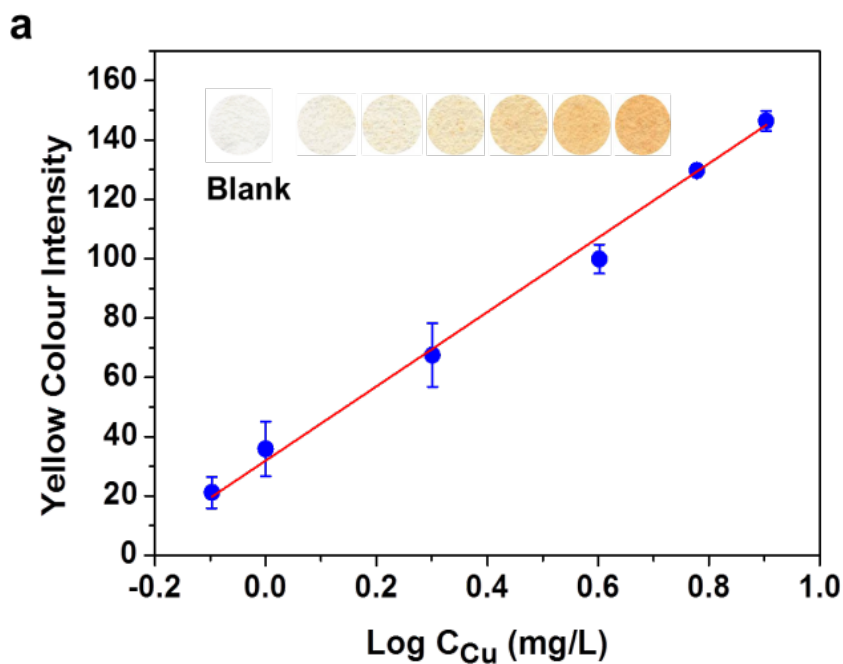
Nickel is another heavy metal which could enter into the water system through mining, manufacturing activities, and through leaching from e-wastes. For a Ni(II) assay, a 10 μL aliquot of dimethylglyoxime (DMG) dissolved in an ethanol solution (80 mM) was first introduced into the “Ni” symbol, followed by an addition of 10 μL of a solution of NaF and $\text{Na}_2\text{S}_2\text{O}_3$ dissolved in Milli-Q water (20 and 80 mg/mL, respectively). The latter solution was used for masking the interference of Cu(II) and naturally existing Fe(III) in water [19,20]. The Ni-DMG complex has a stable pink-magenta colour. When 50 μL of water sample containing ≥ 0.5 mg/L Ni(II) was introduced into the device, the symbol “Ni” became visible. Since the standard of Ni in the Australian and New Zealand guidelines for fresh and marine water quality is 0.2 mg/L (long-term use) or 2 mg/L (short-term use) [26], the appearance of the “Ni” symbol warns the users that the quality of the water is unsafe for long-term purpose (Figure 4c).

5.5.2 Interference study

5.5.2.1 Quantitative validation

To examine the interference tolerance of the paper assays, each metal ion, with and without the presence of interfering ions, was assayed on paper and compared. For this purpose, validation of quantitative information obtained from paper was first carried out using a colorimetric method. A series of solutions with known concentrations of the three heavy metal ions were prepared respectively, including the blank samples for each to get the background data for functionalized papers. Paper substrate was cut into small square pieces to the size of 1 cm \times 1 cm; the assay procedures were the same as the procedures for the text-reporting assays. After finishing the metal identification, a scanner was used to capture the images of the paper squares. The images were then analysed using Adobe Photoshop CS6 to determine the reflective colour density to establish calibration curves for quantification of target heavy metal ion in water: it was transferred to the CMYK model firstly; and then the closest colour to each colourimetric assay was chosen to measure colour intensity [4]. For the copper assay, yellow colour intensity was measured and magenta colour intensity was obtained for the chromium and nickel assays. The colour intensity significantly increases with the increasing of the concentration for each ion. The colour density difference between each heavy metal detection zone and that of the corresponding blank was calculated

and plotted again the heavy metal concentration of the sample to obtain the calibration curve for the metal. Linear curves were fitted for the colour intensity with the logarithm concentration of copper (Figure 5a) and chromium (Figure 5b), and the direct concentration of nickel (Figure 5c). The correlation coefficient R^2 for Cu, Cr and Ni were 0.9936, 0.9840 and 0.9954, respectively.



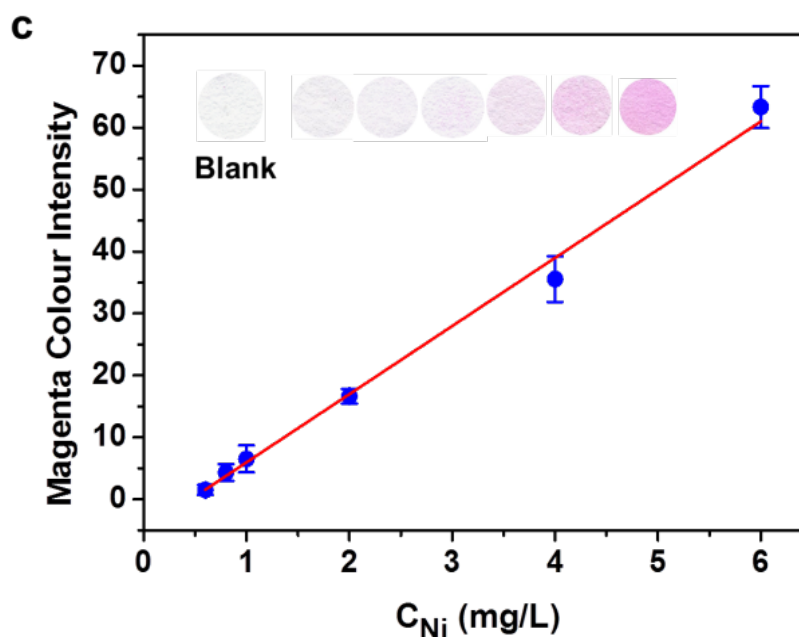


Figure 5. Calibration curves fitted by the measured colour intensity versus the concentration of each ion: a) Copper, concentration from 0.8 to 8 mg/L; b) Chromium, from 0.5 to 4 mg/L; c) Nickel, from 0.6 to 6 mg/L.

5.5.2.2 Interference

The calibration curves obtained in the quantitative validation study (Figure 5) were then used to determine the paper devices' interference tolerance, the results were then compared with those obtained using an ICP-AES. Specifically, for examining interference tolerance of Cu assay on paper, sample solutions containing Cu(II) as the target ion and higher concentrations of Ni(II), Cr(VI), Fe(III), and Zn(II) as interfering ions were prepared. Similar procedures were used to evaluate the interference tolerance of Cr(VI) and Ni(II) assays. Our results show that interfering ions of 10 times the concentration of the target ions do not affect the assay results (Figures 6a-c). Interesting also, assays showed no colour change to samples that contained only interfering ions but no target ions (Figure 6d). Furthermore, other interfering metal ions such as Mn(II) and Co(II) which have similar atomic structure to the target ions as well as Na(I), K(I), Ca(II), and Mg(II), which can exist in high concentrations from some water sources, have also been studied. Results show that interfering ions Na (I) and K(I) of 200 times, Ca(II) and Mg(II) of 100 times, and other transition ions of 10 times the concentration

of 1 mg/L target ion do not affect the assay results (Figure 7). The interference tolerance ratio of different ions when determining 1 mg/L Cu(II), Cr(VI), and Ni(II) is presented in Table 1.

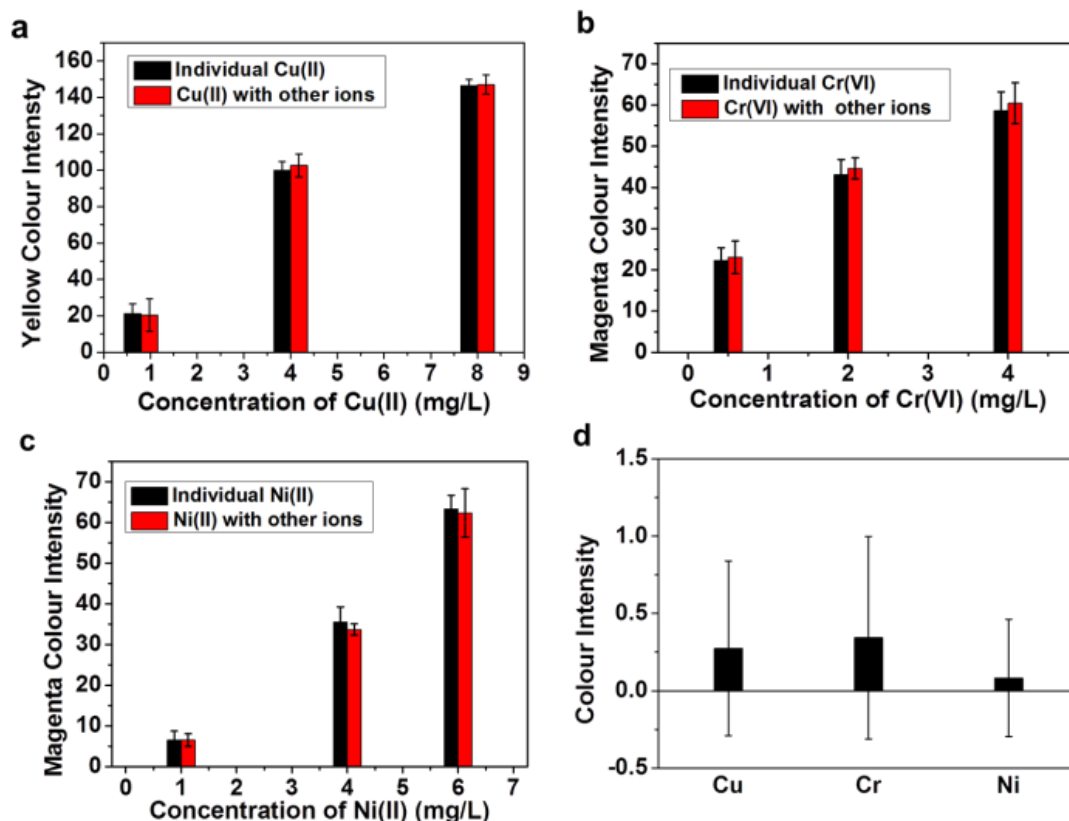


Figure 6. Interference tolerant studies of the paper devices for the three target heavy metal ions in the presence of Cu(II), Cr(VI), Ni(II), Fe(III) and Zn(II) as interfering ions (5 parallel tests for each assay): a) Cu(II) assays of 0.8, 4 and 8 mg/L of Cu(II); b) Cr(VI) assays of 0.5, 2 and 4 mg/L Cr(VI); c) Ni(II) assays of 1, 4 and 6 mg/L of interfering ions; d) The responses of the Cu(II), Cr(VI) and Ni(II) indicator systems to non-target multiple interferent ions solutions. For assays in a) to c), the concentration of each interfering ion was 10 times higher than that of the target ion. For assays in d), samples contained no target ions; the concentrations of all non-target metal ions were 10 mg/L.

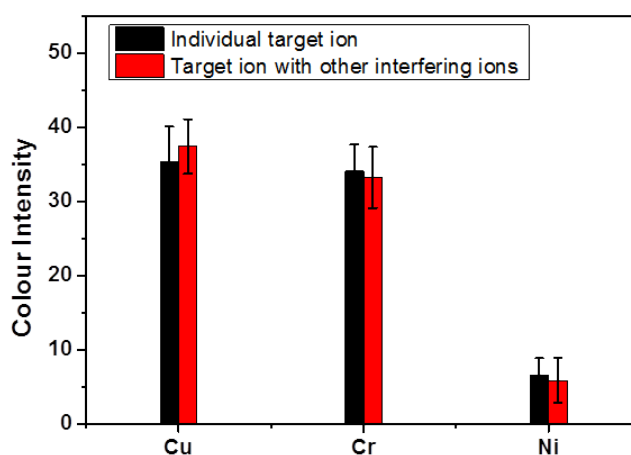


Figure 7. Interference tolerant studies of the paper devices for the three target heavy metal ions in the presence of 10 mg/L Cr (VI), Mn(II), Fe(III), Co(II), Ni(II), Zn(II) for 1 mg/L Cu(II) assay; 10 mg/L Mn(II), Fe(III), Co(II), Ni(II), Cu(II), Zn(II) for 1.0 mg/L Cr(VI) assay; 10 mg/L Cr (VI), Mn(II), Fe(III), Co(II), Cu(II), Zn(II) for 1 mg/L Ni(II) assay, and 200 mg/L Na(I) and K(I), 100 mg/L Ca(II) and Mg (II) for all the three assays.

5.5.3 Pseudo-environmental sample analysis

Pseudoenvironmental samples were prepared to demonstrate the applicability of the paper device for practical water quality monitoring. Tap water from our laboratory was spiked with two different known levels of Cu(II), Cr(VI), and Ni(II) and was then used for determination of the three heavy metal ions. On the one hand, the target ion concentrations were measured using paper squares; images of the paper assays were collected to obtain the colour intensity information using the software; and the concentration of each heavy metal was calculated by means of the best-fitting equation of the corresponding calibration curve (Figure 5). Here paper squares were used to obtain error bar information; text-reporting devices were also used, and results obtained were in good agreement with the paper squares. On the other hand, ICP-AES was used to measure the same samples to compare results with the paper-based assays. Figure 8 shows the determination of Cu(II), Ni(II), and Cr(VI) in tap water with multiple ions by paper-based assays and ICP-AES with 5 parallel tests, respectively. The paper-based assays show a mean error within 10% against results obtained by ICP-AES. The recovery rate of the spiked water samples obtained using our paper device and ICP-AES were compared (Table 2). Data in Table 2 suggested the reliable feasibility

(within 10% error for sample 1 and 5% error for sample 2) of the paper device as a rapid and user-friendly semiquantitative device for environmental monitoring.

Table 1. Tolerance ratio of interference ions for detection of 1 mg/L Cu(II), Cr(VI) and Ni (II).

<i>Interfering ion</i>	<i>10% Tolerance ratio</i>		
	<i>Cu(II)</i>	<i>Cr(VI)</i>	<i>Ni(II)</i>
K(I)	200	200	200
Na(I)	200	200	200
Ca(II)	100	100	100
Mg(II)	100	100	100
Cr(VI)	10	/	10
Mn(II)	10	10	10
Fe(III)	10	10	10
Co(II)	10	10	10
Ni(II)	10	10	/
Cu(II)	/	10	10
Zn(II)	10	10	10

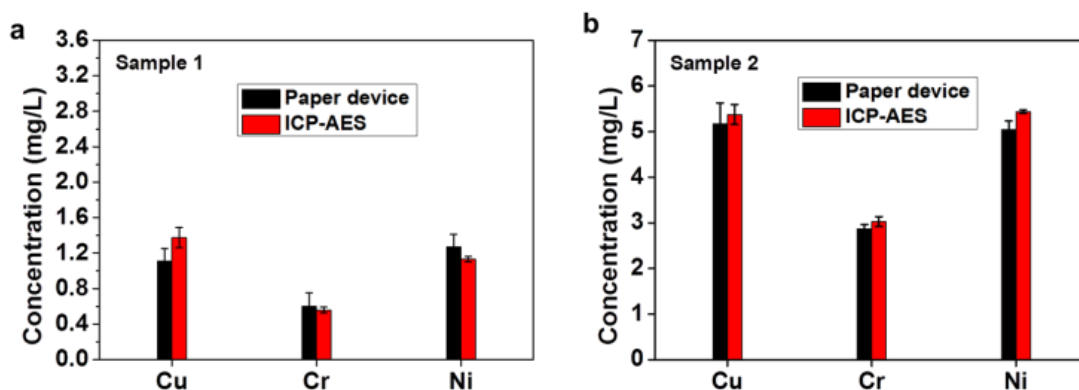


Figure 8. Pseudo-environmental samples analysed by paper-based devices and ICP-AES method: a) tap water with spiking of 1mg/L Cu(II), 0.5 mg/L Cr(VI) and 1mg/L Ni(II); b) tap water with spiking of 5 mg/L Cu(II), 3 mg/L Cr(VI) and 5 mg/L Ni(II).

Table 2. Recovery rate of spike water sample determined by paper device and ICP-AES

Tap water samples	Target ions	Detected ion concentration (mg/L) in non-spiked sample		Detected ion concentration (mg/L) in spiked sample		Spiked ion concentration (mg/L)	Recovery rate	
		Paper	ICP-AES	Paper	ICP-AES		Paper	ICP-AES
Sample 1	Cu(II)	ND*	0.042	1.11	1.38	1.0	111%	134%
	Cr(VI)	ND	0.002	0.55	0.53	0.5	110%	105%
	Ni(II)	ND	0.005	1.13	1.27	1.0	113%	126%
Sample 2	Cu(II)	ND	0.042	5.17	5.37	5.0	103%	106%
	Cr(VI)	ND	0.002	2.87	3.03	3.0	95.7%	101%
	Ni(II)	ND	0.005	5.04	5.44	5.0	101%	109%

* ND: Not detectable, referred as 0 when doing the recovery rate calculation.

Coming back to the periodic table sensor design concept, we fabricated the three chemical symbols on one paper device. We show in Figure 9 that an assay could be performed by simply dipping the device into a water sample and instantaneously obtain the result as a text message. However, we also noticed that while Cu(II) and Ni(II) form water insoluble chelates with their corresponding indicators and remain stable on paper, the colour product 1,5-diphenylcarbazone-Cr(III) or Cr(III)-DPCA complex is water-soluble and could not remain on paper stably. Thus, the Cu and Ni symbols were fabricated on the lower section of the device, whereas the Cr symbol was on the upper section (Figure 9a,b). The Cr(VI) assay requires a separate sample addition process to stop the leaching of the chelate into water (Figure 9c,d).

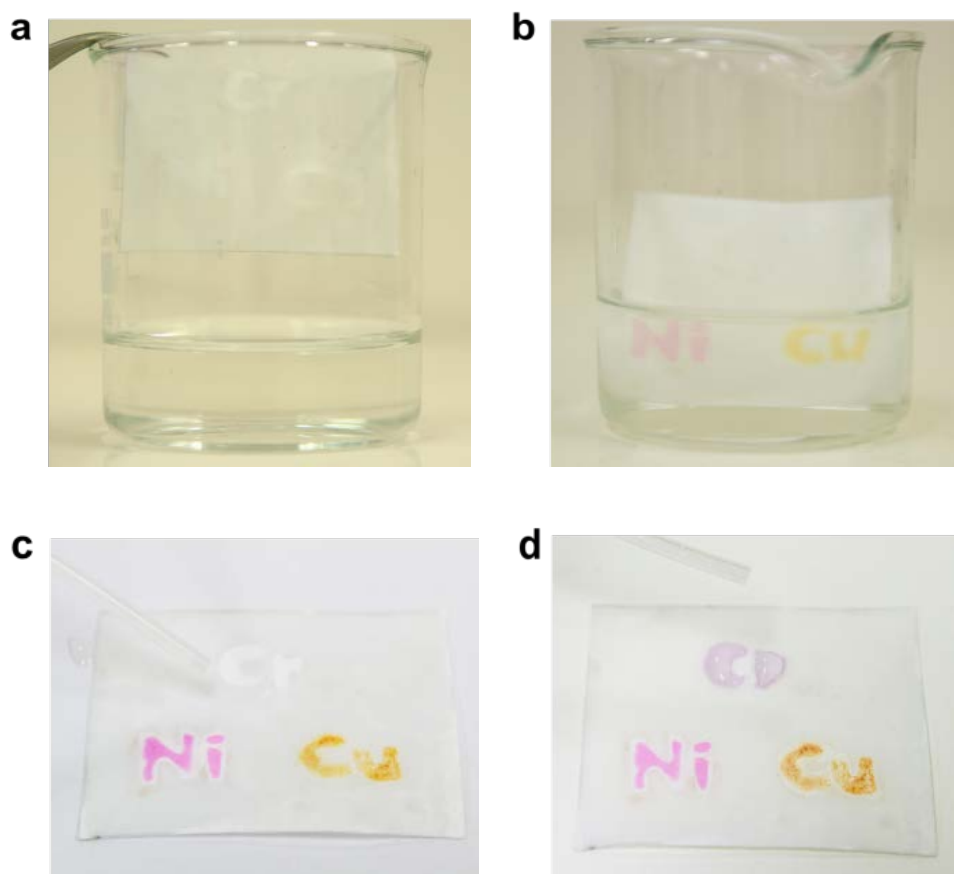


Figure 9. Text-reporting paper device for Cu(II), Ni(II) and Cr(VI) assay in a simulated environmental assay: tap water with striking of 5 mg/L Ni(II), 5 mg/L Cu(II), and 3 mg/L Cr(VI) respectively.

The stability of the three ion-indicator complexes has also been investigated: the Cu(I)-bathocuproine and Ni(II)-DMG complexes showed high stability; colours of these complexes showed no obvious fading after more than 6 months under the ambient laboratory conditions. The Cr(III)-DPCA complex faded significantly after 24 h in the same environment. The different stability of these ion-indicator complexes are related to the stability of the indicators: bathocuproine and DMG are stable compounds, while DPC is light-sensitive. The gradual decomposition of DPC under light is likely to be the cause of instability of the Cr(III)-DPCA complex.

5.6 CONCLUSION

As discussed above, an ideal periodic-table-style paper device for on-site heavy metal monitoring requires the indicator system, and the indicator-metal complex, to be stable and non-leachable by water. The Cu(II) and Ni(II) assays are the two systems that fulfil the requirements. A water sample assay for these two ions can be achieved by simply dipping the device in water; it suits well for Cu and Ni testing, and the results can be stored for a long period. However, the Cr(III)-DPCA complex requires further improvement of its stability. Protection of the DPC indicator and Cr(III)-DPCA complex against light exposure is necessary. It is possible that by significantly reducing the leaching of indicators and the metal ion-indicator complexes through further research, the concept of paper-based text-reporting sensor can be expanded to analyzing other heavy metal ions. It is also expected that an expansion of text-reporting paper sensors beyond this application may be possible in the future, not only for detection of other heavy metal ions but also for a wide range of chemical/biochemical analysis and sensing.

5.7 ACKNOWLEDGMENT

Funding received from Australian Research Council through grants DP1094179 and LP110200973 is gratefully acknowledged. The authors thank Mr. Baiqian Dai for his help with the ICP-AES tests and Dr Junfei Tian for discussions. Ms. Miaosi Li also thanks the Monash University Research and Graduate School and the Faculty of Engineering for postgraduate research scholarships.

5.8 REFERENCES

- [1] <http://www.ewast.com.au/electronic-waste-ewaste-landfill/>
- [2] K. Jomova, M. Valko, *Toxicology*, 2011, **283**: 65-87.
- [3] R. S. Boyd, *J. Chem. Ecol.*, 2010, **36**: 46-58.
- [4] N. Johri, G. Jacquillet, R. Unwin, *Biometals*, 2010, **23**: 783-792.
- [5] V. A. Lemos, A. L. Carvalho, *Environ. Monit. Assess*, 2010, **171**: 255-265.
- [6] D. J. Butcher, *Instrum. Sci. Technol*, 2010, **38**: 458-469.
- [7] J. Feldmann, P. Salaün, E. Lombi, *Environ. Chem.*, 2009, **6**: 275-289.
- [8] A.W. Martinez, S. T. Phillips, M. J. Buttle, G. M. Whitesides, *Angew. Chem. Int. Ed.*, 2007, **46**: 1318-1320.

- [9] A.W. Martinez, S. T. Phillips, E. Carrilho, S. Thomas, H. Sindi, G. M. Whitesides, *Anal. Chem.*, 2008, **80**: 3699-3707.
- [10] X. Li, J. Tian, W. Shen, *Anal. Bioanal. Chem.*, 2010, **396**: 495-501.
- [11] J. L. Delaney, C. F. Hogan, J. Tian, W. Shen, *Anal. Chem.*, 2011, **83**: 1300-1306.
- [12] R. Pelton, TrAC Trends, *Anal. Chem.*, 2009, **28**: 925-942.
- [13] M. S. Khan, G. Thouas, W. Shen, G. Whyte, G. Garnier, *Anal. Chem.*, 2010, **82**: 4158-4164.
- [14] Y. Sameenoi, P. Panymeesamer, N. Supalakorn, K. Koehler, O. Chailapakul, C. S. Henry, Volckens, *J. Environ. Sci. Technol.*, 2013, **47**: 932-940.
- [15] S. M. Z. Hossain, R. E. Luckham, M. J. McFadden, J. D. Brennan, *Anal. Chem.*, 2009, **81**: 9055-9064.
- [16] M. Li, J. Tian, M. Al-Tamimi, W. Shen, *Angew. Chem.Int. Ed.*, 2012, **51**, 5497.
- [17] M. Li, W. L. Then, L. Li, W. Shen, *Anal. Bioanal. Chem.*, 2014, **406**: 669-677.
- [18] S. M. Z. Hossain, J. D. Brennan, *Anal. Chem.*, 2011, **83**: 8772-8778.
- [19] H. Wang, Y. J. Li, J. F. Wei, J. R. Xu, Y. H. Wang, G. X. Zheng, *Anal. Bioanal. Chem.*, 2014, **406**: 2799-2807.
- [20] M. M. Mentele, J. Cunningham, K. Koehler, J. Volckens, C. S. Henry, *Anal. Chem.*, 2012, **84**: 4474-4480.
- [21] P. Rattanarat, W. Dungchai, D. Cate, J. Volckens, O. Chailapakul, C. S. Henry, *Anal. Chem.*, 2014, **86**: 3555-3562.
- [22] C. Sicard, J. D. Brennan, *MRS Bulletin*, 2013, **38**: 331-334.
- [23] A. Nilghaz, D. Ballerini, X. Fang, W. Shen, *Sens. Actuators: B. Chem.*, 2014, **191**: 586-594.
- [24] A. Nilghaz, D. Wicaksono, D. Gustiono, F. Majid, E. Supriyantob, M. Kadir, *Lab Chip*, 2012, **12**: 209-218.
- [25] The Australian government environmental guideline can be viewed or downloaded through the link below:
https://www.nhmrc.gov.au/_files_nhmrc/publications/attachments/eh52_aust_drinking_water_guidelines_update_131216.pdf
- [26] The Australian government environmental guideline can be viewed or downloaded through the link below:
<http://www.environment.gov.au/system/files/resources/e080174c-b267-455e-a8db-d3f79e3b2142/files/nwqms-guidelines-4-vol3.pdf>

Chapter 6

Conclusions and future work

This page is intentionally blank

This thesis has reported two original concepts, the text-reporting method and the sample-only method, both of which significantly enhance the user-friendly, equipment-free and delivered to users (UED) features of low-cost diagnostics. In a series of trials of blood typing and environmental sensing, these concepts have been shown to be highly desirable for professionals or non-professional users, and to meet the WHO's ASSURED criteria.

The direct and unambiguous text-reporting method is the major breakthrough of this thesis. The text-based information is fabricated using a combination of traditional paper sizing (i.e. hydrophobization) chemistry and industrial printing techniques. These fabrication approaches avoid the use of specific or high-capital tools, making the text-reporting method simple and affordable.

The text-reporting method enables the user to communicate with the sensor in a straight-forward manner, allowing untrained users to accurately and rapidly understand the result without professional assistance. It is also of great value to trained users who work in resource-limited situations. Text-reporting devices have potential applications in many areas of chemical and biological analysis, and can contribute to improving the quality of human life.

Because text-based sensors significantly reduce reliance on special equipment and professional personnel when performing an assay, the application of sensors to biomedical diagnosis can help to effectively relieve the pressures on hospitals in developing countries where medical facilities are scarce, and in developed countries where the problems of ageing populations are increasing rapidly. The text-reporting method will also contribute to the development of telemedicine, because the results can be easily stored and transmitted. Text-reporting based telemedicine is an effective solution to eliminate the barriers of distance and improve access to medical services that are often not available in remote rural communities.

The application of the text-reporting method to on-site environmental monitoring reported in this project can also help to improve people's health. On the one hand, the

general public can have easier access to water quality monitoring to satisfy the need of clean water for drinking, recreation and irrigation, which is very closely related to human physical well-being. On the other hand, since the device can provide environmental monitoring information immediately, the relevant government departments can make a much quicker response to contamination, natural disasters and major accidents. This quick response would significantly prevent problems from becoming more severe and threatening public health.

The second original contribution of this research is the concept of “sample-only”, which minimizes users’ efforts in performing a diagnostic assay. A sensor that requires complicated operation and reagent handling by the user usually demands user-training, equipment support and strict delivery conditions, which significantly reduce its adaptability to non-laboratory situations. Therefore, the second distinctive aspect of this research is that it simplifies user’s efforts in existing diagnostics. The “sample-only” method explored in this research effectively addresses the problem.

The sample-only concept is performed on inexpensive substrates such as glass and plastic slides. It enables the sensor to activate immediately upon the sample introduction and report the assay result in a rapid and easy-to-understand manner. Based on this concept, introducing the sample to the sensor is the only effort required from the user. As a result, comprehensive user training on conducting assays and equipment usage can be substantially reduced, and errors in operation can be minimized. In addition, the sample-only concept requires prolonged longevity of the sensor, and the longevity of the device has been remarkably enhanced in this research. With the stable bioactivity of the device, the sample-only method can be effectively conducted.

The achievements of this project have been to establish novel and non-conventional platforms for designing desirable ASSURED analytical devices with various materials. The two main concepts explored in this thesis independently provide effective solutions to the serious UED problems in existing point-of-care diagnostics, and possess enormous potential to be integrated for the development of other improved devices in the future.

Based on the research reported in this thesis, the following future studies are recommended:

- (1) Investigation of new methods to control the paper structure for clearer text-reporting, and expansion of the text-reporting method to many other biochemical, biomedical and chemical diagnosis applications.
- (2) Exploration of new methods and substrates to combine text-reporting and sample-only concepts.
- (3) In environmental sensing, investigation of the increased sensitivity and stability of indicator metal on paper during water monitoring, possibly using combined chemical/physical approaches.
- (4) Design of suitable paper networks for IgG-induced blood typing on paper networks and development of the understanding of the interference of free IgG antibodies in anti-human IgG-sensitized cells interaction.
- (5) Combination of paper and other low-cost materials with telemedicine-based platforms, such as smart phones, tablets, and other portable or wearable sensors, as the use of telemedicine will continue growing globally as an efficient way to avoid complex training for operators administering tests at the point-of-care.

End-users and patients will benefit greatly if future low-cost sensors can be built based on the full design considerations of ASSURED. This is the ultimate goal of our research.

This page is intentionally blank

Appendix I

*Published First and Co-Authored Papers Included
in the Main Body of This Thesis*

This page is intentionally blank

Cite this: *Anal. Methods*, 2015, 7, 1186

A low-cost forward and reverse blood typing device—a blood sample is all you need to perform an assay†

Miaosi Li, Junfei Tian, Rong Cao, Liyun Guan and Wei Shen*

For all user-operated blood typing devices in today's market, including those designed by us in our previous research, a buffer-activation or buffer-washing step is required. The buffer-activation step, as is employed in some commercial blood typing devices, involves dissolving the antibodies deposited in the assaying zones of the device before the introduction of a blood sample for an assay. The buffer-washing step involves washing the blood sample in the assay zone in the end of the assay for result reporting. While all these devices work well, the activation or washing step does reduce the adaptability of those devices to resource-poor areas and under emergent circumstances. In this study, we designed a new device to perform forward and reverse blood typing assays without the buffer-activation or buffer-washing. Low-cost plastic slides were patterned to form channels containing dried grouping antibodies. Blood typing assays can be performed by simply placing a few microlitres of a blood sample into the channels and then tilting the slide. The sample flows along the channel under gravity, dissolving dried antibody and then spreading into a film, unveiling the reaction of red blood cells (RBCs) and antibodies. This device enables easy visual identification of the agglutinated and non-agglutinated RBCs in typically 1 minute. Both forward and reverse blood typing assays can be performed using this device. To optimize the device design, the antibody dissolution profile, assay sensitivity, and device longevity were investigated in this work.

Received 17th November 2014
Accepted 6th December 2014

DOI: 10.1039/c4ay02739f

www.rsc.org/methods

Introduction

In today's world there is an increasing need for affordable healthcare devices which would enable many conventional diagnostic assays to be carried out from home. The home-based and patient-operated assays, if made reliable and rapid, can significantly alleviate the pressure on hospitals and pathological laboratories in developed countries.^{1,2} At the same time, these technologies also carry the hope to minimize the impact of disease outbreaks and to increase the drinking water safety in impoverished areas.^{3–7} This is because the centralised laboratories and hospitals taken for granted in the cities of the developed world are absent in remote and impoverished areas. In the past few years, novel diagnostic devices built on low-cost substrates such as paper, thread, and plastic and glass slides have demonstrated the possibility for such a hope to become reality.^{8–21} These innovations showed the potential impact of low-cost analytical technologies on future human health and environmental care. Among those innovations, a series of blood typing diagnostics based on

paper and thread platforms have been developed.^{19,22–28} The paper- and thread-based devices have significant advantages over the current laboratory- and hospital-based technologies due to their high adaptability to unsupported field conditions, user-friendliness and assaying speed.

Blood typing is a routine clinical test, but also a test of paramount importance for avoiding fatal haemolytic transfusion reactions (HTRs) during surgeries, clinical emergencies and blood transfusions. Equally important, since the world annual blood donations are around 75 million units,¹ routine and rigorous sorting of blood types must be performed in large numbers and speedily. These healthcare and clinical requirements urge the continuous development of accurate, user-friendly and low-cost blood typing technologies.^{29–31}

For ABO and Rh blood groups most clinical techniques are based on the visual observation of haemagglutination reactions, although advanced gene-sequencing technology providing precise determination of blood type through DNA analysis is now available.³² Upon the contact of RBCs with an antibody, the absence of RBC agglutination indicates that there is no haemagglutination reaction; this observation confirms that there are no corresponding antigens on the RBC surface to the grouping antibody. Conversely, if agglutination is observed, it confirms that corresponding antigens to the antibody are present on the RBC surface.

Department of Chemical Engineering, Monash University, Wellington Rd, Clayton, Vic. 3800, Australia.

† Electronic supplementary information (ESI) available. See DOI: 10.1039/c4ay02739f

Table 1 Blood type confirmation by forward and reverse blood typing methods

Reaction of antibodies with blood		Forward blood type	Reaction of reagent cells with serum		Reverse blood type
Anti-A	Anti-B		A1 cells	B cells	
+	–	A	–	+	A
–	+	B	+	–	B
+	+	AB	–	–	AB
–	–	O	+	+	O

Furthermore, for the ABO blood system Landsteiner's rule applies,³¹ which states that, for an individual, if an antigen is present on the surface of his RBCs, the corresponding antibody will be absent from his blood plasma. Instead, the reciprocal antibody will be present in the plasma or serum. For example, an individual of blood type A has A antigen on his RBCs and antibody B in his serum. The normal blood typing assay, also known as the forward blood typing assay, uses blood grouping antibodies to identify the specific antigens on RBCs. Conversely, there is another blood typing assay which determines the antibodies in the serum by using the reagent RBCs with known antigens. This blood typing assay is known as reverse blood typing. Since a reversed blood typing assay determines the interactions between the reagent RBCs and the antibodies in a patient's serum, it also relies on the observation of RBC agglutination. Details to explain the forward and reverse blood typing can be found in Fig. S1 and S2 in the ESI.† In many countries, both forward and reverse blood typing are required to confirm the patient's blood type before a blood transfusion or transplantation is allowed to proceed. The laws that determine blood types by forward and reverse blood typing are shown in Table 1.

Technical designs of blood typing assays therefore focus on using a variety of different methods to differentiate the agglutinated RBCs from the non-agglutinated RBCs. Common methods include the tube test,³³ slide test,³⁴ and column agglutination system (*e.g.* Gel Card).^{35,36} These methods rely on the different sedimentation velocities of agglutinated RBC lumps and non-agglutinated RBCs in a serum suspension, or different migration rates of agglutinated RBC lumps and non-agglutinated RBCs in a gel column of uniform pore size.³¹ The recently reported paper- and thread-based blood typing devices function as a size-based filtration device. Since within these devices the interactions of RBCs and antibodies occur inside the fibre networks of paper and thread, the fibre networks of paper and thread restrict the movement of agglutinated RBC lumps, but do not restrict non-agglutinated RBCs from moving with the serum phase or a carrier phase of buffer. Paper- and thread-based assays allow a short incubation of RBCs with the grouping antibody (typically 20 seconds for ABO and RhD tests), followed by a saline wash.^{19,25,26} The inability of agglutinated RBC lumps to move in a paper fibre network during saline washing makes them easily differentiated from the non-agglutinated RBCs, which can be readily washed out of the fibre network.

In order to further improve the adaptability of paper-based devices to non-laboratory conditions, future designs will need to explore new concepts that can significantly reduce the effort of the user required to perform the blood typing assay. In this work we present a new concept of a blood typing device which does not require the user to apply the saline buffer for activating or washing the device in order to perform an assay. This concept relies on the dissolution of blood grouping antibodies deposited on a non-absorbing substrate by a blood sample, and the subsequent thinning of the sample into a film for blood typing result identification. In the fabrication of the device, channels are formed to guide the blood sample flow. Furthermore, we investigated two factors that affect the performance and sensitivity of the device: the thickness of the blood sample film and the antibody dissolution behaviour. A chromatographic elution method was designed to provide a semi-quantitative estimation of the antibody dissolution profile from the device surface. The antibody longevity on the plastic substrate was studied for one month under ambient laboratory conditions. Apart from performing the general forward blood typing assays, we have also demonstrated the use of our new device to perform reverse blood typing. Presently, reverse blood typing can only be performed in central laboratories and hospitals. This study is the first one to demonstrate reverse blood typing using a low-cost device. We believe that our device concept will allow forward and reverse blood typing to be combined into one user-friendly device.

Experimental

Materials

Plastic slides were purchased from 3M (3M Visual Systems Division, USA). Blood samples were sourced from Red Cross Australia, Sydney. They were stored at 4 °C and used within 7 days of collection. All the antibodies were purchased from ALBA Bioscience, Edinburgh, UK.

The red blood cells required for reverse blood typing, including 15% A1 cells, 15% B cells and 3% C1 cells, were obtained from CSL, Australia; they were concentrated to 45% hematocrit level (the average human whole blood) by centrifugation, stored at 4 °C and used within 30 days. The 0.9% (w/v) NaCl saline solution and the phosphate-buffered saline (PBS) were prepared with AR grade NaCl (Univar) and phosphate (Aldrich), using MilliQ water. Glycerol and Tween 20 were purchased from Aldrich. Surface treatment of the plastic slides was carried out using a plasma reactor (K1050X plasma asher (QuorumEmitech, UK)).

Methods

Blood typing procedure. A blood typing device for use in impoverished regions must allow for direct visual identification of test results; the device should function with a minimum effort from the user and without the need for any equipment. Following these requirements, we explored a new device design concept which provides direct and rapid visual identification of the test result, while minimizing the effort from the user to perform the test. It focuses on eliminating the saline washing step. Fig. 1 describes the advantage of forming a blood sample film on an antibody treated plastic slide for blood typing assays and the device design. Fig. 1(a) and (c) show the result of adding a drop of blood sample into a drop of antibody solution on a plastic slide. Although agglutination of RBCs by the corresponding antibodies had occurred, it could not be visually observed. However, if the slide is tilted to allow the drop to flow under gravity and form a thin film, the user can immediately identify the agglutination of the RBCs by an antibody. Fig. 1(b) and (d) show the flowing blood sample and the grouping antibodies on a tilted plastic slide, clearly showing agglutinated and non-agglutinated RBCs, respectively. In order to reduce the users' efforts to perform the assay, blood grouping antibodies were coated onto the plastic slide so that users are not required to administer antibodies for forward blood typing. This device design principle requires the rapid dissolution of a sufficient quantity of grouping antibodies by the blood sample; therefore the antibody dissolution profile must be verified experimentally.

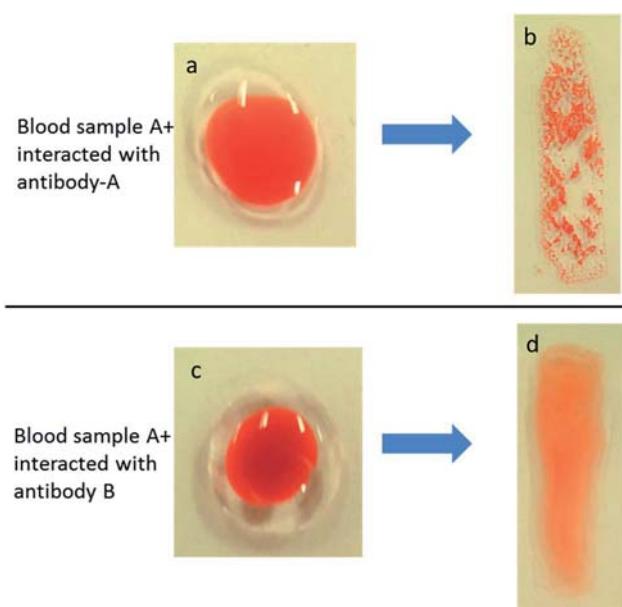


Fig. 1 Demonstration of a blood typing assay of an A+ blood sample on a plastic slide substrate by: (a) placing a drop of blood sample on a drop of anti-A; (b) tilting the substrate to allow the blood sample and anti-A solution to spread into a film, immediately revealing the positive assay result; (c) a drop of A+ blood sample placed on a drop of anti-B; (d) tilting the substrate to reveal the negative assay result.

Plastic slides were first treated with plasma at an intensity of 50 W for 1 minute; a water-resistant pen was then used to draw the boundaries to demarcate the sample flow channels. Three microlitres of antibodies (anti-A, anti-B and anti-D) were dropped respectively on top of the three channels designated to these antibodies, and the slide was tilted to allow antibodies to flow through the channel under gravity. After the antibodies covered the entire length of the channels and were completely dried, 3 μ L of blood sample was dropped from the top of each channel, following the same procedure. Typically, it takes 30 seconds for the blood sample to flow through the entire channel. Antibody-specific agglutination of RBCs can be identified immediately as the blood sample flows through the channels treated with antibodies and forms films. A schematic protocol of the test is shown in Fig. 2.

Quantification of antibody dissolution rates from plastic slides. Since the working principle of the plastic slide device relies on the rapid dissolution of the antibodies deposited on the slide, it is necessary to characterize the dissolution rates of all three antibodies employed for the device design. To do this, PBS buffer was used to perform a controlled dissolution study of all antibodies from the plastic slide surface. Fig. 3 shows the experimental procedure: channels on a plastic substrate were pre-treated with antibody and allowed to dry under ambient conditions. 10 μ L PBS was used to flow through each channel to dissolve the antibody; the contact time was controlled at 30 s. The flow-through PBS solutions containing the dissolved antibodies were collected using Kleenex paper towel; the solutions wetted the paper towel and formed circular wetting zones as shown in Fig. 3.

In order to quantify the dissolved antibodies, antibody concentrations of the collected PBS washing solution were analyzed. We designed the quantification step as follows: a blood sample carrying the corresponding antigen to an antibody was introduced into the zone of the collected PBS washing solution on paper towel. After 30 seconds of incubation time under ambient condition, the edge of the paper was immersed

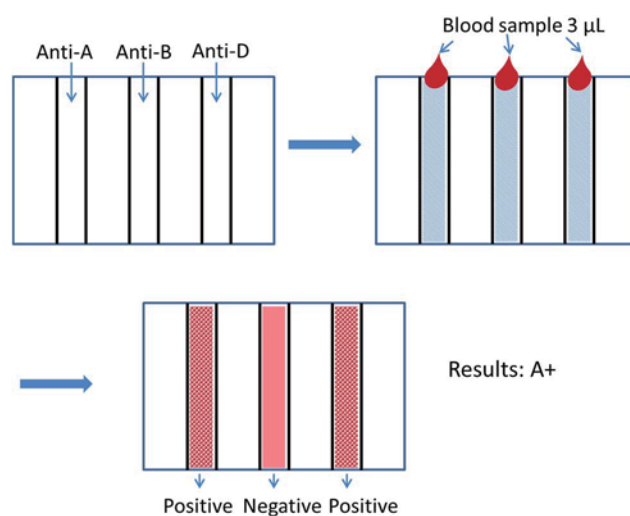


Fig. 2 The designed procedure for blood typing on a plastic slide.

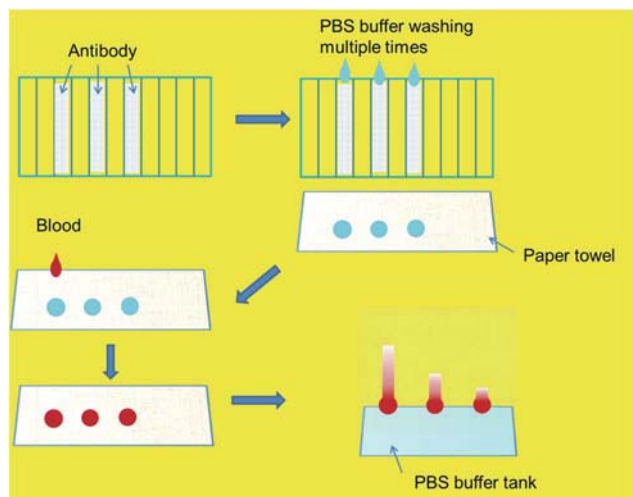


Fig. 3 Schematics of the procedure for studying the antibody dissolution behaviour from the plastic slide. This procedure involves an antibody dissolution step by PBS, followed by quantifying the concentration of the antibodies washed off the plastic slide.

into a chromatography tank containing PBS for elution (Fig. 3), following the method we reported previously.²⁴ If the antibody concentration is high enough, the RBCs of the blood sample will agglutinate, forming a blood stain with a strong colour which cannot be eluted away by PBS. The elution pattern was scanned into a computer and then converted to a monochrome mode (grey scale mode) with the ImageJ software. The optical density of the grey scale image of the blood spot was determined using the software. The gray scale is digitized into 256 steps, which represent different tones from dark to bright in an ascending manner, with 0 being the darkest and 255 being the brightest tone. The optical density of the blood spot therefore provides a simple and semi-quantitative method for determining the antibody dissolution behaviour. An antibody dilution standard calibration curve can be established by determining the optical densities of agglutinated blood spots by a series of step dilutions of an antibody.

Results and discussion

There are in total eight different blood types in the ABO and RhD blood groups; all of them can be clearly identified by the plastic slide method (Fig. 4). After a blood sample was introduced into the channels, it takes typically up to 1 minute for 3 μ L of blood sample to flow through the entire length of the channel. During this process, antibody-specific agglutination of RBCs forms large lumps, which become clearly identifiable when the blood sample flows halfway through the channels, making the assay time with the plastic slide shorter than 1 minute.

Antibody dissolution from the plastic slides

Fig. 5(a) shows the chromatographs of the agglutinated type A blood sample by a serially diluted anti-A; the dilution was made

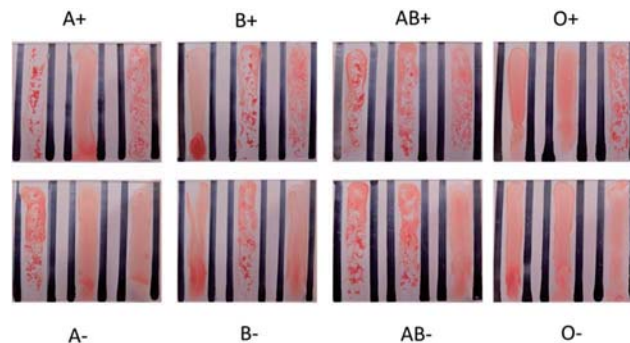


Fig. 4 Assay results reported by the plastic slide device for all 8 ABO and RhD blood groups.

from 1 (original anti-A) to 512 fold. The serial dilution data show that the anti-A retained its activity after being diluted 128 fold. Further dilution, however, weakens the antibody activity, causing weak RBC agglutination. Fig. 5(b) presents the anti-A dilution curve of the blood spot colour density against the dilution factor. Since the concentration of the commercial antibody was unknown, the dilution factor was used as the relative antibody concentration. Fig. 5(c) shows the result of a serial dissolution of anti-A from the plastic slide; the anti-A standard solution was gradually diluted into a series of concentrations and dropped onto the paper towel, followed by the introduction of reagent red blood cell A onto each antibody spot. Then the chromatographic elution method was applied to the paper towel and the colour intensity of each blood spot was tested for building the standard curve of anti-A dilution behaviour, as shown in Fig. 5(a) and (b). The standard curve in Fig. 5(b) shows that a significant loss of anti-A activity to A antigen on the RBC surface by visual evaluation occurred only

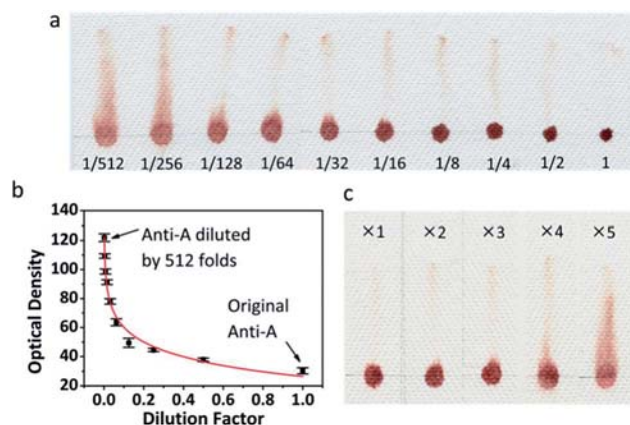


Fig. 5 Antibody dissolution behaviour study for anti-A: (a) anti-A activity as a function of a series of dilutions with PBS; antibody activity can be determined by the reflective optical density of the agglutinated A1 reagent red cell (concentrated from the commercial reagent to a hematocrit level of 45%) on paper. (b) The calibration curve of the A1 cell optical density as a function of anti-A dilution factor; the red curve is the fitting curve of a natural logarithm function (formula (1)); (c) anti-A dissolution behaviour of five consecutive PBS dissolution rinses collected from the plastic substrate.

when it was diluted to 1/128 of its original concentration. This result suggests that the dissolving rate of anti-A is slow, and the following phenomenon provided reasoning. The standard curve in Fig. 5(b) can be fitted to a logarithmic formula (formula (1)) to establish the relationship of the colour density and the relative concentration of the antibody. This standard curve provides a way to quantify the antibody that was washed off the plastic substrate by the saline solution. Since the precise original antibody concentrations were unknown, we could assume that they were C_A , C_B and C_D , and measure the concentration changes caused by the saline dissolution.³⁷ Through measuring the colour density of each blood spot in Fig. 5(c), the relative concentration of anti-A released from the substrate after each saline wash can be calculated; the results are shown in Table 2. Anti-A deposited on the plastic substrate dissolved only 11.1% by the first wash, the remaining anti-A on the substrate still retained sufficient bioactivity for blood typing after another three such washes.

$$\text{Optical density A} = 26.5 - 14.6 \times \ln(f_A - 5.42 \times 10^{-4}); \quad (1)$$

$$f_A = \frac{C'_A}{C_A}$$

where f_A is the dilution factor of anti-A; C'_A is the concentration of anti-A of each dilution.

Following the same procedure for quantifying anti-A, the dissolution behaviour of antibodies B and D has also been quantified. The calibration curve of anti-B dilution showed that anti-B lost its activity after a dilution of 1/16, indicating its weaker activity compared with anti-A (see Fig. S3a in the ESI†). The calibration curve was fitted with formula (2) (Fig. S3b†), which quantitatively showed that the concentration of anti-B in the first saline wash was 23.1% of its original concentration C_B (Table 2). The more efficient dissolution of anti-B by saline solution than of anti-A confirms that anti-B can be dissolved more easily from the plastic slide, therefore anti-B weakened more rapidly than anti-A with the number of washes by saline (Fig. S3c†). As shown in Fig. S1c,† anti-B could sustain three washes and the residual anti-B on the plastic substrate still had sufficient activities for unambiguous blood typing. However, as for anti-D, the dissolution was even more efficient (Fig. S4a and b†), our measurement showed that 92.0% of its original concentration was dissolved (formula (3) and Table 2) and removed from the plastic substrate in the first saline wash; anti-D lost its activity at 1/8 dilution (Fig. S4c†).

$$\text{Optical density B} = 41.4 - 17.2 \times \ln(f_B - 0.02); \quad f_B = \frac{C'_B}{C_B} \quad (2)$$

$$\text{Optical Density D} = 81.1 - 10.7 \times \ln(f_D - 0.03); \quad f_D = \frac{C'_D}{C_D} \quad (3)$$

where f_B and f_D are the dilution factors of anti-B and anti-D; C'_B and C'_D are the concentrations of anti-B and anti-D after each dilution.

According to the definition of reflective optical density used in the printing industry,⁴⁰ the reflective optical density is defined as a logarithmic ratio of the reflected radiation from a printed grey tone on paper to the reflected radiation from the unprinted paper. This is usually presented in the form of logarithm based to 10,⁴⁰ but can be easily converted to the form of natural logarithm:

$$D = -\ln \frac{I}{I_0} \quad (4)$$

where D is the reflective optical density, usually measured with a reflective densitometer in the printing industry, I and I_0 are the reflective radiation intensity from a printed grey tone and from unprinted paper, respectively. In this study grey tones generated by the agglutinated blood spot on paper loaded with different amounts of antibodies create a similar concept for the tones to be quantified by reflective optical density.

Blood spot optical density data (Fig. 5, S3b and c†) can also be correlated with concentrations of corresponding antibody (or dilution) data by logarithm functions, which suggests that optical density data can be correlated with the concentration ratios of the dissolved antibodies. Such correlations have been experimentally given in eqn (1)–(3) and are expected to provide semi-quantitative results for antibody dissolution evaluation.

Sensitivity

The sensitivity of any blood typing device must be investigated for typing blood samples with low concentrations of RBCs. This requirement is essential, as clinically the RBC concentration from blood samples of anaemia patients could be more than 50% lower than those from a healthy patient. Since almost all commonly used blood typing assays rely on the development of large agglutinated RBC lumps, those methods can be less sensitive to samples with low RBC concentrations.

Table 2 The blood spot optical density data and the calculated concentrations of three antibodies of each dissolution from the plastic substrate

Antibody		Number of dissolution washes				
		X1	X2	X3	X4	X5
Anti-A	Colour density	58.7 ± 2.3	62.0 ± 2.8	66.3 ± 2.4	75.8 ± 1.8	99.6 ± 2.6
	Relative concentration	(11.1 ± 1.7)% C_A	(8.9 ± 1.7)% C_A	(6.6 ± 1.1)% C_A	(3.5 ± 0.4)% C_A	(0.7 ± 0.1)% C_A
Anti-B	Colour density	68.3 ± 1.9	76.1 ± 1.6	86.8 ± 2.5	100.5 ± 2.8	
	Relative concentration	(23.1 ± 2.4)% C_B	(15.6 ± 1.3)% C_B	(9.4 ± 1.1)% C_B	(5.5 ± 0.5)% C_B	
Anti-D	Colour density	82.4 ± 1.7	110.6 ± 3.2	143.9 ± 2.2		
	Relative concentration	(92.0 ± 14.3)% C_D	(9.5 ± 1.9)% C_D	(3.2 ± 0.1)% C_D		

The sensitivity study of the plastic slide method was conducted by identifying the agglutination patterns of serially diluted reagent RBCs that carry known antigens. The original RBC samples used for testing were the red cells A1, B and C1. To prepare samples with low RBC concentrations, the suspension medium of the reagent red cells was first removed by centrifugation and then the red cells were diluted to haematocrit of 45% with PBS; this RBC concentration simulates the blood RBC concentration of a healthy individual. Low RBC concentration samples were prepared by diluting this sample by factors of 75%, 50% and 25% with PBS. The diluted blood samples were then used for the sensitivity tests of the device and results are shown in Fig. 6. All positive tests of diluted blood samples A, B and D can still be clearly identified *via* RBC agglutination, even though they were diluted to 25%. These results confirm that the plastic slide blood typing device is able to deliver the equivalent sensitivity of a high performance blood typing device. The film forming process of the blood sample provides a simple way to enhance the sensitivity of blood typing using the plastic slide method.

Antibody longevity on the plastic slide

It was found that the original antibodies gradually lost their activity within 10 days of deposition on plastic slides and allowed to dry. This is because the dried antibodies dehydrated after long exposure to air. As a result, the surface of the channel became more hydrophobic and this significantly reduces the speed of the blood flow in the channel. Fig. 7 shows the hydrophobic development of the slide surface with time. To solve this problem, glycerol and Tween 20 were chosen as additives to prevent antibody dehydration and to increase the channel surface wettability. Glycerol has been used as a traditional additive for protecting biomolecules from denaturing.³⁸

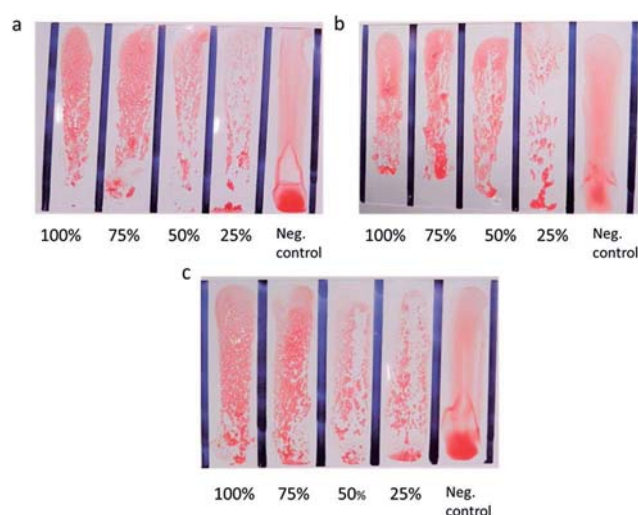


Fig. 6 Sensitivity tests of the plastic slide method by dilution of reagent red blood cell carrying known antigens: (a) A1 cells in the anti-A treated channel; (b) B cells in the anti-B treated channel; (c) C1 cell in the anti-D treated channel. The negative control channel was treated with BSA only.

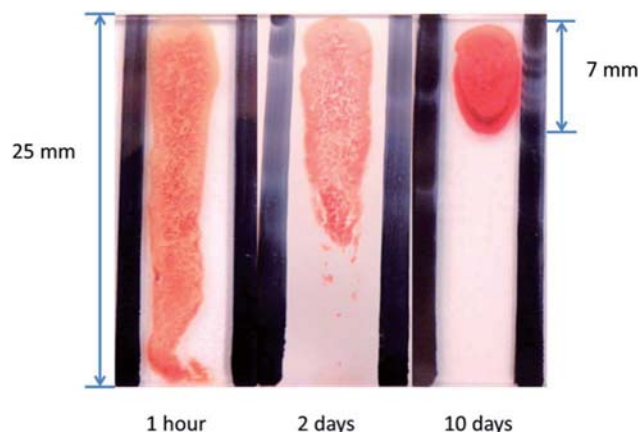


Fig. 7 Lifetime detection for blood group A interaction with the anti-A treated device for different periods.

Its high humectant effect attracts water molecules and prevents biomolecules from dehydration; such a protective effect is most likely related to the presence of 3 hydroxyl groups in the glycerol molecule and its small molecular size. Apart from attracting water molecules, glycerol may also provide direct hydrogen-bonding, like many sugar molecules, to stabilize the biomolecule.³⁹ The addition of Tween 20 as a biologically compatible surfactant is intended to enhance the wettability of the deposited antibody layer on the plastic slide after ageing. Additives with a series of different proportions of glycerol and Tween 20 were mixed with the antibodies to form solutions to treat the channels of the device; the wettability of the channels was tested at different storage times by measurement of the flow length of blood samples in the channels in 30 seconds; results are presented in Table 3. Our results show that antibody solutions containing 20% glycerol, or 10% glycerol and 0.1% Tween 20 enhanced the channel wettability; testing after 30 days of storage showed that the device's wettability was unchanged and all antibodies still retained their activity. We chose 10% glycerol and 0.1% Tween 20 as the preferred additive formulation to perform further experiments. Fig. 8 shows the blood test results obtained after 45 days of storage under ambient temperature and open to air; all the antibodies were still active and gave accurate blood typing within 30 seconds (Fig. 8).

Table 3 The effect of additives on the surface hydrophilicity for blood flowing with the increase of time

Additive	Blood sample flow distance (mm)			
	1 hour	2 days	10 days	30 days
Pure antibody	21	13	8	4
Tween 20 (0.1%)	25	14	3	3
Tween 20 (0.5%)	25	12	3	3
Tween 20 (1%)	20	8	3	3
Glycerol (1%)	25	15	8	4
Glycerol (5%)	25	17	12	6
Glycerol (10%)	25	25	22	20
Glycerol 10% + Tween 20 0.1%	25	25	25	25
Glycerol (20%)	25	25	25	25

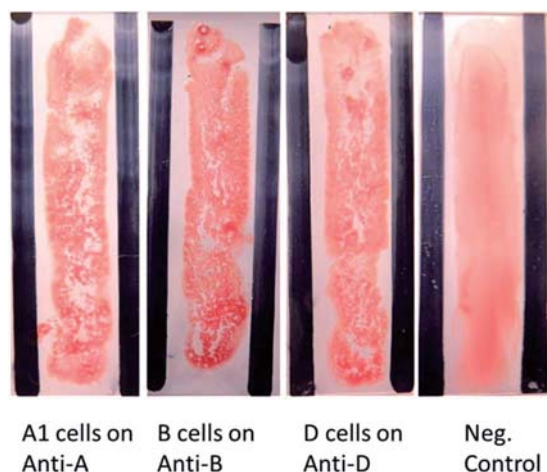


Fig. 8 Antibody activity for its corresponding antigen after being deposited for 45 days on the device surface coated with an additive mixture of 10% of glycerol and 0.1% of Tween 20. Test was conducted under ambient laboratory conditions.

Reverse blood typing using the plastic slide assay

The reverse blood typing assays were also performed using the plastic slide method. Patients' blood serum was first separated from the whole blood sample, which can be prepared by the traditional centrifugation or the new low-cost POC methods on membrane^{41,42} or paper.⁴³ Then the serum samples were dropped into the channels on the plastic slide and allowed to spread throughout the channel. Reagent red blood cells A and B were then pipetted into separate serum-coated channels. By allowing the reagent RBCs to spread in the channel and form a film, the agglutinated RBCs can be clearly identified by the naked eye without any aid (Fig. 9).

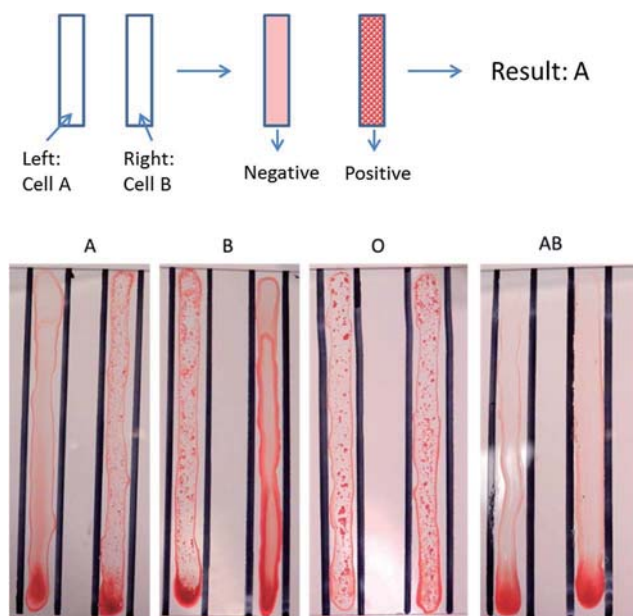


Fig. 9 The reverse blood typing results for identifying ABO blood groups.

Proposed mechanism of RBC agglutination on the plastic slide

The use of film formation as a sensitive method for blood typing takes advantage of the following two processes: firstly, the spreading of blood samples over the antibody coated channel surface provides a large contact area between the blood sample and antibody. The large contact area promotes interactions between the RBCs in the blood sample and the antibodies on the plastic slide; agglutination of RBCs by their corresponding antibodies can therefore occur quickly. Secondly, the relatively slow spreading of blood samples in an antibody treated channel is likely to give sufficient time for the blood sample and antibody to interact and incubate. This, combined with the small thickness of the blood sample film, tends to lead to the formation of sheet-like agglutination lumps, which are very easy to visually identify. The plastic slide device thus offers a sensitive means for rapidly performing both forward and reverse blood typing assays.

Conclusions

In this work we designed and demonstrated a new user-friendly blood typing device. The device was fabricated by patterning the plastic slide with channels treated with different blood grouping antibodies; this design requires the user to simply introduce the blood sample into the channels to complete the blood typing assay, without the need for buffer washing or stirring operations. This device functions by letting the blood sample spread under gravity over a surface treated with blood grouping antibodies. The agglutinated RBC lumps can be rapidly and clearly differentiated from the non-agglutinated RBCs, providing unambiguous visual identification of the positive and negative blood typing assays. This method provides a user-friendly design concept that requires minimum effort from the user to perform an assay to determine the blood type of a patient within 1 minute.

The film-forming principle of this method provides a high level of sensitivity to identify the blood types of samples with low RBC concentrations. Preliminary investigation of the longevity of the device was also conducted; a mixture of glycerol and Tween 20 was chosen as an effective additive mixture to maintain the bioactivity of the antibodies on the device for the testing period of 30 days.

Acknowledgements

This work is supported by the Australian Research Council (ARC). Funding received from ARC through grant numbers DP1094179 and LP110200973 is gratefully acknowledged. The authors thank Haemokinesis for its support through ARC Linkage Project, and Mr Hansen Shen for proof-reading the manuscript. Ms Miaosi Li also thanks the Monash University Research and Graduate School and the Faculty of Engineering for postgraduate research scholarships.

Notes and references

- 1 R. H. Müller and D. L. Clegg, *Anal. Chem.*, 1949, **21**, 1123–1125.
- 2 A. W. Martinez, S. T. Phillips, M. J. Buttle and G. M. Whitesides, *Angew. Chem., Int. Ed.*, 2007, **46**, 1318–1320.
- 3 S. M. Z. Hossain and J. D. Brennan, *Anal. Chem.*, 2011, **83**, 8772–8778.
- 4 S. M. Z. Hossain, C. Ozimok, C. Sicard, S. D. Aguirre, M. Ali, Y. Li and J. D. Brennan, *Anal. Bioanal. Chem.*, 2012, **403**, 1567–1576.
- 5 H. Wang, Y. J. Li, J. F. Wei, J. R. Xu, Y. H. Wang and G. X. Zheng, *Anal. Bioanal. Chem.*, 2014, **406**, 2799–2807.
- 6 P. Rattanarat, W. Dungchai, D. Cate, J. Volckens, O. Chailapakul and C. S. Henry, *Anal. Chem.*, 2014, **86**, 3555–3562.
- 7 S. M. Z. Hossain, R. E. Luckham, M. J. McFadden and J. D. Brennan, *Anal. Chem.*, 2009, **81**, 9055–9064.
- 8 X. Li, J. Tian, G. Garnier and W. Shen, *Colloids Surf., B*, 2010, **76**, 564–570.
- 9 X. Li, J. Tian and W. Shen, *Anal. Bioanal. Chem.*, 2010, **396**, 495–501.
- 10 J. L. Delaney, C. F. Hogan, J. Tian and W. Shen, *Anal. Chem.*, 2011, **83**, 1300–1306.
- 11 X. Li, J. Tian and W. Shen, *Cellulose*, 2010, **17**, 649–659.
- 12 R. Pelton, *TrAC, Trends Anal. Chem.*, 2009, **28**, 925–942.
- 13 S. J. Vella, P. Beattie, R. Cademartiri, A. Laromaine, A. W. Martinez, S. T. Phillips, K. A. Mirica and G. M. Whitesides, *Anal. Chem.*, 2012, **84**, 2883–2891.
- 14 D. Mabey, R. Peeling, A. Ustianowski and M. Perkins, *Nat. Rev. Microbiol.*, 2004, **2**, 231–240.
- 15 X. Li, J. Tian, T. Nguyen and W. Shen, *Anal. Chem.*, 2008, **80**, 9131–9134.
- 16 X. Li, J. Tian and W. Shen, *Lab Chip*, 2011, **11**, 2869–2875.
- 17 J. Tian, D. Kannangara, X. Li and W. Shen, *Lab Chip*, 2010, **10**, 2258–2264.
- 18 A. W. Martinez, S. T. Phillips, E. Carrilho, S. Thomas, H. Sindi and G. M. Whitesides, *Anal. Chem.*, 2008, **80**, 3699–3707.
- 19 D. Ballerini, X. Li and W. Shen, *Anal. Bioanal. Chem.*, 2011, **399**, 1869–1875.
- 20 A. Nilghaz, D. Ballerini and W. Shen, *Biomicrofluidics*, 2013, **7**, 1–13.
- 21 A. Nilghaz, D. Ballerini, X. Fang and W. Shen, *Sens. Actuators, B*, 2014, **191**, 586–594.
- 22 L. Li, J. Tian, D. Ballerini, M. Li and W. Shen, *Colloids Surf., B*, 2013, **106**, 176–180.
- 23 M. S. Khan, G. Thouas, W. Shen, G. Whyte and G. Garnier, *Anal. Chem.*, 2010, **82**, 4158–4164.
- 24 M. Al-Tamimi, W. Shen, R. Zeineddine, H. Tran and G. Garnier, *Anal. Chem.*, 2011, **84**, 1661–1668.
- 25 M. Li, J. Tian, M. Al-Tamimi and W. Shen, *Angew. Chem., Int. Ed.*, 2012, **51**, 5497–5501.
- 26 L. Li, J. Tian, D. Ballerini, M. Li and W. Shen, *Analyst*, 2013, **138**, 4933–4940.
- 27 T. Songjaroen, W. Dungchai, O. Chailapakul, C. S. Henry and W. Laiwattanapaisa, *Lab Chip*, 2012, **12**, 3392–3398.
- 28 M. Li, W. L. Then, L. Li and W. Shen, *Anal. Bioanal. Chem.*, 2014, **406**, 669–677.
- 29 G. Daniels and M. E. Reid, *Transfusion*, 2010, **50**, 281–289.
- 30 N. D. Avent and M. E. Reid, *Blood*, 2000, **95**, 375–387.
- 31 G. Daniels and I. Bromilow, *Essential Guide to Blood Groups*, Wiley-Blackwell, Hoboken, 2007.
- 32 W. Malomgré and B. Neumeister, *Anal. Bioanal. Chem.*, 2009, **393**, 1443–1451.
- 33 B. H. Estridge, A. P. Reynolds and N. J. Walters, *Basic medical laboratory techniques*, Delmar Cengage Learning, Albany, USA, 2000.
- 34 D. Pramanik, *Principles of Physiology*, Academic, Kolkata, 3rd edn, 2010.
- 35 J. H. Spindler, K. H. Ter and M. Kerowgan, *Transfusion*, 2001, **41**, 627–632.
- 36 M. M. Langston, J. L. Procter, K. M. Cipolone and D. F. Stroncek, *Transfusion*, 2001, **39**, 300–305.
- 37 P. Jarujamrus, J. Tian, X. Li, A. Siripinyanond, J. Shiowatana and W. Shen, *Analyst*, 2012, **137**, 2205–2210.
- 38 I. M. Klotz, G. P. Royer and I. S. Scarpa, *Proc. Natl. Acad. Sci. U. S. A.*, 1970, **68**, 263–264.
- 39 C. Manta, N. Ferraz, L. Betancor, G. Antunes, F. Batista-Viera, J. Carlsson and K. Caldwell, *Enzyme Microb. Technol.*, 2003, **33**, 890–898.
- 40 H. Kipphan, *Handbook of printing media*, Springer-Verlag, Berlin, 2001, p. 100.
- 41 X. Yang, O. Forouzan, T. P. Brown and S. S. Shevkoplyas, *Lab Chip*, 2012, **12**, 274–280.
- 42 C. Liu, M. Mauk, R. Gross, F. D. Bushman, P. H. Edelstein, R. G. Collman and H. H. Bau, *Anal. Chem.*, 2013, **85**, 10463–10470.
- 43 T. Songjaroen, W. Dungchai, O. Chailapakul, C. S. Henry and W. Laiwattanapaisa, *Lab Chip*, 2012, **12**, 3392–3398.

Paper-Based Blood Typing Device That Reports Patient's Blood Type "in Writing"***

Miaosi Li, Junfei Tian, Mohammad Al-Tamimi, and Wei Shen*

The British author, J. K. Rowling, presented a visionary idea in her novel "Harry Potter and the Chamber of Secrets" that one can interrogate a piece of paper for information and get unambiguous answers from the paper in writing. Here we report a study, following her vision, on using a low-cost bioactive paper device to perform ABO and rhesus (RhD) blood typing tests and obtain test results from the paper in writing. Paper text patterns are designed and printed to allow interactions between grouping antibodies and red blood cells. Composite text patterns consisting of the bioactive and non-bioactive sections are used to form the letters and symbols for the final display of the testing report. This paper-based blood typing device rapidly reports patient's blood type in unambiguous written text.

Patterned bioactive paper as a tool for biochemical analysis has become a platform for making low-cost and user-operated devices for diagnosis,^[1] point of care (POC),^[1–6] pathogen and biomarker detection,^[1,4,5] and food and drinking water quality testing.^[7] The potential of this platform to deliver affordable, rapid, and user-friendly diagnostic sensors for disease screening, healthcare and drinking water quality evaluation to the developing countries has become increasingly clear.^[1,4,8–10] Over the last five years, there has been an explosion of research in bioactive paper-based low-cost sensor fabrication,^[1,3,4,11–16] electronic transmission of colorimetric assays for real-time diagnosis,^[6,17] as well as new diagnostic and environmental applications using low-cost sensors.^[6,7,18–21] Colorimetric and electrochemical methods are the preferred analytical approaches for bioactive paper sensors, since these methods are proven to be effective in qualitative and semi-quantitative sensing and can be easily adapted onto paper.^[3,6,21,22] However, those studies also revealed certain limitations of those new concepts in their practical applications. Whilst a colorimetric or voltammetric

signal can report the test results, in most situations the results need to be interpreted by trained personnel. This is particularly true if an assay has multiple outcomes and requires careful examination in order for the diagnosis to be made. Therefore, among the many challenges in low-cost diagnostics, unambiguous reporting of the test results by the sensors to the users is critical. Where sensors are used in developing regions for large-scale disease screening, even if we can fabricate sensors that are robust enough to function under an unsupported field condition, misinterpretation of the assay results may still be a significant factor that can compromise the value of low-cost diagnostics.

Are there other means by which we can design and interrogate bioactive paper sensors for diagnostic results? An inspiration can be found in the movie adapted from J. K. Rowling's novel "Harry Potter and the Chamber of Secrets";^[23] Potter interrogated Tom Riddle's Diary by writing on a page of paper in the Diary "Do you know anything about the Chamber of Secrets?"; the paper responded with a "Yes" in writing, instead of with a color change. The artist's vision shows that non-conventional mechanisms of reporting assay results using paper-based sensors should be explored. To the authors' best knowledge, equipment-free bioactive paper-based diagnostic devices capable of reporting multiple conditions in written text from a single test is currently not available. In this study, we present a bioactive paper blood typing device that is capable of reporting ABO RhD blood types rapidly and in written text.

Correct typing of human blood is extremely important in blood transfusion and in events of medical emergency. The blood type of an individual is determined by the presence or absence of certain antigens on the surface of a red blood cell (RBC). In addition, antibodies existing in blood serum protect the body from incompatible and hostile antigens.^[24] The vast majority of techniques for ABO and RhD typing of blood to date have been based upon the principle of haemagglutination reactions between RBCs and antibodies. The absence of agglutination indicates no haemagglutination reaction.^[24] Recently low-cost bioactive paper^[19] and bioactive thread^[18,25] microfluidic sensors have been reported for human blood grouping applications. These devices are also based on the principle of haemagglutination reactions. Through observing the differences in wicking distances of the agglutinated red blood cells and the blood serum, an indication of haemagglutination reaction can be identified. However, paper- and thread-based technologies still require users who have the blood typing knowledge to interpret the result. For the blood typing devices to be more adaptable to conditions in developing countries, they must be able to report results unambiguously to users who may not have the

[*] M. Li,^[+] J. Tian,^[+] Dr. M. Al-Tamimi,^[+] Assoc. Prof. W. Shen
Department of Chemical Engineering, Monash University
Wellington Rd, Clayton, Vic, 3800 (Australia)

[+] These authors contributed equally to this work.

[**] This work is supported by the Australian Research Council (ARC). Funding received from ARC through grant numbers DP1094179 and LP110200973 is gratefully acknowledged. The authors thank Haemokinesis for its support through ARC Linkage Project. M.L. and J.T. thank Monash University Research and Graduate School and the Faculty of Engineering for their postgraduate research scholarships. The authors would like to specially thank Dr. E. Perkins and Dr. W. Mosse of the Department of Chemical Engineering, Monash University for proof reading the manuscript.

Supporting information for this article is available on the WWW under <http://dx.doi.org/10.1002/anie.201201822>.

knowledge to interpret the results based on the first principle. An easy way to bridge this application gap is to design paper-based devices that can report blood typing results to the users in written text.

The text-reporting blood typing device we present here is partly based on the principle of haemagglutination reactions. Its fabrication involves the use of hydrophobic–hydrophilic contrast to form text patterns and to use these text patterns as sites for RBC and antibody interactions. The hydrophobic–hydrophilic contrast will ensure the unambiguous legibility of the text pattern of agglutinated blood to be displayed. In our design the text patterns are made hydrophilic, and antibody solutions are introduced into the corresponding text patterns (e.g. Anti-A into text pattern “A”). In a blood typing assay a blood sample is introduced to all text patterns. To clearly identify the occurrence of haemagglutination reactions inside the hydrophilic text patterns, a saline-washing step is employed. If the antibody in a text pattern is not the corresponding antibody to the antigens carried by RBCs, there will be no haemagglutination reaction; the non-agglutinated RBCs can be easily washed out of the text pattern with the saline solution. Contrary to this, if RBCs have haemagglutination reaction through the antibody-antigen interaction, agglutinated RBC lumps will form inside the fiber matrix of the paper and cannot be washed out by the saline solution.^[26] Those text patterns occupied by the agglutinate RBC lumps therefore have unambiguous legibility with high resolution and contrast.

In devices for ABO RhD blood typing, three antibodies (Anti-A, Anti-B, and Anti-D) are used to display blood typing results by text. The interaction of each antibody with RBCs can have two possible outcomes, that is, “Agglutination” and “No agglutination”. The total number of blood types determinable by the three antibodies will be $2^3 = 8$. Taking an A+ blood sample, for example, the interaction of the A+ blood sample with the three antibodies can be expressed as $\overline{A}BD$, that is, A (agglutination with antibody A occurs), \overline{B} (no agglutination with antibody B), and D (agglutination with antibody D occurs). Following this expression, all different blood types (column 3) determinable by these antibodies through the presence and absence of RBC agglutination (column 2) can be listed in Table 1.

If we use only haemagglutination reactions to design a text-reporting device for blood typing, many blood types cannot be unambiguously reported by text. This situation

includes two circumstances where blood types have no haemagglutination reactions with the grouping antigens, therefore no visually perceivable text patterns can be formed to make the text report. The first circumstance involves all Rh(–) blood types; the lack of interactions of RBCs with Anti-D results in no haemagglutination reaction (i.e. \overline{D}) and therefore cannot form visually perceivable text patterns. The second circumstance involves O-type blood. Since red cells of O-type blood do not carry A and B antigens, they do not have haemagglutination reactions with either Anti-A or Anti-B (i.e. $\overline{A}\overline{B}$). O-type blood cannot be reported in written text formed by haemagglutination reaction only. Table 1 (column 4) lists all five blood types that are associated with these two circumstances. Further design of the devices must overcome these obstacles.

In this study we present a design of a composite text symbol that can report both D and \overline{D} unambiguously. This symbol takes the form of “+”; it consists of a permanent “–” printed using a non-bioactive water-insoluble ink and a bioactive “|” printed using Anti-D (Figure 1 a). In a blood test when a sample is introduced into “|”. If the sample carries D antigen, haemagglutination reaction will occur inside “|” and saline washing will not be able to remove the agglutinated RBCs out of pattern “|”. The composite text symbol will report “+”. On the other hand, if the sample does not carry the RhD antigen, then no haemagglutination reaction will occur. After saline washing, no agglutinated blood sample will be perceivable in “|”; the composite text symbol will report “–” (Figure 1 a). This design fulfills the requirement of using one composite pattern to unambiguously report RhD(+) and RhD(–) in text.

For O-type blood samples, we again employ another composite text symbol to report both “O” and “non-O” types of blood samples. This composite text symbol takes the form of “⊗”; it consists of a permanent letter “O” printed using water-insoluble ink and a “×” printed using an equal-volume mixture of Anti-A and Anti-B (see Figure 1 b). In a blood test when a sample is introduced into “×”, the sample is mixed with Anti-A and Anti-B inside “×”. If the sample carries A-antigen or B-antigen, or both, then haemagglutination reaction will occur inside “×” and saline washing will not be able to remove the agglutinated RBCs out of the pattern. The composite text symbol will report “⊗”. On the other hand, if the sample does not carry A-antigen and B-antigen, then no haemagglutination reaction will occur inside “×”.

Table 1: Blood types that can be reported in text by specific antigen–antibody agglutination reactions before and after implementing our design solutions (see Figure 1).^[a]

No.	Agglutination	Blood types determined by RBC agglutination	RBC antigens unable to be expressed in text by RBC agglutination (and reasons)	RBC antigens unable to be expressed in text after implementing design solution 1	Text reporting after implementing design solutions 1 and 2
1	ABD	AB+			Enabled
2	ABD	A+			Enabled
3	AB \overline{D}	AB–	x (\overline{D})		Enabled
4	A $\overline{B}\overline{D}$	A–	x (\overline{D})		Enabled
5	A $\overline{B}D$	B+			Enabled
6	A $\overline{B}D$	O+	x ($\overline{A}, \overline{B}$)	x ($\overline{A}, \overline{B}$)	Enabled
7	A $\overline{B}\overline{D}$	B–	x (\overline{D})		Enabled
8	ABD	O–	x ($\overline{D}, \overline{A}, \overline{B}$)	x ($\overline{A}, \overline{B}$)	Enabled

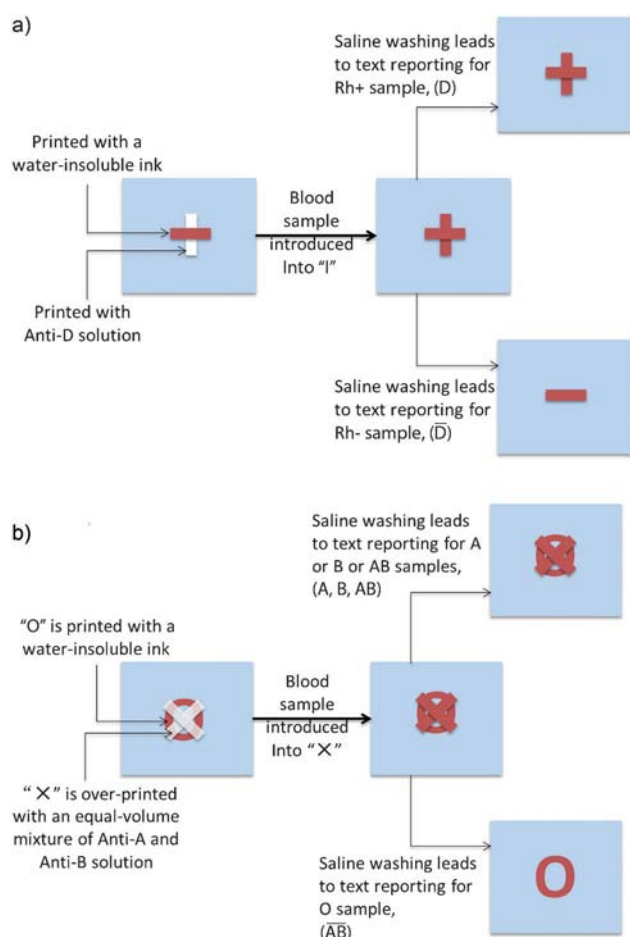


Figure 1. The two design solutions using composite text symbols to report blood test results in text. a) Design solution 1: The composite text symbol for reporting the presence of RhD takes the form of "+"; it consists of a permanent "-" printed using a non-bioactive water-insoluble ink and a "|" printed using Anti-D. b) Design solution 2: The composite text symbol for reporting "O" and "non-O" types of blood samples takes the form of "⊗"; it consists of a permanent letter "O" printed using non-bioactive water-insoluble ink and a "x" printed using an equal-volume mixture of Anti-A and Anti-B.

After saline washing, the composite text symbol will report "O" (Figure 1b). This design fulfills the requirement of using one composite pattern to unambiguously report "O" and "non-O" types of blood samples in text. The three blue dots in the printed device are for positioning purpose.

Negative text patterns consisting of letters "A" and "B" and two text symbols, "x" and "|" were created electronically. A Canon ink jet printer was used to print a 2% (w/v) heptane solution of an alkenyl ketene dimer (AKD)^[3,4] on the paper sample, forming the negative patterns of letters and symbols (see Figure S1 in the Supporting Information). Printing of negative patterns of letters and symbols ensures that these patterns remain hydrophilic and are surrounded by hydrophobic areas. The hydrophilic patterns are, however, invisible. After printing of the hydrophilic patterns, 2.5 μ L of Anti-A, clone 10090; Anti-B, clone 10091; and Anti-D, clone 20093 were introduced into the hydrophilic patterns "A", "B", and "|", respectively, by ink jet printing or writing with a pen

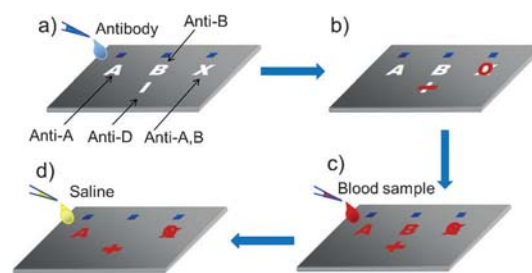


Figure 2. Fabrication and testing procedures of the text-reporting blood-typing devices. Negative patterns of letters and symbols are printed using a heptane solution of an alkenyl ketene dimer; letters and symbols remain hydrophilic and are surrounded by hydrophobic areas (see Figure S1 in the Supporting Information). a) Anti-A and Anti-B are introduced into the corresponding letters. An equal-volume mixture of Anti-A and Anti-B is introduced into "x", and Anti-D is introduced into "I". b) Letter "O" and symbol "-" are printed over "x" and "-", respectively, using a non-bioactive and water-insoluble ink. c) A blood sample is introduced in the device for blood typing test. d) After washing each pattern with 2 \times 50 μ L of saline solution, the blood typing result is reported by the device in text.

(Figure 2a). Two and a half microlitres of an equal-volume mixture of Anti-A and Anti-B were introduced into the pattern "x" (Figure 2a). Then letter "O" was printed using a water-insoluble ink over the hydrophilic and invisible "x" symbol; symbol "-" was also printed with a water-insoluble ink over the hydrophilic and invisible "|" symbol as shown in Figure 2b. The strong hydrophilic–hydrophobic contrast ensures a high resolution of the text patterns formed by antibody solutions. After drying under ambient conditions the device is ready for use. Detailed fabrication steps can be found in the Supporting Information.

In a blood typing assay, 2.5 μ L of blood sample were introduced into each of the antibody-loaded patterns (i.e. A, B, x, and |) with a micropipette (Figure 2c). Twenty seconds were allowed for the antibodies in the letter and symbol patterns to react with the antigens carried by the RBCs. After 20 seconds, two aliquots of 50 μ L saline solution were introduced into each of the letter and symbol patterns. In cases where haemagglutination reactions occur in certain text or symbol patterns, the agglutinated blood sample could not be washed out of those patterns. The agglutinated RBCs formed legible text patterns that report the occurrence of the specific haemagglutination reaction. On the other hand, if the haemagglutination reaction does not occur, the non-agglutinated blood can be easily washed out of the patterns through the vertical flow, leaving no visible trace of the blood sample (Figure 2d). The legible letter and symbol patterns, in combination, form the text report of the blood type of the sample. Figure 3a shows the expected reports for the eight blood types by the device; Figure 3b shows a photo of the actual blood type tests of all eight blood types.

The sensitivity of the bioactive paper text-reporting device was evaluated by testing blood samples (A+ and B+) diluted with saline solution (see Figure S4 in Supporting Information). This method is used to evaluate the sensitivity of blood typing assays for samples from patients with anaemia conditions; these samples have a decreased RBC color

a)	A+	B+	O+	AB+
	• • • A ■ +	• • • B ■ +	• • • O +	• • • AB ■ +
	• • • A ■ -	• • • B ■ -	• • • O -	• • • AB ■ -
	A-	B-	O-	AB-

b)	A+	B+	O+	AB+
	• • • A ✕ +	• • • B ✕ +	• • • O +	• • • AB ✕ +
	• • • A ✕ -	• • • B ✕ -	• • • O -	• • • AB ✕ -
	A-	B-	O-	AB-

Figure 3. a) A schematic of the expected text patterns reported by the blood type device fabricated based on our design. The corresponding blood types are given to assist the reader. b) The actual tests of all eight ABO RhD blood types. The device size is 25 mm×25 mm.

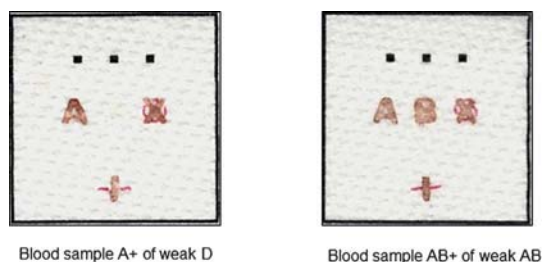


Figure 4. The text reports of weak blood samples using the paper-based text-reporting devices.

intensity. The bioactive paper text-reporting device can confidently identify A and B antigens on RBCs after the blood samples were diluted by a factor of four and D antigens by a factor of two. This level of sensitivity is sufficient, since dilution by a factor of two is considered an adequate threshold for anaemia samples (see the Supporting Information).

A total of 99 samples were tested using the text-reporting device; this sample set contained all eight blood types. All test results using the bioactive paper text-reporting devices matched with the results obtained by the pathological laboratory using the gel card technology. Details of the tested samples are presented in Table 1 in the Supporting Information. Among the samples, two weak samples, a weak AB and a weak D, were confirmed by the pathological laboratory following the gel card protocol. These weak samples were tested using the bioactive paper text-reporting device. The device is able to make clear identification of the blood types of these weak samples and the results match with the confirmation made by the pathological laboratory (see the Supporting Information). Figure 4 shows the test results of the two weak samples by bioactive paper text-reporting

device. The ability of the bioactive paper text-reporting device to confidently identify weak samples is also supported by our recent validation study of paper-based assays for rapid blood typing.^[27]

We show in this study that this bioactive paper text-reporting blood typing device meets the basic requirements of sensitivity, specificity, and text legibility. It is capable of reporting all blood types in the ABO RhD system. This reporting method significantly increases the ability of the device to report the results unambiguously to non-professional users. It is expected that an expansion of text-reporting bioactive paper sensors beyond the ABO RhD blood typing application may be possible. The concept of text-reporting using paper-based devices for low-cost diagnostic applications will be valuable for making affordable, sensitive, specific, rapid, equipment-free, and user-friendly (ASSURED^[10]) devices for developing countries.

Received: March 7, 2012

Published online: April 18, 2012

Keywords: analytical methods · bioactive paper · blood typing · diagnostics

- [1] A. W. Martinez, S. T. Phillips, M. J. Buttle, G. M. Whitesides, *Angew. Chem.* **2007**, *119*, 1340–1342; *Angew. Chem. Int. Ed.* **2007**, *46*, 1318–1320.
- [2] R. H. Müller, D. L. Clegg, *Anal. Chem.* **1949**, *21*, 1123–1125.
- [3] X. Li, J. Tian, W. Shen, *Cellulose* **2010**, *17*, 649–659.
- [4] X. Li, J. Tian, G. Garnier, W. Shen, *Colloids Surf. B* **2010**, *76*, 564–570.
- [5] X. Li, J. Tian, W. Shen, *Anal. Bioanal. Chem.* **2010**, *396*, 495–501.
- [6] J. L. Delaney, C. F. Hogan, J. Tian, W. Shen, *Anal. Chem.* **2011**, *83*, 1300–1306.
- [7] S. M. Z. Hossain, R. E. Luckham, M. J. McFadden, J. D. Brennan, *Anal. Chem.* **2009**, *81*, 9055–9064.
- [8] R. Pelton, *TrAC Trends Anal. Chem.* **2009**, *28*, 925–942.
- [9] <http://www.bioactivepaper.ca>.
- [10] D. Mabey, R. Peeling, A. Ustianowski, M. Perkins, *Nat. Rev. Microbiol.* **2004**, *2*, 231–240.
- [11] X. Li, J. Tian, T. Nguyen, W. Shen, *Anal. Chem.* **2008**, *80*, 9131–9134.
- [12] J. Tian, X. Li, W. Shen, *Lab Chip* **2011**, *11*, 2869–2875.
- [13] J. Tian, D. Kannangara, X. Li, W. Shen, *Lab Chip* **2010**, *10*, 2258–2264.
- [14] K. Abe, K. Suzuki, D. Citterio, *Anal. Chem.* **2008**, *80*, 6928–6934.
- [15] E. M. Fenton, M. R. Mascarenas, G. P. López, S. S. Sibbett, *ACS Appl. Mater. Interfaces* **2009**, *1*, 124–129.
- [16] Y. Lu, W. Shi, L. Jiang, J. Qin, B. Lin, *Electrophoresis* **2009**, *30*, 1497–1500.
- [17] A. W. Martinez, S. T. Phillips, E. Carrilho, S. Thomas, H. Sindi, G. M. Whitesides, *Anal. Chem.* **2008**, *80*, 3699–3707.
- [18] D. Ballerini, X. Li, W. Shen, *Anal. Bioanal. Chem.* **2011**, *399*, 1869–1875.
- [19] M. S. Khan, G. Thouas, W. Shen, G. Whyte, G. Garnier, *Anal. Chem.* **2010**, *82*, 4158–4164.
- [20] V. Leung, A. Shehata, C. Filipe, R. Pelton, *Colloids Surf. A* **2010**, *364*, 16–18.
- [21] A. Apilux, W. Dungchai, W. Siangproh, N. Praphairaksit, C. Henry, O. Chailapakul, *Anal. Chem.* **2010**, *82*, 1727–1732.

- [22] E. Carrilho, S. T. Phillips, S. J. Vella, A. W. Martinez, G. M. Whitesides, *Anal. Chem.* **2009**, *81*, 5990–5998.
 - [23] J. K. Rowling, *Harry Potter and the Chamber of Secrets*, Miracle Productions GmbH and Co. KG, **2002**.
 - [24] V. Joshi, A. Nandedkar, S. Mendburwar, *Anatomy and physiology for nursing and health care*, BI Publications Pvt. Ltd, **2006**.
 - [25] X. Li, J. Tian, W. Shen, *ACS Appl. Mater. Interfaces* **2010**, *2*, 1–6.
 - [26] P. Jarujamrus, J. Tian, X. Li, A. Siripinyanond, J. Shiowatana, W. Shen, *Analyst* **2012**, DOI: 10.1039/c2an15798e.
 - [27] M. Al-Tamimi, W. Shen, R. Zeineddine, H. Tran, G. Garnier, *Anal. Chem.* **2012**, *84*, 1661–1668.
-

This page is intentionally blank

Paper-based device for rapid typing of secondary human blood groups

Miaosi Li · Whui Lyn Then · Lizi Li · Wei Shen

Received: 26 September 2013 / Revised: 4 November 2013 / Accepted: 6 November 2013 / Published online: 28 November 2013
© Springer-Verlag Berlin Heidelberg 2013

Abstract We report the use of bioactive paper for typing of secondary human blood groups. Our recent work on using bioactive paper for human blood typing has led to the discovery of a new method for identifying haemagglutination of red blood cells. The primary human blood groups, i.e., ABO and RhD groups, have been successfully typed with this method. Clinically, however, many secondary blood groups can also cause fatal blood transfusion accidents, despite the fact that the haemagglutination reactions of secondary blood groups are generally weaker than those of the primary blood groups. We describe the design of a user-friendly sensor for rapid typing of secondary blood groups using bioactive paper. We also present mechanistic insights into interactions between secondary blood group antibodies and red blood cells obtained using confocal microscopy. Haemagglutination patterns under different conditions are revealed for optimization of the assay conditions.

Keywords Bioactive paper · Blood typing · Secondary blood groups · Confocal microscopy · Haemagglutination

Introduction

Blood groups were discovered at the beginning of the twentieth century, and for many years they have been considered the best human genetic markers since they carry a significant amount of information for mapping the human genome. To date, 30 blood group systems, including 328 authenticated blood groups, have been classified [1, 2]. The discovery of the ABO blood groups by Landsteiner made blood transfusion

feasible. The later discovery of the RhD antigens led to the understanding and subsequent prevention of haemolytic disease of the newborn (HDN) [3–5]. Although the ABO and RhD groups are the most important systems in transfusion medicine, many other blood group antibodies are also capable of causing haemolytic transfusion reactions or HDN. These blood groups, known as minor or secondary blood groups, are also of great clinical and biological importance in blood transfusion and transplantation [5, 6]. Each of these blood groups contains unique subtype antigens and has a different weight of distribution in the human population [7]. Furthermore, secondary blood groups do not follow the second part of Landsteiner's law—"If an agglutinin is absent in the red cells of a blood, the corresponding agglutinin must be present in the plasma"—which is true only of the ABO groups. Although antibodies A and B are naturally present in human blood serum corresponding to the antigens which they lack, the Rh and secondary antibodies in serum are generated only as a result of an immunization response triggered by transfused red blood cells (RBCs) that carry secondary antigens, or by fetal RBCs leaking into the maternal circulation during pregnancy or during birth [5]. Table 1 summarizes the common secondary blood groups and their subtype antigens. Among these blood groups, some antibodies, such as M, N, Lewis and Lutheran system antibodies, are inactive below 37 °C and are therefore not considered clinically important [5]. Others, however, are as clinically significant as primary blood groups. The mismatching of these blood groups may cause immediate and severe haemolytic transfusion reactions and HDN.

Accurate and rapid identification of human secondary blood groups is important for blood banking and medical procedures under either laboratory or field conditions [8]. Routine minor blood grouping methods rely primarily on the haemagglutination reactions between antigens and antibodies that are performed either manually or by automatic means

M. Li · W. L. Then · L. Li · W. Shen (✉)
Department of Chemical Engineering, Monash University,
Wellington Rd, Clayton, VIC 3800, Australia

Table 1 Common secondary blood group systems

Secondary blood group systems	Antigens
Rh	D*, C, c, E, e
Kell	K, k
P	P ⁱ
Kidd	Jk ^a , Jk ^b
MNS	M, N, S, s
Lewis	Le ^a , Le ^b
Lutheran	Lu ^a , Lu ^b

* Group D is one of the blood groups in the Rh system, but it is not considered as a secondary blood group

[9, 10]. Currently, the commonly used method for secondary blood grouping is based on a gel card test procedure, which requires concentrated RBCs and centrifugation [9]. Because there are a large number of antigens in secondary blood groups, a full identification of the antigens in those groups using this procedure is expensive and requires central laboratory conditions. Other methods, such as slide techniques, although of low cost and equipment-free, are insensitive and therefore are not recommended for initial or definitive antigen determinations, particularly when dealing with neonatal samples [5]. Investigations into novel techniques for rapid and low-cost secondary blood group typing diagnostics are therefore necessary and significant, especially for use in less-industrialized areas, for home care, and for local and temporary blood banking in disaster-response missions.

Recent research on the use of bioactive paper for human blood typing has established a new method for identifying haemagglutination of RBCs [11–16] which relies on using fibre networks in paper with controlled pore sizes to filter out and retain the agglutinated RBC lumps. When a blood sample is introduced onto a piece of paper pretreated with the corresponding grouping antibody, haemagglutination will occur, leading to the formation of agglutinated RBC lumps inside the fibre network [17]. The agglutinated lumps of RBCs are captured by the fibre network and cannot be removed by chromatographic elution with phosphate-buffered saline (PBS) or saline solution, leaving a clearly visible bloodstain on the paper. Conversely, if a blood sample is introduced onto paper treated with non-corresponding grouping antibodies, haemagglutination will not occur and free RBCs can be easily washed out of the fibre network, leaving no discernible stain. This phenomenon forms the foundation of using paper to make low-cost, rapid and user-friendly devices for ABO and RhD blood typing assays [16].

The antigens of some secondary blood groups are found to be less antigenic than the primary blood groups [18]. Those antigens show weaker interactions with their corresponding antibodies, resulting in increased difficulty in their identification in blood grouping assays. Different antibodies [e.g. immunoglobulin G (IgG) instead of immunoglobulin M (IgM)]

available to certain secondary RBC group antigens present further difficulties in blood grouping assays. Although the capabilities of IgG and IgM antibodies in the typing of secondary blood groups have been well understood, RBC responses to bonding with those antibodies are not. In this study, we investigate the secondary blood group antibody–RBC interactions in the fibre network of paper for the purpose of designing highly efficient paper-based secondary blood grouping devices. The confocal microscopy method we developed for paper-based blood grouping assays [17] was used to obtain mechanistic details of RBC behaviour in the interactions with secondary blood group antibodies. Our results elucidate (1) the differences in antibody-specific RBC haemagglutination caused by primary and secondary blood group antibodies, (2) the responses of RBCs to bonding with IgG and IgM antibodies, (3) the time-dependent antibody–antigen interactions in secondary blood grouping, and (4) a concept of secondary blood group assay result reporting using symbols. The protocols and conditions of assaying have also been established and are discussed. The outcome of this work provides microscopic details for the engineering of low-cost, sensitive, specific and rapid paper-based blood grouping devices for secondary human blood groups.

Experimental

Materials and appliances

The paper substrate used in this study was Kleenex paper towel (Kimberly-Clark, Australia). Alkyl ketene dimer (AKD; wax 88 Konz) as a paper hydrophobization reagent was obtained from BASF. AR grade *n*-heptane was obtained from Sigma-Aldrich (Australia); it was used to formulate an inkjet-printable solution for patterning text on paper through the formation of hydrophobic borders. Blood samples were sourced from Red Cross Australia (Sydney). They were stored at 4 °C and used within 7 days of collection. All antibodies were purchased from Alba Bioscience (Edinburgh, UK). The 0.9 % (w/v) NaCl saline solution and the PBS were prepared with AR grade NaCl (Univar) and phosphate (Sigma-Aldrich), using Milli-Q water. Fluorescein isothiocyanate (FITC; isomer I, product number F7250, from Sigma-Aldrich) was used for labelling RBCs [17, 19, 20]. Anhydrous dimethyl sulfoxide (Merck, Australia) was used to dissolve the FITC. Anhydrous D-glucose was provided by Ajax Finechem (Australia).

A reconstructed Canon inkjet printer (Pixma iP3600) was used to print the AKD–*n*-heptane solution onto a Kleenex paper sheet to form the required patterns defined by the hydrophilic–hydrophobic contrast. A series of micropipettes (Eppendorf Research®, 2.5–50 µL) were used to transfer antibodies, blood samples and saline solutions onto the paper device.

A Nikon Ai1Rsi confocal microscope in the Melbourne Centre for Nanofabrication was used to obtain the confocal micrographs. The objective lens used for imaging was a $\times 60$ oil immersion lens.

Symbol patterning onto paper

In our previous work for ABO and RhD blood group tests [16], the fabrication of a paper-based blood grouping device involved patterning letters and symbols as hydrophilic sites for RBC and antibody interactions, surrounded by hydrophobic borders, onto paper. It was done with inkjet printing of AKD onto paper to selectively hydrophobize it. The hydrophobic–hydrophilic contrast allows unambiguously legible text patterns of agglutinated blood to be displayed. Following the international convention, the blood types of the ABO group are reported directly with letters, whereas Rh and other secondary blood groups are reported with the symbol “+” or “-” to indicate either their presence or their absence in RBCs. In this work, for patterning paper for secondary blood grouping, we used “+” and “-” to indicate either a positive or a negative assay result. The symbol consists of a vertical hydrophilic channel and an overlapping horizontal bar printed with water-insoluble ink, as shown in Fig. 1.

An assay for identifying multiple secondary blood groups was performed by introducing 2.5 μL of the corresponding antibodies onto the vertical section of the symbols, and allowing the antibodies to dry under ambient conditions. Two and half microlitres of a blood sample was then introduced onto the vertical channel of all the symbols; a predetermined reaction time was allowed for the antibodies to interact with the RBCs. Subsequently, two 30- μL aliquots of saline solution were introduced onto the vertical section of the cross symbol to wash out the non-agglutinated RBCs.

After washing, the results can be directly read from the device—“+” indicating positive and “-” indicating negative.

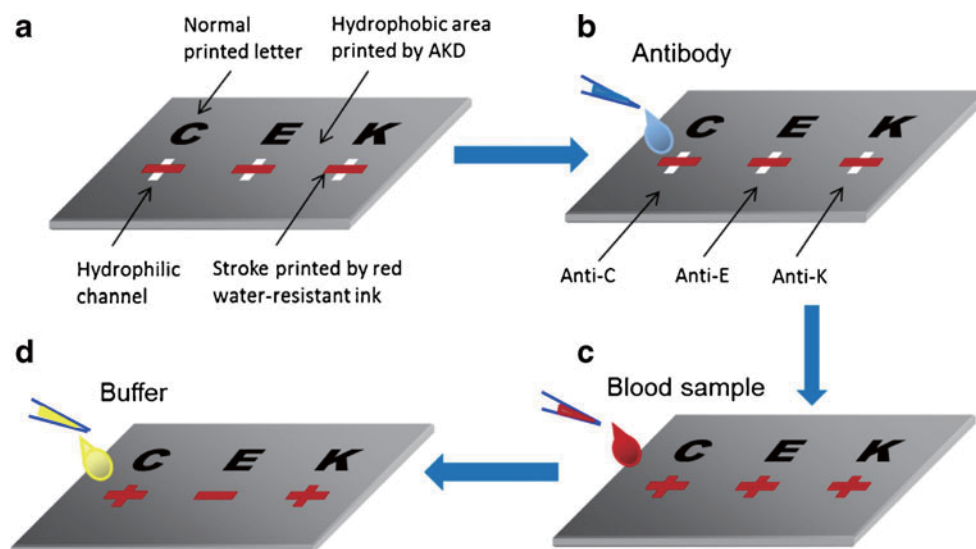
For confocal imaging, RBCs were labelled with FITC using the method reported by Li et al. [17], Hauck et al. [19] and Hudetz et al. [20]. The whole blood sample was first centrifuged at 1,300g relative centrifugal force for 3 min to separate the RBCs from the plasma. The plasma layer was then removed and the RBC layer was washed once with physical saline solution (PSS). FITC was dissolved in dimethyl sulfoxide at a high concentration (40 mg/mL), and was then diluted with CellStab solution to 0.8 mg/mL. This FITC solution and a D-glucose solution in PBS were then added to the RBCs until the concentrations of FITC and D-glucose reached 0.5 mg/mL and 0.4 mg/mL, respectively. This RBC suspension was then incubated in the dark for 2 h to allow FITC to attach onto the cell surface. After incubation, the RBC suspension was washed 13 times with PSS to remove unattached FITC and the RBCs were then resuspended at a haematocrit of around 35 % for further use.

Kleenex paper towel was cut into 10 mm \times 10 mm pieces for use as the test substrate. Ten microlitres of antibody solution was dropped onto paper pieces and allowed to dry, and then 6 μL of labelled RBCs was dropped onto them. A preset reaction time was allowed. Then, 20 μL of PSS was pipetted onto the sample and the sample was immediately placed onto a glass slide for confocal imaging.

Results and discussion

Following the testing procedure illustrated in Fig. 1, a number of secondary blood groups can be assayed on a paper strip; the typical assay results of one blood sample are shown in Fig. 2 by putting the assay papers together. Gel card tests of the same

Fig. 1 Design, fabrication, testing procedures and result reporting of paper diagnostics for secondary blood group typing. AKD alkyl ketene dimer



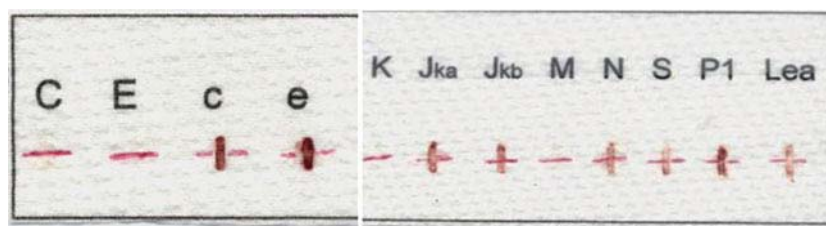


Fig. 2 Paper-based blood group assay designed for identifying 12 antigens in six secondary blood group systems. The blood grouping assay was performed under the same conditions: the reaction time was 30 s and the washing of free red blood cells (RBCs) was done using 0.9 % NaCl

physical saline solution. Reference assays using mainstream technology (gel card) showed that the secondary blood group systems of this blood sample were C(-), E(-), c(+), e(+), K(-), Jka(+), Jkb(+), M(+), N(+), S(+), P1(+), and Lea(+)

blood sample performed in the laboratory of Red Cross Australia were used to compare the results with the results obtained using our paper-based assays.

Two observations can be made. First, with the exception of blood group M, the secondary blood grouping results reported by our paper-based assays matched the gel card results. Second, like the gel card tests, where the clarity of the results of secondary blood groups is less consistent than that of primary blood groups, on paper-based assays the colour intensity of antigen-positive RBCs differs significantly despite all tests being conducted under the same conditions. These results suggest that paper-based sensors are capable of performing assays for secondary blood group antigens and antibodies differ. To further understand the antigen–antibody interactions of secondary blood groups, and to optimize the assay conditions, we focused on the influence of the following factors on RBC agglutination: the antibody–antigen reaction time, antibody types, and washing conditions. Microscopic information obtained with confocal microscopy was compared with information obtained from the visual assays to study the interactions of RBCs in paper.

The effect of the interaction period

The bonding of ABO and RhD antigens with their corresponding antibodies normally occurs instantaneously [16]; therefore, haemagglutination can be visually identified within 30 s [17]. This reaction time, however, is not sufficient for some secondary blood group antigens as they are less antigenic. As a result, the time required for secondary blood group agglutinations to

be visually identifiable ranges from 30 s to 3 min, depending on the antibody–antigen pair. For example, blood groups C and E have strong interactions with their corresponding antibodies within 30 s, whereas blood groups c and e would show false-negative results if the same interaction time of 30 s were allowed. We found that longer interaction times (i.e. 2–3 min) must be allowed for secondary blood groups to improve the clarity of the results (Fig. 3). However, a prolonged reaction time can lead to false-positive results, as excessive exposure of a blood sample to the atmosphere causes aggregation of RBCs. Our study showed that a reaction time up to 3 min is appropriate and adequate for the unambiguous identification of the weaker haemagglutinations.

Confocal microscopy was used to gain a microscopic understanding of haemagglutination processes of RBCs carrying secondary blood group antigens. For comparison, haemagglutination of RBCs by corresponding primary and secondary blood group antibodies was investigated to show the differences in the strength of RBC agglutination. Figure 4 shows four confocal microscopy images taken with a $\times 60$ oil immersion lens. RBCs carrying D(+) (primary) and E(+) (secondary) antigens showed rapid agglutination within 30 s after contact with their corresponding antibodies. RBCs carrying primary blood group D antigens interacted strongly with their corresponding antibodies, leading to strong deformation of RBCs, which formed large lumps; individual RBCs in the lump could not be identified (Fig. 4a). RBCs carrying secondary blood group E antigens showed weaker agglutination than the RBCs carrying group D antigens. Although E(+) RBCs also formed lumps on reacting with the E antibody, cell

Fig. 3 Increasing degrees of haemagglutination of secondary blood group e in antibody-treated paper as a function of time

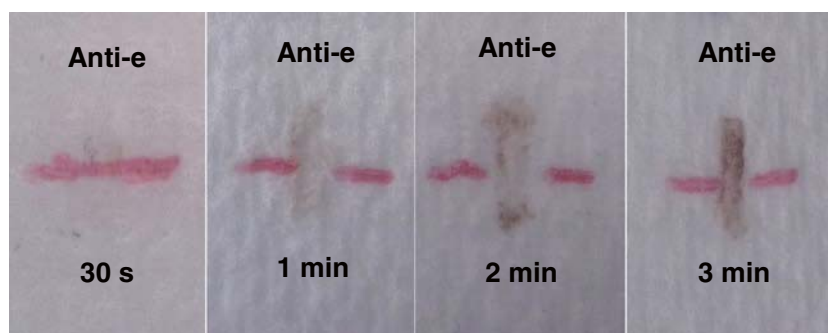
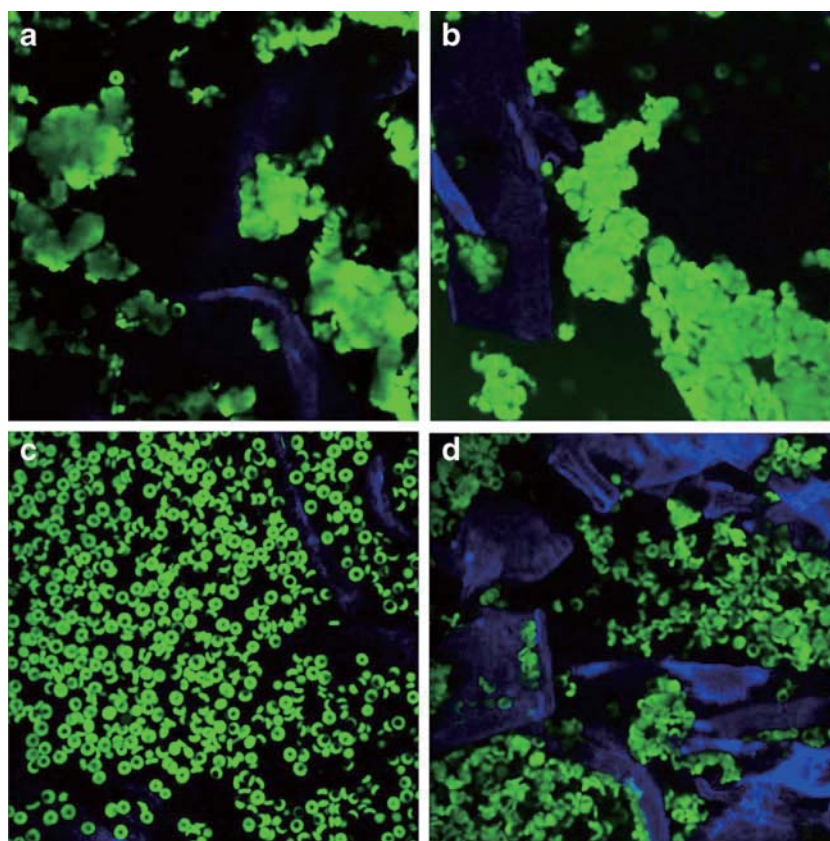


Fig. 4 Haemagglutination behaviour of three blood groups investigated by confocal imaging ($\times 60$ oil immersion lens): **a** RBCs of primary blood group D(+) agglutinated by D antibodies within 30 s; **b** RBCs of secondary blood group E(+) agglutinated by E antibodies within 30 s; **c** RBCs of secondary blood group e(+) did not show any sign of agglutination after reacting with e antibody for 30s; **d** blood group e(+) RBCs showed clear agglutination when reacting with e antibody for 3 min



deformation was less severe than that of the D(+) RBCs (Fig. 4b). The e(+) RBCs showed even weaker agglutination; no agglutination was observable for 30 s of reaction time (Fig. 4c). However, when 3 min of reaction time was allowed, the e(+) RBCs clearly showed agglutination, even though the degree of agglutination was much weaker than for RBCs of the D(+) and E(+) groups (Fig. 4d). These results correlate with the visual assays performed on paper (Fig. 3). More importantly, the confocal microscopy results confirmed the time-dependent haemagglutination reaction of some secondary blood groups. Table 2 summarizes the reaction time required by different secondary blood groups.

The effect of antibody structure

Although some commercial antibodies for secondary blood grouping can easily identify the corresponding secondary blood group antigens through RBC haemagglutination, others

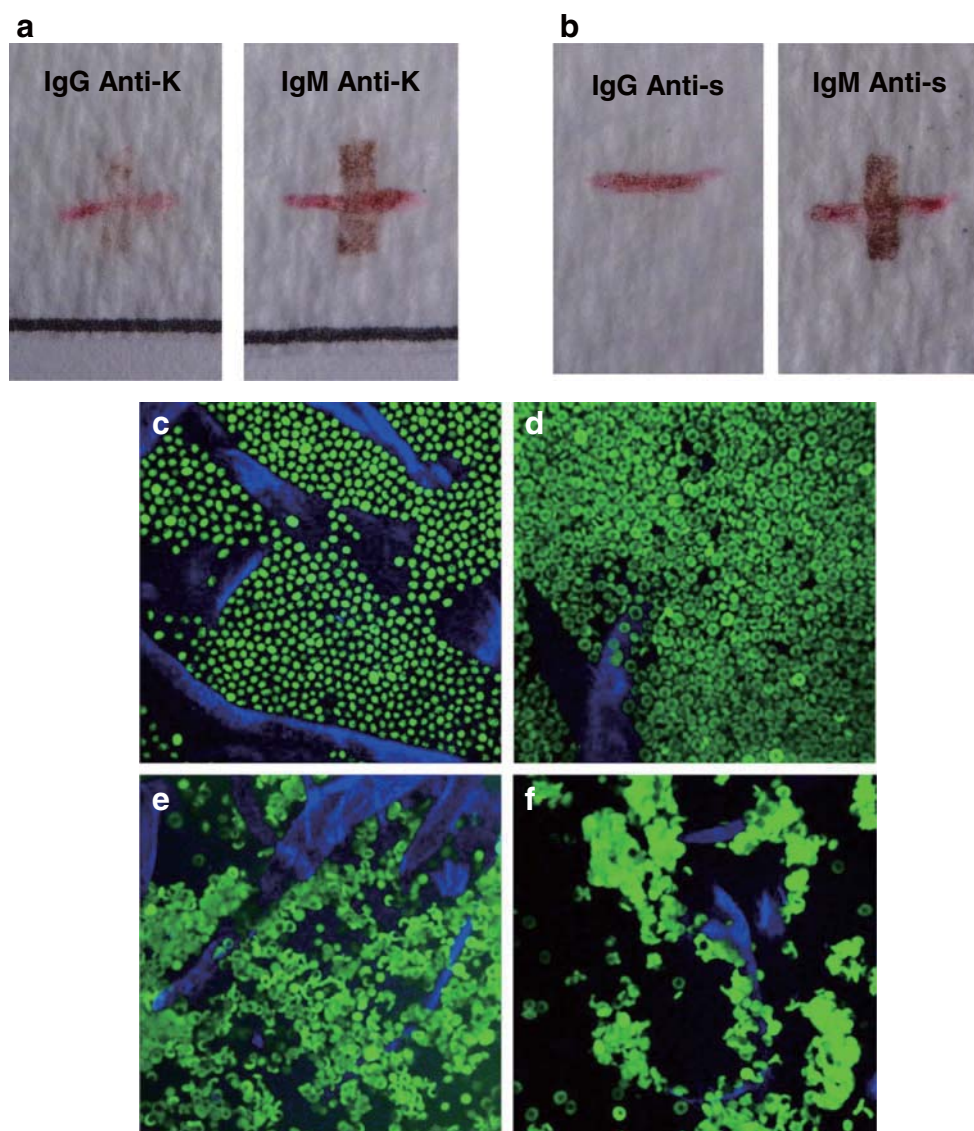
cannot. This is partially due to the structure of antibodies; the IgM and IgG antibodies show a strong performance contrast in causing haemagglutination of RBCs. The commercial products of IgM are monoclonal immunoglobulin which has a pentameric form; each monomer has two binding sites, and IgM therefore has ten sites in total. IgG antibodies, however, are monomers with only two binding sites in total. The molecular dimension of an IgM molecule is also greater than that of an IgG molecule, being 30 nm and 14 nm, respectively [5]. Consequently, the distance between the two binding sites of an IgG molecule is too small to allow it to simultaneously bind with antigens on two RBCs and cause direct agglutination. Generally, IgM antibodies will directly agglutinate antigen-positive RBCs, whereas most IgG antibodies require potentiators or anti-human globulin to effect agglutination [5].

For secondary blood grouping on paper, the IgM antibodies can simultaneously bind to antigens on two RBCs, thus producing sufficiently large agglutinated RBC lumps that can be

Table 2 Agglutination reaction time required by each secondary blood group for the Alba Bioscience antibodies specified in this study

	Blood groups										
	C	c	E	e	K	k	Jk ^a	Jk ^b	P ¹	S	s
Required reaction period	30 s	3 min	30 s	3 min	2 min	30 s	2 min	2 min	30 s	2 min	2 min

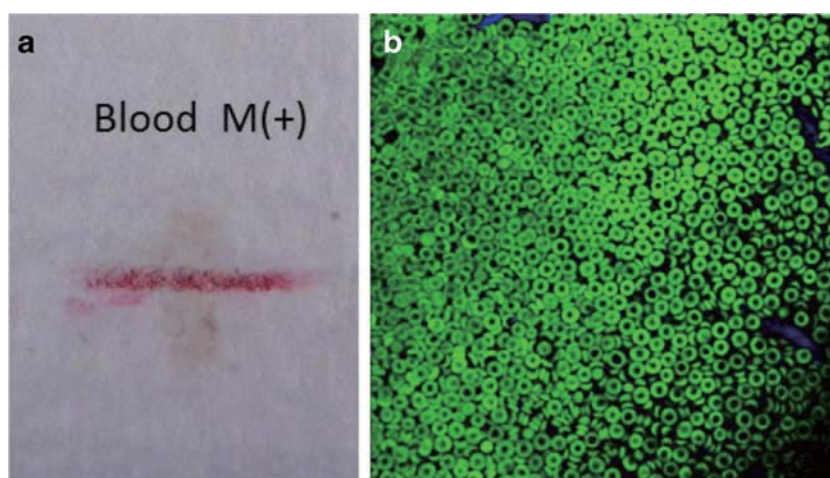
Fig. 5 Comparison of the effect of antibody structures (IgG and IgM) on the visual identification of the test results: **a** for K antigen test; **b** for s antigen test. The confocal images show details of the haemagglutination behaviours of K(+) and s(+) on paper treated with different antibodies: **c** anti-K IgG, **d** anti-s IgG, **e** anti-K IgM and **f** anti-s IgM. The reaction times of all assays were 2 min and a $\times 60$ oil lens was used



immobilized in the porous structure of paper. In contrast, agglutination reactions between IgG and RBC antigens

without anti-human globulin are either extremely weak or do not occur at all, leading to false-negative results. The example

Fig. 6 **a** Visual assay of an M(+) blood sample on paper and **b** confocal image of the same sample. A commercial anti-M IgM obtained from human sera was used for the assay and a reaction time of 3 min was allowed



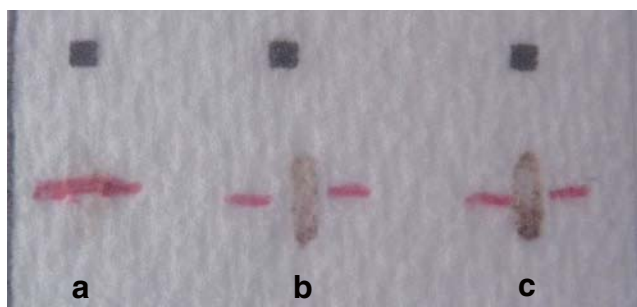


Fig. 7 Identification for agglutinated RBCs of blood group c washed with distilled water (a), 0.9 % NaCl (b), and phosphate-buffered saline (c). An RBC–antibody interaction time of 2 min was allowed

of K antigen in the Kell system is used to illustrate the different performance of antibodies with different structures. Both IgM and IgG antibodies corresponding to K antigen are commercially available. Figure 5a shows a distinct difference in RBC agglutination patterns: whereas IgM causes strong agglutination of the K-positive sample, IgG shows little or no effect. Another example of detecting s antigen (of the MNS system, Table 1) using IgM and IgG antibodies also shows results very similar to those of the K antigen in the Kell system, confirming that the different structures of antibodies can lead to extremely different agglutination behaviours (Fig. 5b).

Confocal microscopy was used to capture the agglutination patterns of the K(+) and s(+) RBCs by IgM and IgG antibodies. Figure 5c and d show agglutination patterns of K(+) and s(+) RBCs after they had been introduced onto papers treated with anti-K IgG and anti-s IgG, respectively. In both cases, no discernible RBC agglutination could be observed. An interesting observation was that K(+) RBCs show strong deformation and crenation when mixed with anti-K IgG. This is because the commercial anti-K IgG reagent was directly obtained and prepared from a donor's plasma. The impurity of the antibody solution might have caused the RBC deformation. After a drop of 10 μ L CellStab solution had been added to the paper, the RBCs regained their natural biconcave disc shape (result not presented), but agglutination of RBCs never occurred. In contrast, when K(+) and s(+) RBCs were introduced onto papers treated with anti-K IgM (Fig. 5e) and anti-s IgM (Fig. 5f), agglutination of RBCs was clearly observed

under the confocal microscope. The confocal microscopy results also show that anti-s IgM causes a stronger degree of agglutination than anti-K IgM (Fig. 5e, f); these results concur with the visual assay on the paper surface (Fig. 5a, b). They provided a clear understanding of the effects of antibody structures on the efficiency of RBC agglutination; such effects were further confirmed on a microscopic level.

In another study, antibody–antigen interactions of secondary blood group M were investigated using confocal microscopy. The motivation of this investigation was to understand why a false-negative result was observed for this blood group in our screening test (Fig. 2). A repeat of the assay on paper showed no RBC agglutination, even though a reaction time of 3 min was allowed (Fig. 6a). The confocal image showed that M(+) RBCs could not be agglutinated by anti-M IgM (Fig. 6b). Although anti-M is IgM antiserum, it is considered as a naturally occurring antibody in the human body, rather than an antibody generated by immunoreactions [21]. This type of antibody is a cold-reacting antibody which is not active at 37 °C, and therefore is regarded as clinically insignificant [5, 21]. In general, the detection of anti-M can be disregarded for transfusion purposes.

The effect of washing conditions

The selection of the washing solution affects the result of secondary blood grouping assays. Firstly, water cannot be used to remove the non-agglutinated blood because of the osmotic effect. Under osmotic pressure, water penetrates into the RBC through its membrane, causing RBC haemolysis by bursting. The agglutinated RBCs therefore can also be removed from the paper (Fig. 7, test a). Secondly, the pH is also an important factor in washing. Under normal circumstances, a washing solution with a pH of about 7 is acceptable because RBCs carry a negative charge and at pH 7–7.5 most antibody molecules have weak positive charges. This enhances the attraction between the RBCs and antibody molecules during the first stage of interaction. Significant lowering of the pH increases the dissociation of the antigen–antibody complexes. This influence of pH levels on the assay result was found to be much more important for secondary blood groups than for primary blood groups; this is due to the weaker antibody–

Table 3 Secondary blood group typing data obtained using paper devices

	Blood type										
	C	E	c	e	P ¹	K	k	Jk ^a	Jk ^b	S	s
Antibody type	IgM	IgM	IgM	IgM	IgM	IgM	IgM	IgM	IgM	IgM	IgM
Reaction period	30 s	30 s	3 min	3 min	30 s	2 min	30 s	2 min	2 min	2 min	2 min
Number of samples	127	127	127	127	79	79	19	30	30	11	11
Matching with the laboratory results (%)	100	100	100	100	100	100	100	100	100	100	100

antigen interactions of secondary blood groups. Figure 7 (tests b and c) shows the washing of the agglutinated RBCs from the paper. Our results show that for the best results of secondary blood grouping assays, PBS should be used for washing.

Five clinically important secondary blood group systems, including 11 blood groups, have been tested under their optimum conditions. Each blood group involved from 11 to more than 100 samples and all test results using the bioactive-paper devices matched the results obtained in a pathology laboratory using gel card technology. Details of the samples tested are presented in Table 3. The accuracy of this paper diagnostic assay for the blood samples studied was 100 %.

Conclusion

We have shown in this study that paper-based diagnostics are capable of testing various clinically important secondary blood types. Compared with the typing of primary blood groups, the major challenges in secondary blood group assaying were identified to be the antibody–RBC interaction time, the antibody types, and the pH of the washing buffer. Visual observation of the agglutination pattern on paper was used to evaluate the degree of agglutination under the conditions of the investigation, and confocal microscopy was used to obtain microscopic information on the agglutination patterns in a fibre network at a cellular level. The microscopic and macroscopic results presented in this work establish a detailed understanding of secondary blood grouping in paper. First, RBCs carrying some secondary blood group antigens require a longer time to react with their corresponding antibodies in order to form a sufficient level of agglutination for unambiguous visual identification on paper. Second, the types of antibodies are important in secondary blood group typing. This work confirmed, at a cellular level, that whereas IgM antibodies are able to cause direct agglutination of RBCs, IgG antibodies are unable to do this. In that case an indirect method must be used. Third, the pH of the washing buffer must be maintained at neutral, or at a slightly basic level, to prevent the undesirable dissociation of the agglutinated RBC lumps during washing.

This work is the first research on using paper-based diagnostics for secondary blood group typing. Of the 11 clinically important secondary blood groups we investigated in this study (Table 3), the results obtained by paper-based devices showed a 100 % match with the mainstream gel card technology. The design concept of the paper assay allows both professionals and non-professionals to easily understand and perform the assay.

Acknowledgments This work was supported by the Australian Research Council (ARC). Funding received from the ARC through grants DP1094179 and LP110200973 is gratefully acknowledged. The authors thank Haemokinesis for its support through the ARC Linkage Project. The authors also thank John Zhu of the Melbourne Centre for Nanofabrication for confocal imaging and technical help, and Hansen

Shen for proofreading the manuscript. M.L., W.L.T. and L.L. thank the Monash University Research and Graduate School and the Faculty of Engineering for postgraduate research scholarships.

Reference

1. Daniels G (2002) Human blood groups, 2nd edn. Blackwell, Oxford
2. Daniels G, Reid ME (2010) Blood groups: the past 50 years. *Transfusion* 50(2):281–289
3. Avent ND, Reid ME (2000) The Rh blood group system: a review. *Blood* 95(2):375–387
4. Westhoff CM (2004) The Rh blood group system in review: a new face for the next decade. *Transfusion* 44(11):1663–1673
5. Daniels G, Bromilow I (2007) Essential guide to blood groups. Wiley-Blackwell, Hoboken
6. Daniels G, Poole J, de Silva M, Callaghan T, MacLennan S, Smith N (2002) The clinical significance of blood group antibodies. *Transfus Med* 12:287–295
7. Thakral B, Saluja K, Sharma RR, Marwaha N (2010) Phenotype frequencies of blood group systems (Rh, Kell, Kidd, Duffy, MNS, P, Lewis, and Lutheran) in north Indian blood donors. *Transfus Apher Sci* 43(1):17–22
8. Malomgré W, Neumeister B (2009) Recent and future trends in blood group typing. *Anal Bioanal Chem* 393(5):1443–1451
9. Harmening DM (1999) Modern blood banking and transfusion practices, 4th edn. Davis, Philadelphia
10. Li L, Tian J, Ballerini D, Li M, Shen W (2013) Superhydrophobic surface supported bioassay—an application in blood typing. *Colloids Surf B: Biointerfaces* 106:176–180
11. Pelton R (2009) Bioactive paper provides a low-cost platform for diagnostics. *Trends Anal Chem* 28(8):925–942
12. Li X, Tian J, Shen W (2009) Paper as a low-cost base material for diagnostic and environmental sensing applications. In: 63rd Appita annual conference and exhibition, Melbourne 19–22 April 2009. Appita, Melbourne, pp 267–271
13. Ballerini D, Li X, Shen W (2012) Patterned paper and alternative materials as substrates for low-cost microfluidic diagnostics. *Microfluidics Nanofluidics* 13(5):769–787
14. Khan MS, Thouas G, Shen W, Whyte G, Garnier G (2010) Paper diagnostic for instantaneous blood typing. *Anal Chem* 82(10):4158–4164
15. Al-Tamimi M, Shen W, Zeineddine R, Tran H, Garnier G (2011) Validation of paper-based assay for rapid blood typing. *Anal Chem* 84(3):1661–1668
16. Li M, Tian J, Al-Tamimi M, Shen W (2012) Paper-based blood typing device that reports patient's blood type “in writing”. *Angew Chem Int Ed* 51:5497–5501
17. Li L, Tian J, Ballerini D, Li M, Shen W (2013) A study of the transport and immobilisation mechanisms of human red blood cells in a paper-based blood typing device studied using confocal microscopy. *Analyst* 138:4933–4940
18. Dean L (2005) Blood groups and red cell antigens. National Center for Biotechnology Information, Bethesda
19. Hauck EF, Apostel S, Hoffmann JF, Heimann A, Kempfski O, Cereb J (2004) Capillary flow and diameter changes during reperfusion after global cerebral ischemia studied by intravital video microscopy. *Blood Flow Metab* 24:383–391
20. Hudetz AG, Feher G, Weigle CGM, Knuese DE, Kampine JP (1995) Video microscopy of cerebrocortical capillary flow: response to hypotension and intracranial hypertension. *Am J Physiol Heart Circ Physiol* 268:H2202–H2210
21. Mais DD (2009) ASCP quick compendium of clinical pathology, 2nd edn. ASCP Press, Chicago



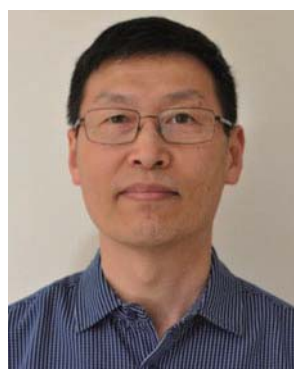
Miaosi Li is a PhD student with the Australia Pulp and Paper Institute in the Department of Chemical Engineering, Monash University, Australia. Her current research is focused on the development of user-friendly diagnostic sensors for the purpose of blood analyses and other biochemical analyses for developing countries.



Lizi Li is a PhD student in the Department of Chemical Engineering, Monash University, Australia. Her current research interests include the optimization of paper structure and surface chemistry for high-performance paper-based blood typing devices and the development of superhydrophobic surface supported bioassays.



Whui Lyn Then is a PhD candidate with BioPRIA in the Department of Chemical Engineering, Monash University, Australia, researching antigen-antibody interactions on paper diagnostics with special focus on paper-based diagnostics for blood typing applications.



Wei Shen is Head of the Surface Engineering Group of the Department of Chemical Engineering, Monash University, Australia. His research interest is focused on paper-based and thread-based analytical devices for diagnostic and environmental applications. The group's aim is to use low-technology innovations to create high-performance devices for real-life analysis.

This page is intentionally blank

The detection of blood group phenotypes using paper diagnostics

W. L. Then, M. Li, H. McLiesh, W. Shen & G. Garnier

Department of Chemical Engineering, BioPRIA, Australian Pulp and Paper Institute (APPI), Monash University, Clayton, Vic., Australia

Vox Sanguinis

Background and Objectives Paper biondiagnostics for blood typing are novel, cheap, fast and easy to use. Agglutinated red blood cells cannot travel through the porous structure of paper, indicating a positive antibody–antigen interaction has occurred. Conversely, non-agglutinated blood can disperse and wick through the paper structure with the ease to indicate a negative result. This principle has been demonstrated to detect blood group phenotypes: ABO and RhD. However, typing for red blood cell antigens such as Rh, Kell, Duffy and Kidd has not yet been explored on paper.

Materials and Methods Two paper testing methods – an elution and a direct flow-through method – were investigated to detect red blood cell antigens excluding the ABO system and RhD. Antigens explored include the following: C, c, E, e, K, k, Fy^a, Fy^b, Jk^a, Jk^b, M, N, S and s, P1, Le^a and Le^b. The variables tested include the following: reaction time and reagent concentration. The importance of antibody type/structure for successful agglutination on paper was confirmed.

Results Some blood group phenotypes showed less agglutination due to weaker antibody–antigen interactions. Most blood groups with antibodies available as IgM, such as C, c, E, e, K and k, and Jk^a and Jk^b, and P1, were successful using both methods. However, other blood groups, especially those with antibodies only available as polyclonal antibodies, were unsuccessful and require further scrutiny.

Conclusion Paper can be used as an alternative blood grouping diagnostic tool for selected blood group phenotypes.

Key words: blood groups, blood typing, haemagglutination, IgG, IgM, paper diagnostics.

Received: 6 May 2014,
revised 12 August 2014,
accepted 13 August 2014

Introduction

Although ABO and RhD are the most important blood group systems in transfusion medicine, many other blood group antibodies can cause serious or fatal haemolytic transfusion reactions (HTRs) or haemolytic disease of the foetus and newborn (HDFN). Current blood typing techniques rely on antibody–antigen interactions to cause red blood cell agglutination for positive identification. Techniques, such as gel columns, are well established. Com-

mon methods for phenotyping blood groups are the tube test and column agglutination test (CAT), which require centrifugation only available under laboratory conditions, unsuitable for in-field and remote testing [1]. Currently, CATs are more widely used, relying on gels or glass beads to visualize agglutination. However, the process requires trained personnel, is more expensive, lengthy and time-consuming to operate. Low-cost and equipment-free methods, such as the glass slide test, can be insensitive and are unsuitable for antigen identification, particularly for neonatal samples [2]. This is especially true when testing for the wide array of clinically significant blood group phenotypes.

For many years, blood groups were the best genetic markers and have played a key role in the mapping of

Correspondence: Gil Garnier, Department of Chemical Engineering, BioPRIA, Australian Pulp and Paper Institute (APPI), Monash University, Clayton, Vic. 3800, Australia

the human genome [3]. Blood group antigens are found on the surface of red blood cells (RBCs). These dictate an individual's blood type. Blood group antibodies are present in the blood plasma and generally result from an immune response triggered by prior exposure, such as previous transfusions or during pregnancy, to the corresponding antigen not located on that individual's RBC surface (alloantibody). There are now 35 blood group systems recognized, with more than 300 blood group antigens, many of which are clinically significant, requiring detection and the identification of antibodies to be performed prior to blood transfusions [3, 4]. The discovery of the ABO blood groups made blood transfusions safe; the disclosure of the RhD antigens led to the understanding and prevention of HDFN [2, 5, 6]. Each of the blood group phenotype systems contains antigens that are unique and have a different frequency depending on the patient's ethnicity [7]. The blood groups and their corresponding alloantibody examined in this study are summarized in Table 1. Aside from these blood groups, some alloantibodies, such as Anti-M, N, P1 and Lewis antibodies, are seldom active at body temperature (37°C) and are generally not considered clinically significant [2]. The mismatching of a blood group antigen in the presence of a clinically significant antibody could cause immediate, delayed or severe HTRs or HDFN, necessitating tests to identify or confirm the presence of these antigens. Prior to blood transfusion, the accurate and fast identification

of the blood group phenotypes is essential for patients who possess an alloantibody [8].

Further development in low-cost minor blood typing methods is necessary, especially for testing in developing countries and the battlefield. Novel paper diagnostic for human blood typing through the haemagglutination of RBCs was developed [9–17]. Paper can be pretreated with a blood typing antibody reagent. When a blood sample is subsequently introduced onto the antibody pretreated paper, if positive, a haemagglutination reaction will occur between the RBCs and corresponding antibody. These blood agglutinates are formed within the porous structure of paper and cannot be removed when washed with solutions such as phosphate-buffered saline (PBS) or 0.9% NaCl saline. Inversely, during negative reactions, the RBCs do not agglutinate and the cells are easily washed away. This phenomenon is the foundation of paper substrates for blood typing which was used to design diagnostics for ABO and RhD blood testing [12].

In this study, paper diagnostics were engineered to identify blood groups using haemagglutination, focusing on common clinically significant blood group phenotypes. The method for phenotyping these blood groups proved not to be as simplistic as the ABO and RhD groups; time-dependent reactions became evident [10, 17]. The influences of antibody types, reaction time, washing conditions and antisera concentration on the identification of blood group phenotype were investigated.

Two separate testing methods were developed using paper, each using different principles regarding the interactions of the analytes, samples and washing method. One method follows the principles of chromatography, allowing the washing solution to elute unbound blood cells laterally along the paper structure (wicking). This method was used for ABO and RhD groups [11]. The second uses the flow-through method [12, 18, 19], which washes through the paper, rather than along, utilizing a filtration mechanism. While each method has been successful when testing ABO and RhD blood types, this is the first report testing paper diagnostics for the detection of blood group phenotypes other than ABO and RhD using both methods.

Materials and methods

Materials and equipment

Professional Kleenex paper towel from Kimberly-Clark, Australia, was employed as paper. Antisera blood typing antibodies were purchased from ALBA bioscience, Edinburgh, United Kingdom, and used as received (Table 1). Washing solutions 0.9% (w/v) NaCl saline and PBS were prepared using MilliQ water, analytical grade NaCl (Uni-

Table 1 Blood groups and the corresponding antibodies used for blood group phenotyping on paper. The antibody structure and clone is also included

Blood system	Blood type	Reagent type	Clone
Rh	C	IgM	P3x25513G8
	E	IgM	DEM1
	c	IgM	H48
	e	IgM	MS-36 and P3GD512
Kell	K	Polyclonal	Polyclonal (human source)
	K	IgM	MS-56
	k	IgM	Lk1
Kidd	Jk ^a	IgM	P3HT7
	Jk ^b	IgM	P3-143
Duffy	Fy ^a	Polyclonal	Polyclonal (human source)
	Fy ^b	Polyclonal	Polyclonal (human source)
MNS	M	IgM	LM1
	N	IgM	LN3
	S	IgM	P3S13JS123
	s	Polyclonal	Polyclonal (human source)
P	P1	IgM	650
Lewis	Le ^a	IgM	LEA2
	Le ^b	IgM	LEB2

var) and PBS tablets (Sigma-Aldrich, Castle Hill, Australia), respectively. Alkyl ketene dimer (AKD) from BASF was used for paper hydrophobization. Analytical grade n-heptane from Sigma-Aldrich was used to formulate ink-jet solution to print text on paper. EDTA blood samples were sourced from Australian Red Cross Blood Service (ARCBS), stored at 4°C and used within 7 days of collection.

Micropipettes (Eppendorf research®, 2.5–50 µl) were used to introduce the antibodies, blood samples and saline solutions on paper. Millipore centrifugation tubes (50 kD cut-off) from Merck, Australia, were used to remove supernatant and increase concentration of the antibodies by filtration.

Method

Two methods were tested: the first was the elution methodology for high-throughput diagnostics in laboratory settings [11] and the second flow-through method used the direct-reporting method suited for remote and emergent situations [12]. These methods differ by the direction of liquid transport within paper during the washing step. The elution method relies on the paper structure to wick saline solution laterally and separate by chromatography along paper, while direct-reporting washes via a flow-through filtration-like method.

Elution

A known antibody reagent is dotted along the bottom of paper (10 µl) before the addition of mixed EDTA blood sample (3 µl) [11]. After a reaction period, ranging from

30 to 120 s, the substrate was hung in a vertical-standing elution tank containing 0.9% NaCl saline solution at a depth of 1 cm. Following an elution period of 5 min, the substrate was removed and dried in the laboratory ($T = 22 \pm 1^\circ\text{C}$; relative humidity = 30–50%) (Fig. 1). Qualitative evaluation of results was conducted visually. Agglutination showed a distinct bloodspot, while non-agglutinated RBCs were defined by the absence of a blood spot and by a clear elution path on paper. Quantitative analysis was achieved using IMAGEJ software (National Institute of Health, Bethesda, MD, USA) to measure colour densities of the blood spot (BS) and elution pathway (EP).

Kleenex paper towel was selected for performance, attainability and cost. Compared with other paper, such as Whatman filter, the results achieved were clearer and more reliable [11, 16].

Flow-Through Direct reporting

Agglutinated cells can form patterns to resemble text or signs. This can be achieved by hydrophobic barriers printed onto the paper prior to the addition of cells. The hydrophobic barrier guides where antisera will be absorbed into the paper. This strong hydrophobic–hydrophilic contrast can be used to border the RBC–antibody interactions on paper, forming shapes or ‘text’ that can be easily read when fabricating a user-friendly blood group device [15]. A reconstructed Canon ink-jet printer (Pixma iP3600) was used to print channels onto paper with an AKD–heptane solution (Fig. 2).

Aliquots of 2.5 µl of antibody solutions were introduced into the corresponding patterns. After the antibody solution was dried, 2.5 µl of blood sample was introduced

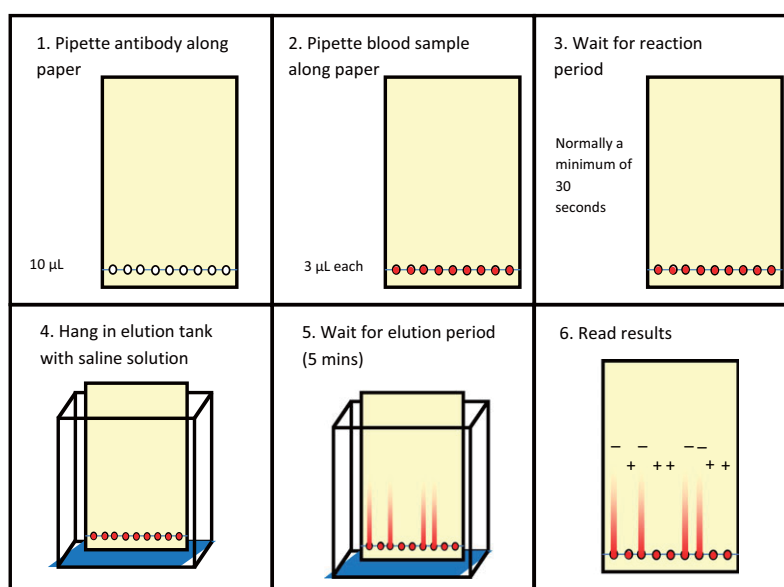


Fig. 1 Methodology for blood group phenotyping using paper via elution.

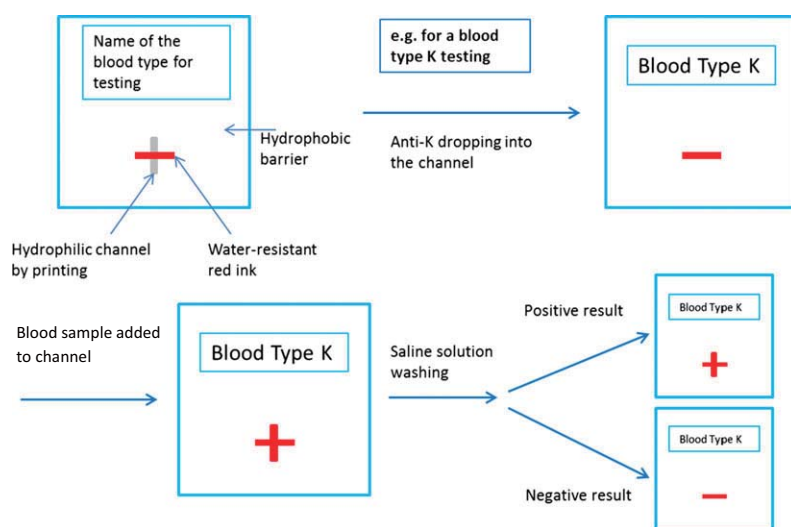


Fig. 2 Fabrication, testing procedures and result reporting of paper diagnostics for antigen detection using example: blood group K.

into the vertical channel. A reaction period was allowed for the antibodies to interact with the RBCs inside the channels. Washing was performed with two 30 μ l aliquots of saline solution introduced into the patterns to wash out non-agglutinated RBCs. The blood types were then read directly. Quantitative analysis used IMAGEJ to measure channel density.

Analysis criteria

Successful testing should easily distinguish positive from negative, while preventing false-positive and false-negative results. For the elution method, a positive result should report a well-defined blood spot (BS) with no RBCs in the elution pathway (EP); conversely, a negative result would have no BS, but show distinct wicking in the EP. The direct-reporting method prints a positive '+' sign, while a negative in the absence of RBCs leaves a negative '-' sign. Two hundred and thirty-six different patient samples were tested. However, not all samples were fully phenotyped. The number of samples for each antigen tested was restrained by blood availability, outlined in Table 2.

To compare the strength of each blood group's antibody-antigen reactions and the testing conditions, the colour densities of the resulting BS were measured using IMAGEJ. Distinct patterns emerged when comparing positive and negative results. Higher density values indicated a positive result (usually >100), while lower values indicated negative samples (<40). Densities between this range (40–100) could be classified as weaker reactions. This distinction was used for the text-reporting method.

However, to analyse the elution method results, the BS alone was insufficient to indicate the interactions of cer-

tain blood groups. In such instances, the BS optical densities bordered the weak reaction threshold. In some cases, the BS for negative and positive looked too similar for accurate determination by the naked eye. It was the presence/absence of an EP that confirmed the result. Therefore, in addition to BS density, an area of the EP 2 cm above the BS was measured. Positive results contained little or no RBCs in EP with low density values. Conversely, negative results showed high densities representing unbound RBCs travelling through paper after washing. This difference was translated into a fraction, the optical density ratio (ODR), comparing density of BS to EP. A higher ODR value (>6.0) indicated positive, while low values (<3.0) indicated negative, with weak reactions between indicated in between (3.0–6.0),

$$\text{ODR} = \frac{\text{BS}}{\text{EP}}.$$

Results

A series of antibody-antigen reaction tests were performed using both procedures to detect blood group phenotypes (Figs 1 and 2). As each antibody-antigen pair behaves differently when tested, each needed to be analysed individually. This differs from the major blood groups (A, B, O and RhD), which react strongly and clearly for most patients; exceptions include the weak subgroup variants [10, 11, 16]. It was found that several factors impacted the interaction strengths observed for each antigen tested. These factors are as follows: (1) reagent type, (2) reaction time, (3) antibody concentration and (4) washing conditions. The washing conditions were found to affect the results of the text-reporting method, but not the elution method. This is due to the effects of directional flow during washing. Table 2 and Fig. 3 depict the

Table 2 Blood group phenotyping using the elution (E) and text-reporting (TR) methods on paper. Blood spot (BS) and elution pathway (EP) are represented as density. Optical density ratio (ODR) compares density EP:BS. Positive is denoted by high density and ODR, negative has lower densities and ODR

Antigen	C	E	c	c	K	K	k
Antibody type	IgM	IgM	IgM	IgM	IgM	Polyclonal	IgM
No. of samples	76	67	54	8	11	53	25
Reaction time (s)	30	30	E:120, TR:180	E:60, TR:180	E: 60, TR:120	120	120
Buffer	NaCl	NaCl	PBS	PBS	NaCl	NaCl	NaCl
No. of samples	31	45	50	41	2	12	23
Elution method	BS	17	14	107	82	97	97
EP	8.2 ± 3.1	51 ± 9.4	44.0 ± 2.4	107 ± 4.63	41 ± 7.7	58 ± 7.0	64 ± 1.7
ODR	17 ± 2.7	32 ± 6.8	32 ± 6.5	6.1 ± 0.48	13 ± 8.8	34 ± 7.1	16 ± 3.1
Text method	152 ± 7.4	28 ± 3.8	145 ± 7.1	135 ± 9.2	106 ± 5.0	35 ± 7.1	131 ± 8.3
Antigen	Fy ^a	Fy ^b	Jk ^a	Jk ^b	P1	Le ^a	Le ^b
Antibody type	Polyclonal	Polyclonal	IgM	IgM	IgM	IgM	IgM
No. of samples	12	8	30	25	40	46	23
Reaction time (s)	120	30	120	120	30	180	180
Buffer	NaCl	NaCl	NaCl	NaCl	NaCl	PBS	PBS
No. of samples	9	3	1	15	26	13	11
Elution method	BS	60 ± 23	40	100 ± 7.5	128 ± 16	N/A	N/A
EP	39 ± 15	33 ± 5.8	35	15 ± 3.6	14 ± 8.8	N/A	N/A
ODR	1.6 ± 0.17	2.0 ± 0.028	1.1	6.8 ± 1.8	12 ± 1.9	N/A	N/A
Text method	36 ± 11	27 ± 4.0	N/A	122 ± 9.8	140 ± 5.7	68 ± 3.1	116 ± 5.9

results achieved for both the elution and text-reporting method for the blood groups investigated (Table 1). However, testing for Duffy groups, Fy^a and Fy^b , MNS groups, and Lewis groups, Le^a and Le^b , was unsuccessful.

Testing conditions

The main variables investigated for optimization include the following: (1) reagent type, (2) reaction time, (3) antibody concentration and (4) washing conditions.

Reagent type

The effect of reagent type was investigated. Certain antibodies are only commercially available as polyclonal (human source), not immunoglobulin M (IgM). IgM antibody reagents are generally monoclonal, containing a pentameric structure, with ten binding sites. IgG antibodies are monomers, containing only two binding sites.

While IgM antibodies show strong agglutination, IgG antibodies generally only sensitize cells without agglutination. This is due to electrostatic repulsion between RBCs. IgM antibodies provide over twice the bridging distance, overcoming the electrostatic double-layer surrounding RBCs. IgM antibodies are expected to exhibit better binding capabilities compared with IgG antibodies, allowing direct agglutination rather than only sensitization to occur. The identification of certain blood groups by direct agglutination using paper is therefore constrained by the commercial availability of IgM antisera.

Reaction time

The reaction time is the time allowed for the antibody sera and RBCs to react. Haemagglutination between ABO and RhD antigens and antibodies can be achieved within 30 s. However, some minor blood group antigens take longer

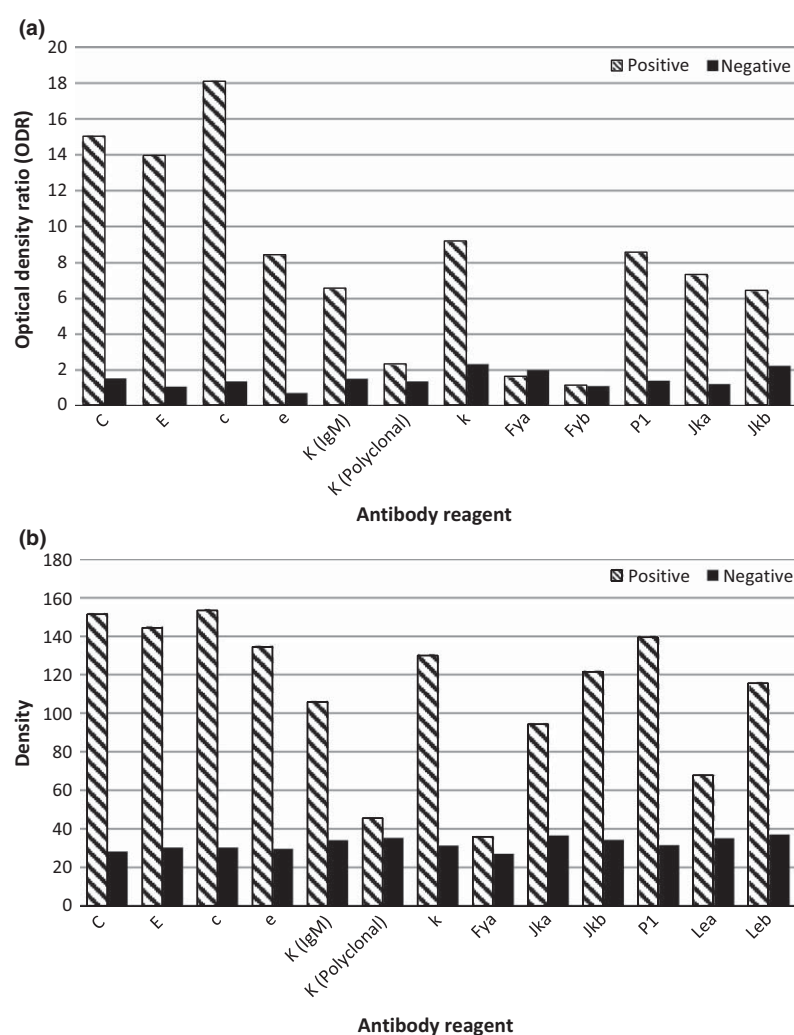


Fig. 3 Blood group phenotyping using (a) elution and (b) text-reporting methods on paper. Blood spot (BS) and elution pathway (EP) are represented as density. Extent of coagulation is represented as optical density ratio (ODR) comparing density EP:BS. Positive is denoted by high density and ODR, negative has lower densities and ODR. (Fy^b was not tested using the text-reporting method.)

than 30 s to bind with their antibodies to show strong haemagglutination for clear identification. Thus, the time the RBC antigens had to bind was extended and compared. Reaction times 30, 60, 120 and 180 s were tested, with optimum conditions reported in Table 2. Reaction times beyond 180 s were not explored as longer reaction times could increase the potential of false positives.

Antibody concentration

The effect of antibody concentration was explored. Antibody concentration was increased by filtering the reagent using Millipore centrifugation tubes. These tubes retain biomolecules 50 kDa or larger and remove supernatant. Increased concentration allows faster collision rates and resulted in stronger agglutination for positive tests. However, this raises the possibility of provoking the prozone effect where agglutination does not occur due to an excess of antibody or antigen.

Washing conditions

Varying the washing buffer was investigated to determine the effect of pH, ionic strength and specificity has on the elution of RBCs and clarity of results. Using the text-reporting method, washing using PBS yielded clearer results, while the effects were nominal for the elution method.

Discussion

Each blood group typing reaction behaved differently when tested, and therefore, each required individual analysis.

Rh blood group system

Apart from the ABO blood groups, the antibodies against the Rh blood group system are the most common clinically significant antibodies. Of these, D is the most immunogenic antigen. The additional antigens investigated within the Rh system which are important when screening patient or donor blood are C, c, E, and e. Testing using paper for these four antigens was successful using the commercial antibody reagent at a standard reaction time of 30 s. The Rh antisera used were all monoclonal IgM (Table 1).

Using the elution method, the C and E antigens were strongly detected (ODR pos: 17 ± 2.7 , neg: 2.9 ± 0.55 ; pos: 16 ± 3.6 , neg: 1.0 ± 1.4 , respectively) (Fig. 3a), only needing 30-s reaction time. However, c and e antigens showed a slightly less clear BS with higher density in the EP. The clarity of tests for c and e improved with longer reaction times of 120 s (ODR pos: 12 ± 3.7 , neg: 1.8 ± 0.39 ; pos: 18 ± 1.5 , neg: 0.72 ± 0.12 , respectively). Extending the RBC–antibody contact time to 2 min or more showed better agglutination with less unbound RBCs able to migrate through the paper structure.

A maximum reaction time of 180 s was selected as longer reaction times could increase false positives. For the elution method for c and e, a 180-s reaction time provided less distinct results with negative ODRs of 1.8 ± 0.39 and 3.0 , respectively. While above the threshold, a lower ODR for negative results provides a clearer result (Fig. 4).

The text-reporting method was similar. C and E had clear and distinct densities (pos: 152 ± 7.4 , neg:

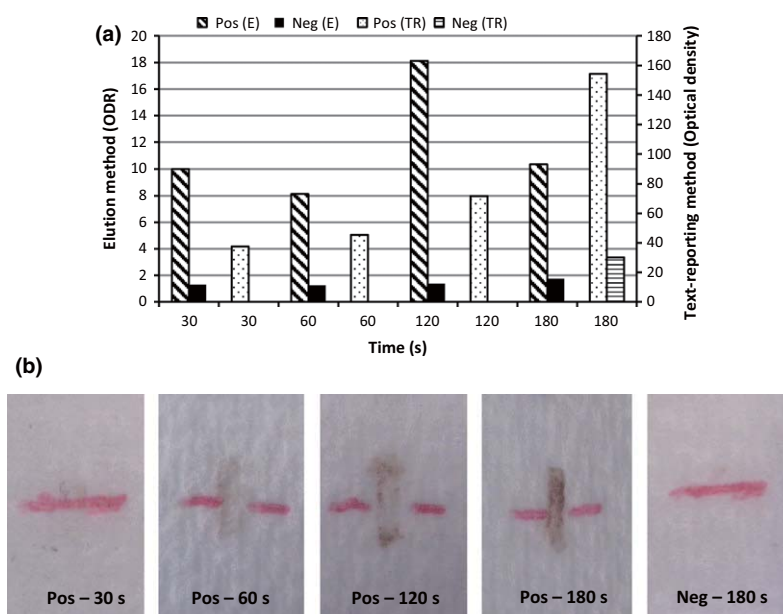


Fig. 4 (a) Effect of time on the reaction period tested with c antigen, comparing elution method (E) and text-reporting method (TR). ODR of E is compared to density of TR. (b) Effect of time on the reaction period tested with c antigen using text-reporting.

28 ± 3.8 ; pos: 145 ± 7.1 , neg: 30 ± 4.9 , respectively). When compared to the BS data of the elution method, the text-reporting method showed a clearer distinction between positive and negative. The c and e tests similarly improved with a longer reaction time of 180 s (pos: 154 ± 5.8 , neg: 30 ± 3.7 ; pos: 135 ± 9.2 , neg: 29 ± 4.2 , respectively) (Fig. 4).

Kell blood group system

Two clinically significant blood group antigens from the Kell system were explored: K and k. Two types of K reagents commercially available were tested: monoclonal IgM and polyclonal (Table 1). The anti-K polyclonal reagents manufactured from human plasma are expected to be composed of IgG antibodies because the immune response against the Kell system produces predominantly IgG antibodies [2]. The efficiency of both reagents was tested with both paper testing methods.

The elution method reported ODR pos: 8.4 ± 5.5 , neg: 2.0 ± 0.46 ; pos: 2.3 ± 0.11 , neg: 1.4 ± 0.39 , for IgM and polyclonal, respectively. The text-reporting method had densities of pos: 106 ± 4.9 , neg: 34 ± 4.0 ; pos: 46 ± 4.1 , neg: 35 ± 7.1 , for IgM and polyclonal, respectively. Interactions between IgM antibodies and the RBCs are strong, and there is no overlap between a positive and a negative test. While both paper methods were accurate with the anti-K IgM antibody, they both failed with polyclonal anti-K (Fig. 5). A clear distinction between positive and negative is fundamental for blood group testing, and only IgM antibodies have systematically achieved such distinction.

In the Saline tube test, IgM antibodies can directly agglutinate antigen-positive red cells, whereas IgG antibodies require anti-human globulin (AHG) to effect agglutination. For both paper testing methods, agglutination between IgG antibodies and RBC antigens without AHG led to false-negative results. As in saline tube test-

ing, this is explained by the greater size of the IgM pentamer able to bridge red cells for electrostatic stabilization. To achieve bridging, the critical length of the antibody must be greater than the electrical layer surrounding the RBC. While IgM antibodies can bridge red cells, where IgG monomers cannot, this allows IgM antibodies to agglutinate red cells in saline solution.

Washing buffer solution affected the clarity of results for the text-reporting method. Using PBS improved the density compared with 0.9% NaCl saline. This is likely due to the directional flow when washing. Only nominal effects were observed for the elution method.

Testing with polyclonal anti-K antisera was used to determine the effect of increasing antibody concentration. Surprisingly, increasing the concentration of the commercial polyclonal antibodies by removing excess serum enhanced reaction clarity. Antibody concentration was increased by filtering the serum to retain biomolecules 50 kDa or larger.

Increasing antibody concentration improved the stoichiometric ratio between antibody and antigen (or RBCs). A higher stoichiometry ratio allows for more colloidal interaction; however, it is costly. This provides a counterpoint to reaction kinetics, as a longer reaction time decreases rapidity and could increase potential false positives.

This worked unexpectedly well, enhancing the clarity for polyclonal anti-K when concentration was doubled (pos: 6.8, neg: 1.4 ± 0.46 with a reaction time of 60 s), with optimum at 120 s (pos: 7.8, neg: 0.61 ± 0.18) (Fig. 6). However, the same method applied to other polyclonal reagents was unsuccessful. Polyclonal anti-K antisera, while assumed to be predominantly IgG antibodies, could contain residual IgM from the original source. Removing the excess supernatant probably increased the IgM concentration in addition to the IgG, thus promoting agglutination. To test this hypothesis, a simple immediate spin tube test and an indirect antiglobulin test (IAT) were

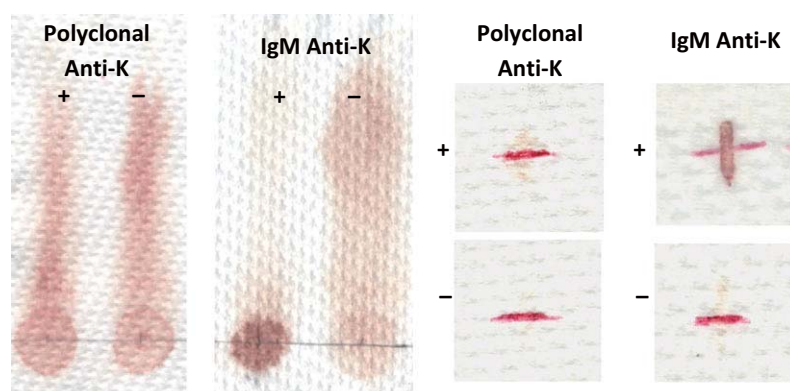


Fig. 5 Comparison of antisera (polyclonal or IgM) effecting identification of testing results for K antigen.

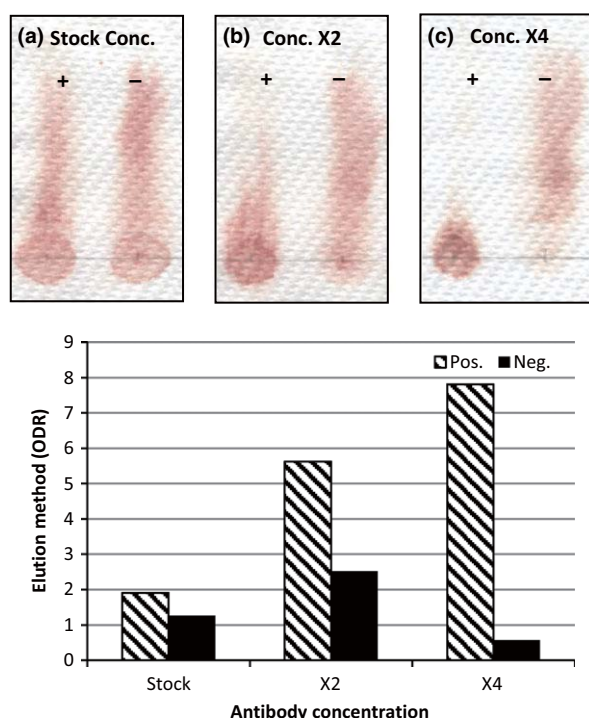


Fig. 6 Effect of anti-K polyclonal concentration on efficacy; (a) at stock solution, (b) double-stock concentration by volume and (c) quadruple stock concentration by volume.

performed with the original polyclonal reagent, against K positive cells. Surprisingly, cell agglutination was observed with both tests, albeit significantly weaker in the immediate spin test. This result indicates that the polyclonal reagent used was predominantly IgG antibodies with some residual IgM antibodies present.

Drawbacks of increasing concentration are as follows: antibody sera are expensive, and not all polyclonal reagents have an IgM component.

Testing for blood group k typing using a monoclonal IgM antibody was straightforward. Much like the Rh groups, results for both the elution and text-reporting methods were clear. For the elution method, positive and negative ODR was 6.4 ± 1.5 and 1.5 ± 0.25 , respectively. Density results for text-reporting method were 131 ± 8.3 and 31 ± 5.0 for positive and negative, respectively (Table 2 and Fig. 3).

Duffy blood group system

Unlike the anti-K antibody reagent, Duffy antibodies, anti-Fy^a and anti-Fy^b, are not available as IgM. Polyclonal Duffy antibody reagents are predominantly IgG [1]. No optimization techniques could achieve clear results as positives reported as (false) negatives. When

reaction time was varied, despite an increased density for positive results, tests for negatives showed an equal increase in density. Attempts to duplicate the improved results seen when concentrating the polyclonal anti-K were unsuccessful for both anti-Fy^a and anti-Fy^b. All results were negative, showing the inability of IgG antibodies to form RBC agglutinates retainable within paper. The antibody structure (IgM vs. IgG) is crucial for successful identification.

Kidd blood group system

The Kidd blood groups studied are Jk^a and Jk^b. The corresponding typing reagents are available as monoclonal IgM antisera and generally showed a clear distinction between positive and negative results. However, the BS achieved was not as defined as desired, requiring optimization. Extending reaction time improved results. Reaction time of 120 s was determined for group Jk^a (ODR pos: 8.3 ± 2.7 , neg: 1.2 ± 0.13 ; pos: 95 ± 6.2 , neg: 37 ± 4.8 ; elution and text-reporting methods, respectively) and Jk^b (ODR pos: 6.8 ± 1.8 , neg: 2.9 ± 1.2 ; pos: 122 ± 10 , neg: 34 ± 6.2 ; elution and text-reporting methods, respectively). Both elution and text-reporting results were accurate.

MNS blood group system

Paper testing for the M, N, S and s antigens was unsuccessful for both methods. The M and N blood groups often reported falsely as 'weak' positives. Numerical data are available as Supplementary Material.

P blood group system

P1 antigen was tested using a monoclonal IgM antibody. Like the C and E antigens, no special optimization was required. The results were clear and easy to distinguish between positive and negative results for both elution and text-reporting (pos: 12 ± 1.9 , neg: 1.7 ± 0.63 ODR; pos: 140 ± 5.7 , neg: 31 ± 5.5 , respectively) (Fig. 3a,b).

Lewis blood group system

Testing the Lewis blood system revealed the importance of the antibody solution composition. Unlike other blood groups, testing with anti-Le^a and anti-Le^b showed anomalous patterns using the elution method. Rather than displaying a clear BS or EP, the blood dispersed irregularly (Fig. 7). This is likely due to potentiators, such as dextran, often added to formulation. Potentiators, consisting of polymers, are often used to enhance the extent of RBC agglutination for low potency antibodies. Potentiators can

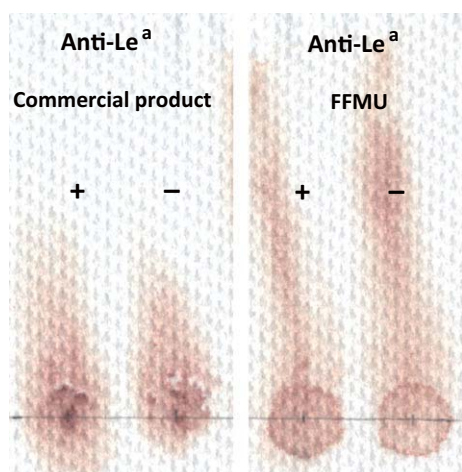


Fig. 7 Dispersion difference between the commercial product and FFMU antibody Le^a.

become problematic for paper tests should they non-specifically retain individual RBC on paper. Instead of absorbing into paper, the antibody solution created a film above the surface, affecting elution and causing irregular dispersion. There was no distinction between positive and negative. The irregular dispersion pattern in paper caused by potentiators was confirmed using 'For Further Manufacturing Use' (FFMU) anti-Le^a, the raw material without potentiators. However, the FFMU anti-Le^a was still unsuccessful for distinguishing positive or negative, due to the lack of potentiators to affect agglutination.

Unlike the elution method, the flow-through method distinguished both positive and negative samples. This is due to directionality and the strength of washing, unaffected by potentiators. The perpendicular washing allowed the saline solution to flow through paper and filtrate, rather than eluting RBCs. Instead, unbound cells could flow through paper. Colour density for Le^a and Le^b using the text-reporting method was pos: 68 ± 3.1 , neg: 35 ± 6.2 ; and pos: 116 ± 5.9 , neg: 37 ± 6.2 , respectively.

Perspective

More than half of the clinically significant blood group phenotypes explored within this study were successfully optimized; the exceptions being Fy^a, Fy^b, S and s. This demonstrates the potential for paper biondiagnostics as a viable alternative for blood group phenotyping. Both testing methods are unique and designed for varying purposes. Successful results for the elution method were more definitive than the flow-through method, better

designed for high-throughput testing. Meanwhile, the flow-through method is ideal for point-of-care testing, especially in remote areas or developing countries. Although in-field testing is unlikely to achieve standard laboratory conditions for temperature and humidity, paper blood typing diagnostics would still provide a cheap, fast and easy to use alternative to current conventional blood grouping methods.

Conclusion

Two paper methods – an elution and a flow-through direct-reporting method – were investigated to determine the blood group phenotype of red blood cells. Clinically significant antigens tested include C, c, E, e, K, k, Fy^a, Fy^b, Jk^a, Jk^b, S and s antigens. The M, N, P1, Le^a and Le^b antigens were also tested. As each group behaved differently, optimization for each antigen was required. This optimization was achieved by controlling the main variables: antibody–antigen reaction time, antibody concentration and changing the washing buffer solution. Antibody class is of the utmost importance on paper. Most antigens with antibodies available as IgM monoclonal antisera were successful with both paper methods (Rh, K (IgM), k, Kidd, P1), though to varying degrees of clarity. Testing with polyclonal antisera was unsuccessful (K and Duffy). Unexpectedly, increasing the antibody concentration of polyclonal anti-K showed a discernible difference between positive and negative results; this was due to increasing the concentration of IgM component. Results were not replicated using polyclonal Duffy antibodies (IgG). Increasing reaction time between antibody and antigens (RBC) showed increased clarity with both methods, while changing washing solution improved testing using the flow-through method. The formulation of the antibody solution is also an important variable for paper testing; any additive able to non-specifically bind RBC to paper affects test sensitivity; this was observed with the Lewis antibodies.

While successful detection was achieved with most IgM antibodies, except Lewis, M, N and S, using both paper assays, polyclonal antibodies, consisting predominantly of IgG, resulted in inconsistent results.

Acknowledgements

The authors are grateful to ARC LP110200973, Haemokinesis and Monash University for funding and D. Bashforth for discussion.

References

- 1 Harmening DM: *Modern Blood Banking and Transfusion Practices*, 4th edn. Philadelphia, PA, F.A. Davis, 1999.
- 2 Daniels G, Bromilow I: *Essential Guide to Blood Groups*. Hoboken, Wiley-Blackwell, 2007.
- 3 Daniels G, Reid ME: Blood Groups: the Past 50 years. *Transfusion* 2010; 50:281–289
- 4 Daniels G: *Human Blood Groups*. Oxford, UK, Blackwell Science, 2002.
- 5 Avent ND, Reid ME: The Rh blood group system: a review. *Blood* 2000; 95:375–387
- 6 Westhoff CM: The Rh blood group system in review: a new face for the next decade. *Transfusion* 2004; 44:1663–1673
- 7 Thakral B, Saluja K, Sharma RR, *et al.*: Phenotype frequencies of blood group systems (Rh, Kell, Kidd, Duffy, MNS, P, Lewis, and Lutheran) in north Indian blood donors. *Transfus Apheres Sci* 2010; 43:17–22
- 8 Malomgré W, Neumeister B: Recent and future trends in blood group typing. *Anal Bioanal Chem* 2009; 393:1443–1451
- 9 Pelton R: Bioactive paper provides a low-cost platform for diagnostics. *Trends Anal Chem* 2009; 28:925–942
- 10 Khan MS, Thouas G, Shen W, *et al.*: Paper diagnostic for instantaneous blood typing. *Anal Chem* 2010; 82:4158–4164
- 11 Al-Tamimi M, Shen W, Zeineddine R, *et al.*: Validation of paper-based assay for rapid blood typing. *Anal Chem* 2011; 84:1661–1668
- 12 Li M, Tian J, Al-Tamimi M, Shen W, *et al.*: Paper-based blood typing device that reports patient's blood type "in writing". *Angew Chem Int Ed* 2012; 51:5497–5501
- 13 Li X, Tian J, Shen W: *Paper as a Low-Cost Base Material for Diagnostic and Environmental Sensing Applications*. In *Appita Conference and Exhibition*. Melbourne, Appita Inc., 2009: 267–271.
- 14 Ballerini D, Li X, Shen W: Patterned paper and alternative materials as substrates for low-cost microfluidic diagnostics. *Microfluid Nanofluid* 2012; 13:769–787
- 15 Su J, Al-Tamimi M, Garnier G: Engineering paper as a substrate for blood typing bio-diagnostics. *Cellulose* 2012; 19:1749–1758
- 16 Reid ME, Lomas-Francis C, Olsson ML: *The Blood Group Antigen Factbook*. London, UK, Academic Press, 2012.
- 17 Li L, Tian J, Ballerini D, *et al.*: A study of the transport and immobilisation mechanisms of human red blood cells in a paper-based blood typing device using confocal microscopy. *Analyst* 2013; 138:4933–4940
- 18 Jarujamrus P, Tian J, Li X, *et al.*: Mechanisms of red blood cells agglutination in antibody-treated paper. *Analyst* 2012; 137:2205–2210
- 19 Li M, Then WL, Li L, *et al.*: Paper-based device for rapid typing of secondary human blood groups. *Anal Bioanal Chem* 2014; 406:669–677

This page is intentionally blank

"Periodic-Table-Style" Paper Device for Monitoring Heavy Metals in Water

Miaosi Li, Rong Cao, Azadeh Nilghaz, Liyun Guan, Xiwang Zhang, and Wei Shen*

Department of Chemical Engineering, Monash University, Wellington Road, Clayton, Victoria 3800, Australia

S Supporting Information

ABSTRACT: If a paper-based analytical device (μ -PAD) could be made by printing indicators for detection of heavy metals in chemical symbols of the metals in a style of the periodic table of elements, it could be possible for such μ -PAD to report the presence and the safety level of heavy metal ions in water simultaneously and by text message. This device would be able to provide easy solutions to field-based monitoring of heavy metals in industrial wastewater discharges and in irrigating and drinking water. Text-reporting could promptly inform even nonprofessional users of the water quality. This work presents a proof of concept study of this idea. Cu(II), Ni(II), and Cr(VI) were chosen to demonstrate the feasibility, specificity, and reliability of paper-based text-reporting devices for monitoring heavy metals in water.



Water contamination is one of the most serious environmental problems facing the world today. The increasing human activities and rapid industrializations are introducing a huge amount of pollutants into the environment, which will undoubtedly contaminate natural water bodies and put human health and ecosystems at risk.¹ Among various pollutants, heavy metals are always one of big concerns due to their severe toxicities so that they have been included in "Blacklist" by the United States Environmental Protection Agency (U.S. EPA).² When these heavy metals enter into the human body, they could easily bind to vital cellular components and accumulate in organisms, resulting in a series of diseases and disorders (e.g., cancers, osteomalacia, kidney malfunction, etc.).^{3,4} As the first step of water pollution prevention, accurate and rapid monitoring of the heavy metals is vital. Ideally monitoring methods are expected to identify point sources of pollutants and the variation of nonpoint sources of pollutants in the environment.

Several methods are widely used for identification and quantification of heavy metals, including colorimetry, atomic absorption spectroscopy (AAS), inductively coupled plasma atomic emission spectroscopy (ICP-AES), inductively coupled plasma mass spectroscopy (ICP-MS), and so on.^{5–7} Although these methods are capable of achieving highly sensitive detection, identification and quantification of heavy metals, they always require the support of well-equipped laboratories and skilled operators, which can be very expensive. Therefore, alternative and inexpensive methods are in demand for field-based or on-site water monitoring by personnel with limited training or even unskilled home-users.

Patterned paper, as a platform technology for making low-cost and user-operated analytical devices, offers a possibility to construct new heavy metal sensors that meet the above-mentioned desirable features. Patterned paper has been used to

make sensing devices for disease screening, point of care (POC), pathogen and biomarker detection, and food and water quality testing.^{8–15} In environment monitoring, research works using paper-based microfluidic devices have, to date, demonstrated the possibility of providing quantification of heavy metals, including Cu, Cd, Hg, Pb, Cr(VI), Ni, etc.^{18–23} These works provide a new approach to monitor heavy metals in water in situations where designated laboratories are not available. However, the assay procedures and result interpretation (involving colorimetric or electrochemical signals) cannot be easily followed and understood by untrained or home users without professional assistance. Besides the high sensor sensitivity and specificity, high portability, rapid detection, and easy result interpretation are highly desirable performance features for new sensing devices. Most recently, researchers have demonstrated that paper-based sensors can be designed to communicate assay results with users via text message, removing errors in assay result interpretation.^{16,17}

One imaginative way to significantly improve the performance of a future paper-based sensor in detecting, quantifying, and reporting heavy metals in water could be to print the chemical symbols of heavy metals with their corresponding and specific indicator systems in a format of the periodic table of elements. Testing of heavy metals in water would simply involve dipping the paper sensor in water, the sensor could then reveal the testing results if the concentrations of heavy metals are higher than legislated standards by showing the chemical symbols of the heavy metals present in water. Such a chemically responsive periodic-table-style paper sensor could be designed to not only provide qualitative answers of what is the

Received: January 6, 2015

Accepted: February 3, 2015

Published: February 3, 2015



water but also provide quantitative (i.e., safe-to-use) information on the heavy metals in water.

Following this idea, we demonstrate the feasibility of paper-based heavy metal sensors, capable of reporting text messages to users if heavy metal concentrations in water reach a legislated unsafe level. We “print” indicator systems for target heavy metals on a patterned paper in chemical symbols of the target metals. This concept can promptly inform even nonprofessional users with clear and unambiguous written warnings against unsafe water. We also demonstrate another use of the same indicator systems to quantify heavy metal concentrations in water. This will enable environmental workers to obtain reliable semiquantitative heavy metal analysis under nonlaboratory conditions and at low-cost.

An ideal paper-based heavy metal sensor for text-reporting has to meet the following performance requirements. First of all, the indicator must be sensitive and form the specific complex with the metal ion to be detected and shows a distinctive color. Second, the indicator system as well as the indicator–metal complex must not be easily leachable into water. Third, the nondetection area of the sensor must be water-repellent. On the basis of these requirements, we chose Cu(II), Cr(VI), and Ni(II) as model heavy metals to demonstrate our idea. The indicator systems for these heavy metals meet the above requirements reasonably well.

Chromatography no. 1 paper was employed to pattern the chemical symbols of Cu, Cr, and Ni by means of generating hydrophilic and hydrophobic boundaries on paper. Computer-generated chemical symbols were first printed on office paper and then soaked in molten wax. After wax treatment, the office paper was allowed to cool down to room temperature. The letters on the wax-loaded office paper was then cut out, forming the cut-out pattern. This office paper was then put on to a piece of chromatography paper and heated with an electric iron, and the wax was transferred to the chromatography paper to form hydrophilic symbols of Cu, Cr, and Ni, surrounded by wax.²⁴ The so-patterned chromatography paper was the final patterned substrate for further construction of the analytical devices. Figure 1 shows the process of fabrication of the patterned

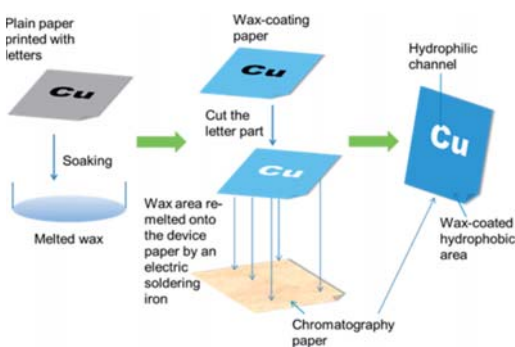


Figure 1. Schematic diagram of the fabrication of patterns of heavy metal chemical symbols on chromatographic paper.

chromatography paper (Supporting Information contains further details). Indicator systems were then added into the chemical symbols of the metals to make the device active.

Cu(II) is one of the most common heavy metals in water, and according to the Australian drinking water guidelines for fresh and marine water quality, Cu concentration in drinking water must not be higher than 1 mg/L.²⁵ Also, the Australian

and New Zealand guidelines for fresh and marine water quality set the standard of Cu(II) in water for irrigation and livestock drinking between 0.2 mg/L (long-term use) and 5 mg/L (short-term use).²⁶ To fabricate a text-reporting Cu(II) sensor, a 10 μ L aliquot of hydroxylamine (0.1 g/mL) in acetic buffer (6.3 M, pH 4.3) was first added into the letter channel. In total, 50 mg of bathocuproine was dissolved in 1 mL of chloroform as the indicator for Cu, and 40 mg PEG 400 was also added into this solution to prevent the detection channel from becoming hydrophobic.²⁰ Before the addition of each solution, the paper device was air-dried for 10 min. Cu(II) forms Cu–bathocuproine complex which has an orange to brown color; the complex is not highly soluble in water.

In a Cu(II) assay, the formation of an orange to brown Cu–bathocuproine complex became visible after 10 μ L aliquot of water sample containing higher than 0.8 mg/mL Cu (II) was dropped onto the device, which displays the “Cu” symbol (Figure 2a). Otherwise, if Cu(II) concentration is below 0.8

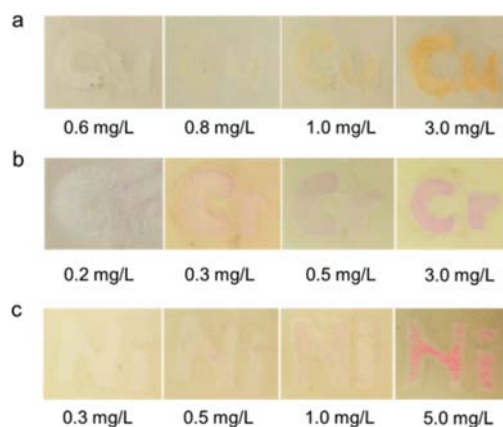


Figure 2. Colorimetric assays showing heavy metal ions of different concentrations: (a) Cu(II), (b) Cr(VI), and (c) Ni(II).

mg/L, the symbol remains colorless. The use of 10 μ L of sample is that it just fills the symbol. The color of the symbol became brighter as the copper concentration increases. This appearance of the “Cu” symbol on the device informs users that Cu(II) concentration is higher than the drinking water standard. In practical use, the device can be simply dipped into a water sample to “read out” the result.

Hexavalent chromium, Cr(VI), is considered as a highly toxic heavy metal ion. A water system contaminated by Cr(VI) can be severely harmful to the environment and humans. For the chromium assay on the paper device, 1,5-diphenylcarbazide (DPC) was dissolved into 50% (v/v) acetone to make the 1 mg/mL solution. The solution was introduced into the “Cr” symbol on paper, followed by an addition of 1% H₂SO₄. Under the acidic conditions, a magenta to purple complex will form when a 10 μ L of Cr(VI) solution is added into the “Cr” symbol. Like the Cu(II) assay, the Cr(VI) assay showed a purple symbol of “Cr” when the Cr(VI) concentration exceeded 0.5 mg/L. By the Australian and New Zealand guidelines for fresh and marine water quality, the trigger value of Cr(VI) in the water resources for purpose of irrigation, livestock drinking and other industries is between 0.1 mg/L (long-term use) and 1 mg/L (short-term use),²⁶ the appearance of “Cr” on the paper (Figure 2b) warns the users against long-term use of the water for their industrial activities.

Nickel is another heavy metal which could enter into the water system through mining, manufacturing activities, and through leaching from e-wastes. For a Ni(II) assay, a 10 μ L aliquot of dimethylglyoxime (DMG) dissolved in an ethanol solution (80 mM) was first introduced into the “Ni” symbol, followed by an addition of 10 μ L of a solution of NaF and Na₂S₂O₃ dissolved in Milli-Q water (20 and 80 mg/mL, respectively). The latter solution was used for masking the interference of Cu(II) and naturally existing Fe(III) in water.^{19,20} The Ni-DMG complex has a stable pink-magenta color. When 50 μ L of water sample containing ≥ 0.5 mg/L Ni(II) was introduced into the device, the symbol “Ni” became visible. Since the standard of Ni in the Australian and New Zealand guidelines for fresh and marine water quality is 0.2 mg/L (long-term use) or 2 mg/L (short-term use),²⁶ the appearance of the “Ni” symbol warns the users that the quality of the water is unsafe for long-term purpose (Figure 2c).

To examine the interference tolerance of the paper assays, each metal ion, with and without the presence of interfering ions, was assayed on paper and compared. For this purpose, validation of quantitative information obtained from paper was first carried out using a colorimetric method which is described in detail in the Supporting Information. Briefly, paper was cut into 1 cm \times 1 cm squares; a series of a heavy metal solution of known concentrations, including blanks, were prepared. Assays of these solutions were performed on paper squares and then scanned to obtain color assay images. Assay images were then analyzed using computer software to determine the reflective color density to establish calibration curves for quantification of target heavy metal ion in water. The calibration curves were then used to determine the paper devices' interference tolerance, the results were then compared with those obtained using an ICP-AES. Specifically, for examining interference tolerance of Cu assay on paper, sample solutions containing Cu(II) as the target ion and higher concentrations of Ni(II), Cr(VI), Fe(III), and Zn(II) as interfering ions were prepared. Similar procedures were used to evaluate the interference tolerance of Cr(VI) and Ni(II) assays. Our results show that interfering ions of 10 times the concentration of the target ions do not affect the assay results (Figure 3a–c). Interesting also, assays showed no color change to samples that contained only interfering ions but no target ions (Figure 3d). Furthermore, other interfering metal ions such as Mn(II) and Co(II) which have similar atomic structure to the target ions as well as Na(I), K(I), Ca(II), and Mg(II), which can exist in high concentrations from some water sources, have also been studied. Results showed that no significant interference could be observed (Figure S4 in the Supporting Information). The interference tolerance ratio of different ions when determining 1 mg/L Cu(II), Cr(VI), and Ni(II) were presented in Table 1.

Pseudoenvironmental samples were prepared to demonstrate the applicability of the paper device for practical water quality monitoring. Tap water from our laboratory was spiked with two different known levels of Cu(II), Cr(VI), and Ni(II) and was then used for determination of the three heavy metals. On the one hand, the target ion concentrations were measured using paper squares (see the Supporting Information); images of the paper assays were collected to obtain the color intensity information using the software; and the concentration of each heavy metal was calculated by means of the best-fitting equation of the corresponding calibration curve (Figure S3 in the Supporting Information). Here paper squares were used to obtain error bar information; text-reporting devices were also

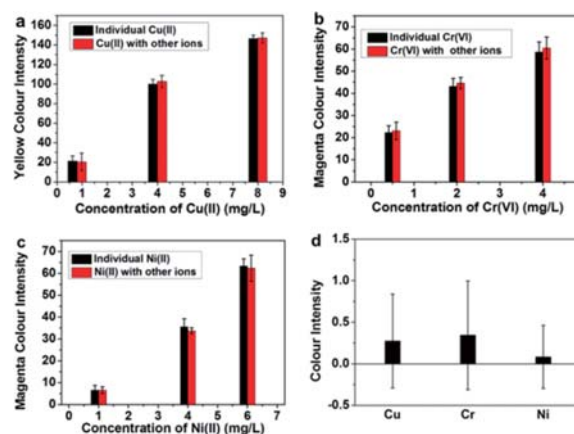


Figure 3. Interference tolerant studies of the paper devices for the three target heavy metal ions in the presence of Cu(II), Cr(VI), Ni(II), Fe(III), and Zn(II) as interfering ions (5 parallel tests for each assay): (a) Cu(II) assays of 0.8, 4, and 8 mg/L of Cu(II); (b) Cr(VI) assays of 0.5, 2, and 4 mg/L Cr(VI); (c) Ni(II) assays of 1, 4, and 6 mg/L of interfering ions; and (d) responses of the Cu(II), Cr(VI), and Ni(II) indicator systems to nontarget multiple interfering agent ions solutions. For assays in parts a–c, the concentration of each interfering ion was 10 times higher than that of the target ion. For assays in part d, samples contained no target ions; the concentrations of all nontarget metal ions were 10 mg/L.

Table 1. Tolerance Ratios of Interference Ions for Detection of 1 mg/L Cu(II), Cr(VI), and Ni(II)

interfering ion	10% tolerance ratio		
	Cu(II)	Cr(VI)	Ni(II)
K(I)	200	200	200
Na(I)	200	200	200
Ca(II)	100	100	100
Mg(II)	100	100	100
Cr(VI)	10		10
Mn(II)	10	10	10
Fe(III)	10	10	10
Co(II)	10	10	10
Ni(II)	10	10	
Cu(II)		10	10
Zn(II)	10	10	10

used, and results obtained were in good agreement with the paper squares. On the other hand, ICP-AES was used to measure the same samples to compare results with the paper-based assays. Figure 4 shows the determination of Cu(II), Ni(II), and Cr(VI) in tap water with multiple ions by paper-

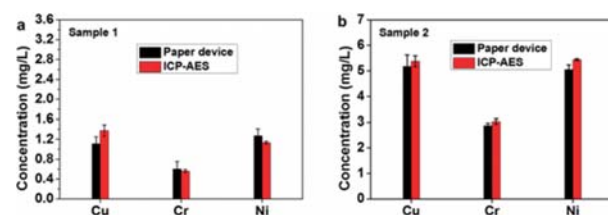


Figure 4. Pseudoenvironmental samples analyzed by paper-based devices and the ICP-AES method: (a) tap water with spiking of 1 mg/L Cu(II), 0.5 mg/L Cr(VI) and 1 mg/L Ni(II); (b) tap water with spiking of 5 mg/L Cu(II), 3 mg/L Cr(VI), and 5 mg/L Ni(II).

based assays and ICP-AES with 5 parallel tests, respectively. The paper-based assays show a mean error within 10% against results obtained by ICP-AES. The recovery rate of the spiked water samples obtained using our paper device and ICP-AES were compared (Table S1 in the Supporting Information), indicating the reliability of the paper assay as a rapid and user-friendly semiquantitative assay for environmental monitoring.

Coming back to the periodic table sensor design concept, we fabricated the three chemical symbols on one paper device. We show in Figure 5 that an assay could be performed by simply

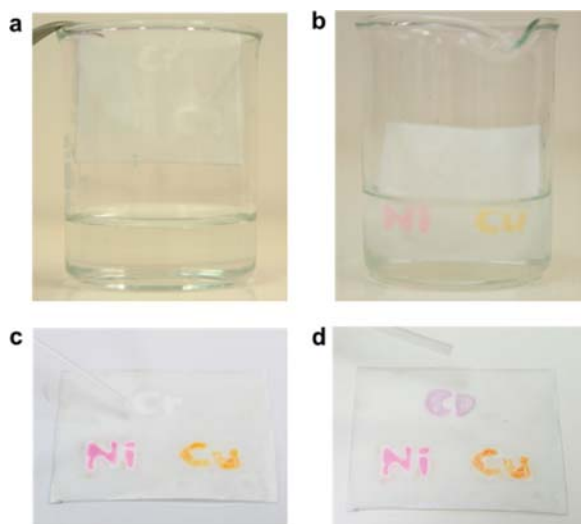


Figure 5. Text-reporting paper device for Cu(II), Ni(II), and Cr(VI) assay in a simulated environmental assay: tap water with striking of 5 mg/L Ni(II), 5 mg/L Cu(II), and 3 mg/L Cr(VI), respectively.

dipping the device into a water sample and instantaneously obtain the result as a text message. However, we also noticed that while Cu(II) and Ni(II) form water insoluble chelates with their corresponding indicators and remain stable on paper, the color product 1,5-diphenylcarbazone-Cr(III) or Cr(III)–DPCA complex is water-soluble and could not remain on paper stably. Thus, the Cu and Ni symbols were fabricated on the lower section of the device, whereas the Cr symbol was on the upper section (Figure 5a,b). The Cr(VI) assay requires a separate sample addition process to stop the leaching of the chelate into water (Figure 5c,d).

The stability of the three ion-indicator complexes has also been investigated: the Cu(II)–bathocuproine and Ni(II)–DMG complexes showed high stability; colors of these complexes showed no obvious fading after more than 6 months under the ambient laboratory conditions. The Cr(III)–DPCA complex faded significantly after 24 h in the same environment. The different stability of these ion–indicator complexes are related to the stability of the indicators: bathocuproine and DMG are stable compounds, while DPC is light-sensitive. The gradual decomposition of DPC under light is likely to be the cause of instability of the Cr(III)–DPCA complex.

As discussed above, an ideal periodic-table-style paper device for on-site heavy metal monitoring requires the indicator system, and the indicator–metal complex, to be stable and nonleachable by water. The Cu(II) and Ni(II) assays are the two systems that fulfill the requirements. A water sample assay for these two ions can be achieved by simply dipping the device in water; it suits well for Cu and Ni testing, and the results can

be stored for a long period. However, the Cr(III)–DPCA complex requires further improvement of its stability. Protection of the DPC indicator and Cr(III)–DPCA complex against light exposure is necessary. It is possible that by significantly reducing the leaching of indicators and the metal ion–indicator complexes through further research, the concept of paper-based text-reporting sensor can be expanded to analyzing other heavy metal ions. It is also expected that an expansion of text-reporting paper sensors beyond this application may be possible in the future, not only for detection of other heavy metal ions but also for a wide range of chemical/biochemical analysis and sensing.

■ ASSOCIATED CONTENT

Supporting Information

Additional information as noted in text. This material is available free of charge via the Internet at <http://pubs.acs.org>.

■ AUTHOR INFORMATION

Corresponding Author

[REDACTED]

Notes

The authors declare no competing financial interest.

■ ACKNOWLEDGMENTS

Funding received from the Australian Research Council through Grants DP1094179 and LP110200973 is gratefully acknowledged. The authors thank Mr. Baiqian Dai for his help with the ICP-AES tests and Dr. Junfei Tian for discussions. Ms. Miaosi Li also thanks the Monash University Research and Graduate School and the Faculty of Engineering for postgraduate research scholarships.

■ REFERENCES

- (1) <http://www.ewast.com.au/electronic-waste-ewaste-landfill/>.
- (2) Jomova, K.; Valko, M. *Toxicology* **2011**, 283, 65.
- (3) Boyd, R. S. *J. Chem. Ecol.* **2010**, 36, 46.
- (4) Johri, N.; Jacquillet, G.; Unwin, R. *Biomaterials* **2010**, 23, 783.
- (5) Lemos, V. A.; Carvalho, A. L. *Environ. Monit. Assess.* **2010**, 171, 255.
- (6) Butcher, D. J. *Instrum. Sci. Technol.* **2010**, 38, 458.
- (7) Feldmann, J.; Salaün, P.; Lombi, E. *Environ. Chem.* **2009**, 6, 275.
- (8) Martinez, A. W.; Phillips, S. T.; Buttle, M. J.; Whitesides, G. M. *Angew. Chem., Int. Ed.* **2007**, 46, 1318.
- (9) Martinez, A. W.; Phillips, S. T.; Carrilho, E.; Thomas, S.; Sindi, H.; Whitesides, G. M. *Anal. Chem.* **2008**, 80, 3699.
- (10) Li, X.; Tian, J.; Shen, W. *Anal. Bioanal. Chem.* **2010**, 396, 495.
- (11) Delaney, J. L.; Hogan, C. F.; Tian, J.; Shen, W. *Anal. Chem.* **2011**, 83, 1300.
- (12) Pelton, R. *TrAC, Trends Anal. Chem.* **2009**, 28, 925.
- (13) Khan, M. S.; Thouas, G.; Shen, W.; Whyte, G.; Garnier, G. *Anal. Chem.* **2010**, 82, 4158.
- (14) Sameenoi, Y.; Panyameesamer, P.; Supalakorn, N.; Koehler, K.; Chailapakul, O.; Henry, C. S.; Volckens, J. *Environ. Sci. Technol.* **2013**, 47, 932.
- (15) Hossain, S. M. Z.; Luckham, R. E.; McFadden, M. J.; Brennan, J. D. *Anal. Chem.* **2009**, 81, 9055.
- (16) Li, M.; Tian, J.; Al-Tamimi, M.; Shen, W. *Angew. Chem., Int. Ed.* **2012**, 51, 5497.
- (17) Li, M.; Then, W. L.; Li, L.; Shen, W. *Anal. Bioanal. Chem.* **2014**, 406, 669–677.
- (18) Hossain, S. M. Z.; Brennan, J. D. *Anal. Chem.* **2011**, 83, 8772.
- (19) Wang, H.; Li, Y. J.; Wei, J. F.; Xu, J. R.; Wang, Y. H.; Zheng, G. X. *Anal. Bioanal. Chem.* **2014**, 406, 2799.

- (20) Mentele, M. M.; Cunningham, J.; Koehler, K.; Volckens, J.; Henry, C. S. *Anal. Chem.* **2012**, *744*, 1.
- (21) Rattanarat, P.; Dungchai, W.; Cate, D.; Volckens, J.; Chailapakul, O.; Henry, C. S. *Anal. Chem.* **2014**, *86*, 3555.
- (22) Sicard, C.; Brennan, J. D. *MRS Bull.* **2013**, *38*, 331–334.
- (23) Nilghaz, A.; Ballerini, D.; Fang, X.; Shen, W. *Sens. Actuators: B. Chem.* **2014**, *191*, S86–S94.
- (24) Nilghaz, A.; Wicaksono, D.; Gustiono, D.; Majid, F.; Supriyantob, E.; Kadir, M. *Lab Chip* **2012**, *12*, 209.
- (25) The guideline can be viewed or downloaded through the government link: https://www.nhmrc.gov.au/_files_nhmrc/publications/attachments/eh52_aust_drinking_water_guidelines_update_131216.pdf.
- (26) The guideline can be viewed or downloaded through the government link: <http://www.environment.gov.au/system/files/resources/e080174c-b267-455e-a8db-d3f79e3b2142/files/nwqms-guidelines-4-vol3.pdf>.

This page is intentionally blank

Appendix II

*Published First Authored Papers Not Included in
the Main Body of This Thesis*

This page is intentionally blank



Charge transport between liquid marbles



Miaosi Li^a, Junfei Tian^a, Lizi Li^a, Aihua Liu^b, Wei Shen^{a,*}

^a Department of Chemical Engineering, Monash University, Wellington Road, Clayton, 3800, Victoria, Australia

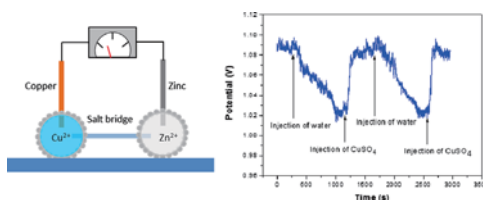
^b Laboratory for Biosensing, Qingdao Institute of Bioenergy & Bioprocess Technology, and Key Laboratory of Bioenergy, Chinese Academy of Sciences, 189 Songling Road, Qingdao 266101, China

HIGHLIGHTS

- Liquid marble was studied as micro reactors.
- Charge and mass transport properties of liquid marble were explored.
- Sample mixing profiles inside a liquid marble were achieved.
- The study indicates that nutrient refilling and waste removal can be realized.
- Liquid marble has the potential use for electric stimulation and reaction monitoring.

GRAPHICAL ABSTRACT

A Daniell Cell was made with liquid marbles. The sample mixing profiles inside liquid marbles were studied and the transport of electric charge and energy between the liquid marble cells was demonstrated. Only microlitres of electrolytes are required to construct an electric cell, showing the liquid marbles can form micro electrochemical reactors.



ARTICLE INFO

Article history:

Received 8 January 2013

Received in revised form

28 March 2013

Accepted 3 April 2013

Available online 18 April 2013

Keywords:

Chemical reactors

Interface

Electrochemistry

Transport processes

Liquid marbles

Continuous sample flow

ABSTRACT

Recent studies on liquid marble applications have shown the possibilities of using liquid marbles as biochemical or biological reactors. These potential applications of liquid marbles generate further interests in the investigation of materials and energy transport between liquid marbles to enable the control and manipulation of the biochemical and biological reactions inside them. In this study, the transport of electric charges between liquid marbles containing electrolyte solutions is demonstrated through a Daniell cell made with liquid marbles. Potential and current comparisons of the Daniell cells made using liquid marbles and solutions in beakers are made. Results show that charge transport between liquid marbles driven by electrochemical reactions is possible. Furthermore, the solution mixing conditions inside a liquid marble is also investigated experimentally and through modeling. The results offer a preliminary appraisal of the internal conditions of liquid marbles as a biological reactor.

Crown Copyright © 2013 Published by Elsevier Ltd. All rights reserved.

1. Introduction

Liquid marble as an interesting interface phenomenon has inspired an abundance of intensive research in recent years after the pioneer study by Quéré and Aussillous was reported in 2001. (Aussillous and Quéré, 2001, 2006; Bormashenko et al., 2009a, 2009b; Dandan and Erbil, 2009; Gao and McCarthy, 2007; Bangi et al., 2010; Rao et al., 2005; Quéré and Aussillous, 2002) A liquid marble is

formed from a liquid drop coated with hydrophobic powder particles; the loosely packed hydrophobic particles form the shell of the liquid marble which prevents any direct contact between the liquid it enwraps and any surface outside the shell. Liquid marbles can therefore maintain a near spherical shape stably on a supporting surface. (Newton et al., 2007; Bormashenko et al., 2009; Dandan and Erbil, 2009) This interesting property has attracted many studies that focused on the fundamental physics (Bormashenko et al., 2009a, 2009b, 2009c, 2011a, 2011b; Aussillous and Quéré, 2006; Dandan and Erbil, 2009; Dupin et al., 2009; Fujii et al., 2010; Arbatan and Shen, 2011; Bormashenko, 2011, 2012; Bajwa et al., 2012; McHale and Newton, 2011) and potential applications (Bormashenko, 2011, 2012; Bajwa et al., 2012; McHale and Newton, 2011; Hapgood et al., 2009;

* Corresponding author.

Bormashenko and Musin, 2009; Zhang et al., 2006; Yao et al., 2011; Tian et al., 2010a, 2010b; Arbatan et al., 2012) of liquid marbles. Among a variety of possible applications, the use of liquid marble as micro reactors has been explored by several groups (Tian et al., 2010a, 2010b; Arbatan et al., 2012; Bormashenko and Balter, 2011). Newton et al. (2007) reported on using the charged Teflon sticks to move liquid marble, demonstrating that motions of marbles can be individually controlled. Bormashenko et al. (2008) investigated the incorporation of Fe_2O_3 nanoparticles in water encapsulated within a polyvinylidene fluoride liquid marble to create a ferrofluidic marble that can be magnetically manipulated. Zhao et al. (2010) showed that liquid marbles enwrapped with hydrophobic Fe_3O_4 nanoparticles can be further controlled by “opening” and “closing” the upper surface of the marble. These reports of liquid marble control further demonstrate that liquid marbles can be used as micro reactors. Tian et al. showed that the porous shell of liquid marbles can be used as micro reactors to detect gas or emit gas (Tian et al., 2010). Bormashenko et al. (2011) also showed that porous liquid marble shells enable gas-triggered reactions to occur inside the liquid marble. More recently, Arbatan et al. (2012a) demonstrated the use of liquid marble as a micro-bioreactor for blood typing. These reports have shown that liquid marbles can be used as micro reactors to carry out chemical and biochemical reactions by either coalescing two marbles containing different reactants into a single marble, or facilitating reactions within one liquid marble while relying on external materials to transport into the liquid marble.

Recently, we have developed new applications of using liquid marbles as biological micro-reactors. (Arbatan et al., 2012b; Tian et al., 2013) Liquid marble can provide one of the simplest micro biological reactors to facilitate the formation of tumor cell spheroids (Arbatan et al., 2012b). The use of liquid marble micro biological reactor for tumor cell spheroid growth is easy and highly efficient: cell aggregation could be clearly observed after 24 h; numerous spheroids formed in a single marble; the yield of cells formation was very high. The confined liquid space inside liquid marble and the hydrophobic marble shell discourage the cell adhesion onto the marble shell, making them to aggregate and forming spheroids. It is possible that the liquid marble method may become a complementary but much more efficient method than the “hanging drop” method that is widely used in biological laboratories for cell spheroid growth, allowing *in vitro* studies of tumor and cancer physiology to be carried out much more easily. Liquid marble also provides a suitable micro-environment for the culturing of microorganisms. This application took advantage of the porous nature of the liquid marble shell; gaseous materials can pass through it, allowing for efficient respirable micro reactors (Tian et al., 2013). The environment in this respirable bioreactor made the growth of aerobic cell more rapidly than that through the traditional way, in the McCartney bottle with shaking incubation. These studies show that the unique structure of liquid marble

provides unexpected advantages over the traditional methods in facilitating biological processes.

In order to explore the full capability of using liquid marble as micro reactors, a wide range of the liquid marble properties must be further investigated. These properties include the movement of liquid marbles as reactant reservoirs; the marble shell compatibility with reactant contained by the liquid marble; and the mass, charge, and energy transport abilities between liquid marbles. It is generally known that stimulations by electric current or potential can be used as a means to manipulate biochemical and biological processes. For this reason, charge transportation between liquid marbles driven by electrochemical processes attracts our attention. The ability to use liquid marbles to transport electric charge between liquid marbles is the first step to the future design of liquid marble micro reactors with functions of generating electric current or potential as the reaction control and monitoring mechanisms. In this study we formed a Daniell cell with liquid marbles and used this micro reactor to investigate the continuous sample flow through liquid marble and sample mixing conditions inside a liquid marble. We envisage that the ability to transport electric charge between liquid marbles will lead to the possible material transport, driven by external electric potential, between liquid marbles for filtration and separation applications in future.

2. Experimental section

A liquid marble Daniell cell was used to demonstrate the conversion of chemical energy into electric energy and the transport of electric charges between liquid marbles. A Daniell cell consists of two half cells of $\text{Zn(s)}|\text{ZnSO}_4$ (α_1 , M) and $\text{Cu(s)}|\text{CuSO}_4$ (α_2 , M). Zinc and Copper electrodes are immersed in zinc sulfate and copper sulfate solutions, respectively. A salt bridge connects the two half cells to enable the continuity of the electric current flow. Fig. 1(a) shows a typical Daniell cell, (http://commons.wikimedia.org/wiki/File:Galvanic_Cell.Svg) while Fig. 1(b) illustrates our design of a liquid marble micro Daniell cell. John Frederic Daniell invented the Daniell cell in 1836; one of his original ideas was to eliminate the generation of H_2 gas by a Voltaic pile. This property of the Daniell cell is well suited for the liquid marble micro Daniell cell, since gas generation may compromise the integrity of the marbles.

Two 50 μL droplets of 0.1 M solutions of copper sulfate and zinc sulfate (both are of AR, Sigma-Aldrich) were rolled over a bed of Polytetrafluoroethylene powder (100 μm , Sigma-Aldrich), respectively, to form two liquid marbles. A 0.2 mm copper wire and a 0.2 mm zinc wire (purity > 99%) were used as electrodes and inserted into the copper sulfate and zinc sulfate marbles, respectively, to form two half cells. An agar salt bridge was prepared to provide electric connection between the two liquid marble half

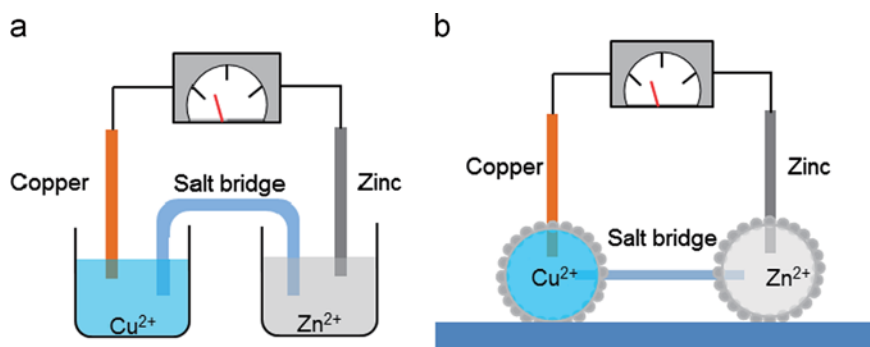


Fig. 1. Schematic of a typical “solutions-in-beakers” Daniell cell (a), (http://commons.wikimedia.org/wiki/File:Galvanic_Cell.Svg) and a liquid marble micro Daniell cell (b).

cells. The salt bridge was made by first heating a mixture of 3% agar in 1 M KNO₃ (w/v) to prepare the agar salt solution. The heated agar salt solution was then filled into a polyethylene tube of 1 mm inner diameter and allowed to cool to room temperature in the tube to form gel. The salt bridge was then put onto a support of suitable height. The two ends of the salt bridge were then inserted into the copper sulfate and the zinc sulfate liquid marbles, respectively, forming a micro liquid marble Daniell cell (Fig. 1(b)). As a comparison, the traditional Daniell Cell made in beakers (Fig. 1(a)) was also formed. The same electrolyte solution, salt bridge and electrode were used in this cell.

To demonstrate the use of a liquid marble as a realistic micro reactor, two micro syringe pumps were used to introduce and withdraw electrolyte solutions from one of the liquid marbles of the Daniell cell. When the two pumps were set at the same flow rate (2 μ L/s), the size of the liquid marble was kept constant and the electrolyte solution flowed through the marble continuously. From measuring the potential variation of the Daniell cell, an experimental evaluation of the sample mixing condition inside the marble was obtained. The data of potential variation measured per second was recorded by a portable data acquisition module (ADVANTECH, USB-4711 A). Mathematical modeling of the sample mixing process was employed to understand the results of the experimental Daniell cell potential change and the solution mixing condition inside the liquid marble.

3. Results and discussions

3.1. Liquid marble Daniell cell potential and charge transport between liquid marbles

The liquid marble Daniell cell can be written as:



The potential of the liquid marble Daniell cell and the current flow through the cell from the cathode to anode was measured using a multimeter (LG, Korea) and was compared with the standard Daniell cell potential, which was calculated using the Nernst Eq. (2), as well as with a Daniell cell formed using beakers shown in Table 1. The calculation of the cell potential also

considers the ion activity coefficient and the Debye–Hückel equation (Eq. (3)) was used Debye and Hückel (1923)

$$E_{\text{Cell}} = E_{\text{Cu}^{2+}/\text{Cu}}^{\ominus} - E_{\text{Zn}^{2+}/\text{Zn}}^{\ominus} + \frac{RT}{nF} \ln \frac{\alpha_{\text{Cu}^{2+}}}{\alpha_{\text{Zn}^{2+}}} \quad (2)$$

$$\ln \gamma_i = -0.509 Z_i^2 \sqrt{I} \quad (3)$$

where E_s : Standard potential of Daniell cell (1) calculated by the Nernst equation; E_b : measured potential of Daniell cell (1) made with the electrolyte solutions in beakers (Fig. 1 (a)); E_m : Potential of the liquid marble micro Daniell cell (1).

The effect of liquid marble size on cell potential was investigated. The liquid droplet volumes ranged from 30 μ L to 100 μ L are appropriate for making liquid marble cell. This is because that it is difficult to fit the salt bridge and an electrode to a liquid marble smaller than 30 μ L, whereas liquid marble greater than 100 μ L loses its spherical shape due to gravity. The electric potentials of Daniell cell (1) formed by liquid marbles of the sizes of 30, 50, 80 and 100 μ L were tested, the potential difference fell in narrow range of ± 0.006 V compared with the value reported in Table 1.

The potential of the Daniell cell formed using beakers is the sum of the electrode potentials and the potentials at the interface between the solution and salt bridge; it is therefore slightly different from the standard Daniell cell potential calculated by the Nernstian equation, which does not consider the latter. The potential of the liquid marble Daniell cell (E_m) is closely comparable with that of the Daniell cell formed using beakers (E_b). This indicates that electric charge transport between the two liquid marble half-cells can be facilitated by the salt bridge and liquid marbles can be used to form electric cells and micro electrochemical reactors. To visually demonstrate the electric charge transport, we used liquid marble Daniell cells to build a battery to power an LED. Since the potential of one liquid marble cell is less than 1.1 V, three cells (4) were connected in series to form a battery pack that has a potential of higher than 3 V.



A schematic of the battery system which is formed with three liquid marble cells is illustrated in Fig. 2(a). The actual liquid marble battery system is shown in Fig. 2(b) the copper electrode of one liquid marble is connected with the zinc electrode of the next liquid marble. An LED is connected to the liquid marble battery series and turned on.

Further investigation of liquid marble Daniell cells was carried out by varying the electrolyte concentrations of each liquid marble. In the first study, we monitored the potential and current change of a liquid marble Daniell cell (5) as a function of the concentration of ZnSO₄ solution (varied from 0.005 to 0.5 M), whilst the concentration of

Table 1
Comparison of potentials of different Daniell cells with the standard Daniell cell potential calculated by the Nernst equation.

Potential (V)	E_s	E_b	E_m
	1.100	1.091 ± 0.002	1.085 ± 0.004

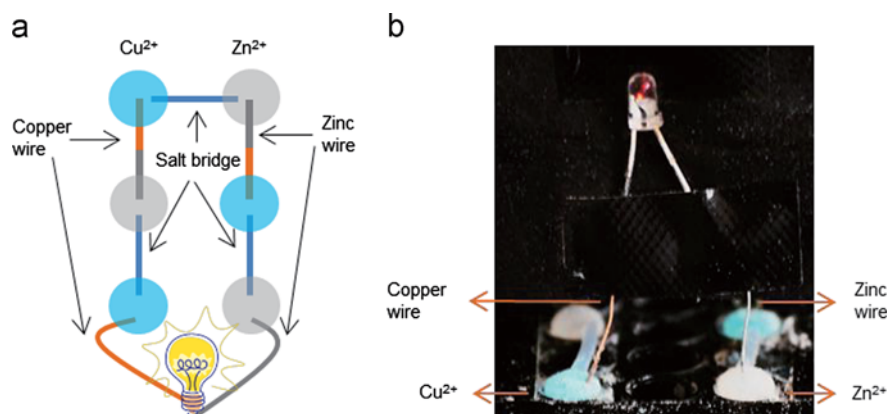


Fig. 2. (a) Schematic of a battery pack formed by liquid marble Daniell cells; (b) LED powered by the liquid marble battery pack.

CuSO₄ solution was held constant at 0.1 M. The potential and current changes of the liquid marble Daniell cell was compared with the potential changes of Daniell cell made using beakers.

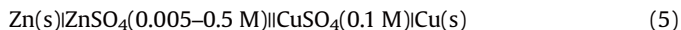


Fig. 3 shows the potential (a) and current (b) variations as functions of the Zn²⁺ concentration in the Daniell cell (5) formed with liquid marbles (triangle points) and with beakers (circular points), respectively. Error bars of each data point were calculated from 8 parallel measurements of 8 cells. Numerical data of cell potentials, currents, standard deviation and standard error of the measurements can be found in the supporting information. The data show that both the cell potential and current increased as the Zn²⁺ concentration increased from 0.005 to 0.2 M, but dropped slightly as the Zn²⁺ concentration further increased to 0.5 M. This is possibly due to a large change of the ionic activity of Zn²⁺ in high concentration ZnSO₄ solutions.

The potential and current change of a liquid marble Daniell cell (6) was also monitored as a function of the concentration of CuSO₄ solution (varied from 0.005 to 0.5 M), while the concentration of ZnSO₄ solution was held unchanged at 0.1 M.

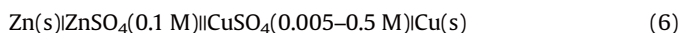


Fig. 4 shows the potential (a) and current (b) variations as functions of the Cu²⁺ concentration variation of the Daniell cell (6) formed with liquid marbles and with beakers, respectively. Error bars of each data point were also calculated from 8 parallel measurements of 8 cells and numerical data are presented in ESI.

A major difference between cell (6) and cell (5) was that the potential and current of cell (6) increase monotonically as the Cu²⁺ concentration increased from 0.005 to 0.500 M. This is most likely due

to the ionic activities of Cu²⁺ in high concentration CuSO₄ solutions being different from the ionic activities of Zn²⁺ in high concentration ZnSO₄ solutions. Data comparison of cell potentials and currents of cell (5) and cell (6) indicates that there is no significant difference between the Daniell cells formed by liquid marbles and by beakers.

3.2. Sample flow control in liquid marble micro reactor

The ability to control the inward and outward sample flows will enable liquid marbles to be used as a realistic micro reactor. Here we demonstrate the use of liquid marble Daniell cell as a micro reactor to monitor the sample flow into and out of a liquid marble. Through monitoring the potential variation of the liquid marble Daniell cell, a preliminary evaluation of the sample mixing condition inside a liquid marble micro reactor can be obtained.

A micro syringe pump was used to pump water and 0.5 M CuSO₄ solution into the CuSO₄ marble of the Daniell cell (4) in alternation at a rate of 2 μL/s; another micro syringe pump withdrew the solution from the CuSO₄ marble at the same pumping rate so that the size of the CuSO₄ marble was kept unchanged. In this process the concentration of ZnSO₄ in the ZnSO₄ marble was kept unchanged at 0.1 M and the ZnSO₄ liquid marble was kept in a sealed container to prevent the concentration change of ZnSO₄ due to water evaporation. The whole experimental setup is illustrated in Fig. 5(a).

The Daniell cell (4) showed a potential of 1.09 V; the cell potential oscillates around 1.09 V as one syringe pump introduced the 0.5 M CuSO₄ solution into the CuSO₄ marble, while the other pump withdrew of the solution out of the marble at the same rate. In this process the amplitude of potential oscillation was ~0.01 V. At 250 s after the experiment began, the introduction of CuSO₄ to

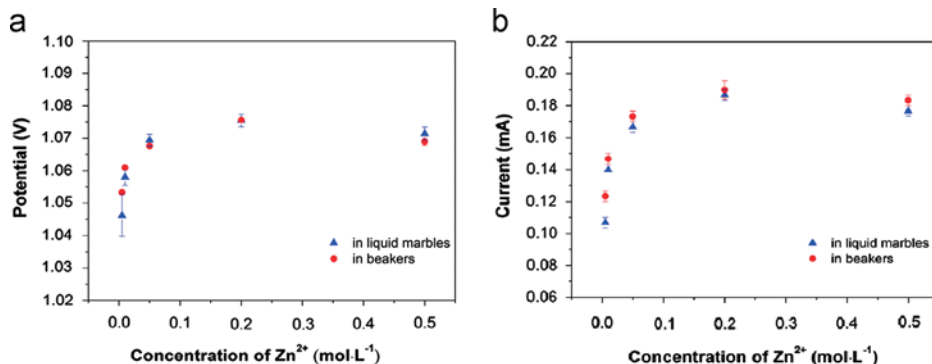


Fig. 3. Potential (a) and current (b) variations of Daniell cell (5) formed with liquid marbles (triangle points) and with beakers (circular points), error bars were calculated from 8 parallel measurements (see ESI).

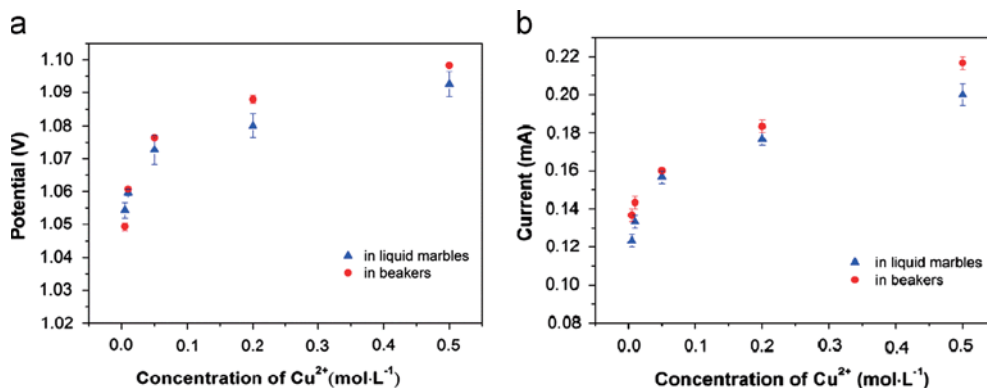


Fig. 4. Potential (a) and current (b) variations of Daniell cell (6) formed with liquid marbles (triangle points) and with beakers (circular points), error bars were calculated from 8 parallel measurements (see ESI).

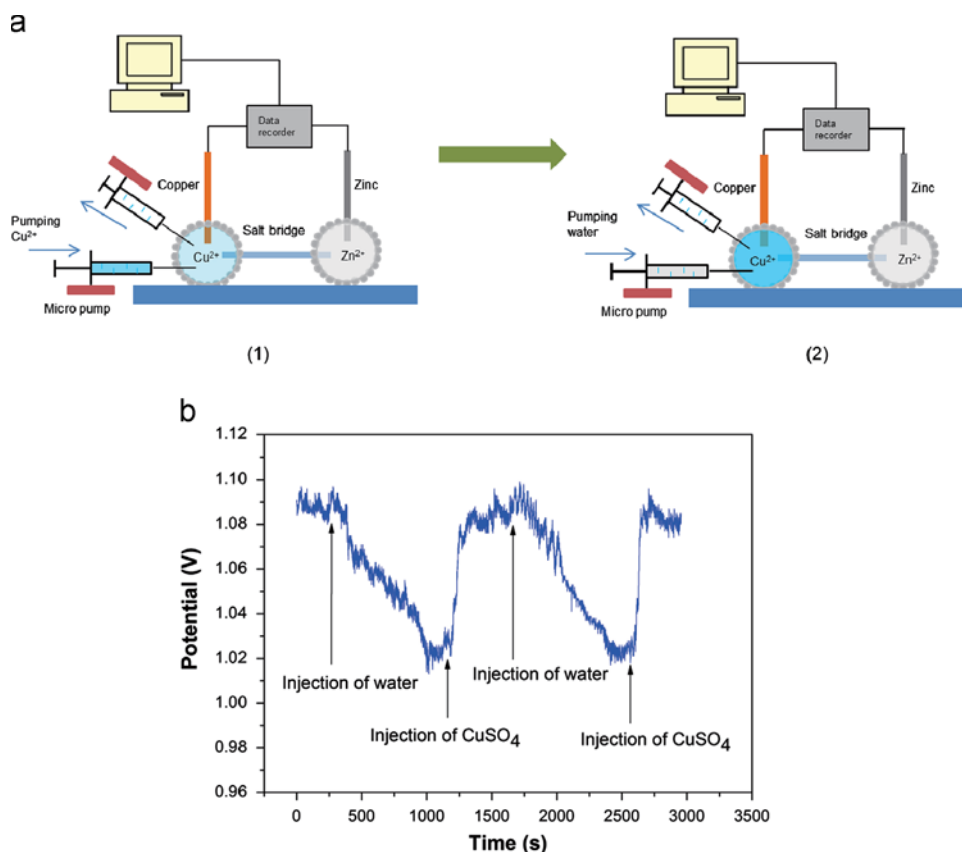


Fig. 5. (a) Experimental set up of sample flow in out of a liquid marble holding CuSO_4 solution: (1) water is introduced into the liquid marble containing 0.5 M CuSO_4 while the mixed solution is withdrawn from the liquid marble by two micropumps with the same rate of 2 $\mu\text{L/s}$; (2) 0.5 M CuSO_4 is then pumped into the same liquid marble while the mixed solution is withdrawn from the liquid marble. (b) Potential variation of liquid marble Daniell cell through the entire pumping process of two cycles.

the CuSO_4 marble was stopped and was replaced with the introduction of water. As water was pumped into the CuSO_4 marble, the potential of the Daniell cell began to drop from 1.09 V, and reached a flat-bottom valley of around 1.025 V after 750 s (Fig. 5(b)). Further introduction of water did not cause further decreases of cell potential. By using the Nernst equation and the standard Nernst Potential E_s of the cell (Table 1), the Cu^{2+} concentration in the CuSO_4 marble can be calculated. However, since the use of Nernst equation for cell potential calculation may be affected by the presence of interface potential between the solution and salt bridge, calculation error is unavoidable. We expect, however, that using the measured liquid marble potential E_m in Table 1 to calculate the Cu^{2+} concentration in the CuSO_4 marble is justifiable and would minimize potential error. This calculation thus gives the Cu^{2+} concentration in the CuSO_4 marble to be 1.99×10^{-4} M.

From 200 s after the cell potential reached the valley, the solution introduction was switched back to 0.5 M CuSO_4 . The cell potential recovered much more rapidly initially compared with its decrease when water was introduced. After around 100 s of rapid increase, the cell potential increase slowed down and after a further 400 s the potential reached the level before the introduction of water. A repeat of such a cycle was performed and the results showed the pattern of potential change was reproducible.

A simple mathematical simulation was conducted to get a preliminary sample mixing appraisal inside the marble. The simulation considered a fixed-volume reactor with one solution inlet and one outlet. The reactor was fed with a 0.5 M CuSO_4 solution; the inlet solution was assumed to have instantaneous mixing with the solution inside the marble. The mixed solution was withdrawn from the reactor via the outlet at the same flow

rate as that of the inlet; this ideal solution flow system was used to simulate the potential changes of the liquid marble Daniell cell as a function of time.

Eq. (7) describes the Cu^{2+} mass flow rate; integration of Eq. (7) leads to the concentration of Cu^{2+} as a function of time, $\text{Cu}^{2+}(t)$, in the CuSO_4 marble (Eq. (8)). By Substituting Eq. (8) into the Nernst equation, a relationship of cell potential as a function of time (Eq. (9)) is obtained.

$$\frac{dm(\text{Cu}^{2+})}{dt} = c(\text{Cu}^{2+})_{en} \nu_{en} - \frac{m(\text{Cu}^{2+})}{V_{mar}} \nu_{ex} \quad (7)$$

$$c_{\text{Cu}^{2+}}(t) = \frac{\frac{c(\text{Cu}^{2+})_{en} \nu_{en} V_{mar}}{\nu_{ex}} - e^{\frac{-(t-A)\nu_{ex}}{V_{mar}}}}{V_{mar}} \quad (8)$$

$$E(t) = E^\circ \left(\frac{\text{Cu}^{2+}}{\text{Cu}} \right) + \frac{RT}{nF} \ln c_{\text{Cu}^{2+}}(t) - E^\circ \left(\frac{\text{Zn}^{2+}}{\text{Zn}} \right) - \frac{RT}{nF} \ln c_{\text{Zn}^{2+}} \quad (9)$$

where $m(\text{Cu}^{2+})$ is mass of Cu^{2+} in the liquid marble; $c(\text{Cu}^{2+})_{en}$ is concentration of Cu^{2+} of the inlet solution into the liquid marble; ν_{en} and ν_{ex} are volume flow rates of the inlet and outlet solutions, respectively; V_{mar} is the volume of the liquid marble; A is constant resulted from the integration.

A plot of the liquid marble Daniell potential as a function of time using Eq. (9) is shown in Fig. 6. This plot simulates two cycles of changing inlet solution from water to 0.5 M CuSO_4 at the flow rate of 2 $\mu\text{L/s}$. At time = 0, reactor contained 0.5 M CuSO_4 solution; as water is added into the reactor the Daniell cell, potential decreases linearly with time from 1.09 V to 1.02 V; this is in good qualitative agreement with the experimental result, although the slopes of the simulation and experimental curves differ

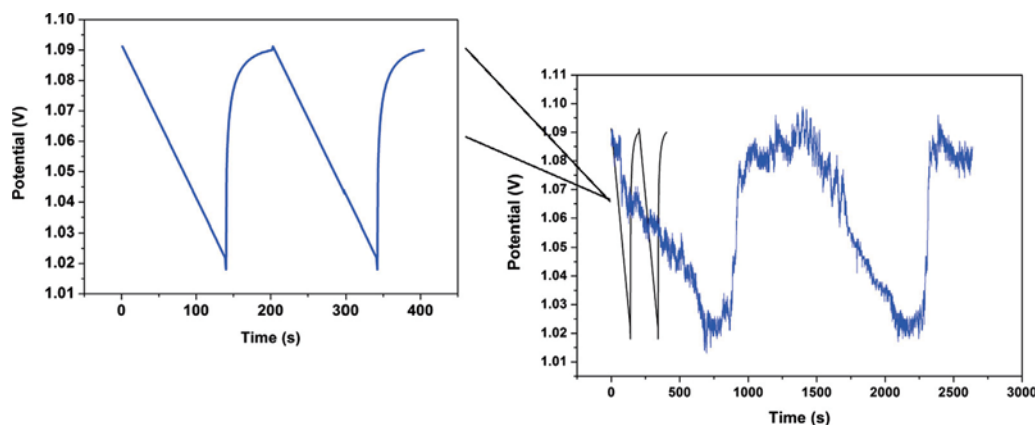


Fig. 6. Mathematical simulation of sample mixing appraisal inside the liquid marble: a plot simulation of the liquid marble Daniell potential as a function of time obtained from the Nernst equation (Eq. (9) overlaid by the experimental data).

significantly, which will be discussed below. From the simulation equations, the linear decrease in cell potential with time only occurs when the Cu^{2+} concentration of the inlet solution is zero. Simple manipulations of Eqs. (7)–(9) will lead to a relationship shown in Eq. (10), given that $v_{en}=v_{ex}$:

$$E(t) = A' + \frac{RT}{nF} \ln \left[c(\text{Cu}^{2+})_{en} + e^{-(t+A)/V_{mar}} \right] \quad (10)$$

In the beginning of the cycle the inlet solution is water and $c(\text{Cu}^{2+})_{en}$ equals to zero; Eq. (10) shows that this condition leads the cell potential to decrease linearly with time. When the inlet sample was switched from water to the 0.5 M Cu^{2+} solution, the variable of the natural logarithm term in Eq. (10) underwent a step change— $c(\text{Cu}^{2+})_{en}$ was abruptly changed from 0 to 0.5 M. This step change of the concentration caused a rapid recovery of the potential in the beginning of the change of $c(\text{Cu}^{2+})_{en}$ to 0.5 M. Since $c(\text{Cu}^{2+})_{en} \neq 0$, the cell potential change with time is linear and the exponential function becomes dominant only as time increases (Eq. (10)).

The qualitative agreement of the experiment result with the mathematical simulation shows that sample mixing inside the liquid marble has occurred. Two points require further comments. First, because of the small size of the liquid marble, the position of the electrode is unavoidably very close to the inlet and outlet solutions. The electrode potential therefore shows significant oscillation, which may be caused by disturbance of the electric double layer around the electrode. Second, the much longer experimental cycle compared to the simulation indicates that sample mixing inside liquid is not instantaneous (Liu and Vecitis, 2012). The concentration of Cu^{2+} at sample inlet is expected to be quite different from that at locations close to the shell of the marble. For this reason, the $c(\text{Cu}^{2+})_{ex}$ is expected to be higher than the simulation value, which is based on the assumption of instantaneous mixing. This is likely the major factor responsible for the much slower experimental sample mixing result than the simulation. Because of the slow sample flow rate, sample mixing inside liquid marble is likely to be dependent considerably upon diffusion. The simulation work provides a preliminary understanding of mass transfer and mixing conditions inside liquid marble; this understanding will trigger further engineering ideas to improve the sample mixing which is useful for the future applications using liquid marbles as a micro reactor.

4. Conclusion

In this study we demonstrated the electric charge transport between liquid marbles by forming a Daniell cell using liquid marbles

and a salt bridge. Charge transport is a relevant property for using liquid marbles to build micro reactors. Only microlitres of electrolytes are required to construct a Daniell cell and a battery pack that can power a LED. The potential and current of the liquid marble Daniell cell are in good agreement with that of the Daniell cell formed with CuSO_4 and ZnSO_4 solutions in beakers. Our investigation also showed that the potential of the liquid marble Daniell cell can be used to monitor the change in Cu^{2+} concentration in the liquid marble. With this idea in mind, we set up a system that provides a continuous flow of Cu^{2+} solutions of different concentrations through the CuSO_4 marble of the Daniell cell and monitored the cell potential by measuring the Daniell cell potential; the results obtained were used as the preliminary evaluation of the sample mixing condition inside a liquid marble. Mathematical modeling shows that sample mixing inside a liquid marble caused by the continuous flow of sample solutions is not instantaneous, but the pattern of sample concentration change inside the marble under the continuous sample flow follows the pattern of mathematical modeling. This study provides the first insights of charge transportation, liquid flow and mixing behavior inside liquid marbles. These insights are useful for designing future liquid marble micro reactors for biochemical and biological applications.

Acknowledgment

Australian Research Council funding (DP1094179) is gratefully acknowledged. ML JT and LL would like to thank Monash University and the Faculty of Engineering for their postgraduate scholarships.

Appendix A. Supplementary Information

Supplementary data associated with this article can be found in the online version at <http://dx.doi.org/10.1016/j.ces.2013.04.003>.

References

- Arbatan, T., Shen, W., 2011. *Langmuir* 27, 12923.
- Arbatan, T., Li, L., Tian, J., Shen, W., 2012a. *Adv. Healthcare Mater.* 1, 80.
- Arbatan, T., Al-Abboodi, A., Sarvi, P.P.Y.C., Shen, W., 2012b. *Adv. Healthcare Mater.* 1, 467–469.
- Aussillous, P., Quéré, D., 2001. *Nature* 411, 924.
- Aussillous, P., Quéré, D., 2006. *Proc. R. Soc. London, Ser. A* 462, 973.
- Bajwa, A., Xu, Y., Hashmi, A., Leong, M., Ho, L., Xu, J., 2012. *Soft Matter* 8, 11604–11608.
- Bangi, U.K.H., Dhre, S.L., Rao, Venkateswara A., 2010. *J. Mater. Sci.* 45, 2944.
- Bormashenko, E., 2011. *Curr. Opinion Colloid Interface Sci.* 16, 266.

- Bormashenko, E., 2012. *Soft Matter* 8, 11018–11021.
- Bormashenko, E., Balter, R., Aurbach, D., 2011. *Int. J. Chem. React. Eng.* 9, S10.
- Bormashenko, E., Musin, A., 2009. *Appl. Surf. Sci.* 255, 6429.
- Bormashenko, E., Pogreb, R., Bormashenko, Y., Musin, A., Stein, T., 2008. *Langmuir* 24, 12119.
- Bormashenko, E., Bormashenko, Y., Musin, A., 2009a. *J. Colloid Interface Sci.* 333, 419.
- Bormashenko, E., Bormashenko, Y., Musin, A., Barkay, Z., 2009b. *ChemPhysChem* 10, 654.
- Bormashenko, E., Pogreb, R., Whyman, G., Musin, A., 2009c. *Colloids Surf. A* 351, 78.
- Bormashenko, E., Bormashenko, Y., Pogreb, R., Gendelman, O., 2011. *Langmuir* 27, 7.
- Bormashenko, E., Pogreb, R., Musin, A., 2011b. *J. Colloid Interface Sci.* 366, 196.
- Dandan, M., Erbil, H.Y., 2009. *Langmuir* 25, 8362.
- Debye, P., Hückel, E., 1923. The theory of electrolytes. I. Lowering of freezing point and related phenomena. *Phys. Z.* 24, 185–206.
- Dupin, D., Armes, S.P., Fujii, S., 2009. *J. Am. Chem. Soc.* 131, 5386.
- Figure was adapted from the original diagram from Wikimedia: (http://commons.wikimedia.org/wiki/File:Galvanic_Cell.Svg).
- Fujii, S., Kameyama, S., Armes, S.P., Dupin, D., Suzuki, M., Nakamura, Y., 2010. *Soft Matter* 6, 635.
- Gao, L., McCarthy, T.J., 2007. *Langmuir* 23, 10445.
- Hapgood, K.P., Farber, L., Michaels, J.N., 2009. *Powder Technol.* 188, 248.
- Liu, H., Vecitis, C.D., 2012. *J. Phys. Chem. C* 116, 374–383.
- McHale, G., Newton, M.I., 2011. *Soft Matter* 7, 5473.
- Newton, M.I., Herbertson, D.L., Elliott, S.J., Shirtcliffe, N.J., McHale, G., 2007. *J. Phys. D: Appl. Phys.* 40, 20.
- Quéré, D., Aussillous, P., 2002. *Chem. Eng. Technol.* 25, 925.
- Rao, A.V., Kulkarni, M.M., Bhagat, S.D., 2005. *J. Colloid Interface Sci.* 285, 413.
- Tian, J., Arbatan, T., Li, L., Shen, W., 2010a. *Chem. Eng. J.* 65, 347.
- Tian, J., Arbatan, T., Li, X., Shen, W., 2010b. *Chem. Commun.* 46, 4734.
- Tian, J., Fu, N., Chen, D., Shen, W., 2013. *Colloids Surf. B* 106, 187–190.
- Yao, X., Gao, J., Song, Y., Jiang, L., 2011. *Adv. Funct. Mater.* 21, 4270.
- Zhang, C., Xu, J., Ma, W., Zheng, W., 2006. *Biotechnol. Adv.* 24, 243.
- Zhao, Y., Fang, J., Wang, H., Wang, X., Lin, T., 2010. *Adv. Mater.* 22, 707–710.

This page is intentionally blank

Appendix III

*Published Co-Authored Papers Not Included in the
Main Body of This Thesis*

This page is intentionally blank

Understanding Thread Properties for Red Blood Cell Antigen Assays: Weak ABO Blood Typing

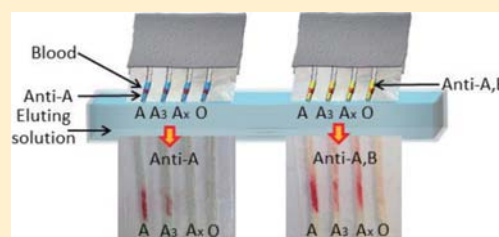
Azadeh Nilghaz, Liyuan Zhang, Miaosi Li, David R. Ballerini, and Wei Shen*

Department of Chemical Engineering, Monash University, Clayton Campus, Victoria 3800, Australia

Supporting Information

ABSTRACT: “Thread-based microfluidics” research has so far focused on utilizing and manipulating the wicking properties of threads to form controllable microfluidic channels. In this study we aim to understand the separation properties of threads, which are important to their microfluidic detection applications for blood analysis. Confocal microscopy was utilized to investigate the effect of the microscale surface morphologies of fibers on the thread’s separation efficiency of red blood cells. We demonstrated the remarkably different separation properties of threads made using silk and cotton fibers. Thread separation properties dominate the clarity of blood typing assays of the ABO groups and some of their weak subgroups (A_x and A_3). The microfluidic thread-based analytical devices (μ TADs) designed in this work were used to accurately type different blood samples, including 89 normal ABO and 6 weak A subgroups. By selecting thread with the right surface morphology, we were able to build μ TADs capable of providing rapid and accurate typing of the weak blood groups with high clarity.

KEYWORDS: thread, microfluidics, chromatographic separation, surface morphology, weak ABO blood typing



1. INTRODUCTION

In recent time, thread has been employed as a low-cost substrate for the fabrication of microfluidic diagnostics.^{1,2} Several studies have reported applications of qualitative immunoassays³ and semiquantitative analyses of biomedical and environmental samples.^{4–6} Other studies have explored ideas of building controllable flow valves, mixers, and thread networks to mitigate sample flow for more advanced thread-based microfluidic sensor applications.^{7,8} These studies provide a good understanding of the wetting, liquid transport, as well as color display properties of threads,⁹ which are essential for the engineering of functional microfluidic thread-based analytical devices (μ TADs). Additionally, the use of μ TADs for blood typing has been reported by our group.¹⁰ Our study shows that threads made from suitable fibers, once treated with blood grouping antibodies, can be used as efficient diagnostic devices to provide normal ABO and RhD blood typing analysis.

The basic principle of using μ TADs to perform blood typing assays is that when a blood sample is introduced onto a thread that has been treated with a blood grouping antibody, the antibody is dissolved into the plasma phase of the sample. If the RBCs of the sample carry the antigen corresponding to the antibody that the thread has been treated with, then the RBCs will agglutinate predominantly in the interfiber spaces of the thread. Conversely, if the RBCs do not carry the corresponding antigens to the antibodies introduced onto the thread, they will not agglutinate and remain as free cells, moving with the wicking plasma phase along the interfiber gap capillaries. This difference can be easily identified by the naked eye. In assay device design, however, blood typing applications not only require the threads to have desirable liquid transport properties but must also allow

for the clear separation of agglutinated RBCs from the plasma phase to provide a final assay result of high clarity for visual identification.

Although using thread for blood typing has been validated for normal ABO and RhD groups,¹⁰ the underlying transport mechanisms of RBCs in threads are still not fully understood. We observed that assays performed with threads made of different fibers can have surprisingly large differences in their level of clarity; these observations could not be explained by results we obtained from macroscopic assaying experiments. This highlights the importance of gaining a better understanding of the fundamental properties of fiber for thread-based sensor design.

Clinically, the ABO blood group system has a number of subgroups; in type A blood, there are subgroups A_1 , A_2 , A_3 , A_x , etc. Among these, A_3 and A_x are considered weak subgroups. RBCs of weak groups carry a much smaller number of antigens, which leads to weak hemeagglutination reactions when they are exposed to group A antibodies.¹¹ That in turn will lead to the formation of comparatively small agglutinated RBC aggregates in a positive assay, which can be difficult to differentiate from a negative assay. Correct typing of weak ABO subgroups is therefore difficult to achieve, even in professional laboratories; success being heavily reliant on the availability of special equipment and experienced clinical staff.¹² These difficulties have been well-documented in immunological blood grouping research and in clinical practice.¹² Some alternate methods give

Received: August 31, 2014

Accepted: November 17, 2014

Published: November 17, 2014

the weak subgroups mixed field hemeagglutination, which could lead to the weak groups being mistyped as group O, A or B by using a device with insufficient power to clearly differentiate weakly agglutinated RBCs from free ones. This is dangerous both when individuals with weak ABO types receive blood, and when their blood is donated for transfusion into others. More worryingly, individuals of group A_x almost exclusively possess the anti- A_1 antibody in their blood serum. If, as a result of mistyping, a patient of group A_x receives transfusion from a group- A_1 individual, the risk of a hemolytic transfusion reaction is significant because the A_1 antigen is one of the strongest antigens and will have strong hemeagglutination reaction with A_1 antibodies.^{13–15} Despite the seemingly small fraction of the population (1:5,100 or 0.02%) who possess these weak subgroups, it is important to consider that more than 107 million units of blood donations are collected each year, which means that ~21 000 could be expected to contain blood of weak ABO subgroups, with the same proportion among the recipients of blood transfusions.^{13–15}

The key thread property that governs the clarity of blood analysis is its separation ability which, to date, has not been investigated in depth. Thread-based blood analysis takes advantage of the presence of interfiber gaps in thread, which provide the capillary driving force for liquid wicking.⁵ Liquid samples can therefore be delivered to the designated locations in a microfluidic device for analyte identification or quantification.⁵ However, a successful thread-based blood typing device requires a thread to provide both the capillary wicking driving force and separation power to differentiate agglutinated RBC lumps from free RBCs in the wicking serum phase. The interfiber channels in a thread are helically structured and run almost parallel to one another; they form relatively simple microfluidic systems for sample wicking. If a thread is used for the purpose of separating particles from a liquid phase, the fiber morphology may play an important role because it defines the wall of the capillary channels, which, in the case of blood typing, affect the transport behavior of the free and agglutinated RBCs.

To design low-cost, high-performance thread-based sensors for blood analysis, the selection of fibers with desirable properties requires careful consideration. In this study, silk and cotton threads with different morphologies,^{16–19} have been investigated and employed for typing of ABO blood samples and its weak subgroups, A_3 and A_x , using a chromatographic elution method.^{20,21} The influence of threads' morphological properties on their performance as a size-based RBC lump separator has also been investigated using confocal microscopy. The confocal microscopic examination provides an insight into the separation mechanism of the agglutinated RBCs from free ones on each thread. Furthermore, the optimal pH of the buffer solution and eluting time have been established with respect to differentiating A_x and A_3 subgroups from each other, and from normal A and O blood types. Finally, the blood typing results have been presented with barcode shaped symbols to provide a simple means for data interpretation by lay personnel without the requirement of special training.

2. EXPERIMENTAL SECTION

Materials, Reagents, and Blood Samples. Hydrophobic silk fibers and cotton threads were obtained from the School of Fashion and Textiles, RMIT University, Melbourne, Australia. Blood samples were received from the Red Cross, Australia, which were collected from adult donors. The groups of all samples were already confirmed

by the Red Cross using a mainstream laboratory blood typing technology (Gel Card). The blood samples were stored at 4 °C in Vacutainer test tubes containing lithium-heparin anticoagulant and used within 10 days of collection. Blood typing antibodies were received from the ALBA Clone, UK; anti-A Clone (Z001), anti-D blend (Z041), anti-B FFMU, and anti-A,B (Z021); they were stored at 4 °C and used as received. A physiological saline solution (PSS) was prepared from analytical grade (AR) by dissolving 0.9 g of NaCl in 100 mL of water. Ammonia solution was used to adjust the pH of the buffer solution before elution. All reagents used for preparing buffer solutions were purchased from Sigma-Aldrich. Anhydrous D-glucose was obtained from AJAX Chemicals Ltd., Australia. Fluorescein isothiocyanate (FITC, isomer I) and anhydrous dimethyl sulfoxide (DMSO) were purchased from Sigma-Aldrich and MERCK Chemicals Ltd., Australia, respectively. ID-CellStab red cell stabilization solution was obtained from BioRad, Australia. The confocal images were captured with a Nikon Ai1Rsi confocal microscope in the Melbourne Centre for Nanofabrication. Water used for all dilutions was purified with Milli-Q water.

Methods. Choice of Thread. To evaluate our hypothesis, that fiber morphology plays a significant role in a thread's separation abilities in blood typing assays, cotton and silk threads with differing surface morphologies¹⁹ were selected as models for this study. We obtained the ready-to-use cotton thread, and made hand-spun silk thread following the cotton thread's constructional parameters (around 200 fibers and 5 twists per centimeter). The surface morphologies of the threads were examined using a Scanning Electron Microscope (SEM) (Figure 1). The threads were then treated in a vacuum plasma reactor (K1050X plasma asher (Quorum Emitech, UK)) for 60 s at an intensity of 50W to increase their wettability.⁵

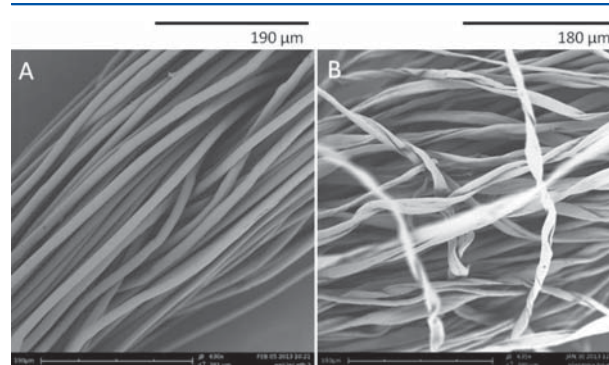


Figure 1. SEM images showing morphologies of (A) silk and (B) cotton threads.

Device Fabrication and Blood Typing Method. Blood typing devices were fabricated by affixing cotton and silk threads to a sticky holder. These threads form “multi-elution columns” parallel to one another.^{3,4} Prior to a blood typing test, 2 μ L of a commercial blood typing antibody (anti-A, anti-B, anti-A,B, and anti-D on first, second, third, and fourth thread, respectively) was deposited on one end of each thread and allowed to dry at ambient temperature (~23 °C) for 10 min. Half a microliter of whole blood (40% hematocrit)¹¹ was introduced on each thread at the same spot where the antibody was introduced, and allowed 40 s for RBCs and the antibody to interact. Half a microliter of blood sample can stain around 0.5–0.7 cm of the thread, a length that is readily visible to the naked eye and is enough to react with antibody and generate a definitive assay result. Errors due to micro pipetting can therefore be monitored, such that small variations within the above range do not affect the assay result. The lower ends of threads were then dipped into 100 μ L of the elution buffer. The buffer acts as a chromatographic mobile phase that elutes the free (nonagglutinated) RBCs along the thread, whereas agglutinated RBC lumps become immobilized in the interfiber gaps of the thread.

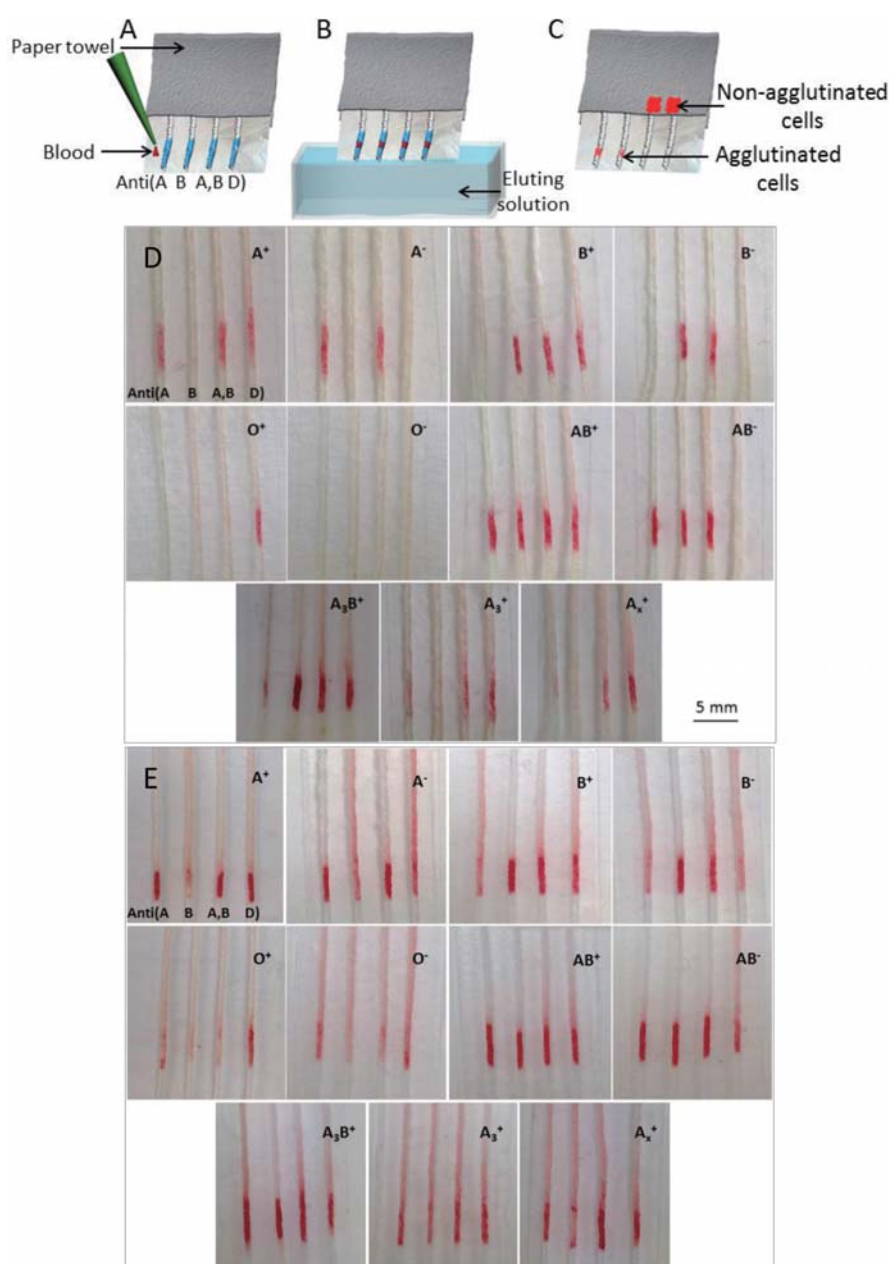


Figure 2. Schematic diagram showing (A–C) the blood typing method on thread. (A) Blood typing antibody (anti-A, anti-B, anti-A,B, and anti-D) and whole blood sample were deposited on each thread before (B) eluting with buffer. (C) Positive and negative results after elution. Images of ABO blood typing and its weak subgroups on (D) silk and (E) cotton threads. The threads for each test were pretreated with four different blood grouping antibodies; anti-A, anti-B, anti-A,B, and anti-D, respectively.

The blood sample introduction spots were then captured using a digital camera (Apple iPhone 5, auto color photo setting without flash light; object distance of 10 cm).

Confocal Microscopy Study of RBCs in Thread. The mechanism of how the surface morphology of fibers interferes with the blood typing results on threads has been investigated using a fluorescent confocal microscope. Fluorescent labeling of RBCs for confocal microscopy was performed as previously described.²² In short, 10 mg of FITC was dissolved in 250 μ L of Dimethyl sulfoxide (DMSO) and then diluted with ID-CellStab solution to obtain a FITC concentration of 0.8 mg/mL. A 0.6 mL of this solution, mixed into 40 μ L of D-glucose solution (10 mg/mL), was added to 0.4 mL of RBCs before incubating for 2.5 h, with mixing at a low centrifuge force of 100 g to prevent the RBCs from settling down. Afterward, stained RBCs were washed with

PSS a total of 10 times to remove unbound FITC (with centrifugation at 1300 g for 3 min after each wash). These stained RBCs were resuspended to 40% hematocrit with ID-CellStab solution.

To ensure that the blood staining protocol does not significantly affect the activity of the RBC antigens, we performed blood typing assays using whole blood and stained RBCs from the same sample on thread. A 0.5 μ L sample of whole and stained blood was introduced to antibody treated silk thread and then eluted using the elution buffer. The degree of agglutination was examined by capturing and transferring the images to Adobe Photoshop for color intensity analysis. As shown in Figure S1 in the Supporting Information, staining has caused slight changes in the RBC agglutination color density on thread. However, such changes are not significantly enough to affect the visual identification of the assay results in any way.

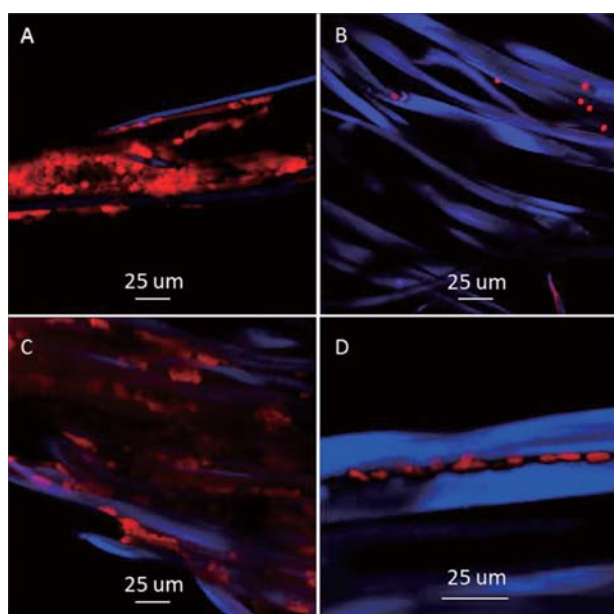


Figure 3. Confocal images of (A, C) agglutinated and (B, D) free RBCs on silk and cotton threads after buffer elution for 60 s. Agglutinated RBCs are immobilized in the interfiber gaps of (A) silk and (C) cotton threads. (B) Free RBCs are almost thoroughly removed from silk thread by buffer elution. (D) On cotton thread; however, RBCs are stuck in intrafiber gaps, creating a permanent red stain.

The conventional glass slide technique was also performed (see Figure S2 in the Supporting Information). Images captured using the confocal microscope demonstrated that stained RBCs still formed aggregates as expected in the presence of antigen-specific antibody (see Figure S2A in the Supporting Information), but shows no agglutination when the antibody present is nonspecific (see Figure S2B in the Supporting Information).

Effects of Buffer Elution Ph and Elution Time on Blood Typing. To improve the blood typing results on thread, we compared the color intensities (measured as the mean intensity of red color in RGB format in Adobe Photoshop 5.5) of the blood spots after elution with buffer solutions of different pH values for different durations of time. The buffer solutions were prepared by diluting PSS with 0.1 mM of ammonia solution to obtain serial elution buffers with different pH values (8, 9, and 10). The buffer solutions were then used to elute the blood spots for different durations of time (10, 30, 60, 90, and 120 s). The best condition was selected and used to identify the blood typing tests. In all assays, a 0.5 μ L of blood sample was introduced onto the antibody treated thread, incubated for 40 s before being eluted with a buffer solution.

Identification of Weak A Subgroups. Because anti-A could not reliably identify weak A subgroups such as A_x and A_3 , we decided to use both anti-A and anti-A,B to build the blood typing devices.²³ Two sets of threads were treated using anti-A and anti-A,B. Half a microlitre of whole blood was introduced onto each thread and left to incubate for 40 s. Thread was then eluted with a buffer solution for 60 s. The degree of the A_x and A_3 reactions with anti-A and anti-A,B has been used to differentiate them from each other and from the normal A and O blood types. The blood typing results were evaluated by the naked eye to determine the highest degree of agglutination.

Generating Barcode-Shaped Symbols. An easy method for interpreting blood typing results is beneficial for the successful application of microfluidic thread-based blood typing devices. Herein, in order to provide a simple interpretation, a set of barcode shaped symbols have been designed and then matched to each blood type. The symbols include white, black, and gray lines resembling the

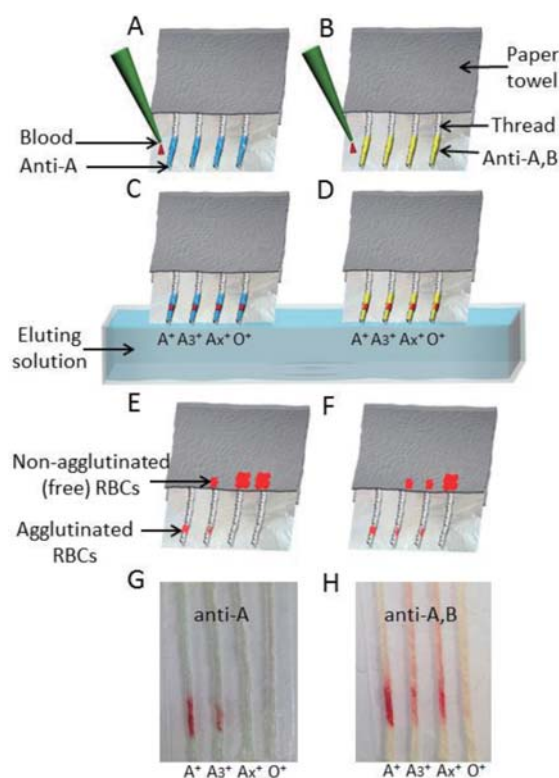


Figure 4. Schematic diagram showing the identification of weak A subgroups on silk thread using two blood grouping antibodies: (A, C, E, G) with anti-A, and (B, D, F, H) with anti-A,B. The assay procedures are described as follows: (A, B) Introducing blood on the antibody treated thread. (C, D) Devices before elution. (E, F) Devices after elution. (G, H) Final assay results. As shown, the degree of each hemeagglutination reaction for A_x , A_3 , A, and O is different.

negative, positive and weak reactions of RBCs with different blood typing antibodies, respectively.

3. RESULTS AND DISCUSSION

Effect of Morphological Structure on Separation Properties of Thread. Morphological structures of silk (Figure 1A) and cotton (Figure 1B) threads were investigated using SEM. The silk fiber surface is smooth with no intrafiber gaps or lobes.¹⁹ Thread constructed with silk has regular and continuous microfluidic channels formed by interfiber gaps.¹⁹ The regular channels provide a possibility for the separation of agglutinated and free RBCs through silk thread during elution. In comparison, cotton thread is made of hollow, ribbonlike, cellulose fibers with intrafiber gaps on their surface.¹⁹ The intrafiber gaps in cotton thread provide rather irregular microfluidic channels that trap or mechanically immobilize RBCs within the thread. This makes cotton thread an unsuitable substrate for blood typing purpose.

Normal ABO and Its Weak Subgroups Blood Typing Using Different Threads. The blood samples were introduced onto antibody treated threads and eluted with buffer solution of pH = 9 for 60 s (Figure 2A–C). Specific antibody–antigen reactions produced agglutinated RBCs including blood type A with anti-A and anti-A,B, blood type B with anti-B and anti-A,B and blood samples of type RhD⁺ with anti-D.²⁰ After elution, a clear separation of agglutinated and free RBCs by silk thread could be observed. This is because

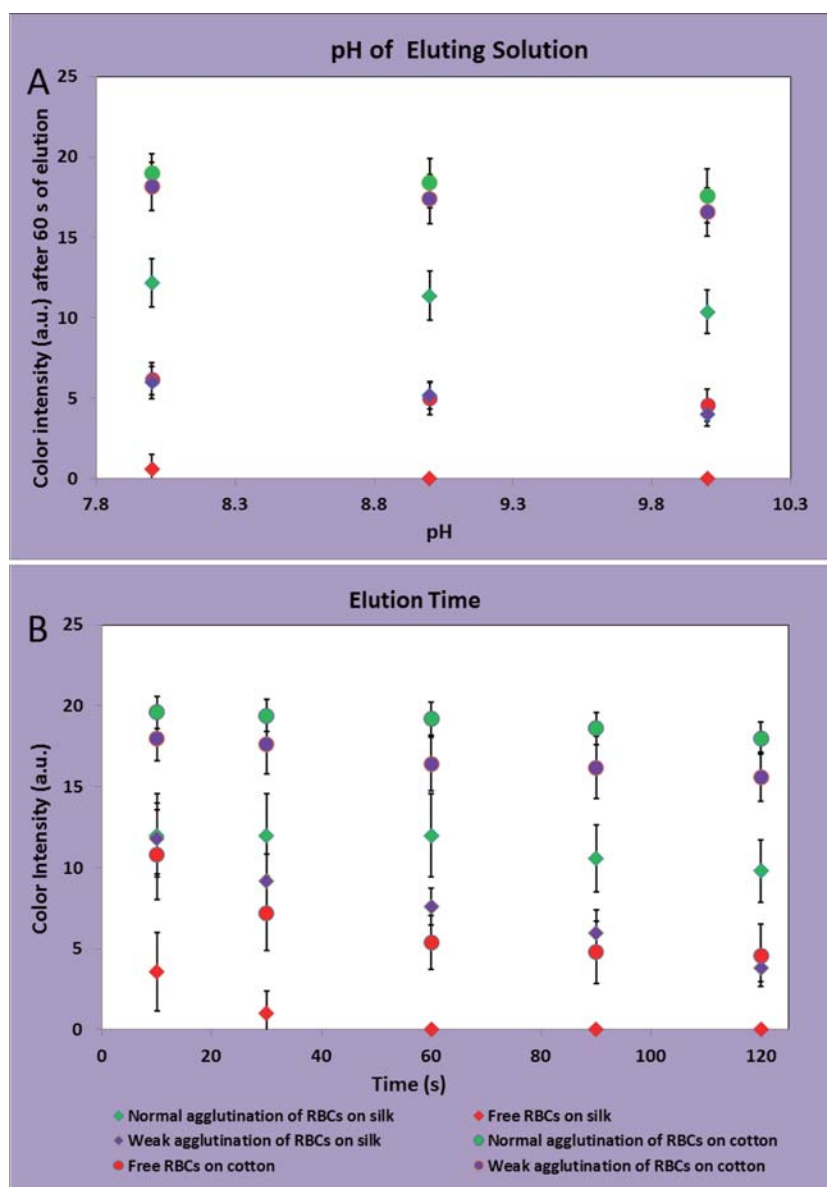


Figure 5. Improvement of blood typing assay on silk and cotton threads using the elution method. (A) Samples were eluted using buffer solution of different pH values for 60 s. (B) Samples were eluted using a buffer (pH 9) for different durations.

that interfiber channels in silk thread provide an efficient separation of the agglutinated RBCs from the free ones, making silk a suitable substrate for blood typing (Figures 2D and 3A, B).

However, in cotton thread, the free RBCs became stuck within the intrafiber gaps; making it difficult for cotton thread to differentiate the agglutinated and free RBCs (Figures 2E and 3C, D). Free RBCs are able to fold and enter into pores of an average diameter of $\sim 3 \mu\text{m}$.²⁴ In addition, RBCs can travel horizontally or perpendicularly with respect to the fiber surface during elution and become entrapped in intrafiber gaps of different sizes. Figure 3D shows disclike RBCs lodged into a narrow intrafiber gap on the surface of a cotton fiber. This situation can get worse in weak ABO blood typing, as mixed field agglutination reaction always occurs and a very clear separation of small agglutinated lumps from free RBCs is required. In such circumstances, the differentiation of normal and weak reactions is almost impossible. Figure 3D also shows

that material affinity interactions between the cotton fiber surface and RBC are weak, because no free RBCs could be observed on the smooth cotton fiber surface. Therefore, mechanical entrapment of RBCs by intrafiber gaps is the major mechanism responsible for the low clarity of blood typing assay.

Effect of Different Antibodies in Weak A Subgroup Blood Typing. Through using the elution method to investigate the potencies of specific antibodies for weak A subgroups, we found a suitable surface for detection of A_x and A_3 . As is shown in Figure 4, the RBCs of A_3 samples agglutinated on silk threads pretreated with anti-A and anti-A₃B, but more weakly than normal A. A_x samples, however, agglutinated more strongly on the thread with deposited anti-A₃B rather than anti-A. The use of two antibodies in our design is suitable for A_x and A_3 blood typing purposes and can be used as a key for differentiating A_3 and A_x from each other and from normal A and O groups.

Table 1. Summary of the Efficacy of Blood Typing of normal ABO and Its Weak Subgroups for Blood Samples from 95 Donors Using Silk Thread^a

blood type	RBCs immobilization with anti-A	RBC immobilization with anti-B	RBC immobilization with anti-A,B	RBC immobilization with anti-D
A ⁺ (n = 24)	24/24	0/24	24/24	24/24
A ⁻ (n = 9)	9/9	0/9	9/9	0/9
B ⁺ (n = 6)	0/6	6/6	6/6	6/6
B ⁻ (n = 5)	0/5	5/5	5/5	0/5
AB ⁺ (n = 3)	3/3	3/3	3/3	3/3
AB ⁻ (n = 2)	2/2	2/2	2/2	0/2
O ⁺ (n = 25)	0/25	0/25	0/25	25/25
O ⁻ (n = 15)	0/15	0/15	0/15	0/15
A ₃ ⁺ (n = 1)	1/1	0/1	1/1	1/1
A ₃ B ⁺ (n = 3)	3/3	3/3	3/3	3/3
A _x ⁺ (n = 2)	0/2	0/2	2/2	2/2

^aTable is adapted with permission from ref ²⁰. Copyright 2011 American Chemical Society.

Effects of Elution Buffer pH and Elution Time on Blood Typing. To obtain unambiguous results of blood typing, buffer solutions with different pH values (8, 9, and 10) have been used to elute RBCs from antibody treated silk and cotton threads for 60 s. Figure 5A shows that the main effect determining the assay clarity is the fiber type (or fiber surface morphology), which is in consistence with the results in Figure 3 and the above discussion. pH, however, has a secondary effect to the assay clarity on silk. Figure 5A shows that as the pH increases to 9 and higher, the negative assays on silk become clean (color density = 0), this increases the assay clarity on silk thread. The most likely reason is that silk fiber and free RBCs carry weak acidic groups which dissociate more strongly at high pH, this causes stronger charge repulsion between the silk fiber and the RBCs, allowing free RBCs to be eluted away from silk fiber surfaces more thoroughly.

With regard to eluting time, a buffer solution (pH = 9) has been used to elute the RBCs from threads for different durations (10, 30, 60, 90, and 120 s). As shown in Figure 5B, the optimal elution time is around 60 s. Under this condition, free RBCs of negative assays could be removed from the silk thread completely, while in positive assays of weak blood groups, the small agglutinated RBC clusters were not significantly dissociated. This condition therefore produced weak blood group assays of the highest clarity. Elution time longer than 60 s produced slightly weaker color density for positive assays of weak blood groups, which is most likely caused by the dissociation of small agglutinated RBC clusters of the weak groups. Ninety five blood samples of different groups were assayed with 60 s elution time using the silk thread, the results (Table 1) were in full agreement with the assays performed by the Red Cross Australia. In all cases, the specific antibody–antigen reactions produced the immobilized hemagglutinated RBCs on silk thread surface; no nonspecific reaction between antibodies and RBCs were observed. Interestingly, silk thread can also report unambiguous positive assays for normal and weak blood groups if elution times longer than 60 s are used. This is because that the clarity of silk thread assays are high, all negative assays have zero color density, making the color densities of positive assays to stand out clearly.

Barcode Shaped Symbols. To have an easy blood typing result interpretation, we provided a set of printed patterns similar to barcodes to confirm the result of each blood test by visual matching. In Table 2, the black and gray lines refer to the strong and weak agglutination reactions between antibody and RBCs, respectively. The white lines however represent negative

Table 2. Barcode Shaped Symbols Provided for Easy Interpretation of Blood Typing Results^a

Blood group	Symbol
A ⁺ (n = 24)	
A ⁻ (n = 9)	
B ⁺ (n = 6)	
B ⁻ (n = 5)	
AB ⁺ (n = 3)	
AB ⁻ (n = 2)	
O ⁺ (n = 25)	
O ⁻ (n = 15)	
A ₃ ⁺ (n = 1)	
A ₃ B ⁺ (n = 3)	
A _x ⁺ (n = 2)	

^aThe white, black, and grey symbols refer to the negative, positive, and weak antibody–antigen reactions, respectively.

agglutination reactions between the blood samples with antibody. Only one symbol is used in each case to show the blood type (Figure 2D and Table 2), which can be useful for easy result interpretation, especially in the region with a lack of trained personnel.

4. CONCLUSIONS

In this study, the effect of the surface morphologies of silk and cotton fibers on the separation properties of threads made from these fibers has been investigated for the application of blood typing based on the principal of chromatographic elution. Blood typing devices made of silk thread deliver significantly higher assay clarity than those made of cotton thread. SEM study shows that cotton fibers have irregular intrafiber gaps of several microns in width, whereas silk fibers have no intrafiber gaps. This surface morphological difference between silk and

cotton fibers significantly affect the migration behavior of free RBCs in these threads. Confocal microscopic investigations showed that intrafiber gaps on cotton fiber surfaces can mechanically trap free RBCs; cotton thread therefore provides poor separation power to differentiate the agglutinated RBCs from the free ones. This makes blood typing assays using cotton thread very low clarity and unsuitable for visual identification. In contrast, silk fibers, having a smooth surface do not trap RBCs; silk threads therefore provide much more efficient separation power for differentiating free RBCs from agglutinated ones. The high clarity blood typing assays by silk threads are well-suited for visual identification. This study provides new insights into the selection of the right threads for building sensors with the desired performance.

The degree of RBC agglutination with different antibodies on silk thread has also been used as a strategy to differentiate six samples of the weak A blood types from one another and from the normal ABO red blood cells. The ability to differentiate different weak ABO groups from the normal ABO groups is a very important, as it will reduce transfusion mistakes for weak ABO group patients. Silk thread delivers results for both weak and normal ABO groups that can be easily interpreted by the naked eye with the aid of a matching chart.

■ ASSOCIATED CONTENT

■ Supporting Information

Comparison of whole blood samples and stained red blood cells (RBCs) in blood typing assays on thread; Confocal images of FITC stained red blood cells on glass slide. This material is available free of charge via the Internet at <http://pubs.acs.org>.

■ AUTHOR INFORMATION

Corresponding Author

Notes

The authors declare no competing financial interest.

■ ACKNOWLEDGMENTS

This work is supported by the Australian Research Council Grant (ARC DP1094179) and (ARC LP1120973). A.N., M.L., and D.R.B. gratefully acknowledge the research scholarships provided by Monash University and the Department of Chemical Engineering. This work was performed in part at the Melbourne Centre for Nanofabrication (MCN) in the Victorian Node of the Australian National Fabrication Facility (ANFF).

■ REFERENCES

- (1) Nilghaz, A.; Ballerini, D. R.; Shen, W. Exploration of Microfluidic Devices Based on Multi-Filament Threads and Textile Microfluidic Nanofluids: A Review. *Biomicrofluidics* **2013**, *7*, 051501–051516.
- (2) Ballerini, D. R.; Li, X.; Shen, W. Patterned Paper and Alternative Materials as Substrates for Low-Cost Microfluidic Diagnostics. *Microfluids Nanofluids* **2012**, *13*, 769–787.
- (3) Zhou, G.; Mao, X.; Juncker, D. Immunochromatographic Assay on Thread. *Anal. Chem.* **2012**, *84*, 7736–7743.
- (4) Nilghaz, A.; Ballerini, D. R.; Fang, X. Y.; Shen, W. Semi-quantitative Analysis on Microfluidic Thread-Based Analytical Devices by Ruler. *Sens. Actuators B* **2013**, *191*, 586–594.
- (5) Li, X.; Tian, J.; Shen, W. Thread as a Versatile Material for Low-Cost Microfluidic Diagnostics. *ACS Appl. Mater. Interfaces* **2010**, *2*, 1–6.
- (6) Reches, M.; Mirica, K. A.; Dasgupta, R.; Dickey, M. D.; Butte, M. J.; Whitesides, G. M. Thread as a Matrix for Biomedical Assays. *ACS Appl. Mater. Interfaces* **2010**, *2*, 1722–1728.

- (7) Ballerini, D. R.; Li, X.; Shen, W. Flow Control Concepts for Thread-Based Microfluidic Devices. *Biomicrofluidics* **2011**, *5*, 0141051–01410513.
- (8) Safavieh, R.; Zhou, G. Z.; Juncker, D. Microfluidics Made of Yarns and Knots: From Fundamental Properties to Simple Networks and Operations. *Lab Chip* **2011**, *11*, 2618–2624.
- (9) Wang, N.; Zha, A.; Wang, J. Study on the Wicking Property of Polyester Filament Yarns. *Fiber Polym.* **2008**, *9*, 97–100.
- (10) Ballerini, D. R.; Li, X.; Shen, W. An Inexpensive Thread-Based System for Simple and Rapid Blood Grouping. *Anal. Bioanal. Chem.* **2011**, *399*, 1869–1875.
- (11) Dean, L. *Blood Groups and Red Cell Antigens*; National Center for Biotechnology Information: Bethesda, MD, 2005.
- (12) Musa, R.; Ahmed, S.; Hashim, H.; Ayob, Y.; Asidin, N. H.; Choo, P. Y.; Al-Joudi, F. S. Red Cell Phenotyping of Blood from Donors at the National Blood Center of Malaysia. *Asian J. transfus. sci.* **2011**, *6*, 3–9.
- (13) Klein, H. G.; Spahn, D. R.; Carson, J. L. Red Blood Cell Transfusion in Clinical Practice. *Lancet* **2007**, *370*, 415–426.
- (14) Watkins, W. M. The ABO Blood Group System: Historical Background. *Transfusion Med.* **2001**, *11*, 243–265.
- (15) Thakral, B.; Saluja, K.; Bajpai, M.; Sharma, R. R.; Marwaha, N. Importance of Weak ABO Subgroups. *Science* **2005**, *36*, 32–34.
- (16) Leal-Egaña, A.; Scheibel, T. Silk-Based Materials for Biomedical Applications. *Biotechnol Appl. Biochem* **2010**, *55*, 155–167.
- (17) Meinel, L.; Hofmann, S.; Karageorgiou, V.; Kirker-Head, C.; McCool, J.; Gronowicz, G.; Zichner, L.; Langer, R.; Vunjak-Novakovic, G.; Kaplan, D. L. The Inflammatory Responses of Silk Films in Vitro and in Vivo. *Biomaterials* **2005**, *26*, 147–155.
- (18) Jin, H.-J.; Kaplan, D. L. Mechanism of Silk Processing in Insects and Spiders. *Nature* **2003**, *424*, 1057–1061.
- (19) Craig Burton, S. *Critical Evaluation of Wicking in Performance Fabrics, in Polymer, Textile and Fiber Engineering*; Georgia Institute of Technology: Atlanta, GA, 2004.
- (20) Al-Tamimi, M.; Shen, W.; Zeineddine, R.; Tran, H.; Garnier, G. Validation of Paper-Based Assay for Rapid Blood Typing. *Anal. Chem.* **2011**, *84*, 1661–1668.
- (21) Li, M.; Tian, J.; Al-Tamimi, M.; Shen, W. Paper-Based Blood Typing Device That Reports Patient's Blood Type "in Writing. *Angew. Chem., Int. Ed.* **2012**, *51*, 5497–5501.
- (22) Li, M.; Then, W.; Li, L.; Shen, W. Paper-Based Device for Rapid Typing of Secondary Human Blood Groups. *Anal. Bioanal. Chem.* **2014**, *406*, 669–677.
- (23) Harmening, D. *Modern Blood Banking and Transfusion Practices*; Davis Company: Philadelphia, PA, 2012.
- (24) Reinhart, W. H.; Huang, C.; Vayo, M.; Norwich, G.; Chien, S.; Skalak, R. Folding of Red Blood Cells in Capillaries and Narrow Pores. *Biorheology* **1991**, *28*, 537–549.

This page is intentionally blank



Short communication

Superhydrophobic surface supported bioassay – An application in blood typing

Lizi Li¹, Junfei Tian¹, Miaosi Li, Wei Shen*

Department of Chemical Engineering, Monash University, Clayton Campus, VIC 3800, Melbourne, Australia

ARTICLE INFO

Article history:

Received 8 September 2012

Received in revised form 15 January 2013

Accepted 18 January 2013

Available online 30 January 2013

Keywords:

Superhydrophobic surface

Liquid drop micro reactor

Bioassay

Blood typing

Digital image analysis

ABSTRACT

This study presents a new application of superhydrophobic surfaces in conducting biological assays for human blood typing using a liquid drop micro reactor. The superhydrophobic substrate was fabricated by a simple printing technique with Teflon powder. The non-wetting and weak hysteresis characteristics of superhydrophobic surfaces enable the blood and antibody droplets to have a near-spherical shape, making it easy for the haemagglutination reaction inside the droplet to be photographed or recorded by a digital camera and then analyzed by image analysis software. This novel blood typing method requires only a small amount of blood sample. The evaluation of assay results using image analysis techniques offers potential to develop high throughput operations of rapid blood typing assays for pathological laboratories. With the capability of identifying detailed red blood cell agglutination patterns and intensities, this method is also useful for confirming blood samples that have weak red blood cell antigens.

Crown Copyright © 2013 Published by Elsevier B.V. All rights reserved.

1. Introduction

The superhydrophobic phenomenon and fabrication of artificial superhydrophobic surfaces have attracted intense research in recent years. The strong water-repellent property of superhydrophobic surfaces forces water droplets to assume large contact angles ($>150^\circ$) and can be designed to have very weak hysteresis on those surfaces [1–4]. Superhydrophobic surfaces have many practical applications such as self-cleaning [5,6], anti-wetting [7], water-repellence [8,9], oil–water separation [10], anti-freezing [4] and fluid-drag reduction [11].

While numerous studies have been directed towards the fabrication and applications of superhydrophobic surfaces for water-repellence, anti-wetting and oil–water separation, some research works have focused on utilizing the water droplet supported by superhydrophobic surfaces for practical applications. The non-wetting and weak hysteresis characteristics of superhydrophobic surfaces enables a lab-on-chip analytical sensor to be designed; aqueous droplets containing analytes can be manipulated for analytical purposes, such as sample storage, transport, mixing and splitting on a lab-on-chip device [12]. More recently, several researchers explored the use of aqueous droplets on superhydrophobic pedestals as a micro-scale reactor to perform chemical reactions and the growth of crystals [13,14].

The near-spherical shape of an aqueous droplet on a superhydrophobic surface allows for a sufficient elevation of its centre of gravity so that a micro-scale physical transformation or biochemical reaction occurring inside the droplet can be clearly observed and recorded from the side view. The superhydrophobic surface supported micro-scale analytical or diagnostic reactors require materials of low-cost and are easy to be transformed into an automated high volume biochemical assays. To date, however, there is little information about superhydrophobic surface supported biochemical assays in literature.

To clearly observe a living reaction inside an aqueous droplet from the side view, the droplet needs to have a sufficient height on the supporting surface; for this reason a hydrophobic surface or a superhydrophobic surface is required. Eq. (1) and Fig. 1(a) describe the height of a droplet and its contact angle with the supporting surface.

$$h = R[1 + \sin(\theta - 90^\circ)] \quad (1)$$

where h is the height of the drop, R is the radius of the drop and θ is the contact angle of the drop on the surface. If the gravity effect is neglected, the height of a drop on a surface can be calculated by Eq. (1). Fig. 1(b) shows the plot of the droplet height and its contact angle with the supporting surface. For a droplet having a radius of 1.68 mm ($\sim 20 \mu\text{L}$) on a hydrophobic surface ($\theta = 120^\circ$), the height is 2.52 mm. For the same droplet on a superhydrophobic surface ($\theta = 150^\circ$), the height of the droplet increases 3.13 mm. The difference in droplet height on superhydrophobic and hydrophobic surfaces is moderate, and further increase in contact angle beyond 150° results in only a very small increase in droplet height. Therefore, for the purpose of only acquiring side views of

* Corresponding author.

¹ Lizi Li and Junfei Tian contributed equally as co-first authors.

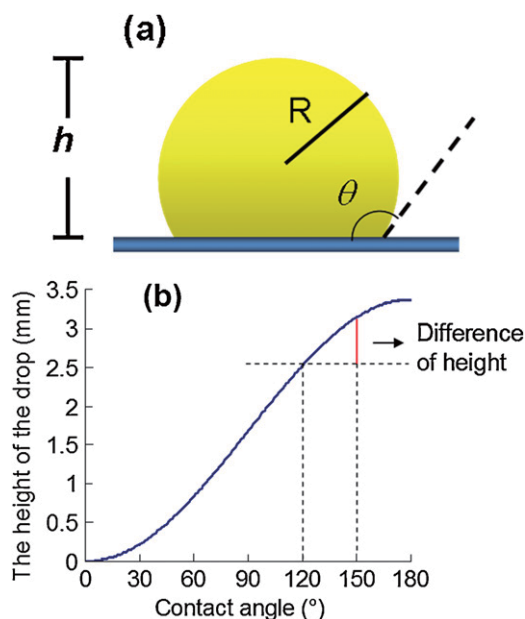


Fig. 1. (a) Scheme of the side-view profile of a water droplet on a (super-) hydrophobic surface (R and h are the radius and the height of the droplet, respectively; θ is the contact angle); (b) a plot of the height of a 20 μL droplet on a supporting surface with respect of its contact angle with the surface (gravity effect is not considered). The red line shows the difference of the heights of water droplets on a hydrophobic surface ($\theta = 120^\circ$) and a superhydrophobic surface ($\theta = 150^\circ$).

a droplet, a highly hydrophobic surface would be sufficient. However, a significant advantage of using superhydrophobic surface for biochemical assay is that the liquid sample can easily roll off the surface after test; this prevents the surface from being contaminated. For some assays, this advantage may be important, since the superhydrophobic supporting surface may be reused. This highly useful function of superhydrophobic surfaces needs to be further explored to enable chemical and biological reactions, and biochemical assays to be conducted in a high throughput capacity and at low cost.

In this study, we demonstrate the use of superhydrophobic surfaces for biological assays through making observations of the haemagglutination reaction of human red blood cells (RBC) and blood typing assay. Accurate and rapid typing of human blood is not only of great importance for blood transfusion and transplantation medicine [15], but also critically important for blood banking, and for screening or cross-checking donors' blood samples. For the later, in particular, high throughput methods are required to process large number of samples rapidly. Although the lateral flow and the Gel Card technologies are the mainstream technologies currently in use in hospitals and pathological laboratories, diagnostic industry has never stopped exploring new technologies [16,18–21,24–26]. In this work superhydrophobic substrate was fabricated by using a simple contact printing method developed in our laboratory [17]; the substrate is inexpensive and disposable, suitable for use as a laboratory consumable item. In a blood typing application, the haemagglutination reaction inside the blood sample droplet can be imaged by using a digital camera and suitable software can be used for the blood type identification. The use of digital camera allows photos of an assay to be kept for retrieval and analysis, and it has the potential to reveal detailed agglutination process if camera with high magnification is used. Further automation in assay result evaluation will provide a new potential method for rapid blood typing assays of high throughput operation, with the capability of providing magnified photo and video footage of the agglutination reaction,

which will be of a significant diagnostic aid to the identifying of blood samples whose RBCs carry weak antigens.

2. Material and methods

Teflon powder with an average particle size of 35 μm was obtained from Sigma–Aldrich. The polymer film used in this study was a commercial overhead transparency (Xerox). A UV curable flexographic post-print varnish (UV 412) was received as a gift from Flint Inks (Flint Group Australia). Six blood samples (type A+, A–, B+, AB+, O+ and O–) were received from a pathological laboratory, following the ethical protocols. All blood samples were stored in Vacutainer® test tubes containing lithium–heparin anticoagulant at 4 °C and used within 5 days of collection. Epiclone™ anti-A, anti-B and anti-D monoclonal grouping reagents were sourced commercially from the Commonwealth Serum Laboratory, Australia. Anti-A and anti-B are colour-coded cyan and yellow solutions respectively, while anti-D is a clear colourless solution. All monoclonal grouping reagents were also stored at 4 °C.

2.1. Fabrication of superhydrophobic Teflon powder surface on polymer film

The superhydrophobic surface on polymer film was fabricated by a contact printing method developed in our laboratory [17]. A thin layer of UV curable flexographic post-print varnish was uniformly transferred onto the transparency film with a roller. Teflon powder was then dusted onto the film and adhered to the uncured varnish. The film was then passed through a UV curing station. Upon curing, the UV varnish tightly glued the Teflon powder particles on the film. The micron-scale roughness of Teflon particles on the film formed the required superhydrophobic surface.

2.2. Observation of haemagglutination reaction inside the blood sample drop

Blood samples of two types, A+ and B+, were chosen to demonstrate the time dependency of haemagglutination reaction with anti-B solution inside near-spherical blood droplets supported by the superhydrophobic surface. 10 μL of each blood sample was placed on the superhydrophobic surface using a micropipette (Eppendorf research®). The same volume of anti-B solution was then injected into the blood droplet with a micropipette, and gently stirred with the micropipette-head. The droplets were then monitored for haemagglutination reaction for 180 s with a digital microscopy camera (Moticam 2500); photographs were taken at 30 s intervals from the beginning of the blood sample and antibody mixing.

2.3. Blood typing assay on superhydrophobic surfaces

The experimental procedure of performing a blood typing assay is similar to observing the haemagglutination reaction except that three droplets of each blood sample were taken and mixed with three different antibody reagents; anti-A, anti-B and anti-D. The sample blood type can be identified from the pattern of the haemagglutination reaction(s) with the three antibodies. Photos of the sample droplets taken by the camera provide clear identification of the occurrence of a haemagglutination reaction.

A simple colour density measurement method is presented in this study to digitally determine the changes of colour intensities of the blood sample droplets after being mixed with antibody solutions. This method can potentially be used to automate this blood typing assay for high throughput applications.

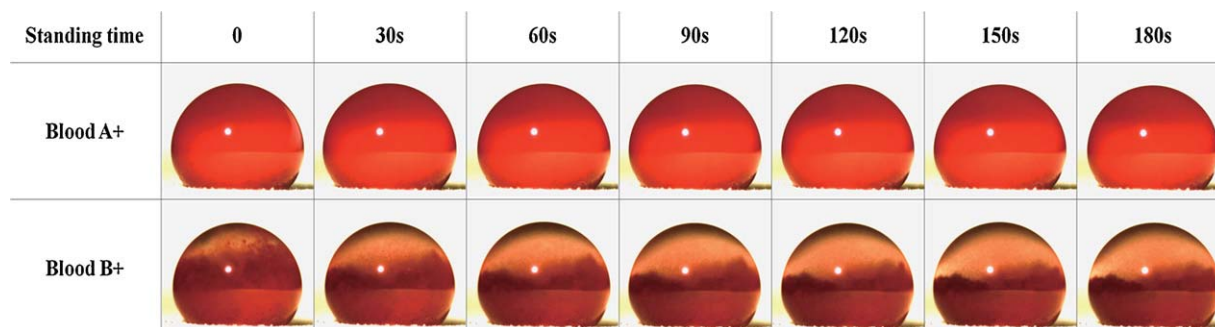


Fig. 2. Photos of two 10 μ L blood droplets (A+ and B+) mixed with 10 μ L anti-B reagent. Haemagglutination was immediately observed inside the droplet of B+ blood sample (second row), due to the specific interaction between anti-B and the B-antigen carried by RBCs of the B+ sample. There was, however, no haemagglutination in the droplet of A+ blood sample during the entire 180 s standing time (first row), since anti-B is not a specific antibody to the antigen carried by the RBCs of the A+ sample.

3. Results and discussion

3.1. Contact angle characterization of the superhydrophobic Teflon powder surface

Contact angle measurements were used to characterize the printed Teflon powder surface. Water, a blood sample and antibody solutions were used as liquids for contact angle measurements. Contact angles for water, blood (A+), anti-A, anti-B and anti-D with the Teflon powder surface were determined to be $158.6^\circ \pm 1.0^\circ$, $153.1^\circ \pm 2.2^\circ$, $154.1^\circ \pm 3.2^\circ$, $155.8^\circ \pm 1.3^\circ$ and $148.5^\circ \pm 0.2^\circ$, respectively. This data is the average of 5 measurements and the standard deviations are also given.

From the contact angle data of water with the surface it can be seen that the printed Teflon powder surface was superhydrophobic since the water contact angle was significantly higher than 150° . The blood and antibody solutions also showed contact angles greater than or close to 150° . The only liquid that has the lower than 150° contact angle was the anti-D solution. The slightly lower contact angle of anti-D solution compared to that of the other antibody solutions may be related to its formulation being different from other antibody solutions. However, it can be found that such a small difference in contact angle between the blood sample and the antibody solutions means that there is a negligible difference in the practical application of observing haemagglutination reactions inside the sample droplets.

3.2. Observation of haemagglutination inside the blood sample droplet

To observe the haemagglutination reaction inside blood sample droplets, anti-B was introduced into two blood samples of A+ and B+ types. As anti-B was introduced into the drop of blood sample type B+, the specific antibody-antigen interaction resulted in an immediate haemagglutination of RBCs – a clear separation of agglutinated RBC lumps from the plasma phase can be observed inside the blood sample drop immediately after the anti-B introduction (Fig. 2).

As time progressed to 90 s, the agglutination reaction led to the clearing of the top part of B+ sample droplet. Further standing of the sample to 180 s showed little further change in RBC separation. In contrast to the reaction of B+ blood sample with anti-B, the mixing of A+ blood sample with anti-B (a non-specific antibody) resulted in no haemagglutination reaction and therefore no separation of the RBCs inside the sample droplet (Fig. 2). Haemagglutination of RBCs is the indication of the occurrence of specific interactions between the antigen present on the surface of the red blood cells and the corresponding antibody present or added in the plasma phase. Therefore haemagglutination of RBCs in the presence

of blood typing antibodies provides identification of the blood type of the sample. Results in Fig. 2 provide rapid and clear identification of the blood types of the samples. With the use of a digital camera, it is also possible for the captured images to be digitally analyzed to identify the blood types of the samples in an automated way for high throughput blood typing service application. Depending on the assay, the superhydrophobic substrate may be disposed of after use, or reused after allowing the sample drop to roll off the surface.

3.3. Blood typing using superhydrophobic surfaces as a low-cost supporting substrate

The clear observation of haemagglutination reaction inside a blood sample droplet shows that a superhydrophobic substrate in general can be used to support micro reactors for biochemical assays. We further demonstrate the use of superhydrophobic surface for ABO and RhD blood typing assays. The use of superhydrophobic surfaces for blood typing may offer significant economic advantage, since the cost of such a surface is low.

Recently, low-cost paper- and thread-based blood typing platforms have been reported [18–21]. Paper- and thread-based blood typing devices greatly reduce the cost and the time required for performing blood typing assays; they are particularly suitable for making user-operated devices for developing countries. As an alternative platform, superhydrophobic surface-based blood typing assays offer the following advantages: (1) Superhydrophobic surfaces combined with an imaging system allow automated high throughput equipment to be built at a moderate to low cost. (2) Such equipment provides detailed visual haemagglutination patterns of samples, which may be further used for evaluation of haemagglutination reaction through image analysis. (3) Haemagglutination reactions inside the sample drop provide the possibility of extracting the plasma phase from the samples for other assays.

Six blood samples were assayed using the superhydrophobic surface supported blood typing assay. For each blood sample, three sample droplets were placed on the superhydrophobic surface; these droplets were respectively mixed with anti-A, anti-B and anti-D following the protocol described in Section 2. The samples droplets were then observed for haemagglutination reactions. Fig. 3 shows images of the assaying results of the six blood samples; haemagglutination reaction can be easily identified from the photos taken from the side view of the droplets. Based on the pattern of haemagglutination reactions in Fig. 3, blood types of the samples were identified as being A+, A–, B+, AB+, O+ and O–. These results were in total agreement with the blood typing results obtained by the pathological laboratory using the Gel Card technology.

To explore the possible automation of using the superhydrophobic surface supported bioassay for high throughput blood typing

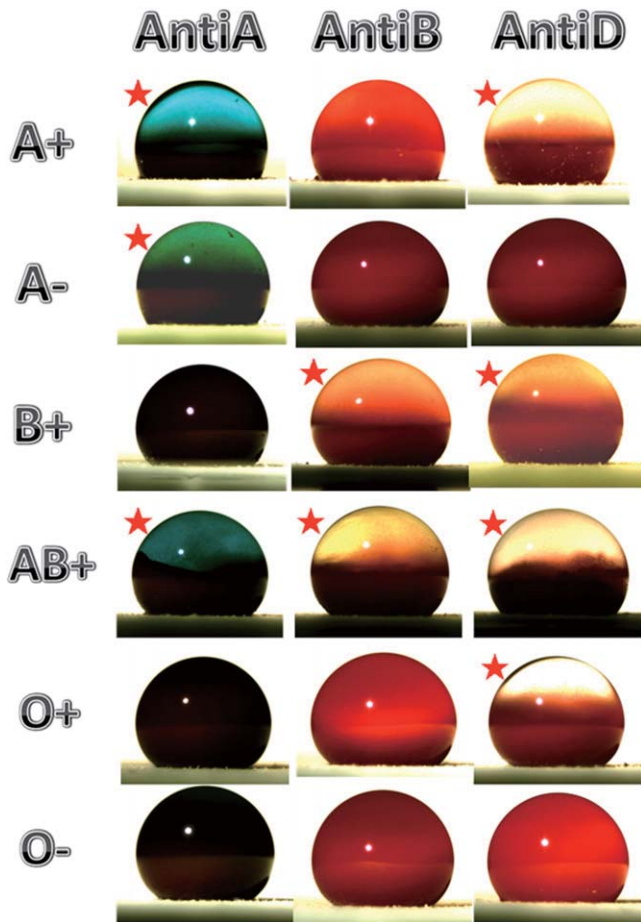


Fig. 3. Photos of the blood agglutination of the six blood samples (A+, A−, B+, AB+, O+ and O−) when they are respectively mixed with three antibodies (Anti-A, Anti-B and Anti-D) on superhydrophobic surface. The red star represents blood aggregation was found in that photo. The blood type can be determined by observing the aggregation of blood with different antibodies.

assays, images in Fig. 4 were digitally processed and identification of haemagglutination via image analysis was pursued by using Adobe Photoshop. The image analysis was performed on a standard square of 5 mm × 5 mm in the top part of the droplet image; the average colour intensity of the magenta channel was measured from the square. The choice of measuring the magenta channel is based on its large dynamic range [22], which is capable of providing more accurate measurement of the sample. Table 1 shows the magenta intensity of the analyzed area of each image. The magenta colour intensity measured from the images of the sam-

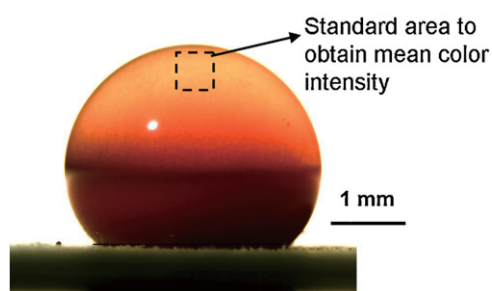


Fig. 4. Illustration of the measurement of colour intensity (magenta channel). The blood aggregation can be detected by comparing the colour intensity of the standard area in the images of different drops. From the identified aggregation of blood caused by their corresponding antibodies, the type of blood can be determined.

Table 1

The magenta intensity of the standard area in each image of Fig. 3.

	Anti-A	Anti-B	Anti-D
A+	7.18 ± 0.75	219.52 ± 0.13	0.06 ± 0.04
A−	70.22 ± 2.93	253.04 ± 0.53	253.23 ± 0.26
B+	225.36 ± 0.28	101.52 ± 1.98	94.81 ± 0.76
AB+	147.52 ± 1.63	61.63 ± 1.89	6.38 ± 1.89
O+	219.65 ± 0.57	253.79 ± 0.41	0.23 ± 0.15
O−	220.10 ± 1.60	252.39 ± 0.67	252.80 ± 0.04

ple drops shows strong contrast; samples with haemagglutination correspond to colour intensity values much lower than saturation, whereas samples with no haemagglutination show magenta colour intensity close to saturation.

In order for the haemagglutination status to be evaluated digitally, a colour intensity threshold of 180 was introduced to differentiate haemagglutination from non-haemagglutination. This threshold level was chosen as it is numerically around 40 above the highest colour intensity of the non-agglutinated sample and around 40 below the lowest colour intensity of the agglutinated sample. With this threshold level it is possible to digitally identify the haemagglutination reaction in a blood sample drop after the addition of antibody solution. The combination of the superhydrophobic supporting surface, the simple camera system and the software system presents a design concept of an automated blood typing device capable of high throughput analysis of blood samples. The digitized results obtained using this system can deliver direct blood typing result and also can be transmitted by mobile phone [23] or other electronic devices to a remote facility should it be necessary.

4. Conclusion

In this study we investigated a new application of using superhydrophobic surfaces to conduct biological assays. By using a superhydrophobic surface as a supporting surface for liquid droplets, a human blood typing assay was conducted. The non-wettable property of the superhydrophobic surface by blood samples and antibody solutions makes the blood and antibody droplets assume a near spherical shape, providing an excellent side view for the haemagglutination reaction to be observed inside the droplet. By observing the presence or absence of the haemagglutination reaction, specific antibody–RBC interactions can be identified; this method can be used for rapid blood typing. By using a camera and a simple image analysis system, haemagglutination inside the blood sample droplets can be digitally identified. This capability potentially makes the superhydrophobic surface supported blood typing assay suitable for high throughput assay applications. We believe that the superhydrophobic surface supported micro reactor concept can be developed into more applications for chemical or biological assays.

Acknowledgements

This work is supported by Australian Research Council Grants (ARC LP0990526 and LP110200973). Authors thank Haemokinesis for its support through an ARC Linkage Project. The authors would like to specially thank Dr. Emily Perkins, Department of Chemical Engineering and Mr Hansen Shen, student of the Faculty of Law of Monash University for proof reading the manuscript. Lizi Li, Junfei Tian and Miaosi Li thank Monash University Research and Graduate School and the Faculty of Engineering for their postgraduate research scholarships.

Appendix A. Supplementary data

Supplementary data associated with this article can be found, in the online version, at <http://dx.doi.org/10.1016/j.colsurfb.2013.01.049>.

References

- [1] X. Hong, X.F. Gao, L. Jiang, Application of superhydrophobic surface with high adhesive force in no lost transport of superparamagnetic microdroplet, *J. Am. Chem. Soc.* 129 (2007) 1478–1479.
- [2] X. Zhang, F. Shi, J. Niu, Y. Jiang, Z. Wang, Superhydrophobic surfaces: from structural control to functional application, *J. Mater. Chem.* 18 (2008) 621–633.
- [3] A. Tuteja, W. Choi, M. Ma, J.M. Mabry, S.A. Mazzella, G.C. Rutledge, G.H. McKinley, R.E. Cohen, Designing superoleophobic surfaces, *Science* 318 (2007) 1618–1622.
- [4] X. Yao, Y. Song, L. Jiang, Applications of bio-inspired special wettable surfaces, *Adv. Mater.* 23 (2011) 719–734.
- [5] R. Bossey, Self-cleaning surfaces – virtual realities, *Nat. Mater.* 2 (2003) 301–306.
- [6] V.A. Ganesh, H.K. Raut, A.S. Nair, S. Ramakrishna, A review on self-cleaning coatings, *J. Mater. Chem.* 21 (2011) 16304–16322.
- [7] T.L. Sun, L. Feng, X.F. Gao, L. Jiang, Bioinspired surfaces with special wettability, *Acc. Chem. Res.* 38 (2005) 644–652.
- [8] X.M. Li, D. Reinhoudt, M. Crego-Calama, What do we need for a superhydrophobic surface? A review on the recent progress in the preparation of superhydrophobic surfaces, *Chem. Soc. Rev.* 36 (2007) 1350–1368.
- [9] P. Roach, N.J. Shirtcliffe, M.I. Newton, Progress in superhydrophobic surface development, *Soft Matter* 4 (2008) 224–240.
- [10] L. Feng, Z. Zhang, Z. Mai, Y. Ma, B. Liu, L. Jiang, D. Zhu, A super-hydrophobic super-oleophilic coating mesh film for the separation of oil and water, *Angew. Chem.* 116 (2004) 2046–2048.
- [11] H. Mertaniemi, V. Jokinen, L. Sainiemi, S. Franssila, A. Marmur, O. Ikkala, R.H.A. Ras, Superhydrophobic tracks for low-friction, guided transport of water droplets, *Adv. Mater.* 23 (2011) 2911–2914.
- [12] B. Balu, A.D. Berry, D.W. Hess, V. Breedveld, Patterning of superhydrophobic paper to control the mobility of micro-liter drops for two-dimensional lab-on-paper applications, *Lab Chip* 9 (2009) 3066–3075.
- [13] B. Su, S. Wang, Y. Song, L. Jiang, A miniature droplet reactor built on nanoparticle-derived superhydrophobic pedestals, *Nano Res.* 4 (2011) 266–273.
- [14] B. Su, S. Wang, J. Ma, Y. Song, L. Jiang, Clinging-microdroplet patterning upon high-adhesion, pillar-structured silicon substrates, *Adv. Funct. Mater.* 21 (2011) 3297–3307.
- [15] G. Daniels, M.E. Reid, Blood groups: the past 50 years, *Transfusion* 50 (2010) 281–289.
- [16] J.K.M. Duguid, I.M. Bromilow, New technology in hospital blood banking, *J. Clin. Pathol.* 46 (1993) 585–588.
- [17] J. Tian, X. Li, W. Shen, Printed two-dimensional micro-zone plates for chemical analysis and ELISA, *Lab Chip* 11 (2011) 2869–2875.
- [18] M.S. Khan, G. Thouas, W. Shen, G. Whyte, G. Garnier, Paper diagnostic for instantaneous blood typing, *Anal. Chem.* 82 (2010) 4158–4164.
- [19] M. Al-Tamimi, W. Shen, R. Zeineddine, H. Tran, G. Garnier, Validation of paper-based assay for rapid blood typing, *Anal. Chem.* 84 (2012) 1661–1668.
- [20] D.R. Ballerini, X. Li, W. Shen, An inexpensive thread-based system for simple and rapid blood grouping, *Anal. Bioanal. Chem.* 399 (2011) 1869–1875.
- [21] T. Arbatan, L. Li, J. Tian, W. Shen, Liquid marbles as micro-bioreactors for rapid blood typing, *Adv. Healthcare Mater.* 1 (2012) 80–83.
- [22] A.W. Martinez, S.T. Phillips, E. Carrilho, S.W. Thomas, H. Sindi, G.M. Whitesides, Simple telemedicine for developing regions: camera phones and paper-based microfluidic devices for real-time, off-site diagnosis, *Anal. Chem.* 80 (2008) 3699–3707.
- [23] J.L. Delaney, C.F. Hogan, J. Tian, W. Shen, Electrogenated chemiluminescence detection in paper-based microfluidic sensors, *Anal. Chem.* 83 (2011) 1300–1306.
- [24] M. Li, J. Tian, M. Al-Tamimi, W. Shen, Paper-based blood-typing device that reports patient's blood type in writing, *Angew. Chem. Int. Ed.* 51 (2012) 5497–5501.
- [25] P. Jarujamrus, J. Tian, X. Li, A. Siripinyanond, J. Shiowatana, W. Shen, Mechanisms of antibody and red blood cell interactions in paper-based blood typing devices, *Analyst* 137 (2012) 2205–2210.

This page is intentionally blank

Barcode-Like Paper Sensor for Smartphone Diagnostics: An Application of Blood Typing

Liyun Guan,[†] Junfei Tian,[†] Rong Cao,[†] Miaosi Li,[†] Zhaoxiang Cai,[‡] and Wei Shen^{*,†}

[†]Department of Chemical Engineering, [‡]Clayton School of Information Technology, Monash University, Wellington Rd., Clayton, Melbourne, Victoria 3800, Australia

S Supporting Information

ABSTRACT: This study introduced a barcode-like design into a paper-based blood typing device by integrating with smartphone-based technology. The concept of presenting a paper-based blood typing assay in a barcode-like pattern significantly enhanced the adaptability of the assay to the smartphone technology. The fabrication of this device involved the use of a printing technique to define hydrophilic bar channels which were, respectively, treated with Anti-A, -B, and -D antibodies. These channels were then used to perform blood typing assays by introducing a blood sample. Blood type can be visually identified from eluting lengths in bar channels. A smartphone-based analytical application was designed to read the bar channels, analogous to scanning a barcode, interpret this information, and then report results to users. The proposed paper-based blood typing device is rapidly read by smartphones and easy for the user to operate. We envisage that the adaptation of paper-based devices to the widely accepted smartphone technology will increase the capability of paper-based diagnostics with rapid assay result interpretation, data storage, and transmission.



Paper-based analytical devices (PADs) have generated great interest in the field of medical diagnostics in recent years because they demonstrate great potential to develop affordable, rapid, and practical diagnostic sensors for resource-limited areas.^{1–5} Numerous research works have been reported, covering methods of paper sensor fabrication,^{6,7} analyte-specific assays,⁸ and various result-reporting ideas, including colorimetric,⁹ fluorescent,¹⁰ electroluminescent,¹¹ and electrochemical,¹² as well as text-reporting.¹³ Among the analyte-specific assays, PADs were demonstrated to be able to provide semiquantitative to quantitative analysis.^{14–16} Recently, PADs, investigated as a class of field-based, equipment-free blood typing devices, have achieved the same accuracy but have been proven to be much more rapid than the mainstream blood typing technologies.^{13,17} These developments show that current research has produced a wide range of new concepts for making paper-based devices a new platform that does not require hospital and laboratory support. Among these concepts, several have been extensively developed and have almost reached commercialization.^{18,19}

Most PADs research focuses on the development of stand-alone devices that function under nonlaboratory conditions.^{20–22} While in this direction many innovative ideas have been explored and reported, it should be noted that PADs will be more successful if they can be adapted to existing technologies that are ubiquitous in modern society. From the early days of PADs research, it was proposed that camera phones can significantly enhance low-cost diagnostics by connecting the users who perform the tests with professionals

who receive the results and provide medical instructions.^{23,24} The extremely high acceptance of smartphone technology by the human population in both developed and developing countries makes this technology a valuable infrastructure for any other technology to build upon.²⁵ The adaptation of PADs to smartphone technology, particularly through software innovation, will significantly enhance the power of PADs as a platform technology for diagnostic applications through providing simple analytical tools, increasing coverage and connection between users and professionals, and allowing data sorting, storage, and management for local and temporary medical facilities in remote medical emergencies and disaster response missions.

In this study, we applied a barcode reading concept to adapt paper-based blood typing assays to smartphone technology. Blood typing is a routine clinical assay in surgical procedures, medical emergencies, and blood transfusions, as well as in blood banking.²⁶ Our group has reported a series of studies on the fabrication of new types of PADs and thread-based analytical devices for blood typing.^{27–29} These studies have demonstrated new stand-alone blood typing devices that can be operated by users without the need of any supporting instrument. While the stand-alone devices promise a superior platform to the mainstream hospital-based technologies in

Received: September 3, 2014

Accepted: October 10, 2014

Published: October 10, 2014

providing health care to home-based users and users living in impoverished areas, adaptation to smartphones through software innovation will provide further advantages to paper-based blood typing technology in digital data sorting, storage, and transmission. It is anticipated that the use of software will be an effective means of reducing human error in data sorting and storage. In this work, we developed a simple software for smartphones and used it for paper-based blood typing assays.

EXPERIMENTAL SECTION

Reagents and Apparatus. Antibodies against RBC antigens approved for human blood grouping were obtained from the Commonwealth Serum Laboratory (CSL), Australia. They were IgM antibodies commercialized under the names of Epiclone Anti-A, Anti-B, and Anti-D (IgM) FFMU Concentrate. All of them are transparent solutions. Phosphate-buffered physiological salt solution (PBS, pH 7.4), sourced from Sigma-Aldrich, Australia, was used as the diluent for all antibody solutions. Alginic acid sodium salt (NaAlg) was acquired from Sigma-Aldrich, Australia. Anti-A and Anti-B were diluted to 1/5 with PBS solution for use in our study. All antibodies were stored at 4 °C.

Blood samples acquired from adult volunteers of a known blood group were provided by Red Cross, Australia. Samples were stored in Vacutainer tubes containing heparin, citrate, and EDTA and refrigerated at 4 °C; they were used within 10 days of collection. Reagent red blood cells Revercell (15% A1, 15% B red blood cells) and Abtectcell III (3% R1R1, 3% R2R2, and 3% rr red blood cells) were purchased from CSL Limited, Australia, stored at 4 °C and used within 30 days of delivery. All blood samples, including reagent blood cells, were diluted to 15% with PBS for performing blood typing assays in our printed barcode paper devices. Ultrapure water (≥ 18.2 M Ω) purified by a Milli-Q System (Millipore, Bedford, MA, USA) was used for the preparation of all solutions. Kleenex paper towels (Kimbley-Clark, Australia) with a basis weight of 34 g/m² and an apparent thickness of 140 μ m were purchased from a local supermarket.

Bar Pattern Design for Blood Typing. Alkyl ketene dimer (Precis900, Hercules Australia Pty Ltd.) was used as the cellulose hydrophobization reagent. Analytical-grade *n*-heptane (Sigma-Aldrich, Australia) was used as the solvent for the dimers. The Kleenex paper, cut into A4 size, was selected as the substrate to fabricate the bar pattern paper-based blood typing devices. The fabrication procedure involves using a reconstructed commercial desktop ink jet printer (Canon Pixma ip4500) to print computer-generated patterns onto the paper with an ink solution of alkyl ketene dimer–heptane (3%, v/v) according to previous works.³⁰ The printed paper was heat-treated in an oven at 105 °C for 1 h to allow the hydrophobicity of the printed area on paper to fully develop. In this work, the device was fabricated with three separate channel patterns, which were labeled with the printed letters “A”, “B”, and “D”. Each pattern consisted of a bar channel (0.3 cm \times 5 cm), a buffer rinsing zone ($r = 0.2$ cm), and a bridging channel linking these two (Figure 1). The channel patterns were hydrophilic and used for the assaying application.

Preparation of Antibody-Loaded Bar Channels. Before loading antibodies, the bar channels were treated with NaAlg for the purpose of enhancing antibody loading efficiency. NaAlg solutions with concentrations of 0%, 0.01%, 0.05%, and 0.1% (w/v) were prepared using Millipore-purified water. The patterned paper devices were divided into four groups; the

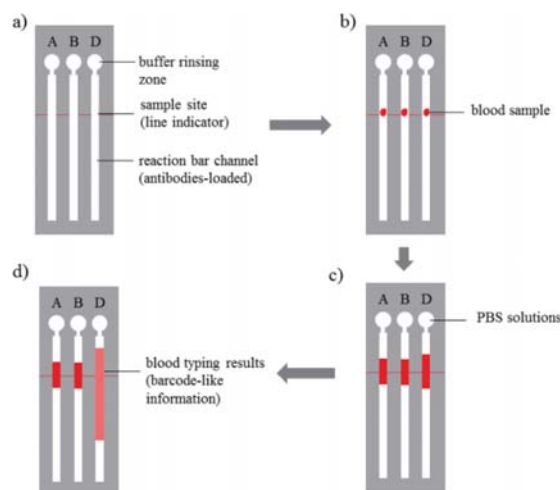


Figure 1. Schematic diagram of the barcode-like blood typing device. (a) Anti-A, Anti-B, and Anti-D antibodies were introduced into the reaction bar channels. (b) 3 μ L of blood samples was introduced in the sample sites for the blood typing test and allowed to wick and react for 30 s. (c) 10 μ L of PBS solutions was added as eluting buffer for 1 min of elution. (d) Reading the blood typing test results.

channels of each group were treated with 10 μ L of each of the four NaAlg solutions, respectively. All the papers modified with NaAlg solutions were dried for 30 min at room temperature.

All channels marked with “A” (channel “A”) in all four groups of NaAlg-treated papers were treated with Anti-A; 10 μ L of diluted Anti-A antibodies were uniformly deposited into the entire channel length. Likewise, for channels “B” and “D”, 10 μ L of Anti-B and 10 μ L of Anti-D antibodies were deposited into the “B” and “D” channels of all papers, respectively. All the paper devices were dried for 1 h at room temperature.

Covalent antibody immobilization involves two steps: activating the NaAlg-modified paper surface using EDC-NHS chemistry and then conjugating it with the antibody molecules. In the paper surface activation step, 20 μ L of an equal-volume mixture of 20 mg/mL EDC and 12 mg/mL NHS solutions was uniformly deposited into each channel and the activation reaction was allowed 30 min for completion in an environment with a controlled high humidity. After activation, each channel was rinsed with 60 μ L of H₂O three times. For the conjugation of antibodies, all of the “A” bar channels were uniformly deposited with 10 μ L of diluted Anti-A antibodies and allowed 1 h for conjugation at 50% humidity. Similarly, bar channels “B” and “D” of all groups were deposited with 10 μ L of Anti-B and 10 μ L of Anti-D, respectively, under the same conditions, for conjugation reactions. At the end of the conjugation reactions, each channel was rinsed three times using 60 μ L of PBS and then allowed to dry for 1 h at room temperature.

Water Drop Penetration Time (WDPT) Measurement.

To evaluate the influence of paper surface modification on paper wettability, a water drop penetration time test was adopted. The untreated and antibody-conjugated Kleenex paper towel was cut into 1 cm \times 1 cm squares for water penetration time testing. A contact angle instrument (Data-physics OCA230, Germany) was used to take video of the water drop penetration process. The experimental procedure was as follows: a piece of a paper square was horizontally fixed to the measurement platform; a 3 μ L water droplet was delivered onto the paper surface by a syringe; the drop landing

and penetration processes were recorded at a frame speed of 56 frames/s; the final penetration time was calculated by the system software from the video data. Three measurements were taken for each paper sample.

Blood Typing Using the Barcode-Like Paper Device. A volume of 3 μL of prediluted 15% blood samples was introduced into each channel via its sampling site indicated by the red line (Figure 1); red blood cells were permitted to react with the antibody in the channel for 30 s. Then, a volume of 10 μL of PBS buffer solution was introduced onto the rinsing zone and allowed to elute through the channel by capillary wicking for 1 min. The testing assay was then scanned and interpreted by smartphone-based technology.

Smartphone-Based Analysis Design. The mobile software designed for carrying out the preset analytical procedures (app) was developed on the Android platform. The software was coded with Java using ADT (Android development tools), and the functions of the smartphone were controlled through APIs (application programming interfaces). The app can be supported by Android version 2.2 and above. The app was designed to read the information in each bar channel along its length, since the blood penetration along the channel gives the most distinguishable difference between a positive and negative result. In this study, a Google Nexus 5 smartphone (Google Android version 4.4) was used to read the final blood typing results.

RESULTS AND DISCUSSION

The Sensor Design Concept. Paper-based analytical devices have been designed for ABO/RhD blood grouping based on the principle of hemagglutination reaction between RBCs and antibodies.³¹ When a blood sample wicks into the fiber network of paper treated with the corresponding antibody, hemagglutination will occur within the fiber network which will lead to the formation of large lumps that lock inside the fiber network and cannot be eluted out. Therefore, when hemagglutination occurs in the bar channels of our blood typing device (Figure 1), buffer elution will not elute the agglutinated RBC lumps along the channel, leaving a short bar of blood stain with a strong color. The deep red color came from the aggregated red blood cells. In contrast to this, when RBCs contact a noncorresponding antibody inside the fiber network, no hemagglutination will occur. Free RBCs can be eluted along the channel by PBS solution, forming a diluted bar of much greater length along the channel (Figure 1). For the purpose of interpreting an assay result, if we can distinguish a "short" bar from a "long" bar in a channel, it will be possible to identify whether hemagglutination has occurred in this channel or not. Therefore, making sure the "short" and "long" information are distinguishable is an important consideration when designing this sensor.

However, the length difference between agglutinated (positive, "P") and nonagglutinated (negative, "N") RBCs was not significant enough to be clearly identified (Figure S-1a, Supporting Information), since the limited volume of blood samples cannot provide enough driving force for non-agglutinated RBCs to continue penetrating forward. Therefore, we introduced PBS buffer solutions as eluting buffer into channels to supply a driving force for free RBCs to continue to move forward. The RBCs eluting length difference between positive and negative tests was distinct: agglutinated RBCs formed a short eluting length in the bar channel, while nonagglutinated RBCs led to a much longer eluting length

(Figure S-1b, Supporting Information). Such difference makes this sensor viable for accurate identification by smartphone-based analysis. In the final design of this blood typing assay (Figure 1), three separate patterns labeled with "A", "B", and "D" were designed for the identification of A, B, and D antigens, respectively, to determine ABO and RhD blood types.

Sensor Development. On the basis of the above sensor design concept, a smartphone-based app was designed to read the RBC eluting length in a channel. To ensure unambiguous results identification using this design idea, different physicochemical channel modifications have been considered. Emphasis is given to the design of the bar channels to provide the negative and positive tests with a significant sample eluting length difference for easy and fast identification by the software. This relies on detailed consideration of channel surface treatment to enhance the antibody sorption and wetting ability of paper. For this reason, different paper surface modification methods have been investigated to obtain the maximum eluting length difference between positive and negative tests.

Physical or Chemical Immobilization. Physical and chemical methods for antibody immobilization were investigated so that the method capable of producing a larger difference between the positive and negative assays could be selected. The chemistry applied here is the EDC/NHS activating agent pair which is commonly used for the coupling of primary amines with carboxyl groups to yield amide bonds. Since there are sparse carboxyl groups on the paper, NaAlg was used to increase carboxyl groups on paper because of its great biocompatibility and the retention of NaAlg has been proven to be satisfactory.³² However, the antibody-treated channels with chemical coupling have failed to retain a sufficient amount of antibody on the paper surface for performing a blood typing assay. Also, this approach causes a decrease of paper wettability as shown by the water drop penetration test (WDPT) (Table S-1, Supporting Information). These undesirable outcomes make the chemical coupling approach unsuitable, since poor paper wettability prevents the blood sample from wicking into the fiber network and contacting antibody molecules. In contrast to this, antibodies physically immobilized on paper can be freely released from the fiber matrix into the blood samples to effectively collide and react with RBCs to allow hemagglutination reactions to occur.

NaAlg Concentration. Among the systems that were considered above, physical immobilization was judged to be the only appropriate method to provide a suitable surface modification for the sensor design. To optimize the physical immobilization of NaAlg, the bar channels were first modified with 0% (w/v) NaAlg (Figure S-2,1, Supporting Information), 0.01% (w/v) NaAlg (Figure S-2,2, Supporting Information), 0.05% (w/v) NaAlg (Figure S-2,3, Supporting Information), and 0.1% (w/v) NaAlg (Figure S-2,4, Supporting Information), followed by treatment with Anti-A antibodies (Figure S-2a, Supporting Information), Anti-B antibodies (Figure S-2b, Supporting Information), and Anti-D antibodies (Figure S-2c, Supporting Information). Both positive (Figure S-2, "P", Supporting Information) and negative (Figure S-2, "N", Supporting Information) assays were performed by, respectively, introducing antigen-positive and -negative RBCs in bar channels modified with different concentrations of NaAlg and the corresponding antibodies. As shown in Figure S-2, Supporting Information, all positive assays had shorter bar lengths than the negative reactions. Although antigen-positive and -negative blood samples could be distinguished among all

the NaAlg modified channels, the modification that led to the greatest difference was selected for more accurate identification. Therefore, 0.05% NaAlg was chosen for the final sensor design since the length difference was the greatest with this concentration (Figure 2).

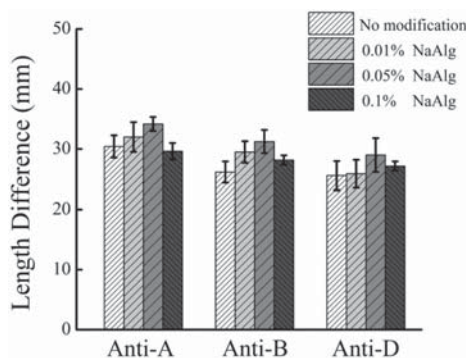


Figure 2. Eluting length difference in “A”, “B”, and “D” reaction bar channels modified with different concentrations of NaAlg. Bar channels based on untreated paper were used as controls (No modification by NaAlg). “A”, “B”, and “D” channels were, respectively, loaded with Anti-A, Anti-B, and Anti-D antibodies. The error bars represent the standard deviation of five tests.

Sensor Validation. The final paper-based blood typing device was designed under optimum conditions based on the above results. Figure 3 shows a photo of the actual tests of all

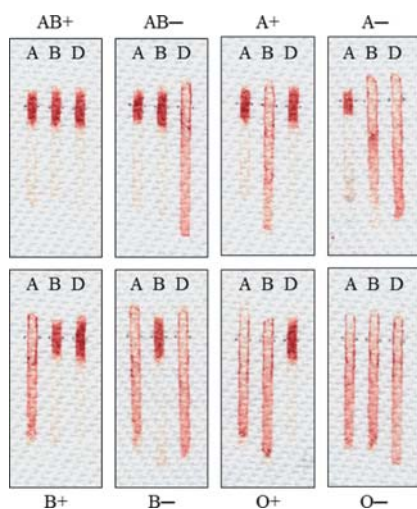


Figure 3. Actual assays of all eight ABO/RhD blood types by the optimized barcode-like paper-based blood typing device.

eight ABO/RhD blood types by our blood typing device. Figure 4 shows the average eluting lengths of positive and negative assays in A, B, and D channels. The measured bar lengths for the positive assays were: A, 9.9 ± 1.2 mm; B, 12 ± 1.6 mm; D, 13.4 ± 1 mm. By comparison, the bar lengths for the negative assays were: A, 42.6 ± 1.6 mm; B, 42.2 ± 1.3 mm; D, 42.5 ± 1.7 mm. The distinct length difference between positive and negative assays makes this device possible for easy result interpretation by smartphone-based analysis.

Smartphone-Based Analysis. To rapidly identify the eluting length information resulting from a blood type assay,

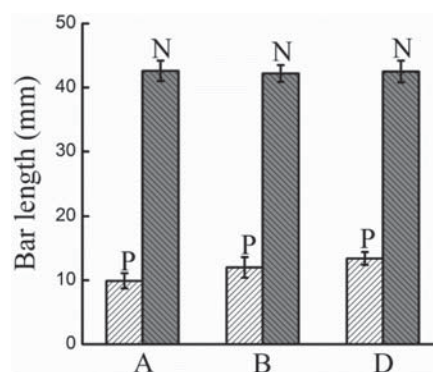


Figure 4. Average eluting lengths for positive (P) and negative (N) reactions in “A”, “B” and “D” channels.

smartphone-based analysis software (app) was developed. The basic principle of the identification process is as follows: If a short RBC eluting length appears in one channel, it will be encoded as “1” by the app; on the contrary, if a long eluting length occurs in the channel, it will be encoded as “0”. On the basis of this design, all eight blood types are encoded as “AB +”/“1 1 1”, “AB -”/“1 1 0”, “A +”/“1 0 1”, “A -”/“1 0 0”, “B +”/“0 1 1”, “B -”/“0 1 0”, “O +”/“0 0 1”, and “O -”/“0 0 0”. The code messages will be presented from the “A”, “B”, and then “D” channel for further interpretation. Therefore, for instance, when acquiring code message “1 1 0”, the app will interpret it as blood type “AB -”.

To quantitatively assess whether one channel message is “1” or “0”, references with eluting lengths of positive and negative assays of this channel will be required for comparison purposes. The app designed in this study has preloaded references which were obtained from statistical analyses based on a large amount of known blood samples; therefore, after acquiring the eluting lengths of the target blood assay, the app will compare the lengths with the references, transfer the length data to code messages, and then interpret the code messages into the corresponding blood type.

The basic statistical analysis principles used to obtain references are described as follows: (1) assume both the eluting length values of negative (L_n) and positive (L_p) reactions in one channel, respectively, follow normal distributions: $L_n \sim N_0(\mu_0, \sigma_0^2)$ with unknown mean μ_0 and unknown variance σ_0^2 and $L_p \sim N_1(\mu_1, \sigma_1^2)$ with unknown mean μ_1 and unknown variance σ_1^2 ; (2) on the basis of data measured from negative reactions (sample size is Q) in this channel, get the sample mean \bar{L}_n and sample standard deviation s_n . Since the true value of standard deviation σ_0 is unknown, the distribution of the sample mean \bar{L}_n follows the t distribution (t_n) with mean μ_0 and standard deviation ($s_n/(Q)^{1/2}$); (3) on the basis of data measured from positive reactions (sample size is Q) in this channel, get the sample mean \bar{L}_p and sample standard deviation s_p . Similarly, since the true value of standard deviation σ_1 is unknown, the distribution of the sample mean \bar{L}_p follows the t distribution (t_p) with mean μ_1 and standard deviation ($s_p/(Q)^{1/2}$); (4) two t distributions (t_n and t_p) obtained from step (2) and step (3) are taken as the references for testing whether the length value is “0” or “1”. For instance, two basic steps will be run by this app for determining the code message of the “A” channel: (1) Get the average value of eluting length in the “A” channel of target sample; (2) At a significance level of 0.01, if

the value only falls into the confidence intervals for the mean μ_0 based on t_n distribution of “A” channels, get message “0”; if the value merely falls into the confidence intervals for the mean μ_1 based on t_p distribution of “A” channels, get message “1”; if the value fall into the confidence intervals of both t_n and t_p distribution, the one whose sample mean value is closer to the tested value will be chosen; otherwise, do not report the result.

This app was tested on a Google Nexus 5 smartphone for identifying blood assays (Figure 5) in this study. The blood

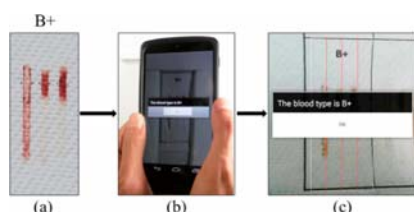


Figure 5. Testing results based on smartphone-based analysis. (a) Blood typing test result (B+) is shown in bar channels, (b) reading the result using the Android app, and (c) obtaining the blood result with text on the screen.

type of the target assays will be displayed and reported with text on the smartphone screen. For simple operation of this app, three scanning channels, which were indicated by three red solid lines, have been designed for, respectively, scanning “A”, “B”, and “D” channels. One simple instruction to operate this app is to use the camera of the smartphone to make sure the three indicating red lines of the app match with the “A”, “B”, and “D” bar reaction channels of the paper-based device. Figure 6 shows that the snapshots of all eight ABO/RhD blood group

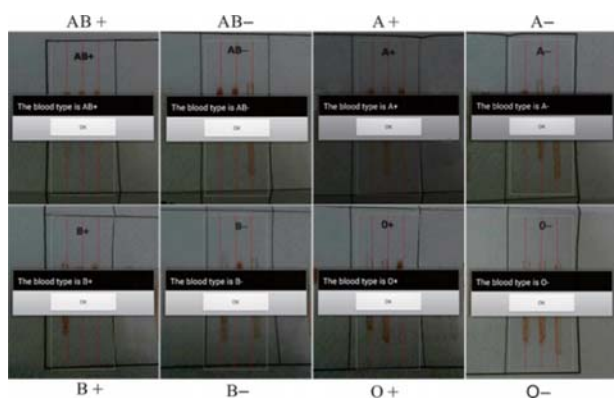


Figure 6. All eight ABO/RhD blood types were reported by the Android system-based smartphone app.

types were successfully text-reported by this Android app. This barcode-like design makes smartphone-based analysis easier and more reliable through reading the length information, which is less affected by environmental factors (such as light source, temperature, etc.) compared to other forms of signals such as colorimetric and electric.

Validation for Blood Typing. A total of 98 blood samples were assayed using this barcode-like blood typing device. All samples were also assayed in the pathological laboratory of Red Cross Australia using the mainstream blood typing technologies. These samples contain all the 8 blood types in the ABO

blood typing system. All results agree with those reported by the Red Cross Australia. All results are shown in Table S-2, Supporting Information.

CONCLUSIONS

In this study, a barcode reading concept has been applied for the first time in designing paper-based devices by adapting to smartphone-based technology. This sensor design has been used for the application of blood typing. Users can obtain all eight ABO/RhD blood types as text messages on the screen of the smartphone, without the need of further interpretation. The specific barcode-like design of the paper-based device makes smartphone-based analysis more reliable by reading the bar length information. In addition, by utilizing smartphone technology, test results from paper sensors can be automatically saved in e-form and transferred conveniently between users and professionals. It is expected that paper-based technology with smartphone diagnostics will be greatly expanded and applied as a diagnostic platform for medical and environmental applications.

ASSOCIATED CONTENT

Supporting Information

Additional figures and tables. This material is available free of charge via the Internet at <http://pubs.acs.org>.

AUTHOR INFORMATION

Corresponding Author

* [Redacted]

Notes

The authors declare no competing financial interest.

ACKNOWLEDGMENTS

This work is supported by Australian Research Council Grant (ARC DP1094179 and LP 110200973). Authors thank Haemokinesis for its support through the ARC Linkage Project and Mr. Hansen Shen for proof reading the manuscript. Postgraduate research scholarships from Monash University of Graduate Research and Faculty of Engineering are gratefully acknowledged.

REFERENCES

- (1) Fu, E.; Lutz, B.; Kauffman, P.; Yager, P. *Lab Chip* **2010**, *10*, 918–920.
- (2) Martinez, A. W.; Phillips, S. T.; Whitesides, G. M.; Carrilho, E. *Anal. Chem.* **2010**, *82*, 3–10.
- (3) Ali, M. M.; Aguirre, S. D.; Xu, Y.; Filipe, C. D. M.; Pelton, R.; Li, Y. *Chem. Commun.* **2009**, *43*, 6640–6642.
- (4) Tan, S. N.; Ge, L. Y.; Tan, H. Y.; Loke, W. K.; Gao, J. R.; Wang, W. *Anal. Chem.* **2012**, *84*, 10071–10076.
- (5) Tian, J. F.; Li, X.; Shen, W. *Lab Chip* **2011**, *11*, 2869–2875.
- (6) Carrilho, E.; Martinez, A. W.; Whitesides, G. M. *Anal. Chem.* **2009**, *81*, 7091–7095.
- (7) Li, X.; Tian, J. F.; Nguyen, T.; Shen, W. *Anal. Chem.* **2008**, *80*, 9131–9134.
- (8) Luckham, R. E.; Brennan, J. D. *Analyst* **2010**, *135*, 2028–2035.
- (9) Hossain, S. M. Z.; Brennan, J. D. *Anal. Chem.* **2011**, *83*, 8772–8778.
- (10) Noor, M. O.; Shahmuradyan, A.; Krull, U. J. *Anal. Chem.* **2013**, *85*, 7502–7511.
- (11) Wang, S. M.; Ge, L.; Song, X. R.; Yu, J. H.; Ge, S. G.; Huang, J. D.; Zeng, F. *Biosens. Bioelectron.* **2012**, *31*, 212–218.
- (12) Dungchai, W.; Chailapakul, O.; Henry, C. S. *Anal. Chem.* **2009**, *81*, 5821–5826.

- (13) Li, M. S.; Tian, J. F.; Al-Tamimi, M.; Shen, W. *Angew. Chem., Int. Ed.* **2012**, *51*, 5497–5501.
- (14) Tian, J. F.; Li, X.; Shen, W. *Lab Chip* **2011**, *11*, 2869–2875.
- (15) Zhang, Y.; Zhou, C.; Nie, J.; Le, S.; Qin, Q.; Liu, F.; Li, Y.; Li, J. *Anal. Chem.* **2014**, *86*, 2005–2012.
- (16) Li, X.; Tian, J. F.; Shen, W. *Cellulose* **2010**, *17*, 649–659.
- (17) Guan, L. Y.; Cao, R.; Tian, J. F.; McLiesh, H.; Garnier, G.; Shen, W. *Cellulose* **2014**, *21*, 717–727.
- (18) Tian, J. F.; Kannangara, D.; Li, X.; Shen, W. *Lab Chip* **2010**, *10*, 2258–2264.
- (19) Abbas, A.; Brimer, A.; Slocik, J. M.; Tian, L. M.; Naik, R. R.; Singamaneni, S. *Anal. Chem.* **2013**, *85*, 3977–3983.
- (20) Mabey, D.; Peeling, R. W.; Ustianowski, A.; Perkins, M. D. *Nat. Rev. Microbiol.* **2004**, *2*, 231–240.
- (21) Lutz, B.; Liang, T.; Fu, E.; Ramachandran, S.; Kauffman, P.; Yager, P. *Lab Chip* **2013**, *13*, 2840–2847.
- (22) Pelton, R. *Trends Anal. Chem.* **2009**, *28*, 925–942.
- (23) Delaney, J. L.; Doeven, E. H.; Harsant, A. J.; Hogan, C. F. *Anal. Chim. Acta* **2013**, *790*, 56–60.
- (24) Hong, J. I.; Chang, B. Y. *Lab Chip* **2014**, *14*, 1725–1732.
- (25) Zhu, H. Y.; Isikman, S. O.; Mudanyali, O.; Greenbaum, A.; Ozcan, A. *Lab Chip* **2013**, *13*, 4890–4890.
- (26) Daniels, G.; Bromilow, I. *Essential Guide to Blood Groups*; Blackwell: Hoboken, NJ, 2007.
- (27) Ballerini, D. R.; Li, X.; Shen, W. *Anal. Bioanal. Chem.* **2011**, *39*, 1869–1875.
- (28) Su, J. L.; Al-Tamimi, M.; Garnier, G. *Cellulose* **2012**, *19*, 1749–1758.
- (29) Li, L. Z.; Tian, J. F.; Ballerini, D.; Li, M. S.; Shen, W. *Analyst* **2013**, *138*, 4933–4940.
- (30) Li, X.; Tian, J. F.; Garnier, G.; Shen, W. *Colloids Surf., B* **2010**, *76*, 564–570.
- (31) Khan, M. S.; Thouas, G.; Shen, W.; Whyte, G.; Garnier, G. *Anal. Chem.* **2010**, *82*, 4158–4164.
- (32) Alkasir, R. S. J.; Ornatska, M.; Andreescu, S. *Anal. Chem.* **2012**, *84*, 9729–9737.

A study of the transport and immobilisation mechanisms of human red blood cells in a paper-based blood typing device using confocal microscopy†

Cite this: *Analyst*, 2013, **138**, 4933

Lizi Li, Junfei Tian, David Ballerini, Miaosi Li and Wei Shen*

Recent research on the use of bioactive paper for human blood typing has led to the discovery of a new method for identifying the haemagglutination of red blood cells (RBCs). When a blood sample is introduced onto paper treated with the grouping antibodies, RBCs undergo haemagglutination with the corresponding grouping antibodies, forming agglutinated cell aggregates in the paper. A subsequent washing of the paper with saline buffer could not remove these aggregates from the paper; this phenomenon provides a new method for rapid, visual identification of the antibody-specific haemagglutination reactions and thus the determination of the blood type. This study aims to understand the mechanism of RBC immobilization inside the paper which follows haemagglutination reactions. Confocal microscopy is used to observe the morphology of the free and agglutinated RBCs that are labelled with FITC. Chromatographic elution patterns of both agglutinated and non-agglutinated RBCs are studied to gain insight into the transport behaviour of free RBCs and agglutinated aggregates. This work provides new information about RBC haemagglutination inside the fibre network of paper on a microscopic level, which is important for the future design of paper-based blood typing devices with high sensitivity and assaying speed.

Received 22nd April 2013

Accepted 3rd June 2013

DOI: 10.1039/c3an00810j

www.rsc.org/analyst

Introduction

Accurate and rapid determination of human blood groups is imperative for many medical procedures such as blood transfusion and organ transplantation.¹ Blood groups are classified based on inherited differences (polymorphisms) in antigens on the surface of the red blood cells (erythrocytes). The International Society of Blood Transfusion (ISBT) recognises 328 different antigens and 30 major blood group systems, among which the ABO and Rhesus systems are of the greatest clinical importance.² Without ABO compatibility testing, around one third of unscreened blood transfusions would lead to potentially fatal haemolytic transfusion reactions. The RBC antigen D of the Rh system is considered to be the most common culprit, also causing haemolytic disease of the foetus and in newborns (HDFN).²

The majority of techniques for determining the ABO and Rh blood type are based on the principle of observing haemagglutination between RBC antigens and serum antibodies. Haemagglutination occurs when multi-armed antibodies bind to the particular binding sites on the antigens of RBCs, adhering cells together and leading to the formation of larger blood

lumps that cannot be stably suspended in the plasma. Currently, the most common assays used for the identification of blood groups include the slide test, tube test, micro plate and solid phase assays, as well as the column agglutination system.^{3–8} Recently, advanced blood typing assays based on gene sequencing of DNA^{9,10} and flow cytometry¹¹ have been reported. Blood typing assays that are currently used in hospitals and pathological laboratories are capable of sensitively and specifically identifying blood types; they are reliable and robust.¹² However, few point-of-care assays can be done without either dedicated laboratory instruments or the direct handling of the antibodies by the personnel who carry out the tests (such as the slide and tube tests).^{13,14} In addition, the equipment-based assays usually take a long time (10–30 min), and the costs are high.^{7,12} A disadvantage common to all blood typing assays is that it is difficult for non-professionals and lay-users to interpret the assay result, since currently available blood typing devices require users to have some knowledge of blood typing and an understanding of the device working principle. It follows that the availability of simple, rapid, cheap, and reliable methods for blood typing would be of significant benefit for point-of-care applications, such as bedside compatibility checks, fast blood typing in emergency scenarios, and in developing regions or remote locations where there may be no access to laboratory facilities.¹⁴

Paper is a material fabricated from cellulosic fibres, which are easy-accessible, recyclable, environment-friendly and of

Department of Chemical Engineering, Monash University, Wellington Rd, Clayton, Vic. 3800, Australia.

† Electronic supplementary information (ESI) available: Separated confocal signals of fibres and RBCs for Fig. 4. See DOI: 10.1039/c3an00810j

low-cost.¹⁵ The promising use of paper for environmental and diagnostic applications has been strongly highlighted.^{16–18} Recently, innovations in the use of bioactive paper to perform blood typing assays have been reported in the literature;^{14,19–21} these innovations are based on a new mechanism for identifying haemagglutination. Khan *et al.*¹⁹ found that agglutinated blood samples resulting from antibody-specific haemagglutination reactions transport differently in the porous structure of paper than stable blood samples with well dispersed red cells. They observed that agglutinated RBCs in paper could not be eluted chromatographically by the wicking of blood serum. This observation marked the discovery of a new blood typing method which relies on the visual identification of red cell transport behaviour in paper which led to a new concept for fabricating low-cost blood typing devices. Following work by Ballerini *et al.*²² showed that the same principle could be used to fabricate inexpensive thread-based blood typing devices.

Jarujamrus *et al.*²⁰ investigated the separation of the agglutinated RBCs from the blood serum phase in filter paper. They took a biochemical approach and analysed the amount of antibody that could be washed off from an antibody-treated filter paper. Their hypothesis was that a blood sample introduced onto a piece of antibody-treated paper could re-dissolve a fraction of antibody deposited and dried on the fibre surface. The re-dissolved antibody molecules could then engage in specific interactions with the RBCs, leading to haemagglutination within paper. Jarujamrus *et al.*²⁰ showed that between 34 and 42% of antibody molecules carried by the antibody-treated paper could be re-dissolved by saline solution or a blood sample. Al-Tamimi *et al.*¹⁴ reported a chromatographic elution technique for blood typing. Their results showed that agglutinated RBCs in paper were immobilised within the paper structure and could not be eluted by saline solution, while non-agglutinated RBCs could be eluted easily. Their results again showed that agglutinated RBC lumps inside the paper have drastically different transport behaviour from non-agglutinated RBCs (Fig. 1). Al-Tamimi *et al.*¹⁴ and Su *et al.*²³ have also

shown that the efficiency of chromatographic separation of agglutinated and non-agglutinated RBCs on paper could be increased by controlling the thickness and porosity of the paper.

More recently, Li *et al.*²¹ applied this difference in transport behaviour between agglutinated and non-agglutinated RBCs in paper to design the first text-reporting blood typing device. This design presented a new concept of adding grouping antibodies onto paper which had printed patterns of text and symbols (*i.e.* to dose anti-A into the printed text pattern “A”). If the RBCs of a blood sample undergo haemagglutination reaction due to anti-A in the text pattern “A”, agglutination of RBCs would occur inside the patterned “A” zone; the deep crimson red colour formed by the agglutinated RBCs could not be washed away by saline solution and the paper will report the blood type of this sample with a letter “A” formed by the colouring effect of the agglutinated RBCs. This design enables non-professional users who may not have the knowledge of blood typing to identify blood types; it is suitable for developing countries where trained medical professionals may not be always available. The text-reporting blood typing concept using bioactive paper has since been explored by the diagnostic industry as a new class of sensitive, rapid and user-friendly device.

In this study we focus on understanding the mechanism of haemagglutination-induced immobilization of RBCs in antibody-treated bioactive paper. Microscopic evidence will be sought to understand (a) the morphology of the non-agglutinated RBCs in the fibre network of paper, (b) the morphology, size and distribution of agglutinated RBC aggregates formed after haemagglutination in the fibre network and (c) the transport behaviour of individual RBCs and large agglutinated RBC lumps driven by the wicking saline solution in paper. Confocal microscopy is used to observe RBCs and agglutinated RBC lumps in the fibre network of paper. The results of this study revealed details of RBC agglutination inside the fibre network of paper with clarification on a cellular level. The immobilisation mechanism of the agglutinated RBC lumps inside the paper is established. Information obtained from this study will be used to guide future device designs, particularly the design of the paper structures suitable for the low-cost blood typing papers.

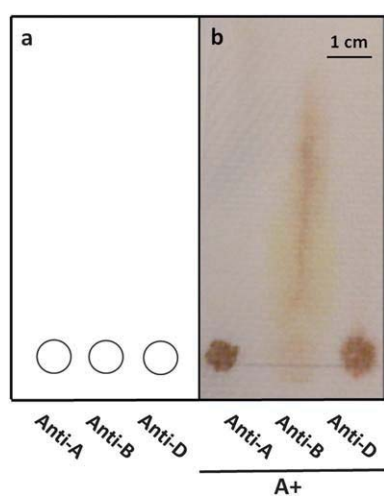


Fig. 1 An example of paper-based assay for rapid blood typing. (a) A schematic diagram of the anti-body treated paper. (b) An actual test result of blood A+.¹⁴

Experimental

Materials

Anti-coagulated blood samples were acquired from adult volunteers of known blood group by Dorevitch Pathology, Australia. All blood samples were stored in Vacutainer® tubes containing heparin, citrate and EDTA at 4 °C, and used within 5 days of collection. Epiclone™ anti-A, anti-B and anti-D monoclonal grouping reagents were sourced commercially from the Commonwealth Serum Laboratory, Australia. Anti-A and anti-B are transparent solutions, coloured cyan and yellow respectively, while anti-D is a clear colourless solution. Monoclonal grouping reagents were also kept at 4 °C. Kleenex paper towel with a basis weight of 34 g m⁻² and a thickness of 140 μm was purchased from Kimberly-Clark, Australia. Analytical grades of NaCl, KCl, Na₂HPO₄, and KH₂PO₄ were obtained from Sigma-Aldrich and used for preparation of physiological salt

solution (PSS) and phosphate-buffered physiological salt solution (PBS, pH 7.4). Fluorescein isothiocyanate (FITC, isomer I, product number: F7250) from Sigma-Aldrich was used for labelling RBCs. Anhydrous dimethyl sulphoxide (DMSO, from MERCK Chemicals Ltd, Australia) was employed to dissolve the FITC. Anhydrous D-glucose was provided by AJAX Chemicals Ltd., Australia. Microscope immersion oil was purchased from Sigma-Aldrich, Germany.

Methods

Red blood cells were labelled using the methods reported by Hauck *et al.*²⁴ and Hudetz *et al.*²⁵ Firstly, whole blood was centrifuged at 800 r min^{-1} for 10 minutes and the plasma layer was removed. The red cells collected from the bottom of the centrifuge tube were then washed with PSS and incubated in PBS with D-glucose (0.5 mg ml^{-1}) and FITC (0.4 mg ml^{-1}) for 3 hours. The labelled cells were then washed with PSS twice and re-suspended at a hematocrit of 45%. The testing papers were prepared by introducing $10\text{ }\mu\text{L}$ of antibody solution onto $10\text{ mm} \times 10\text{ mm}$ squares of Kleenex paper towel and allowing the antibody to penetrate and dry for 1 minute. In order to form the agglutinated blood lumps inside the paper sheet, $8\text{ }\mu\text{L}$ of labelled and re-suspended blood sample was pipetted onto the paper from the opposite side to which the antibody was introduced. Thirty seconds were given for the interaction between RBCs and the antibody within paper. After that, the sample was placed onto a glass slide for confocal imaging. The microscopic images were recorded from the side which the blood was introduced into. A Nikon Ai1Rsi Confocal Microscope in the facilities at the Melbourne Centre for Nanofabrication was used for generating the confocal micrographs. The objective lenses employed for imaging were $20\times$ dry lens and $60\times$ oil immersion lens. Images of red blood cells within the antibody-treated paper were captured as x-y images or a series of x-y images with stepped variation in the z-direction for construction of 3D images (or z-stack images). The resolution of all images was 1024×1024 pixels and the step width for the z-stack images was $0.125\text{--}0.250\text{ }\mu\text{m}$.

In order to gain a better understanding of the transport behaviour of agglutinated and non-agglutinated RBCs on paper, an experiment of chromatographic elution with PSS was performed. Briefly, $10\text{ }\mu\text{L}$ of antibody solution and $3\text{ }\mu\text{L}$ of blood sample were dropped on a glass slide and allowed to react for 30 seconds. The mixture of blood and antibody was then transferred from the glass slide onto a piece of Kleenex paper around 2 cm from the lower edge of the paper, and allowed to absorb completely for 1 minute. The Kleenex paper was then suspended in PSS in a chromatography tank about 1 cm from its lower edge to ensure the blood spot remained above the buffer surface and the saline solution was allowed to elute up through the paper by capillary wicking for 10 minutes. The paper was then allowed to dry at room temperature on a blotting paper for another 10 minutes and the elution patterns of RBCs were characterized by observing the presence of RBCs at different points away from the original blood sample spot with the confocal microscope.

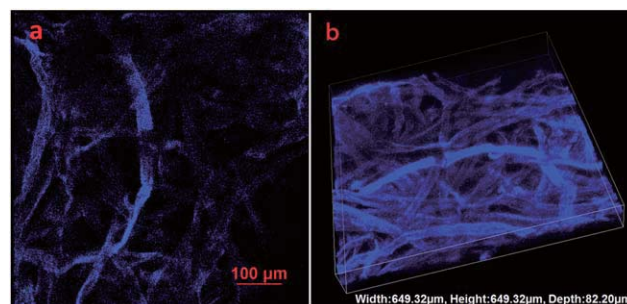


Fig. 2 2D (a) and 3D (b) confocal images of lignocellulosic fibers within paper captured by $20\times$ dry lens.

Results and discussion

Observation of red blood cells in paper by confocal microscopy

In this confocal microscopy study a 405 nm laser was used to observe the fibre network of the Kleenex paper. The excitation wavelength of this laser beam is able to generate fluorescent emission in the blue spectral region from lignocellulosic fibres of the Kleenex paper; the fluorescent emission enabled clear images of the fibre network in the paper to be generated at a satisfactory resolution. Fig. 2a shows a 2D image from a single confocal scan of the Kleenex paper sample. Fig. 2b shows a 3D reconstruction of a series of 2D scans from the same paper sample; all scans were obtained using a $20\times$ dry lens. These results clearly show that the distribution of fibres in the Kleenex paper is even but random. The width of the lignocellulosic fibres that form the Kleenex paper is around $20\text{ }\mu\text{m}$ to $30\text{ }\mu\text{m}$; the spaces between these fibres form the porous structure of paper.

Fig. 3a and b show the FITC-labelled RBCs in the Kleenex paper and on top of a glass slide, respectively. FITC is widely used to attach a fluorescent label to proteins *via* the amine group. The isothiocyanate group in FITC reacts with amino terminals and primary amines in proteins. Isomer I of FITC was used in this study; it has the thiocyanate group on the fourth carbon of the benzene ring. This isomer has been reported to be suitable for labelling red blood cells.^{24,25} Our results as shown in Fig. 3a and b are in good agreement with those reports. A

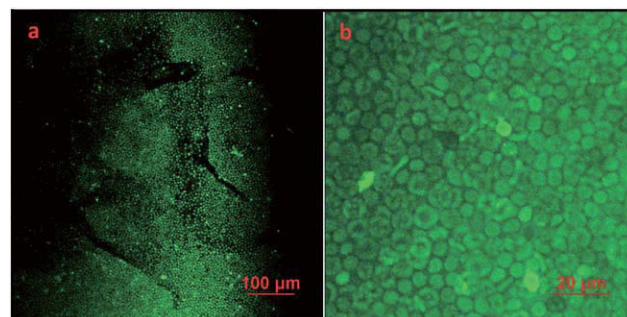


Fig. 3 Confocal images of RBCs labelled with FITC within paper (a) and on a slide glass (b) captured by $20\times$ dry lens.

fluorescent emission spectrum is generated from the FITC-labelled red blood cells with a 488 nm laser line by the multiline argon-ion laser of the Nikon Ai1Rsi Confocal Microscope; this excitation wavelength is close to the absorption peak of FITC. As a result, the distribution of FITC-labelled RBCs in the porous structure of the paper can be clearly imaged by confocal microscopy (Fig. 3, by 20 \times dry lens). Fortunately, the 488 nm laser line cannot excite fluorescent emission from the lignocellulosic fibres, therefore the fibre network of the paper appears as dark spaces as shown in Fig. 3a. Fig. 3b shows an enlarged confocal image of FITC-labelled RBCs observed using a 20 \times dry lens on a glass slide; it shows the morphology of RBCs after the FITC labelling. The RBCs retain the shape of centrally depressed disks, with diameters of 6–8 μm and a thickness of 2 μm . These figures demonstrate that FITC-labelling of the RBCs does not change the morphology of the RBCs and that confocal microscopy is a suitable technique for obtaining detailed, cellular level information of RBC behaviour in paper made of lignocellulosic fibres. It is expected that, by combining the blue fluorescent emission signal from the fibre with the green fluorescent signal from the FITC-labelled red blood cells, a full picture of the RBCs in paper can be obtained.

The activity of the red blood cell antigen after FITC labelling

The FITC labelling of the red blood cells does not have any noticeable effect on the activity of the RBC antigens on the surface of the red cells. This was confirmed by comparing the reactions of whole blood and FITC-labelled RBCs drawn from the same source with the corresponding antibodies on glass

slides (results are not shown). Under the same assaying conditions, FITC labelling does not cause discernible differences in the sizes of the agglutinated RBC aggregates nor in the time required for the RBCs to agglutinate after coming into contact with their corresponding antibodies.

Mechanisms of red blood cell immobilisation in antibody-treated paper

Fig. 4a and b show the two-dimensional confocal micrographs of RBCs of type O+ introduced into a paper sample treated with anti-A reagent acquired using a 20 \times dry lens and a 60 \times oil immersion lens respectively. These figures combine the signals from the lignocellulosic fibres in paper (blue) and the FITC-labelled RBCs (green), and provide a much clearer visual identification of positions of the RBCs within the fibre network. Since O+ red blood cells do not carry the A antigen, no haemagglutination is expected to occur. Results shown in Fig. 4a and b reveal that the O+ RBCs distribute rather uniformly in the spaces of the fibre network of the paper treated with anti-A. Fig. 4c shows a 3D confocal image of type O+ RBCs in paper treated with anti-A; it shows that red blood cells have penetrated through the fibre network and reached around the middle of the paper sheet. However, the RBCs remain free of any morphological change.

Fig. 4d and e show two examples of 2D confocal images of type O+ RBCs in anti-D treated papers acquired using 20 \times dry and 60 \times oil immersion lenses. Strong changes in both the RBC distributions in the fibre network and cell morphology show the occurrence of haemagglutination of type O+ RBCs with anti-D.

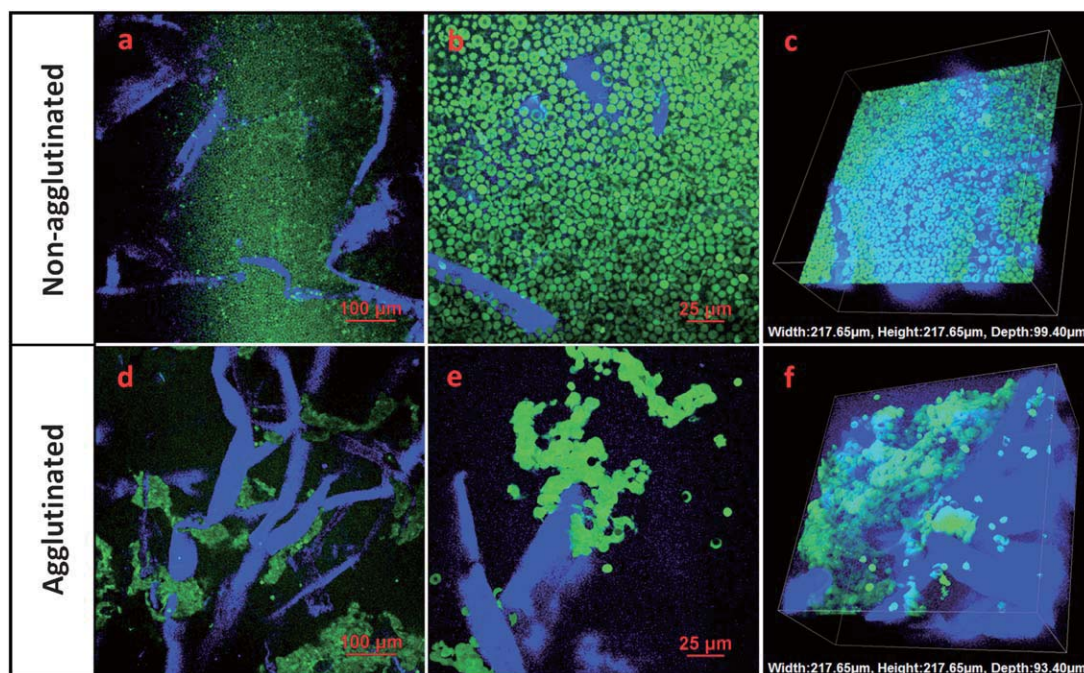


Fig. 4 Confocal images of non-agglutinated and agglutinated RBCs within paper. (a) 2D image of non-agglutinated RBCs captured by 20 \times dry lens. (b) 2D image of non-agglutinated RBCs captured by 60 \times oil lens. (c) 3D image of non-agglutinated RBCs captured by 60 \times oil lens; (d) 2D image of agglutinated RBCs captured by 20 \times dry lens. (e) 2D image of agglutinated RBCs captured by 60 \times oil lens. (f) 3D image of agglutinated RBCs captured by 60 \times oil lens. The separate (non-combined) images of paper and labelled RBCs can be found in the ESI.†

Several observations may be made regarding the mechanism of RBC haemagglutination inside paper. First, the sizes of agglutinated RBC lumps vary significantly. Most lumps contain hundreds of RBCs, while others contain only a few. The bonding of antibody molecules with the RBCs appears to be strong, since some RBCs appear to have lost their natural disk-like shape when they become agglutinated. However, haemagglutination of RBCs does not cause massive haemolysis of the cells; this is supported by the observation that although cells formed aggregates, the profiles of cells can still be identified.

Secondly, many RBCs have moved toward one another during haemagglutination to form large lumps. The movement of red cells freed large areas of the fibre surface from cell coverage (Fig. 4d and e). Fig. 4f also shows that there are a few single red blood cells that apparently adhere to the fibre surface. This raises the possibility that some individual red cells could undergo interactions directly with the antibody molecules adsorbed on the fibre surface and become immobilised there. While this possibility does exist, the fibre surface coverage by such individual cells is small; these adsorbed, individual cells make negligible visual contribution to the assay result. These observations support the conclusion of a previous study by Jarujamrus *et al.*,²⁰ who found that a significant fraction of antibody molecules introduced into an antibody-treated paper could be washed off from the fibre surface by saline solution or by the serum phase of a blood sample. Therefore the dominant mechanism of RBC agglutination inside an antibody-treated paper is through the haemagglutination caused by the released antibody molecules from the fibre surface.

Thirdly, the confocal results show that the major mechanism for the immobilisation of the agglutinated RBC lumps inside the fibre network is the strong adhesion of the lumps to the fibres and mechanical entrapment. Fig. 4d–f show that large agglutinated RBC lumps of the dimension similar to those of the interfibre pores were formed inside the paper and the entrapment and adhesion of those lumps occurred mostly at the gaps and pores between fibres. These factors make the chromatographic elution of the lumps practically impossible. The confocal results are in full agreement with the conclusion by Al-Tamimi *et al.*,¹⁴ they provide detailed microscopic evidence of the working mechanism of this new blood typing method using bioactive paper.

An application study of blood elution patterns in paper using the confocal method

One design of bioactive paper-based blood typing devices for identification of haemagglutination in paper is based on paper chromatography.¹⁴ Grouping antibodies (anti-A, anti-B and anti-D) are first spotted at 2 cm above the bottom edge of a piece of Kleenex paper, then a blood sample is introduced onto the grouping antibody spot; the spot containing antibody and the blood sample is referred to as the “antibody and blood sample zone”. The Kleenex paper is then dipped into a chromatographic tank, with the bottom edge slightly submerged into the saline solution. The saline solution penetrates through the interfibre pores of the paper towel, wicking across spots of

grouping antibodies and the blood samples within the spots. If haemagglutination occurs in the antibody spots, the agglutinated blood sample will not be eluted up by the rising saline solution. If haemagglutination does not occur, the blood sample will be eluted out of the grouping antibody spot, forming an elongated, visible chromatographic track of blood. The difference in the elution behaviours of the blood sample provides an easy and accurate method for the identification of the blood type.¹⁴

In practice, however, two elution bands may be observed. The first band can be observed close to the elution front of saline solution and the second band can be observed behind the first band. In some assays, these two bands could be observed simultaneously; in other assays only one could be observed. Fig. 5 shows a schematic description of this phenomenon. Confocal microscopy was used to investigate the two bands to gain an understanding of this phenomenon.

In this study, FITC-labelled RBCs were used to perform the chromatographic elution blood typing assays. The FITC-labelled RBCs were first mixed with each of the grouping antibodies on separate glass slides to ensure complete reaction; the mixture of blood and antibody reagent was then spotted onto the Kleenex paper and chromatographic elution was begun. This procedure was adopted in this investigation because the two bands could be reproducibly observed in all assays. The chromatographic elution patterns of the A+ blood sample with anti-A, anti-B and anti-D, as well as the patterns of the B+ blood sample with the three antibodies, are presented in Fig. 6. In all negative assays two bands can be observed simultaneously, whereas in all positive assays only the first band can be observed.

For confocal microscopy investigation, samples of blood of type A+ and B+ reacting with anti-B reagent were adopted to represent non-agglutinated and agglutinated groups for chromatographic elution experiments by saline solution. The confocal image taken from the antibody and blood sample zone

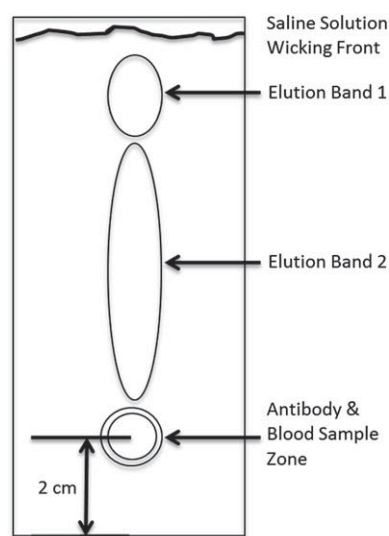


Fig. 5 A schematic diagram of the observed elution bands of RBCs on antibody-treated paper.

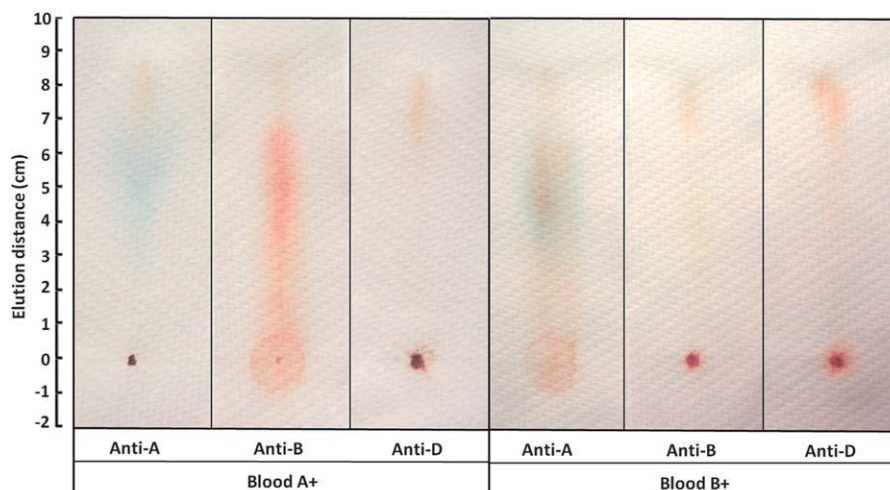


Fig. 6 Chromatographic elution patterns of A+ and B+ blood samples reacting with grouping antibodies anti-A, anti-B, and anti-D.

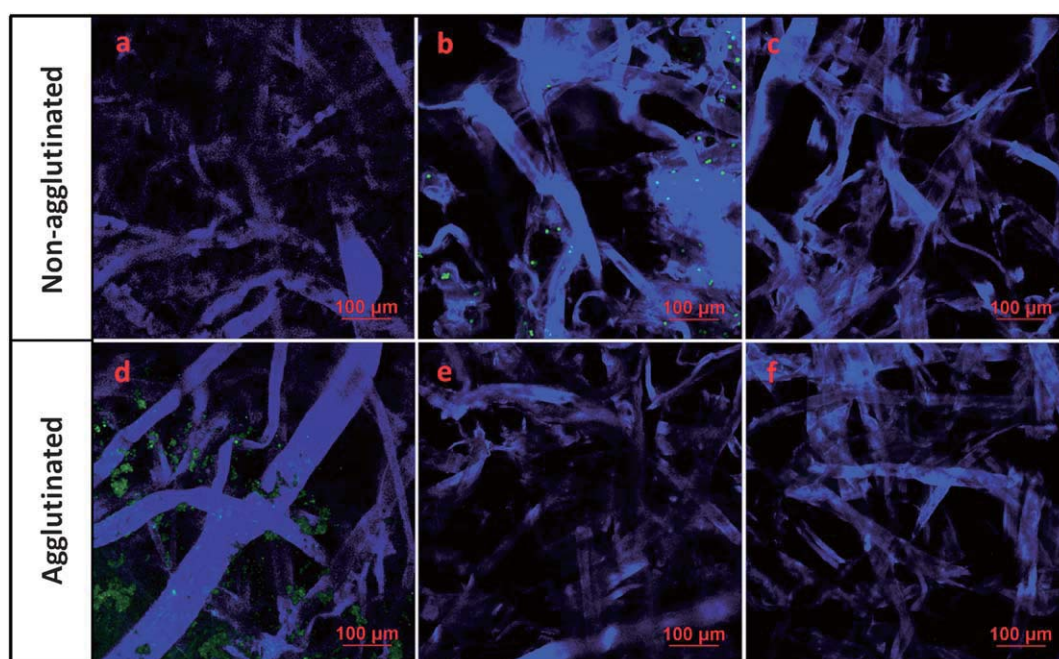


Fig. 7 Confocal images of chromatographic elution patterns of non-agglutinated RBCs at an elution distance of 0 cm (a), 5 cm (b), and 8 cm (c) and agglutinated RBCs at an elution distance of 0 cm (d), 5 cm (e) and 8 cm (f).

of the positive assay is shown in Fig. 7d. Large lumps of agglutinated red blood cells are observed inside pores surrounded by fibres; this observation is consistent with the findings in Fig. 4. Another confocal image taken from the second band of the negative assay shows sparsely populated single red cells and small clusters formed by a few red cells on the fibre surface (Fig. 7b). This band therefore consists of the eluted, non-agglutinated RBCs. Further confocal images taken from the position of the second band of a positive assay failed to identify any RBCs (Fig. 7e). This is because most of the RBCs have been agglutinated in the spotting point in the antibody and blood sample zone; only a very small number of free RBCs are

available in this zone for chromatographic elution. Therefore it is very difficult to find free RBCs from the position of the second band. The confocal result is in good agreement with the elution pattern of positive assays observed in Fig. 6.

Confocal images of the first bands of all negative and positive assays did not show any cells, despite Fig. 6 showing that the first bands of all assays have a weak blood colour. An explanation is that the first band is the elution band of haemoglobin from the internal fluid of ruptured RBCs; this band has the deep red colour of blood but not due to the presence of non-ruptured RBCs. To support this explanation, chromatographic elution of two haemolysed blood samples of type A+ and

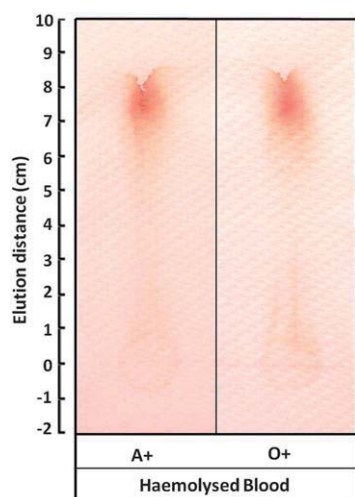


Fig. 8 Chromatographic elution patterns of haemolysed blood samples of A+ and O+.

O+ was conducted under the same conditions. The haemolysed blood samples were obtained by mixing 3 μL of blood and 10 μL of distilled water for 5 minutes. The activity of haemolysed blood samples was evaluated by adding their corresponding grouping antibodies. The absence of haemagglutination reactions proved that the haemolysis of the RBCs had occurred. The chromatographic elution patterns of haemolysed blood samples of type A+ and O+ are shown in Fig. 8. The presence of only the first band confirms that it is indeed caused by the haemoglobin released after haemolysis of RBCs.

In this application study, the confocal microscopy method was used to investigate the two chromatographic elution bands and the spotting zone of blood typing assays on paper for the details of their composition. Confocal micrographs reveal that the rupture of RBCs occurred in the spotting zone. Haemoglobin released by the ruptured cells was eluted by the saline solution faster than the free RBCs and small cell clusters resulting in the first band close to the elution front, while free RBCs form the second elution band.

Conclusions

A confocal microscopy method was developed to study the mechanism of the agglutination of RBCs in a paper-based blood typing device. This work shows that confocal microscopy is a suitable technique for providing the details of RBC agglutination at the cellular level inside the fibre network of paper. Human RBCs can be labelled with FITC without the antigens on the surface of the red cells losing their activity. Two laser beams of differing wavelength were used to excite fluorescent signals with two different emission wavelengths in lignocellulosic fibres and FITC-labelled red cells. These confocal signals were collected by different channels and converted into 2D and 3D confocal images for investigation of the fibre network, RBCs, and the different distributions of free RBCs and agglutinated blood lumps inside the fibre network. The non-agglutinated RBCs do not undergo morphological change, distributing rather

uniformly in the spaces of the fibre network and staying around the middle of the paper sheet. On the other hand, the agglutinated RBCs are deformed, forming blood aggregates immobilised randomly at different positions on the fibre surface.

A Kleenex paper towel was used as the substrate to prepare the paper-based blood typing device. The size of the interfibre pores of the Kleenex paper was shown by confocal micrographs to be much larger than the RBCs; the RBCs can thus be eluted by saline solution either vertically or laterally through the interfibre pores. RBCs undergo haemagglutination inside paper that was treated with the corresponding antibody. It has been confirmed by the confocal study that the release of antibody molecules from the fibre surface by dissolution is the main mechanism that causes haemagglutination. Haemagglutination of RBCs in the fibre network results in the formation of large lumps of aggregated cells, which become immobilised by mechanical entrapment within the interfibre pores. These aggregates could not be eluted by saline solution and thus result in the visual effect of the blood colouring becoming fixed on the paper. The non-agglutinated RBCs can be eluted by saline solution, therefore leaving no colour on paper after elution.

The confocal method was used to understand the chromatographic bands formed when blood samples are eluted in paper. This confocal method will be a powerful tool for understanding antibody and RBC interaction and for designing more sensitive bioactive paper-based blood typing devices in the future.

Acknowledgements

This work is supported by Australian Research Council Grants (ARC DP1094179 and LP110200973). Authors thank Haemokinosis for its support through an ARC Linkage Project. Authors also thank staff of MCN for Confocal training and usage and Dr M. Al-Tamini of the Department of Chemical Engineering for information on red cell tagging. Ms Lizi Li, Ms Miaosi Li and Mr David Ballerini acknowledge the Monash University Research and Graduate School and the Faculty of Engineering for post-graduate research scholarships.

Notes and references

- 1 G. Daniels and M. E. Reid, *Transfusion*, 2010, **50**, 281–289.
- 2 G. Daniels and I. Bromilow, *Essential Guide to Blood Groups*, Wiley-Blackwell, Chichester, West Sussex, UK, 2010.
- 3 D. Pramanik, *Principles of Physiology*, Academic Publishers, Kolkata, India, 2010.
- 4 B. H. Estridge, A. P. Reynolds and N. J. Walters, *Basic Medical Laboratory Techniques*, Cengage Learning, Albany, NY, USA, 2000.
- 5 F. Llopis, F. Carbonell-Uberos, M. C. Montero, S. Bonanad, M. D. Planelles, I. Plasencia, C. Riola, T. Planells, C. Carrillo and A. De Miguel, *Vox Sang.*, 1999, **77**, 143–148.
- 6 J. H. Spindler, H. Kluter and M. Kerowgan, *Transfusion*, 2001, **41**, 627–632.
- 7 Y. Lapierre, D. Rigal, J. Adam, D. Josef, F. Meyer, S. Greber and C. Drot, *Transfusion*, 1990, **30**, 109–113.

- 8 M. M. Langston, J. L. Procter, K. M. Cipolone and D. F. Stroncek, *Transfusion*, 1999, **39**, 300–305.
- 9 D. J. Anstee, *Blood*, 2009, **114**, 248–256.
- 10 J. Petrik, *Vox Sang.*, 2001, **80**, 1–11.
- 11 J. D. Roback, S. Barclay and C. D. Hillyer, *Transfusion*, 2003, **43**, 918–927.
- 12 D. Harmening, *Modern blood banking and transfusion practices*, F.A. Davis, Philadelphia, PA, 1999.
- 13 F. Giebel, S. M. Picker and B. S. Gathof, *Transfus. Med. Hemother.*, 2008, **35**, 33–36.
- 14 M. Al-Tamimi, W. Shen, R. Zeineddine, H. Tran and G. Garnier, *Anal. Chem.*, 2012, **84**, 1661–1668.
- 15 L. Neimo, *Papermaking Chemistry*, Fapet Oy, Helsinki, Finland, 1999.
- 16 X. Li, J. Tian, T. Nguyen and W. Shen, *Anal. Chem.*, 2008, **80**, 9131–9134.
- 17 X. Li, J. Tian, G. Garnier and W. Shen, *Colloids Surf., B*, 2010, **76**, 564–570.
- 18 Z. H. Nie, F. Deiss, X. Y. Liu, O. Akbulut and G. M. Whitesides, *Lab Chip*, 2010, **10**, 3163–3169.
- 19 M. S. Khan, G. Thouas, W. Shen, G. Whyte and G. Garnier, *Anal. Chem.*, 2010, **82**, 4158–4164.
- 20 P. Jarujamrus, J. Tian, X. Li, A. Siripinyanond, J. Shiowatana and W. Shen, *Analyst*, 2012, **137**, 2205–2210.
- 21 M. S. Li, J. F. Tian, M. Al-Tamimi and W. Shen, *Angew. Chem., Int. Ed.*, 2012, **51**, 5497–5501.
- 22 D. R. Ballerini, X. Li and W. Shen, *Anal. Bioanal. Chem.*, 2011, **399**, 1869–1875.
- 23 J. L. Su, M. Al-Tamimi and G. Garnier, *Cellulose*, 2012, **19**, 1749–1758.
- 24 E. F. Hauck, S. Apostel, J. F. Hoffmann, A. Heimann and O. Kempfski, *J. Cereb. Blood Flow Metab.*, 2004, **24**, 383–391.
- 25 A. G. Hudetz, G. Feher, C. G. M. Weigle, D. E. Knuese and J. P. Kampine, *Am. J. Physiol.: Heart Circ. Physiol.*, 1995, **268**, H2202–H2210.

Strategy To Enhance the Wettability of Bioactive Paper-Based Sensors

Junfei Tian,[†] Purim Jarujamrus,[‡] Lizi Li,[†] Miaosi Li,[†] and Wei Shen^{*,†}

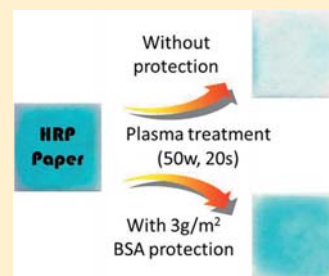
[†]Department of Chemical Engineering, Monash University, Wellington Road, Clayton, Vic. 3800, Australia

[‡]Department of Chemistry and Center for Innovation in Chemistry, Faculty of Science, Mahidol University, Rama VI Road, Bangkok 10400

Supporting Information

ABSTRACT: This paper reports a potential method that can restore the wettability of bioactive paper-based sensors while maintaining their bioactivity. This study is driven by the need to increase the wettability of the antibody-loaded blood typing paper devices in order to increase the blood typing assaying speed using such paper devices. Plasma treatment is used to improve the wettability of bioactive paper; the protective effect of bovine serum albumin (BSA) to biomolecules against plasma deactivation is investigated. In the first stage, horseradish peroxidase (HRP) was used as a model biomolecule, because of the convenience of its quantifiable colorimetric reaction with a substrate. By using this protection approach, the inactivation of biomolecules on paper during the plasma treatment is significantly slowed down. This approach enables plasma treatment to be used for fabricating paper-based bioactive sensors to achieve strong wettability for rapid penetration of liquid samples or reagents. Finally, we demonstrate the use of plasma treatment to increase the wettability of antibody treated blood typing paper. After the treatment, the blood typing paper becomes highly wettable; it allows much faster penetration of blood samples into the plasma treated testing paper. Antibodies on the paper are still sufficiently active for blood typing and can report patients' blood type accurately.

KEYWORDS: paper-based, bioactivity, wettability, low-cost diagnostics, blood typing, plasma treatment



INTRODUCTION

The recent rapid advancement in bioactive paper-based diagnostics has shown enormous promise of this new platform technology in improving human health in the developing world.^{1–5} Some novel proof of concept studies focusing on specific diagnostic assays and methods of assay result transmissions have demonstrated that paper-based diagnostics have superior application potentials to many currently available technologies in obtaining rapid diagnoses under the unsupported field conditions.^{2,4,6} Major research and development groups in this field have estimated that real applications of bioactive paper diagnostics are getting closer to becoming reality, although there are still hurdles to overcome.^{7–9}

Among the engineering considerations of an up-scaled production of bioactive paper devices, a top priority is to retain all the required properties of the substrate and biomolecular materials in a fabrication process so that the performances of the fabricated devices are at their optimum. For most bioactive paper-based devices, paper wettability and paper bioactivity are two of the most important properties, which determine the performance of the devices. In the fabrication of some devices, it was found that the introduction of bioactive reagents can significantly reduce the wettability of bioactive paper, seriously compromising the performance of the device in a diagnostic test.

An example from our recent experience is the bioactive paper device for blood typing.^{6,10,11} The working principle of a paper-based blood typing device relies on the introduction of blood

typing antibodies into the paper first. Penetration of antibody solution into the pores of the paper results in deposition of antibody molecules and an additive, such as BSA, on the fiber surface. The so-formed bioactive blood typing paper is expected to function when a blood sample is added onto the paper. First, the blood will redissolve the deposited antibody from the fiber surface into the blood serum. The dissolved antibody will be able to interact with the antigens on the surface of the red blood cells (RBCs). The antibody-RBC interaction may either cause agglutination of the red cells or have no effect on them. With the aid of saline washing, the agglutination or non-agglutination of RBCs will be revealed.^{6,10,11}

This simple design has confronted an unexpected problem of reduced wettability of the antibody loaded paper by the blood sample when antibodies from commercial sources are used.¹⁰ Figure 1 shows the degree of poor wetting of the antibody-loaded paper compared with paper without antibody. The poor wettability of the paper significantly reduces the speed of liquid penetration. An easy and upscalable solution for restoring the wettability of the paper could be by plasma treatment. In a plasma environment, energetic electrons, ions, and radical species impinge on the surface, leading to physical and chemical changes of the surface in three main ways: 1) Etching. Plasma treatment is used to remove materials from solid surfaces. 2)

Received: August 18, 2012

Accepted: November 14, 2012

Published: November 14, 2012

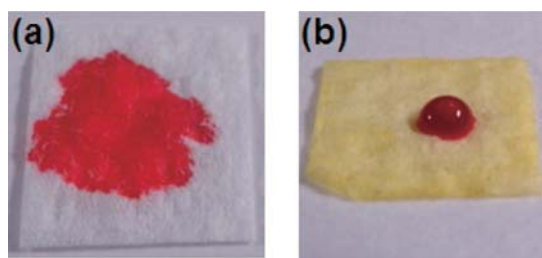


Figure 1. (a) 4 μ L of blood penetrates into untreated paper and (b) 4 μ L of blood stands on an antibody treated paper.

Activation. It is used to chemically and/or physically modify the surfaces so that the modified surfaces carry active species. 3) Coating. It is used to deposit a thin film of material on solid surfaces.¹² Martinez et al. and Abo et al. respectively demonstrated the use of plasma treatment as a step of μ PADs fabrication to increase channel wettability.^{1,13} Li et al. and Tian et al. also used plasma treatment to increase the wettability of the thread-based microfluidic device and V-groove microfluidic device on polymer film by removing the contaminant deposits on the surface.^{14,15} In another study by Li et al., plasma treatment has been utilized as a patterning method to selectively etch hydrophilic patterns onto a piece of hydrophobic filter paper to create the μ PADs.³ After plasma treatment, the sample delivery channels and detection areas of these devices become highly wettable. Aqueous solution of biomolecules and detection reagents can be easily loaded into the paper by absorption, to form a complete sensor.

While plasma treatment is an easy and matured technology for surface treatment to increase materials' wettability, it can significantly reduce the activity of biomolecules.^{16–18} Plasma treatment has been widely used as a method for biodecontamination.^{17,19,20} Von Keudell showed that plasma treatment can efficiently inactivate a range of biocontaminants including micro-organisms, bacteria and proteins, etc.¹⁶ Plasma treatment allows energetic particles to destroy or modify surface chemical bonding of materials, causing a variety of proteins to denature.

In our bioactive paper studies, however, we found that plasma treatment imposes a much weaker destructive effect on blood typing antibodies than expected. Blood typing antibodies do not lose their functions in blood typing assays. This surprising observation was found to be reproducible. One possible reason for this observation is the presence of certain protection additives in the antibody reagent. Based on the supplier's specification, the antibodies contain 1–5% BSA as a protection additive. There are reported bioactivity protection methods in the literature, but most of these methods focus on the protection of the activity and stability of proteins and enzymes from the inhibition induced by temperature, soluble additives, and even radiation.^{21–24} In those methods, BSA is a widely used stabilizer that prevents the thermally induced inactivation of biomolecules. Moreover, BSA has also been reported to have a protection effect on enzyme activity from the inhibition caused by a toxicant. Our hypothesis is that BSA may contribute to the protection for antibody during the plasma treatment. If the destructive effect of plasma to biomolecules can be reduced through a simple method, then plasma treatment can be used to improve the wettability of bioactive papers; it will greatly improve the fabrication of low-cost sensors.

In this paper, we used horseradish peroxidase (HRP) as a model biomolecule to demonstrate the influence of plasma treatment to the activity of biomolecules on paper. The choice of HRP is based on the fact that its activity can be visually shown by using a suitable liquid substrate; HRP therefore provides an easy way to assess the activity loss of the biomolecule. We compared the activity of HRP paper loaded with a range of concentrations of HRP solutions before and after plasma treatment. The effect caused by plasma with increasing treatment time on the activity of HRP paper loaded with a given concentration of HRP solution was also studied. An effective strategy that can protect the biomolecules on paper from being deactivated by plasma treatment was investigated. This strategy offers a significant flexibility to the fabrication of bioactive paper based sensors; this flexibility allows the enhancement of the device's wettability and the addition of bioactivity to the paper to be performed in any desired sequence, effectively reducing practical fabrication constraints in device production.

EXPERIMENTAL SECTION

Materials and Equipment. Horseradish peroxidase (HRP) (Type I, lyophilized powder, 100 KU) was obtained from Sigma-Aldrich. HRP powder was dissolved in phosphate-buffered saline (PBS, pH 7.4) to make stock solution (1 mg/mL). A liquid substrate system of HRP, 3,3',5,5'-tetramethylbenzidine (TMB), was obtained from Sigma-Aldrich and used for HRP activity analysis. The activity of enzymatic paper containing HRP molecules can be calorimetrically assessed by using TMB substrate. After applying the liquid substrate to an HRP loaded enzymatic paper, the enzyme-catalyzed reaction will occur. The intensity of the blue color developed through this reaction reflects the activity of HRP in paper. The blue color of the reacted substrate was then scanned into a computer, and the activity of HRP was quantitatively analyzed using computer software.

Commercial antibody solutions of red blood cell antigens A, B, and D (Epiclone Anti-A, Anti-B, and Anti-D monoclonal grouping reagents) were obtained from CSL, Australia. Anti-A and Anti-B are color-coded blue and yellow solutions, respectively, whereas Anti-D is a clear solution. These antibodies are made of immunoglobulin M (IgM). Normal saline (0.85 g NaCl in 100 mL of deionized water (18.2 M Ω cm⁻¹)) was used as diluent and washing solution in this study. Blood samples were collected from 3 adult volunteers; the samples were kept in standard plastic vials containing lithium heparin anticoagulant. Antibody solutions and blood samples were stored at 4 $^{\circ}$ C, and blood samples were used within 5 days.

Filter papers (Whatman grade 4) were cut into 1 cm \times 1 cm squares for fabricating HRP and HRP-BSA paper. A Kleenex paper towel was cut into 5 mm \times 5 mm squares which were used as the base substrate for making the blood typing device, while standard blotting papers (drink coaster blotting, 280 g/m²) were used to remove excess liquids during device preparation.

K1050X plasma asher (Quorum Emitech, U.K.) was used for plasma treatment. The vacuum level for the treatment was 6 \times 10⁻¹ mbar. The paper samples were always placed in the center of the chamber during the treatment for a consistent effect of treatment.

Test of Activity of HRP Paper without Plasma Treatment. HRP stock solution was diluted with to get serially diluted HRP standard solutions with the concentrations of 0, 1, 2, 3, and 4 μ g/mL. About 10 mL of HRP solution in a plastic Petri dish (I.D. = 8.5 cm) was used for soaking paper. Five filter paper squares were respectively soaked in each diluted HRP solution for 2 s. The wet paper squares were not blotted. They were put onto a piece of plastic film and dried in a fume hood for 20 min. After drying, each paper square received an addition of 15 μ L of TMB liquid substrate solution. These paper squares carrying TMB were then placed into a dark box for 2 min to develop color changes of the substrate on paper. Color intensity of scans of the filter paper squares was measured using Adobe Photoshop

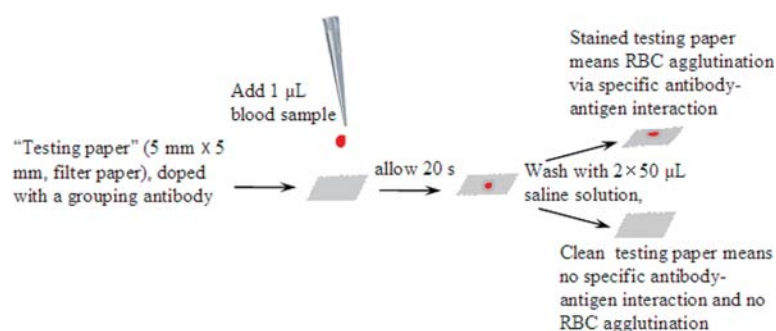


Figure 2. A schematic diagram showing blood typing test protocol using paper and result interpretation.

CS software; the calibration curve was then obtained. Error bars (relative standard deviation) were obtained from five repeats of the whole experiment.

Test of Activity of HRP-BSA Paper without Plasma Treatment. Seven filter paper squares (1 cm × 1 cm) were soaked in diluted HRP solution (4 µg/mL) and dried in a fume hood for 20 min. Then, 15 µL of BSA solution with the concentrations of 0.1%, 0.2%, 0.5%, 1%, 2%, 3%, and 4% (w/v) were deposited onto each square, respectively. After drying in the fume hood for 20 min, 15 µL of TMB liquid substrate solution was added onto each of the filter paper squares. These filter paper squares were then incubated for 2 min to allow the color development. Finally, the filter paper squares were scanned to get clear images. Error bars (relative standard deviation) were obtained from five repeats of the whole experiment.

Test of Activity of HRP Paper after Plasma Treatment. *Paper Loaded with Different Concentrations of HRP Solution Treated with Plasma for a Fixed Treatment Time.* HRP stock solution was diluted to standard solutions with the concentrations of 0, 1, 2, 3, and 4 µg/mL. Five filter paper squares (1 cm × 1 cm) were soaked in each diluted HRP solution and dried in a fume hood for 20 min. Then, the paper squares were plasma treated (50 W) for 60 s. Plasma treatment was activated in vacuum, with a background air pressure of 6×10^{-1} mbar. TMB liquid substrate was added to the paper squares following the same procedure used in the previous section.

Paper Loaded with a Known Fixed Concentration of HRP Solution Treated with Plasma for Different Times. Six filter paper squares (1 cm × 1 cm) were soaked in diluted HRP solution (4 µg/mL) and dried in a fume hood for 20 min. Then, the paper squares were plasma treated (50 W) for 0, 5, 10, 20, 40, and 60 s, respectively. TMB liquid substrate was added to the paper squares following the same procedure used in the previous section.

Test of Activity of HRP-BSA Paper with Plasma Treatment. *Paper Loaded with a Fixed Concentration of HRP Solution and BSA Solution Treated with Plasma for a Fixed Treatment Time.* Ten filter paper squares (1 cm × 1 cm) were soaked in diluted HRP solution (4 µg/mL) and dried in a fume hood for 20 min. Then, 15 µL of BSA solution with the concentration of 2% (w/v) was deposited onto these squares. After drying in the fume hood for 20 min, the paper squares were plasma treated (50 W) for 0, 5, 10, 20, 40, 60, 80, 100, 200, and 300 s, respectively. TMB liquid substrate was added to the paper squares following the same procedure used in the previous section.

Paper Loaded with a Fixed Concentration of HRP Solution and Different Concentrations of BSA Solution Treated with Plasma for a Fixed Treatment Time. Seven filter paper squares (1 cm × 1 cm) were soaked in diluted HRP solution (4 µg/mL) and dried in a fume hood for 20 min. Then, 15 µL of BSA solution with the concentration of 0.1%, 0.2%, 0.5%, 1%, 2%, 3%, and 4% (w/v) were deposited onto each paper square, respectively. After drying in the fume hood for 20 min, the paper squares were plasma treated (50 W) for 20 s. TMB liquid substrate was added to the paper squares following the same procedure used in the previous section.

Quantification of the Activity of Bioactive Paper from Scanned Images. After each test, the colored paper squares were imaged with a desktop scanner (Epson Perfection 2450, color photo setting), then imported into Adobe Photoshop software, and

converted into CMYK mode. The mean cyan intensity was obtained using the histogram function. This is because the cyan channel can provide a larger dynamic range than other channels and further increases the accuracy of the analysis of the developed color on the paper squares. The ultimate mean intensity value was generated by subtracting the measured average intensity of the colored paper squares from the mean intensity of the blank control.

Blood Typing by Using Plasma Treated Testing Paper. A 5 mm × 5 mm Kleenex paper square was cut and treated by doping it with 3.5 µL of undiluted (1×) commercial grouping antibody agent and allowed to dry in a fume hood for 10 min. This Kleenex paper square was then treated in a vacuum plasma reactor for 1 min, at an intensity of 50 W. The vacuum level for the treatment was 6×10^{-1} mbar. A further 3.5 µL of undiluted (1×) commercial grouping antibody agent was then introduced to the paper square (double dope). The plasma treatment was then repeated once again. The antibody-treated papers (with 2 × plasma treatments) are referred to as the “testing papers” and are shown as the white squares in Figure 2. The testing papers treated with Anti-A, Anti-B, and Anti-D are specifically referred to as “paper A”, “paper B”, and “paper D”, respectively.

A one-microliter blood sample was introduced onto the antibody treated testing paper (Figure 2). Most of the sample was absorbed by the testing paper. The nonabsorbed blood sample passed through the testing paper and was absorbed by blotting paper. Twenty seconds was given to allow interactions of RBCs with the antibody in paper. After that, the testing paper was placed onto another blotting paper. Two aliquots of 50 µL saline solution aliquot saline solution were gradually introduced by a micropipet onto the blood sample-loaded testing paper; the saline solution penetrated through the testing paper and was absorbed by the blotting paper underneath the testing paper. The testing paper was then separated from the blotting paper for visual inspection. Visible blood stain on the testing paper indicates that RBC agglutination occurred and the test is positive. On the other hand, if no blood stain is observable on the testing paper, RBC agglutination did not occur, and the test is negative. Following this principle an ideal testing-result-matrix is presented in Figure S1.

RESULTS AND DISCUSSION

Effect Plasma Treatment of HRP Activity. Proteins, including enzymes, can be denatured when they are exposed to extreme conditions such as high temperature, mechanical forces, radiation, plasma treatment, chemicals, and many transition metal ions. Figures 3 (a) and 3 (b) clearly show that plasma treatment has the effect of deactivating the HRP paper. Since the TMB solution was added onto HRP paper, the blue color was developed resulting from the enzyme–substrate reaction (Figure 3 (a)). The HRP activity is indicated by the intensity of the blue color. Figure 3 (c) shows the activity of HRP paper treated with a series of concentrations of HRP solution. However, after 60 s plasma treatment (50 W), the blue color intensity was greatly reduced indicating a significant

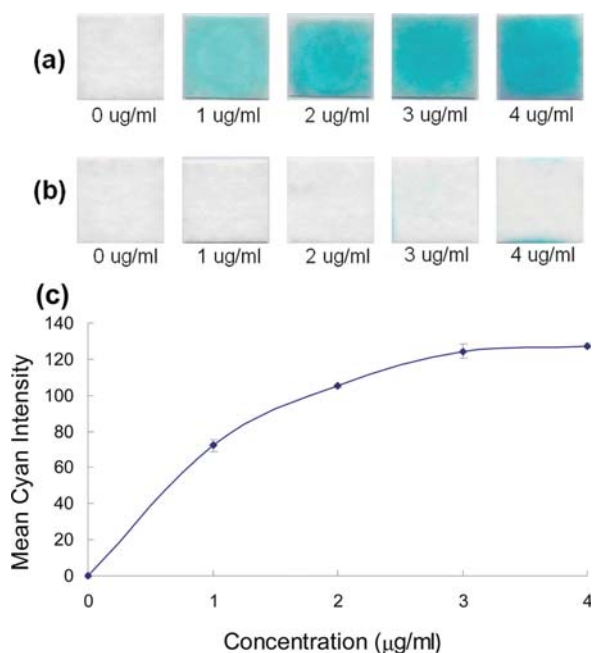


Figure 3. The comparison of the activities of a series of HRP paper squares (a) without plasma treatment and (b) with plasma treatment (50 W, 60 s); (c) measured mean cyan intensity of catalytic product on HRP paper. (a) First, paper squares were treated with different concentrations of HRP solution and dried in a fume hood. Then, 15 μL TMB was added on the squares. Image was obtained after 2 min incubation. (b) First, paper squares were treated with different concentrations of HRP solution and dried in a fume hood. Then, these paper squares were treated with plasma (50 W) for 60 s. After that, 15 μL TMB was added on the squares. Image was obtained after 2 min incubation.

loss of enzymatic activity (Figure 3 (b)). This observation clearly shows the devastating loss of HRP activity in paper by plasma treatment.

To quantify the effect of plasma treatment on the activity loss of HRP, the dried HRP paper, which was prepared by soaking the paper in 4 $\mu\text{g/mL}$ HRP solution, was chosen for further investigation; the paper squares were treated with plasma (50 W) for different times, and the HRP activity was measured in the same way. Figure 4 shows the rapid loss of HRP activity on paper with the increase of plasma treatment time. It can be seen from Figure 4 that there is a sharp decline of mean cyan intensity with the increasing treatment time from 0 to 10 s,

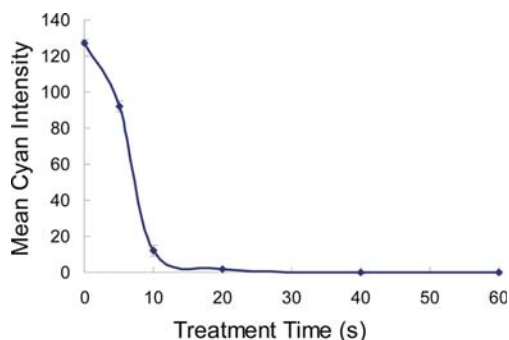


Figure 4. The effect of plasma treatment on the activity of HRP on paper.

showing that deactivation of HRP occurred in a very short time under plasma treatment. After 20 s of plasma treatment, HRP was almost completely deactivated. This study indicates the activity of HRP is extremely susceptible to plasma treatment.

Protection of HRP from Total Inactivation Caused by Plasma Treatment. The above results are in agreement with many studies reported in the literature that plasma treatment has devastating effects on activities of biointerfaces. In fabrication of low-cost diagnostic devices such as bioactive paper devices, however, it is ideal that bioactivities can be protected from total inactivation by plasma treatment. At least two scenarios can be perceived where such protection will be necessary. First, if bioactivities can be protected from plasma inactivation, then the fabrication process can be carried out with more flexibility; plasma treatment of the device does not have to be performed before the addition of bioactive reagents into the device. Second, the biochemical method used for protecting the plasma inactivation could be used as a method of patterning of bioactivity. In this study, however, we focus on proving the concept of using BSA to protect the bioactivity from total inactivation by plasma treatment.

In order to quantitatively evaluate the protective action of BSA against the inactivation of HRP paper caused by plasma treatment, a range of concentrations of BSA solution was prepared to create a protective layer over the HRP paper. In order to understand the addition of BSA to the activity of HRP on the paper, HRP activities on paper with and without BSA were compared. It can be seen from Figure 5 (a) that the

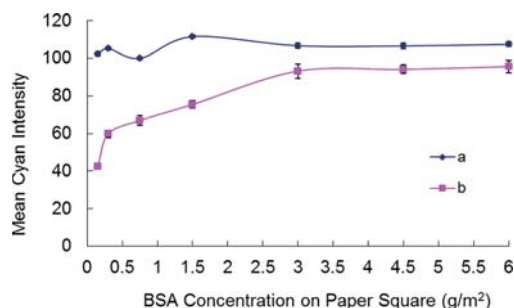


Figure 5. The protective action of BSA on HRP paper: (a) untreated HRP-BSA paper and (b) plasma (50 W, 20 s) treated HRP-BSA paper. Filter paper squares were soaked in 4 $\mu\text{g/mL}$ HRP solution. After drying, these squares were dosed with 15 mL of different concentrations of BSA solution. After drying in a fume hood for 20 min, HRP-BSA paper was fabricated. The calibration curve to convert color intensity to equivalent concentration of HRP solution ($\mu\text{g/mL}$) can be seen in Figure S3.

addition of a BSA layer over the HRP paper slightly reduced the activity of HRP, nevertheless the HRP still remain active. A possible reason for this observation may be that the protective layer of BSA slows down the penetration of the TMB solution, which restricted the accessibility of TMB to the HRP molecules that are covered by the BSA layer. Therefore, the shorter reaction time led to a slightly weaker development of color.

The most interesting result can be seen in Figure 5(b), which clearly shows that HRP molecules on the HRP-BSA paper retain a substantial level of activity after plasma treatment (50 W, 20 s). Compared with Figure 4, the inactivation of HRP on paper is significantly slowed down. This result suggests that the protection layer of BSA offers protection to HRP in paper against damage by plasma treatment. The effect of protection

could be improved with the increase of the concentration of BSA up to approximately 2 wt %. Fifteen microliters of 2 wt % BSA solution can provide a BSA layer with the concentration of 3 g/m² on paper square. Further increase of BSA concentration solution beyond 2 wt % offers little improvement of the protection of HRP in paper. The results show that a stable protection layer which was made of 2 wt % BSA solution offers a significant level of protection to HRP against plasma deactivation of HRP although such protection is not 100%. The HRP activity that survived the plasma treatment shows that BSA offers a practical means to protect the bioactivity in paper, and the level of protection is sufficient to maintain its bioactive function. The possible mechanism of the protection of HRP by BSA may be due to the physical barrier effect of BSA which shields the HRP molecules from the direct exposure to the energetic particles in the plasma environment.

Kylián et al. studied the plasma etching of a deposited BSA layer on a silica surface. They found that the deposited BSA layer can be etched away by plasma treatment.²⁵ However, the reduction of BSA layer under the plasma treatment was not instantaneous; instead, it was shown to be a gradual process with the increase of the amount of plasma treatment (i.e., intensity \times time).

Figure 6 compares the stability between HRP paper and HRP-BSA paper under plasma treatment. With increasing

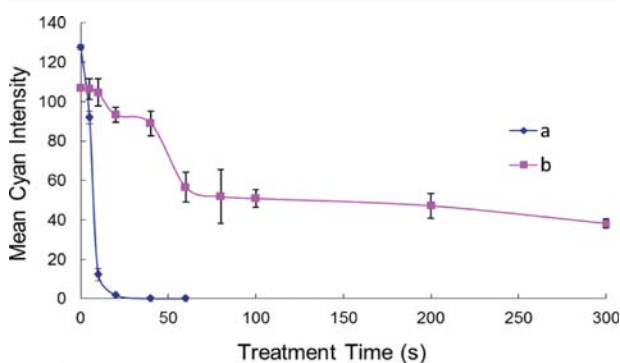


Figure 6. The stability of HRP paper (a) and HRP-BSA paper (b) under plasma treatment (50 W). Filter paper squares were soaked in 4 μ g/mL HRP solution. After drying, these squares were treated with 15 mL of BSA solution (2 wt %). After drying in fume hood for 20 min, the preparation of an HRP-BSA paper sample was completed. The calibration curve to convert color intensity to equivalent concentration of HRP solution (μ g/mL) can be seen in Figure S4.

treatment time, the intensity of developed cyan color of the catalytic product on HRP-BSA paper was reduced. The trend shown by Figure 6 (b) indicates that the activity of the HRP-BSA paper underwent slower loss with the increase of plasma treatment time, compared with the HRP paper without BSA. This result shows that BSA has a positive protection effect on HRP activity against plasma treatment. Normally, 20–30 s of plasma treatment (50 W) can significantly improve the wettability of low-wettable paper. After 20–30 s of plasma treatment at 50 W, the measurement of HRP catalyzed color change shows that greater than 70% of color intensity can still be observed. This color intensity corresponds to near 40% of enzyme activity. Even after 300 s of plasma treatment at 50 W, measurement of HRP catalyzed color change shows that greater than 40% of color intensity can still be observed indicating that there is still an amount of enzyme molecules remaining active.

This finding shows the stability of HRP-BSA paper is greatly improved over HRP paper, whose activity was almost completely lost after 20 s of plasma treatment at 50 W.

Plasma Treatment of Papers Carrying Blood Grouping Antibodies. We return to the practical application of improving blood wettability of blood typing paper that carries the blood typing antibodies. As was mentioned earlier, when blood typing antibodies from stated source are introduced on the paper, the blood wettability of the paper reduces significantly (Figures 7 (a) and 7 (b)). Such a reduction in



Figure 7. Profile of blood in/on (a) paper; (b) antibody paper (contact angle = 122.2°); and (c) plasma treated antibody paper. (a) Kleenex paper square without any treatment. (b) Kleenex paper square treated by adding antibody solution twice. (c) Kleenex paper square treated using the same treatment procedure as blood typing paper. Four microliters of blood was deposited onto each paper square respectively. After 3 s, images were taken to compare the status of blood sample on each paper. Blood penetrated into paper (a) and plasma treated antibody paper (c) in less than 3 s. However, water does not completely penetrate into antibody paper (b) within 30 s.

blood wettability negatively impacts on the performance of the blood typing paper, since slow penetration of sample will slow down the assaying speed. The most effective way to overcome this problem is to restore the wettability of the paper.

Blood typing antibodies from stated source contain 1–5% BSA as the stabilization reagent.¹⁰ Because of the hydrophobic nature of BSA, its adsorption on cellulose fiber surfaces will reduce wettability. However, based on our study of the HRP-BSA system, the wettability of the paper carrying blood typing antibodies should be restored by plasma treatment and the blood typing antibody molecules should still be active. Followed by this hypothesis, paper carrying blood typing antibodies were plasma treated for 60 s at 50 W. After the treatment, the blood wetting of the paper was restored; a blood sample can completely penetrate into the treated paper within 3 s (Figure 7 (c)). This level of wettability fulfills the blood penetration requirement of blood typing paper.

Figure 8 shows the blood typing results using the plasma treated papers (50 W, 60 s). These results show that plasma treatment can be used as a method to improve the wettability of bioactive papers, provided that appropriate protection measures are taken to prevent the plasma deactivation of the biomolecules.

CONCLUSION

The concept of using plasma treatment to improve the wettability of bioactive paper for rapid spreading and penetration of liquid sample into paper was investigated. Plasma treatment is shown to rapidly deactivate HRP molecules on paper. In this study, we found that BSA can act as a molecular chaperone to protect HRP in paper against inactivation caused by plasma treatment. The successful protection of biomolecules by BSA enables plasma treatment to be used as a part of the fabrication process for the mass production of paper-based sensors in which strong wettability of bioactive areas such as detection areas on a device is

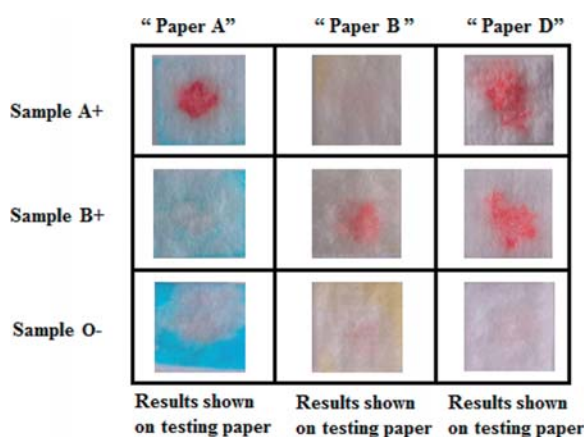


Figure 8. Testing of blood types using testing papers treated with $2 \times 3.5 \mu\text{L}$ of commercial antibodies. Paper A, Paper B, and Paper D, all showing expected results ($1 \mu\text{L}$ blood sample, plasma treatment).

required. We also demonstrated a real bioactive paper application of blood typing paper. Plasma treatment of antibody loaded papers greatly increases the blood penetration rate into the paper and at the same time leaves a sufficient level of antibody activity to agglutinate RBCs that carry the corresponding antigens. Plasma treatment of the blood typing papers shows that this method may be further developed into a fabrication step in mass production of bioactive paper diagnostics where devices must have a high level of wettability and sufficient bioactivity. This study shows that the sequence of plasma treatment and the introduction of bioactive reagents onto paper may no longer be an engineering restriction in sensor production. These two fabrication steps can be implemented in any sequence to suit the engineering of the best production efficiency.

■ ASSOCIATED CONTENT

● Supporting Information

Four figures: (1) Figure S1. A schematic of an ideal blood typing testing-result-matrix of antibody-specific agglutination of RBCs on testing paper; (2) Figure S2. A schematic of the process for evaluating the protection of HRP paper by BSA from plasma treatment; (3) Figure S3. The protective action of BSA on HRP paper. (a) Untreated HRP-BSA paper; (b) Plasma (50 W, 20 s) treated HRP-BSA paper; (4) Figure S4. The stability of HRP paper (a) and HRP-BSA paper (b) under plasma treatment (50 W). This material is available free of charge via the Internet at <http://pubs.acs.org>.

■ AUTHOR INFORMATION

Corresponding Author

* [Redacted]

Notes

The authors declare no competing financial interest.

■ ACKNOWLEDGMENTS

This work is supported by Australian Research Council Grant (ARC DP1094179 and LP110200973). Authors thank Haemokinesis for its support through ARC Linkage Project. The authors would like to specially thank Dr. E. Perkins in the Department of Chemical Engineering, Monash University for proofreading the manuscript. J.T., L.L., and M.L. thank Monash University Research and Graduate School and the Faculty of

Engineering for their postgraduate research scholarships. P.J. is grateful for the research grants from the Thailand Research Fund (TRF) through the Royal Golden Jubilee PhD Program (RGJ) and Center of Excellence for Innovation in Chemistry (PERCH-CIC), Commission on Higher Education, Ministry of Education.

■ REFERENCES

- (1) Martinez, A. W.; Phillips, S. T.; Butte, M. J.; Whitesides, G. M. *Angew. Chem., Int. Ed.* **2007**, *46*, 1318–1320.
- (2) Martinez, A. W.; Phillips, S. T.; Whitesides, G. M.; Carrilho, E. *Anal. Chem.* **2010**, *82*, 3–10.
- (3) Li, X.; Tian, J.; Nguyen, T.; Shen, W. *Anal. Chem.* **2008**, *80*, 9131–9134.
- (4) Pelton, R. *TrAC, Trends Anal. Chem.* **2009**, *28*, 925–942.
- (5) Tian, J.; Shen, W. *Chem. Commun.* **2011**, *47*, 1583–1585.
- (6) Li, M.; Tian, J.; Al-Tamimi, M.; Shen, W. *Angew. Chem., Int. Ed.* **2012**, *51*, 5497–5501.
- (7) Mukhopadhyay, R. *Chem. World* **2010**, *7*, 50–53.
- (8) McMaster University Daily News. <http://dailynews.mcmaster.ca/article/bioactive-paper-closer-to-commercialization/> (accessed Nov 5, 2012).
- (9) Paper Money Web site. <http://www.globalpapermoney.org/bioactive-paper-research-receives-added-funding-for-bioactive-paper-development-cms-5380> (accessed Nov 5, 2012).
- (10) Jarujamrus, P.; Tian, J.; Li, X.; Siripinyanond, A.; Shiowatana, J.; Shen, W. *Analyst* **2012**, *137*, 2205–2210.
- (11) Al-Tamimi, M.; Shen, W.; Zeineddine, R.; Tran, H.; Garnier, G. *Anal. Chem.* **2011**, *84*, 1661–1668.
- (12) Pykönen, M.; Silvaani, H.; Preston, J.; Fardim, P.; Toivakka, M. *Colloids Surf., A* **2009**, *352*, 103–112.
- (13) Abe, K.; Suzuki, K.; Citterio, D. *Anal. Chem.* **2008**, *80*, 6928–6934.
- (14) Li, X.; Tian, J.; Shen, W. *ACS Appl. Mater. Interfaces* **2010**, *2*, 1–6.
- (15) Tian, J.; Kannangara, D.; Li, X.; Shen, W. *Lab Chip* **2010**, *10*, 2258–2264.
- (16) von Keudell, A.; Awakowicz, P.; Benedikt, J.; Raballand, V.; Yanguas-Gil, A.; Opretzka, J.; Flötgen, C.; Reuter, R.; Byelykh, L.; Halfmann, H.; Stapelmann, K.; Denis, B.; Wunderlich, J.; Muranyi, P.; Rossi, F.; Kylián, O.; Hasiwa, N.; Ruiz, A.; Rauscher, H.; Sirghi, L.; Comoy, E.; Dehen, C.; Challier, L.; Deslys, J. P. *Plasma Processes Polym.* **2010**, *7*, 327–352.
- (17) Rauscher, H.; Kylián, O.; Benedikt, J.; von Keudell, A.; Rossi, F. *ChemPhysChem* **2010**, *11*, 1382–1389.
- (18) Fumagalli, F.; Kylián, O.; Amato, L.; Hanuš, J.; Rossi, F. *J. Phys. D: Appl. Phys.* **2012**, *45*, 135203.
- (19) Birmingham, J. G.; Hammerstrom, D. J. *IEEE Trans. Plasma Sci.* **2000**, *28*, 51–55.
- (20) Rossi, F.; Kylián, O.; Hasiwa, M. *Plasma Processes Polym.* **2006**, *3*, 431–442.
- (21) Eremin, A. N.; Budnikova, L. P.; Sviridov, O. V.; Metelitsa, D. I. *Appl. Biochem. Microbiol.* **2002**, *38*, 151–158.
- (22) Gronczewska, J.; Biegniewska, A.; Zięta, M. S.; Skorkowski, E. F. *Comp. Biochem. Physiol., Part C: Toxicol. Pharmacol.* **2004**, *137*, 307–311.
- (23) Marini, I.; Moschini, R.; Corso, A.; Mura, U. *Cell. Mol. Life Sci.* **2005**, *62*, 3092–3099.
- (24) D'Souza, S. E.; Altekar, W.; D'Souza, S. F. *World J. Microbiol. Biotechnol.* **1997**, *13*, 561–564.
- (25) Kylián, O.; Benedikt, J.; Sirghi, L.; Reuter, R.; Rauscher, H.; von Keudell, A.; Rossi, F. *Plasma Processes Polym.* **2009**, *6*, 255–261.

Surface Modification of Cellulose Paper for Quantum Dot-based Sensing Applications

Liyun Guan,^a Junfei Tian,^a Rong Cao,^a Miaosi Li,^a Zhangxiong Wu,^b Azadeh Nilghaz,^a Wei Shen^{a,*}

Cellulose paper specimens with and without surface modification were compared in order to study their physicochemical compatibility with quantum dots (QDs) for biochemical sensing applications. Silane and chitosan modification methods were applied. The distribution of QDs deposited on untreated paper, and papers modified with silane and chitosan were investigated in order to understand the interaction between QDs and fibre. Modified papers were shown to significantly reduce the undesirable redistribution of QDs during paper drying. The retention ability and thermal resistance of QDs to the loss of fluorescence on modified papers were also studied for the purpose of determining the most suitable paper surface modification for developing QD-Paper-based analytical devices (QD-PADs). Furthermore, chitosan-modified paper was used to design QD-PADs to quantify glucose concentration in aqueous samples; the quenching effect of the enzymatic product on the fluorescent emission of QDs was used as the indicator system. The change of fluorescence of QDs was measured by a simple in-house constructed fluorescence imaging system. The detection limit of glucose was 5 mg/dL, which is comparable with other reported paper sensors for detection of glucose.

Keywords: Cellulose Paper; Surface Modification; Quantum Dots; Paper-based Analytical Devices; Glucose Sensing

Contact information: a: Department of Chemical Engineering, Monash University, Wellington Rd., Clayton, Vic. 3800, Australia; b: School of Chemical and Environmental Engineering, College of Chemistry, Chemical Engineering and Materials Science, Soochow University, Suzhou, Jiangsu Province 215123, China; *Corresponding author

INTRODUCTION

In recent years cellulose paper has attracted the interest of those working in the field of developing paper-based analytical devices (PADs) for diagnostics applications (Balu *et al.* 2009; He *et al.* 2013). Made of cheap and widely available cellulose fibre (Hubbe *et al.* 2008), paper is a suitable material for manufacturing analytical sensors on a large scale to meet the demand of diagnostics from human populations living in developing regions. The rapid advancement of PADs research can be attributed to the unique physicochemical properties of paper including: compatibility with biological samples (Tan *et al.* 2012); easy surface modification to immobilize proteins, DNA, and other molecules (Xiao and Huang 2011; Araujo *et al.* 2012); and controllable wettability for transporting fluids (Tian *et al.* 2010). Historically, concepts of using paper for chemical assay tests have been explored from as early as 1937 (Yagoda 1937). Since 2007, paper-based diagnostics have been re-discovered and pursued by many research groups globally; a trend initiated by the Whitesides Group (Martinez *et al.* 2007).

During the development of PADs several techniques have been reported for qualitative or semi-quantitative sensing applications, such as colorimetric (Xiao *et al.* 2013), electrochemical (Dungchai *et al.* 2009), chemiluminescent (Liu *et al.* 2013), and fluorescent methods (Ma *et al.* 2012). At the same time, a variety of sensor probes, whose properties change when they interact with analytes, have been adapted to these methods and used to indicate the functions of paper sensors (Li *et al.* 2012; Liu *et al.* 2013). The performances of probes applied in PADs are extremely important for obtaining accurate assay results. Quantum dots (QDs) have been considered to have great potential as fluorescence probes for biosensing (Hai *et al.* 2013; Chen *et al.* 2013). In particular, the comparable dimensions of QDs and biomolecules, such as proteins and DNA, enable the preparation of biocompatible QD-bioconjugates with special recognition functions (Li *et al.* 2011). Their excellent properties such as photo-stability and broad absorption spectra, together with high surface activity, make QDs advantageous probes in the development of biochemical sensors (Li *et al.* 2011).

Recently, a few studies have been published about the combination of QD probes with cellulose paper for sensing applications (Niu *et al.* 2011; Yuan *et al.* 2012; Noor *et al.* 2013). Yuan *et al.* reported the use of polymer QD-enzyme hybrids on PADs to detect the presence of a substrate with corresponding enzymes (Yuan *et al.* 2012). Noor *et al.* proposed a paper-based solid phase nucleic acid hybridization assay using immobilized QDs as donors in fluorescence resonance energy transfer (Noor *et al.* 2013). The QDs and QD conjugates were immobilized onto the surface of paper through imidazole ligands modification chemistry. These works successfully demonstrated applications of PADs using QDs as sensing probes. In this study, we further investigated the physicochemical compatibility between cellulose paper and QDs. Different surface modifications of cellulose paper were studied to evaluate their effects on QD particles distribution, retention ability and thermal stability for sensing applications. A simple fluorescence imaging system has been constructed in-house in order to obtain the fluorescence characteristics of the QDs on cellulose paper. Furthermore, QD-Paper-based analytical devices (QD-PADs) based on these studies have been successfully developed for glucose detection with fluorescence intensity change of QD probes.

EXPERIMENTAL

Reagents and Apparatus

Chitosan (medium molecular weight) and 3-aminopropyltrimethoxysilane (APTMS, >97%) were purchased from Sigma Aldrich. Phosphate buffer solution (PBS) tablets and Tween 20 were obtained from Sigma Aldrich. Tween-20 (0.5%, v/v) was spiked into 0.01 mol/L pH 7.4 PBS solutions as wash buffer (PBST). Ultra-pure water (>18.0 M Ω) was obtained from a Milli-Q integral water purification system. All reagents were used without further purification. Carboxyl group functionalized CdS_xSe_{1-x}/ZnS alloyed quantum dots (QDs) (λ_{em} = 630 nm) were acquired from Sigma Aldrich.

Whatman No.1 filter paper (diameter = 20 mm) was obtained from Sigma Aldrich; this grade of filter paper is made of pure cellulose fibres. The paper was cut into different sizes for further use. K1050X Plasma Asher (Quorum Emitech, U.K.) was used for plasma treatment. The vacuum level for the treatment was 0.6 mbar and the paper was placed in the center of the chamber for 30 s of treatment.

Surface Modification of Cellulose Paper

Silane Modification

The preparation procedures for silane modified paper can be summarized as follows (Li *et al.* 2010; Koga *et al.* 2011; Jin *et al.* 2011, 2012): a volume of 3 mL 2.5% (v/v) 3-aminopropyltrimethoxysilane (APTMS) was prepared using 80% (v/v) ethanol solvent, and thus was hydrolyzed to form reactive silanol groups. Then 20 pieces of paper squares (1 cm \times 1 cm), after plasma treatment, were immersed in the resulting solution for 2 h, followed by thorough washing with ethanol. Subsequently, the solvent was evaporated in the fume hood at room temperature for 10 min. The obtained paper squares were thermally treated at 110 °C for 3 h.

Chitosan Modification

To prepare chitosan modified paper, a volume of 10 mL 0.1% (w/v) chitosan was freshly prepared using a weak acid solution. Then 20 μ L of chitosan solution were uniformly deposited on 1 cm \times 1 cm paper squares, and then dried at room temperature for 1 h. Subsequently, each paper square was washed three times with 20 μ L of ultrapure water, and then dried at room temperature. The chitosan retention was reported to be strong, due to the opposite charges of the chitosan and cellulose with the former being cationic and the latter being anionic (Wang *et al.* 2012; Xiao *et al.* 2013).

Preparation and Characterization of QDs on Cellulose Paper

Fluorescence and SEM characterization

Papers with APTMS- and chitosan-modification were prepared following the above procedures in Section “Surface Modification of Cellulose Paper”. Untreated filter paper, APTMS- and chitosan-modified filter papers were cut into 1 cm \times 1 cm squares for further QDs compatibility studies. Then 4 μ L of 0.02 mg/mL QDs were dropped into the center of each paper square and allowed to dry at room temperature for 20 min.

For the purpose of collecting the fluorescence signals of QDs on the paper, a simple fluorescent imaging system (Fig. 1) was constructed in-house to capture the fluorescence signals.

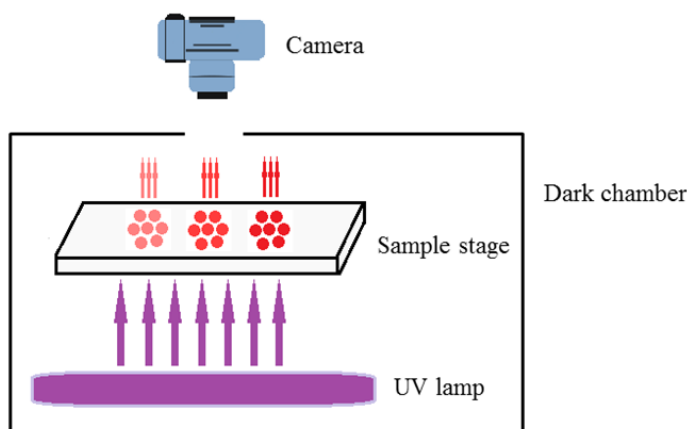


Fig. 1. The Schematic diagram of the fluorescence imaging system assembled in-house.

The in-house built fluorescent imaging system was comprised of a 365 nm emission UV-lamp, a sample stage and a digital camera. The UV-lamp, used as an excitation light source, was placed at the bottom of a dark chamber and the sample stage

was fixed above the UV-lamp. After turning on the light source, the UV light passed through the optically transparent sample stage and excited the fluorescence of the samples. The fluorescence signals emitted from the samples were captured by the camera right on the top of the sample stage. Before each fluorescence test, the light source was turned on and warmed up for 15 min to allow the stabilization of the radiation intensity.

The cellulose papers with and without QDs were further investigated by a MECM Nova NanoSEM scanning electron microscope (SEM) in order to observe the morphology of cellulose paper and the distribution of QDs on the cellulosic structure of paper. A volume of 4 μL 1 mg/mL, instead of 0.02 mg/mL QDs, was dropped onto each paper square for preparing samples for SEM study.

Retention Tests by Washes with Aqueous Solution

The retention ability of QDs on APTMS- and chitosan-modified cellulose papers was also investigated following the procedures below: three aliquots of 40 μL 0.5% PBST solution were introduced onto each testing paper, while standard blotting papers (drink coaster blotting, 280 g/m^2) were used to remove liquid during the washing process. The fluorescence of QDs on paper squares before and after washing were measured using the above in-house built fluorescence imaging system.

The quantitative analyses were carried out following the description in Section “The Quantitative Analysis Technique”.

Temperature Treatment of QDs on Cellulose Paper

Immediately after preparation, three groups of paper squares loaded with QDs were treated at temperatures of 4 $^{\circ}\text{C}$, 25 $^{\circ}\text{C}$ and 45 $^{\circ}\text{C}$. The fluorescence signals of these paper squares were respectively measured after 0 h, 24 h, 36 h and 60 h of treatment. The quantitative analyses were performed following the procedures described in Section “The Quantitative Analysis Technique”.

Development of QD-PADs for Glucose Detection

Chitosan-modified paper squares (0.5 cm \times 0.5 cm) were employed to make QD-PADs for detecting glucose. Five hundred microliters of QD suspension (0.04 mg/mL) was mixed with 500 μL of glucose oxidase (100 U/mL). A volume of 2 μL of the above suspension was dropped onto the center of each chitosan-modified paper square, and allowed to dry for 15 min under room temperature (Gill *et al.* 2008). Then several 1.2 μL volumes of glucose solution, with concentrations of 0, 5, 10, 20, 50, 100, 150, 200 mg/dL, were respectively introduced onto each paper square, and then allowed to react for 15 min under a controlled high humidity.

The fluorescence images of all the paper squares were captured by the in-house built fluorescence imaging system. Quantitative analyses were performed following the descriptions in Section “The Quantitative Analysis Technique”.

The Quantitative Analysis Technique

The test paper squares with QDs fluorescence images were imported into Adobe Photoshop. The mean red intensity of the reaction spot was obtained using the histogram function of the software. Error bars (standard deviation) were obtained from five repeats of all the tests.

RESULTS AND DISCUSSION

Characterization of QDs on Cellulose Paper

Fluorescence characterization

The fluorescence emission performance of QDs on cellulose paper, with and without modification, was investigated using the above system (Fig. 1). Fig. 2 shows the fluorescence images of untreated paper (Fig. 2, b1), APTMS- (Fig. 2, b2), and chitosan-modified paper (Fig. 2, b3). The blue color in these images was the background UV light source, and the red color is the fluorescence of QDs. In Fig. 2, b1, an extremely weak red color spread around the edge of the paper surface and could be easily observed by the naked eye. This was because QD nanoparticles dried on the untreated cellulose paper tend to migrate with the solvent phase (PBS solutions). In contrast to this, clear red fluorescence signals of QDs were captured in the center of both APTMS- (Fig. 2, b2) and chitosan-modified papers (Fig. 2, b3), which indicates that QDs were well restricted within the center range of modified papers. Whatman #1 filter paper used in this study was made of pure cellulose fibres with no additives such as strengthening or whitening agents. The basic structure of untreated paper is composed of cellulose fibers that are firmly bond together through hydrogen bonding (Sahin and Arslan 2008). This kind of paper has inactive, slightly anionic surface with a low, negative, surface-charge density (Wang *et al.* 2012). In this situation, negative-charged COOH—QDs particles have a weak tendency to strongly attach to the paper surface by the physical immobilization method. Therefore, when QDs particles were dropped onto the untreated cellulose paper, QDs will be carried by the mobile phase (PBS solution) wicking front and spread to the edge of the paper. However, the surface chemistry property of paper will change after modification processes due to the introduction of active functional groups, which enhance the charge interaction between QDs particles and the paper surface. Hence, QD particles will be left behind from the solvent phase wicking front and immobilized in the center area of paper (Fig. 2, b2 and b3).

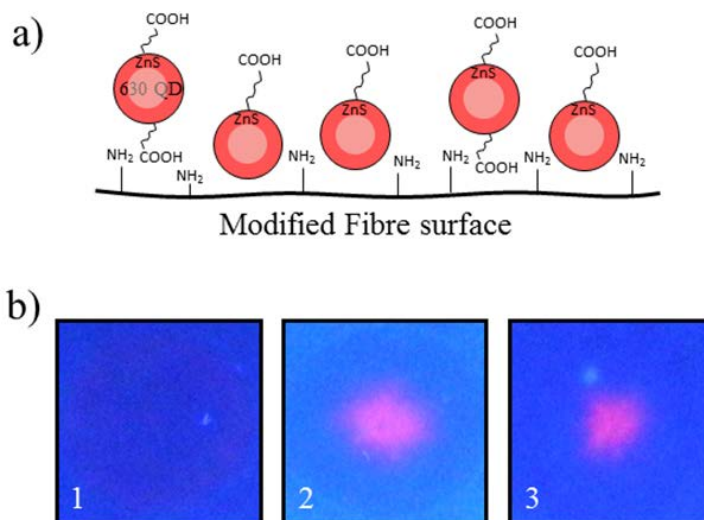


Fig. 2. a) Possible schemes of the QDs captured by modified cellulose paper' b) Fluorescence images of QDs on cellulose paper (1) without modification, (2) with APTMS-modification, (3) with chitosan modification

It was observed that the average size of the formed colored QD spots on APTMS-modified paper was larger than that on chitosan-modified paper. Additionally, it was also noticed that the size of QDs on APTMS-modified papers was less uniform than that on chitosan-modified papers, and thus the reproducibility of QD spot sizes on APTMS-modified papers was not as consistent (not presented). The APTMS modification method in this study applied a silane coupling technique through the reaction between silanol groups (Si—OH) of APTMS and groups (mainly hydroxyl groups C—OH) of cellulose paper.

The relatively low reactivity of existing groups (mainly C—OH groups) on paper will greatly affect the amount of introduced groups with APTMS treatment processes (Pelton 2009). However, as a physical modification approach, the chitosan modification method can be applied reproducibly with uniform coating on the surface of paper. As a result, the outsourcing active groups in the cellulosic network of APTMS-modified paper are less densely distributed compared to that of chitosan-modified paper. Therefore, QD particles have a stronger interaction with chitosan modified paper; this difference is the main reason for the difference of QD spots between the two modified papers.

SEM Characterization

The porous fibre network structures of papers remained after modification with APTMS and chitosan (Fig. 3). Figure 3 shows the SEM images of untreated papers, papers with APTMS-modification, and papers with chitosan-modification loaded with QDs. QD particles show different distributions on non-modified and modified papers (Fig. 3). Abundant QD particles were observed around the edges of untreated paper (Fig. 3, a2) while very a small quantity of particles could be observed around the center of the paper (Fig. 3, a1). However, the distribution of QDs was the opposite in the cases of APTMS- and chitosan-modified papers; most QD particles were found gathered around the center of the modified papers (Fig. 3, b1 and c1). The results are consistent with the above fluorescence characterization studies, indicating that surface modification can result in immobilization of QD particles to any point of interest on paper (*e.g.* to the center area of the paper square in this study).

In addition, particles tend to attach to the cellulose fibres rather than staying in pores of fibre network (Fig. 3, b1 and c1), suggesting that most of the active groups of APTMS and chitosan have been modified onto the fibres. Furthermore, QD particles have been found to be more closely packed on chitosan-modified paper (Fig. 3, c1) than that on APTMS-modified paper (Fig. 3, b2). The results illustrate that the charge interaction between QD particles and a chitosan-modified fibre surface was stronger than their interaction with a fibre surface modified with APTMS. The former captured more QD particles at points of interest.

QD particle aggregates were observed on modified paper. Their sizes were greater than separate QD particles (about 6 nm), and they lose the ability to produce fluorescence signals (Liu *et al.* 2012). One reason for the formation of large particles could be that a part of the original aqueous QD suspension had started to form aggregates, which has been observed and reported previously (Noh *et al.* 2010). Another reason, which is more likely, is that the high concentration of QD suspension applied to the paper surface for SEM tests had aggregated during the drying process.

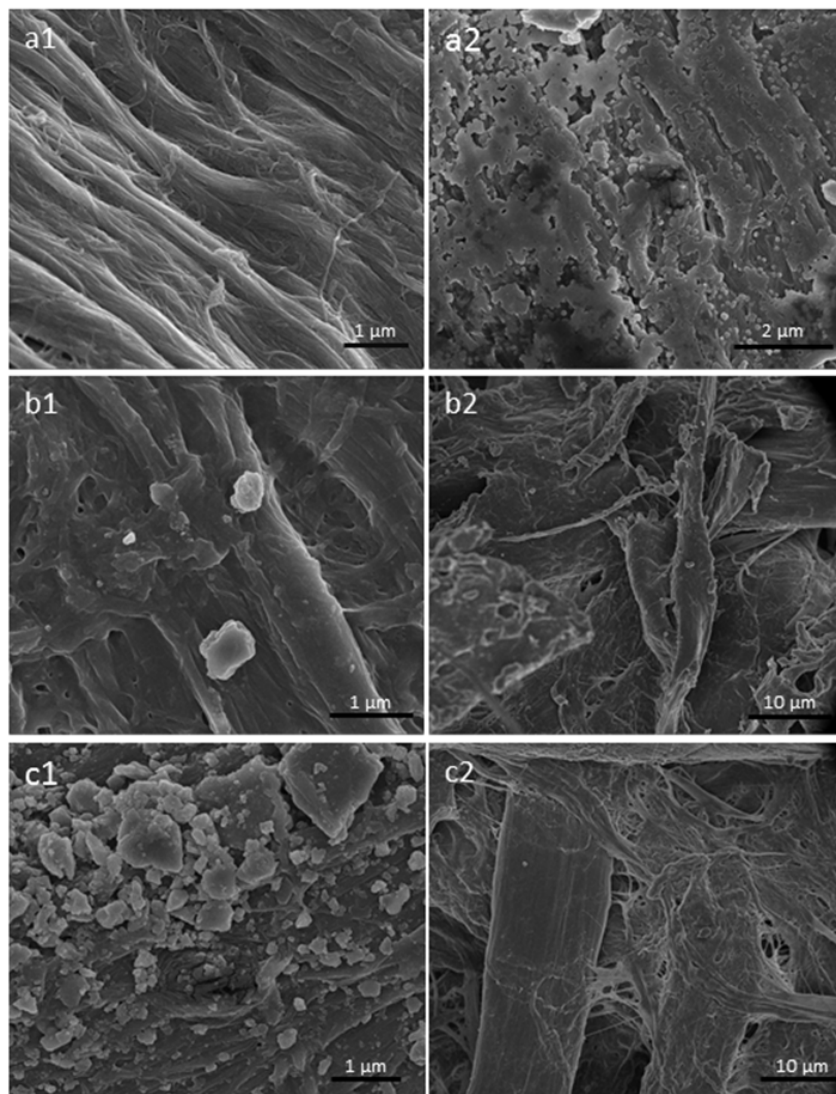


Fig. 3. SEM images of the (a1) center and (a2) edge areas of untreated cellulose paper; (b1) center and (b2) edge areas of APTMS-modified paper; (c1) center and (c2) edge areas of chitosan-modified paper. All the papers were loaded with QDs particles for SEM tests.

Retention of QDs on Modified Cellulose Paper

The retention ability of QD probes on a paper substrate is critical to the performance of QD-PADs. This is because when an analyte solution is introduced onto the detection point of the sensor, QD probes with weak bonding to fibres could be eluted away from the detection point, leading to signal distortion in the detection zone. To study the retention of QDs on the two modified papers, 0.5% PBST solutions were applied to wash modified papers loaded with QDs. The more QD particles retained after washing means the stronger interaction between QDs and paper. In this study, the red intensity measured from the QD spots is the fluorescence intensity of QDs. Figure 4 shows the fluorescence intensity changes of modified papers with QDs after washing. The fluorescence intensity decreased by 26.5% on APTMS-modified paper (Fig. 4, left), while for QDs on chitosan-modified paper (Fig. 4, right), the intensity dropped by 18.2%. This result indicates that the retention ability of QDs on chitosan-modified paper was

greater than that on APTMS-modified paper, which was further evidence that the interaction between QDs and chitosan-modified paper is stronger.

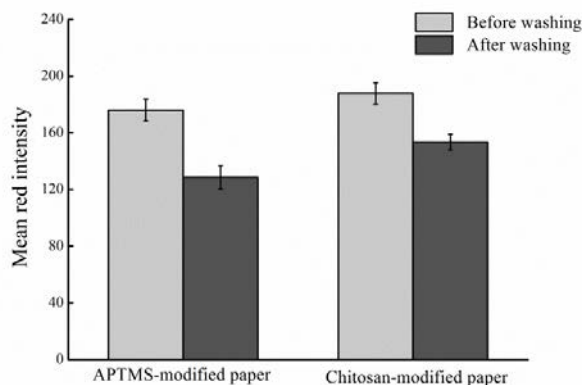


Fig. 4. The fluorescence intensity of QDs on APTMS-modified (left) and chitosan-modified (right) cellulose paper before and after washing with PBST buffer solutions

Thermal Stability of QDs on Modified Paper

Since thermal stability is a very important performance indicator of PADs for sensor applications (Guan *et al.* 2014), both APTMS- and chitosan-modified papers loaded with QDs were aged at different temperatures to test their thermal stability. Thermal stability was evaluated by measuring the red intensities of QDs spots formed in the center of the paper before and after aging. Figure 5 shows little intensity change of QDs bounded to both modified papers after aging at 4 °C; in contrast to this, a significant decrease in fluorescent intensity was observed when the papers were treated at 45 °C. Intensity decrease of QD spots on papers also occurred with a treatment temperature of 25 °C, however, it was less than that with the treatment temperature of 45 °C. The results indicate that QDs fixed in a cellulosic network could remain relatively stable at low temperatures, but a rise of temperature will lead to partial loss of fluorescence. Moreover, the results showed that the intensity decrease of QDs on APTMS-modified paper (Fig. 5a) was much greater than that on chitosan-modified paper (Fig. 5b) after aging at 45 °C. It is therefore most likely that the temperature-driven fluorescence loss of QDs on chitosan-modified paper is slower than that on APTMS-modified paper because of the stronger interaction between QD particles and the former paper.

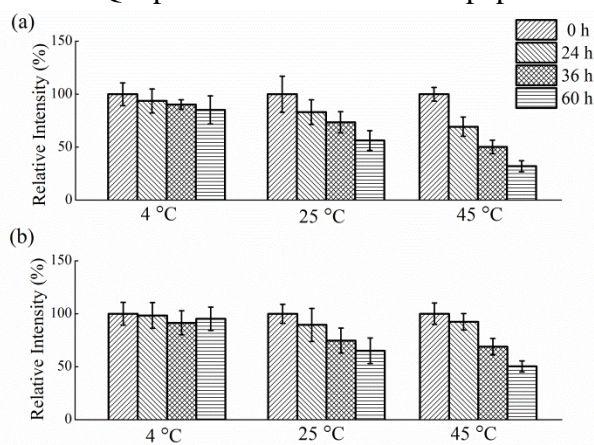


Fig. 5. The fluorescence intensity of QDs on (a) APTMS-modified and (b) Chitosan-modified cellulose paper after at 4 °C, 25 °C and 45 °C temperature treatment with different time

Development of QD-PADs for Glucose Detection

To design practical QD-PADs, the primary consideration is immobilizing QDs in the detection zones of the paper to reduce QD migration. However, QDs deposited on untreated cellulose filter paper will migrate with the solvent and mostly gather around the edge of the paper. These migrated QDs were no longer suitable for any sensor applications. Yuan *et al.* (2012) attempted to solve this problem by encapsulating QDs with opposite-charged polymer. The present study shows that suitably modified papers could well solve the migration problem of QDs. Therefore in this study, chitosan-modified paper was selected to fabricate QD-PADs for demonstrating sensor application.

QDs have been reported as a sensitive probe for hydrogen peroxide, and further used in the detection of glucose with glucose oxidase as the catalyst to produce hydrogen peroxide (Wu *et al.* 2010). The possible mechanism that stimulates the fluorescence quenching of QDs is the oxidation of S^{2-} surface states, which presumably yields Zn^{2+} surface traps for the electrons (Gill *et al.* 2008). Figure 6a shows the fluorescence quenching effect of the QDs on the chitosan-modified paper by different concentrations of glucose. The calibration curve (Fig. 6a) represents the quenching effect of glucose yields $I_0/I = 1.139 + 0.0069C_{glucose}$ ($r^2 = 0.95$), where I_0 is the mean red intensity of QD-PADs when the concentration of glucose is 0, and I is the measured mean red intensity for the target sample. The detection limit of glucose is 5 mg/dL and the detection linear range is between 20 mg/dL and 200 mg/dL. Compared with the previous methods utilizing the glucose oxidase and QDs-polymer co-immobilization method in normal filter paper (Yuan *et al.* 2012), a lower detection limit of glucose was obtained in this study. Also in comparison to the solution-based method, this study largely reduces the usage of QDs and other reagents.

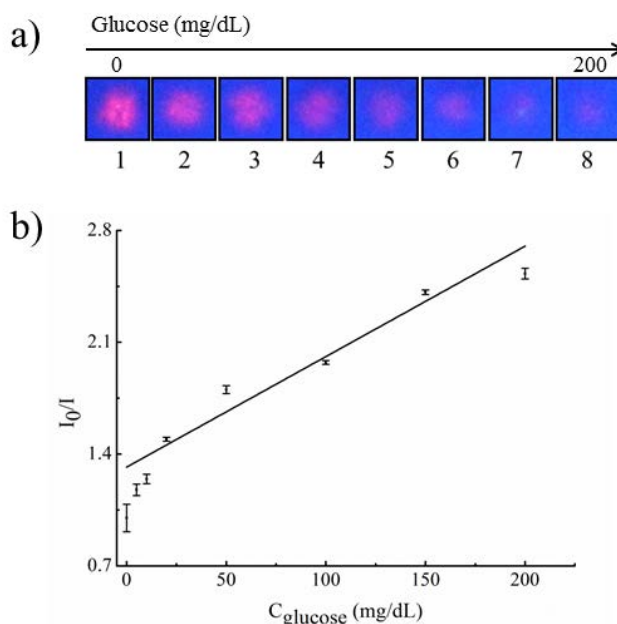


Fig. 6. a) Response of QD-PADs using chitosan-modified paper to different concentrations of glucose 0, 5, 10, 20, 50, 100, 150, 200 mg/dL (from 1 to 8); b) corresponding calibration curve

CONCLUSIONS

1. This study investigated the physicochemical compatibility between QD particles and cellulose papers for the purpose of developing reproducible QD-PADs. The migration problem of QDs moving with the solvent phase in the fibre network structure of paper was greatly reduced by modifying the surface of cellulose. The retention ability and thermal stability of QD probes on paper have been studied as critical performance indicators of QD-PADs.
2. QD-PADs using chitosan-modified paper was demonstrated for glucose detection and the detection limit is comparable with reported paper-based glucose sensors.
3. This work provides an important framework for the development of QD-PADs and it is expected that QD-PADs can lay a foundation for further developing practical and stable sensor for diagnostic and analytical applications.

ACKNOWLEDGMENTS

This work is supported by Australian Research Council Grant (ARC DP1094179 and LP 110200973). Authors thank Mr. Hansen Shen for proof reading the manuscript. Postgraduate research scholarships from Monash University of Graduate Research and Faculty of Engineering are also gratefully acknowledged.

REFERENCES CITED

- Araujo, A. C., Song, Y. J., Lundeberg, J., Stahl, P. L., and Brumer, H. (2012). "Activated paper surface for the rapid hybridization of DNA through capillary transport," *Anal. Chem.* 84(7), 3311-3317. DOI: 10.1021/ac300025v
- Balu, B., Berry, A. D., Hess, D. W., and Breedveld, V. (2009). "Patterning of super hydrophobic paper to control the mobility of micro-liter drops for two-dimensional lab-on-paper applications," *Lab. Chip* 9(21), 3066-3075. DOI: 10.1039/B909868B
- Chen, Z. Z., Ren, X. L., Meng, X. W., Tan, L. F., Chen, D., and Tang, F. Q. (2013). "Quantum dots-based fluorescent probes for turn-on and turn-off sensing of butyrylcholinesterase," *Biosens. Bioelectron.* 44, 204-209. DOI: 10.1016/j.bios.2013.01.034
- Dungchai, W., Chailapakul, O., and Henry, C. S. (2009). "Electrochemical detection for paper-based microfluidics," *Anal. Chem.* 81(14), 5821-5826. DOI: 10.1021/ac9007573
- Gill, R., Bahshi, L., Freeman, R., and Willner, I. (2008). "Optical detection of glucose and acetylcholine esterase inhibitors by H₂O₂-sensitive CdSe/ZnS quantum dots," *Angew. Chem. Int. Edit* 47(9), 1676-1679. DOI: 10.1002/anie.200704794
- Guan, L. Y., Cao, R., Tian, J. F., McLiesh, H., Garnier, G., and Shen, W. (2014). "A preliminary study on the stabilization of blood typing antibodies sorbed into paper," *Cellulose*, 21(1), 717-727. DOI: 10.1007/s10570-013-0134-x
- Hubbe, M. A., Pawlak, J. J., and Koukoulas, A. A. (2008). "Paper's appearance: A review," *BioResources*. 3(2), 627-665.

- Hai, H., Yang, F., and Li, J. P. (2013). "Electrochemiluminescence sensor using quantum dots based on G-quadruplex aptamer and the detection of Pb^{2+} ," *Rsc Adv.* 3(32), 13144-13148. DOI: 10.1039/C3RA41616J
- He, Q. H., Ma, C. C., Hu, X. Q., and Chen, H. W. (2013). "Method for fabrication of paper-based microfluidic devices by alkylsilane self-assembling and UV/O₃-patterning," *Anal. Chem.* 85(3), 1327-1331. DOI: 10.1021/ac303138x
- Jin, C., Yan, R., and Huang, J. (2011). "Cellulose substance with reversible photo-responsive wettability by surface modification," *J. Mater. Chem.* 21, 17519-17525. DOI: 10.1039/C1JM13399C
- Jin, C., Jiang, Y., Niu, T., and Huang, J. (2012). "Cellulose-based material with amphiphobicity to inhibit bacterial adhesion by surface modification," *J. Mater. Chem.* 22, 12562-12567. DOI: 10.1039/C2JM31750H
- Koga, H., Kitaoka, T., and Isogai, A. (2011). "In situ modification of cellulose paper with amino groups for catalytic applications," *J. Mater. Chem.* 21(25), 9356-9361. DOI: 10.1039/C1JM10543D
- Li, S., Wei, Y., and Huang, J. (2010). "Facile fabrication of superhydrophobic cellulose materials by a nanocoating approach," *Chem. Lett.* 39(1), 20-21. DOI: 10.1246/cl.2010.20
- Liu, W., Cassano, C. L., Xu, X., and Fan, Z. H. (2013). "Laminated paper-based analytical devices (LPAD) with origami-enabled chemiluminescence immunoassay for cotinine detection in mouse serum," *Anal. Chem.* 85(21), 10270-10276. DOI: 10.1021/ac402055n
- Li, M. S., Tian, J. F., Al-Tamimi, M., and Shen, W. (2012). "Paper-based blood typing device that reports patient's blood type 'in writing'," *Angew. Chem. Int. Edit* 51(22), 5497-5501. DOI: 10.1002/anie.201201822
- Liu, H., Li, X., and Crooks, R. M. (2013). "Paper-based slipPAD for high-throughput chemical sensing," *Anal. Chem.* 85(9), 4263-4267. DOI: 10.1021/ac4008623
- Li, Y. Q., Guan, L. Y., Wang, J. H., Zhang, H. L., Chen, J., Lin, S., Chen, W., and Zhao, Y. D. (2011). "Simultaneous detection of dual single-base mutations by capillary electrophoresis using quantum dot-molecular beacon probe," *Biosens. Bioelectron.* 26(5), 2317-2322. DOI: 10.1016/j.bios.2010.10.002
- Li, Y. Q., Guan, L. Y., Zhang, H. L., Chen, J., Lin, S., Ma, Z. Y., and Zhao, Y. D. (2011). "Distance-dependent metal-enhanced quantum dots fluorescence analysis in solution by capillary electrophoresis and its application to DNA detection," *Anal. Chem.* 83(11), 4103-4109. DOI: 10.1021/ac200224y
- Liu, J. B., Yang, X. H., Wang, K. M., He, X. X., Wang, Q., Huang, J., and Liu, Y. (2012). "Aggregation control of quantum dots through ion-mediated hydrogen bonding shielding," *Acs Nano.* 6(6), 4973-4983. DOI: 10.1021/nn300517k
- Martinez, A. W., Phillips, S. T., Butte, M. J., and Whitesides, G. M. (2007). "Patterned paper as a platform for inexpensive, low-volume, portable bioassays," *Angew. Chem. Int. Edit* 46(8), 1318-1320. DOI: 10.1002/anie.200603817
- Ma, Y. X., Li, H., Peng, S., and Wang, L. Y. (2012). "Highly selective and sensitive fluorescent paper sensor for nitroaromatic explosive detection," *Anal. Chem.* 84(19), 8415-8421. DOI: 10.1021/ac302138c
- Ma, W., Qin, L. X., Liu, F. T., Gu, Z., Wang, J., Pan, Z. G., James, T. D., and Long, Y. T. (2013). "Ubiquinone-quantum dot bioconjugates for in vitro and intracellular complex I sensing," *Sci. Rep.* 3, 1537. DOI: 10.1038/srep01537

- Noor, M. O., Shahmuradyan, A., and Krull, U. J. (2013). "Paper-based solid-phase nucleic acid hybridization assay using immobilized quantum dots as donors in fluorescence resonance energy transfer," *Anal. Chem.* 85(3), 1860-1867. DOI: 10.1021/ac3032383
- Noh, M., Kim, T., Lee, H., Kim, C. K., Joo, S. W., and Lee, K. (2010). "Fluorescence quenching caused by aggregation of water-soluble CdSe quantum dots," *Colloid Surface A* 359(1-3), 39-44. DOI: 10.1016/j.colsurfa.2010.01.059
- Niu, T., Gu, Y., and Huang, J. (2011). "Luminescent cellulose sheet fabricated by facile self-assembly of cadmium selenide nanoparticles on cellulose nanofibers," *J. Mater. Chem.* 21, 651-656. DOI: 10.1039/C0JM02356F
- Pelton, R. (2009). "Bioactive paper provides a low-cost platform for diagnostics," *TrAC-Trend Anal. Chem.* 28(8), 925-942. DOI: 10.1016/j.trac.2009.05.005
- Sahin, H. T., and Arslan, M. B. (2008). "A study on physical and chemical properties of cellulose paper immersed in various solvent mixtures," *Int. J. Mol. Sci.* 9(1), 78-88. DOI: 10.3390/ijms9010078
- Tian, J. F., Kannangara, D., Li, X., and Shen, W. (2010). "Capillary driven low-cost V-groove microfluidic device with high sample transport efficiency," *Lab. Chip* 10(17), 2258-2264. DOI: 10.1039/C003728A
- Tan, S. N., Ge, L. Y., Tan, H. Y., Loke, W. K., Gao, J. R., and Wang, W. (2012). "Paper-based enzyme immobilization for flow injection electrochemical biosensor integrated with reagent-loaded cartridge toward portable modular device," *Anal. Chem.* 84(22), 10071-11076. DOI: 10.1021/ac302537r
- Wang, S. M., Ge, L., Song, X. R., Yu, J. H., Ge, S. G., Huang, J. D., and Zeng, F. (2012). "Paper-based chemiluminescence ELISA: Lab-on-paper based on chitosan modified paper device and wax-screen-printing," *Biosens. Bioelectron.* 31(1), 212-218. DOI: 10.1016/j.bios.2011.10.019
- Wu, P., He, Y., Wang, H. F., and Yan, X. P. (2010). "Conjugation of glucose oxidase onto Mn-doped ZnS quantum dots for phosphorescent sensing of glucose in biological fluids," *Anal. Chem.* 82(4), 1427-1433. DOI: 10.1021/ac902531g
- Xiao, W., Xu, J., Liu, X., Hu, Q., and Huang, J. (2013). "Antibacterial hybrid materials fabricated by nanocoating of microfibril bundles of cellulose substance with titania/chitosan/silver-nanoparticle composite films," *J. Mater. Chem. B* 1, 3477-3485. DOI: 10.1039/C3TB20303D
- Xiao, W., Luo, Y., Zhang, X. H., and Huang, J. G. (2013). "Highly sensitive colourimetric anion chemosensors fabricated by functional surface modification of natural cellulose substance," *Rsc Adv.* 3(16), 5318-5323. DOI: 10.1039/C3RA00074E
- Xiao, W., and Huang, J. G. (2011). "Immobilization of oligonucleotides onto zirconia-modified filter paper and specific molecular recognition," *Langmuir* 27(20), 12284-12288. DOI: 10.1021/la203150f
- Yagoda, H. (1937). "Applications of confined spot tests in analytical chemistry," *Anal. Chem.* 9(2), 79-82. DOI: 10.1021/ac50106a012
- Yuan, J. P., Gaponik, N., and Eychmuller, A. (2012). "Application of polymer quantum dot-enzyme hybrids in the biosensor development and test paper fabrication," *Anal. Chem.* 84(11), 5047-5052. DOI: 10.1021/ac300714j

Article submitted: November 13, 2014; Peer review completed: January 3, 2015; Revised version received and accepted: January 19, 2015; Published: January 23, 2015.